

Asymmetric Photoredox Catalysis with Chiral-at-Rhodium Complexes

A DISSERTATION

In

Chemistry

Presented to the Faculties of Philipps-Universität Marburg in Partial Fulfillment
of the Requirements for the Degree of Doctor of Science
(Dr. rer. nat.)

Jiajia Ma

Anhui, P. R. China

Marburg/Lahn 2018

Die vorliegende Dissertation entstand in der Zeit von October 2014 bis April 2018 am Fachbereich Chemie der Philipps-Universität Marburg unter der Betreuung von Herrn Prof. Dr. Eric Meggers.

Vom Fachbereich Chemie der Philipps-Universität Marburg (Hochschulkenziffer: 1180) als Dissertation am _____ angenommen.

Erstgutachter:	Prof. Dr. Eric Meggers
Zweitgutachter:	Prof. Dr. Armin Geyer
weitere Mitglieder Prüfungskommission:	Prof. Dr. Jörg Sundermeyer

Tag der mündlichen Prüfung: 07.08.2018

Acknowledgements

It's really a gorgeous life experience to pursue my doctoral degree in the Meggers group at Philipps-Universität Marburg. I would like to express my deepest gratitude to everybody who has helped and supported me over the past several years.

My sincere appreciation goes first and foremost to my advisor Prof. Meggers, for his constant encouragement and supervision over both my M.Sc. and Ph.D. studies. He has walked me through all the stages of my scientific research during past seven years. His extensive knowledge and dedication towards scientific research have made a great impact on me as well as the entire group, thereby triggering me to pursue an academic career in my future.

Next, I am grateful to Prof. Geyer and Prof. Sundermeyer for referring this thesis and participating in the defense committee.

I would appreciate all of the sweet colleagues in the Meggers and Höbenreich groups as well as the collaborators from the department and other institutes. Thanks a lot to Dr. Lilu Zhang, Dr. Sabrina Höbenreich, Ina Pinnschmidt, Marcel Hemming and Andrea Tschirch, for their kind help. Thanks a lot to Xiaodong Shen, Xiao Zhang, Shipeng Luo, Xiaoqiang Huang, Jiahui Lin and Lifang Zhao, for their sparking inspirations and helpful cooperation on my research. Thanks a lot to Anthony R. Rosales and Prof. Olaf Wiest for the computational investigation on the β -C(sp³)-H functionalization project. Thanks a lot to Dr. Klaus Harms, Radostan Riedel and Michael Marsch for the measurement and analysis of all the single crystals. Thanks a lot to Dr. Xiulan Xie for the analysis of NMR spectra. Thanks a lot to Erik Winterling for translating the abstract into German version. Thanks a lot to all of the former group members, Haohua Huo, Chuanyong Wang, Yuzheng, Wei Zuo, Nathalie Nett, Jens Henker, Melanie Helms, Rajathees Rajaratnam, Cornelia Ritter, Markus Dörr, Elisabeth Martin, Francisco Fávoro de Assis, Timo Völker, Thomas Cruchter, Tabea-Melanie Faber and Bo Zhang, for their kind help. Besides, I really appreciate for the help and company from the other current group members, Qi Zhang, Jie Qin, Yuqi Tan, Zijun Zhou, Sabine Dewel, Yvonne Grell, Yubiao Hong, Chenhao Zhang, Thomas Mietke, Tianjiao Cui, Yuanze Tang, Xingwen Zheng and Xin Nie.

At last, I would like to appreciate my lovely families and especially my wife Yan Zhang for their constant support and endless encouragement.

All the best wishes for my friends and families!

Publications and Poster Presentations

Publications:

1. J. Ma, J. Lin, L. Zhao, K. Harms, M. Marsch, X. Xie, E. Meggers, Synthesis of β -Substituted γ -Aminobutyric Acid Derivatives via Enantioselective Photoredox Catalysis, *Angew. Chem. Int. Ed.* **2018**, DOI: 10.1002/anie.201804040.
2. J. Ma[‡], X. Zhang[‡], X. Huang, S. Luo, E. Meggers, Preparation of Chiral-at-Metal Catalysts and Their Use in Asymmetric Photoredox Chemistry, *Nat. Protoc.* **2018**, *13*, 605. (‡ Equal contribution)
3. J. Ma, X. Xie, E. Meggers, Catalytic Asymmetric Synthesis of Fluoroalkyl-Containing Compounds by Three-Component Photoredox Chemistry, *Chem. Eur. J.* **2018**, *24*, 259.
4. J. Ma, A. R. Rosales, X. Huang, K. Harms, R. Riedel, O. Wiest, E. Meggers, Visible-Light-Activated Asymmetric β -C-H Functionalization of Acceptor-Substituted Ketones with 1,2-Dicarbonyl Compounds, *J. Am. Chem. Soc.* **2017**, *139*, 17245. (featured in *Synfacts* **2018**, 0157)
5. J. Ma, K. Harms, E. Meggers, Enantioselective Rhodium/Ruthenium Photoredox Catalysis *en Route* to Chiral 1,2-Aminoalcohols, *Chem. Commun.* **2016**, *52*, 10183.
6. J. Ma, X. Shen, K. Harms, E. Meggers, Expanding the Family of bis-Cyclometalated Chiral-at-Metal Rhodium(iii) Catalysts with a Benzothiazole Derivative, *Dalton Trans.* **2016**, *45*, 8320.

Poster Presentation:

“20th European Symposium on Organic Chemistry (ESOC 2017)”, Poster: Visible-Light-Induced Catalytic Asymmetric β -C(sp³)-H Activation of Acceptor-Substituted Ketones, 2nd-6th July **2017**, Cologne, Germany.

Abstract

Chiral transition metal catalysts in which the chirality exclusively originates from a stereogenic metal center witness a more recent advance and their excellent catalytic performance has been demonstrated through applications into diverse enantioselective transformations, especially visible-light-activated photoredox reactions. This thesis deals with the synthesis of new chiral-at-metal rhodium Lewis acid catalysts and their applications in enantioselective photoredox chemistry.

1) Synthesis of a new member of the rhodium-based chiral Lewis acids family, named **RhS**, with exclusive octahedral centrochirality which features the Λ -configuration (left-handed propeller) and Δ -configuration (right-handed propeller) has been accomplished. Both enantiomers Λ - and Δ -**RhS** contain two cyclometalating 5-*tert*-butyl-2-phenylbenzothiazoles in addition to two exchange-labile acetonitriles with a hexafluorophosphate counterion, were synthesized conveniently through a chiral-auxiliary-mediated strategy. Compared with the previously developed Λ/Δ -**RhO** complexes bearing corresponding benzoxazoles, the Λ/Δ -**RhS** have been recognized as better chiral Lewis acid catalysts due to the higher steric congestion directed by the benzothiazole ligands, in which the longer C–S bonds over C–O bonds position the steric bulky tertiary butyl groups closer to the substrate coordination site (chapter 3.1). Subsequently, the newly developed chiral-at-rhodium Lewis acids were applied to visible-light-activated asymmetric photoredox catalysis as discussed in chapters 3.2-3.5.

2) The chiral Lewis acid Λ -**RhS** combined with the photoredox catalyst [Ru(bpy)₃](PF₆)₂ enabled the visible-light-activated redox coupling of α -silylalkyl amines with 2-acyl imidazoles to afford, after desilylation, 1,2-amino-alcohols in yields of 69–88% and with high enantioselectivities (54–99% ee). The reaction is proposed to proceed *via* single electron transfer (SET) between the α -silylamine (electron donor) and the rhodium-chelated 2-acyl imidazole (electron acceptor), followed by a stereocontrolled radical–radical recombination (chapter 3.2).

3) A new and simple commercially available photoredox mediator 4,4'-difluorobenzil was developed to cooperate with the chiral-at-rhodium Lewis acids Λ/Δ -**RhS**. This synergistic catalytic system permits an enantioselective three-component photoreaction to provide the fluoroalkyl-containing products under dual C–C bond formation with high enantioselectivities (up to 98% ee) and modest diastereoselectivities (up to 6:1 dr). Excellent diastereoselectivities (up to >38:1 dr) for natural chiral compound derivatives were observed. The photoexcited 4,4'-difluorobenzil is

proposed to enable the single electron oxidation of sodium perfluoroalkyl sulfinates under the generation of corresponding perfluoroalkyl radicals which are trapped by electron-rich vinyl ethers to deliver α -oxy carbon-centered radicals. These nucleophilic radical species are involved in a subsequent Rh-catalyzed radical conjugate addition with acceptor-substituted alkenes (chapter 3.3).

4) The single chiral-at-rhodium Lewis acids catalyzed radical conjugate addition of α -amino alkyl radicals with acceptor-substituted alkenes provided the C–C formation products in good yields (up to 89%) and with excellent enantioselectivities (up to 97% ee) under visible-light-activated photocatalyst-free conditions. The α -amino alkyl radicals are generated from simple glycine derivatives upon single electron reduction triggered by the photoreductant Hantzsch ester. This methodology is recognized as a practical and versatile avenue to access diverse pharmaceutically demanding chiral β -substituted γ -aminobutyric acid analogs, including previously inaccessible derivatives containing fluorinated quaternary stereocenters. Synthetically valuable applications are demonstrated by providing straightforward access to the pharmaceuticals or related bioactive compounds (*S*)-pregabalin, (*R*)-baclofen, (*R*)-rolipram and (*S*)-nebracetam (chapter 3.4).

5) Visible-light-activated enantioselective β -C(sp³)-H functionalization of 2-acyl imidazoles and 2-acylpyridines with 1,2-dicarbonyl compounds catalyzed by a single chiral-at-rhodium Lewis acid Δ -**RhS** derivative was developed. The C–C bond formation products are obtained in high yields (up to 99%) and with excellent stereoselectivities (up to >20:1 dr and up to >99% ee). Experimental and computational studies support a mechanism in which a photoactivated Rh-enolate intermediate, produced through the coordination of an acceptor-substituted ketone to the central rhodium in the presence of base, transfers a single electron to the 1,2-dicarbonyl compound followed by deprotonation at β position of initial ketone and a subsequent stereocontrolled radical-radical recombination. The chiral-at-rhodium Lewis acid is capable of serving a dual function as a chiral catalyst and a photoredox (pre)catalyst (chapter 3.5).

Zusammenfassung

Chirale Übergangsmetallkatalysatoren, welche nur achirale Liganden koordinieren und bei denen die Chiralität des gesamten Komplexes auf ein stereogenes Metallzentrum zurückgeführt werden kann, bilden eine neuere Klasse von asymmetrischen Übergangsmetallkatalysatoren. Ihre ausgezeichneten katalytischen Fähigkeiten wurde durch die Anwendungen in verschiedenen enantioselektiven Umwandlungen demonstriert, insbesondere auch in lichtaktivierten Photoredoxreaktionen. Diese Arbeit beschäftigt sich mit der Synthese neuartiger Rhodium-basierter chiraler Lewis-Säurekatalysatoren mit ausschliesslich metallzentrierter Chiralität und deren Anwendungen in der enantioselektiven Photoredoxchemie.

1) Die Synthese eines neuen Mitglieds der Familie Rhodium-basierter chiraler Lewis-Säuren wurde entwickelt. Der neue Komplex wurde **RhS** genannt. Mit einer ausschliesslich oktaedrischen Zentrochiralität weist der racemische Komplex eine Λ -Konfiguration (linksdrehender Propeller) und Δ -Konfiguration (rechtsdrehender Propeller) auf. Die beiden Enantiomere, Λ - und Δ -**RhS**, enthalten zwei cyclometallisierende 5-*tert*-Butyl-2-phenylbenzothiazole, zwei austauschbaren Acetonitrile und ein Hexafluorophosphat-Gegenion. Sie wurden mit Hilfe einer Chirales-Auxiliar-vermittelten Strategie enantiomerenrein synthetisiert. Im Vergleich zu den zuvor entwickelten Λ/Δ -**RhO**-Komplexen, die entsprechende Benzoxazole tragen, wurden Λ/Δ -**RhS** als bessere chirale Lewis-Säure-Katalysatoren ermittelt. Dies kann mit einer höheren sterischen Abschirmung erklärt werden. Durch die im Vergleich zu den C-O-Bindungen im Benzoxazol längeren C-S-Bindungen der Benzothiazole befinden sich die *tert*-Butylgruppen von **RhS** näher am Reaktionszentrum (Kapitel 3.1). Anschließend wurden die neu entwickelten chiralen Rhodium-Lewis-Säuren auf die durch sichtbares Licht aktivierte asymmetrische Photoredoxkatalyse angewendet, wie es in den Kapiteln 3.2-3.5 beschrieben wurde.

2) Die mit dem Photoredoxkatalysator $[\text{Ru}(\text{bpy})_3](\text{PF}_6)_2$ kombinierte chirale Lewis-Säure Λ -**RhS** ermöglichte die durch sichtbares Licht aktivierte Redoxkupplung von α -Silylalkylaminen mit 2-Acylimidazolen. Nach der Desilylierung wurden 1,2-Aminoalkohole mit Ausbeuten von 69% bis 88% und mit hohen Enantioselektivitäten (54-99% ee) erhalten. Es wird vorgeschlagen, dass die Reaktion über einen Einzelelektronentransfer (SET) zwischen dem α -Silylalkylamin (Elektronendonator) und dem Rhodium-Chelat-2-Acylimidazol (Elektronenakzeptor) verläuft, gefolgt von einer stereokontrollierten Radikal-Radikal-Rekombination (Kapitel 3.2).

3) Ein neuer und kommerziell erhältlicher Photoredox-Vermittler 4,4'-Difluorbenzil wurde entwickelt. Dieser Vermittler kann mit den chiralen Rhodium-Lewis-Säuren Λ/Δ -**RhS** kooperieren. Dieses synergistische katalytische System ermöglichte eine enantioselektive Drei-Komponenten-Photoreaktion, um die fluoralkylhaltigen Produkte unter dualer C–C-Verknüpfung mit hohen Enantioselektivitäten (bis zu 98% ee) und moderaten Diastereoselektivitäten (bis zu 6: 1 dr) zu liefern. Ausgezeichnete Diastereoselektivitäten (bis zu > 38: 1: 1 dr) für natürliche chirale Verbindungsderivate wurden beobachtet. Es wird vorgeschlagen, dass das photoangeregte 4,4'-Difluorbenzil die Einzelelektronenoxidation von Natriumperfluoralkylsulfonaten unter Erzeugung von entsprechenden Perfluoralkylradikalen ermöglicht, die durch elektronenreiche Vinylether abgefangen werden, um α -Oxy-Kohlenstoff-zentrierte Radikale zu liefern. Diese nucleophilen Radikalspezies sind an einer anschließenden Rh-katalysierten radikalkonjugierten Addition mit Akzeptor-substituierten Alkenen beteiligt (Kapitel 3.3).

4) Unter durch sichtbares Licht aktivierten Photokatalysator-freien Bedingungen lieferte die durch chirale Rhodium-Lewis-Säuren katalysierte radikalische Addition von γ -Aminoalkylresten mit Akzeptor-substituierten Alkenen die C–C-Bildungsprodukte in guten Ausbeuten (bis zu 89%) und mit ausgezeichneten Enantioselektivitäten (bis zu 97% ee). Die α -Aminoalkylreste wurden aus einfachen Glycinderivaten bei der durch den Photoreduktanten-Hantzsch-Ester ausgelösten Einzelelektronenreduktion erzeugt. Diese Methode wird als ein praktischer und vielseitiger Weg angesehen, um Zugang zu verschiedenen pharmazeutisch anspruchsvollen chiralen β -substituierten γ -Aminobuttersäure-Analoga zu erhalten, einschließlich bisher unerreichbarer Derivate, die fluorierte quartäre Stereozentren enthalten. Synthetisch wertvolle Anwendungen wurden durch einen einfachen Zugang zu den Pharmazeutika oder verwandten bioaktiven Verbindungen (*S*)-Pregabalin, (*R*)-Baclofen, (*R*)-Rolipram und (*S*)-Nebracetam (Kapitel 3.4) demonstriert.

5) Eine durch sichtbares Licht aktivierte enantioselektive β -C(sp³)-H-Funktionalisierung von 2-Acylimidazolen und 2-Acylpyridinen mit 1,2-Dicarbonylverbindungen wurde entwickelt, welche von einem einzigen chiralen Rhodium-Lewis-Säure- Δ -RhS-Derivat katalysiert wird. Die C–C-Bindungsbildungsprodukte wurden in hohen Ausbeuten (bis zu 99%) und mit ausgezeichneten Stereoselektivitäten (bis zu > 20: 1 dr und bis zu > 99% ee) erhalten. Experimentelle und theoretische Untersuchungen stützen den folgenden Mechanismus. Zuerst bildet sich ein Rh-Enolat-Intermediat in Gegenwart einer Base durch Koordination eines Akzeptor-substituierten Ketons an das zentrale

Rhodium. Das photoaktivierte Rh-Enolat-Intermediat überträgt ein einzelnes Elektron auf die 1,2-Dicarbonylverbindung. Nach der Deprotonierung an β -Position des anfänglichen Ketons kommt es zu einer stereokontrollierten Rekombination der beiden Radikale. Die chirale Rhodium-Lewis-Säure ist in der Lage, eine doppelte Funktion als chiraler Katalysator und als Vorläufer des Photoredox-Katalysators zu erfüllen (Kapitel 3.5).

Table of Contents

Acknowledgements.....	I
Publications and Poster Presentations	III
Abstract	V
Zusammenfassung.....	VII
Table of Contents.....	XI
Chapter 1: Theoretical Part.....	1
1.1 Introduction.....	1
1.2 Asymmetric Photoredox Chemistry with Organocatalysts.....	4
1.3 Asymmetric Photoredox Chemistry with Transition Metal Catalysts	20
1.4 Asymmetric Photoredox Chemistry with Traditional Lewis Acid Catalysts	23
1.5 Asymmetric Photoredox Chemistry with Chiral-at-Metal Lewis Acid Catalysts	26
1.6 Conclusions.....	31
Chapter 2: Aim of the Work.....	34
Chapter 3: Results and Discussion.....	37
3.1 Synthesis of the New Chiral-at-Rh Lewis Acid Catalyst Λ/Δ -RhS	37
3.1.1 Synthetic Design.....	37
3.1.2 Synthesis and Characterization.....	39
3.1.3 Evaluation of Catalytic Activity of Λ -RhS	42
3.1.4 Conclusions	44
3.2 Cooperative Rhodium/Ruthenium Asymmetric Photoredox Catalysis to Access Chiral 1,2-Aminoalcohols.....	45
3.2.1 Research Background and Reaction Design.....	45
3.2.2 Initial Experiments and Reaction Development	48
3.2.3 Substrate Scope	50
3.2.4 Mechanistic Study	52
3.2.5 Conclusions	54
3.3 Synthesis of Fluoroalkyl-Containing Compounds through Enantioselective Three-Component Photoredox Reaction	56
3.3.1 Research Background and Reaction Design.....	56
3.3.2 Initial Experiments and Reaction Development	60
3.3.3 Substrate Scope	62
3.3.4 Mechanistic Study	65
3.3.5 Conclusions	68

3.4 Synthesis of β-Substituted γ-Aminobutyric Acid Derivatives through Enantioselective Photoredox Catalysis	70
3.4.1 Research Background and Reaction Design.....	70
3.4.2 Initial Experiments and Reaction Development.....	73
3.4.3 Scope of γ -Aminobutyric Acid Analogs.....	75
3.4.4 Synthetic Applications.....	77
3.4.5 Conclusions	78
3.5 Asymmetric β-C–H Functionalization of Acceptor-Substituted Ketones through Single Rh-based Photoredox Catalysis.....	80
3.5.1 Research Background and Reaction Design.....	80
3.5.2 Initial Experiments and Reaction Development.....	82
3.5.3 Substrate Scope	84
3.5.4 Synthetic Transformation	86
3.5.5 Mechanistic Study	87
3.5.6 Conclusions	94
Chapter 4: Summary and Outlook	96
4.1 Summary	96
4.2 Outlook.....	102
Chapter 5: Experimental Part.....	104
5.1 Materials and Methods.....	104
5.2 Synthesis of the New Chiral-at-Rh Lewis Acid Catalyst Λ/Δ-RhS	107
5.2.1 Synthesis of Rhodium-Based Catalysts Λ -RhS and Δ -RhS.....	107
5.2.2 Rhodium-Catalyzed Asymmetric Reactions.....	111
5.2.3 Determination of Enantiomeric Purities of the Rhodium Catalysts	112
5.2.4 Investigation of the Configurational Stability of the Rhodium Catalyst	114
5.2.5 Single Crystal X-Ray Diffraction Studies	118
5.3 Cooperative Rhodium/Ruthenium Asymmetric Photoredox Catalysis to Access Chiral 1,2-Aminoalcohols.....	122
5.3.1 Synthesis of Substrates.....	122
5.3.2 Rhodium-Catalyzed Redox Coupling Reactions Activated by Visible Light.....	131
5.3.3 Mechanistic Studies.....	147
5.3.4 Single Crystal X-Ray Diffraction Studies	149
5.4 Synthesis of Fluoroalkyl-Containing Compounds through Enantioselective Three-Component Photoredox Reaction	153
5.4.1 Synthesis of Substrates.....	153
5.4.2 Optimization of Conditions.....	159
5.4.3 Rhodium-Catalyzed Asymmetric Three-Component Photoredox Reactions	162
5.4.4 Mechanistic Experiments	184
5.4.5 Gram Scale Reaction and Catalyst Recovery	188
5.4.6 Assignment of Absolute and Relative Configurations.....	189

5.5 Synthesis of β-Substituted γ-Aminobutyric Acid Derivatives via Enantioselective Photoredox Catalysis	196
5.5.1 Synthesis of Substrates	196
5.5.2 Rhodium-Catalyzed Giese-Type Reaction Activated by Visible Light	205
5.5.3 Synthetic Applications.....	226
5.5.4 Assignment of Absolute Configuration.....	235
5.6 Asymmetric β-C–H Functionalization of Acceptor-Substituted Ketones through Single Rh-based Photoredox Catalysis	240
5.6.1 Synthesis of a Derived Chiral-at-Rhodium Lewis Acid Catalyst	240
5.6.2 Synthesis of Substrates	246
5.6.3 Rhodium-Catalyzed β -(sp ³)-C–H Functionalization Activated by Visible Light	255
5.6.4 Removal of Directing Group	283
5.6.5 Mechanistic Experiments	284
5.6.6 Single Crystal X-Ray Diffraction Studies	287
Chapter 6: Appendices.....	292
6.1 List of Abbreviations	292
6.2 List of Figures.....	295
6.3 List of Tables	302
6.4 List of New Compounds	303
Statement.....	311
Curriculum Vitae.....	312

Chapter 1: Theoretical Part

1.1 Introduction

Over the past century, photochemistry has witnessed significant progress to lead the discovery of diverse unconventional synthetic methodologies in organic chemistry. In contrast with the well-established ultraviolet (UV) light mediated photosynthesis, the visible-light-induced photocatalysis is a more recent advance. Utilizing visible light, ideally sunlight, as driving forces contents the quest for renewable and clean sources of energy in modern organic synthesis, which in turn, affords fruitful synthetic protocols under sufficiently mild conditions. Remarkably, most of these unusual protocols are inaccessible under thermal control. Among the mechanistic scenarios of photocatalysis, including energy transfer, atom transfer and single electron transfer (SET), the SET-based photoredox catalysis has attracted much attention from the broad organic chemistry community.¹

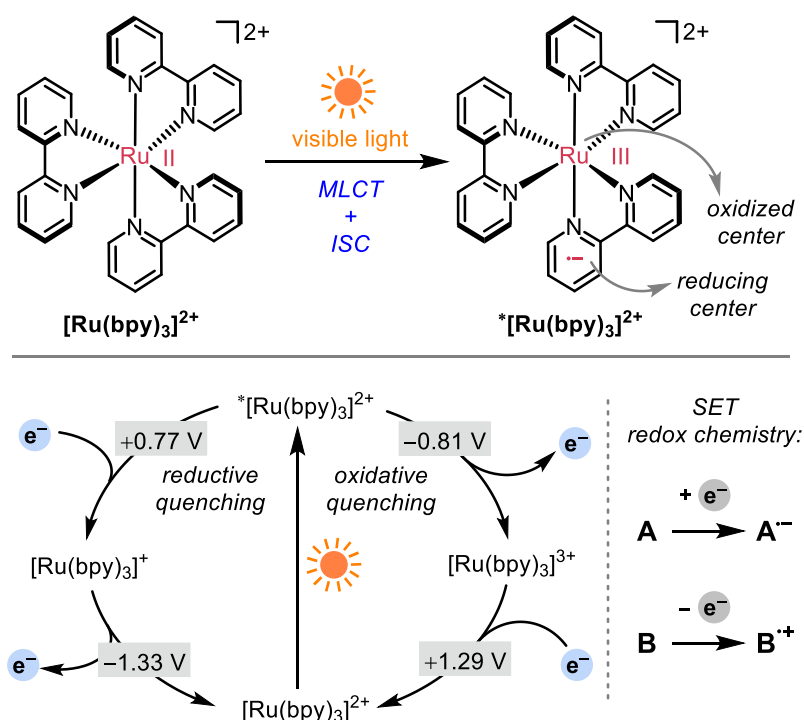


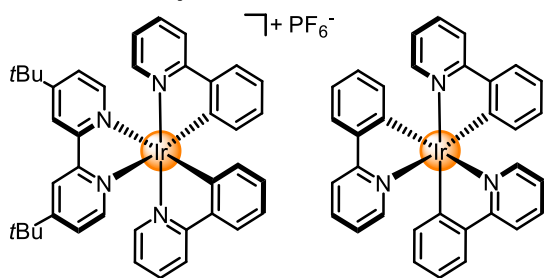
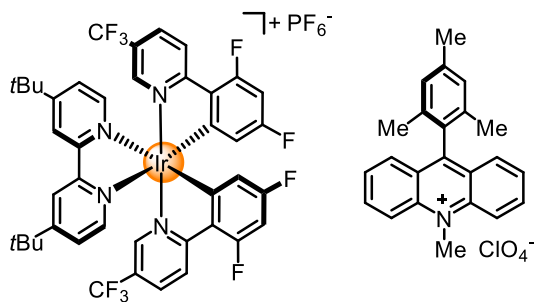
Figure 1. Visible-light-induced photoredox catalytic processes as exemplified by $[\text{Ru}(\text{bpy})_3]^{2+}$. MLCT = metal to ligand charge transfer. ISC = intersystem crossing. SET = single electron transfer

With respect to the term of photoredox catalysis, typically, transition metal complexes, such as the commonly used $\text{Ru}(\text{bpy})_3^{2+}$ at substoichiometric amounts, upon absorption of a photon at visible region,

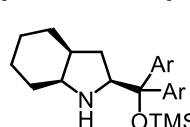
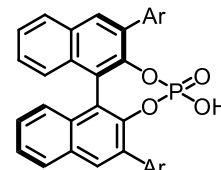
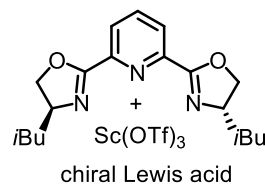
an electron on the non-bonding metal-centered orbital (HOMO) could be excited to the π system of the ligand framework (LUMO), defined as metal to ligand charge transfer (MLCT) (**Figure 1**). Subsequent intersystem crossing affords a long-lived triplet state photocatalyst which constitutes an ideal source of electrochemical potential to promote single electron transfer (SET) events with organic substrates or other reaction partners. Namely, this excited photocatalyst could either donate a high-energy electron out (termed as oxidative quenching) or accept a single electron (termed as reductive quenching). Nevertheless, the resulted catalyst at the reduced or oxidized state features the strong thermodynamic driving force back to the original ground state, thereby promoting a second reverse-path SET event. The overall process would provide radical cations or anions which could directly undergo the chemical bond formations. Alternatively, these intermediates, upon subsequent transformation, afford thermodynamically relatively stable species that engage into diverse synthetic processes. One of the most interesting aspects of the visible-light-induced photoredox catalysis is the combination with asymmetric catalysis. Namely, the forementioned photogenerated intermediates could undergo the formation of carbon-carbon or carbon-heteroatom bonds under the stereocontrol of a chiral catalyst. The photoredox catalyst and asymmetric catalyst could derive either from the identical or a separated source.

However, over the past decades the development of highly enantioselective photoreactions remains as a formidable challenge, mainly due to the high reactivity of the photogenerated intermediates as well as the low activation barriers of the following bond formation processes. Alongside with the renaissance of the photoredox catalysis in the recent years, tremendous success has been achieved using the conventional or emerging catalytical techniques. The following section will highlight representative examples on asymmetric photoredox catalysis based on the types of the chiral catalysts, including organocatalysts, transition metal catalysts, traditional Lewis acids and the emerging chiral-at-metal catalysts (**Figure 2**).

Photoredox catalysts:

Ir(ppy)₂(dtbbpy)PF₆*fac*-Ir(ppy)₃Ir(dF(CF₃)ppy)₂(dtbbpy)PF₆[Acr-Mes]ClO₄

Asymmetric catalysts:

Ar = 3,5-(CF₃)₂-C₆H₃
chiral amineAr = 2,4,6-(iPr)₃C₆H₂
chiral phosphoric acid

chiral Lewis acid

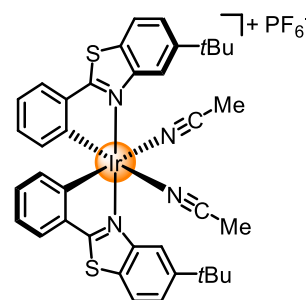
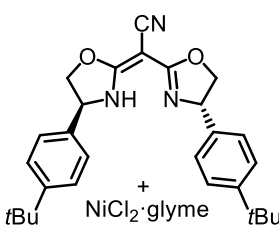
Λ-IrS
chiral-at-Ir Lewis acidNiCl₂:glyme
chiral transition metal

Figure 2. Representative photoredox and asymmetric catalysts. The chiral-at-iridium Lewis acid and the chiral amine (only in special cases) constitute dual functions of photoredox/asymmetric catalyst.

1.2 Asymmetric Photoredox Chemistry with Organocatalysts

Organocatalysis triggered the leading invention of the visible-light-induced enantioselective photoredox chemistry, and has been demonstrated as one of the most powerful architectures.² The following sections will briefly review the organo-catalyzed photoredox reactions.

1) Covalent interaction catalysts: chiral amine and *N*-heterocyclic carbene

Due to the dedicated work from several research groups, the chiral amine has been demonstrated as one of the most impressive tools to promote the asymmetric photoredox catalysis. The chiral amine mediated enamine catalysis could cooperate smoothly with the visible-light-induced photoredox catalysis. Alternatively, in some cases, the electron-rich enamine intermediate (donor) would interact with the electron-deficient substrate (acceptor), thereby affording the transient electron donor acceptor (EDA) complex. This colored complex is capable of absorbing visible light, subsequently undergoing internal single electron exchange. Very recent reports reveal that the chiral enamine and iminium ion could even get directly excited under the irradiation with visible light and then trigger the single electron reduction/oxidation of suitable substrates, respectively.

In 2008, MacMillan and co-workers reported the first example on intertwining the visible-light-activated photoredox catalysis with asymmetric enamine catalysis.³ The enantioselective α -alkylation of aldehydes with electron-deficient α -bromo carbonyl compounds proceeded efficiently in the presence of Ru(bpy)₃Cl₂ and chiral imidazolidinone under the irradiation of a household 15 W compact fluorescent lamp (CFL) (**Figure 3**). The methodology was later proved to be of reproducible and robust by switching from the Ru-based photoredox catalyst to the Eosin Y and semiconductors.⁴

This cooperative photoredox/enamine catalysis was further demonstrated as a versatile approach for the α -functionalization of aldehydes including trifluoromethylation⁵ and cyanoalkylation⁶. Especially, the α -cyanoalkylated aldehydes are valuable feedstocks for the synthesis of a wide range of medicinally relevant heterocycles and other derivatives. For instance, the natural product (–)-burshehemin was obtained from an oxonitrile product over four steps in overall 80% yield and with excellent stereoselectivity (>30:1 dr, 94% ee).

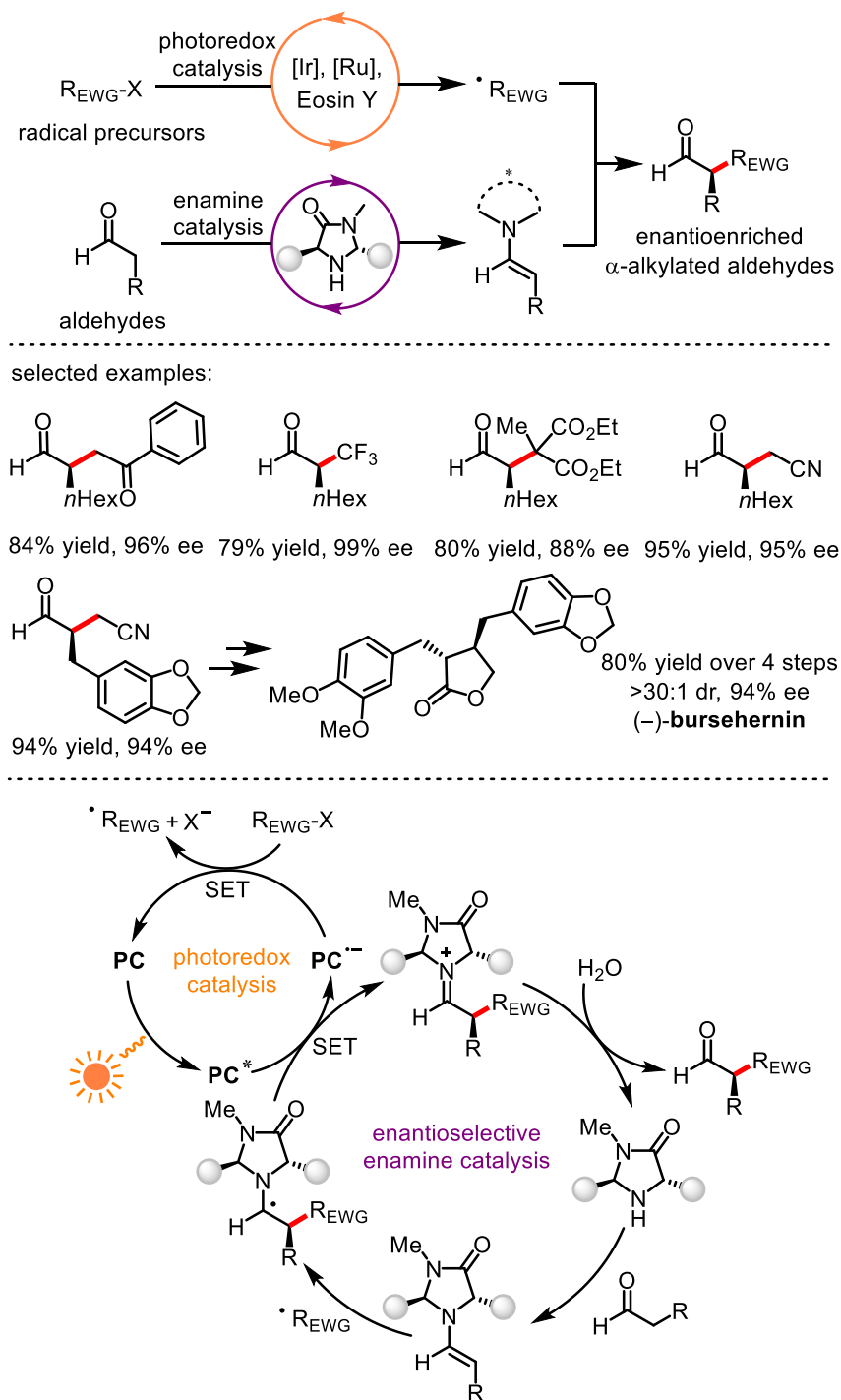


Figure 3. α -Alkylation of aldehydes enabled by dual photoredox/enamine catalysis.

A proposed reaction mechanism is outlined in **Figure 3**. Accordingly, the electrophilic radical species which was generated by single electron reduction mediated a photoredox catalytic cycle, could react towards an enamine intermediate under the formation of C–C bond. The produced α -aminoalkyl radical was further converted into an iminium ion by promoting a single electron reduction to the photoredox cycle, alternatively to the electron-deficient bromo compounds (chain

mechanism). The iminium ion was hydrolyzed to deliver the α -alkylated product accompanied with the regeneration of the chiral imidazolidinone which would enable a new enantioselective enamine catalytic cycle. Luo and co-workers later extended this dual photoredox/enamine catalysis system to the asymmetric α -alkylation of β -dicarbonyl compounds to forge the all-carbon quaternary stereocenters with excellent enantioselectivities.⁷

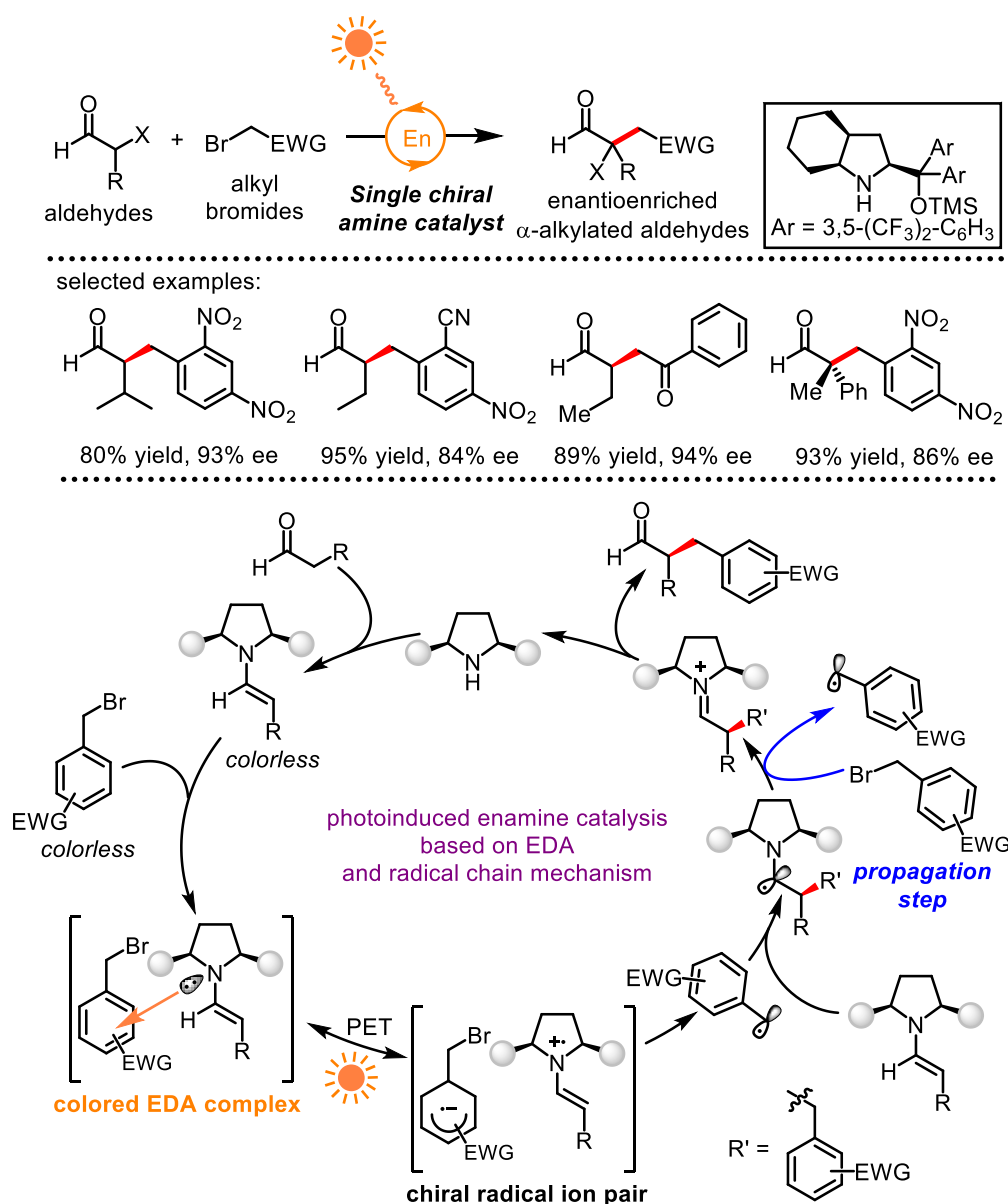


Figure 4. Enantioselective α -alkylation of aldehydes through photoexcited EDA and radical chain mechanism. EDA = electron donor acceptor. PET = photoinduced electron transfer

Subverting the idea on using cooperative catalysis to trigger the asymmetric photoredox chemistry, Melchiorre's group reported a unique enantioselective photoreaction scheme in the absence of any photoredox catalyst, while based on a single chiral secondary amine catalyst. This single catalyst

mediated photoredox reaction gave rise to the enantioenriched α -alkylated aldehydes, as well with high efficiency (**Figure 4**).⁸ The elaborated mechanism investigation revealed that the colorless electron-rich enamine intermediate (donor) interacted with the electron-deficient organobromide compound (acceptor) to deliver an electron-donor-acceptor (EDA) complex in the nonpolar solvent. This colored complex was capable of absorbing visible light, followed by a single electron transfer (SET) between the two components to afford a radical ion pair. Subsequently, the organobromide-based radical anion underwent a heterolytic fragmentation to provide an electrophilic alkyl radical which was interfaced with a new chiral enamine to generate to generate an α -aminoalkyl radical. This electron rich radical species then promoted the direct single electron reduction of organobromide compound to provide an iminium ion and an electrophilic alkyl radical, which process was identified as “radical chain mechanism”.⁹ Upon hydrolysis of the iminium ion, the enantioenriched α -alkylated aldehydes were afforded and accompanied with the regeneration of the chiral secondary amine. This unusual EDA-based strategy was later applied into the enantioselective α -alkylation of ketones with a cinchona-based primary amine catalyst.¹⁰

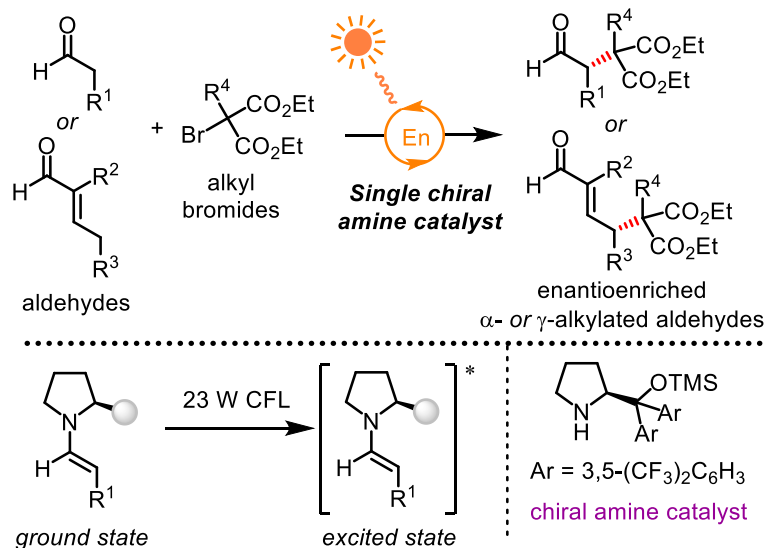


Figure 5. Single chiral amine catalyzed enantioselective photoredox chemistry through the direct photoexcitation of enamine. CFL = compact fluorescent lamp.

Interestingly, Melchiorre and co-workers later found the enamine intermediate capable of photoexcitation by absorbing light in the near-UV region under the irradiation of 23 W CFL, which then triggered the single electron reduction of bromomalonate (**Figure 5**).¹¹ Mechanistic investigations revealed that the photoexcited enamine served as a sacrificial initiator of a radical chain

propagation pathway. Besides, MacMillan group also reported that a single chiral primary amine was capable of enabling the asymmetric photoredox chemistry, namely catalyzing the enantioselective α -amination of aldehydes using (ODN)-*N*-functionalized carbamates as aminyl radical precursors (ODN=2,4-dinitrophenylsulfonyloxy).¹² However, the authors didn't discuss the possibility of EDA complex formation, the direct excitation of enamine and the radical chain mechanism in this report.

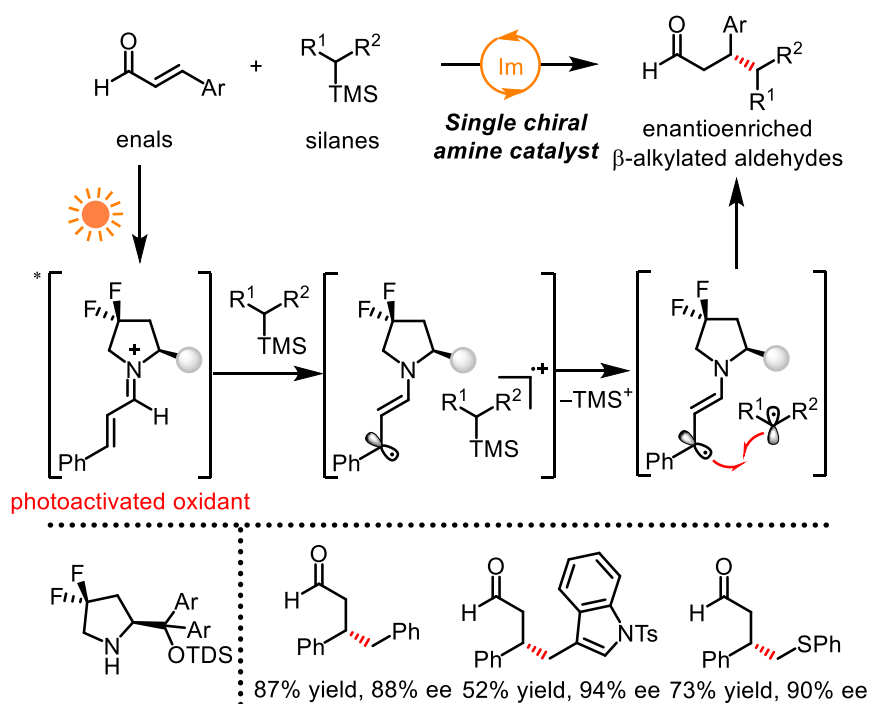


Figure 6. β -Alkylation of aldehydes through photoexcited iminium ion intermediate enabled by single chiral amine catalyst. TMS = trimethylsilyl. TDS = hexyl-dimethylsilyl.

Later, inspired by the observation that the iminium ion is capable of absorbing visible light and triggers photochemical events in the biological system, Melchiorre's group reported the utilization of this chemical process to enable the enantioselective β -alkylation of enals with the silanes in high yields and good enantioselectivities (**Figure 6**).¹³ There are two key issues in this chemical transformation: 1) the iminium ion absorbing the visible light while the individual reaction partner not and 2) the high oxidation potential of the photoexcited iminium ion. A single electron transferred from the silane to the photoexcited iminium ion, after desilylation, affording two radical species. These two radicals recombined, thereby providing the chiral β -alkylated aldehydes.

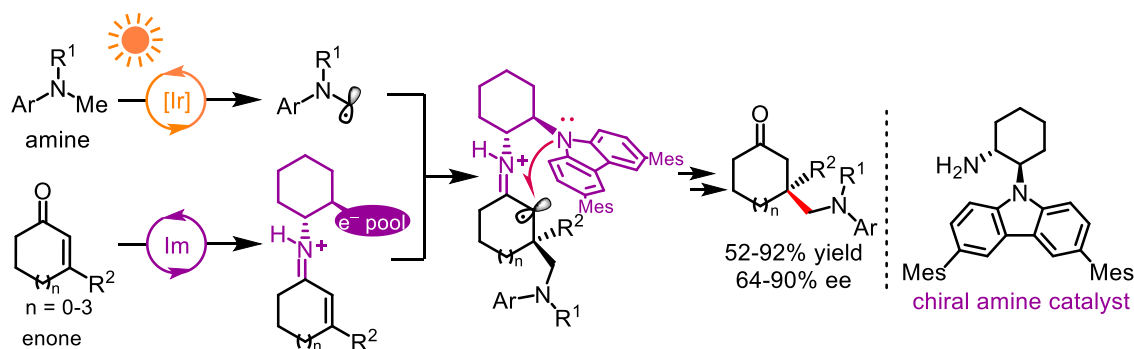


Figure 7. Enantioselective radical conjugate addition reaction enabled by dual photoredox/enamine catalysis. [Ir] = Ir[dF(CF₃)ppy]₂(dtbbpy)PF₆.

Using the dual catalysis strategy, Melchiorre and co-workers disclosed another interesting photoreaction to accomplish the construction of often challenging all-carbon quaternary stereocenters (**Figure 7**).¹⁴ The photogenerated α -aminoalkyl radical reacted towards the iminium ion which was produced by condensation of chiral amine catalyst and β,β -disubstituted cyclic enone. The following stereocontrolled radical conjugate addition provided the C–C formation products containing all-carbon quaternary stereocenters in good enantioselectivities (64–90% ee). The key to success for this reaction is tailored design of the chiral amine catalyst, thereby the introduced redox-active carbazolyl being capable of triggering the rapid intramolecular single electron transfer (SET) between the electron-rich carbazole moiety and the short-lived α -iminyl radical cation. This electron-relay process prevented the highly reactive α -iminyl radical cation to undergo the undesired radical elimination (β -scission), therefore giving back to the α -aminoalkyl radical and the iminium ion.

Turning back to the cooperative enamine/photoredox catalysis, MacMillan's group further extended this strategy to enable the β -C(sp³)–H activation of aldehydes and ketones, however, only providing one example of β -arylation products with unsatisfactory enantioselectivity (50% ee) using a cinchona-based primary amine catalyst.¹⁵ As outlined in **Figure 8**, this reaction scheme was built within the redox coupling between the cyclohexanone and the 1,4-dicyanobenzene. Accordingly, the cyclohexanone, upon condensation with the chiral amine catalyst, afforded an enamine intermediate. This electron-rich intermediate would exchange a single electron with electron deficient 1,4-dicyanobenzene molecular which process was mediated by an electron shuttle, photoexcited *fac*-Ir(ppy)₃. A subsequent unique stereocontrolled radical-radical coupling provided the corresponding β -aryl ketone with the enantioselectivity of 50% ee. Coupling reagent scope of this photoinduced β -functionalization protocol was further extended to the ketones¹⁶, enones¹⁷ and imines¹⁸. However,

all of the corresponding C–C formation products with these reagents were obtained in racemic form. Overall, the β -functionalization of saturated carbonyl compounds using dual photoredox/enamine catalysis still remains as a formidable challenge. The invention of new catalytic techniques would lead to the solution of this puzzle.

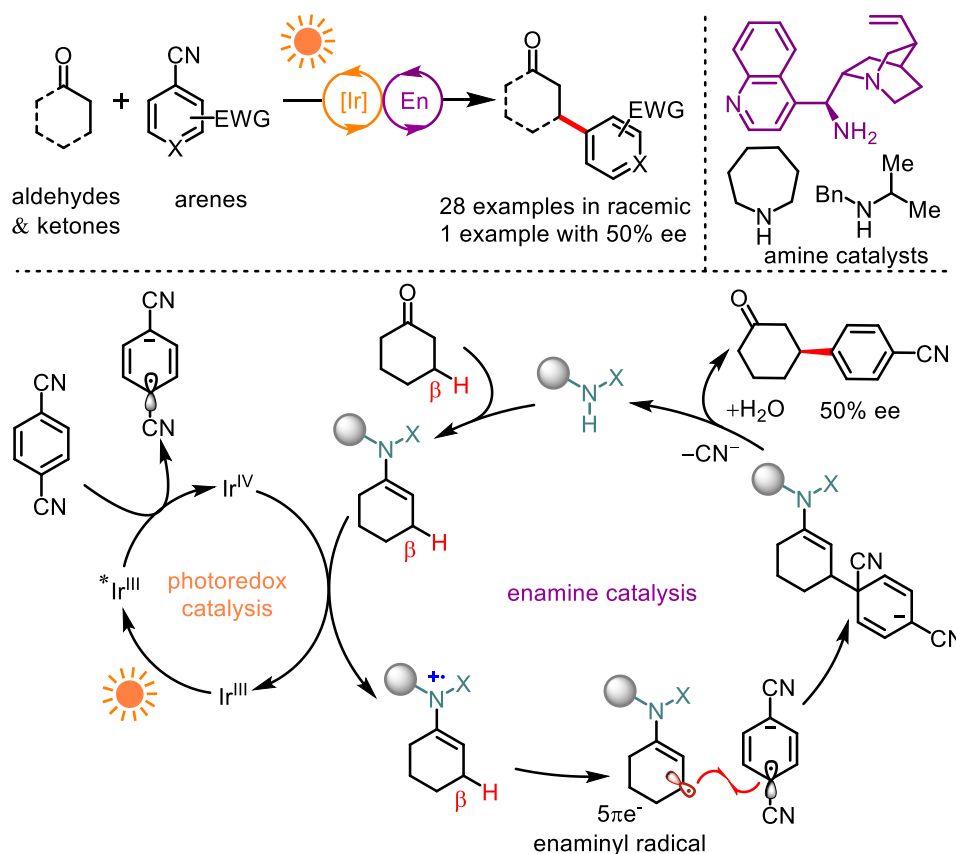


Figure 8. β -Arylation of the aldehydes and ketones enabled by dual photoredox/enamine catalysis. [Ir] = *fac*-Ir(ppy)₃.

While the chiral-amine-based dual asymmetric photoredox catalysis was established, the MacMillan's group turned to investigate a triple catalysis system containing an additional hydrogen atom transfer (HAT) catalytic cycle. This triple catalysis scheme provided the α -alkylated aldehydes with good outcome through the trapping of $3\pi e^-$ enaminy radical cation intermediates using simple olefins (**Figure 9**).¹⁹

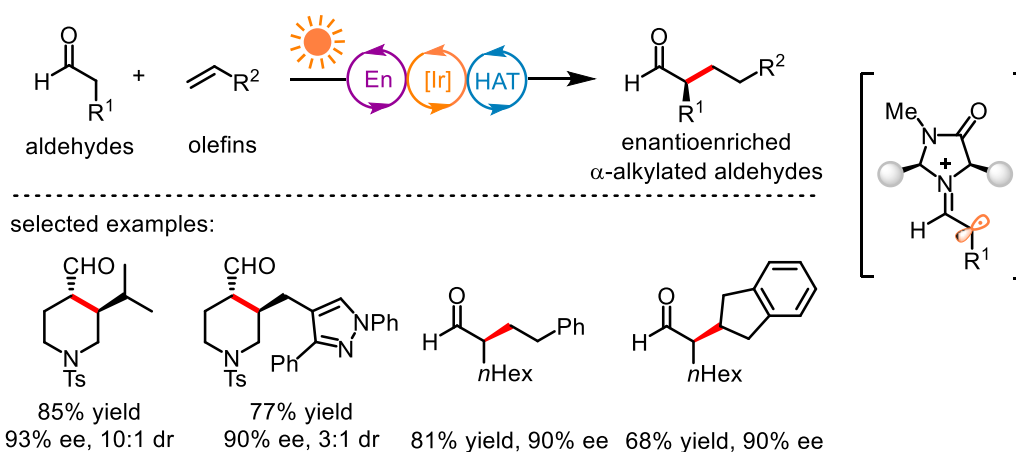


Figure 9. α -Alkylation of aldehydes enabled by triple photoredox/enamine/HAT catalysis.

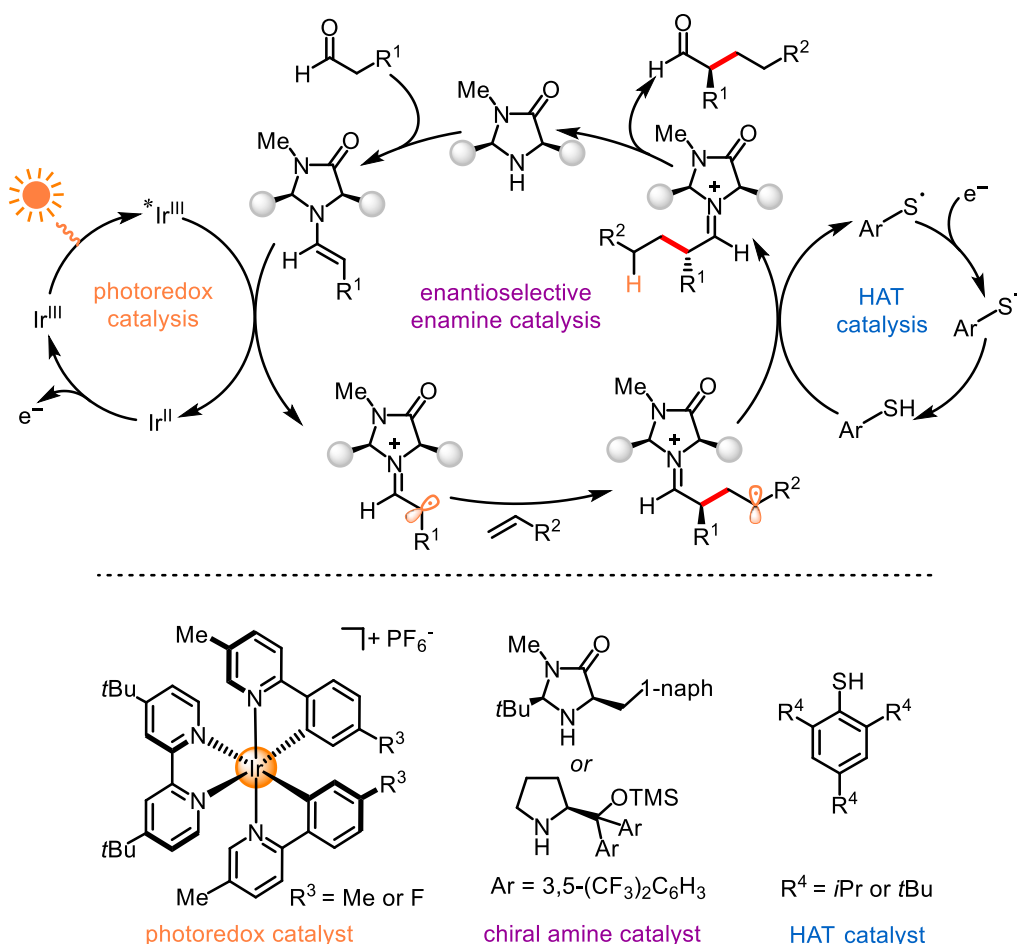


Figure 10. Proposed mechanism for triple photoredox/enamine/HAT catalysis.

The proposed mechanism is outline in **Figure 10**. Accordingly, condensation of the chiral amine catalyst and an aldehyde substrate would deliver an electron-rich enamine intermediate, which could quench the visible-light-excited iridium-based photocatalyst by single electron reduction. From which process an electrophilic $3\pi e^-$ enaminyll radical cation intermediate along with a reductive Ir^{II} species

were generated. This $3\pi e^-$ enamyl radical cation intermediate added rapidly to the simple olefin under the C–C formation within the chiral environment directed by the amine catalyst to afford a second alkyl radical. The produced nucleophilic radical was supposed to abstract a hydrogen atom from a thiophenol constituting an acidic and weak S–H (BDE = 78 kcal mol⁻¹). Subsequently, the target enantioenriched aldehyde product was liberated from the iminium ion by hydroxylation and the chiral amine catalyst was regenerated which would trigger a new catalytic cycle. While the thiyl radical was reduced by the above mentioned Ir^{II} species followed by protonation to produce the HAT catalyst thiophenol as well as the ground state Ir-based photoredox catalyst.

In 2012, a dual photoredox/chiral *N*-heterocyclic carbene (NHC) catalysis protocol was demonstrated by Rovis' group to enable the enantioselective α -acylation of tertiary amines (**Figure 11**).²⁰ The photoredox catalyst Ru(bpy)₃Cl₂ in combination with the external stoichiometric amount of oxidant *m*-dinitrobenzene (*m*-DNB) would provide the iminium ion from the tertiary amine under the double single electron oxidation. Meanwhile, the condensation of chiral *N*-heterocyclic carbene (NHC) catalyst with the aldehydes afforded the nucleophilic Breslow intermediate which could intercept with forementioned iminium ion, upon elimination of NHC, thereby producing the chiral α -amino ketones. This photoredox scheme constituted a net oxidation mechanism using *m*-DNB as terminal oxidant.

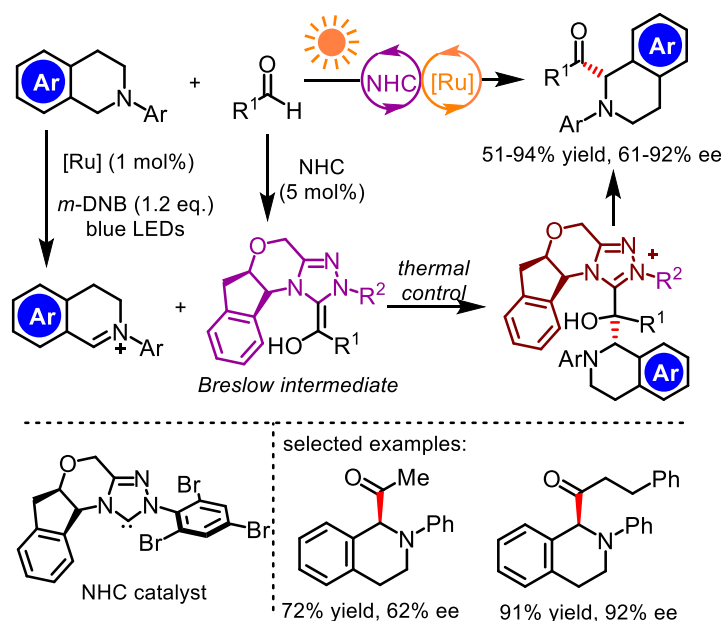


Figure 11. Asymmetric α -acylation of tertiary amines enabled by dual photoredox/NHC catalysis. [Ru] = Ru(bpy)₃Cl₂. NHC = *N*-heterocyclic carbene.

2) Non-covalent interaction catalysts: chiral Brønsted acid, thiourea and ammonium ion

The chiral Brønsted acid has been recognized as another powerful architecture for enantioselective cooperative photocatalysis. In 2013, Knowles group²¹ demonstrated the pioneering contribution to this field. As shown in **Figure 12**, the enantioselective intramolecular reductive coupling of ketones and hydrazones was demonstrated by using cooperative photoredox/Brønsted acid catalysis to provide the *syn* 1,2-amino alcohols in high yields (45–96%) and with excellent enantioselectivities (77–95% ee).

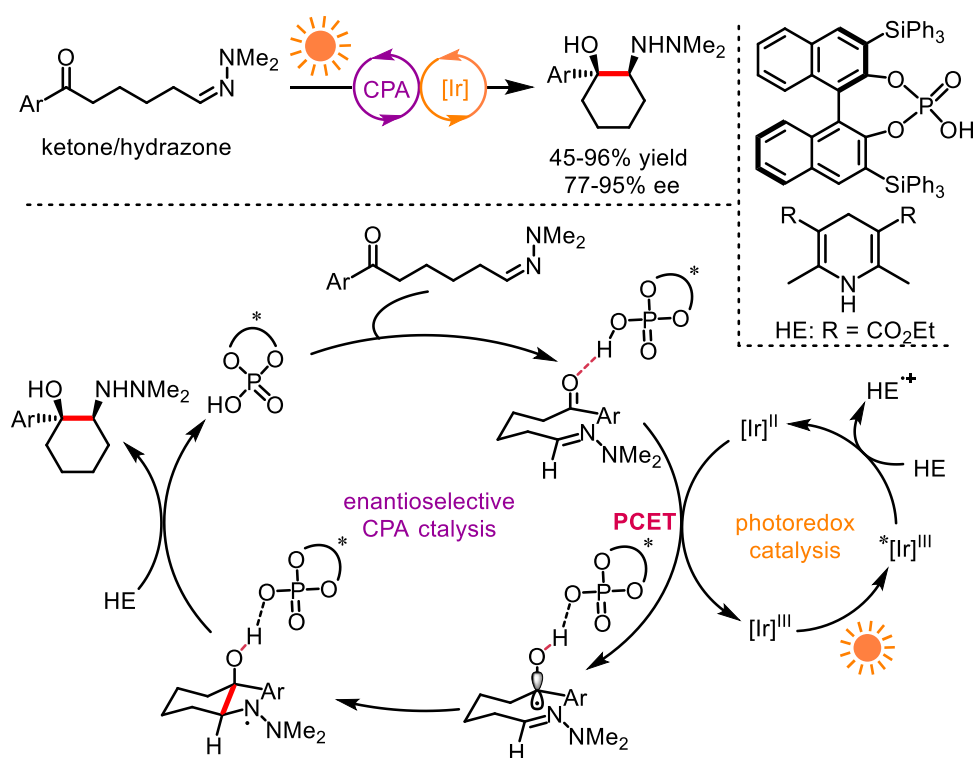


Figure 12. Enantioselective synthesis of *syn* 1,2-amino alcohols through dual photoredox/Brønsted acid catalysis. CPA = chiral phosphoric acid. PCET = proton-coupled electron transfer. [Ir] = [Ir(ppy)₂(dtbbpy)]PF₆. HE = Hantzsch ester.

Mechanistically, the chiral phosphoric acid (CPA) associated with the ketone moiety through hydrogen-bonding interaction. This adduct accepted a single electron from the highly reducing [Ir]^{II} species which was generated from the reductive quenching of photoredox catalyst [Ir(ppy)₂(dtbbpy)]PF₆. The single electron reduction was in concert with the proton transfer from the CPA to the oxygen anion of the produced ketyl radical, which process was defined as proton-coupled electron transfer (PCET). The following stereocontrolled C–C formation, single electron reduction of the nitrogen-centered radical and the CPA catalyst release would provide the target *syn* 1,2-amino

alcohols

Very recently, Jiang²² and co-workers reported that a chiral phosphoric acid (CPA) and a photoactivated dicyanopyrazine-derived chromophore (DPZ) dual catalysis system could enable a radical conjugate addition-protonation process between *N*-aryl glycines with α -branched 2-vinylpyridines and 2-vinylquinolines (**Figure 13**). This reaction afforded a range of chiral α -tertiary azaarenes with high yields (up to 97%) and excellent enantioselectivities (up to >99%), and even applied to a two-step synthesis of an enantiomerically pure pharmaceutical (*R*)-pheniramine with high efficiency (76% yield and 91% ee).

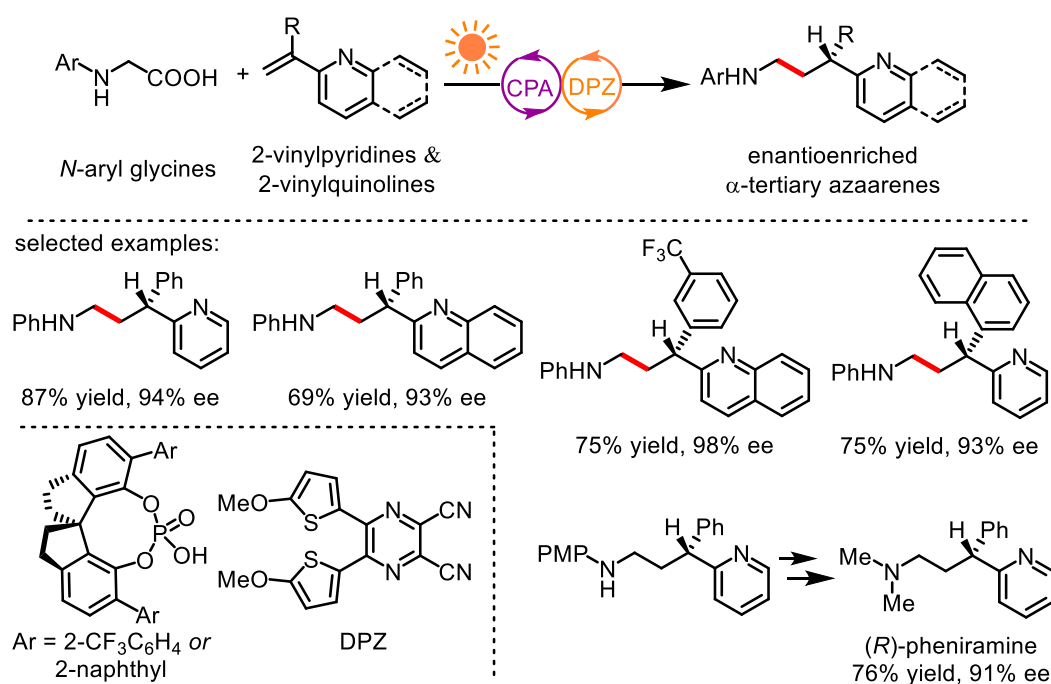


Figure 13. Radical conjugate addition-enantioselective protonation by dual photoredox/Brønsted acid catalysis.

Intrigued by the versatile spread of *N*-heterocycles including pyridines and quinolines in the enantioenriched bioactive molecules, Phipps group²³ developed an alternative strategy of CPA/photoredox catalysis for the involvement of these heterocycles in the enantioselective Minisci-type reaction by providing α -heterocyclic amines with high yields and excellent enantioselectivities (**Figure 14**).

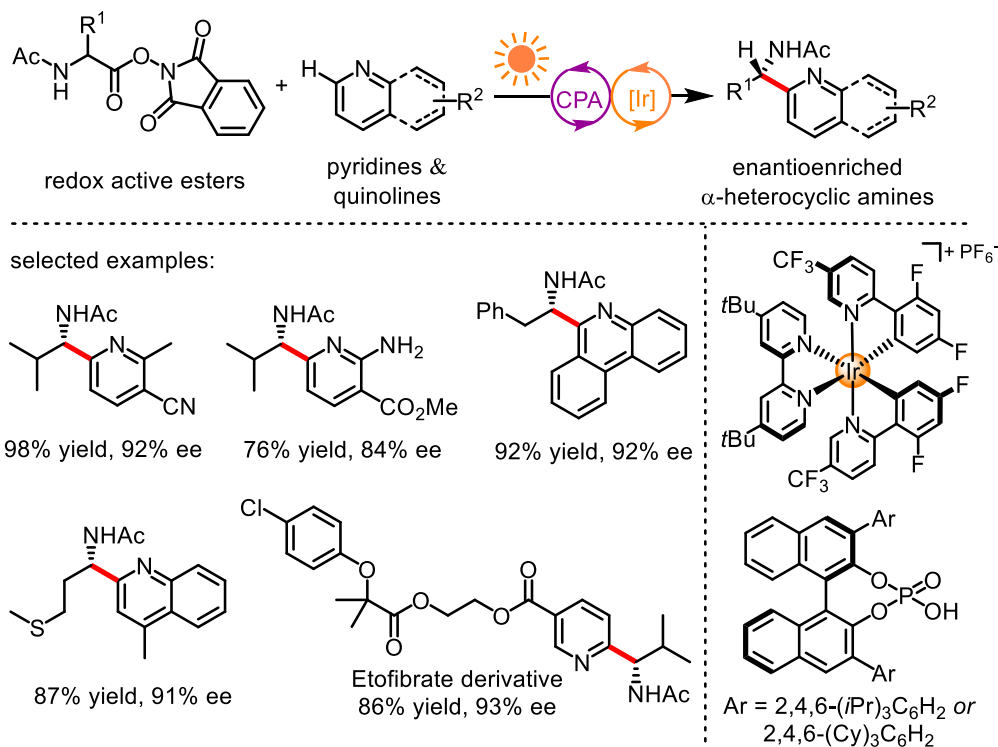


Figure 14. Enantioselective Minisci-type reaction through dual photoredox/Brønsted acid catalysis.

The proposed reaction mechanism is shown in **Figure 15**. Accordingly, the chiral phosphoric acid (CPA) could bind to the *N*-heteroarenes by hydrogen-bonding interaction thus providing the SOMO activation. And the formed conjugate ion of CPA would remain to associate with the pyridinium cation through electrostatic and hydrogen bonding interactions, as well incorporated the incoming of the photogenerated α -aminoalkyl radical. The following radical conjugate addition proceeded smoothly under the CPA-directed chiral environment, and most importantly, the phosphate promoting the deprotonation at the α -position of amino radical cation to render the radical-conjugate-addition step irreversible. While the resulting C–C formation radical intermediate promoted a single electron to the photoredox cycle and followed by deprotonation to deliver the target chiral α -heterocyclic amines.

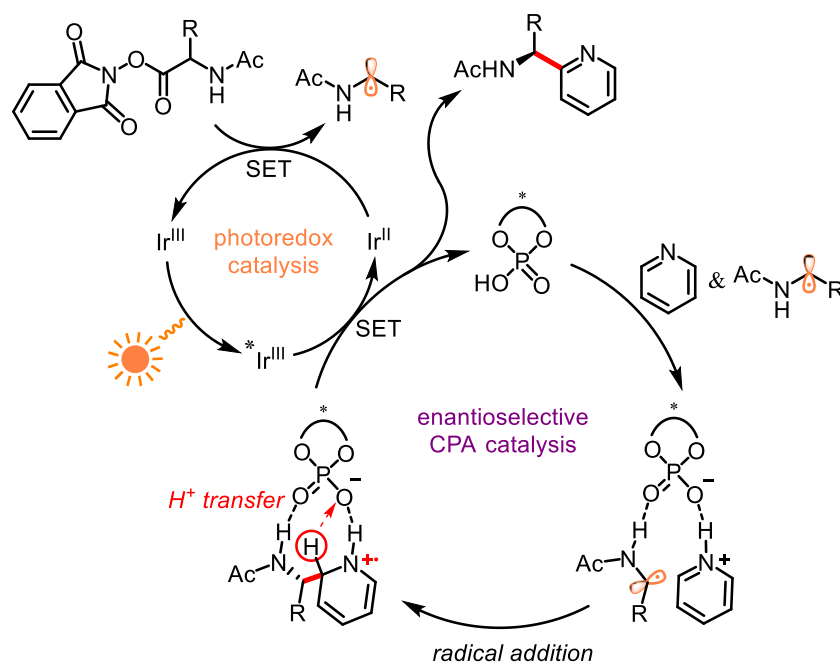


Figure 15. Proposed mechanism for dual photoredox/Brønsted acid catalysis promoted Minisci-type reaction.

The Brønsted acid catalyst would cooperate very well with the photoredox catalyst, and as well trigger the asymmetric catalysis in the absence of any photocatalyst, thereby utilizing the substrate which was capable of interacting with some other reactive compounds to afford specific electron-donor-acceptor (EDA) complex. A related report was disclosed by Jiang's group, in which the benzil and amine substrates would deliver an EDA complex which was amendable to be excited by visible light.²⁴ With a single electron transferring from donor to acceptor, a ketyl radical would bound to a chiral Brønsted acid catalyst, after hydrogenation and protonation, afforded the enantioenriched alcohol in high efficiency.

Besides chiral phosphoric acids (CPAs), chiral arylaminophosphonium salts were also introduced into asymmetric photocatalysis. For example, Ooi and co-workers reported a remarkable cooperative catalysis of chiral arylaminophosphonium ions and Ir-based photocatalysts for achieving a highly enantioselective redox coupling of *N*-arylaminoethanes with *N*-sulfonyl imines.²⁵ The photoredox catalytic cycle could be imitated by both the reductive^{25a} and the oxidative quenching events^{25b}. As shown in **Figure 16**, the photoexcited Ir(III)-based photocatalysts, due to their intrinsic electrochemical properties could be quenched by the *N*-arylaminoethanes (reductive quenching) or the *N*-sulfonyl imines (oxidative quenching), to afford the Ir(II) and Ir(IV) species. These species would further trigger single electron transfer events, thereby producing the prochiral radical anions or

amino radical cations. Nevertheless, the chiral arylaminophosphonium salt would interact with the produced the prochiral radical anions to give the chiral ion pairs. Concurrently, the α -amino alkyl radicals were formed upon the deprotonation/desilylation of the corresponding amino radical cations. Afterwards, the cross coupling reactions between the above two radicals proceeded under the stereocontrol of the chiral arylaminophosphonium. Enantioenriched 1,2-diamine derivatives were obtained in high yields (60–90% for reductive quenching and 28–86% for oxidative quenching) and with high enantioselectivities (85–98% ee for reductive quenching and 78–97% ee for oxidative quenching).

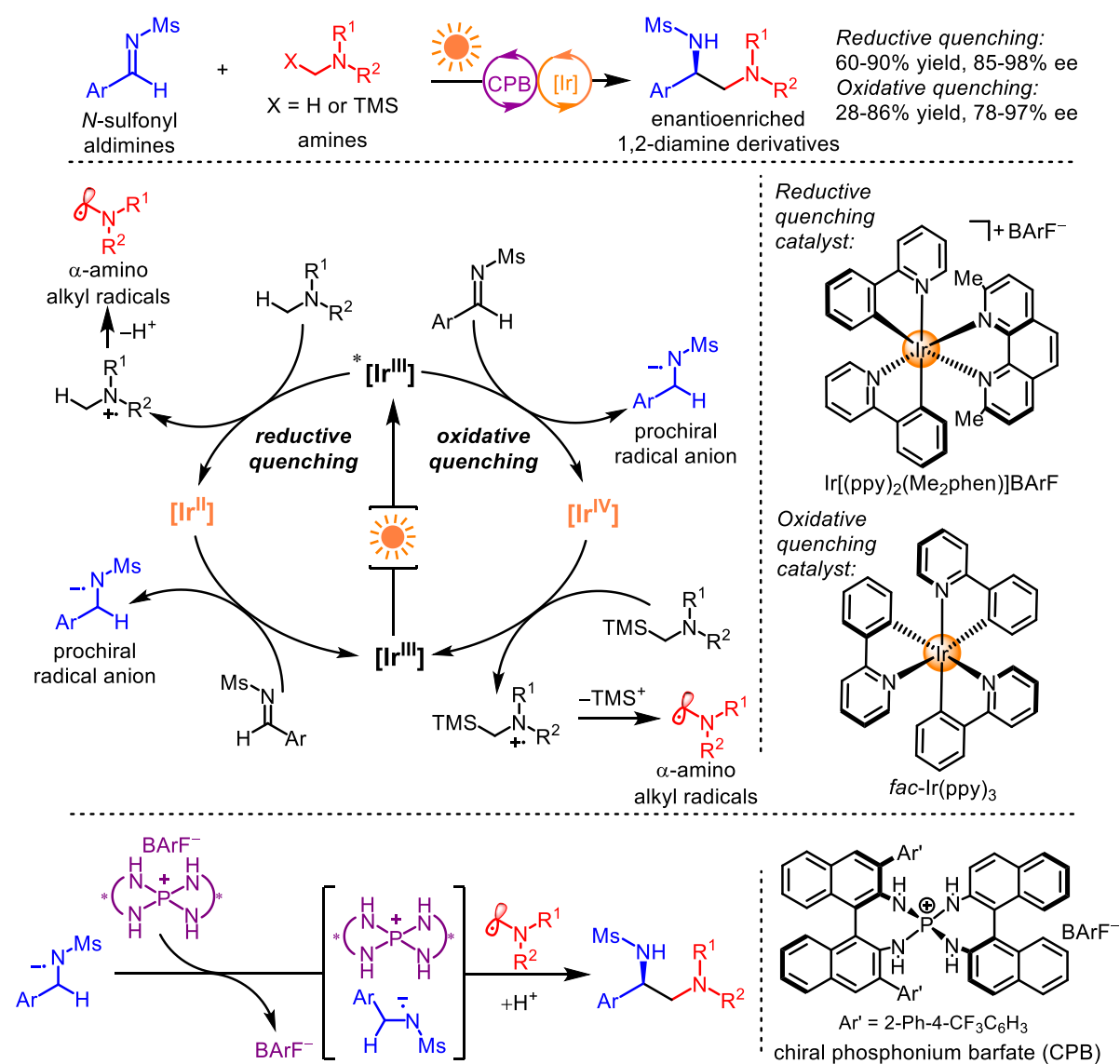


Figure 16. Dual photoredox/Brønsted acid catalysis promoted enantioselective redox coupling of N -arylaminoethanes with N -sulfonyl imines.

In 2014, Stephenson and Jacobsen reported a sequential photoredox (1st step) and chiral anion-bonding (2nd step) catalytic approach to trigger the enantioselective Mukaiyama Mannich reaction.²⁶ As shown in **Figure 17**, initially, the photoinduced net oxidation catalysis with CCl_4 as terminal oxidant afforded the racemic α -chloroamines; subsequently, upon switching the reaction conditions as well as adding the chiral thiourea catalyst and the silyl enol ether, the enantioenriched β -amino esters were obtained in good yields (11–72%) and with high enantioselectivities (42–99% ee). The chiral thiourea was proposed to form the counterion pair between H-bonded chloride anion and the iminium cation, thereby providing the stereocontrol under C–C formation process.

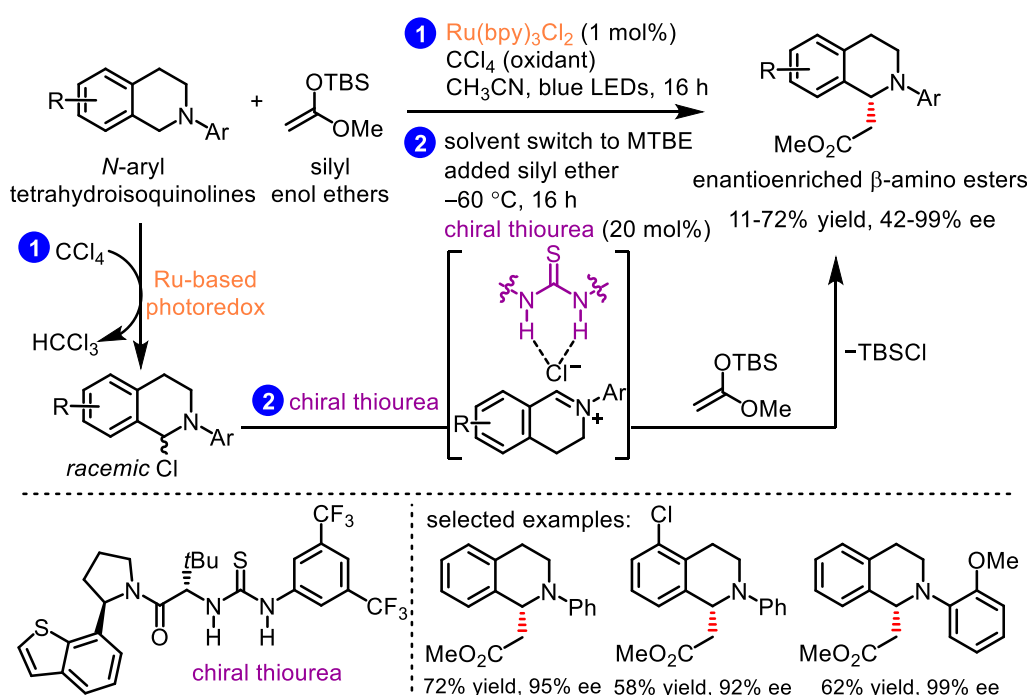


Figure 17. Enantioselective Mukaiyama Mannich reaction through sequential photoredox and chiral anion-bonding catalysis.

Interestingly, a chiral phase transfer catalyst (PTC) was demonstrated to be applicable in the asymmetric photoredox catalysis in the absence of photocatalyst, thereby permitting the enantioselective perfluoroalkylation of cyclic β -ketoesters (**Figure 18**).²⁷ This reaction was proposed to proceed through a visible-light-activated electron-donor-acceptor (EDA) complex which was formed between a PTC-stabilized enolate intermediate and the perfluoroalkyl iodide.

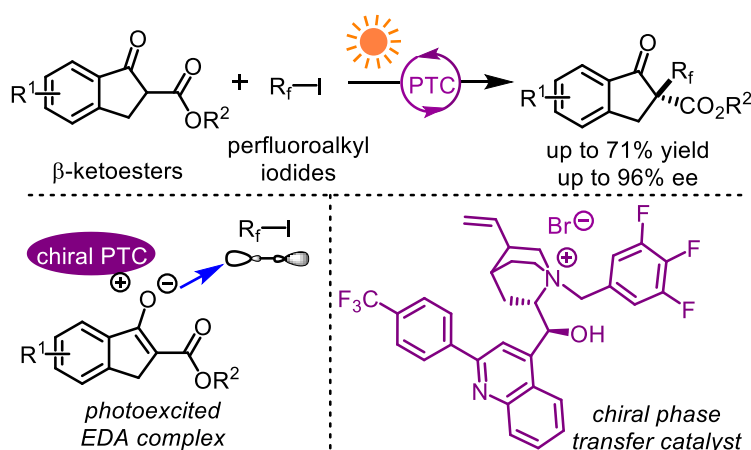


Figure 18. Single chiral phase transfer catalyst (PTC) enabled enantioselective perfluoroalkylation of cyclic β -ketoesters.

Just recently, Luo's group reported a single organic chiral ion pair catalyst was capable of promoting enantioselective anti-Markovnikov hydroetherification of alkenols in high yields and with moderate enantioselectivities under visible-light-activated photoredox conditions (**Figure 19**).²⁸ Mechanistically, a chiral ion pair acridinium photoredox catalyst get excited upon irradiation of the visible light and then reductively quenched by the alkene to regenerate the organophotoredox catalyst as well as produce a cation-radical intermediate. Concurrently, the chiral phosphate ion exchanged from the excited photocatalyst to the cation-radical intermediate. The follow-up deprotonation and C–O formation would be under the control of the chiral phosphate ion. While the C–O formation radical species abstracted a hydrogen atom from the 2-phenylmalononitrile, the enantioenriched substituted tetrahydrofuran was obtained with high yield and moderate enantioselectivity. Even though this chiral ion pair catalyst design is fantasy, the reaction outcome remains as the unsatisfactory stage.

Soon after, Nicewicz's group reported a similar strategy to trigger the enantioselective cation radical Diels-Alder reaction by employing a single chiral ion pair catalyst comprised of a pyrilium salt and a chiral *N*-triflyl phosphoramidate anion. However, the reaction outcome is as well sluggish.²⁹

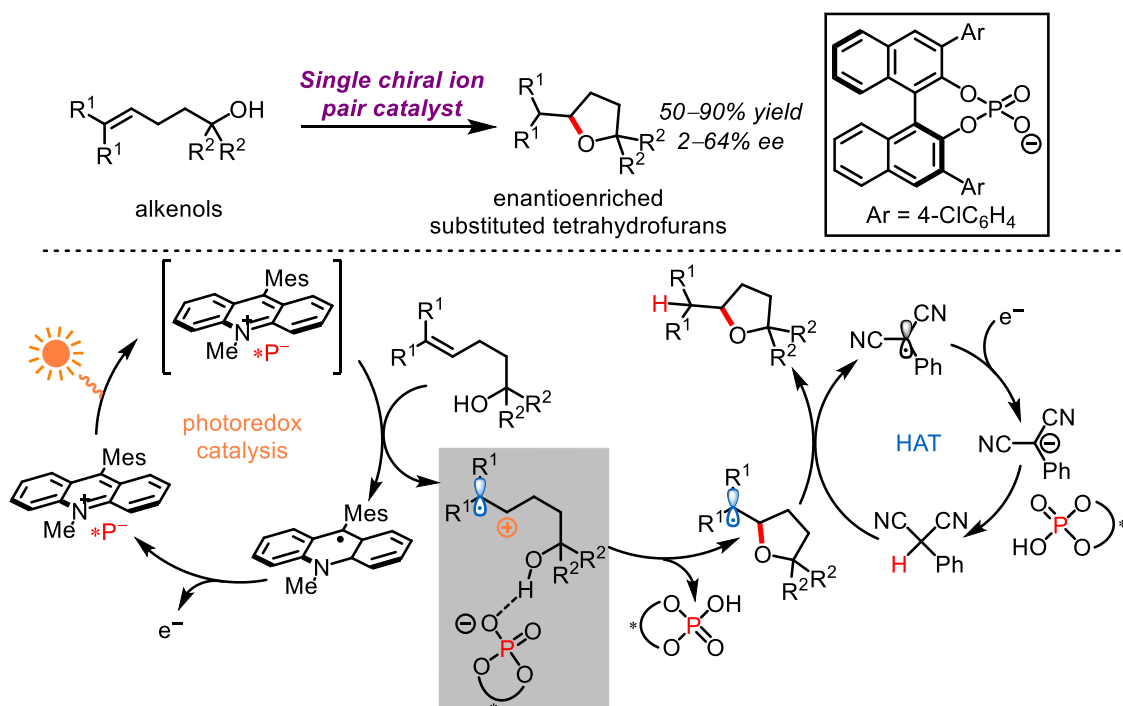


Figure 19. Enantioselective anti-Markovnikov hydroetherification of alkenols through single chiral ion pair catalyst.

1.3 Asymmetric Photoredox Chemistry with Transition Metal Catalysts

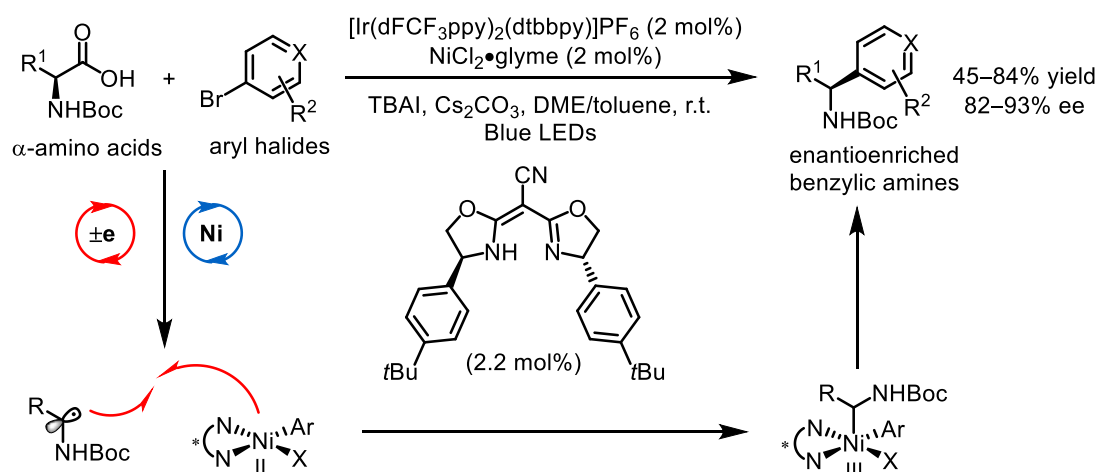


Figure 20. Enantioselective decarboxylative C^{sp}³-C^{sp}² cross-coupling reaction enabled by dual photoredox/nickel catalysis

In 2016, Fu's and MacMillan's groups reported the merger of synergistic photoredox and nickel catalysis to accomplish the enantioselective decarboxylative C^{sp}³-C^{sp}² cross-coupling, thereby providing an efficient access to valuable chiral benzylic amines.³⁰ As shown in **Figure 20**, the abundant feedstock α-amino acids and aryl halides coupled under the cooperation of chiral nickel

catalysis and Ir-based photoredox catalysis to produce the C–C formation products with good reaction outcome (45-84% yield and 82-93% ee). Accordingly, the α -amino acid undergoes a well-established visible-light-activated decarboxylation to afford an α -aminoalkyl radical; concurrently, the nickel catalyst would react towards the aryl halide to give a Ni(II)-aryl complex, which interfaced the α -aminoalkyl radical. The resulting diorganonickel(III) adduct then undergoes a reductive elimination process under the induction of the chiral environment directed by a semicorrin-like ligand, thereby producing the target benzylic amines.

Later in 2017, Rovis' and Doyle's groups reported an alternative dual photoredox/nickel catalysis scheme though the similar strategy (**Figure 21**).³¹ The cyclic *meso*-anhydrides underwent enantioselective desymmetrization with the benzyl trifluoroborates under the cooperation of chiral nickel catalysis and organo photoredox catalysis to provide *trans* keto-acids as major isomer (6:1- >20:1) in high enantioselectivities (36-94% ee) and good yields (34-90%). Within this protocol, the Ni(0) catalyst first reacted with the anhydride through oxidative addition under a stereocontrolled fashion to afford a Ni(II) complex. Subsequently, this Ni(II) species would intercept with the benzylic radical generated by oxidative organo photoredox catalysis to deliver the Ni(III) complex. With the following reductive elimination, the target product *trans* keto-acid was obtained and the nickel catalysis was regenerated.

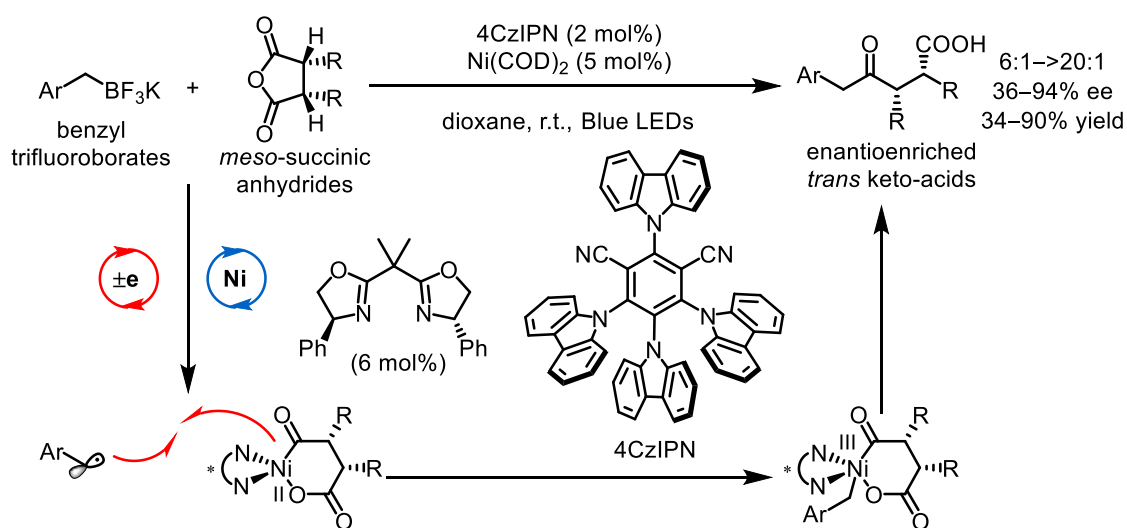


Figure 21. Enantioselective desymmetrization of cyclic *meso*-anhydrides enabled by dual photoredox/nickel catalysis.

With respect to the single transition metal mediated photoredox chemistry, Fu and co-workers

introduced an elegant catalytic strategy by using single copper catalysis to promote the cross-coupling between racemic tertiary alkyl chloride electrophiles with amines to forge quaternary stereocenters with high yields and excellent enantioselectivities (**Figure 22**).³² This report represents the first example involving the asymmetric base metal catalysis with visible-light-induced photoredox catalysis employing a single *in situ* assembled chiral catalyst. The proposed reaction mechanism is outlined in **Figure 22**. Accordingly, a copper(I)-amine complex get excited under the irradiation of visible light, subsequently transferred a single electron to the alkyl chloride under the formation of an alkyl radical and a Cu(II) species. The nucleophilic Cu(II) complex would react towards the electrophilic alkyl radical under the formation of C–N bond through an outer- or innersphere pathway. Afterwards, a Cu(I) intermediate was generated and then trapped by the amines to trigger a catalytic cycle. The employed simple CuCl salt and the phosphine ligand highlighted this work significantly.

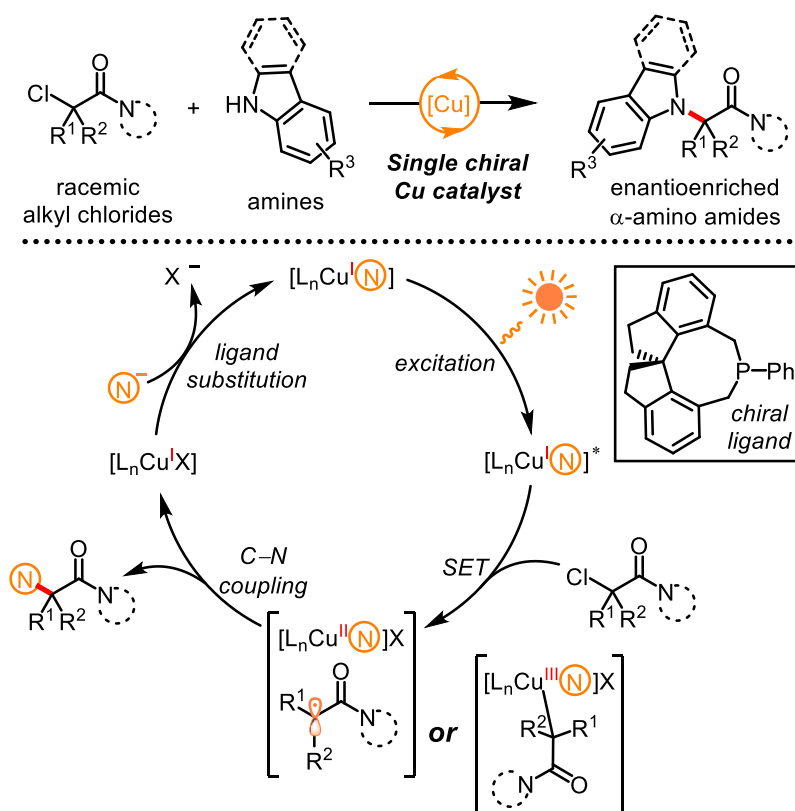


Figure 22. Enantioselective cross-coupling of racemic tertiary alkyl chlorides with amines enabled by visible-light-activated single copper catalysis.

1.4 Asymmetric Photoredox Chemistry with Traditional Lewis Acid Catalysts

Yoon's group contributed pioneering efforts on merging enantioselective Lewis acid catalysis with photocatalysis for quite a lot of chemical transformations, including photocycloadditions³³, and radical conjugate addition.³⁴ For example, Yoon showcased the highly enantioselective [2+2] photocycloaddition of enones through a dual photoredox/Lewis acid catalysis strategy (**Figure 23**). This protocol provided the corresponding non-racemic cyclobutanes with moderate diastereoselectivities (1.5:1 to 9:1 dr) and excellent enantioselectivities (84–97% ee). Interestingly, an imine-based chiral ligand and a corresponding reduced amine-based one provided the reverse configuration at the β position of produced cyclobutanes. The key aspect of this reaction scheme was the Eu-based Lewis acid, upon coordination to the enone, decreased the reductive potential of which, thereby rendering it amendable to be reduced under Ru-based photoredox conditions. This elegant reaction design has suppressed the un-catalyzed background reactions completely.

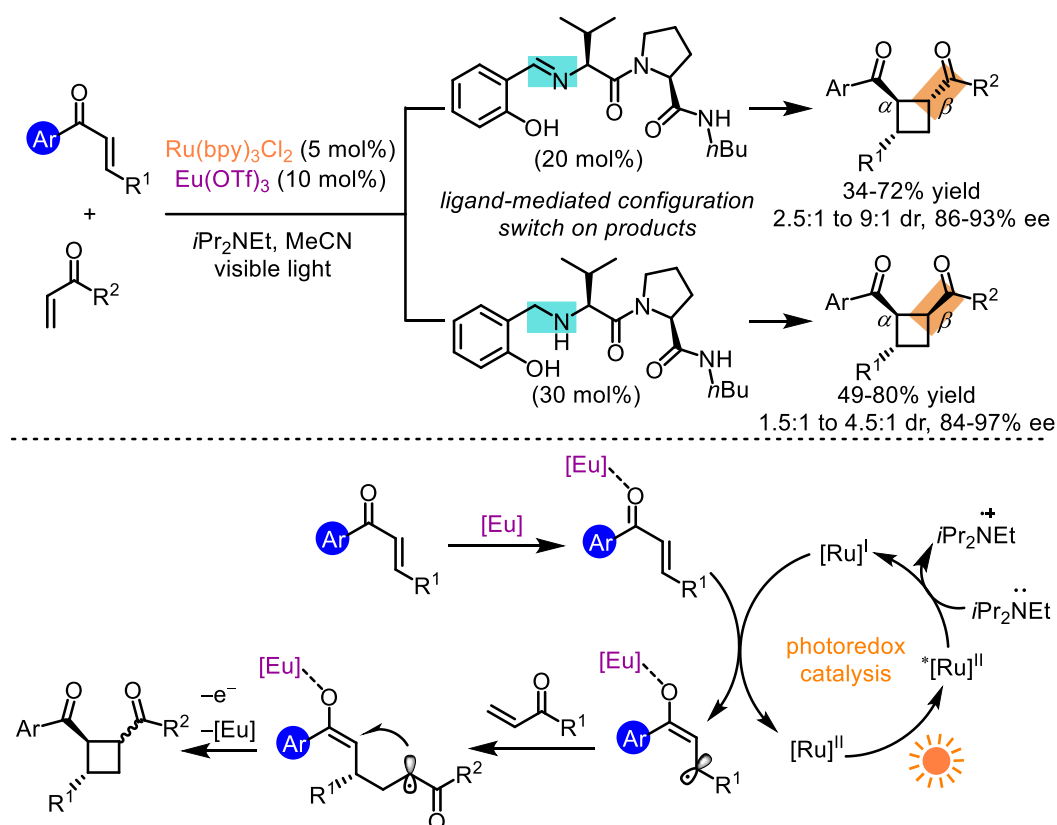


Figure 23. Enantioselective [2+2] cycloaddition enabled by dual photoredox/Lewis acid catalysis.

Later in 2015, Yoon reported a highly enantioselective radical conjugate addition reaction between the α -amino alkyl radical and the Michael acceptor (**Figure 24**).³⁴ The Ru-based photoredox

catalysis was employed to permit the generation of the nucleophilic α -amino alkyl radical species from α -silylalkyl amines, which subsequently added to the enone, while the asymmetric Lewis acid catalyst provided good stereocontrol over this radical conjugate addition process.

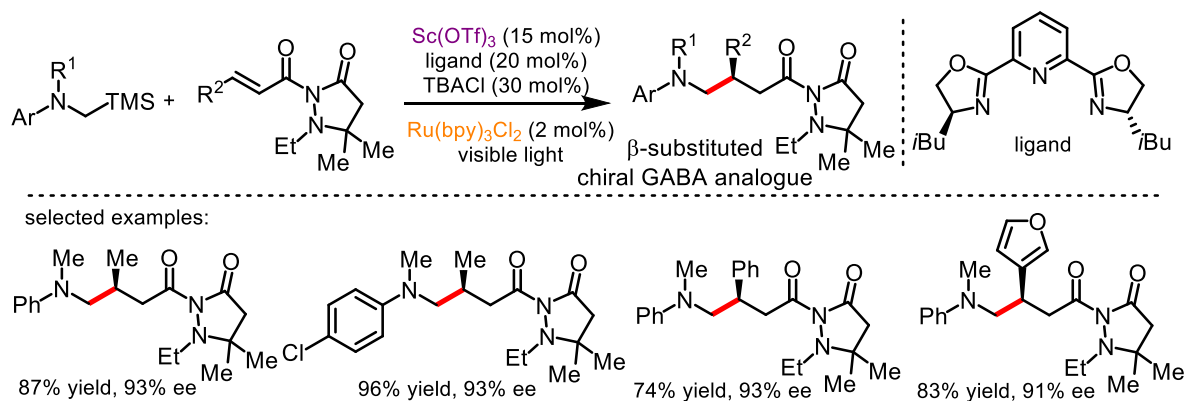


Figure 24. Enantioselective radical conjugate addition reaction enabled by dual photoredox/Lewis acid catalysis.

On the other hand, base metal Lewis acid was also applicable in the enantioselective photochemistry, even constituted the dual role of photoredox and asymmetric catalyst. Gong and co-workers disclosed a unique asymmetric photoredox scenario by using the simple Ni^{II} -DBFOX catalyst (**Figure 25**).³⁵ This single nickel catalyst system, upon visible-light-excitation, was capable of initiating single electron transfer (SET) events from α -silyl alkylamines and concurrently activating the α,β -unsaturated carbonyl compounds with bidentate coordination interaction. The follow-up radical conjugate addition of the α -amino alkyl radical to the Ni-bound enone proceeded enantioselectively under the chiral environment arranged by the DBFOX ligand. Notably, similar with Melchiorre and Yoon's work on the enantioselective radical conjugate addition reaction discussed above, the herein produced non-racemic C–C formation products were also recognized as the analogues of pharmaceutically important β -substituted chiral γ -aminobutyric acids (GABAs). However, the limited amine substrate scope on aryl versions hampered the access to the free or generally protected amino moiety; therefore the transformation to chiral GABAs can't be realized.

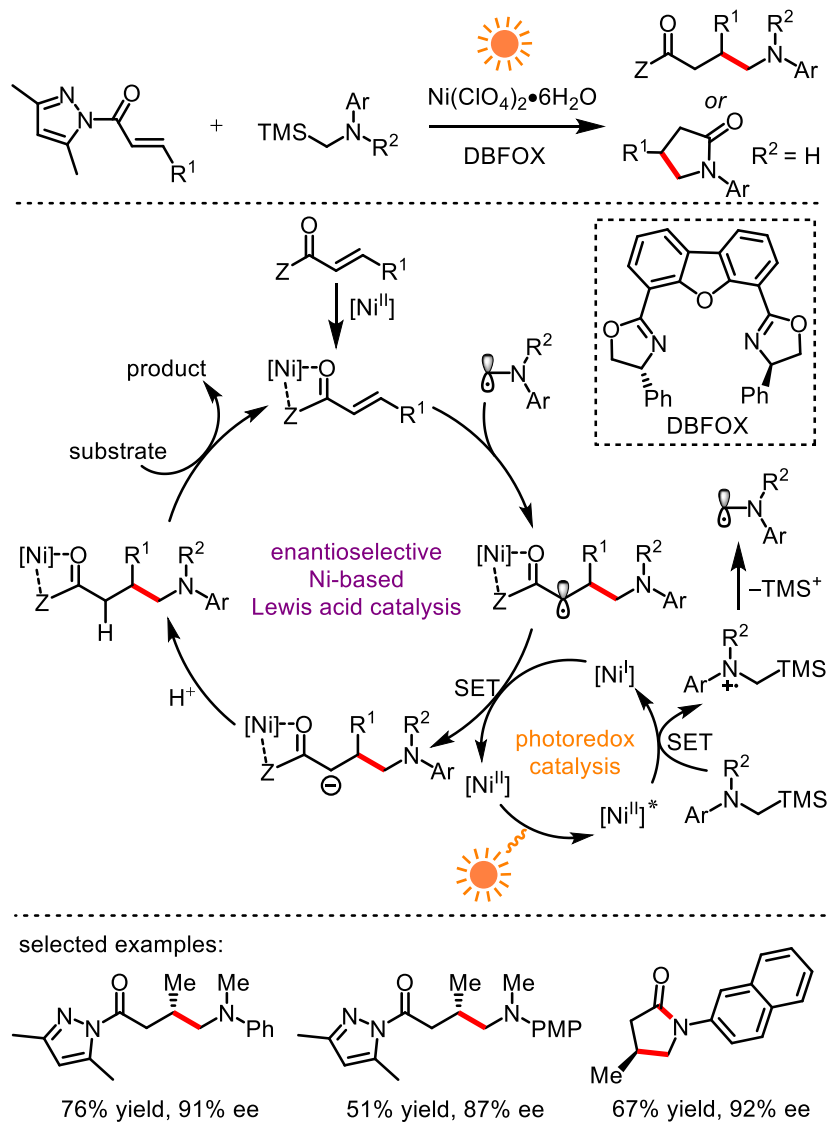


Figure 25. Enantioselective radical conjugate addition reaction enabled by single Ni-based Lewis acid catalyst under visible-light-activated photoredox conditions.

1.5 Asymmetric Photoredox Chemistry with Chiral-at-Metal Lewis Acid Catalysts

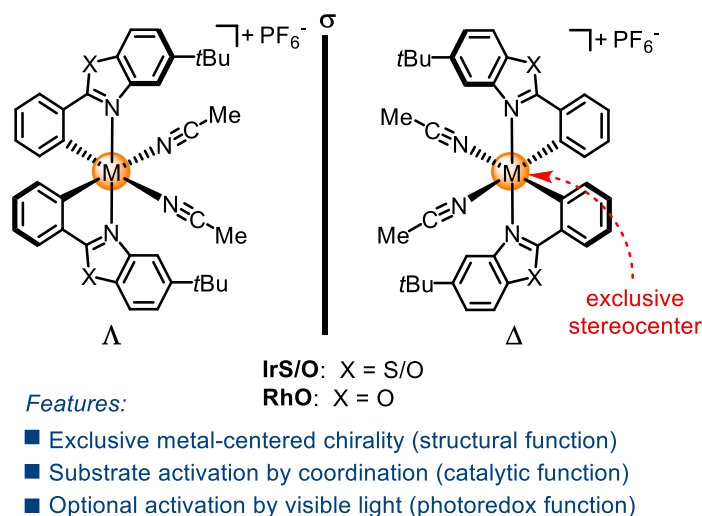


Figure 26. Structures of chiral-at-metal iridium and rhodium Lewis acid catalysts.

Meggers group recently introduced a new class of chiral-at-metal Lewis acid (**Figure 26**) which comprised the functions of photoactivation, substrate activation and asymmetric induction in one catalyst, and was demonstrated to be capable of enabling versatile visible-light-activated photoredox reactions.

In 2014, the former group members Haohua Huo and Xiaodong Shen reported a unique catalytic scheme in which the chiral-at-Ir Lewis acid Λ -**IrS/IrO** could integrate asymmetric catalysis with photoredox catalysis.³⁶ Mechanistic investigations revealed that the chiral iridium(III) complex upon coordinating to a 2-acyl imidazole delivers an *in situ* assembled photoactive species (enolate intermediate, **Figure 27**) with the assistance of a weak base. This photoactive enolate species can be activated by visible light and promotes a single electron transfer (SET) to the electron-deficient organobromo compounds under the release of corresponding electrophilic carbon-centered radicals. The iridium enolate intermediate does not only serve as the photoactive species but also constitutes a key intermediate in the catalytic cycle by reacting with the generated electrophilic radicals to provide the C–C formation products after protonation and liberation from the metal center. High catalytic reactivity of the chiral-at-Ir catalyst Λ -**IrS** was observed by obtaining the α -alkylation products with up to quantitative yield and 99% ee. However, the initially developed related benzoxazole catalyst Λ -**IrO** showed inferior enantioselectivity. Subsequently, the benzothiazole catalyst Λ -**IrS** was successfully employed for enantioselective α -trichloromethylations of 2-acyl imidazoles and 2-acyl

pyridines with excellent enantioselectivities of up to >99% ee.³⁷ Herein the related benzoxazole catalyst Λ -**IrO** again provided inferior results compared with Λ -**IrS**. This observation was attributed to a decreased steric shielding of the catalytic site due to the shorter C–O bonds in the benzoxazole moieties compared to the C–S bonds of benzothiazoles which leads to less steric hindrance of the two *tert*-butyl groups.³⁸

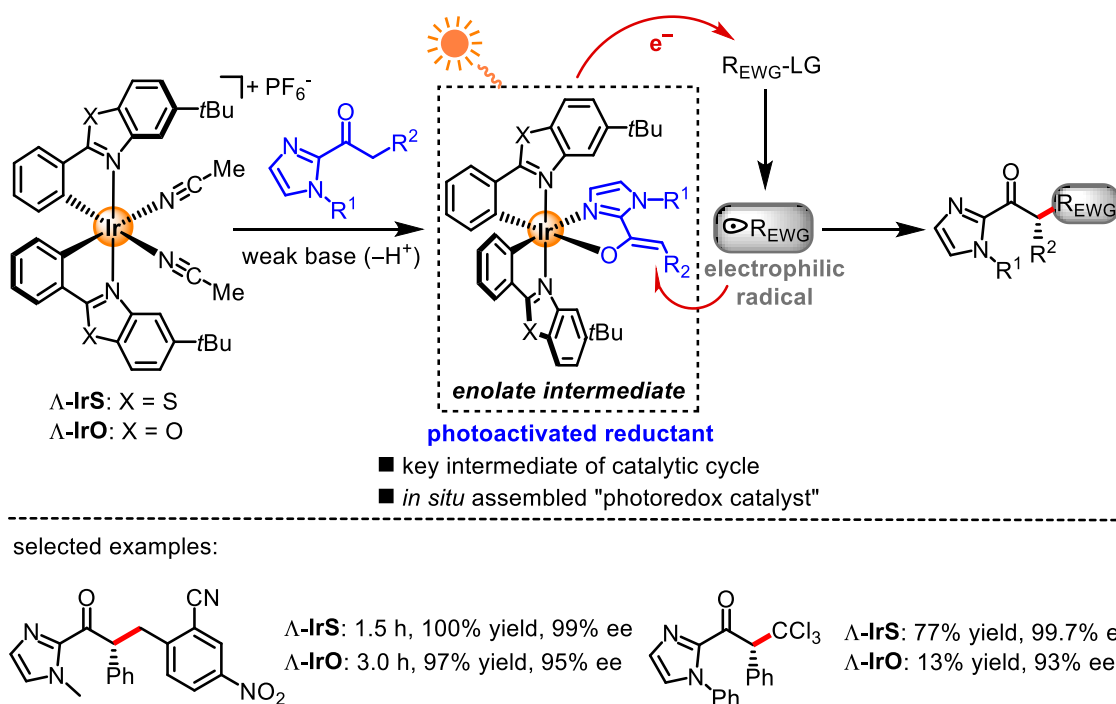


Figure 27. Enantioselective photoredox reactions enabled by single chiral-at-Ir Lewis acid catalysts.

In this discussed photoredox chemistry (**Figure 27**) the visible-light-excited *in situ* assembled photoactive species was oxidatively quenched, whereas in further investigations, our former group member Chuanyong Wang disclosed a complementary reductive quenching scheme (**Figure 28**). For instance, the Ir-based Lewis acid Λ -**IrO** was found to be capable of catalyzing the enantioselective redox coupling reaction of 2-acyl imidazoles with α -silyl alkylamines under net oxidative photoredox conditions.³⁹ A further redox neutral example demonstrated a unique stereocontrolled radical-radical recombination reaction scheme.⁴⁰ Accordingly, the photoactivated iridium-bound trifluoromethyl ketone could permit a single electron oxidation from a tertiary amine under the formation of an iridium-bound ketyl radical and an amino radical cation which undergo fast α -deprotonation to produce an α -aminoalkyl radical. The following radical-radical cross-coupling between the α -aminoalkyl radical and the ketyl radical proceeds smoothly to access 1,2-amino alcohols after

proton transfer, in an enantio- and diastereoselective (if applicable) fashion with up to 99% ee and 10:1 dr. However, a strong electron-withdrawing group CF_3 , which apparently enhances the oxidative potential of the *in situ* assembled photoactive species, was essential for this transformation.

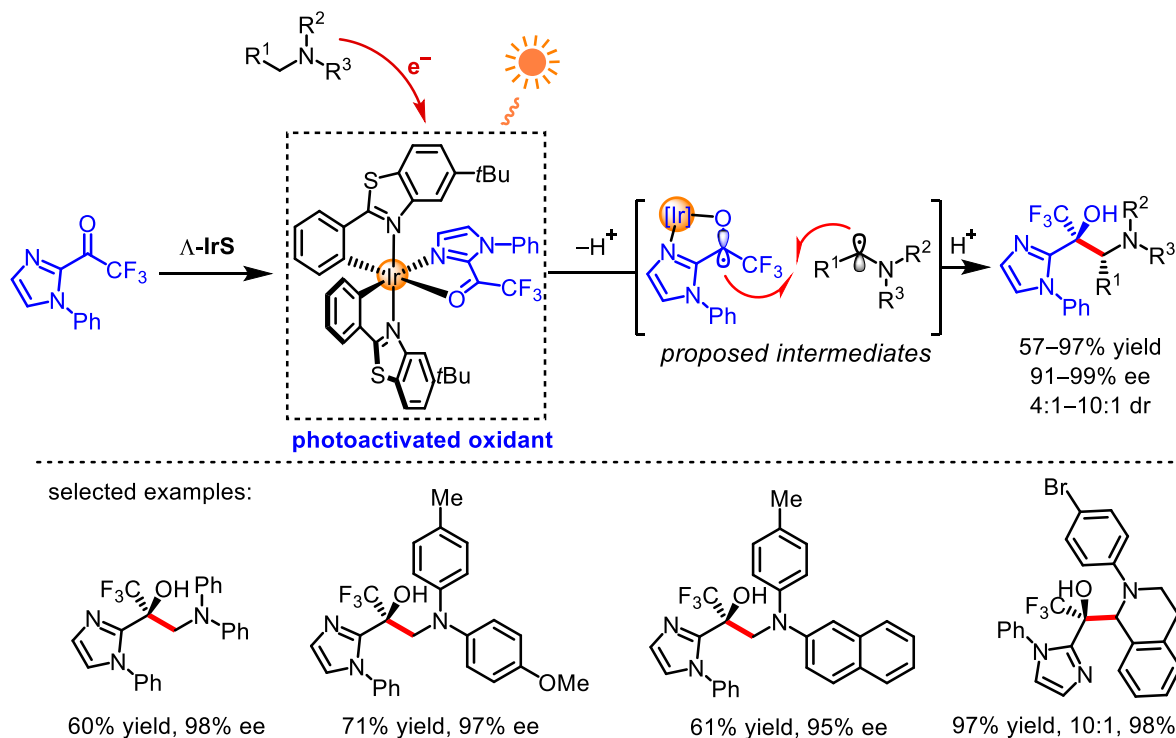


Figure 28. Single chiral-at-Ir Lewis acid catalyst $\Lambda\text{-IrS}$ mediated asymmetric radical-radical cross-coupling reactions under photoredox conditions.

With respect to the Rh-based asymmetric photoredox catalysis, the former group member Wei Yuan found that the chiral-at-rhodium(III) catalyst $\Lambda\text{-RhO}$ was capable of assembling a photoactivated oxidant (**Rh-I**) *in situ*, thereby promoting a highly enantioselective cross-dehydrogenative-coupling (CDC) reaction.⁴¹ As shown in **Figure 29a**, the tertiary amine, upon undergoing twice single electron oxidation through Rh-based photoredox catalysis in the presence of air, delivered an iminium ion. This electrophilic intermediate would intercept with the rhodium-enolate species (**Rh-II**), followed by the catalyst release, affording β -amino carbonyl compounds in good yields (35-81%) and with excellent enantioselectivities (79-97% ee). Soon later, Kang and co-workers reported that a $\Lambda\text{-RhO}$ derivative could trigger the enantioselective radical conjugate addition reaction to provide γ -amino carbonyl compounds (**Figure 29b**).⁴² The reaction is supposed to be initiated by the coordination of the enone to the Rh-based Lewis acid and the resulting adduct (**Rh-IV**) is photoexcited and then promotes single electron oxidation of the tertiary amine. The produced α -aminoalkyl radical then react with the

Rh-bound enone (**Rh-IV**), thus giving rise to the C–C formation product **Rh-V**. Upon the late stage electron/proton transfer and catalyst release, the γ -amino carbonyl compounds were obtained in moderate diastereoselectivities (52:48 to 93:7 dr) and excellent enantioselectivities (90->99% ee). However, a different mechanism can be envisioned. Accordingly, the single electron exchange between the tertiary amine and the excited **Rh-IV** might afford an α -aminoalkyl radical accompanied with a Rh-bound enol radical, followed by a stereocontrolled radical-radical recombination. Possibly, the radical-radical recombination pathway and the radical conjugate addition mechanism compete with each other.

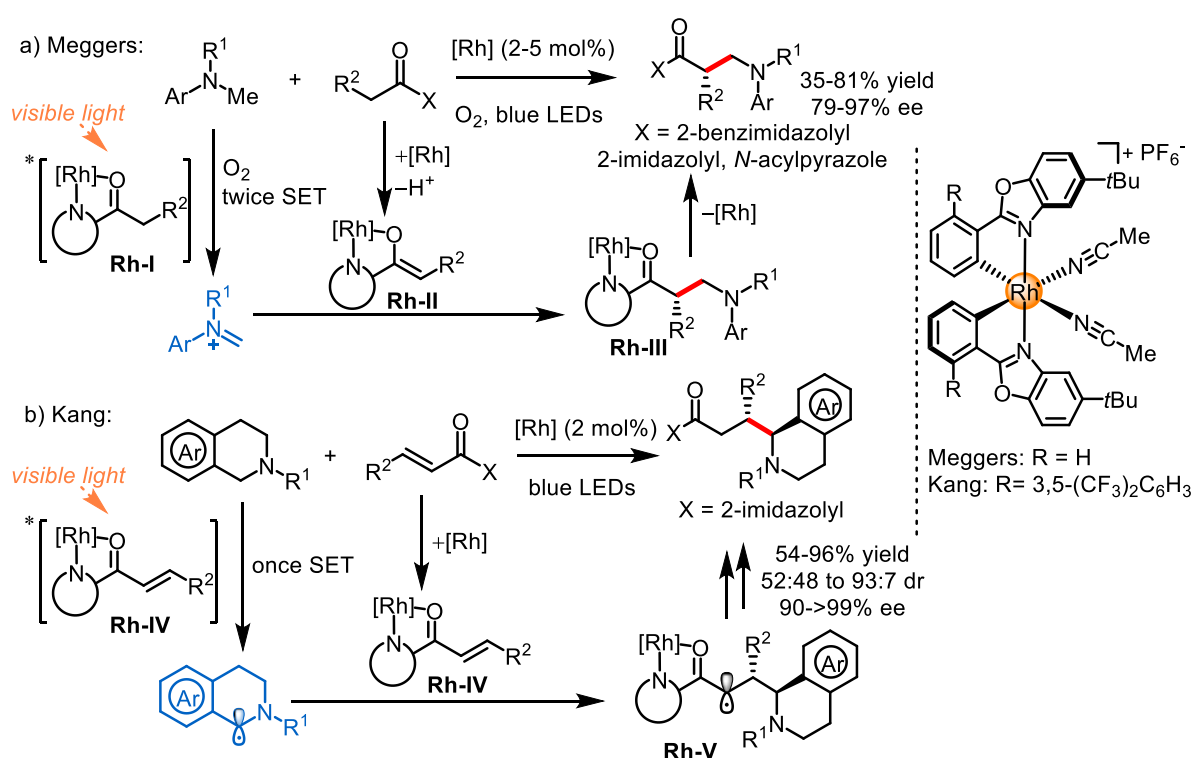


Figure 29. a) Enantioselective cross-dehydrogenative-coupling (CDC) reaction mediated by single chiral-at-rhodium complex Δ -**RhO**; b) enantioselective radical conjugate addition reaction mediated by single Δ -**RhO** derivative.

In addition, the former group member Xiaodong Shen found that the Rh-based Lewis acid (Δ -**RhO**) was also capable of triggering visible-light-induced photoredox catalysis through an oxidative quenching pathway which complemented the forementioned reductive quenching scenario.⁴³ As shown in **Figure 30**, the enantioselective α -amination of 2-acyl imidazoles was accomplished by using (ODN)-*N*-functionalized carbamates (ODN=2,4-dinitrophenylsulfonyloxy)¹² under the chiral-at-Rh Lewis acid catalyzed photoredox conditions. The C–N bond formation products were

obtained with high yields (52-99%) and excellent enantioselectivities (92-98%).

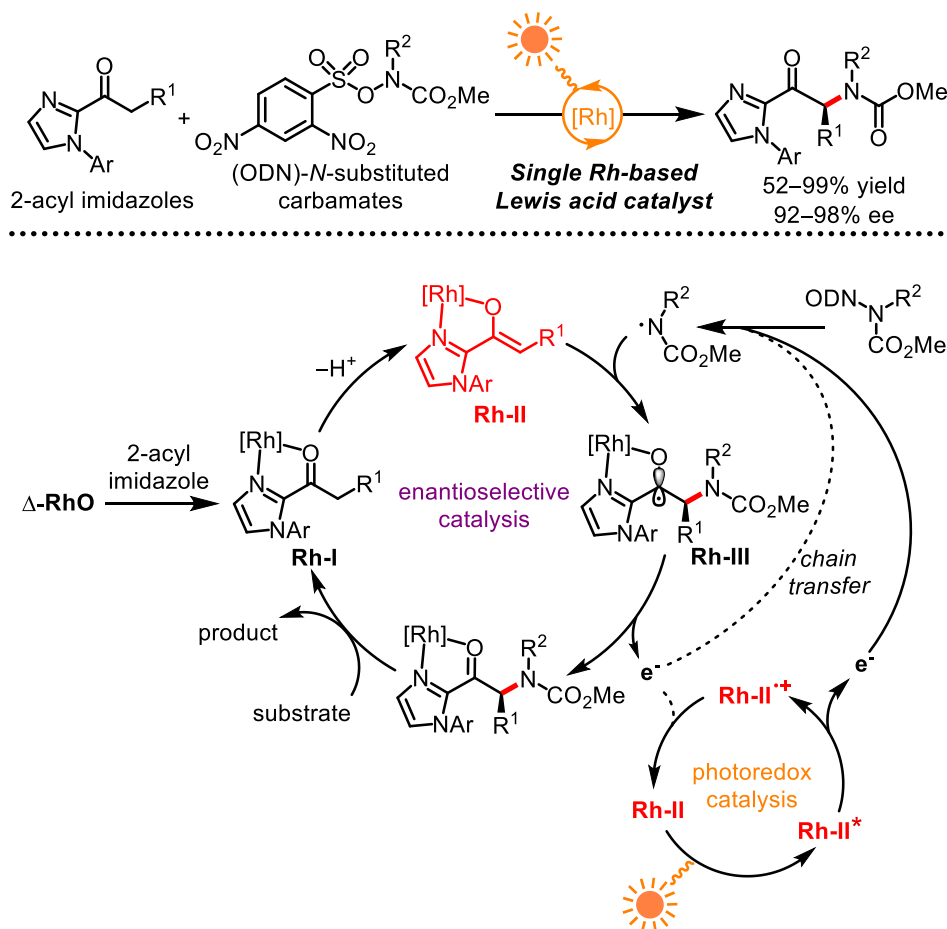


Figure 30. Single chiral-at-Rh Lewis acid catalyst mediated enantioselective photoredox reaction. ODN = 2,4-dinitrophenylsulfonyloxy.

Mechanistically, the chiral-at-Rh complex (Δ -**RhO**) is supposed to coordinate to the 2-acyl imidazole, and upon deprotonation, delivers a Rh-stabilized enolate intermediate (**Rh-II**). Under the irradiation of 24 W blue LEDs (455 nm), this intermediate gets photoexcited and constitutes an electron (re)initiator, thereby promoting a single electron to the (ODN)-N-functionalized carbamate (ODN = 2,4-dinitrophenylsulfonyloxy). After fragmentation, a highly electrophilic aminyl radical is produced and subsequently reacts with the intermediate **Rh-II**. The C-N bond formation is under the control of the chiral environment directed by octahedral coordination geometry. This process provided the Rh-bound ketyl radical intermediate (**Rh-III**) which is a highly reductive agent, thereby being capable of transferring a single electron to the photoredox cycle to regenerate the ground state rhodium complex. Alternatively, the intermediate (**Rh-III**) could directly promote the single electron reduction of the substrate (ODN)-N-functionalized carbamate, thereby furnishing the concept of “chain transfer”.⁴⁴

Notably, the related congener **IrO** could not catalyze this transformation at all. This observation could be traced back to the higher ligand-exchange kinetics of the Rh-based Lewis acid than the Ir-based one, which was crucial to match the highly reactive aminyl radicals.

1.6 Conclusions

Visible-light-induced catalytic enantioselective photochemistry has been at the forefront of chemical research over the past decade. Chemists from the broad synthetic chemistry community provided considerable contributions on the development of diverse elegant protocols. Within these emerging catalytic tools, organocatalysis is dominant. The leading breakthrough was achieved by using a cooperative strategy with dual enamine and photoredox catalysis to promote the enantioselective α -functionalization of ketones and aldehydes. Sometimes, mechanistically, the single chiral amine can comprise the dual role of asymmetric induction and photoactivation upon interaction with the substrates. Compatibility of chiral Brønsted acids with asymmetric photoredox catalysis was demonstrated by stereocontrolled transformations of carbonyl derivatives and aza-arenes. The generality of other techniques for organo-catalyzed asymmetric photoredox chemistry, including *N*-heterocyclic carbene catalysis, hydrogen bonding catalysis and so on, is still quite narrow and needs to be further extended.

Transition metal catalysis as one of the most powerful tools to forge enantioselective photoreactions, showcased its potential by permitting the stereocontrolled formation of C–C/N bonds in several cases. Another interesting chiral catalyst architecture is the traditional Lewis acid. Recent publications reveal that the metal salts associated with the chiral ligands could promote asymmetric photoredox catalysis with or without a separated photoredox catalyst, to trigger a variety of chemical transformations.

The Meggers group introduced a class of unusual chiral-at-metal Lewis acid catalysts in which the chirality originates exclusive from the stereogenic metal center. These chiral-at-metal complexes have already been demonstrated as quite useful catalytic tools to promote diverse enantioselective photoreactions through integrating the dual functions of photoredox and asymmetric catalysis, thereby leading to novel asymmetric photoreactions.

Reference

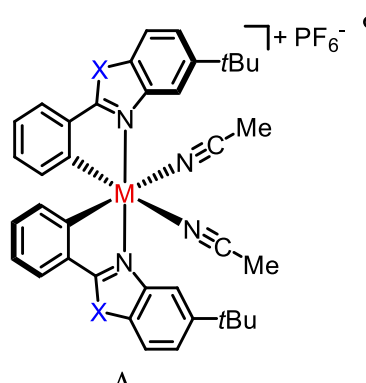
- 1 For selected reviews, see: a) J. Xuan, W.-J. Xiao, *Angew. Chem. Int. Ed.* **2012**, *51*, 6828; b) J. W. Tucker, C. R. J. Stephenson, *J. Org. Chem.* **2012**, *77*, 1617; c) C. K. Prier, D. A. Rankic, D. W. C. MacMillan, *Chem. Rev.* **2013**, *113*, 5322; d) M. N. Hopkinson, B. Sahoo, J.-L. Li, F. Glorius, *Chem. Eur. J.* **2014**, *20*, 3874; e) R. Brimiouille, D. Lenhart, M. M. Maturi, T. Bach, *Angew. Chem. Int. Ed.* **2015**, *54*, 3872; f) E. Meggers, *Chem. Commun.* **2015**, *51*, 3290; g) J. W. Beatty, C. R. J. Stephenson, *Acc. Chem. Res.* **2015**, *48*, 1474; h) C. Wang, Z. Lu, *Org. Chem. Front.* **2015**, *2*, 179; i) L. Zhang, E. Meggers, *Acc. Chem. Res.* **2017**, *50*, 320; j) Y.-Q. Zou, F. M. Hormann, T. Bach, *Chem. Soc. Rev.* **2018**, *47*, 278.
- 2 M. Silvi, P. Melchiorre, *Nature* **2018**, *554*, 41.
- 3 D. A. Nicewicz, D. W. C. MacMillan, *Science* **2008**, *322*, 77.
- 4 a) N. Matthias, F. Stefan, K. Burkhard, Z. Kirsten, *Angew. Chem. Int. Ed.* **2011**, *50*, 951; b) C. Maria, N. Matthias, F. Stefan, H. Christoph, K. Susanne, D. Stephan, P. Arno, Z. Kirsten, K. Burkhard, *Angew. Chem. Int. Ed.* **2012**, *51*, 4062; c) R. Paola, M. A. Alba, A. Josep, P. Emilio, P. M. A., *Angew. Chem. Int. Ed.* **2014**, *53*, 9613.
- 5 D. A. Nagib, M. E. Scott, D. W. C. MacMillan, *J. Am. Chem. Soc.* **2009**, *131*, 10875.
- 6 E. R. Welin, A. A. Warkentin, J. C. Conrad, D. W. C. MacMillan, *Angew. Chem. Int. Ed.* **2015**, *54*, 9668.
- 7 Y. Zhu, L. Zhang, S. Luo, *J. Am. Chem. Soc.* **2014**, *136*, 14642.
- 8 E. Arceo, I. D. Jurberg, A. Álvarez-Fernández, P. Melchiorre, *Nat. Chem.* **2013**, *5*, 750.
- 9 A. Bahamonde, P. Melchiorre, *J. Am. Chem. Soc.* **2016**, *138*, 8019.
- 10 E. Arceo, A. Bahamonde, G. Bergonzini, P. Melchiorre, *Chem. Sci.* **2014**, *5*, 2438.
- 11 M. Silvi, E. Arceo, I. D. Jurberg, C. Cassani, P. Melchiorre, *J. Am. Chem. Soc.* **2015**, *137*, 6120.
- 12 G. Cecere, C. M. König, J. L. Alleva, D. W. C. MacMillan, *J. Am. Chem. Soc.* **2013**, *135*, 11521.
- 13 a) M. Silvi, C. Verrier, Y. P. Rey, L. Buzzetti, P. Melchiorre, *Nat. Chem.* **2017**, *9*, 868; b) C. Verrier, N. Alandini, C. Pezzetta, M. Moliterno, L. Buzzetti, H. B. Hepburn, A. Vega-Peñaloza, M. Silvi, P. Melchiorre, *ACS Catal.* **2018**, *8*, 1062.
- 14 J. J. Murphy, D. Bastida, S. Paria, M. Fagnoni, P. Melchiorre, *Nature* **2016**, *532*, 218.
- 15 M. T. Pirnot, D. A. Rankic, D. B. C. Martin, D. W. C. MacMillan, *Science* **2013**, *339*, 1593.
- 16 F. R. Petronijević, M. Nappi, D. W. C. MacMillan, *J. Am. Chem. Soc.* **2013**, *135*, 18323.
- 17 J. A. Terrett, M. D. Clift, D. W. C. MacMillan, *J. Am. Chem. Soc.* **2014**, *136*, 6858.
- 18 J. L. Jeffrey, F. R. Petronijević, D. W. C. MacMillan, *J. Am. Chem. Soc.* **2015**, *137*, 8404.
- 19 A. G. Capacci, J. T. Malinowski, N. J. McAlpine, J. Kuhne, D. W. C. MacMillan, *Nat. Chem.* **2017**, *9*, 1073.
- 20 D. A. DiRocco, T. Rovis, *J. Am. Chem. Soc.* **2012**, *134*, 8094.

- 21 L. J. Rono, H. G. Yayla, D. Y. Wang, M. F. Armstrong, R. R. Knowles, *J. Am. Chem. Soc.* **2013**, *135*, 17735.
- 22 Y. Yin, Y. Dai, H. Jia, J. Li, L. Bu, B. Qiao, X. Zhao, Z. Jiang, *J. Am. Chem. Soc.* **2018**, *140*, 6083.
- 23 R. S. J. Proctor, H. J. Davis, R. J. Phipps, *Science* **2018**, *360*, 419.
- 24 L. Lin, X. Bai, X. Ye, X. Zhao, C.-H. Tan, Z. Jiang, *Angew. Chem. Int. Ed.* **2017**, *129*, 14030.
- 25 a) D. Uraguchi, N. Kinoshita, T. Kizu, T. Ooi, *J. Am. Chem. Soc.* **2015**, *137*, 13768; b) T. Kizu, D. Uraguchi, T. Ooi, *J. Org. Chem.* **2016**, *81*, 6953.
- 26 G. Bergonzini, C. S. Schindler, C.-J. Wallentin, E. N. Jacobsen, C. R. J. Stephenson, *Chem. Sci.* **2014**, *5*, 112.
- 27 Ł. Woźniak, J. J. Murphy, P. Melchiorre, *J. Am. Chem. Soc.* **2015**, *137*, 5678.
- 28 Z. Yang, H. Li, S. Li, M.-T. Zhang, S. Luo, *Org. Chem. Front.* **2017**, *4*, 1037.
- 29 P. D. Morse, T. M. Nguyen, C. L. Cruz, D. A. Nicewicz, *Tetrahedron* **2018**, *74*, 3266.
- 30 Z. Zuo, H. Cong, W. Li, J. Choi, G. C. Fu, D. W. C. MacMillan, *J. Am. Chem. Soc.* **2016**, *138*, 1832.
- 31 E. E. Stache, T. Rovis, A. G. Doyle, *Angew. Chem. Int. Ed.* **2017**, *56*, 3679.
- 32 Q. M. Kainz, C. D. Matier, A. Bartoszewicz, S. L. Zultanski, J. C. Peters, G. C. Fu, *Science* **2016**, *351*, 681.
- 33 a) J. Du, K. L. Skubi, D. M. Schultz, T. P. Yoon, *Science* **2014**, *344*, 392; b) A. G. Amador, E. M. Sherbrook, T. P. Yoon, *J. Am. Chem. Soc.* **2016**, *138*, 4722.
- 34 L. Ruiz Espelt, I. S. McPherson, E. M. Wiensch, T. P. Yoon, *J. Am. Chem. Soc.* **2015**, *137*, 2452.
- 35 X. Shen, Y. Li, Z. Wen, S. Cao, X. Hou, L. Gong, *Chem. Sci.* **2018**, *9*, 4562.
- 36 H. Huo, X. Shen, C. Wang, L. Zhang, P. Röse, L.-A. Chen, K. Harms, M. Marsch, G. Hilt, E. Meggers, *Nature* **2014**, *515*, 100.
- 37 H. Huo, C. Wang, K. Harms, E. Meggers, *J. Am. Chem. Soc.* **2015**, *137*, 9551.
- 38 X. Shen, H. Huo, C. Wang, B. Zhang, K. Harms, E. Meggers, *Chem. Eur. J.* **2015**, *21*, 9720.
- 39 C. Wang, Y. Zheng, H. Huo, P. Röse, L. Zhang, K. Harms, G. Hilt, E. Meggers, *Chem. Eur. J.* **2015**, *21*, 7355.
- 40 C. Wang, J. Qin, X. Shen, R. Riedel, K. Harms, E. Meggers, *Angew. Chem. Int. Ed.* **2016**, *55*, 685.
- 41 Y. Tan, W. Yuan, L. Gong, E. Meggers, *Angew. Chem. Int. Ed.* **2015**, *54*, 13045.
- 42 S.-X. Lin, G.-J. Sun, Q. Kang, *Chem. Commun.* **2017**, *53*, 7665.
- 43 X. Shen, K. Harms, M. Marsch, E. Meggers, *Chem. Eur. J.* **2016**, *22*, 9102.
- 44 M. A. Cismesia, T. P. Yoon, *Chem. Sci.* **2015**, *6*, 5426.

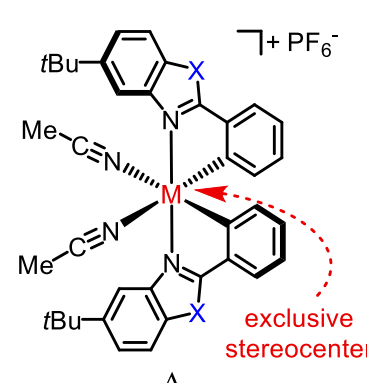
Chapter 2: Aim of the Work

Chiral transition metal complexes play a prominent role as catalysts for the asymmetric synthesis of non-racemic compounds.¹ The required chirality typically originates from chiral mono- or multidentate ligands within the coordination sphere of the metal catalyst. Chiral transition metal catalysts in which the chirality exclusively originates from a stereogenic metal center witness a more recent development especially by the contribution from the Meggers research group.² With the elaborated efforts of the former group members Haohua Huo, Xiaodong Shen and Chuanyong Wang, a new family of chiral-at-metal iridium (dubbed **IrO**³ and **IrS**⁴) and rhodium (dubbed **RhO**⁵) Lewis acid catalysts were introduced (**Table 1**).

Table 1. Structures of chiral-at-metal Lewis acids.



Λ



Δ

Entry	Complex	M	X	Remarks
1	Λ- and Δ- IrO	Ir	O	ref. 3
2	Λ- and Δ- IrS	Ir	S	ref. 4
3	Λ- and Δ- RhO	Rh	O	ref. 5
4	Λ- and Δ- RhS	Rh	S	<i>unknown</i>

These C_2 -symmetrical complexes contain two cyclometalating 5-*tert*-butyl-2-phenylbenzoxazoles or the analogous benzothiazoles, in addition to two labile acetonitrile ligands. The cyclometalating ligands create a propeller-type geometry with left-handed (Λ enantiomer) and right-handed (Δ enantiomer) screw sense. Importantly, a key aspect of the overall catalyst design is the strongly σ -donating phenyl ligands, which create a strong ligand field going along with a high ligand activation energy thereby rendering the bis-cyclometalated propeller unit configurationally inert (important for

retaining the catalyst's chirality), while at the same time the strong kinetic *trans*-effect of the phenyl ligands labilize the coordinated acetonitrile ligands (important for catalysis). Meggers and several other groups demonstrated over the past several years that these bis-cyclometalated iridium(III) and rhodium(III) complexes and derivatives thereof are very versatile catalysts for a variety of asymmetric transformations, ranging from enolate chemistry and conjugate additions to asymmetric transfer hydrogenations.^{2d} An especially interesting aspect of this class of catalysts is their ability to become activated by visible light thereby catalyzing asymmetric photoreactions.⁶

1) Expanding the family of chiral-at-metal Lewis acid catalysts

In previous investigations on the catalytic activity of these chiral-at-metal Lewis acids, two interesting observations are noticeable. Firstly, the Rh-based Lewis acid (**RhO**) often show higher catalytic activity than the Ir-based one (**IrO**) which can be rationalized with a more rapid ligand exchange kinetics of the rhodium complex. Secondly, the **IrS** comprising the cyclometalating benzothiazole ligands often displays higher asymmetric induction than its benzoxazole congener **IrO** which can be explained with an improved steric congestion directed by the benzothiazoles, in which the longer C–S bonds over C–O arranges the steric bulky tertiary butyl groups closer to the substrate coordination site.⁷ Therefore, it would be highly desirable to access the other type of Rh-based Lewis acid catalyst containing the benzothiazole ligand (dubbed **RhS**).

2) Discovering novel visible-light-induced asymmetric transformations

Visible-light-induced asymmetric photoredox catalysis has been demonstrated as a powerful synthetic tool to access enantioenriched molecules.⁶ However, discovery of novel enantioselective photoreactions is mainly hampered by the development of new chiral catalysts which could get photoexcited directly upon interaction with substrates or cooperate harmoniously with an external achiral photocatalyst. Therefore, the other goal of this thesis is to make use of the chiral-at-rhodium complex **RhS** for discovering new methodologies in the field of asymmetric photoredox chemistry. The potential higher turnover frequencies of **RhS** compared to **IrS** should be an advantage for reactions involving short-lived photogenerated intermediates. The to be expected less favorable photophysical properties of **RhS** compared to **IrS** will be compensated by complementing with suitable photoactive species, thus furnishing the concept of “asymmetric cooperative photoredox

catalysis” as demonstrated also by other groups.⁸ Overall, a new chiral-at-metal Lewis acid catalyst might lead to the discovery of some unconventional new photoreactions.

References

- 1 a) P. J. Walsh, M. C. Kozlowski, *Fundamentals of asymmetric catalysis*, University Science Books: Sausalito, California, **2009**; b) K. A. Jørgensen, M. Johannsen, S. Yao, H. Audrain, J. Thorhauge, *Acc. Chem. Res.* **1999**, *32*, 605; c) S. Kanemasa, M. Hasegawa, F. Ono, *Chem. Rec.* **2007**, *7*, 137.
- 2 a) M. Fontecave, O. Hamelin, S. Ménage, *Top. Organomet. Chem.* **2005**, 271; b) L. Gong, L.-A. Chen, E. Meggers, *Angew. Chem. Int. Ed.* **2014**, *53*, 10868; c) Z.-Y. Cao, W. D. Brittain, J. S. Fossey, F. Zhou, *Catal. Sci. Technol.* **2015**, *5*, 3441; d) L. Zhang, E. Meggers, *Acc. Chem. Res.* **2017**, *50*, 320.
- 3 H. Huo, C. Fu, K. Harms, E. Meggers, *J. Am. Chem. Soc.* **2014**, *136*, 2990;
- 4 H. Huo, X. Shen, C. Wang, L. Zhang, P. Röse, L.-A. Chen, K. Harms, M. Marsch, G. Hilt, E. Meggers, *Nature* **2014**, *515*, 100.
- 5 C. Wang, L.-A. Chen, H. Huo, X. Shen, K. Harms, L. Gong, E. Meggers, *Chem. Sci.* **2015**, *6*, 1094.
- 6 a) E. Meggers, *Chem. Commun.* **2015**, *51*, 3290; b) R. Brimiouille, D. Lenhart, M. M. Maturi, T. Bach, *Angew. Chem. Int. Ed.* **2015**, *54*, 3872; c) M. H. Shaw, J. Twilton, D. W. MacMillan, *J. Org. Chem.* **2016**, *81*, 6898; d) A. F. Garrido-Castro, M. C. Maestro, J. Alemán, *Tetrahedron Lett.* **2018**, *59*, 1286.
- 7 X. Shen, H. Huo, C. Wang, B. Zhang, K. Harms, E. Meggers, *Chem. Eur. J.* **2015**, *21*, 9720.
- 8 a) M. N. Hopkinson, B. Sahoo, J.-L. Li, F. Glorius, *Chem. Eur. J.* **2014**, *20*, 3874; b) K. L. Skubi, T. R. Blum, T. P. Yoon, *Chem. Rev.* **2016**, *116*, 10035.

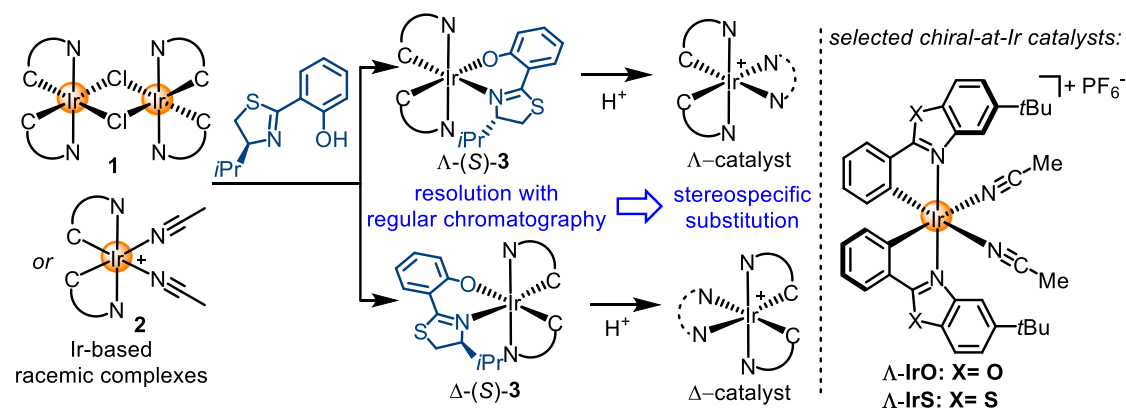
Chapter 3: Results and Discussion

3.1 Synthesis of the New Chiral-at-Rh Lewis Acid Catalyst Λ/Δ -RhS

3.1.1 Synthetic Design

Chiral-at-metal transition metal complexes devoid of any ligand-based chirality are traditionally resolved into their enantiomers by crystallizing salts with chiral counterions so that the often different solubility of the diastereomeric salts can be exploited.¹ However, in order to not solely rely on unpredictable solubility differences of diastereomeric salts, our research group developed a chiral-auxiliary-mediated strategy² which was initially used for the asymmetric synthesis of chiral ruthenium complexes³ and later applied into the synthesis of enantiopure chiral-at-metal iridium and rhodium complexes including the metal templated “organocatalysts”⁴ and Lewis acids.⁵

a) synthetic strategy for chiral-at-Ir “organocatalysts” and Lewis acids



b) synthetic strategy for chiral-at-Rh Lewis acid Λ -RhO

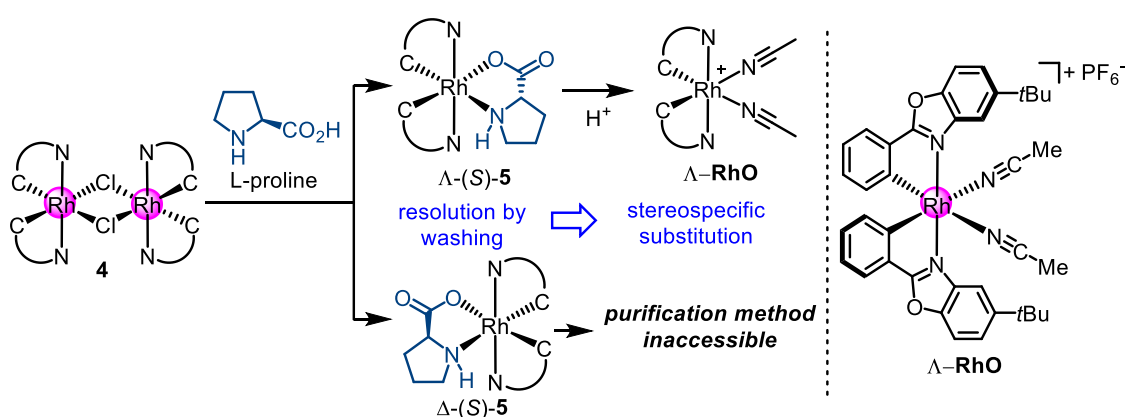


Figure 31. Synthetic strategies for chiral-at-metal iridium and rhodium catalysts.

With respect to the synthesis, as shown in **Figure 31a**, the racemic Ir-based complexes **1** or **2**,

which were prepared from cyclometalating reaction of $\text{IrCl}_3 \cdot x\text{H}_2\text{O}$ and corresponding ligands, reacted towards the chiral auxiliary salicylthiazoline to provide a mixture of two diastereomeric complexes Λ -(*S*)-**3** and Δ -(*S*)-**3**. These two diastereoisomers were then resolved by the regular silica gel chromatography, followed by stereospecific substitution under the acidic conditions to deliver the target enantiopure complexes. This synthetic protocol has provided very efficient access to a variety of metal-templated “organocatalysts”⁴ and the chiral-at-iridium Lewis acid catalysts (Λ/Δ -**IrO** and Λ/Δ -**IrS**)^{5, 6}. However, in the later research on the resolution of Rh-based complexes, Chuanyong Wang found that the most frequently used thiazoline- and oxazoline-based chiral auxiliaries in Meggers lab couldn’t deliver any stable diastereomeric complexes which were suitable for the resolution or purification on the standard silica gel chromatography⁷. C. Wang next turned to another type of naturally abundant auxiliary, enantiopure α -amino acids. As shown in **Figure 31b**, introducing the L-proline to the rhodium center afforded two diastereomeric rhodium prolinato complexes Λ -(*S*)-**5** and Δ -(*S*)-**5**, which again showed limited stability on the column chromatography. However, these two complexes displayed distinct solubility in the mixed solvent of $\text{CH}_2\text{Cl}_2/\text{Et}_2\text{O}$, thereby the insoluble Λ -(*S*)-**5** was isolated by washing out the soluble Δ -(*S*)-**5**. The following acid-induced stereospecific substitution afforded the enantiopure chiral-at-rhodium Lewis acid Λ -**RhO**. The opposite configurational catalyst Δ -**RhO** was obtained through the D-proline-mediated synthetic route.⁸ A drawback of this method needed to be pointed out is that the soluble diastereomers (Δ -(*S*)-**5** and Λ -(*R*)-**5**) can’t be obtained in sufficient purity due to the inaccessible purification method in the Meggers lab.

Intrigued by these established synthetic strategies for chiral-at-metal iridium and rhodium complexes, the author of this thesis decided to investigate the synthesis of the potentially highly active catalysts Λ/Δ -**RhS** using the forementioned chiral-auxiliary-mediated synthetic protocol.

3.1.2 Synthesis and Characterization

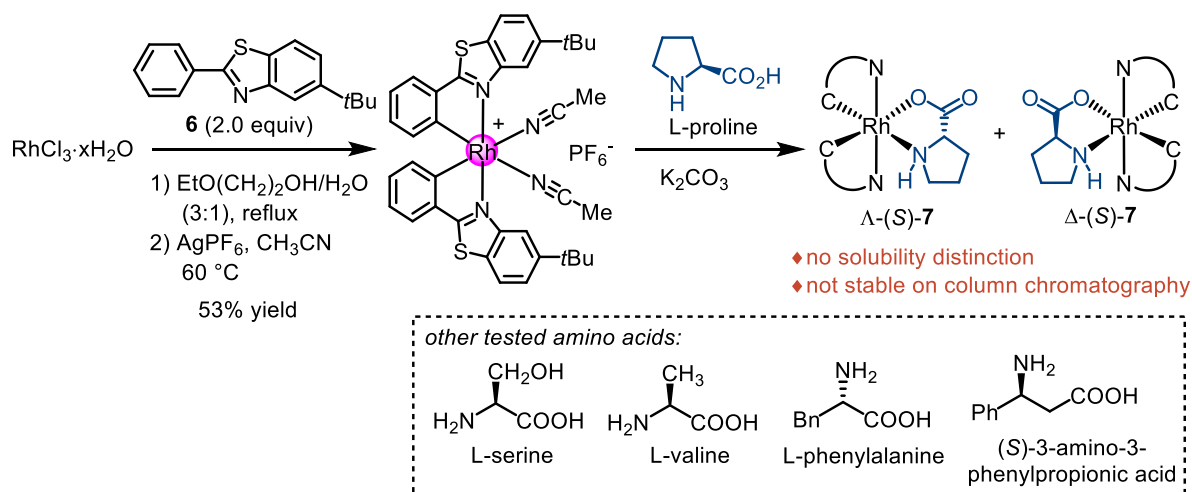


Figure 32. Attempts on resolution of *rac*-**RhS** using enantiopure amino acids.

In line with C. Wang's work on the auxiliary-mediated synthesis of chiral-at-rhodium catalysts Λ/Δ -**RhO**, the enantiopure L-proline should be the first choice for Λ/Δ -**RhS**. The synthesis started with rhodium trichloride hydrate which was first converted into *rac*-**RhS** (1.70 g, 53% yield, data from Xiaoqiang Huang) by reaction with 2 equiv of 5-*tert*-butyl-2-phenylbenzothiazole **6**, followed by treatment with 2.0 equiv. of AgPF_6 in MeCN (**Figure 33**). The *rac*-**RhS** was then reacted with the L-proline to provide a mixture of diastereomeric isomers Λ -(S)-**7** and Δ -(S)-**7**. Unfortunately, these two complexes didn't show any applicable solubility distinction in a range of screened solvents or the combination thereof, and as well were not stable on the stand column chromatography. Moreover, screening other natural or unnatural amino acids didn't lead to any resolution of the corresponding diastereomers.

After running into a stone wall on using enantiopure amino acids as chiral auxiliaries, the author of this thesis decided to turn back to the oxazoline mediated strategy. Upon analyzing reasons of the instability of oxazoline-coordinated rhodium complexes in C. Wang's research, the cleavage of Rh–O ionic bond under acidic conditions should be the key aspect. Taking this into account, a monofluorinated salicyloxazoline (*S*)-**8**⁹ was introduced in which the fluorine would decrease the basicity of the oxygen, therefore most likely hampering the cleavage of Rh–O ionic bond under acidic conditions, especially upon interaction with the silica gel on column chromatography. The realization of this proposal was accomplished as outlined in **Figure**.^{6, 10} Accordingly, the *rac*-**RhS** was reacted with the auxiliary (*S*)-**8** to afford diastereomers Λ -(*S*)-**9** and Δ -(*S*)-**9**, which unexpectedly, displayed

completely distinct solubility in EtOH (**Figure 34**). More gratifyingly, both isomers were stable on the silica gel chromatography as expected. Overall, combining the washing with silica gel chromatography strategies, the *rac*-**RhS** got readily resolved into pure diastereomers Λ -(*S*)-**9** (44% yield) and Δ -(*S*)-**9** (46% yield). Configurations were assigned based on the crystal structure of Λ -(*S*)-**9** as shown in **Figure 35**. Following stereospecific substitutions in acetonitrile provided straightforward access to the enantiopure chiral-at-rhodium Lewis acids Λ -**RhS** and Δ -**RhS** (90% yield and >99:1 er for each one).

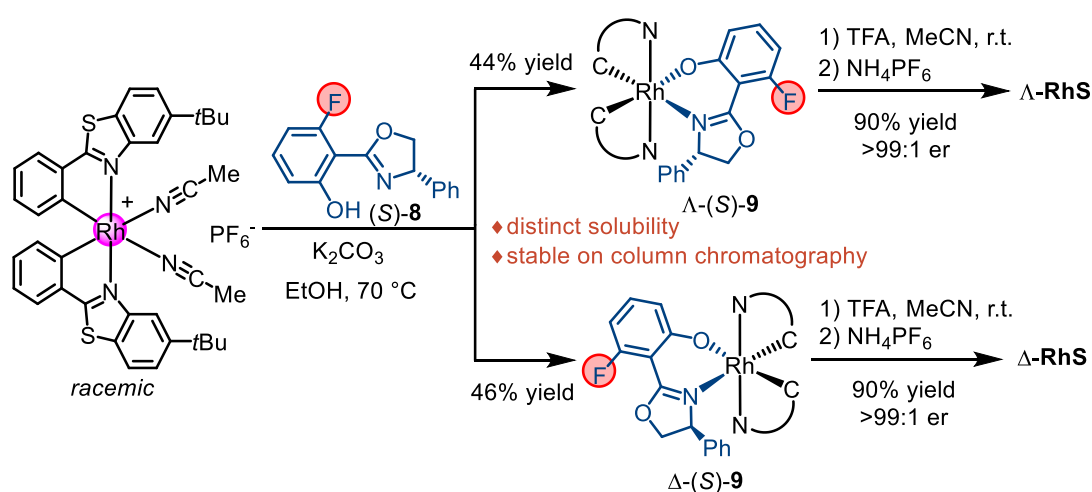


Figure 33. Chiral-auxiliary-mediated synthesis of enantiomerically pure Λ - and Δ -**RhS**.

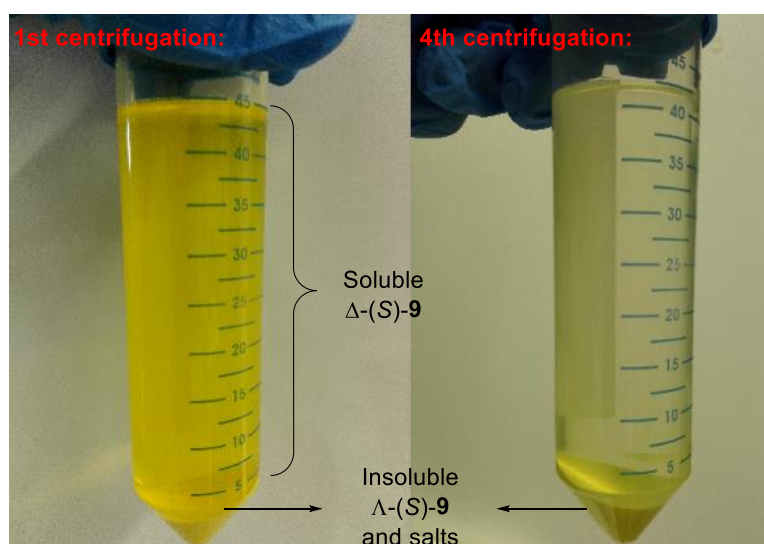


Figure 34. Reaction system after first time centrifugation (left) and after washing by EtOH for another three more times (right).

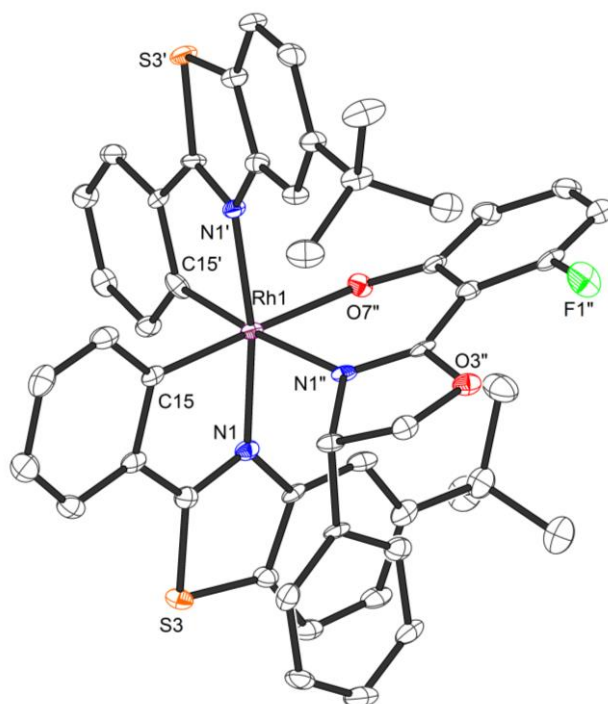


Figure 35. Crystal structure of the auxiliary complex Λ -(S)-9. ORTEP drawing with 50% thermal ellipsoids.

CD spectra of the complexes Λ - and Δ -RhS are shown in **Figure 36** and confirm their mirror-imaged structures. HPLC performed on chiral stationary phase validate the high enantiomeric purity of the individual enantiomers (**Figure 37**). For the Δ -enantiomer an e.r. of 99.9:0.1 was determined, while peak tailing prevents an accurate validation of the Λ -enantiomer and was estimated as >99:1 e.r.

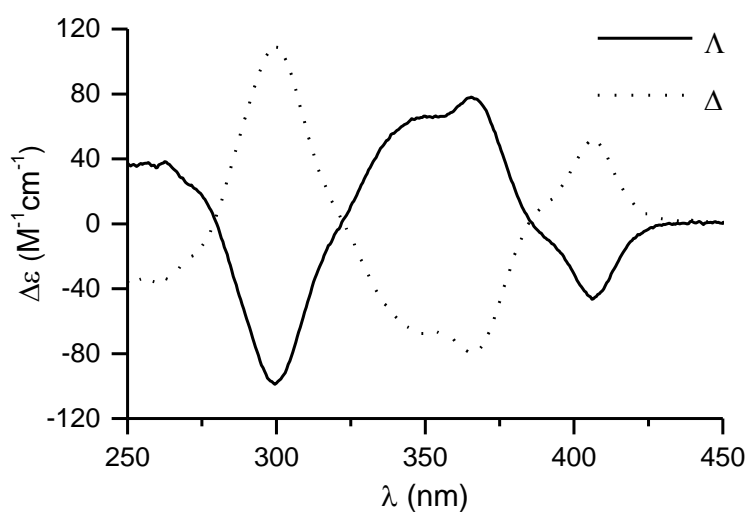


Figure 36. CD spectra of Λ - and Δ -RhS recorded in $\text{CH}_3\text{OH}:\text{CH}_2\text{Cl}_2$ (4:1).

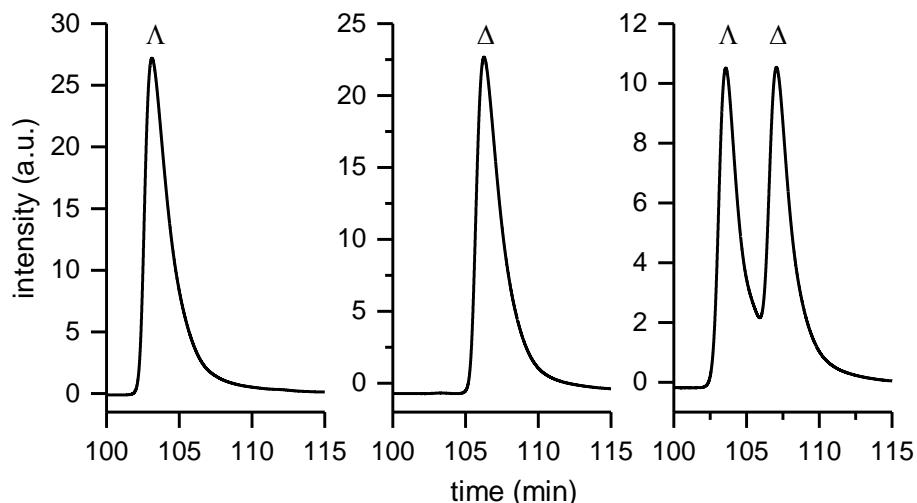


Figure 37. HPLC traces of racemic, Λ - and Δ -RhS. HPLC conditions: Daicel Chiralpak IB, 250 x 4.6 mm, column temp. = 25 °C, abs = 254 nm, flow rate = 0.6 mL/min, solvent A = 0.1% aqueous TFA, solvent B = MeCN, gradient = 40% to 50% B in 180 min.

3.1.3 Evaluation of Catalytic Activity of Λ -RhS

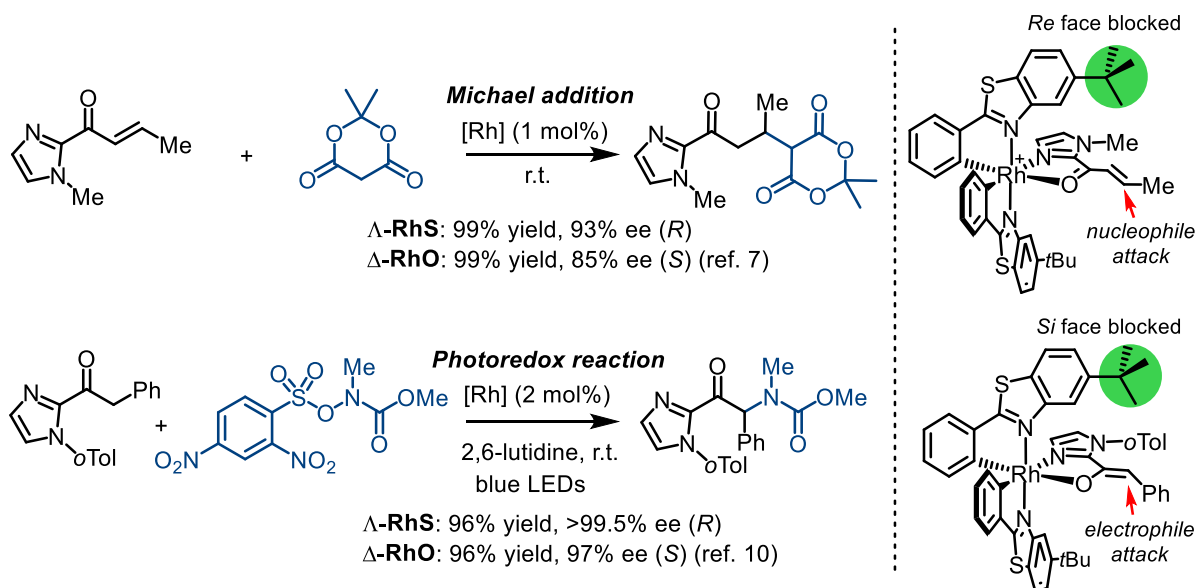


Figure 38. Comparison of catalytic activity of Λ -RhS and Δ -RhO.

Preliminary investigation on the catalytic performance of the newly prepared chiral-at-rhodium Lewis acids Λ/Δ -RhS is outline in **Figure 38**. Accordingly, the enantioselective Michael addition reaction of Meldrum's acid and 2-acyl imidazole catalyzed by the Δ -RhO provided the C–C formation product (*S* configuration) in 99% yield and 85% ee (conducted by C. Wang).⁸ However, using the Λ -RhS instead, an increased enantioselectivity (93% ee with *R* configuration) was obtained with unchanged yield (99%). Another comparison was demonstrated using a photoredox reaction. The

Δ -**RhO** catalyzed asymmetric α -amination of 2-acyl imidazole under photoredox conditions provided the target C–N product in excellent enantioselectivity (97% ee),¹¹ while the Λ -**RhS** gave an even better stereocontrol (>99.5% ee) (conducted by Xiaodong Shen).

The improved catalytic activity of **RhS** over **RhO** is attributed to higher steric congestion directed by the benzothiazole ligands, in which the longer C–S bonds over C–O bonds, arranged the steric bulky tertiary butyl groups closer to the exchange-labile acetonitrile ligands. As outlined in **Figure 39**, the superimposed crystal structures of Λ -**RhS** and mirror-imaged Δ -**RhO** (contributed by Dr. K. Harms), not only confirmed the assigned metal-centered configuration of Λ -**RhS** but also revealed differences in how two *tert*-butyl groups flank the coordination site around the two acetonitrile ligands. In comparison with **RhO**, the *tert*-butyl groups of **RhS** are in closer proximity to the labile acetonitriles as quantified by a 0.9 Å shorter intramolecular distance between quaternary carbons of the two *tert*-butyl groups in **RhS** (10.5 Å) over **RhO** (11.4 Å). This is consistent and analogous with a comparison of the related benzooxazole and benzothiazole iridium complexes.¹²

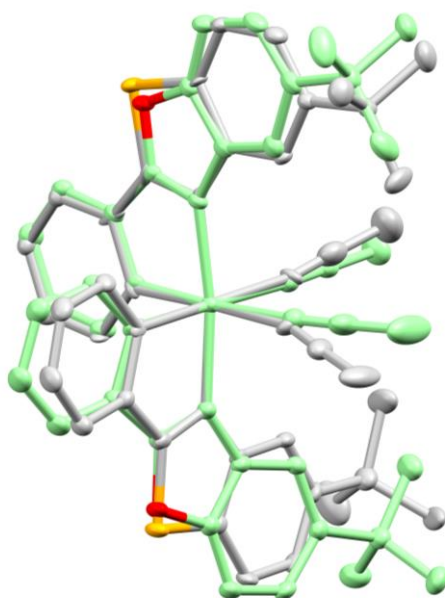


Figure 39. Superimposed crystal structure of Λ -**RhS** (grey) with inverted Δ -**RhO** (green). Fitted are the central metal together with the metal-bound atoms. Atoms are displayed as 50% thermal ellipsoids.

3.1.4 Conclusions

Herein the synthesis of new chiral-at-metal benzothiazole complexes Λ/Δ -**RhS** has been accomplished, which expands the family of bis-cyclometalated rhodium(III) complexes for applications in asymmetric catalysis. Compared with the previously reported benzoxazole complexes Λ/Δ -**RhO**, the benzothiazole ligands in Λ/Δ -**RhS** provide a higher steric congestion around the labile acetonitrile ligands, thereby making Λ/Δ -**RhS** as superior asymmetric catalysts. Applications of the new chiral Lewis acid catalysts to other interesting asymmetric photoredox transformations would be presented in the following chapters.

References

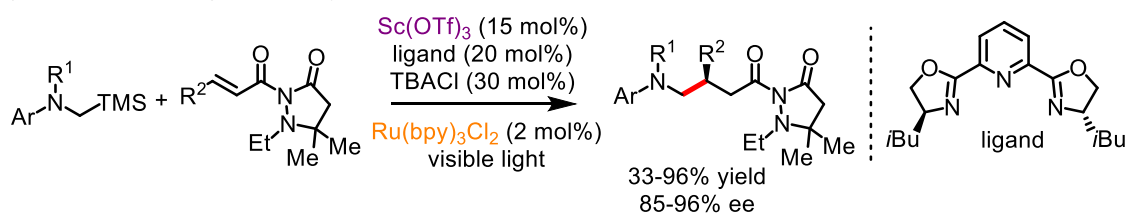
- 1 a) M. Fontecave, O. Hamelin, S. Ménage, *Top. Organomet. Chem.* **2005**, 271; b) L. Gong, L.-A. Chen, E. Meggers, *Angew. Chem. Int. Ed.* **2014**, 53, 10868; c) Z.-Y. Cao, W. D. Brittain, J. S. Fossey, F. Zhou, *Catal. Sci. Technol.* **2015**, 5, 3441.
- 2 E. Meggers, *Chem. Eur. J.* **2010**, 16, 752.
- 3 L. Gong, M. Wenzel, E. Meggers, *Acc. Chem. Res.* **2013**, 46, 2635.
- 4 For selected examples, see: a) L.-A. Chen, W. Xu, B. Huang, J. Ma, L. Wang, J. Xi, K. Harms, L. Gong, E. Meggers, *J. Am. Chem. Soc.* **2013**, 135, 10598; b) J. Ma, X. Ding, Y. Hu, Y. Huang, L. Gong, E. Meggers, *Nat. Commun.* **2014**, 5, 4531; c) W. Xu, M. Arieno, H. Löw, K. Huang, X. Xie, T. Cruchter, Q. Ma, J. Xi, B. Huang, O. Wiest, L. Gong, E. Meggers, *J. Am. Chem. Soc.* **2016**, 138, 8774; for a review, see: d) L. Gong, L. A. Chen, E. Meggers, *Angew. Chem. Int. Ed.* **2014**, 53, 10868.
- 5 L. Zhang, E. Meggers, *Acc. Chem. Res.* **2017**, 50, 320.
- 6 J. Ma, X. Zhang, X. Huang, S. Luo, E. Meggers, *Nat. Protoc.* **2018**, 13, 605.
- 7 C. Wang, E. Meggers, *Asymmetric Catalysis With Octahedral Chiral-at-Metal Iridium and Rhodium Complexes*. Philipps-Universität Marburg, **2016** (Ph.D. thesis).
- 8 C. Wang, L.-A. Chen, H. Huo, X. Shen, K. Harms, L. Gong, E. Meggers, *Chem. Sci.* **2015**, 6, 1094.
- 9 E. Marchi, R. Sinisi, G. Bergamini, M. Tragni, M. Monari, M. Bandini, P. Ceroni, *Chem. Eur. J.* **2012**, 18, 8765.
- 10 J. Ma, X. Shen, K. Harms, E. Meggers, *Dalton Trans.* **2016**, 45, 8320.
- 11 X. Shen, K. Harms, M. Marsch, E. Meggers, *Chem. Eur. J.* **2016**, 22, 9102.
- 12 a) H. Huo, C. Fu, K. Harms, E. Meggers, *J. Am. Chem. Soc.* **2014**, 136, 2990; b) H. Huo, X. Shen, C. Wang, L. Zhang, P. Röse, L.-A. Chen, K. Harms, M. Marsch, G. Hilt, E. Meggers, *Nature* **2014**, 515, 100; c) X. Shen, H. Huo, C. Wang, B. Zhang, K. Harms, E. Meggers, *Chem. Eur. J.* **2015**, 21, 9720.

3.2 Cooperative Rhodium/Ruthenium Asymmetric Photoredox Catalysis to Access Chiral 1,2-Aminoalcohols

3.2.1 Research Background and Reaction Design

Photoinduced Enantioselective Radical Conjugate Addition

a) Yoon's work using dual catalysts:



b) H. Huo's initial attempt using single catalyst:

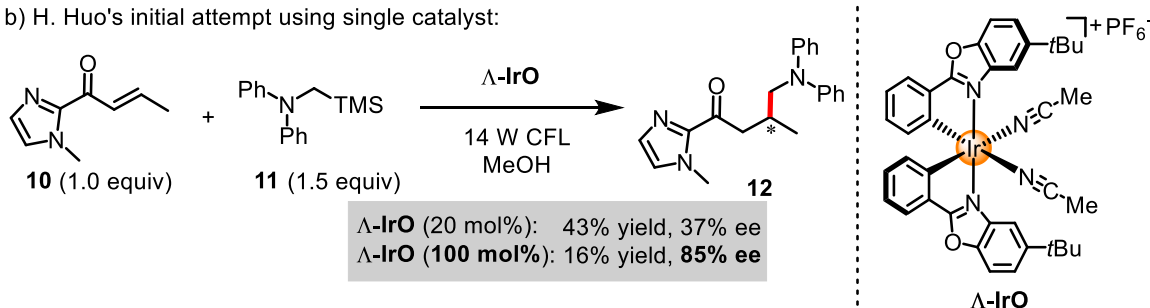


Figure 40. Photoinduced catalytic enantioselective radical conjugate addition by Yoon and the former group member H. Huo.

The catalytic enantioselective radical conjugate addition reaction was a formidable challenge when the author of this thesis started to pursue his doctoral degree in Meggers group. This can be attributed mainly to the strong uncontrollable background reaction which results from the high reactivity of the involved alkyl radicals.¹ A limited number of examples existed. Sibi and co-workers disclosed that the magnesium bisoxazoline complex (5% mol) as chiral Lewis acid was capable of catalyzing radical conjugate addition of isopropyl radical to an oxazolidinone cinnamate with good outcome (92% yield and 90% ee).² Recently, Yoon's group reported that a dual photoredox/Lewis acid catalysis could promote the highly enantioselective radical conjugate addition of α -aminoalkyl radicals to α,β -unsaturated carbonyl compounds (**Figure 40a**).³ With respect to the research of the Meggers group, H. Huo found that the previously developed single chiral-at-iridium Lewis acid Λ -IrO with a loading of 20 mol% could catalyze a similar transformation to provide the C–C formation product **12** in 43% yield and with inferior enantioselectivity of 37% ee under photoredox conditions. While using stoichiometric amount of Λ -IrO (100 mol%), a satisfactory enantioselectivity was obtained (85% ee).⁴

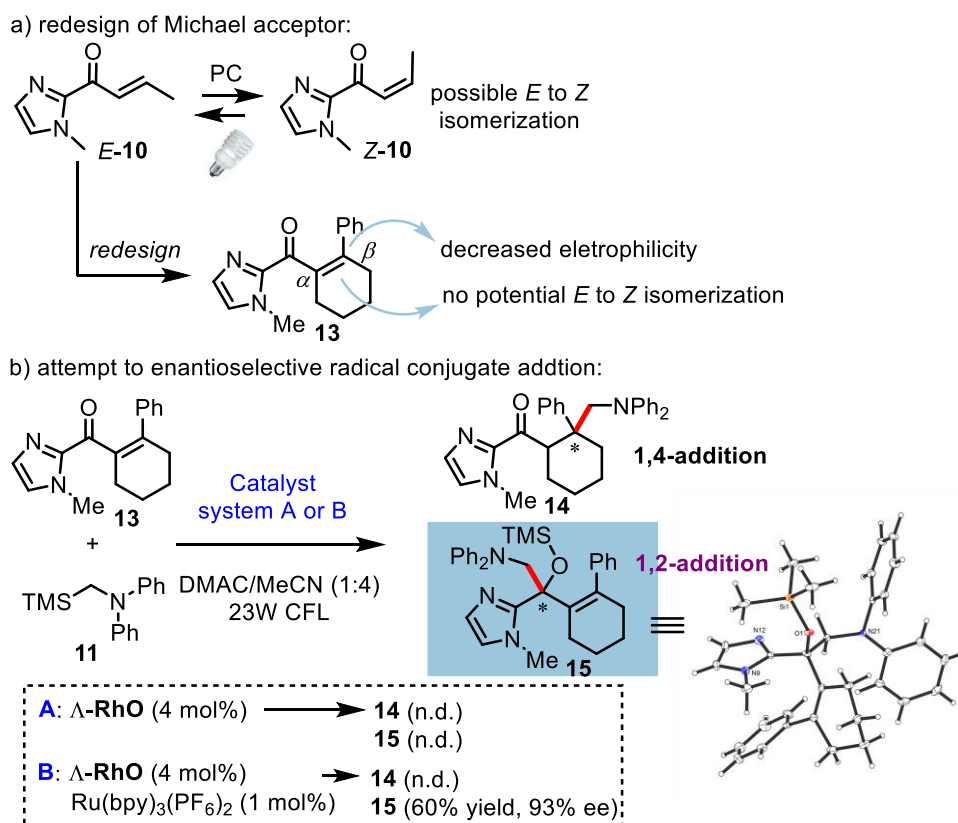


Figure 41. a) Substrate redesign; b) attempt to enantioselective radical conjugate addition. n.d. = not detected. PC = photocatalyst

Intrigued by these results, especially the work of H. Huo, the author of this thesis decided to further investigate the potential of photoinduced enantioselective radical conjugate additions by using the chiral-at-metal catalysts developed in the Meggers group. Considering that the strong uncatalyzed background reaction was the key challenge, it was reasonable to introduce a redesigned Michael acceptor with lower reactivity which should be beneficial to decrease the background or other undesired side reactions. Moreover, with respect to the employed substrate *E-10* in H. Huo's initial attempt, a photoinduced isomerization reaction of *E* to *Z* was possible⁵ and these two isomers would deliver the products with opposite absolute configurations under Λ -IrO catalyzed conditions (**Figure 41a**). The overall result was the diminution of the enantioselectivity of the target C–C formation product. Taking these aspects into account, a new cyclohexene-based Michael acceptor **13** was introduced, which contained two substituents at the β carbon, therefore decreasing its electrophilicity. And the cyclic configuration afforded the alkene without *E* and *Z* isomerization.

As discussed in chapter 1.5, the chiral-at-rhodium complex **RhO** which provided high turnover frequency over **IrO/S** in ligand exchange processes, showed excellent catalytic activity for

photoinduced enantioselective α -amination reactions.⁶ Inspired by this observation, the newly designed α,β -unsaturated carbonyl compound **13** was subjected to a reaction with the α -silyl alkyl amine **11** in the presence of Λ -**RhO** (4 mol%) under the irradiation of 23 W CFL. Disappointingly, no target C–C formation product **14** was observed. However, upon the addition of an established photoredox catalyst $\text{Ru}(\text{bpy})_3(\text{PF}_6)_2$ (1 mol%) to the reaction, unexpectedly, an 1,2-addition product was isolated as the silyl ether **15** in 60% yield and 93% ee, whereas no 1,4-addition was observed. The structure of **15** identified as chiral 1,2-aminoalcohol analogue was confirmed by X-ray crystallography. Even though the initially designed radical conjugate addition was not accomplished, the herein obtained 1,2-aminoalcohol analogue (**15**) was found to be structurally related to the products reported by C. Wang as discussed in chapter 1.5, in which the ketone substrates was limited to compounds containing $\alpha\text{-CF}_3$ groups.⁷ The author of this thesis then wondered if it is possible to use the herein unexpected dual catalysis strategy to expand the limited substrate scope of C. Wang's work to alkyl- and arylsubstituted ketones (**Figure 42**).

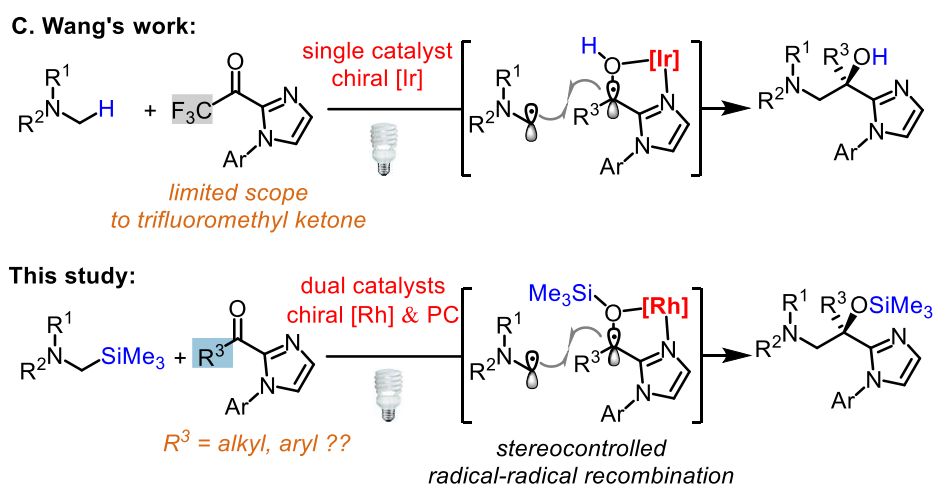


Figure 42. Catalytic enantioselective synthesis of 1,2-aminoalcohol under photoredox conditions. PC = photoredox catalyst.

3.2.2 Initial Experiments and Reaction Development

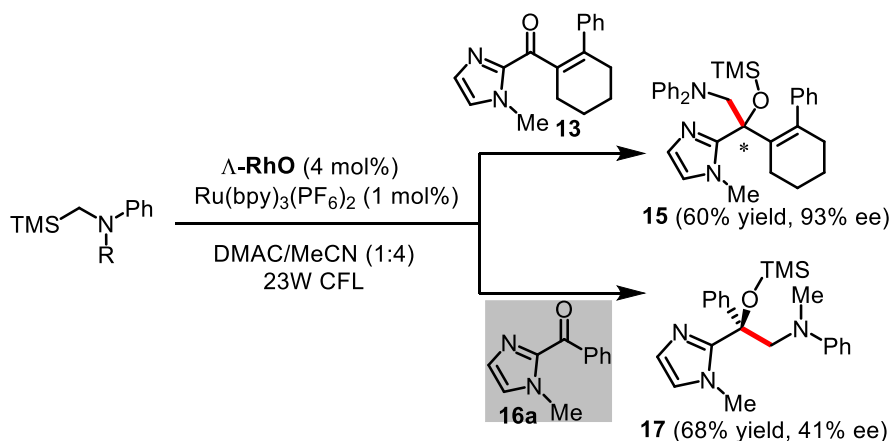
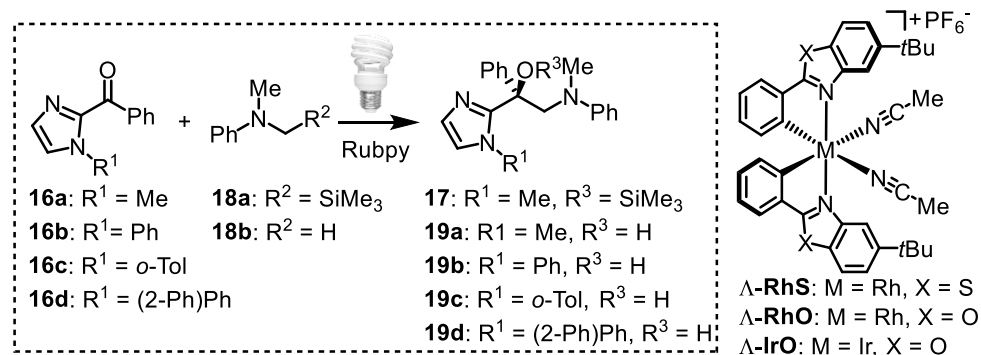


Figure 43. Photoinduced enantioselective redox coupling reaction using the general ketone **16a**.

The investigation on expanding the scope of photoinduced redox coupling reaction started with the acceptor-substituted ketone **16a**. As outlined in **Figure 43**, the chiral-at-metal rhodium-based Lewis acid Λ -RhO⁸ together with the established photocatalyst [Ru(bpy)₃]²⁺ (Rubpy)⁹ catalyzed the reaction of **16a** with the α -silylalkyl amine to provide the C–C formation product **17** in good yield of 68% and decreased enantioselectivity of 41%. With this promising result using the general ketone **16a**, the author of this thesis moved to the dedicated optimization and the result is shown in **Table 2**. Accordingly, removing the trimethylsilyl (TMS) group with TBAF ahead of the workup increased the yield of the corresponding alcohol **19a** to 73% (entry 2). The enantioselectivity of the aminoalcohol coupling product was then stepwise improved by increasing the steric bulk of the substituent at the imidazole nitrogen (R¹, entries 3–5), with the best result obtained for a 2-phenylphenyl substituent, reaching 93% ee. Importantly, replacing the rhodium-catalyst with the analogous iridium congener Λ -IrO¹⁰ abolished product formation, both in the presence or absence of an additional photocatalyst (entries 6 and 7). This can probably be traced back to a different spin localization/delocalization in the iridium ketyl intermediate. Finally, the newly developed second-generation chiral-at-metal rhodium-based Lewis acid Λ -RhS,¹¹ in which the benzoxazole ligands are replaced with benzothiazoles, provided in combination with [Ru(bpy)₃]²⁺ the best results with 76% yield and 95% ee for the reaction **16d** + **18a** → **19d** (entry 8). Control experiments confirm that this reaction requires both visible light and the ruthenium photocatalyst (entries 9 and 10). Furthermore, the TMS group appears crucial for this reaction as a related amine (**18b**) devoid of any silyl group suppressed product

formation completely (entry 11).

Table 2. Reaction development and control experiments.



entry	cat.	PC ^b	<i>hν</i> ^c	cpd 16	cpd 18	<i>t</i> (h)	yield (%) ^d	ee (%) ^e
1	Λ - RhO	Rubpy	yes	16a	18a	14	68 (17)	41
2	Λ - RhO	Rubpy	yes	16a	18a	14	73 (19a)	41
3	Λ - RhO	Rubpy	yes	16b	18a	14	74 (19b)	82
4	Λ - RhO	Rubpy	yes	16c	18a	14	73 (19c)	88
5	Λ - RhO	Rubpy	yes	16d	18a	14	72 (19d)	93
6	Λ - IrO	Rubpy	yes	16d	18a	24	50 (19d)	0
7	Λ - IrO	none	yes	16d	18a	24	43 (19d)	3
8	Λ - RhS	Rubpy	yes	16d	18a	5	76 (19d)	95
9	Λ - RhS	Rubpy	none	16d	18a	20	n.r.	n.d.
10	Λ - RhS	none	yes	16d	18a	20	n.r.	n.d.
11	Λ - RhS	Rubpy	yes	16d	18b	20	n.r.	n.d.

^aReaction conditions: To a mixture of **16a-d** (0.1 mmol), [Ru] (1.0 mol% or none), and catalyst (4 mol% or none) in MeCN/DMAC (4:1) (1ml) was added the amine **18a-b** (0.15 mmol). The reaction mixture was stirred at r.t. under nitrogen and, except for entry 9, irradiated with a 23 W CFL. Afterwards, the solvent was evaporated to dryness and the residue was redissolved in THF, then treated with TBAF (0.5 mmol). The TBAF addition was omitted for entry 1. ^bRubpy = [Ru(bpy)₃](PF₆)₂. ^c23 W CFL. ^dIsolated yields. n.r. = no reaction. ^eDetermined by HPLC on chiral stationary phase. n.d. = not determined. PC = photoredox catalyst.

3.2.3 Substrate Scope

Having obtained the optimized reaction conditions, the substrate scope with respect to α -trimethylsilylalkyl amines (**Figure 44**) was next investigated. Accordingly, both the para- and meta-methylated *N*-phenyl moiety of the α -silylamines afforded the individual products (**19e-f**) in good yields (81-82%) and with excellent enantioselectivities (97-98%). A benzyl substituted α -silylamine also exhibited good tolerance by providing **19g** in 78% yield and with 93% ee. Notably, the reaction between 2-acyl imidazole and the 1,2,3,4-tetrahydroquinoline derivative provided the 1,2-amino alcohol (**19h**) with a satisfactory result (70% yield and 95% ee). Gratifyingly, the *N,N*-diaryl α -silylamines have been applied into this chemistry successfully (**19i-j**), despite a relatively longer reaction time was necessary when the bis(4-(*tert*-butyl)phenyl) substituted α -silylamine involved.

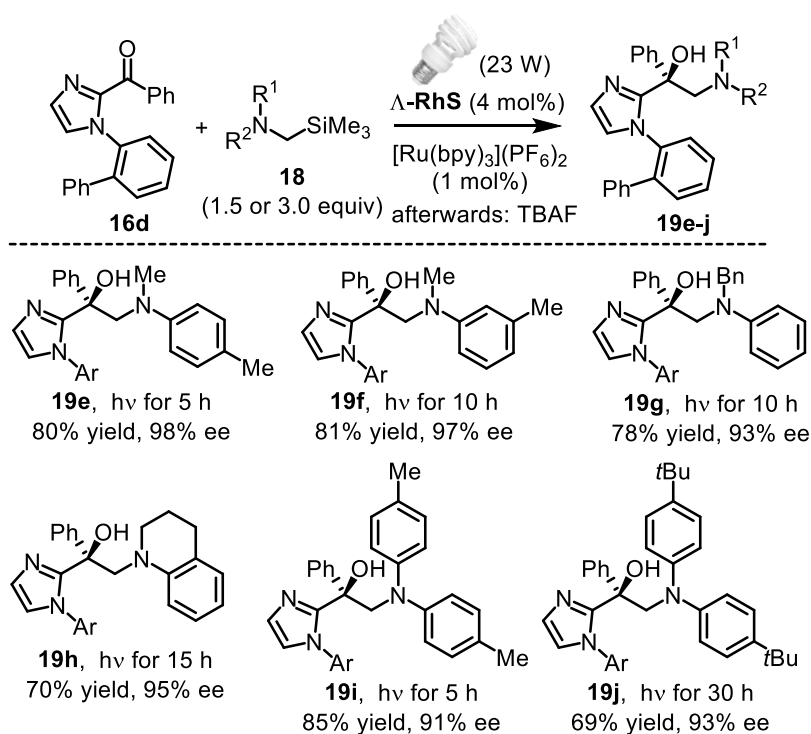


Figure 44. Substrate scope with respect to α -silylalkyl amines.

Next, the substrate scope with respect to 2-acyl imidazoles was evaluated. **Figure 45** reveals that both aromatic as well as aliphatic substituents at the acyl group are tolerated, providing the respective 1,2-amino alcohols **19k-s** in 70-88% yield and with enantioselectivities of 54-99% ee. With respect to substituents in the aromatic moiety, methyl groups (products **19k** and **19l**) and a phenyl group (product **19q**) provide excellent enantioselectivities of 96-98% ee. An acetoxy substituent also afforded the

product **19p** with high yield and high enantioselectivity. However, more strongly electron withdrawing or electron accepting substituents lead to inferior results. For example, while a chloro substituent still provides the product **19m** with high yield (88%) and satisfactory enantioselectivity (93% ee), a methyl ester or methoxy group in *para*-position provided the products **19n** and **19o** only with 54% ee and 86% ee, respectively.

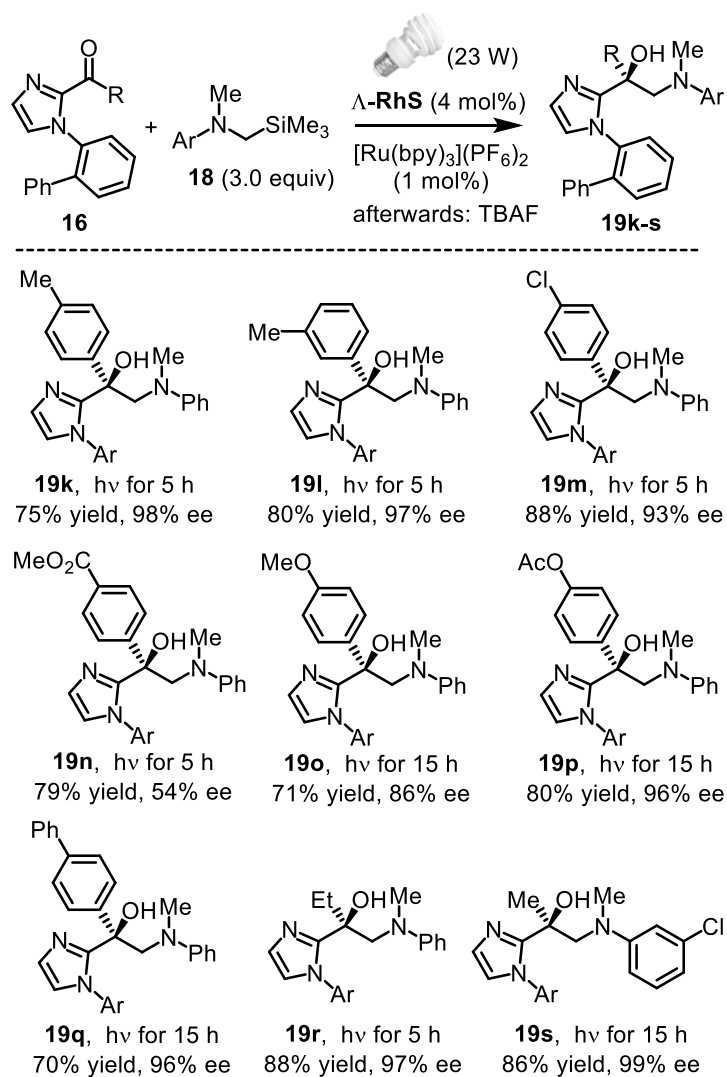


Figure 45. Substrate scope with respect to 2-acyl imidazoles.

3.2.4 Mechanistic Study

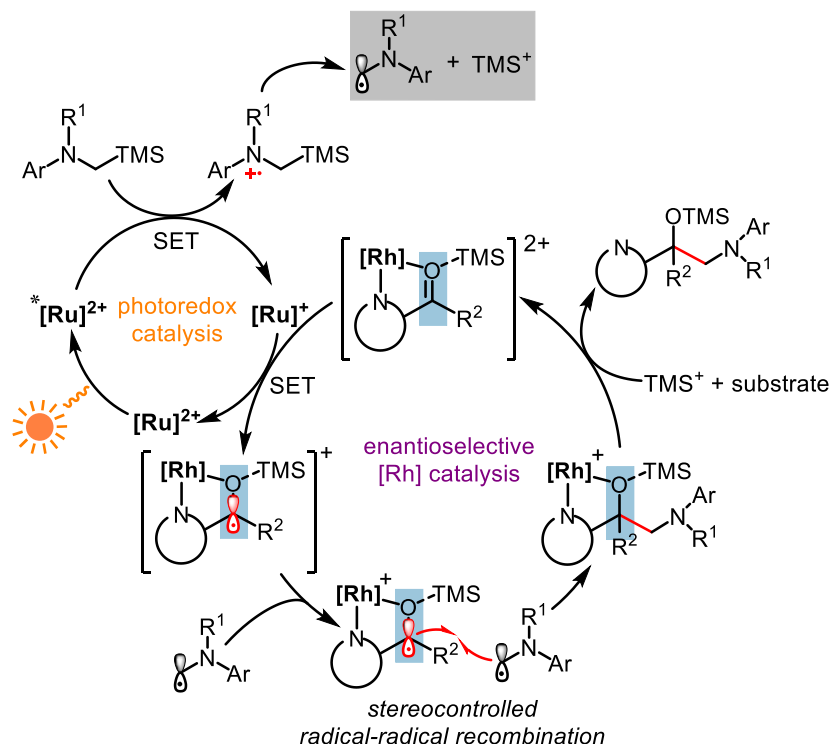


Figure 46. Proposed mechanism for the observed silyl effect in the visible-light activated Rh/Ru dual catalysis. SET = single electron transfer.

A proposed mechanism is illustrated in **Figure 46**. Accordingly, visible light activated $[\text{Ru}(\text{bpy})_3]^{2+}$ ($E_{1/2}^{\text{PC}^*/\text{PC}^-} = +0.77$ V vs SCE in MeCN) oxidizes in a well-established mechanism the α -silylamine ($E_p = \sim 0.41$ V vs SCE in MeCN) to the corresponding radical cation, which subsequently undergoes a rapid desilylation to provide an α -aminomethyl radical.¹² Notably, a related *N,N*-dimethyl aniline constitutes a much higher oxidative potential ($E_p = \sim 0.75$ V vs SCE in MeCN) compared with the α -silylamine.¹³

To take into account the observed silyl effect, the released trimethylsilyl group is proposed to be captured by the rhodium-coordinated 2-acyl imidazole (intermediate **I**) to afford the very electron deficient silylated intermediate **II**. This is followed by an electron transfer from the reduced photocatalyst to regenerate the catalyst in the ground state and provide a rhodium coordinated, silylated ketyl (intermediate **III**), which then undergoes a radical-radical recombination with the α -aminomethyl radical to form the rhodium-coordinated C–C coupling product (intermediate **IV**). Replacement of the product (**19**) by a new substrate (**16**) will then initiate a new catalytic cycle. Thus,

in this mechanism, $\text{Ru}(\text{bpy})_3(\text{PF}_6)_2$ serves as a light-activated electron shuttle between the α -silylalkyl amine (electron donor) and the 2-acyl imidazole (electron acceptor), followed by a radical-radical coupling, in which the stereochemistry is controlled by the chiral rhodium Lewis acid. **Figure 47** shows a crystal structure of a derivative of intermediate **I** and the structure of the proposed intermediate **III** which can rationalize the observed *S*-configuration of the products.

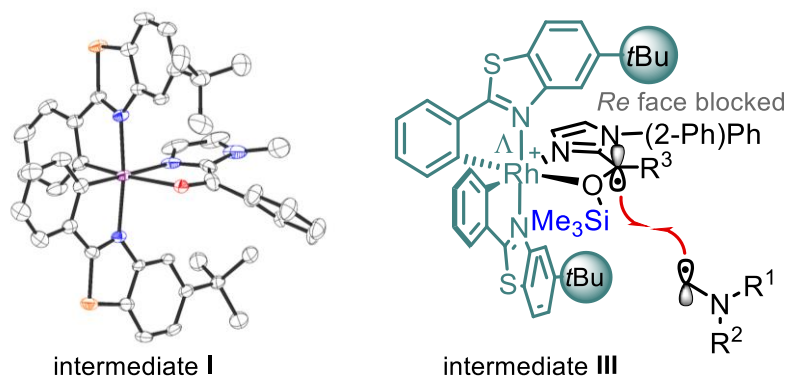


Figure 47. Crystal structure of a derivative intermediate **I** and the proposed structure of intermediate **III** with the indicated stereocontrolled radical-radical recombination.

Mechanistic experiments are shown in **Figure 48**. Control experiments demonstrate that the silyl group, although crucial for observing the C–C coupling product with a 2-acyl imidazole, is actually not required for the production of intermediate α -aminomethyl radicals. Accordingly, the radical species generated from both α -silylmethylamine **18a** and the dimethyl amine **18b** are trapped by an electron deficient alkene to give the product **20** in comparable yield (**Figure 48a**). Additionally, in the presence of the photoredox catalyst $\text{Ru}(\text{bpy})_3(\text{PF}_6)_2$ (1 mol%), reaction of the α -silylmethylamine **18a** with the 2-acyl imidazole **16a** provides the redox coupling product silyl ether with 30% yield, while the dimethyl amine affords no product under the same conditions (**Figure 48b**). Moreover, an amine substrate (**18c**) with the more bulky bis(cyclopropyl)methylsilyl group afforded only 7% yield of the aminoalcohol. Overall, these experiments support the mechanistic picture that the trimethylsilyl group exerts an important role as an additional Lewis acid^{14,15} to activate the rhodium-coordinated 2-acyl imidazole and facilitates a reduction by lowering the ligand-centered LUMO, whereas the related di(cyclopropyl)-methylsilyl group is too bulky to interact with the rhodium-coordinated substrate and the *N,N*-dimethyl aniline can't deliver a second Lewis acid in the reaction system even though undergoing smooth single electron oxidation.

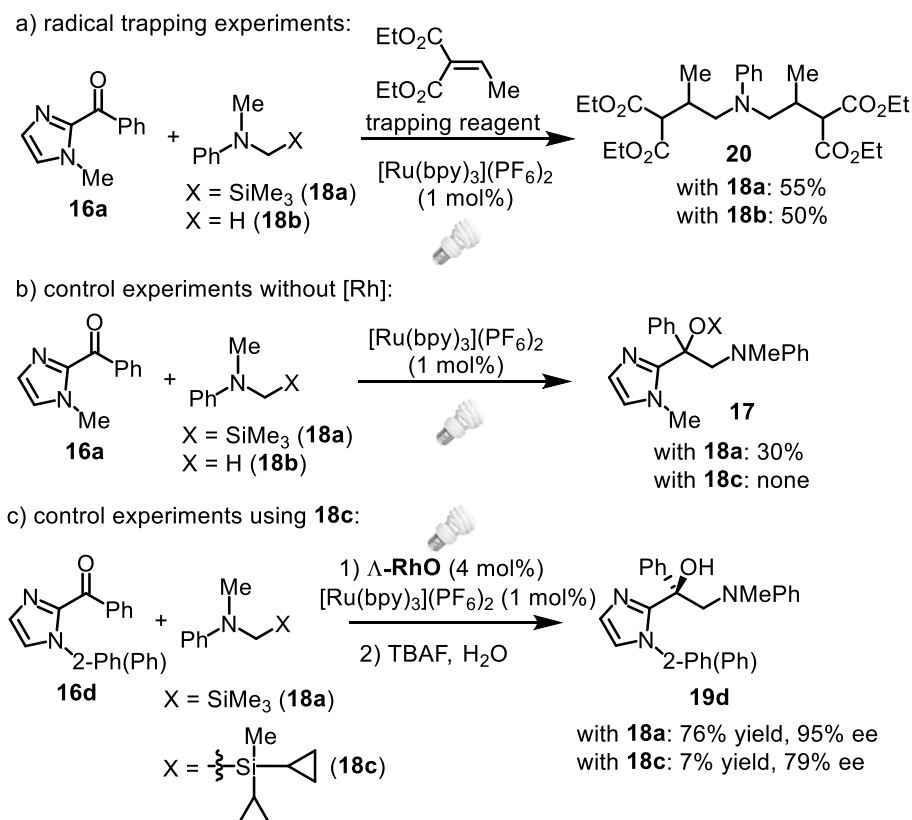


Figure 48. Mechanistic experiments.

3.2.5 Conclusions

A visible-light-driven enantioselective radical-radical cross-coupling was discovered by cooperativity between a rhodium-based chiral Lewis acid and a ruthenium photoredox catalyst and in which a trimethylsilyl group appeared to play a crucial role as an *in situ* released Lewis acid. This protocol expands the substrate scope to a much broader scheme compared with the previous work by C. Wang. In this way synthesized diverse nonracemic 1,2-aminoalcohols represent a reductive Umpolung of the carbonyl reactivity triggered by a photoinduced electron transfer.¹⁶

References

- 1 For a review on enantioselective radical reactions, see: J. Zimmerman, M. P. Sibi, *Top. Curr. Chem.* **2006**, *263*, 107.
- 2 M. P. Sibi, J. Ji, J. H. Wu, S. Gürtler, N. A. Porter, *J. Am. Chem. Soc.* **1996**, *118*, 9200.
- 3 L. Ruiz Espelt, I. S. McPherson, E. M. Wiensch, T. P. Yoon, *J. Am. Chem. Soc.* **2015**, *137*, 2452.
- 4 H. Huo, E. Meggers, *Asymmetric Catalysis with Chiral-at-Metal Complexes: From non-Photochemical Applications to Photoredox Catalysis*. Philipps-Universität Marburg, **2016** (Ph.D. thesis).

- 5 J. B. Metternich, R. Gilmour, *J. Am. Chem. Soc.* **2015**, *137*, 11254.
- 6 X. Shen, K. Harms, M. Marsch, E. Meggers, *Chem. Eur. J.* **2016**, *22*, 9102.
- 7 C. Wang, J. Qin, X. Shen, R. Riedel, K. Harms, E. Meggers, *Angew. Chem. Int. Ed.* **2016**, *55*, 685.
- 8 a) C. Wang, L.-A. Chen, H. Huo, X. Shen, K. Harms, L. Gong, E. Meggers, *Chem. Sci.* **2015**, *6*, 1094; b) Y. Tan, W. Yuan, L. Gong, E. Meggers, *Angew. Chem. Int. Ed.* **2015**, *54*, 13045.
- 9 a) J. W. Tucker, C. R. J. Stephenson, *J. Org. Chem.* **2012**, *77*, 1617; b) C. K. Prier, D. A. Rankic, D. W. C. MacMillan, *Chem. Rev.* **2013**, *113*, 5322.
- 10 H. Huo, C. Fu, K. Harms, E. Meggers, *J. Am. Chem. Soc.* **2014**, *136*, 2990.
- 11 a) J. Ma, X. Shen, K. Harms, E. Meggers, *Dalton Trans.* **2016**, *45*, 8320; b) J. Ma, X. Zhang, X. Huang, S. Luo, E. Meggers, *Nat. Protoc.* **2018**, *13*, 605.
- 12 For the oxidation of α -silylamines through visible-light-activated photoredox catalysis, see: a) Y. Miyake, K. Nakajima, Y. Nishibayashi, *J. Am. Chem. Soc.* **2012**, *134*, 3338; b) Y. Miyake, Y. Ashida, K. Nakajima, Y. Nishibayashi, *Chem. Commun.* **2012**, *48*, 6966; c) Y. Miyake, Y. Ashida, K. Nakajima, Y. Nishibayashi, *Chem. Eur. J.* **2014**, *20*, 6120; d) L. Ruiz Espelt, I. S. McPherson, E. M. Wiensch, T. P. Yoon, *J. Am. Chem. Soc.* **2015**, *137*, 2452.
- 13 B. E. Cooper, W. J. Owen, *J. Organomet. Chem.* **1971**, *29*, 33.
- 14 For reviews covering silicon-based Lewis acids, see: a) H. Emde, D. Domsch, H. Feger, U. Frick, A. Göz, H. H. Hergott, K. Hofmann, W. Kober, K. Krägeloh, T. Oesterle, W. Steppan, W. West, G. Simchen, *Synthesis* **1982**, *1982*, 1; b) A. D. Dilman, S. L. Ioffe, *Chem. Rev.* **2003**, *103*, 733; c) H. F. T. Klare, M. Oestreich, *Dalton Trans.* **2010**, *39*, 9176; d) T. Stahl, H. F. T. Klare, M. Oestreich, *ACS Catal.* **2013**, *3*, 1578.
- 15 For selected examples regarding in situ generated silylium ions as Lewis acids, see: a) G. A. Olah, A. Husain, B. G. B. Gupta, G. F. Salem, S. C. Narang, *J. Org. Chem.* **1981**, *46*, 5212; b) M. B. Boxer, H. Yamamoto, *J. Am. Chem. Soc.* **2006**, *128*, 48; c) P. Garca-Garca, F. Lay, P. Garca-Garca, C. Rabalakos, B. List, *Angew. Chem. Int. Ed.* **2009**, *48*, 4363; d) A. Takahashi, H. Yanai, M. Zhang, T. Sonoda, M. Mishima, T. Taguchi, *J. Org. Chem.* **2010**, *75*, 1259; e) H. Yanai, A. Takahashi, T. Taguchi, *Chem. Commun.* **2010**, *46*, 8728; f) M. Michalska, O. Songis, C. Taillier, S. P. Bew, V. Dalla, *Adv. Synth. Catal.* **2014**, *356*, 2040; g) I. Ramakrishna, G. S. Grandhi, H. Sahoo, M. Baidya, *Chem. Commun.* **2015**, *51*, 13976; h) T. Gatzemeier, M. van Gemmeren, Y. Xie, D. Höfler, M. Leutzsch, B. List, *Science* **2016**, *351*, 949.
- 16 For the reductive umpolung of carbonyl compounds by visible light photoredox catalysis, see: a) K. T. Tarantino, P. Liu, R. R. Knowles, *J. Am. Chem. Soc.* **2013**, *135*, 10022; b) L. J. Rono, H. G. Yayla, D. Y. Wang, M. F. Armstrong, R. R. Knowles, *J. Am. Chem. Soc.* **2013**, *135*, 17735; c) M. Nakajima, E. Fava, S. Loescher, Z. Jiang, M. Rueping, *Angew. Chem. Int. Ed.* **2015**, *54*, 8828; d) E. Fava, A. Millet, M. Nakajima, S. Loescher, M. Rueping, *Angew. Chem. Int. Ed.* **2016**, *55*, 6776; e) W. Li, Y. Duan, M. Zhang, J. Cheng, C. Zhu, *Chem. Commun.* **2016**, *52*, 7596.

3.3 Synthesis of Fluoroalkyl-Containing Compounds through Enantioselective Three-Component Photoredox Reaction

3.3.1 Research Background and Reaction Design

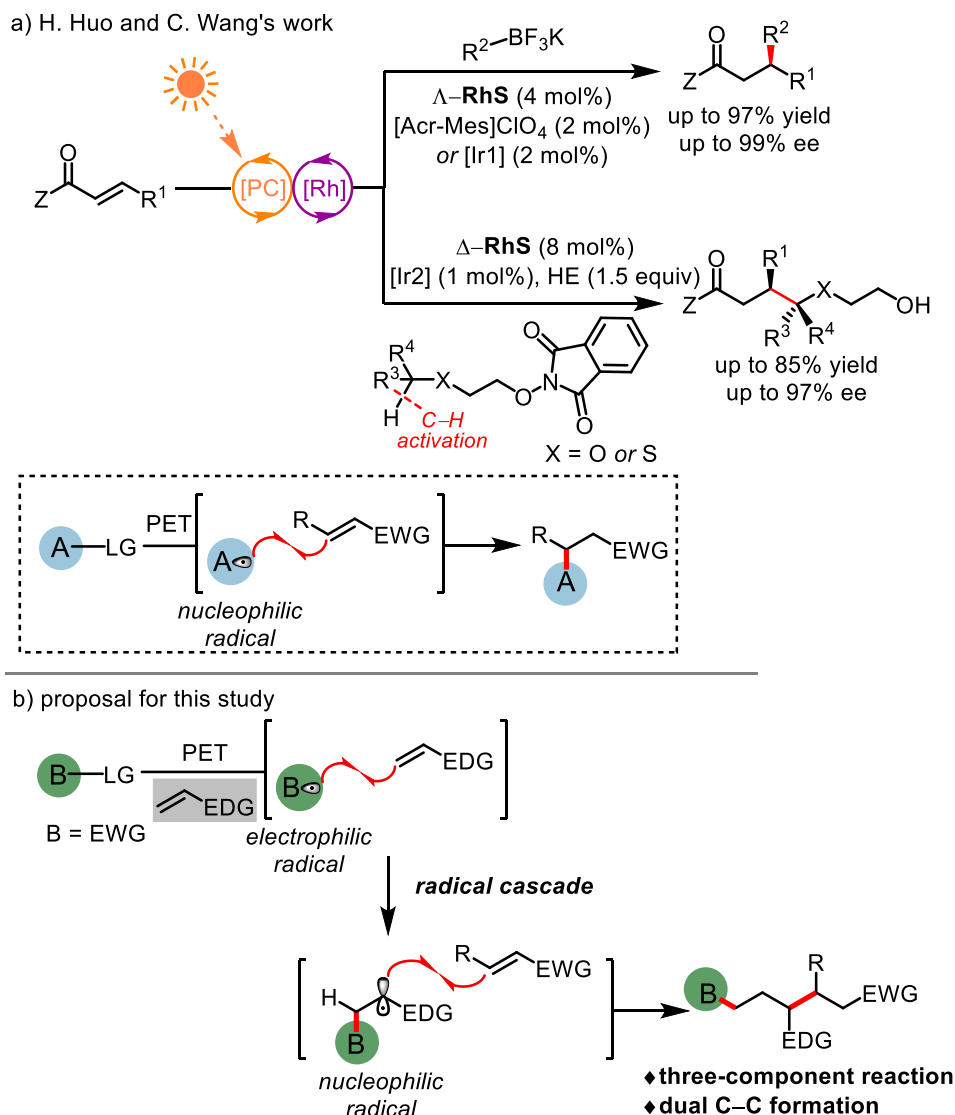


Figure 49. a) H. Huo and C. Wang's work on photoinduced radical conjugate addition reaction; b) proposal for this study. PC = photoredox catalyst. [Ir1] = Ir(dF(CF₃)ppy)₂(bpy)PF₆. [Ir2] = *fac*-Ir(ppy)₃. PET = photoinduced electron transfer. EWG = electron withdrawing group. EDG = electron donating group.

In 2016, the former group member H. Huo accomplished the visible-light-induced enantioselective radical conjugate addition of organotrifluoroborates and acceptor-substituted alkenes by using the cooperative catalysis of chiral-at-rhodium Lewis acid Δ -**RhS** and established photoredox catalysts (**Figure 49a**).¹ C. Wang further extended this elegant methodology to the functionalization of C(sp³)-H bonds through intramolecular 1,5-hydrogen atom transfer (1,5-HAT).² Both of these two

reaction schemes provided the C–C formation products with excellent enantioselectivities (up to 99% and 97% ee, respectively) by suppressing the often prevailing racemic background reaction, which typically needed to be counterbalanced with high catalyst loadings. With respect to the mechanism, a nucleophilic radical **A** is thought to be typically produced upon the release of a leaving group triggered by photoinduced electron transfer (PET). This radical species is supposed to add to the rhodium-bound acceptor-substituted alkenes to provide the C–C formation products in a catalytic enantioselective fashion. Inspired by this mechanistic scenario, the author of this thesis became interested in the development of methods for generating nucleophilic radicals. As illustrated in **Figure 49b**, a radical cascade pathway was proposed for the generation of a nucleophilic radical. Accordingly, this new design started with the production of an electrophilic radical under photoredox conditions, which was subsequently trapped by an electron-rich olefin to deliver the nucleophilic radical species. This species is an equivalent of intermediate **A** in the previous work and would then add to the Michael acceptor under the stereocontrol of the chiral-at-rhodium Lewis acid catalyst. Overall, this newly proposed radical cascade scheme would trigger a catalytic asymmetric three component photoredox reaction which provides the non-racemic dual C–C formation products in highly efficient fashion.

On the other hand, the author of this thesis was also quite interested in the discovery of new photoredox catalysts or mediators which are simple and readily available. In 2016, the Li group reported a practical photochemical method for the trifluoromethylation of unactivated arenes and heteroarenes using acetone (UV activation) and diacetyl (visible-light activation) as simple photoredox initiators or mediators.³ In particular, diacetyl as a simple commercially available material is very appealing for visible-light-induced single electron transfer (SET) but the requirement to use it as a cosolvent poses a significant drawback. The author of this thesis then envisioned that some other α -diketones⁴ with improved photoredox properties would be applicable to the forementioned three-component photoredox reaction at a substoichiometric amount.

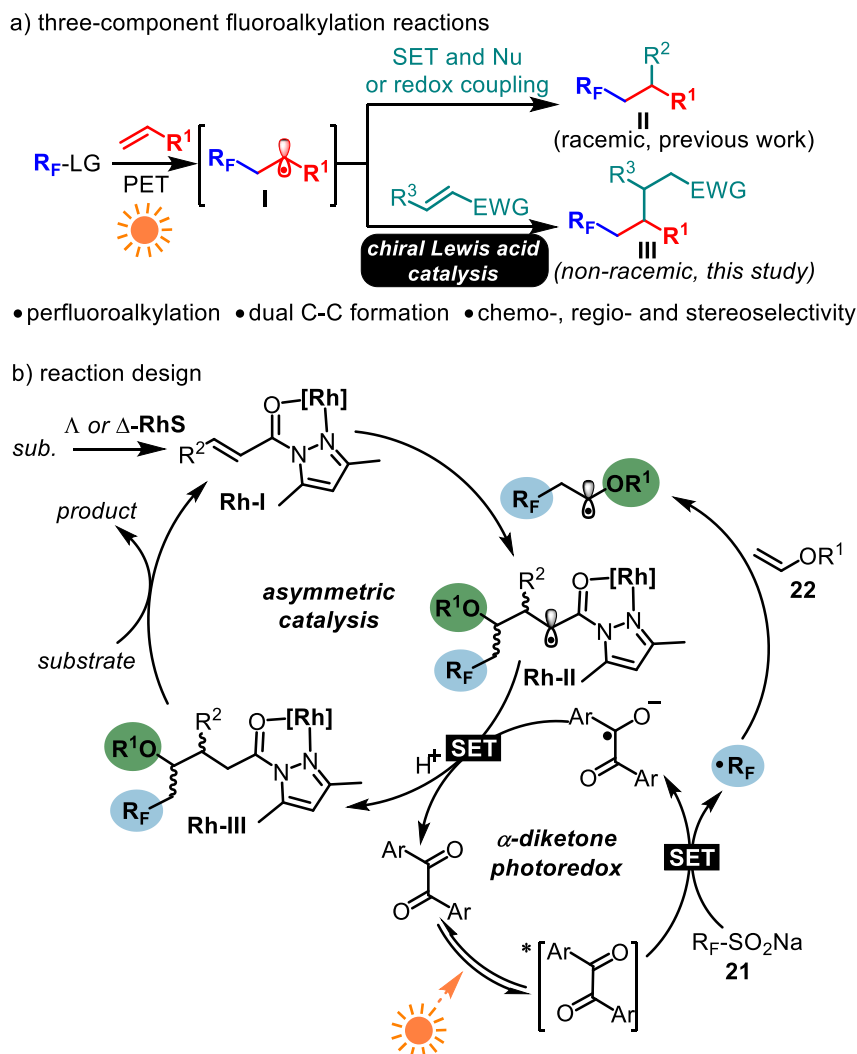


Figure 50. a) Previous work and this study on visible-light-induced three-component fluoroalkylation reactions; b) Reaction design based on asymmetric Lewis acid catalysis in combination with α -diketone organophotoredox chemistry. PET = photoinduced electron transfer. SET = single electron transfer.

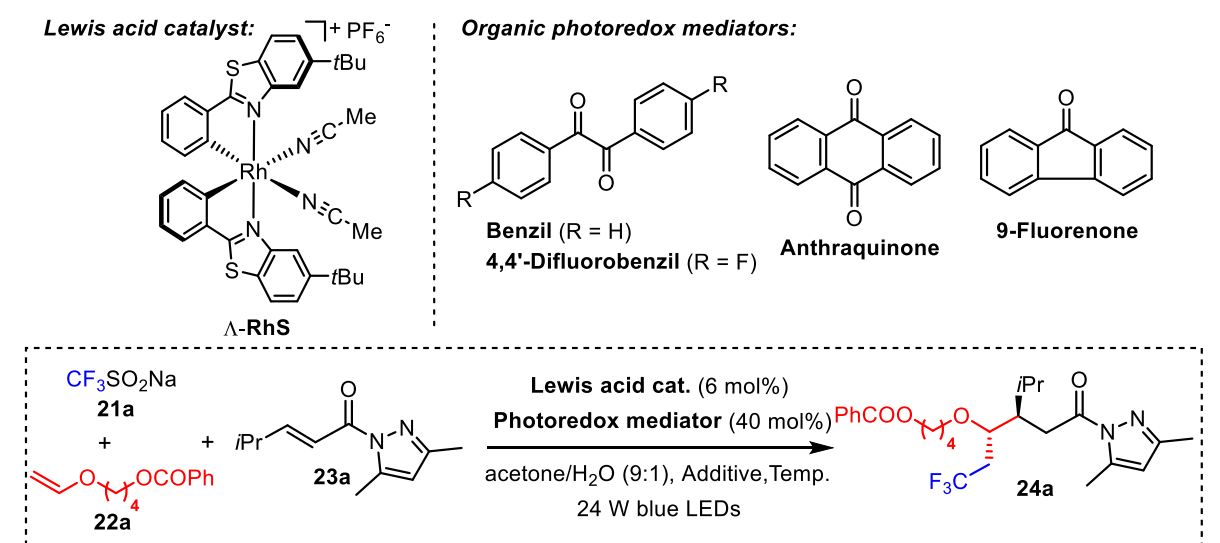
While turning to the photoredox reaction using three or multiple components, the visible-light-induced three-component fluoroalkylations have witnessed increasing popularity because perfluoroalkyl radicals can be generated conveniently under photoredox conditions and are then used in the context of multicomponent reactions (MCRs)⁵ for the efficient synthesis of organofluorine compounds.⁶ For example, Akita and coworkers introduced an elegant three-component oxytrifluoromethylation under photoredox conditions to efficiently difunctionalize C–C double bonds in a regioselective fashion.⁷ Magnier and Masson further extended this approach to the more challenged oxyperfluoroalkylation by using S-perfluoroalkyl sulfilimino iminiums as versatile fluorinated radical source.⁸ In all these cases, the reactions are initiated by the generation of perfluoroalkyl radicals through photoinduced electron transfer (PET), followed by their addition to

alkenes⁹ which leads to the formation of secondary radicals (intermediate **I** in **Figure 50a**). These secondary radicals are then often oxidized by single electron transfer (SET) and trapped with a nucleophile to furnish the racemic three-component product **II**. Xiao and Chen described an alternative three-component radical cascade process in which the secondary radicals (intermediate **I**) were directly trapped by aryldiazonium salts and later underwent single electron oxidation to deliver various trifluoromethylated azo compounds under photoredox conditions.¹⁰ Despite the vast efforts that have been devoted to racemic visible-light-induced multicomponent-based perfluoroalkylation,¹¹ catalytic asymmetric versions remain elusive, presumably due to the challenge of achieving satisfactory asymmetric inductions with highly reactive free radicals. However, beyond photoredox chemistry, X.-Y. Liu¹² and G. Liu¹³ recently reported several examples concerning the catalytic asymmetric synthesis of trifluoromethyl containing compounds based on MCRs in which Cu(I) is proposed to initiate single electron transfer (SET) from Togni's [CF₃⁺] reagent.

Overall, inspired by all these studies, the author of this thesis therefore envisioned a new Rh-catalyzed three-component enantioselective radical conjugate addition reaction using α -diketones as photoredox mediators. The reaction design is outlined in **Figure 50b**. Accordingly, a photoexcited α -diketone, presumably bearing an extended π -system with aryl substituents to improve visible light absorption and stabilize radical anion intermediates, should be quenched reductively by the Langlois reagent¹⁴ or related sodium perfluoroalkyl sulfinates (**21**)¹⁵ to generate a perfluoroalkyl radical along with ketyl radical. The electron-deficient fluorinated radical is then selectively trapped by the electron-rich terminal alkene **22** to provide under C–C bond formation an α -oxyl carbon-centered radical species which subsequently engages in a rhodium-catalyzed asymmetric addition to an acceptor-substituted alkene (**Rh-I**→**Rh-II**) to create a second C–C single bond in an enantioselective and diastereoselective fashion. SET from the reduced photoredox mediator (ketyl intermediate) to the rhodium-coordinated radical (**Rh-II**) followed by protonation then provides the rhodium-coordinated product (**Rh-III**) accompanied with a regenerated α -diketone. After dissociation of the product the rhodium catalyst can engage in a new catalytic cycle. This visible-light-activated three-component radical cascade reaction would provide structurally complex organofluorine building blocks in an efficient fashion under conditions of asymmetric catalysis.

3.3.2 Initial Experiments and Reaction Development

Experimental study started by investigating the reaction Langlois reagent **21a**, vinyl ether **22a**, and α,β -unsaturated *N*-acylpyrazole **23a** under photoredox conditions (**Table 3**). Encouragingly, the combination of Λ -**RhS**¹⁶ (6 mol%) and the organic photoredox mediator benzil¹⁷ (40 mol%) enabled the asymmetric three-component fluoroalkylation reaction to provide **24a** under dual C–C bond formation, but only in 10% yield, with a limited diastereoselectivity (2:1), and a low enantioselectivity of 40% ee for each diastereomer (entry 1). No desired product was observed by employing the chiral Lewis acid catalyst Λ -**RhS** (6 mol%) in the absence of benzil (entry 2). The yield and enantioselectivity were improved somewhat to 19% by adding NH_4PF_6 as a proton transfer mediator (entry 3). We next rationalized that electron-withdrawing groups introduced into benzil should be beneficial due to an increased oxidation potential. Interestingly, when we used 4,4'-difluorobenzil instead of benzil the yield remained unchanged at 19% but the enantioselectivity increased significantly to 67% ee (entry 4). When we conducted the reaction at a reduced temperature of 5–7 °C, a satisfactory yield of **24a** of 64% and an excellent enantioselectivity of 96% ee for each formed diastereomer (2:1 dr) was achieved (entry 5). Notably, these two diastereomers could be resolved by regular column chromatography on silica gel. Several control experiments were conducted to show the superiority of the herein employed chiral Rh-based Lewis acid catalyst in combination with the inexpensive organic photoredox mediator 4,4'-difluorobenzil. For example, $\text{Sc}(\text{OTf})_3$ (20 mol%) or $\text{Cu}(\text{OAc})_2$ (20 mol%) instead of Λ -**RhS**, provided a decreased yield (26%, entry 6) or no product formation (entry 7), respectively. Meanwhile, product formation was completely abolished with other ketones, such as anthraquinone¹⁸ and 9-fluorenone¹⁹, which have been well-established for photoinduced hydrogen atom transfer (entries 8 and 9). Other control experiments verified that visible light and oxygen-free conditions were essential for this chemical transformation (entries 10 and 11). More details concerning the optimization of conditions, comparison with other photoredox mediators as well as light sources are available in the Experimental Part.

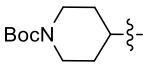
Table 3. Reaction development and control experiments^a

entr	catalyst	photoredox mediator	T (°C)	additive	<i>hν</i> ^b	yield (%) ^c	dr ^d	ee (%) ^e
1	Λ-RhS	benzil	25	none	yes	10% (20 h)	2:1	40/40
2	Λ-RhS	none	25	none	yes	0 (48 h)	n.a.	n.a.
3	Λ-RhS	benzil	25	NH ₄ PF ₆	yes	19% (20 h)	2:1	51/51
4	Λ-RhS	4,4'-difluorobenzil	25	NH ₄ PF ₆	yes	19% (20 h)	2:1	67/67
5	Λ-RhS	4,4'-difluorobenzil	5-7	NH₄PF₆	yes	64% (28 h)	2:1	96/96
6 ^f	Sc(OTf) ₃	4,4'-difluorobenzil	5-7	NH ₄ PF ₆	yes	26% (48h)	2:1	n.a.
7 ^f	Cu(OAc) ₂	4,4'-difluorobenzil	5-7	NH ₄ PF ₆	yes	0 (48 h)	n.a.	n.a.
8	Λ-RhS	anthraquinone	5-7	NH ₄ PF ₆	yes	0 (48 h)	n.a.	n.a.
9	Λ-RhS	9-fluorenone	5-7	NH ₄ PF ₆	yes	0 (48 h)	n.a.	n.a.
10	Λ-RhS	4,4'-difluorobenzil	5-7	NH ₄ PF ₆	no	0 (48 h)	n.a.	n.a.
11 ^g	Λ-RhS	4,4'-difluorobenzil	5-7	NH ₄ PF ₆	yes	0 (48 h)	n.a.	n.a.

^aReaction conditions: **21a** (0.6 mmol), **22a** (0.3 mmol) and **23a** (0.1 mmol), Rh catalyst (6 mol%), and α -diketone (40 mol%) in acetone/H₂O (9:1, v/v, 0.1 M) were stirred at the indicated temperature for 20–48 h under an atmosphere of nitrogen, unless otherwise noted. ^bLight source: 24 W blue LEDs. ^cIsolated yields; reaction time provided in brackets. ^dDetermined by ¹⁹F NMR analysis of the crude products. ^eDetermined by HPLC analysis on a chiral stationary phase; ee of both diastereomers are shown. ^f20 mol% of Sc(OTf)₃ and Cu(OAc)₂ were employed respectively. ^gReaction was conducted under air. n.a. = not applicable.

3.3.3 Substrate Scope

Table 4. Substrate scope with respect to *N*-acylpyrazoles and sodium perfluoroalkyl sulfonates^a

entry	R _F	R ¹	R ²	t (h)	yield (%) ^b	dr ^c	ee (%) ^d
1 ^e	CF ₃ (21a)	Bz(CH ₂) ₄ O (22b)	<i>i</i> Pr (23a)	30	70 (24b)	2.1:1	92 / 93
2	CF ₃ (21a)	Bz(CH ₂) ₄ O (22b)	3-pentyl (23b)	48	57 (24c)	1.7:1	95 / 95
3 ^f	CF ₃ (21a)	Bz(CH ₂) ₄ O (22b)	cyclopentyl (23c)	30	53 (24d)	1.9:1	97 / 94
4 ^f	CF ₃ (21a)	Bz(CH ₂) ₄ O (22b)	cyclohexyl (23d)	30	65 (24e)	2.0:1	96 / 90
5	CF ₃ (21a)	Bz(CH ₂) ₄ O (22b)	<i>t</i> Bu (23e)	66	47 (24f)	6.0:1	96 ^h
6	CF ₃ (21a)	BnO(CH ₂) ₄ O (22c)	Et (23f)	14	26 (24g)	1.7:1	70 / 78
7	CF ₃ (21a)	Bz(CH ₂) ₄ O (22b)	BocN  (23g)	28	86 (24h)	2.0:1	94 / 92
8 ^g	C ₄ F ₉ (21b)	Bz(CH ₂) ₄ O (22b)	<i>i</i> Pr (23a)	38	51 (24i)	2.7:1	91 / 91
9 ^g	C ₆ F ₁₃ (21c)	BzO(CH ₂) ₄ O (22a)	<i>i</i> Pr (23a)	30	42 (24j)	2.6:1	90 / 87

^aReaction conditions: sodium perfluoroalkyl sulfonates **21a-c** (0.6 mmol), vinyl ethers **22a-c** (0.3 mmol) and *N*-acylpyrazoles **23a-g** (0.1 mmol), Λ -**RhS** (6 mol%), 4,4'-difluorobenzil (40 mol%) in acetone/H₂O (9:1, v/v, 0.1 M) at 5-7 °C for 14–66 h under an atmosphere of nitrogen, under irradiation with 24 W blue LEDs, unless otherwise noted. ^bIsolated yields. ^cDetermined by ¹⁹F NMR analysis. ^dDetermined by HPLC analysis on a chiral stationary phase; ee of both diastereomers are shown. ^e Λ -**RhS** (4 mol%) was employed. ^f Λ -**RhS** (8 mol%) was employed. ^g Δ -**RhS** (4 mol%) and 4,4'-difluorobenzil (25 mol%) were employed. ^hEe of major diastereomer shown.

Next, the substrate scope with respect to α,β -unsaturated *N*-acylpyrazoles and sodium perfluoroalkyl sulfonates was evaluated. **Table 4** shows that the asymmetric three-component fluoroalkylation reactions afforded the desired dual C–C bond formation products **24b–j** in 26–86% yields, 1.7:1–6.0:1 dr and 70–97% ee. A tertiary alkyl group at the alkene (product **24f**) provided good diastereoselectivity (6:1) as well as excellent enantioselectivity (96% ee). However, the ethyl substituent gave inferior results (product **24g**, 26 % yield, 1.7:1 dr, 70% / 78% ee) which could be traced back to the decomposition of the corresponding α,β -unsaturated *N*-acylpyrazole substrate **23f** (see Experimental Part). The perfluoroalkylation products **24i** and **24j** were obtained with satisfactory

results (42–51% yields, 2.6:1–2.7:1 dr and 87–91% ee) with a relatively low loading of Δ -**RhS** (4 mol%) and 4,4'-difluorobenzil (25 mol%). Notably, except for **24d** and **24g**, all other chiral fluorinated products could be purified by regular column chromatography to obtained >10:1 or even >20:1 dr for the main stereoisomer.

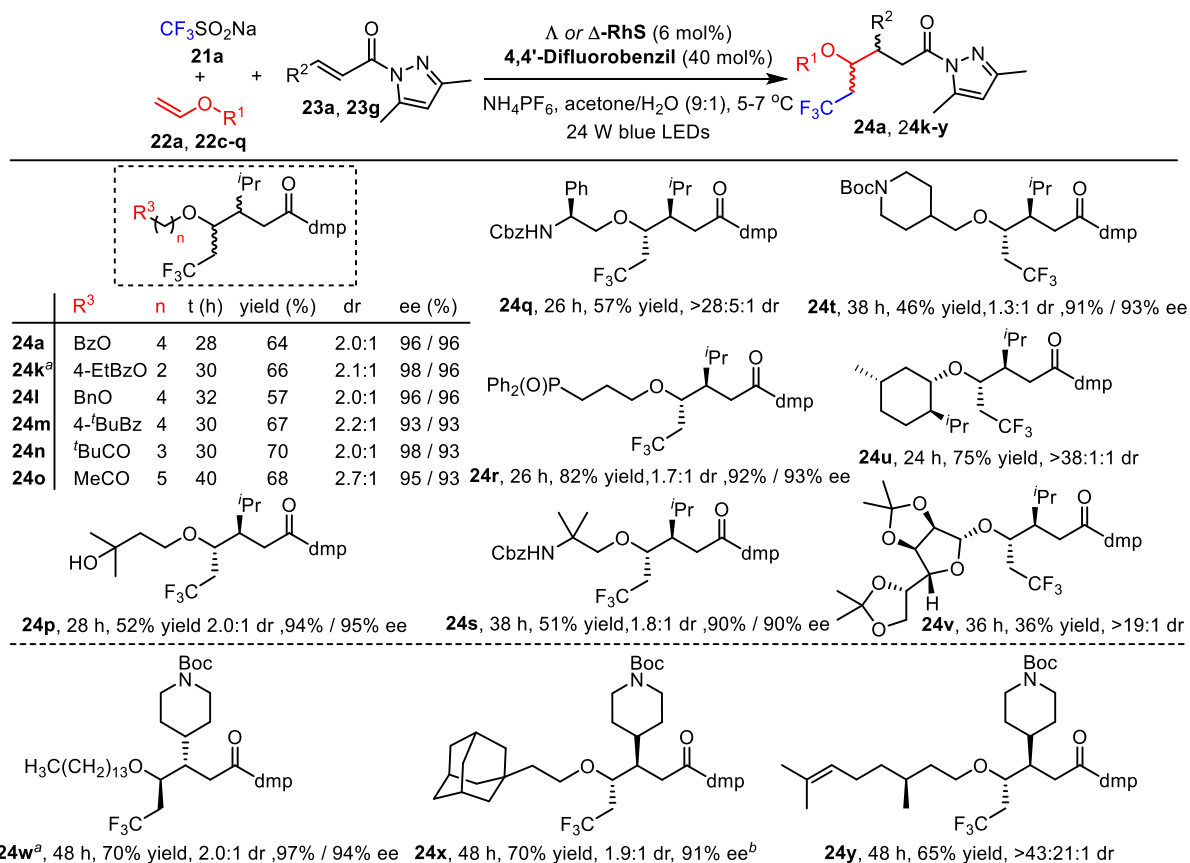


Figure 51. Substrate scope with respect to vinyl ethers. ^a Δ -**RhS** (6 mol%) was employed. ^bEe of major diastereomer was available. dmp= 3,5-dimethylpyrazole. The absolute and relative configuration of compound **24k** was determined as described in the Experimental Part and all other compounds were assigned accordingly.

Furthermore, a wide range of vinyl ethers were investigated under our developed photoredox conditions, thus providing the dual C–C bond formation adducts in yields of 36–82%, with 1.3:1–2.7:1 dr, and 90–98% ee, and with excellent diastereoselectivities of >28:5:1–>38:1:1 for chiral vinyl ethers (**Figure 51**). Good tolerance for various functional groups including ester, ketone, hydroxyl, amide and phosphine oxide (**24a**, **24k–t**) was observed. In particular, a set of natural compound derivatives (**24q**, **24u–v**, **24y**) were compatible with this protocol, thereby implying the versatility of our method even in the context of more complex molecules. Notably, the product **24q**, **24u–v** and **24y** with natural chirality, which were produced in high diastereoselectivities under asymmetric catalysis conditions,

could be further purified by regular column chromatography to obtained >50:1 dr, and all other chiral fluorinated products could be obtained with >10:1 or even >20:1 dr for the main stereoisomer by simple chromatography.

Finally, to further demonstrate the utility of this methodology, a gram-scale reaction was performed along with the recovery of both the organic photoredox mediator and the Lewis acid catalyst (Figure 52). Compared to the original smaller scale catalytical reaction, each diastereomer of **24w** was isolated in somehow decreased yield (37% for major, 15% for minor, 1.0 g in total), but still identical enantioselectivities (97% and 94% ee, respectively). The 4,4'-difluorobenzil was isolated by column chromatography in 84% yield. Importantly, the chiral Lewis acid catalyst Δ -**RhS** was recovered by assistance of a chiral auxiliary **25** to afford Δ -(*R*)-aux-**RhS** (70% yield, > 99:1 dr) after filtration and washing according to our previously developed method^{12a}.

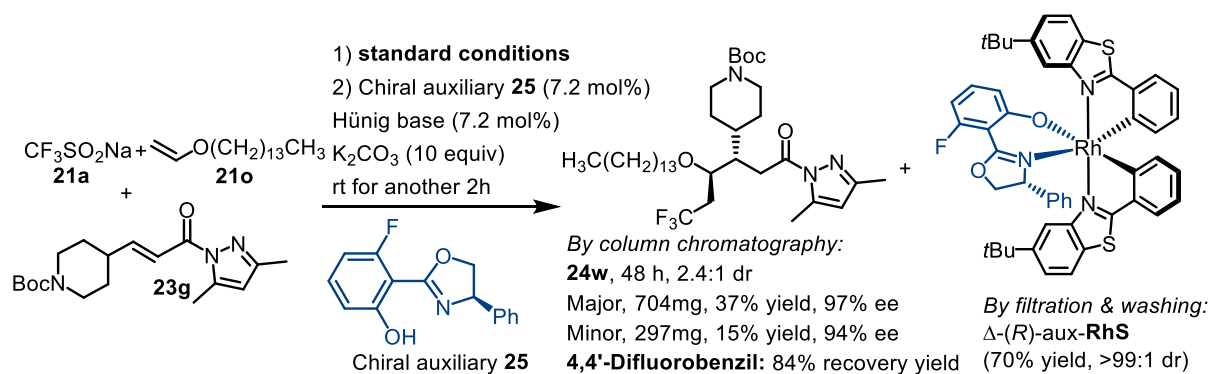


Figure 52. Gram-scale reaction and catalysts recovery.

3.3.4 Mechanistic Study

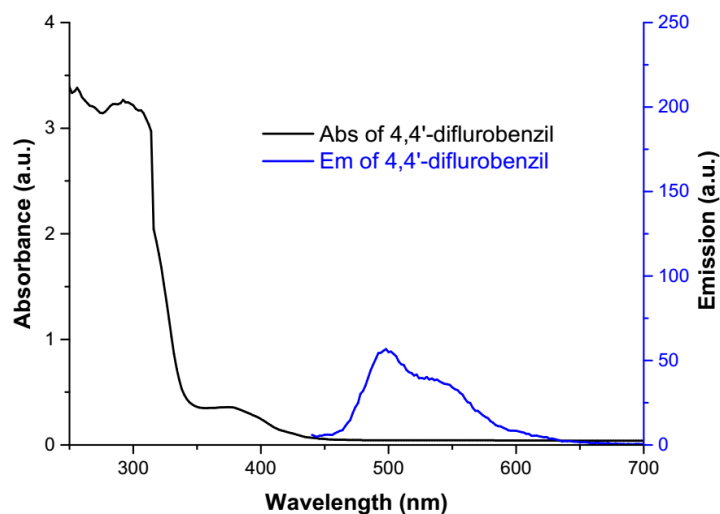


Figure 53. UV-Vis absorption (black) and luminescence emission (blue) spectra of 4,4'-difluorobenzil were collected in acetone/H₂O (9:1, v/v, 4 mM), $\lambda_{\text{ex}} = 400$ nm.

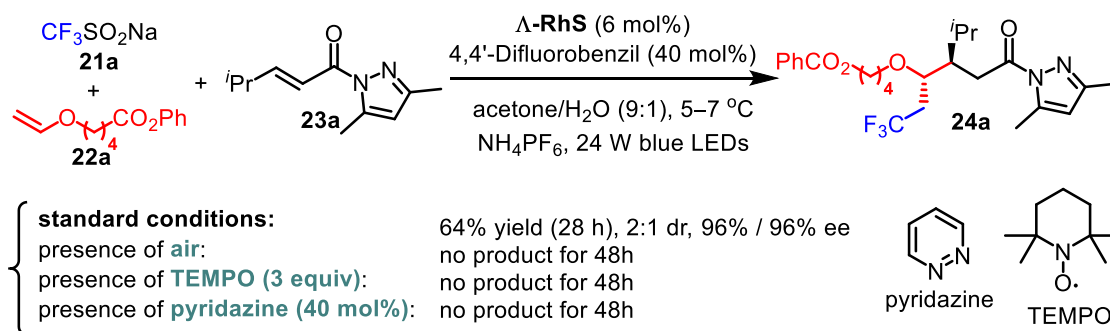


Figure 54. Probing radical pathway.

Several experiments support the proposed function of 4,4'-difluorobenzil as a visible-light-activated photoredox mediator. A UV/Vis absorption and emission spectrum of 4,4'-difluorobenzil is shown in **Figure 53** and reveals that this chromophore indeed absorbs visible light with a long wavelength absorption maximum at $\lambda_{\text{max}} = 380$ nm and a shoulder reaching into the blue region. Conducting the reaction in the presence of air, the radical inhibitor TEMPO (3 equiv) or the triplet quencher pyridazine (40 mol%) affords no desired C–C formation product **4a** which provides indicator for a radical pathway (**Figure 54**).

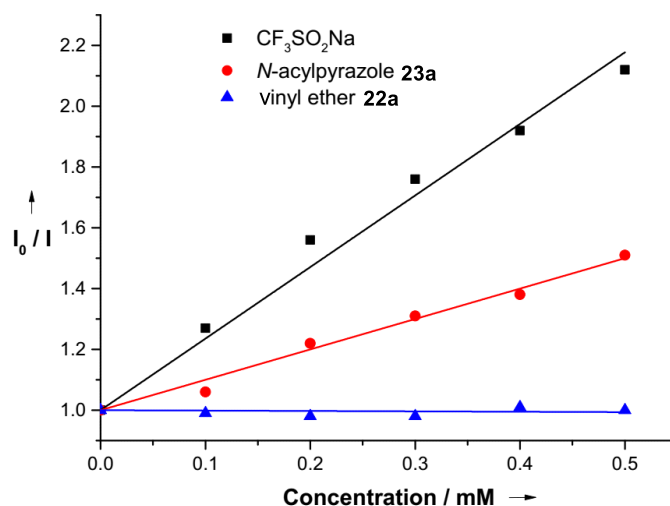


Figure 55. I_0 and I are respective luminescence intensities in the absence and presence of the indicated concentrations of the corresponding quenchers, 4,4'-difluorobenzil was dissolved in acetone/H₂O (9:1, v/v, 4 mM), $\lambda_{\text{ex}} = 375$ nm.

Although 1,2-dicarbonyl compounds typically engage in hydrogen atom transfer (HAT) upon photoactivation, several aspects support a visible-light-induced SET over HAT. Firstly, a Stern-Volmer plot revealed that Langlois reagent ($E_{\text{ox}} = + 1.05$ V vs SCE in MeCN)²⁰ efficiently quenches the photoexcited 4,4'-difluorobenzil ($E_{1/2}^{\text{PC}^*/\text{PC}^{*-}} = > 1.22$ V vs SCE in MeCN) in a concentration dependent manner, which is indicative for SET quenching and cannot be explained by HAT (**Figure 53b**). In contrast, vinyl ether **22a** was not capable of quenching the excited state of 4,4'-difluorobenzil, whereas the quenching with the pyrazole substrate **23a** was less efficient and can be explained with energy transfer.

Secondly, the direct reaction of Langlois reagent **21a** with 4,4'-difluorobenzil in the presence of visible light afforded the compound **26** as the main product (42% yield) which supports a mechanism that photoexcited 4,4'-difluorobenzil induces a single electron transfer from Langlois reagent, followed by a radical-radical coupling (**Figure 56**). And the standard reaction provided a side product **27** in a yield of about 9%, which is also proposed to be formed by radical-radical recombination between the intermediate **I** and **II**.

A final support of 4,4'-difluorobenzil as a SET over HAT mediator came from a comparison with anthraquinone and 9-fluorenone, which are well-established HAT inducers upon photoactivation but were not capable of enabling the here reported reaction (Table 1, entries 8 and 9). Taken together, all here discussed experiments provide strong evidence for the role of 4,4'-difluorobenzil as a photoredox

mediator.

However, the extinction coefficient of the substrate-coordinated rhodium complex ($\epsilon_{420} = 2338 \text{ M}^{-1}\text{cm}^{-1}$) is approximately hundred-fold higher compared to 4,4'-difluorobenzil ($\epsilon_{420} = 22.8 \text{ M}^{-1}\text{cm}^{-1}$) (see Experimental Part), so that the involvement of a mechanism in which the substrate-coordinated rhodium complex serves as a photosensitizer to first absorb the visible light and to then transfer the triplet energy to ground state 4,4'-difluorobenzil cannot be excluded.

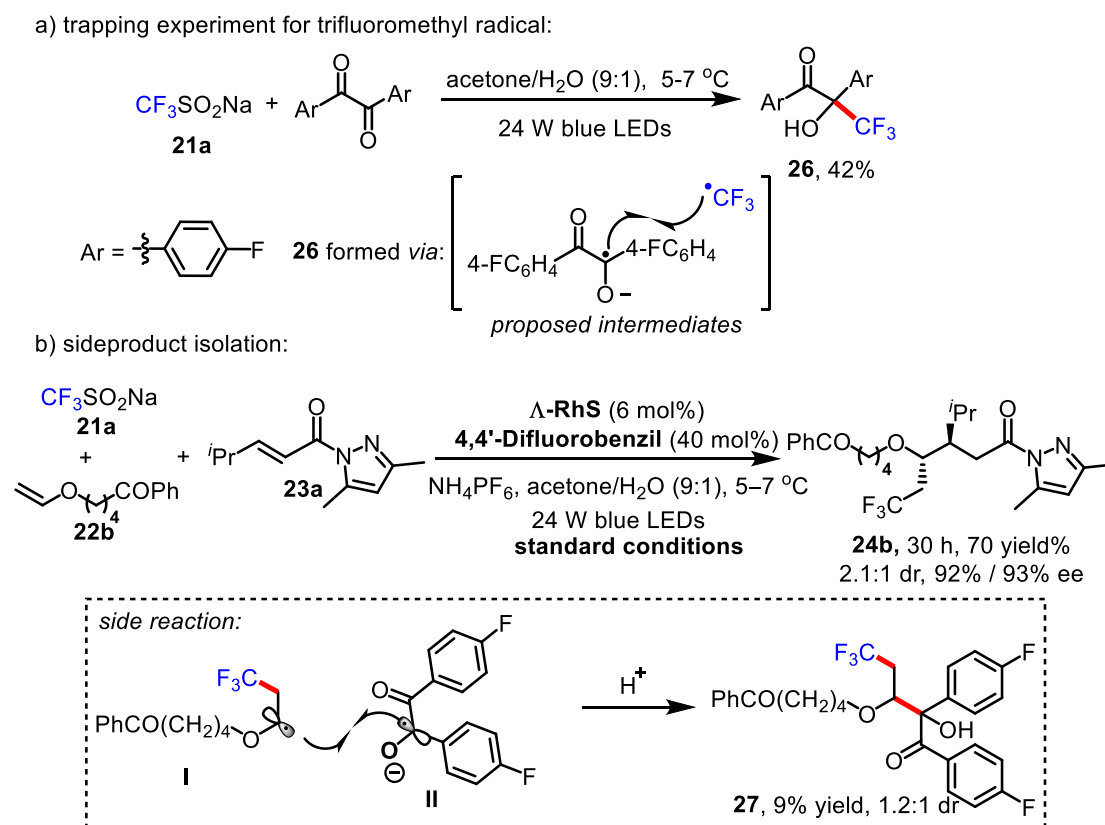


Figure 56. Radical trapping experiment.

The here described role of α -diketones acting as photoredox mediators is distinct from previous reports in which mono- and 1,2-dicarbonyl compounds were mainly employed for light-activated hydrogen atom transfer (HAT) or triplet energy transfer. For example, Chen et al. reported an approach for benzylic C–H mono- and difluorination catalyzed by 9-fluorenone and xanthone, respectively, in which photoexcited diarylketones play a crucial role to selectively abstract a benzylic hydrogen atom.¹⁹ Melchiorre et al. reported *p*-anisaldehyde as a triplet sensitizer to enable the intermolecular atom transfer radical addition (ATRA) of haloalkanes onto olefins.²¹ In other examples, phenyl glyoxylic acid and its corresponding ethyl ester were reported to permit efficient hydroacylation of

dialkyl azodicarboxylates by activating the involved aldehydes via photoinduced hydrogen atom transfer (HAT).²² Besides, benzil and other α -diketones have long been known as triplet sensitizers²³ for the isomerization of stilbenes²⁴ and the epoxidation of olefins²⁵. Just recently, Ooi reported an unusual photoredox ketone catalysis in which a thioxanthone catalyst acted as a photo-excited reductant and permitted C–H imidation and acyloxylation of arenes.²⁶

3.3.5 Conclusions

Herein a chiral-at-rhodium Lewis acid catalyzed asymmetric three-component fluoroalkylation reaction was introduced which proceeded under visible light activation with the simple organic photoredox mediator 4,4'-difluorobenzil. This process opens a new avenue to the catalytic asymmetric synthesis of trifluoromethyl and perfluoroalkyl-containing compounds from easily accessible starting materials. Moreover, the employed chiral Lewis acid catalyst and the simple organic photoredox mediator can be recovered by operationally simple work-up procedures.

References

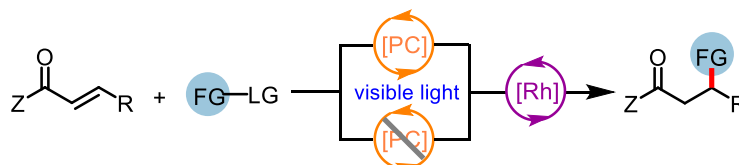
- 1 H. Huo, K. Harms, E. Meggers, *J. Am. Chem. Soc.* **2016**, *138*, 6936.
- 2 C. Wang, K. Harms, E. Meggers, *Angew. Chem. Int. Ed.* **2016**, *55*, 13495.
- 3 L. Li, X. Mu, W. Liu, Y. Wang, Z. Mi, C.-J. Li, *J. Am. Chem. Soc.* **2016**, *138*, 5809.
- 4 C. Bibaut-Renaud, D. Burget, J. P. Fouassier, C. G. Varelas, J. Thomatos, G. Tsagaropoulos, L. O. Ryrfors, O. J. Karlsson, *J. Polym. Sci., Part A: Polym. Chem.* **2002**, *40*, 3171.
- 5 a) B. Ganem, *Acc. Chem. Res.* **2009**, *42*, 463; b) G. van der Heijden, E. Ruijter, R. V. A. Orru, *Synlett* **2013**, *24*, 666.
- 6 a) M.-Y. Cao, X. Ren, Z. Lu, *Tetrahedron Lett.* **2015**, *56*, 3732; b) T. Koike, M. Akita, *Acc. Chem. Res.* **2016**, *49*, 1937; c) X. Pan, H. Xia, J. Wu, *Org. Chem. Front.* **2016**, *3*, 1163; d) T. Courant, G. Masson, *J. Org. Chem.* **2016**, *81*, 6945; e) S. Garbarino, D. Ravelli, S. Protti, A. Basso, *Angew. Chem. Int. Ed.* **2016**, *55*, 15476.
- 7 Y. Yasu, T. Koike, M. Akita, *Angew. Chem. Int. Ed.* **2012**, *51*, 9567.
- 8 M. Daniel, G. Dagousset, P. Diter, P.-A. Klein, B. Tuccio, A.-M. Goncalves, G. Masson, E. Magnier, *Angew. Chem. Int. Ed.* **2017**, *56*, 3997.
- 9 For a review on addition of CF₃ towards unsaturated moieties, see: E. Merino, C. Nevado, *Chem. Soc. Rev.* **2014**, *43*, 6598.
- 10 X.-L. Yu, J.-R. Chen, D.-Z. Chen, W.-J. Xiao, *Chem. Commun.* **2016**, *52*, 8275.
- 11 Selected examples on visible-light-induced multicomponent-based fluoroalkylations, see a) R.

- Tomita, Y. Yasu, T. Koike, M. Akita, *Angew. Chem. Int. Ed.* **2014**, *53*, 7144; b) A. Carboni, G. Dagousset, E. Magnier, G. Masson, *Org. Lett.* **2014**, *16*, 1240; c) G. Dagousset, A. Carboni, E. Magnier, G. Masson, *Org. Lett.* **2014**, *16*, 4340; d) A. Carboni, G. Dagousset, E. Magnier, G. Masson, *Synthesis* **2015**, *47*, 2439; e) L. Jarrige, A. Carboni, G. Dagousset, G. Levitre, E. Magnier, G. Masson, *Org. Lett.* **2016**, *18*, 2906; f) R. Tomita, T. Koike, M. Akita, *Chem. Commun.* **2017**, *53*, 4681; g) Y.-Y. Liu, X.-Y. Yu, J.-R. Chen, M.-M. Qiao, X. Qi, D.-Q. Shi, W.-J. Xiao, *Angew. Chem. Int. Ed.* **2017**, *56*, 9527; h) W. Kong, H. An, Q. Song, *Chem. Commun.* **2017**, *53*, 8968; i) X. Geng, F. Lin, X. Wang, N. Jiao, *Org. Lett.* **2017**, *19*, 4738.
- 12 a) P. Yu, J. S. Lin, L. Li, S. C. Zheng, Y. P. Xiong, L. J. Zhao, B. Tan, X. Y. Liu, *Angew. Chem. Int. Ed.* **2014**, *53*, 11890; b) T. Li, P. Yu, Y.-M. Du, J.-S. Lin, Y. Zhi, X.-Y. Liu, *J. Fluorine Chem.* **2017**, *203*, 210; c) L. Li, L. Ye, S.-F. Ni, Z.-L. Li, S. Chen, Y.-M. Du, X.-H. Li, L. Dang, X.-Y. Liu, *Org. Chem. Front.* **2017**, *4*, 2139.
- 13 a) F. Wang, D. Wang, X. Wan, L. Wu, P. Chen, G. Liu, *J. Am. Chem. Soc.* **2016**, *138*, 15547; b) L. Wu, F. Wang, X. Wan, D. Wang, P. Chen, G. Liu, *J. Am. Chem. Soc.* **2017**, *139*, 2904.
- 14 a) M. Tordeux, B. Langlois, C. Wakselman, *J. Org. Chem.* **1989**, *54*, 2452; b) B. R. Langlois, E. Laurent, N. Roidot, *Tetrahedron Lett.* **1991**, *32*, 7525.
- 15 L. Cui, Y. Matusaki, N. Tada, T. Miura, B. Uno, A. Itoh, *Adv. Synth. Catal.* **2013**, *355*, 2203.
- 16 a) J. Ma, X. Shen, K. Harms, E. Meggers, *Dalton Trans.* **2016**, *45*, 8320; b) Ma, X. Zhang, X. Huang, S. Luo, E. Meggers, *Nat. Protoc.* **2018**, *13*, 605.
- 17 Y. Nishigaichi, T. Orimi, A. Takuwa, *J. Organomet. Chem.* **2009**, *694*, 3837.
- 18 L. Cui, N. Tada, H. Okubo, T. Miura, A. Itoh, *Green Chem.* **2011**, *13*, 2347.
- 19 J.-B. Xia, C. Zhu, C. Chen, *J. Am. Chem. Soc.* **2013**, *135*, 17494.
- 20 L. Zhu, L.-S. Wang, B. Li, B. Fu, C.-P. Zhang, W. Li, *Chem. Commun.* **2016**, *52*, 6371.
- 21 E. Arceo, E. Montroni, P. Melchiorre, *Angew. Chem. Int. Ed.* **2014**, *53*, 12064.
- 22 a) G. N. Papadopoulos, D. Limnios, C. G. Kokotos, *Chem. -Eur. J.* **2014**, *20*, 13811-13814; b) G. N. Papadopoulos, C. G. Kokotos, *Chem. -Eur. J.* **2016**, *22*, 6964; c) G. N. Papadopoulos, C. G. Kokotos, *J. Org. Chem.* **2016**, *81*, 7023.
- 23 a) G. S. Hammond, J. Saltiel, A. A. Lamola, N. J. Turro, J. S. Bradshaw, D. O. Cowan, R. C. Counsell, V. Vogt, C. Dalton, *J. Am. Chem. Soc.* **1964**, *86*, 3197; b) S. Jockusch, H.-J. Timpe, W. Schnabel, N. Turro, *J. Phys. Chem. A* **1997**, *101*, 440.
- 24 a) Y. Tokunaga, K. Akasaka, K. Hisada, Y. Shimomura, S. Kakuchi, *Chem. Commun.* **2003**, 2250; b) M. R. Ams, C. S. Wilcox, *J. Am. Chem. Soc.* **2007**, *129*, 3966; c) V. Serreli, C.-F. Lee, E. R. Kay, D. A. Leigh, *Nature* **2007**, *445*, 523.
- 25 N. Shimizu, P. D. Bartlett, *J. Am. Chem. Soc.* **1976**, *98*, 4193.
- 26 C. B. Tripathi, T. Ohtani, M. T. Corbett, T. Ooi, *Chem. Sci.* **2017**, *8*, 5622.

3.4 Synthesis of β -Substituted γ -Aminobutyric Acid Derivatives through Enantioselective Photoredox Catalysis

3.4.1 Research Background and Reaction Design

a) proposal for PC-free asymmetric radical conjugate addition:



b) reports on HE as photoreductant:

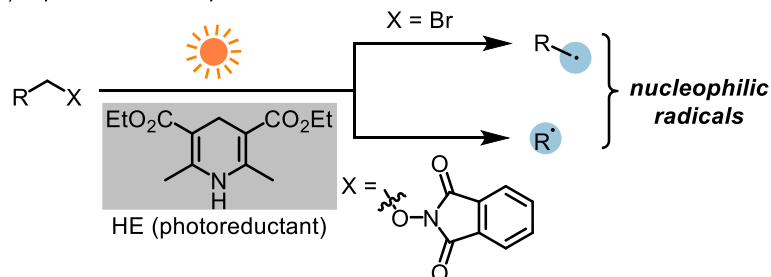


Figure 57. a) Proposal for photoredox-catalyst-free asymmetric radical conjugate addition; b) reports on using Hantzsch ester (HE) as visible-light-activated photoreductant. PC = photoredox catalyst. LG = leaving group. [Rh] = chiral-at-rhodium Lewis acids Λ/Δ -RhS.

As discussed in chapter 3.3, former group members H. Huo and C. Wang disclosed two elegant enantioselective radical conjugate addition reaction schemes (classified as Giese reaction), respectively, by using the chiral-at-rhodium Lewis acid in combination with a photoredox catalyst.¹ The author of this thesis further extended this dual catalysis system to the enantioselective three-component fluoroalkylation reaction.² Notably, the Kang group recently reported a single chiral-at-rhodium Lewis acid capable of catalyzing enantioselective photoredox reaction of *N*-aryl-tetrahydroisoquinolines with acceptor-substituted alkenes.³ However, the mechanism of this reaction is not completely clear and the proposed radical conjugate addition mechanism might compete with a radical-radical recombination pathway.⁴ Additionally, the limited substrate scope of using *N*-aryl-tetrahydroisoquinolines and inferior diastereoselectivities render this method of questionable utility.

Intrigued by these studies, the author of this thesis holds a great interest on the development of asymmetric radical conjugate addition reactions under photoredox-catalyst-free conditions for some practical applications (**Figure 57a**). An inspiration was sparked by the reports on using commercially

available Hantzsch ester (HE) as a visible-light-activated photoreductant (**Figure 57b**). For example, Cheng and Li reported that a bromo compound underwent single electron reduction which was promoted by visible-light-activated HE to afford an alkyl radical.⁵ Chen recently found that HE upon interaction with an *N*-alkoxyphthalimide molecular delivered an electron donor acceptor (EDA) complex with enhanced photophysical properties.⁶ This complex can get excited directly under the irradiation with visible light, followed by internal single electron exchange and fragmentation, affording a carbon-centered radical. Interestingly, the produced radical species in these two protocols are highly nucleophilic, and should be amendable to a Rh-catalyzed radical conjugate addition reaction scheme.

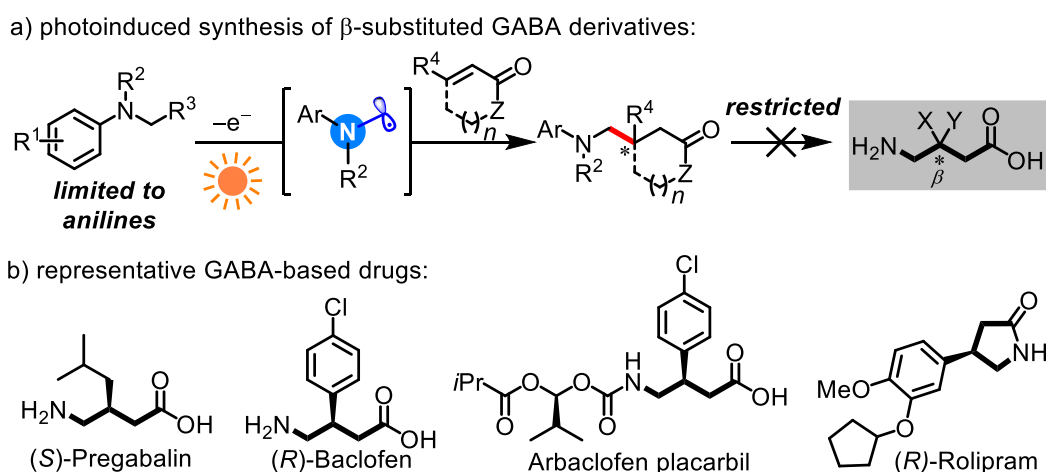


Figure 58. a) Approaches to non-racemic γ -amino carbonyl derivatives through photoinduced radical conjugate addition reaction; b) representative β -substituted GABA-based drugs.

Moreover, the photoinduced enantioselective radical conjugate addition reaction of nucleophilic α -aminoalkyl radicals to Michael acceptors has recently been recognized as an avenue to pharmaceutically valuable β -substituted γ -aminobutyric acids (GABAs) (**Figure 58a**). As discussed before, Yoon and coworkers reported that aromatic α -silylalkyl amines, upon undergoing single electron oxidation mediated by Ru-based photoredox catalyst, could deliver α -aminoalkyl radicals.⁷ These radicals subsequently engaged in the enantioselective conjugate addition to α,β -unsaturated alkenes catalyzed by Sc-based chiral Lewis acid. Melchiorre later reported a dual photoredox/organo catalysis system as an approach to β -substituted GABA analogs, but substrates were limited to aromatic tertiary amines and to cyclic enones.⁸ However, due to the employment of aniline as α -aminoalkyl radical precursors in these reports, no practical synthetic transformations have been

accomplished to access the GABA-based drugs, such as (*R*)-baclofen⁹, (*S*)-pregabalin¹⁰, arbaclofen placarbil¹¹, and (*R*)-rolipram¹² (**Figure 58b**). Thus, despite the noteworthy progress, the currently narrow substrate scope and limited follow-up functional group interconversions render these methods of low utility.

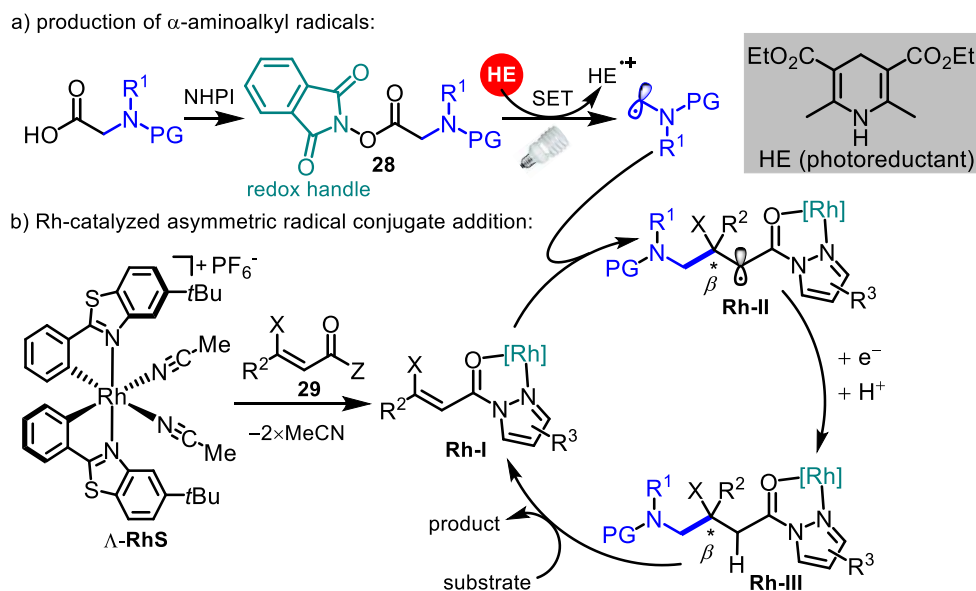
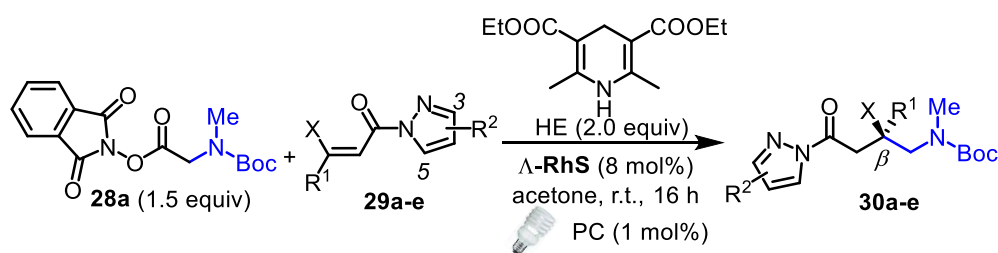


Figure 59. Reaction design for the synthesis of β -substituted γ -aminobutyric acid analogs. HE = Hantzsch ester. PG = protecting group. NHPI = *N*-hydroxyphthalimide.

Overall, inspired by all the aspects discussed above, the author of this thesis introduced a reaction proposal on the practical synthesis of β -substituted γ -aminobutyric acids (GABAs) through Rh-catalyzed enantioselective radical conjugate addition, in which the HE is supposed to act as photoreductant to promote the formation of α -aminoalkyl radicals. Accordingly, a glycine derivative *N*-(acyloxy)phthalimide (**28**)¹³ bearing an easily removable *N*-protected group and an *O*-phthalimide ester group as the redox handle, might provide easily accessible and very general precursors of a large variety of α -aminoalkyl radicals upon single electron reduction promoted by the photoreductant HE. The produced radicals would subsequently be interfaced with established chiral-at-rhodium Lewis acid catalyzed radical conjugate addition, α,β -unsaturated *N*-acylpyrazoles **29** (intermediate **Rh-I**) to provide intermediate **Rh-II**, which after reduction and protonation afford the Rh-bound products (**Rh-III**).¹⁴ Replacement of the product by another substrate leads to a new catalytic cycle. This visible-light-activated single Rh-catalyzed asymmetric radical conjugate addition could provide access to general enantiopure β -substituted γ -aminobutyric acid analogs in an efficient fashion.

3.4.2 Initial Experiments and Reaction Development

Table 5. Reaction development and control experiments^a

entry	compound 29			PC	yield (%) ^b	ee (%) ^c
	X	R ¹	R ²			
1	H	Me	3,5-di-Me (29a)	none	86 (30a)	94
2	H	Me	3,5-di-Me (29a)	<i>fac</i> -Ir(ppy) ₃	89 (30a)	91
3	H	Ph	3,5-di-Me (29b)	none	54 (30b)	90
4	H	Ph	3-Me (29c)	none	84 (30c)	95
5	Me	Ph	3-Me (29d)	none	0 (30d)	n.a.
6 ^d	F	Ph	3-Me (29e)	none	70 (30e)	93
7 ^e	H	Ph	3-Me (29c)	none	0 (30c)	n.a.
8 ^f	H	Ph	3-Me (29c)	none	14 (30c)	93

^aReaction conditions: **28a** (0.30 mmol), **29a-e** (0.20 mmol), Δ -RhS (0.016 mmol), and Hantzsch ester (HE) (0.40 mmol) in acetone (1.0 mL, 0.2 M) were stirred at r.t. for 16 hours under N₂ and irradiated with 23 W CFL unless otherwise noted. ^bIsolated yield. ^cDetermined by HPLC analysis on a chiral stationary phase. ^d Δ -RhS (0.016 mmol) and 2 mL of acetone were employed (0.1 M). ^eReaction conducted in the dark. ^fReaction assembled under air, then sealed the tube. r.t. = room temperature. n.a. = not applicable. PC = photoredox catalyst.

The experimental study started by investigating the reaction of *N*-(acyloxy)phthalimide **28a** with α,β -unsaturated *N*-acylpyrazole **29a** under photoredox conditions (Table 5). In the presence of chiral-at-Rh Lewis acid catalyst Δ -RhS and Hantzsch ester (HE) as the photoreductant under the irradiation with a household 23 W CFL, the C–C formation product **30a**, identified as a β -methyl γ -aminobutyric acid analog, was isolated in 86% yield and 94% ee (entry 1). For comparison, when a photoredox catalyst *fac*-Ir(ppy)₃ (1 mol%) was added, the product **30a** was obtained with even decreased enantioselectivity (91% ee) (entry 2). This observation indicates that the accelerated production of α -aminoalkyl radical with additional photocatalyst might bring with stronger uncatalyzed background.

Next, the tolerance of a β -phenyl (**29b**) instead of a β -methyl group (**29a**) in α,β -unsaturated *N*-acylpyrazoles was investigated, which showed a more limited scope in our previous reports,^{1,2} but would lead to an important class of potentially bioactive β -aryl γ -aminobutyric acids. As a result, using *N*-acylpyrazole **29b** as substrate, the C–C formation product **30b** was afforded with inferior yield (54%) and decreased enantioselectivity (90% ee) (entry 3). But when we modified the substituents on the pyrazole moiety, we found that employing a 3-Me-substituted pyrazolyl (**29c**) instead of the 3,5-bis-substituted pyrazolyl (**29b**) not only improved the yield (84%) but also afforded an excellent enantioselectivity (95% ee) (entry 4).¹⁵ A β -disubstituted β -methyl- β -phenyl alkene (**29d**) could not deliver any C–C formation product under these optimized conditions (entry 5). However, a disubstituted β -fluorine- β -phenyl α,β -unsaturated *N*-acylpyrazole **29e** delivered the target product **30e** in 70% yield and 93% ee accompanied with the formation of a fluorinated quaternary stereocenter, which is a formidable challenge in the field of asymmetric photocatalysis²⁴ (entry 5). Control experiments verified that visible light (entry 7) is essential for this transformation. Under air atmospheric conditions, **30c** was produced but in a strongly diminished yield (entry 8).

Even though β -methyl- β -phenyl alkene (**29d**) couldn't afford any C–C formation product, the author of this thesis still would like to investigate the tolerance of some other β,β -disubstituted *N*-acylpyrazoles to forge all-carbon quaternary stereocenters. Unfortunately, with elaborated efforts, it proved to be not applicable to γ -aminobutyric acid analogs bearing β -all-carbon quaternary stereocenters under the developed reaction conditions. Even a β -chlorine- β -phenyl substituted α,β -unsaturated *N*-acylpyrazole was not tolerated. The tested β,β -disubstituted *N*-acylpyrazoles are listed below:

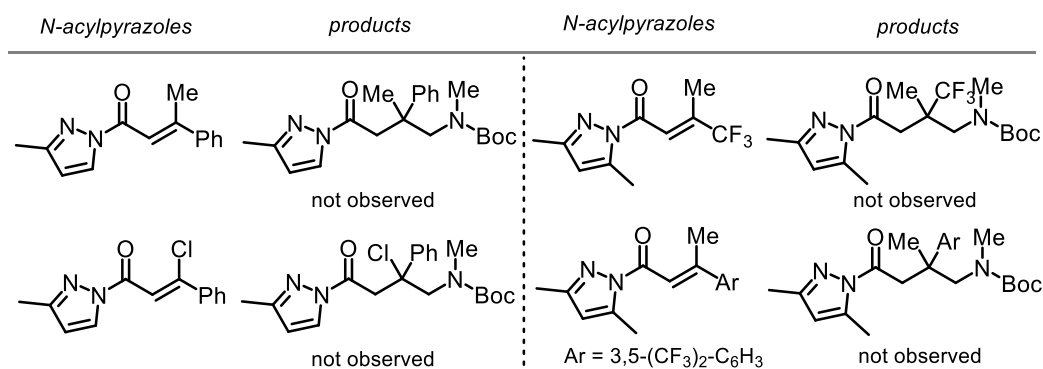


Figure 60. Limitations of the developed methodology.

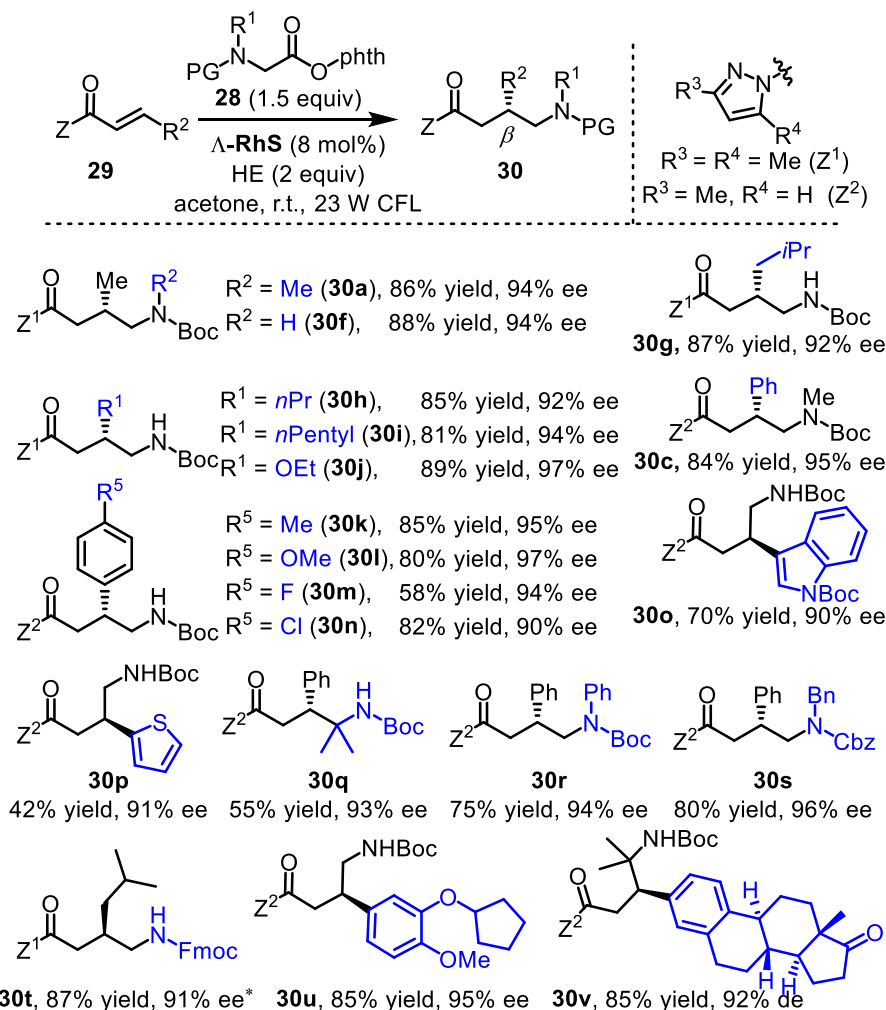
3.4.3 Scope of γ -Aminobutyric Acid Analogs

Figure 61. Scope with respect to synthesis of β -alkyl and β -aryl substituted γ -aminobutyric acid analogs. * Δ -RhS was employed.

Encouraged by the success on enantioselective synthesis of the representative β -alkyl (**30a**), β -aryl (**30c**) and β -fluorine- β -aryl (**30e**) γ -aminobutyric acid analogs, the author of this thesis next investigated the generality of this approach. The scope with respect to the synthesis of β -alkyl and β -aryl substituted γ -aminobutyric acid analogs is outlined in **Figure 61**. The α,β -unsaturated N -acylpyrazoles display good tolerance with respect to substituents at the β -position, including various alkyl groups (**30g-i**), an ethoxy group (**30j**), electron-rich phenyl moieties (**30k-l**, **30u**), as well as electron-deficient substituents (**30m-n**). Heteroaromatic rings, like an indolyl (**30o**) and a thienyl moiety (**30p**) lead to the target products with satisfactory results. Furthermore, N -(acyloxy)phthalimides accompanied with different N -protected amino moieties could also enable

this transformation smoothly by affording products **30q-t** with 55-87% yields and 91-96% ee. It is worth noting that an estrone derived *N*-acylpyrazole (**28r**) provided the corresponding γ -aminobutyric acid analogy (**30v**) with high yield (85%) and excellent diastereoselectivity (92% de). This observation demonstrates that our protocol is applicable for the incorporation of bioactive motifs to the side chain of γ -aminobutyric acid.

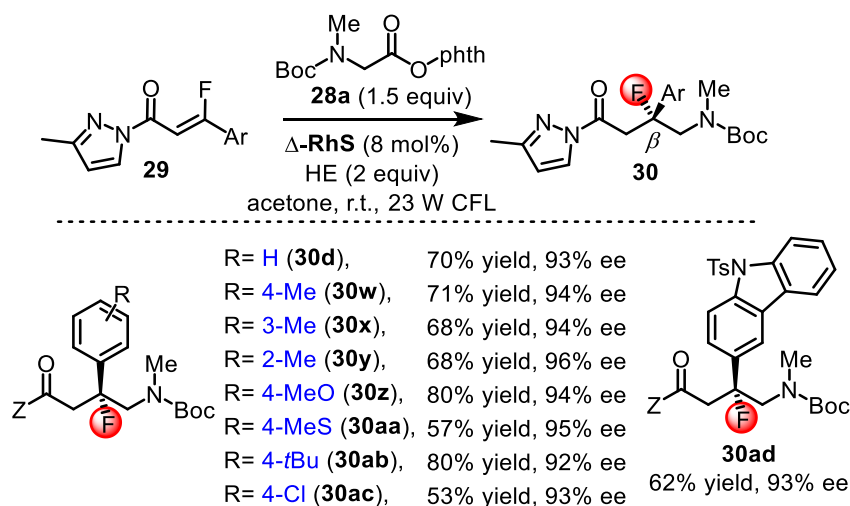


Figure 62. Substrate scope with respect to synthesis of β -fluorine- β -aryl substituted γ -aminobutyric acid analogs.

The scope with respect to synthesis of β -fluorine- β -aryl γ -aminobutyric acid analogs is outlined in **Figure 62**. Accordingly, substituents at different positions of the phenyl moiety show little influence on the reaction outcome by providing **30w-y** in good yields (68-71%) and excellent enantioselectivities (94-96% ee). Electron-donating groups (**30z-30aa**), a bulky *tert*-butyl group (**30ab**), and a chlorine (**30ac**) were also accommodated. Additionally, a carbazole moiety was tolerated well by affording the C–C formation product **30ad** in 62% yield and 93% ee.

3.4.4 Synthetic Applications

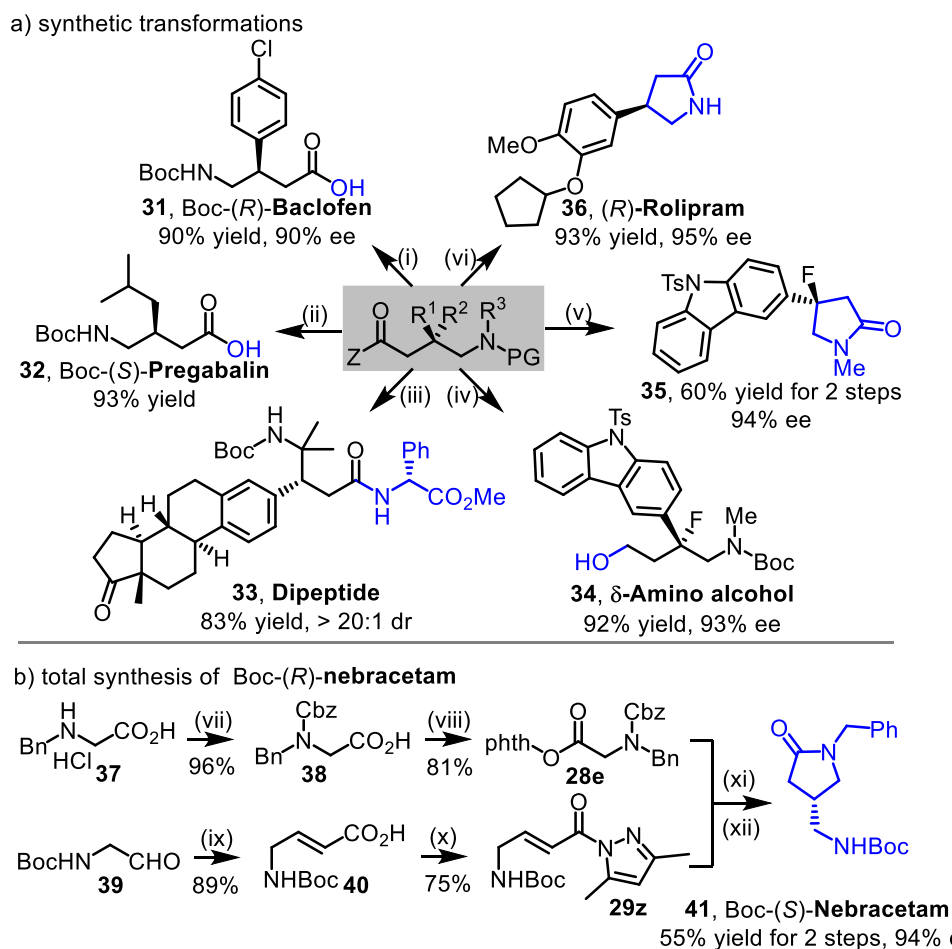


Figure 63. Synthetic applications. Reaction conditions: (i) LiOH, THF/H₂O; (ii) LiOH, THF/H₂O; (iii) *D*-Phenylglycine methyl ester hydrochloride, Et₃N, HOBT; (iv) NaBH₄; (v) Pd/C, H₂ (1 atm); (vi) LiCl, MeOH then TFA followed by Et₃N; (vii) Diethylphosphonoacetic acid, LHMDs; (viii) 3,5-Dimethylpyrazole, T₃P, Et₃N; (ix) *N*-Benzyloxycarbonyloxy succinimide; K₂CO₃; (x) NHPI, DCC, DMAP; (xi) Δ -RhS, HE, 23 W CFL; (xii) Pd/C, H₂ (1 atm). More details are available in Experimental Part.

With a range of β -substituted γ -aminobutyric acid analogs in hand, the synthetic application of this protocol was evaluated (**Figure 63**, see details in the Experimental Part). The pyrazole moiety can easily be transformed into a broad range of functionalities under mild conditions. For example, treating **30n** with LiOH in THF/H₂O at room temperature, after cleaving the pyrazole group, provided the corresponding *N*-protected γ -aminobutyric acid Boc-(*R*)-baclofen (**31**) in excellent yield (90%) and unchanged enantioselectivity (90% ee). Boc-(*S*)-pregabalin (**32**) could be obtained efficiently by the same method. Furthermore, compound **30v** was converted to the dipeptide **33** in 83% yield and as a single diastereomer by reacting with *D*-phenylglycine methyl ester. A δ -amino alcohol (**34**) and a

γ -lactam (**35**) bearing fluorinated quaternary stereocenters were obtained smoothly under mild transformation conditions. Additionally, the γ -aminobutyric acid analog **30u** was converted into the anti-inflammatory drug (*R*)-rolipram (**36**) in 93% yield and without any loss of enantioselectivity (95% ee). To further demonstrate the practicability of our protocol, the synthetic route to Boc-(*S*)-nebracetam which is an enantiopure form of a *N*-protected nootropic drug¹⁶, is shown in **Figure 63b**. Accordingly, the C–C coupling partners **28e** and **29z** were synthesized over two steps from commercially available materials **37** and **39**, respectively, and were then subjected to the developed asymmetric radical conjugate addition reaction, followed by a cyclization, thereby delivering the Boc-(*S*)-nebracetam (**41**) with 94% ee and 55% yield over the two steps. Overall, the herein outlined synthetic applications clearly demonstrate that our approach is very versatile for the synthesis of structurally diverse enantiopure β -substituted γ -aminobutyric acids and their derivatives.

3.4.5 Conclusions

In conclusion, a highly practical and versatile synthetic access to the pharmaceutically important class of β -substituted GABA analogs was introduced. The methodology is based on catalytic asymmetric photoredox catalysis using a simple glycine derivative as the precursor for α -aminoalkyl radicals which are then engaged in highly enantioselective rhodium-catalyzed Giese-type radical conjugate additions. The commercially available HE acts as the visible-light-activated reductant to promote single electron transfer events. Furthermore, for the first time enantioselective radical conjugate additions to β -fluorine- β -aryl substituted α,β -unsaturated enones are achieved which provides a potentially very valuable access to GABA analogs with β -fluorinated quaternary stereocenters.

References

- 1 a) H. Huo, K. Harms, E. Meggers, *J. Am. Chem. Soc.* **2016**, *138*, 6936; b) C. Wang, K. Harms, E. Meggers, *Angew. Chem. Int. Ed.* **2016**, *55*, 13495.
- 2 J. Ma, X. Xie, E. Meggers, *Chem. -Eur. J.* **2018**, *24*, 259.
- 3 S.-X. Lin, G.-J. Sun, Q. Kang, *Chem. Commun.* **2017**, *53*, 7665.
- 4 Z. Zhou, Y. Li, B. Han, L. Gong, E. Meggers, *Chem. Sci.* **2017**, *8*, 5757.
- 5 W. Chen, H. Tao, W. Huang, G. Wang, S. Li, X. Cheng, G. Li, *Chem. -Eur. J.* **2016**, *22*, 9546.

- 6 J. Zhang, Y. Li, F. Zhang, C. Hu, Y. Chen, *Angew. Chem. Int. Ed.* **2015**, *55*, 1872.
- 7 L. Ruiz Espelt, I. S. McPherson, E. M. Wiensch, T. P. Yoon, *J. Am. Chem. Soc.* **2015**, *137*, 2452.
- 8 a) J. J. Murphy, D. Bastida, S. Paria, M. Fagnoni, P. Melchiorre, *Nature* **2016**, *532*, 218. For the report with only two examples with merely 71% and 75% ee by the same group, see: b) M. Silvi, C. Verrier, Y. P. Rey, L. Buzzetti, P. Melchiorre, *Nat. Chem.* **2017**, *9*, 868.
- 9 N. G. Bowery, D. R. Hill, A. L. Hudson, A. Doble, D. N. Middlemiss, J. Shaw, M. Turnbull, *Nature* **1980**, *283*, 92.
- 10 R. B. Silverman, *Angew. Chem. Int. Ed.* **2008**, *47*, 3500.
- 11 F. Xu, G. Peng, T. Phan, U. Dilip, J. L. Chen, T. Chernov-Rogan, X. Zhang, K. Grindstaff, T. Annamalai, K. Koller, M. A. Gallop, D. J. Wustrow, *Bioorg. Med. Chem. Lett.* **2011**, *21*, 6582.
- 12 S. Takeo, H. Hayashi, M. Tadokoro, K. Takagi, K. Miyake, N. Takagi, S. Oshikawa, *Bio. Pharm. Bull.* **1997**, *20*, 36.
- 13 For selected recent examples on using *N*-(acyloxy)phthalimides as carbon-centered radical precursors under photoredox conditions, see: a) Y. Slutskyy, L. E. Overman, *Org. Lett.* **2016**, *18*, 2564; b) Y. Jin, H. Yang, H. Fu, *Org. Lett.* **2016**, *18*, 6400; c) A. Fawcett, J. Pradeilles, Y. Wang, T. Mutsuga, E. L. Myers, V. K. Aggarwal, *Science* **2017**, *357*, 283; d) L. Candish, M. Teders, F. Glorius, *J. Am. Chem. Soc.* **2017**, *139*, 7440; e) Y. Zhao, J.-R. Chen, W.-J. Xiao, *Org. Lett.* **2018**, *20*, 224; f) A. Tlahuext-Aca, L. Candish, R. A. Garza-Sanchez, F. Glorius, *ACS Catal.* **2018**, *8*, 1715. See also the pioneering studies: g) K. Okada, K. Okamoto, M. Oda, *J. Am. Chem. Soc.* **1988**, *110*, 8736; h) K. Okada, K. Okamoto, N. Morita, K. Okubo, M. Oda, *J. Am. Chem. Soc.* **1991**, *113*, 9401. See the examples on using *N*-(oxaly)phthalimides, see: i) G. L. Lackner, K. W. Quasdorf, L. E. Overman, *J. Am. Chem. Soc.* **2013**, *135*, 15342; j) G. L. Lackner, K. W. Quasdorf, G. Pratsch, L. E. Overman, *J. Org. Chem.* **2015**, *80*, 6012. For a review, see: k) J. Xuan, Z. G. Zhang, W. J. Xiao, *Angew. Chem. Int. Ed.* **2015**, *54*, 15632; *Angew. Chem.* **2015**, *127*, 15854.
- 14 a) J. Ma, X. Shen, K. Harms, E. Meggers, *Dalton Trans.* **2016**, *45*, 8320; b) J. Ma, X. Zhang, X. Huang, S. Luo, E. Meggers, *Nat. Protoc.* **2018**, *13*, 605. For a review, see: c) L. Zhang, E. Meggers, *Acc. Chem. Res.* **2017**, *50*, 320.
- 15 X. Huang, X. Li, X. Xie, K. Harms, R. Riedel, E. Meggers, *Nat. Commun.* **2017**, *8*, 2245.
- 16 S. Shorvon, *The Lancet* **2001**, *358*, 1885.

3.5 Asymmetric β -C–H Functionalization of Acceptor-Substituted Ketones through Single Rh-based Photoredox Catalysis

3.5.1 Research Background and Reaction Design

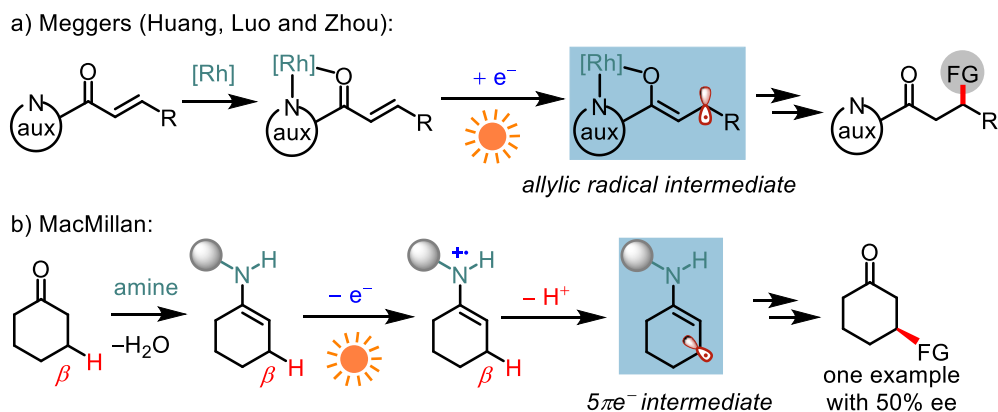


Figure 64. a) Production of rhodium stabilized allylic radical intermediate under photoredox conditions as accomplished by the group members Huang, Luo and Zhou; b) MacMillan's report on the β -C(sp³)-H functionalization through a photogenerated $5\pi e^-$ intermediate.

In 2017, the group members X. Huang and S. Luo introduced a unique reaction design to enable the enantioselective β -alkylation of enones under visible-light-activated photoredox conditions.¹ In this reaction scheme, the enone substrate, upon coordination to chiral-at-rhodium Lewis acid, constituted a decreased reductive potential, therefore undergoing a mild single electron reduction (**Figure 64a**). This process provided the key intermediate, Rh-stabilized allylic radical species, which experienced the follow up radical trapping with an allyl sulfone and proton transfer to deliver the non-racemic C–C formation product. Concurrently, Z. Zhou in his Master thesis at Xiamen University disclosed a highly enantioselective β -amination protocol through proton-coupled electron transfer (PCET) mechanism under asymmetric photoredox conditions, in which the Rh-stabilized allylic radical species was again proposed as the key reaction intermediate to undergo a stereocontrolled radical-radical recombination.² The photogenerated Rh-stabilized allylic radical species in these two reports were then recognized to be both structurally and reactively related to the $5\pi e^-$ intermediate in MacMillan's work as discussed in chapter 1.2. As shown in **Figure 64b**, MacMillan and coworkers developed a photoredox-catalyzed β -C(sp³)-H functionalization protocol in which the saturated carbonyl compound (e.g. cyclohexanone), upon condensation with amine catalyst, underwent single

electron oxidation to afford an enaminy radical cation. The following deprotonation of the generated radical cation at the β -position of initial carbonyl substrate gave rise to the key $5\pi e^-$ intermediate. With the similar reactivity as discovered by X. Huang, S. Luo and Z. Zhou, this $5\pi e^-$ intermediate could be involved into interesting reactions including radical trapping with electron-deficient alkenes³ and radical recombination with second radical species⁴. However, most of these transformations have been accomplished in the racemic form. Only one asymmetric example in β -arylation reactions was accessed by using a chiral amine catalyst, affording the corresponding C–C formation product in an unsatisfactory enantioselectivity of 50% ee.

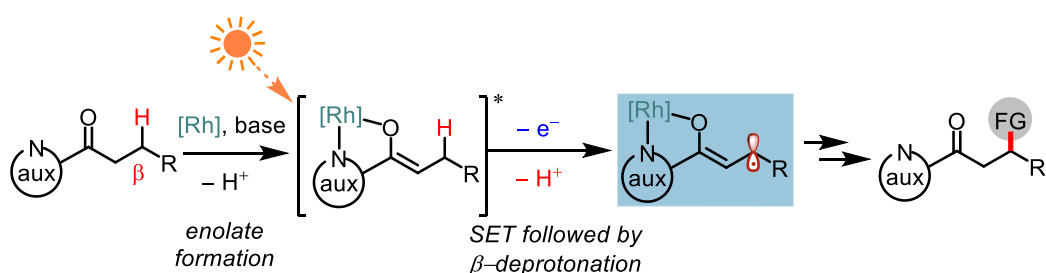


Figure 65. Proposal for chiral-at-rhodium Lewis acid catalyzed enantioselective β -C(sp³)-H functionalization under photoredox conditions.

Intrigued by all this precedence, the author of this thesis introduced a new proposal on the enantioselective β -C(sp³)-H functionalization of acceptor-substituted ketones using the chiral-at-rhodium Lewis acid catalyst. As proposed in **Figure 65**, an acceptor-substituted ketone would coordinate to the Rh-based Lewis acid in a bidentate fashion, in the presence of base, to deliver a Rh-enolate intermediate. This chemistry has been well established by the efforts of the Meggers lab and several other groups.⁵ The obtained neutral Rh-enolate intermediate would then get excited under visible light irradiation, thereby constituting a strong photoexcited reducing agent. By interacting with a suitable electron acceptor, this photoexcited Rh-enolate intermediate would donate a single electron to the acceptor, followed by a deprotonation at the β -position of the initial ketone substrate, to provide the forementioned Rh-stabilized allylic radical species, a rhodium enolate radical anion. This key intermediate would be subsequently involved in a stereocontrolled bond formation reaction. Overall, the herein proposed chiral-at-rhodium Lewis acid catalyzed enantioselective β -C(sp³)-H functionalization under photoredox conditions might provide a new avenue to access non-racemic molecules in a sustainable fashion.

3.5.2 Initial Experiments and Reaction Development

Inspired by using ketones as single electron acceptor in photochemical reactions,⁶ the experimental investigation started with the reaction of 2-acyl imidazole **42a** with a set of different carbonyl compounds **43a-f** in the presence of the chiral-at-rhodium catalyst Δ -**RhS1**⁷ (4 mol%) and DABCO (20 mol%) under the irradiation with blue LEDs (**Table 6**). Surprisingly, the course of the reaction strongly depended on the structure of the carbonyl compounds. Whereas no product was observed with benzophenone (**43a**) (entry 1), fluorenone (**43b**) provided the homocoupling product **44** in 40% yield (entry 2). Using the 1,2-diketone benzil (**43c**), the homocoupling product **44** was even formed in a yield of 73% and with excellent diastereoselectivity (>20:1 dr) and enantioselectivity (>99% ee) (entry 3). This asymmetric β -C(sp³)-H functionalization was encouraging, however, homocouplings are typically of more limited utility and the author of this thesis thus seeking to establish a more versatile heterocoupling. Revealingly, the α -ketoester **43d** in the presence of Δ -**RhS1**, gave a complete switch in the reaction outcome. No homocoupling product **44** was detected but instead the heterocoupling product **45a** formed in high yield (95%) with excellent enantioselectivity (98% ee) and moderate diastereoselectivity of 5.5:1 (entry 4). Exchanging the methyl ester (**43d**) with a more bulky *tert*-butyl (**44e**) or cyclohexyl (**44f**) ester afforded slightly improved diastereoselectivities of 5.9:1 (product **45b**) and 6.4:1 (product **45c**), respectively (entries 5 and 6). We next modified the rhodium catalyst and found that introducing a phenyl group into the cyclometalating ligand, providing the catalyst Δ -**RhS2**,⁸ not only improved the diastereoselectivity to 10.0:1 but afforded also a perfect enantioselectivity (>99% ee) at high yield (98%) (entry 7). It is worth noting that a related iridium complex (Δ -**IrS**), which is known to enable photoactivated enolate photoredox chemistry,⁹ failed to promote this catalytic, asymmetric β -functionalization (entry 8). Control experiments verified that visible light and oxygen-free conditions are essential for this transformation (entry 9).

Table 6. Reaction development and control experiments^a

Reaction scheme: **42a** reacts with **43a-f** (R¹, R²) in the presence of a chiral catalyst (4 mol %) and DABCO (20 mol %) in acetone at room temperature for 16 h under blue LEDs to yield **44** (Homo-coupling) and **45a-c** (Cross-coupling).

Structures of Z groups: **43a** (R³ = Ph), **43b** (R³ = 1-naphthyl), **43c-f** (R³ = Ph, OMe, OtBu, OCy).

Structure of the chiral catalyst: Δ -**IrS** (M = Ir, R⁴ = H), Δ -**RhS1** (M = Rh, R⁴ = H), Δ -**RhS2** (M = Rh, R⁴ = Ph).

entry	catalyst	43a-f	NMR yield (%) ^b		dr ^c	ee (%) ^d
			44	45		
1	Δ - RhS1	43a	0	0	n.a.	n.a.
2	Δ - RhS1	43b	40	0	n.d.	n.d.
3	Δ - RhS1	43c	73	0	>20:1	>99
4	Δ - RhS1	43d	0	95 (45a)	5.5:1	98
5	Δ - RhS1	43e	0	95 (45b)	5.9:1	98
6	Δ - RhS1	43f	0	98 (45c)	6.4:1	98
7	Δ - RhS2	43f	0	98 (45c)	10.0:1	>99
8	Δ - IrS	43f	0	0	n.a.	n.a.
9 ^e	Δ - RhS2	43f	0	0	n.a.	n.a.

^aReaction conditions: **42a** (0.1 mmol), **43a-f** (0.3 mmol), chiral Lewis acid catalyst (0.004 mmol), and DABCO (0.02 mmol) in acetone (1 mL) stirred at r.t. for 16 h under N₂ and irradiated with blue LEDs (24 W) unless otherwise noted. ^bDetermined by ¹H NMR of the crude products. ^cDetermined by ¹H NMR analysis of the crude main product. ^dDetermined by HPLC analysis of the crude main product on a chiral stationary phase; ee of major diastereomer is shown. ^eReaction conducted in the dark or under air. r.t. = room temperature. n.d. = not determined. n.a. = not applicable.

3.5.3 Substrate Scope

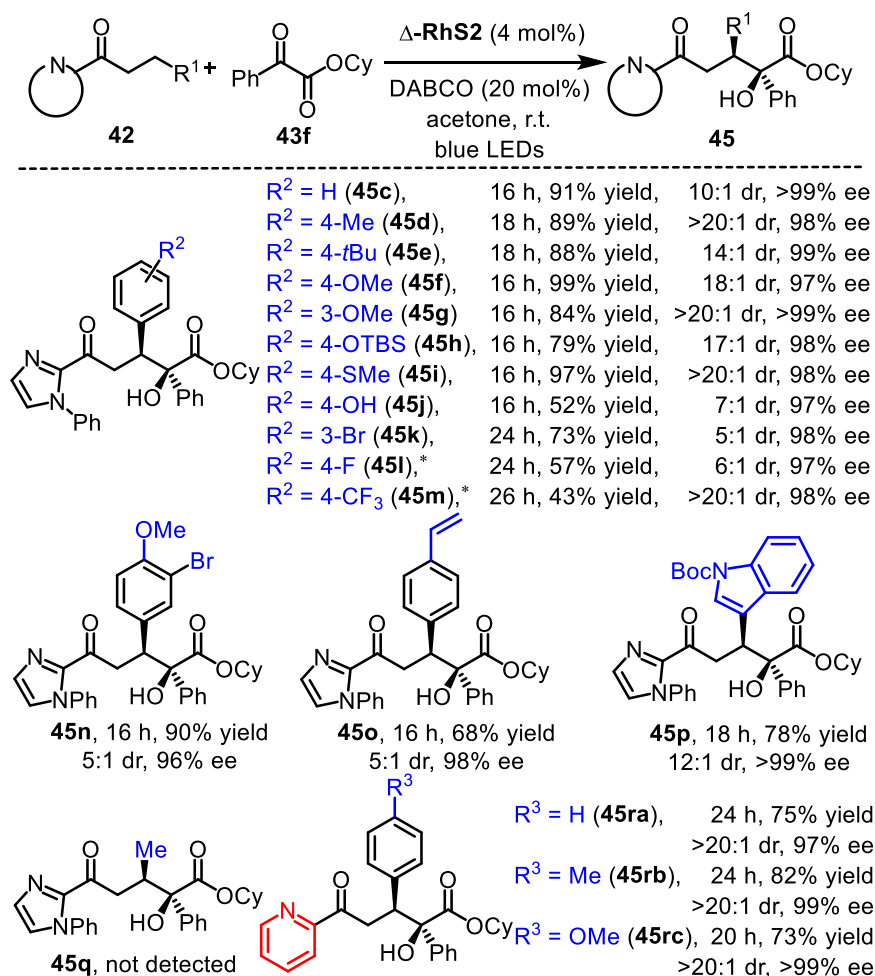


Figure 66. Substrate scope with respect to 2-acyl imidazoles and 2-acyl pyridines. Structure of **45i** was determined by X-ray crystallography and all other compounds were assigned accordingly. *Reaction was performed at 50 °C.

The substrate scope with respect to the acceptor-substituted ketones (**Figure 66**) was next evaluated. 2-Acyl imidazoles (products **45c-p**) have good tolerance for various functional groups including alkyl groups (**45d** and **45e**), ethers (**45f-h**, **45m**), a thioether (**45i**), a hydroxyl (**45j**), bromines (**45k** and **45n**), an olefin (**45o**), and an indole moiety (**45p**). Strongly electron-withdrawing groups (**45l**, **45m**) lead to more sluggish reactions but provided satisfactory results upon heating to 50 °C. 2-Acyl pyridines were also found to be tolerated well by providing the C–C formation products (**45ra-rc**) with excellent diastereo- and enantioselectivities (>20:1 dr and 97 to >99% ee). It is worth noting that six of these products were obtained with an enantiomeric excess of 99% or higher.

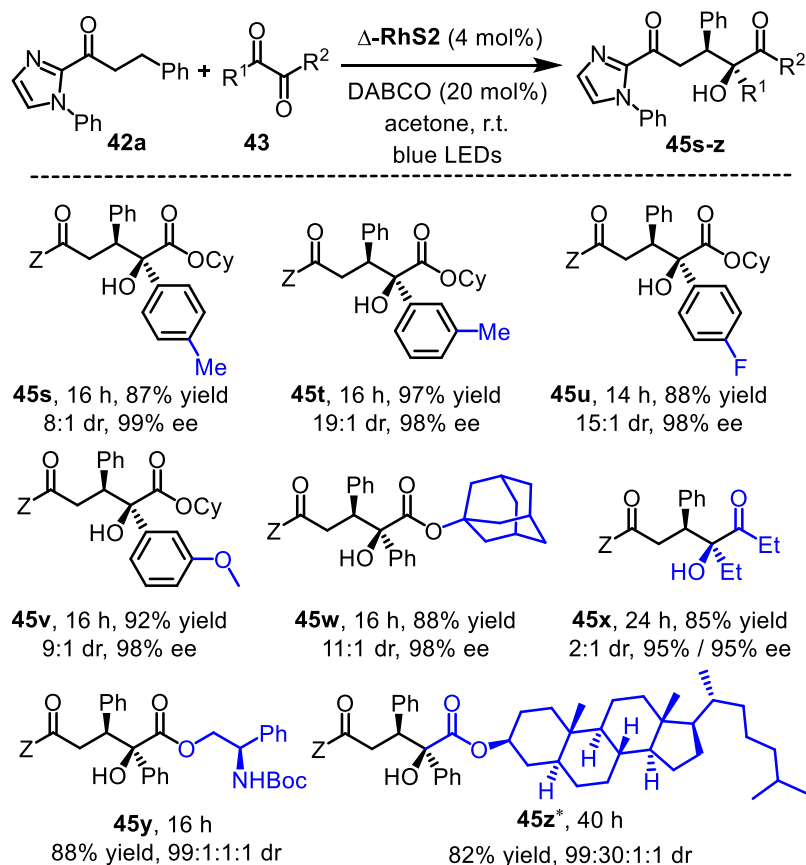


Figure 67. Substrate scope with respect to 1,2-dicarbonyl compounds. *Acetone/CH₂Cl₂ (1:1, vol/vol) was used as solvent. Z = 2-(*N*-phenyl imidazole).

The scope of asymmetric functionalization of β -methylene with respect to 1,2-dicarbonyl compounds is shown in **Figure 67**. The C–C coupling products **45s-w** were obtained in yields of 87-97% with 9:1 to 19:1 dr and excellent 98-99% ee. 1,2-Dicarbonyl compounds as simple as 3,4-hexanedione could also enable this transformation by affording product **45x** in 85% yield with 2:1 dr and 95% ee for both diastereomers. Furthermore, two chiral α -ketoesters provide the expected products **45y** and **45z** in good yields of 88% and 82% and with excellent diastereoselectivities of 99:1:1:1 and 99:30:1:1, respectively. This demonstrates the versatility of this catalytic approach in the context of complex molecules.

However, when introducing a methyl group at the β -position, no C–C formation product (**45q**) was formed and the starting material was recovered with 95% yield (analyzed by ¹H NMR). Apparently, the aryl moiety at the β -position of the carbonyl group is required to facilitate the β -H activation. The limitation of the moieties at the β -position as well as the *N*-heteroaryl rings was further investigated, and the result was outlined in **Figure 68**.

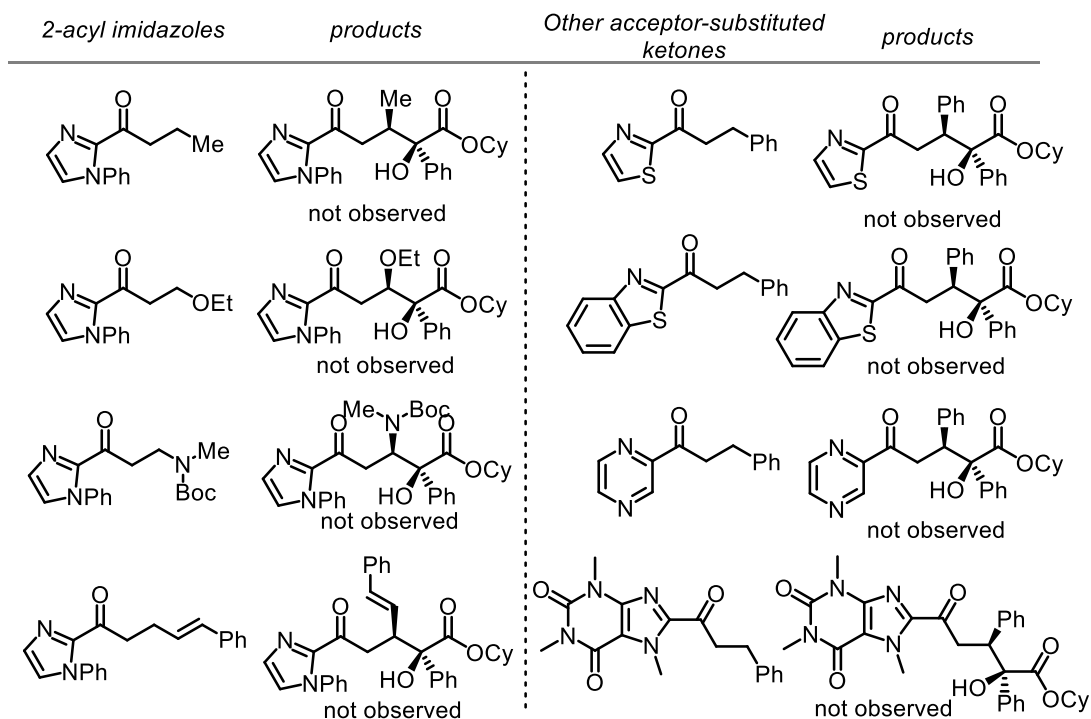


Figure 68. Limitations of the substrate scope.

3.5.4 Synthetic Transformation

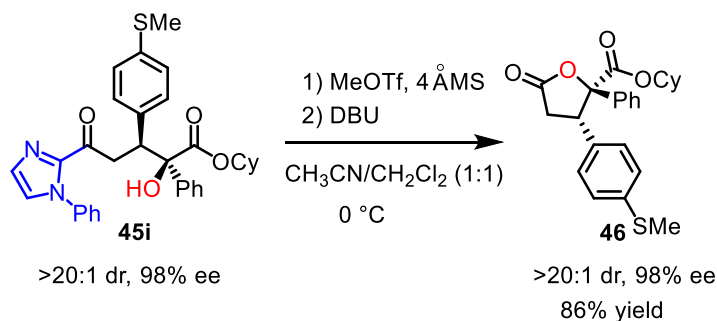


Figure 69. Removal of directing group.

As shown in **Figure 69**, the directing imidazole group was cleaved smoothly by a methyl triflate induced conversion to provide the corresponding γ -lactone **46** without any loss of the enantioselectivity (98% ee) and diastereoselectivity (>20: 1 dr).

3.5.5 Mechanistic Study

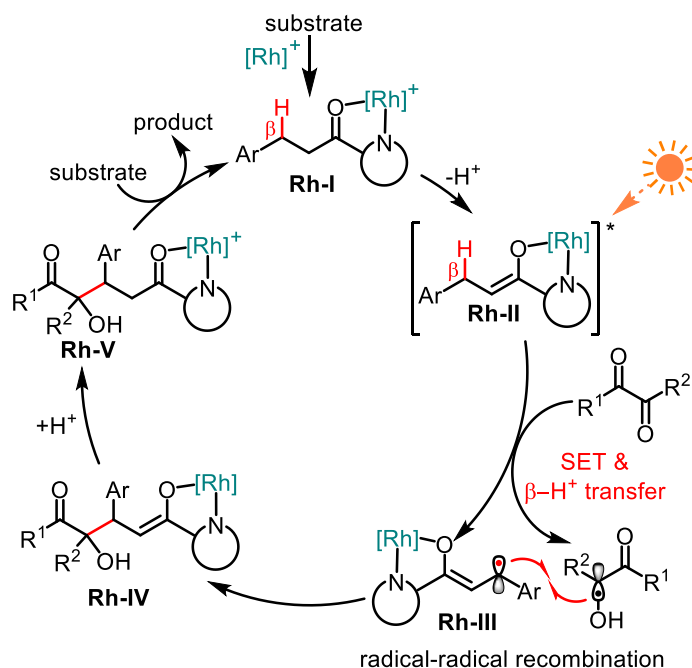


Figure 70. Proposed mechanism.

A proposed mechanism is outlined in **Figure 70**. The catalytic cycle is initiated by the bidentate coordination of substrate **42a** to the Rh-catalyst (**Rh-I**) followed by a base-induced deprotonation to provide the key intermediate Rh-enolate **Rh-II**. The extinction coefficient at 420 nm for the intermediate Rh-enolate is 3-4 orders of magnitudes higher compared to the ketoester **44d** which disfavors a direct excitation of the 1,2-dicarbonyl compound followed by HAT¹⁰ and instead supports a mechanism through photoexcited **Rh-II** (see Experimental Part). Calculated and measured redox potentials are consistent with a reduction of the ketoester **44d** by photoexcited **Rh-II**, followed by a proton transfer, to produce the stabilized, persistent β -carbon-centered radical intermediate **Rh-III**¹¹ accompanied with formation of α -hydroxy radical. In the case of using ketoesters **44d-f**, a stereocontrolled radical-radical recombination¹² occurs to provide the cross-coupling intermediate **Rh-IV**, and after protonation to give the Rh-coordinated product (**Rh-V**). Apparently, the radical-radical recombination efficiency depends on the nature of the α -hydroxy radical and effects the switch between homo- and heterocoupling.

A number of observations support the proposed mechanism. Control experiments in the dark, under air, or in the presence of the radical scavengers TEMPO or BHT, all completely suppressed the C-C bond formation (**Table 6** and **Figure 71a**), thereby supporting a radical mechanism. A determined

quantum yield of 0.08 is consistent with the absence of a chain process. Radical and enolate intermediate trapping experiments were conducted by adding phenyl vinyl ketone **47** as a trapping reagent (**Figure 71b**). In these experiments, the C–C bond formation product **48** was isolated in 40% yield and with 87% ee, supporting the intermediate formation of the enolate intermediate (**Rh-II**), which is then trapped by compound **47**. Interestingly, a dual C–C formation product **49** was also obtained in 37% yield and with >10:1 dr and 92% ee, together with some amounts of the homocoupling product **3**, which is supportive of the formation of the electron-rich Rh-enolate radical intermediate **Rh-III**.

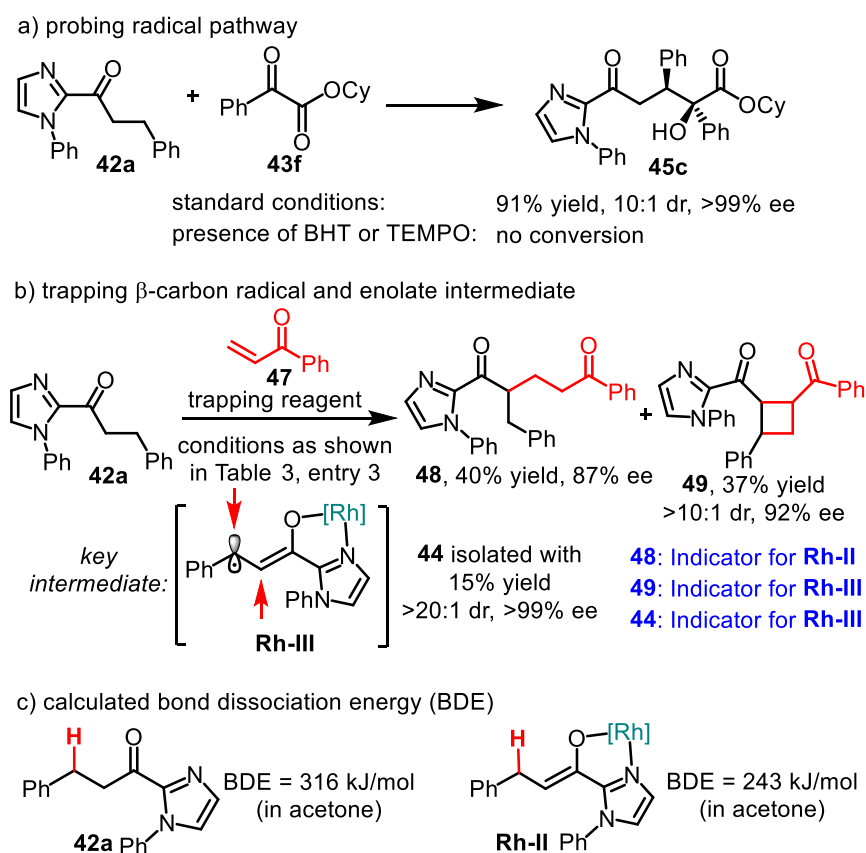


Figure 71. An overview of mechanistic studies.

It is worth noting that computational studies of the key Rh-enolate (**Rh-II**) intermediate at M06/6-31g*/LANL2DZ//6-311++G**/LANL2DZ+CPCM level of theory show that the bond dissociation energy (BDE) of the β -C(sp³)-H in **Rh-II** is lowered by 73 kJ/mol (316 kJ/mol for **42a** vs 243 kJ/mol for **Rh-II**) (**Figure 71c**), thus rendering a direct hydrogen atom abstraction by a photoexcited 1,2-dicarbonyl compound an alternative for generating the same radical intermediates. However, the Rh-enolate intermediate **Rh-II** serves as a very efficient light-harvesting antenna which will suppress direct photoactivation of the dicarbonyl reaction partner and therefore renders a stepwise

electron- and proton-transfer initiated by photoactivated Rh-enolate **Rh-II** more likely. The computational study was conducted by Anthony R. Rosales, a Ph.D. student from Prof. Olaf Wiest's research group at the University of Notre Dame. Other mechanistic investigations including the comparison of different light sources, bases, solvents and the redox potentials of key reaction partners are listed as following:

1) Trapping of the Intermediates

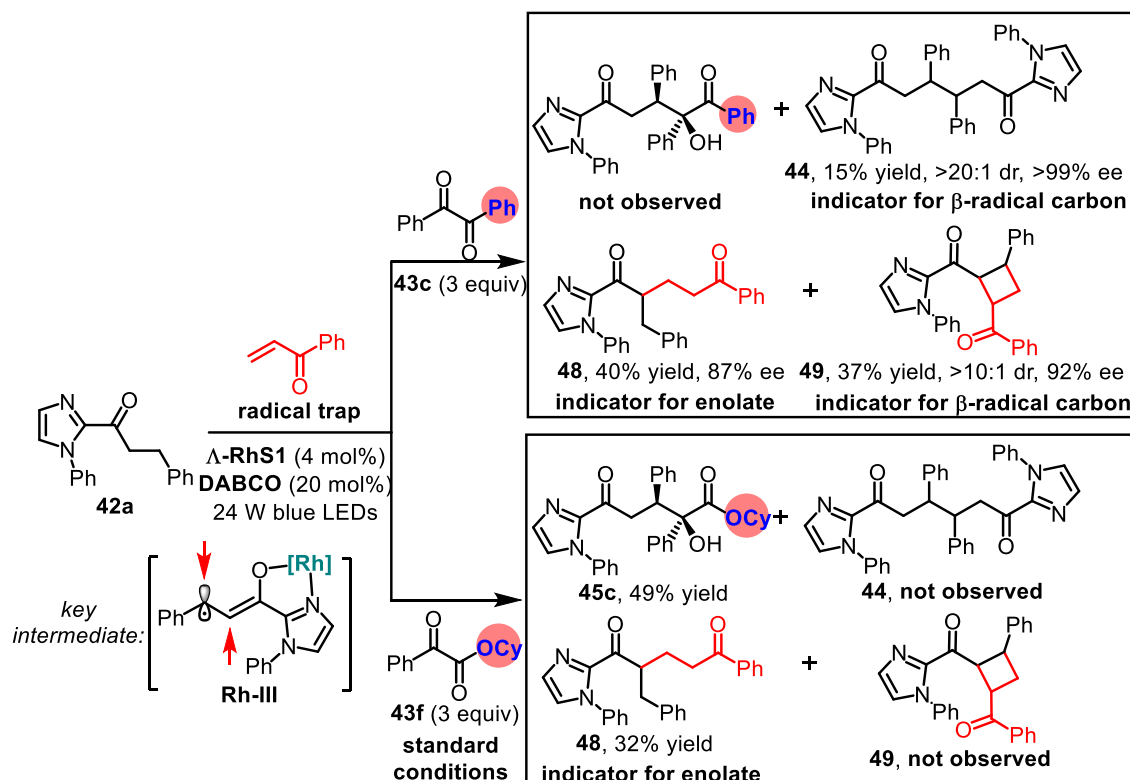


Figure 72. Trapping experiments under the conditions with benzil (**44c**) and α -ketoester (**44f**).

Radical trapping experiments were conducted under the condition with benzil (**44c**) and α -ketoester (**44f**), respectively, which are outline in **Figure 72**. Under standard conditions using a ketoester instead of benzil, the hetero-coupling was dominant and thus reduced the yield of the trapping product **48** and completely suppressed **49**.

Additionally, the formation route of cyclobutane product **49** was clearly demonstrated in **Figure 73**. In this proposal benzil serves as the terminal oxidant and becomes reduced to benzoin.

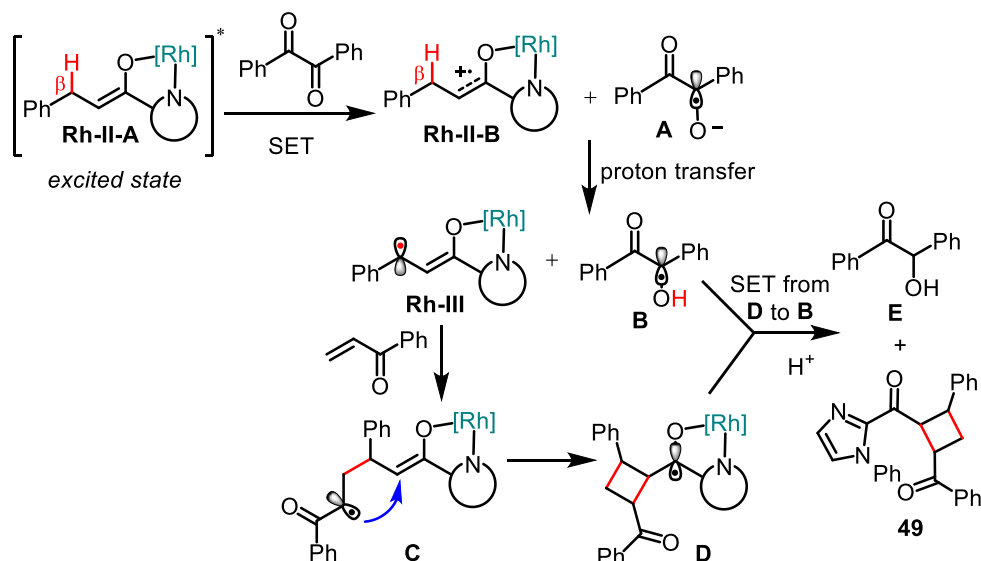
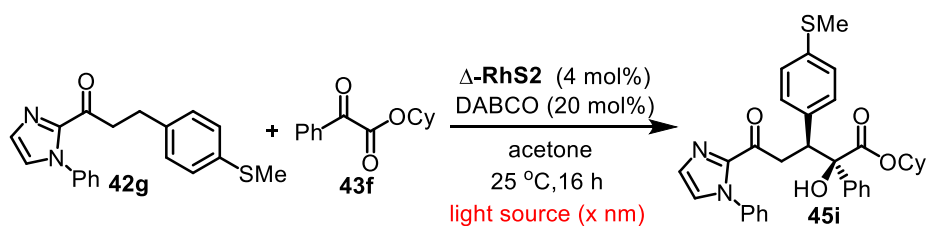


Figure 73. Formation route of cyclobutane product **49**.

2) Comparison of Different Light Sources

As shown in **Table 7**, the reaction proceeded faster using LEDs with shorter emission wavelength (emission maxima shown). However, the enantioselectivities decreased somewhat so that blue LEDs with an emission maximum at 450 nm provided the best compromise out of reaction time and enantiomeric excess.

Table 7. Comparison of different light sources^a



Entry	Light source	Yield (%) ^b	dr ^c	ee (%) ^d
1	450 nm	95 (16 h)	>20:1	98
2	400 nm	>95 (10 h)	>20:1	97
3	390 nm	>95 (10 h)	>20:1	96

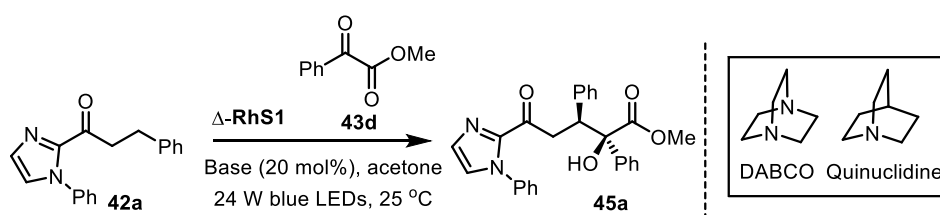
^aReaction conditions: **42g** (0.05 mmol), **43f** (0.3 mmol), Δ -**RhS2** (4 mol%) and DABCO (20 mol%) in acetone (0.5 mL, 0.1 M) were stirred at r.t. for the indicated time under N₂ with the irradiation of different light source. ^bYields were determined by ¹H NMR analysis of the reaction mixtures with an internal standard. ^cDetermined by ¹H NMR analysis of the crude products. ^dDetermined by HPLC analysis on a chiral stationary phase; ee of major diastereomer is shown.

3) Comparison of Different Bases

Reactions were performed in the presence of different Brønsted bases. As shown in **Table 8**, in the presence of DABCO, the C–C formation product **45a** was afforded smoothly (entry 1). However, in the absence of DABCO, the product formation was abolished completely (entry 2). Na₂HPO₄ (entry 3) and 2,6-lutidine (entry 4) enabled the transformation but with inferior results. The base DIEPA promoted this reaction with satisfactory yield of 86% and stereocontrol of 5.0:1 dr and 88% ee. Quinuclidine could promote this transformation more efficiently (92% yield and 93% ee).

MacMillan's group recently reported that quinuclidine can serve as a HAT reagent after oxidation to the amine radical cation.¹³ One therefore needs to consider that DABCO might serve as a HAT mediator in the here reported system. However, since other bases can also promote this transformation, a significant involvement of DABCO as a HAT mediator is unlikely.

Table 8. Comparison of different bases^a



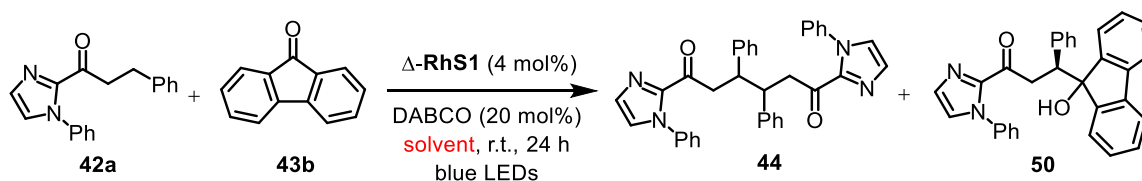
Entry	Base	Yield (%) ^b	dr ^c	ee (%) ^d
1	DABCO	95 (16 h)	5.5:1	98
2	none	n.d.	n.a.	n.a.
3	Na ₂ HPO ₄	18 (40 h)	2.0:1	60
4	2,6-Lutidine	52 (40 h)	4.2:1	37
5	DIPEA	86 (24 h)	5.0:1	88
6	Quinuclidine	92 (16 h)	5.2:1	93

^aReaction conditions: **42a** (0.1 mmol), **43d** (0.3 mmol), Δ -**RhS1** (4 mol%) and bases (20 mol%) in acetone (1 mL, 0.1 M) were stirred at r.t. for indicated time under N₂ with the irradiation of 24 W blue LEDs. ^bYields were determined by ¹H NMR analysis of the reaction mixtures with an internal standard; reaction time provided in brackets. ^cDetermined by ¹H NMR analysis of the crude products. ^dDetermined by HPLC analysis on a chiral stationary phase; ee of major diastereomer is shown. n.d. = not detected. n.a. = not applicable.

4) Comparison of Different Solvents

As shown in **Table 9**, solvents (DMSO, NMP, DMA and DMF with similar polarity) with viscosities higher than acetone favored radical-radical recombination product **8** (hetero-coupling) when using 9-fluorenone (**2b**) as substrate. The competition between homo- and hetero-coupling might be determined by the ability of the radical pair (**Rh-III** and α -hydroxy radical) to reorient itself during random motions.¹⁴ As solvent viscosity increases, using for example DMSO, DMF, DMA, or NMP, the reorientational motions is reduced and thereby favoring heterocoupling over homocoupling. Instead, when the radical pair escapes the cage (e.g. due to faster diffusion and higher radical stabilities), homo-coupling can compete with the desired hetero-coupling.

However, it is noteworthy that benzil (**2c**) does not afford any hetero-coupling regardless of the employed solvents. We speculate that benzil promotes two-electron oxidation of two molecules of Rh-enolate to deliver the homo-coupling product as well as benzoin.

Table 9. Comparison of different viscous solvents^a

Entry	Solvent	Polarity	Viscosity (cP)	Yield (%) ^b		ee (%) ^d (50)
				44	50	
1	(CH ₂ OH) ₂	6.9	25.7	0	0	n.a.
2	DMSO	7.2	1.99	13	20	n.d.
3	NMP	6.7	1.67	<5	63	n.d.
4	DMA	6.5	0.95	12	45	n.d.
5	DMF	6.4	0.80	<5	55 ^c	94%
6	acetone	5.4	0.32	40	0	n.a.

^aReaction conditions: **43a** (0.1 mmol), **44b** (0.3 mmol), Δ -RhS1 (4 mol%) and DABCO (20 mol%) in different solvents (1 mL, 0.1 M) were stirred at r.t. for 24 h under N₂ with the irradiation of 24 W blue LEDs. ^bDetermined by ¹H NMR of crude products. ^cIsolated yield. ^dDetermined by HPLC analysis on a chiral stationary phase. n.a. = not applicable; n.d. = not determined.

5) Determination of Quantum Yield

The quantum yield of the reaction **42g**+**43f**→**45c** was determined by a method and setups developed by Prof. Dr. Eberhard Riedle's Group.¹⁵ As light source 400 nm LEDs were employed. A powermeter was used as detector.

Step 1: The radiant power of light transmitted by the cuvette with a blank solution was measured as $P_{blank} = 29.16$ mW.

Step 2: The reaction mixture of **1g** (64.4 mg, 0.20 mmol), **2f** (139.2 mg, 0.60 mmol), *rac*-**RhS** (7.0 mg, 4.0 mol%) and DABCO (4.5 mg, 20 mol%) in acetone (2.0 mL, 0.1 M) was filled into a fluorescence cuvette with a stirring bar and septum and degassed by bubbling with nitrogen (5 min). Then, the cuvette was put into the setups and illuminated with the 400 nm LEDs. The transmitted radiant power $P_{sample} = 0.28$ mW was noted. The transmitted radiant power was monitored during the irradiation and remained constant.

Step 3: After illumination for 3 hours ($t = 3 \times 3600$ s), the amount of the formed **45c** was determined as 8.601×10^{-5} mol ($N_{product}$) by ¹H NMR.

Step 4: The overall quantum yield can be calculated as following:

$$\begin{aligned} \text{Quantum Yield} &= \frac{N_{product}}{N_{photon}} = \frac{N_A \times N_{product}}{\frac{P_{absorbed} \times t}{\frac{h \times c}{\lambda}}} = \frac{h \times c \times N_A \times N_{product}}{(P_{blank} - P_{sample}) \times t \times \lambda} \\ &= \frac{6.626 \times 10^{-34} \text{ Js} \times 2.998 \times 10^8 \text{ ms}^{-1} \times 6.022 \times 10^{23} \text{ mol}^{-1} \times 8.601 \times 10^{-5} \text{ mol}}{(29.16 - 0.28) \times 10^{-3} \text{ Js} \times 3 \times 3600 \text{ s} \times 400 \times 10^{-9} \text{ m}} = 0.083 \end{aligned}$$

A quantum yield of <1 is in agreement with the expected closed catalytic cycle, as outlined in the proposed mechanism, no chain process is possible whereas one photon is required for each C–C bond formation event.¹⁶

6) Comparison of Redox Potentials

As shown in **Figure 74**, published reduction potentials of **43a**¹⁷, **43b**¹⁸, **43c-d**¹⁹ and **43l** were converted to Normal Hydrogen Electrode (NHE) as reference. The oxidation potentials of Ir-enolate and Rh-enolate²⁰ were also recalculated accordingly. The excited state reduction potential of Rh-enolate' was estimated as -1.48 V using the E^{00} energy of the homologous iridium complex.

A comparison of the listed redox potential demonstrates that an electron transfer from the rhodium-enolate intermediate **Rh-II** to fluorenone, the used 1,2-diketones, and 1,2-ketoesters is thermodynamically feasible. However, a reduction of benzophenone is endergonic and consistent with our results that benzophenone did not engage in the photoreaction.

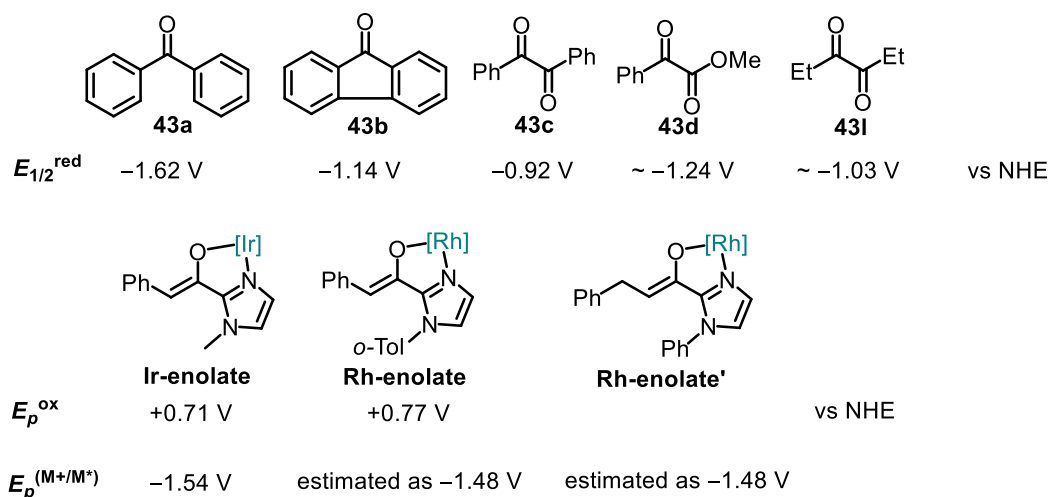


Figure 74. Redox potentials vs Normal Hydrogen Electrode (NHE).

3.5.6 Conclusions

In conclusion, herein a new strategy for the catalytic, asymmetric β -C(sp³)-H functionalization of the carbonyl substrates 2-acyl imidazoles and 2-acylpyridines was developed. According to the mechanistic study, visible light excitation of a rhodium enolate intermediate initiates a single electron transfer to a 1,2-dicarbonyl compound, followed by proton transfer, and subsequent stereocontrolled radical-radical recombination. This method should be of practical value for the asymmetric functionalization of β -C(sp³)-H bonds.

Reference

- 1 X. Huang, S. Luo, O. Burghaus, R. D. Webster, K. Harms, E. Meggers, *Chem. Sci.* **2017**, 8, 7126.

- 2 Z. Zhou, Y. Li, B. Han, L. Gong, E. Meggers, *Chem. Sci.* **2017**, *8*, 5757.
- 3 J. A. Terrett, M. D. Clift, D. W. C. MacMillan, *J. Am. Chem. Soc.* **2014**, *136*, 6858.
- 4 a) M. T. Pirnot, D. A. Rankic, D. B. C. Martin, D. W. C. MacMillan, *Science* **2013**, *339*, 1593; b) F. R. Petronijević, M. Nappi, D. W. C. MacMillan, *J. Am. Chem. Soc.* **2013**, *135*, 18323; c) J. L. Jeffrey, F. R. Petronijević, D. W. C. MacMillan, *J. Am. Chem. Soc.* **2015**, *137*, 8404.
- 5 L. Zhang, E. Meggers, *Acc. Chem. Res.* **2017**, *50*, 320.
- 6 a) D. Ravelli, M. Fagnoni, A. Albin, *Chem. Soc. Rev.* **2013**, *42*, 97; b) N. A. Romero, D. A. Nicewicz, *Chem. Rev.* **2016**, *116*, 10075; c) C. Chen, *Organic & Biomolecular Chemistry* **2016**, *14*, 8641. See also ref. **4b**.
- 7 a) J. Ma, X. Shen, K. Harms, E. Meggers, *Dalton Trans.* **2016**, *45*, 8320; b) J. Ma, X. Zhang, X. Huang, S. Luo, E. Meggers, *Nat. Protoc.* **2018**, *13*, 605.
- 8 For related modifications, see for examples: a) S.-W. Li, J. Gong, Q. Kang, *Org. Lett.* **2017**, *19*, 1350; b) S.-X. Lin, G.-J. Sun, Q. Kang, *Chem. Commun.* **2017**, *53*, 7665.
- 9 H. Huo, X. Shen, C. Wang, L. Zhang, P. Röse, L.-A. Chen, K. Harms, M. Marsch, G. Hilt, E. Meggers, *Nature* **2014**, *515*, 100.
- 10 a) J.-B. Xia, C. Zhu, C. Chen, *J. Am. Chem. Soc.* **2013**, *135*, 17494; b) D. Limnios, C. G. Kokotos, *Adv. Synth. Catal.* **2017**, *359*, 323; c) N. J. Turro, T.-J. Lee, *J. Am. Chem. Soc.* **1969**, *91*, 5651.
- 11 For Lewis acid stabilized enolate radicals as reactive intermediates applied into asymmetric catalysis, see: J. Du, K. L. Skubi, D. M. Schultz, T. P. Yoon, *Science* **2014**, *344*, 392. See also ref. **1** and **2**.
- 12 a) D. Uraguchi, N. Kinoshita, T. Kizu, T. Ooi, *J. Am. Chem. Soc.* **2015**, *137*, 13768; b) T. Kizu, D. Uraguchi, T. Ooi, *J. Org. Chem.* **2016**, *81*, 6953; c) C. Wang, J. Qin, X. Shen, R. Riedel, K. Harms, E. Meggers, *Angew. Chem. Int. Ed.* **2016**, *55*, 685; d) M. Silvi, C. Verrier, Y. P. Rey, L. Buzzetti, P. Melchiorre, *Nat. Chem.* **2017**, *9*, 868.
- 13 M. H. Shaw, V. W. Shurtleff, J. A. Terrett, J. D. Cuthbertson, D. W. C. MacMillan, *Science* **2016**, *352*, 1304.
- 14 a) R. Braslau, N. Naik, H. Zipse, *J. Am. Chem. Soc.* **2000**, *122*, 8421; b) H. Fischer, H. Paul, *Acc. Chem. Res.* **1987**, *20*, 200.
- 15 U. Megerle, R. Lechner, B. König, E. Riedle, *Photochem. Photobiol. Sci.* **2010**, *9*, 1400.
- 16 a) M. D. Kärkäs, B. S. Matsuura, C. R. J. Stephenson, *Science* **2015**, *349*, 1285; b) M. A. Cismesia, T. P. Yoon, *Chem. Sci.* **2015**, *6*, 5426.
- 17 B. D. Mahoney, N. A. Piro, P. J. Carroll, E. J. Schelter, *Inorg. Chem.* **2013**, *52*, 5970.
- 18 S. Li, M. Aljhdli, H. Thakellapalli, B. Farajidizaji, Y. Zhang, N. G. Akhmedov, C. Milsmann, B. V. Popp, K. K. Wang, *Org. Lett.* **2017**, *19*, 4078.
22. G. A. Russell, S. A. Weiner, *J. Am. Chem. Soc.* **1967**, *89*, 6623.
- 20 X. Huang, R. D. Webster, K. Harms, E. Meggers, *J. Am. Chem. Soc.* **2016**, *138*, 12636.

Chapter 4: Summary and Outlook

4.1 Summary

In this thesis, the synthetic access to previously elusive single enantiomers of octahedral chiral-at-Rh Lewis acids has been accomplished through a chiral-auxiliary-mediated synthetic strategy. The obtained chiral Lewis acids Λ/Δ -**RhS** contain two cyclometalating 2-phenylbenzothiazole ligands and two liable acetonitrile ligands, in which the chirality originates exclusively from the stereogenic central metal. The benzothiazole-containing **RhS** is a superior chiral Lewis acid catalyst compared to its benzoxazole congener which can be rationalized with a higher steric congestion around the catalytic site.

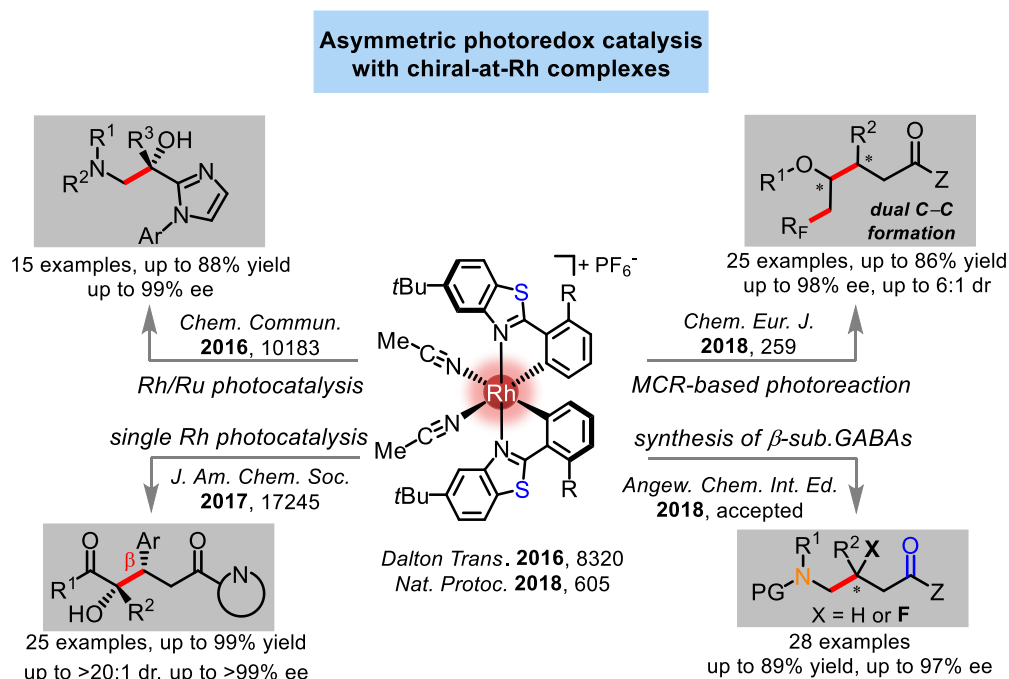


Figure 75. An overview for this thesis. Only the Δ -configuration is shown. MCR = multicomponent reaction. GABAs = γ -aminobutyric acids

The excellent catalytic activity of the Lewis acid catalyst has been demonstrated through diverse visible-light-induced asymmetric photoredox reactions. Accordingly, the Lewis acid Λ -**RhS** cooperated with an external photoredox catalyst/mediator provides access to the enantioenriched 1,2-aminoalcohols and fluoroalkyl-containing compounds. In particular, this unique chiral-at-rhodium Lewis acid catalysis system provides a practical avenue to pharmaceutically demanding enantioenriched β -substituted γ -aminobutyric acids. Further investigations revealed that Δ -**RhS** or

related derivatives are capable of promoting the enantioselective β -C(sp³)-H functionalization of acceptor-substituted ketones through integrating the dual functions of asymmetric and photoredox catalyst.

1) Synthesis of the New Lewis acid catalyst Λ/Δ -RhS

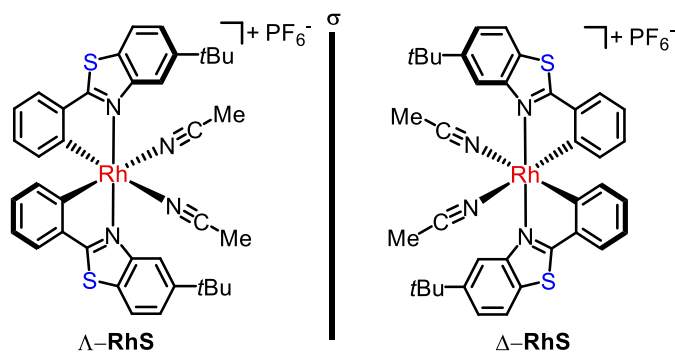


Figure 76. Chiral Lewis acid catalyst Λ/Δ -RhS.

The synthesis of Lewis acid catalyst Λ/Δ -RhS was accomplished through a chiral-auxiliary-mediated strategy (**Figure 77**). Key aspect of this synthetic strategy is the employment of a fluorinated auxiliary (*S*)-**8** which provides two diastereomers with distinct solubility and sufficient stability for purification using the standard silica gel chromatography. Upon the acid induced replacement of the coordinated auxiliary ligand with two acetonitriles, the diastereomers are converted into individual enantiomers Λ -RhS and Δ -RhS with perfect optical purities (>99:1 er).

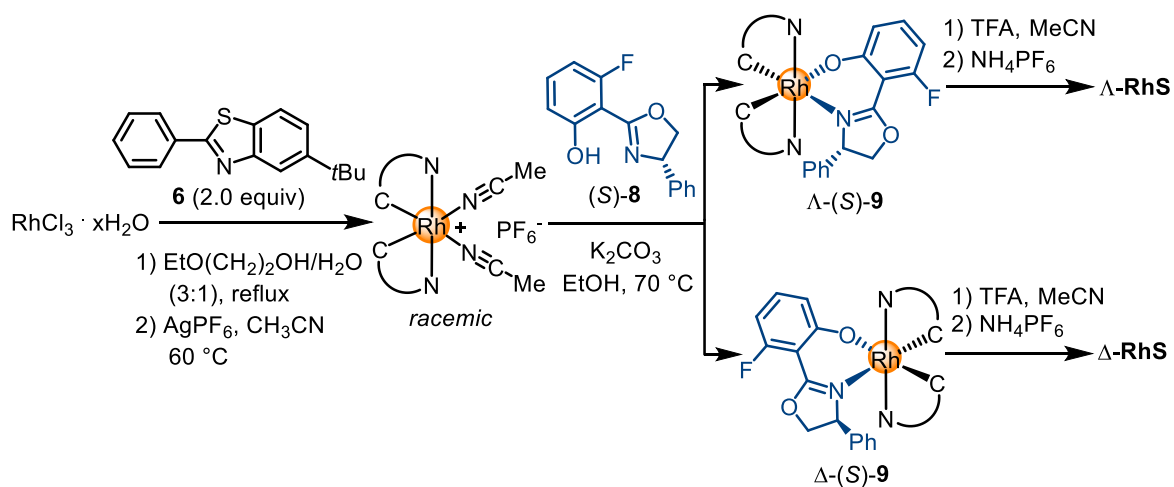


Figure 77. Synthetic route to chiral Lewis acid catalyst Λ/Δ -RhS.

2) Cooperative rhodium/ruthenium asymmetric photoredox catalysis to access chiral 1,2-aminoalcohols

Asymmetric cooperative Rh-based Lewis acid catalysis with Ru-based photoredox catalysis provides synthetic access to non-racemic 1,2-aminoalcohols in good yields (up to 88%) and with excellent enantioselectivities (up to 99% ee). The Ru-photocatalyst is proposed to constitute an electron shuttle, thereby triggering a single electron from the α -silylamine (electron donor) to the Rh-chelated 2-acyl imidazole (electron acceptor). The following stereocontrolled radical–radical recombination affords the C–C formation product (**Figure 78**).

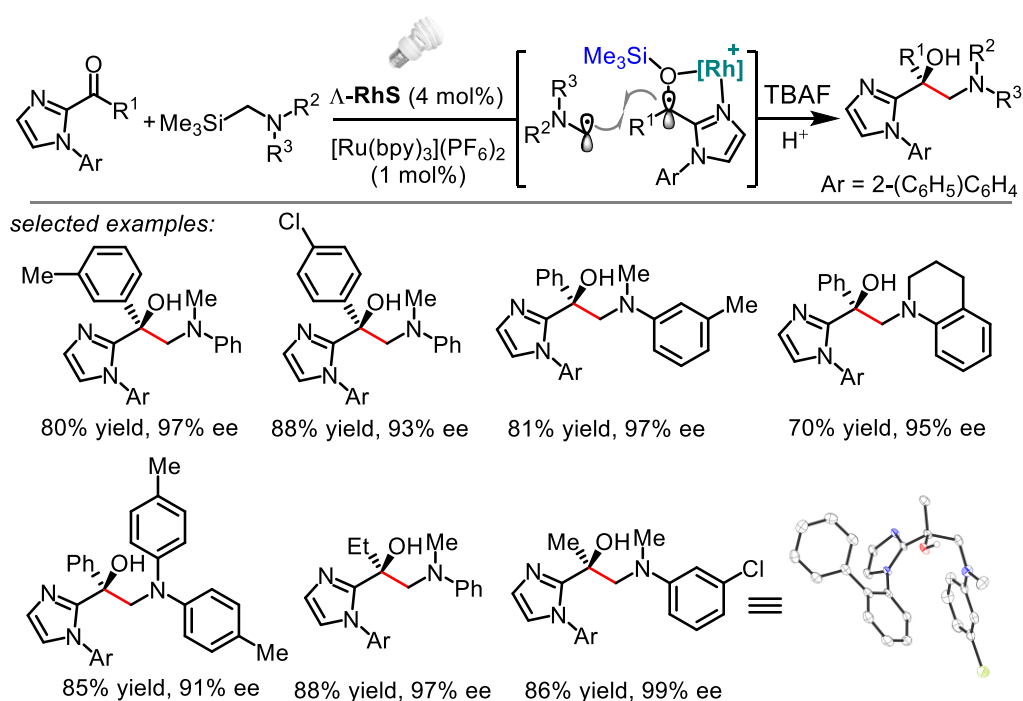


Figure 78. Cooperative rhodium/ruthenium photoredox catalysis to access chiral 1,2-aminoalcohols.

3) Synthesis of fluoroalkyl-containing compounds through enantioselective three-component photoredox reaction

The cooperative strategy by using chiral-at-rhodium Lewis acid was further extended to a visible-light-induced asymmetric three-component fluoroalkylation reaction, in which the photoredox process was mediated by the inexpensive, commercially available organic photoredox mediator 4,4'-difluorobenzil. This three-component fluoroalkylation scheme provided a range of complex fluoroalkyl-containing chiral compounds under dual C–C bond formation with high enantioselectivities (up to 98% ee) and modest diastereoselectivities (up to 6:1 dr). Excellent diastereoselectivities (up to >38:1 dr) for natural chiral compound derivatives were observed. Broad substrate scope, excellent functional group tolerance, scalability of the reaction, along with the option to recover the chiral catalyst and photoredox mediator revealed the practicability of this methodology in organic synthesis for the rapid synthesis of fluorinated chiral molecules.

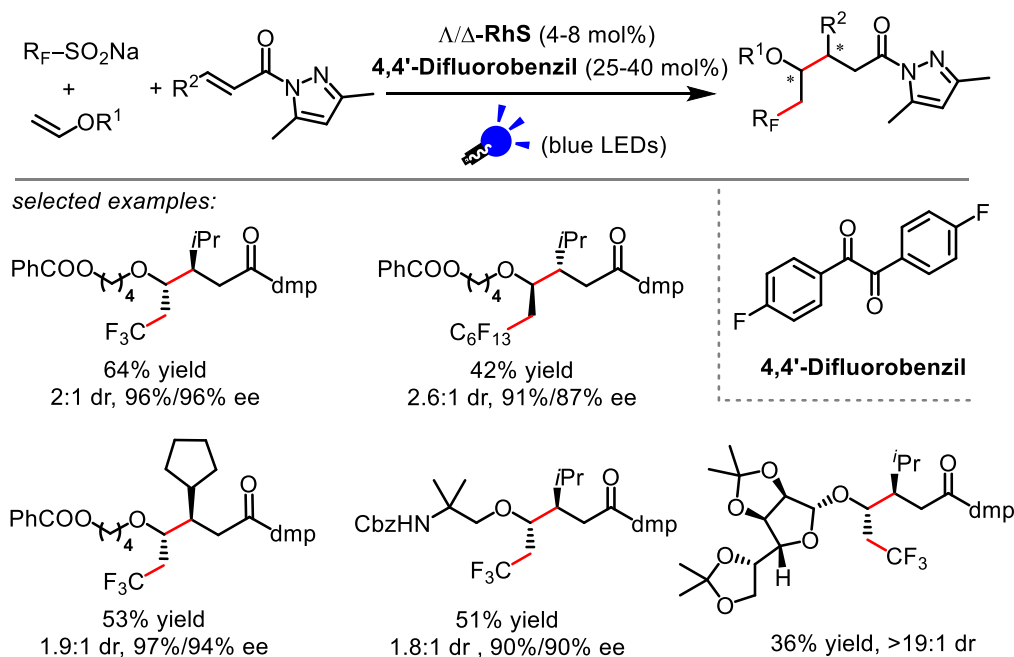


Figure 79. Synthesis of fluoroalkyl-containing compounds through enantioselective three-component photoredox chemistry. dmp = 3,5-dimethylpyrazolyl.

4) Synthesis of β -Substituted γ -Aminobutyric Acid Derivatives through Enantioselective Photoredox Reaction

The Rh-based Lewis acid photocatalysis system was later recognized as a practical avenue to the pharmaceutically demanding β -substituted γ -aminobutyric acids (GABAs) and their derivatives. The protocol is based on Rh-catalyzed radical conjugate addition of an acceptor-substituted alkene with an α -aminoalkyl radical which was produced from simple glycine derivatives upon single electron reduction mediated by photoreductant Hantzsch ester. Diverse β -substituted GABA analogs, including previously inaccessible derivatives containing fluorinated quaternary stereocenters, were accessed with high efficiency (good yields of 42–89% and excellent enantioselectivities of 90–97% ee). Synthetically valuable applications were demonstrated by providing straightforward synthetic access to the pharmaceuticals or related bioactive compounds (*S*)-pregabalin, (*R*)-baclofen, (*R*)-rolipram and (*S*)-nebracetam (**Figure 80**).

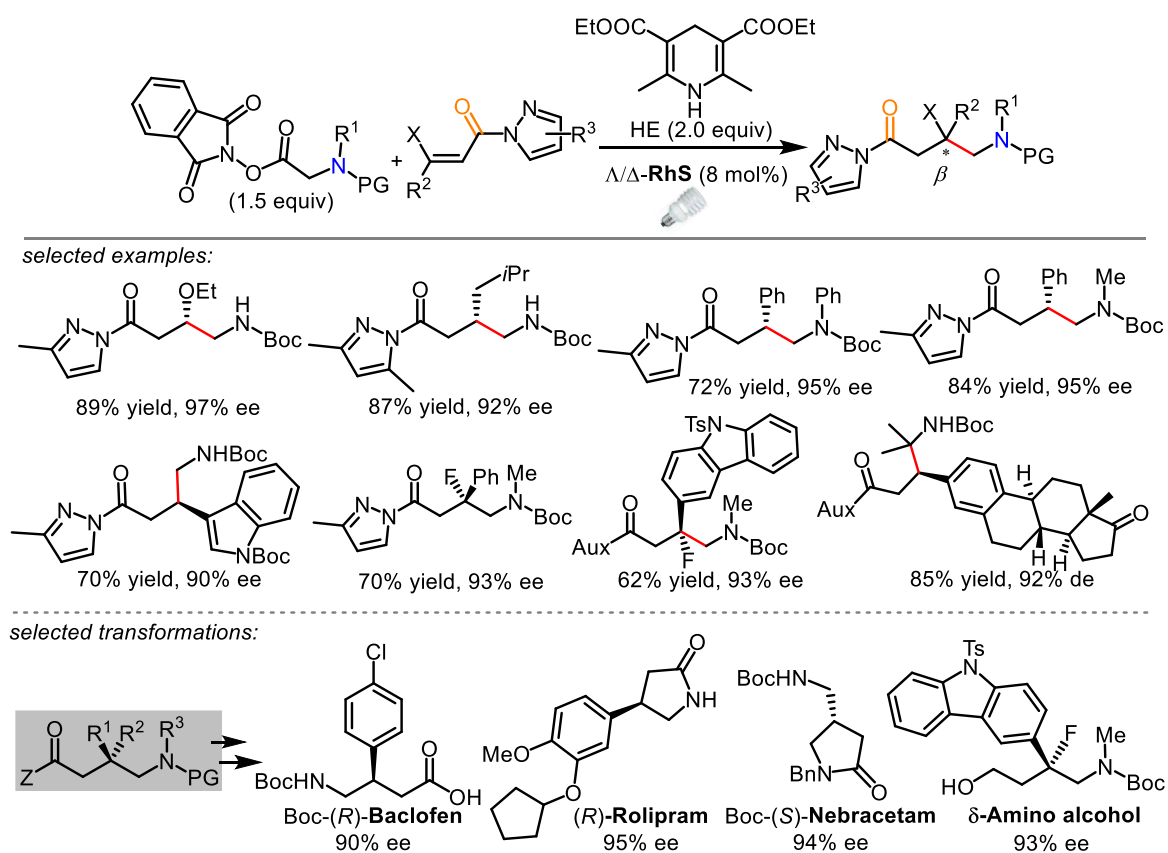


Figure 80. Synthesis of β -substituted GABA derivatives through enantioselective photoredox catalysis. Aux = 3-methyl pyrazolyl.

5) Asymmetric β -C–H functionalization of acceptor-substituted ketones through single Rh-based photoredox catalysis

The enantioselective β -C(sp³)-H functionalization of acceptor-substituted ketones with 1,2-dicarbonyl compound was accomplished by using a single chiral-at-rhodium Lewis acid Δ -**RhS** derivative as catalyst. The C–C bond formation products were obtained in high yields (up to 99%) and with excellent stereoselectivities (up to >20:1 dr and up to >99% ee). Experimental and computational studies support a mechanism in which visible light excitation of a rhodium enolate intermediate initiates a single electron transfer to a 1,2-dicarbonyl compound, followed by proton transfer, and subsequent stereocontrolled radical-radical recombination.

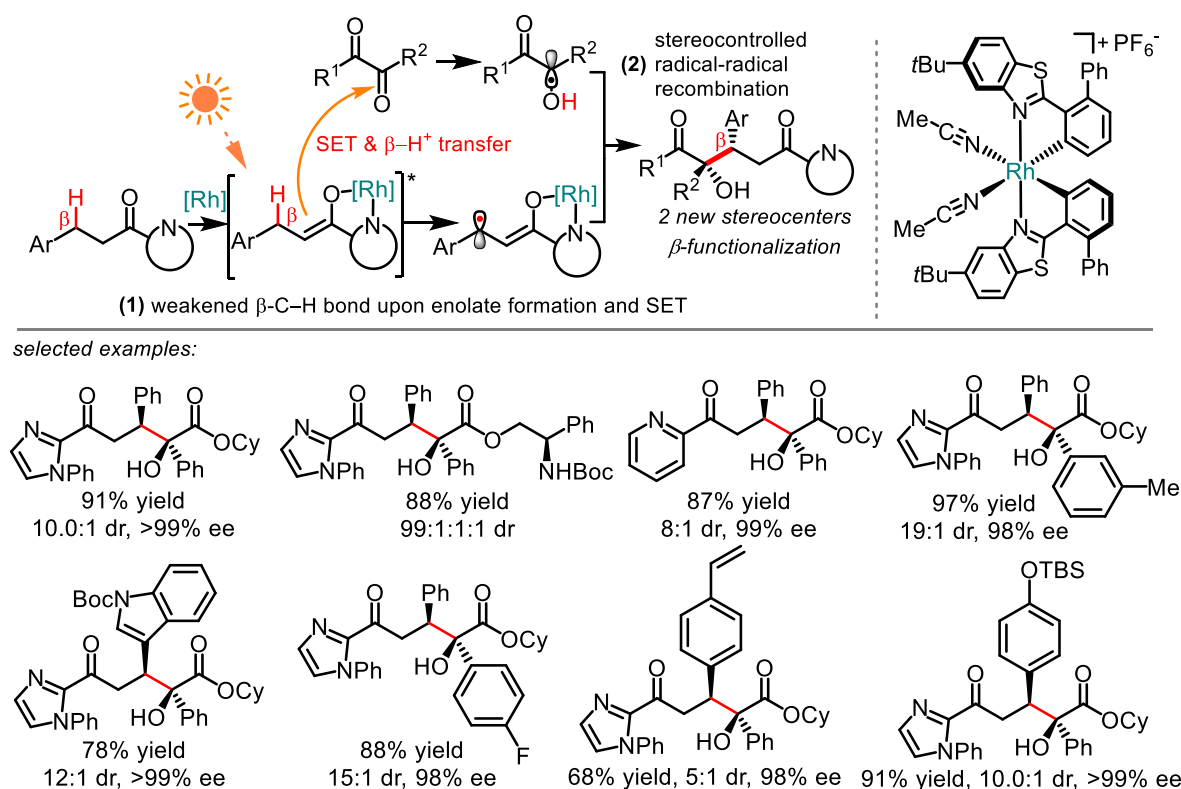


Figure 81. Single chiral-at-Rh Lewis acid catalyzed β -C(sp³)-H functionalization under photoredox conditions.

4.2 Outlook

Considering the unmet demand and the limited techniques, further experiments on the more profound investigations of the herein introduced chiral-at-rhodium Lewis acid catalysis system is desirable. Apparently in this thesis the unique catalytic system has been demonstrated as a versatile tool for organic synthesis, and therefore it should be of high value for further broad synthetic applications.

1) Extend the herein developed β -C(sp³)-H alkylation protocol to carbon-heteroatom bond construction: The strategy of enantioselective β -C(sp³)-H functionalization with asymmetric photoredox catalysis might be further extended beyond the herein disclosed β -alkylation, but to a borylation or trifluoromethylthiolation through tuning reaction conditions and involved co-substrates. Accordingly, it's supposed that the photoexcited rhodium enolate intermediate donates a single electron to an suitable electron shuttle (e.g. benzil) rather than a co-substrate to afford an allylic radical which might be trapped by a boronic ester¹ or acid² under the stereocontrolled formation of C-B bond. Alternatively, a single electron might exchange between the photoexcited enolate intermediate (donor) and the electron-deficient Phth-SCF₃³ substrate (acceptor) to afford the rhodium stabilized allylic radical and trifluoromethylthionyl radical. A following stereocontrolled radical-radical recombination reaction would deliver a C-S formation product. Overall, the herein developed visible-light-activated enantioselective β -C(sp³)-H functionalization protocol should constitute high potential for applications in the valuable carbon-heteroatom bond construction.

2) Exploit new substrate activation mode in enantioselective photoredox catalysis: Despite the versatile catalytic activity of chiral-at-rhodium Lewis acid in asymmetric photoredox catalysis has been disclosed in this thesis, a current limitation is existed, namely the requirement of one substrate with bidentate N,O-based metal-binding site, such as 2-acyl imidazoles, 2-acyl pyridines, and *N*-acyl pyrazoles. Therefore, development of new substrate activation method in the rhodium catalyzed photoredox chemistry is of interest. The former group member Luo recently found a chiral-at-rhodium complex was capable of promoting enantioselective alkynylation of aromatic aldehydes, in which a rhodium acetylide intermediate might be formed.⁴ It's supposed herein that this neutral rhodium acetylide intermediate, upon photoexcitation, could be highly reducing, thereby triggering single electron reduction of suitable co-substrate (e.g. *N*-(acyloxy)phthalimide) to deliver an alkyl radical.

And a photogenerated prochiral nucleophilic alkyl radical would then react with the rhodium acetylide in a stereocontrolled fashion.⁵ While in the presence of stoichiometric amounts of sacrificial oxidant, a photogenerated α -aminoalkyl radical then undergoes a single electron oxidation event to provide an iminium ion which might be trapped by acetylide intermediate.⁶ Overall, the rhodium acetylide intermediate is potentially applicable in the enantioselective photoredox catalysis, thereby leading to broader synthetic applications.

Reference

- 1 A. Fawcett, J. Pradeilles, Y. Wang, T. Mutsuga, E. L. Myers, V. K. Aggarwal, *Science* **2017**, *357*, 283.
- 2 D. Hu, L. Wang, P. Li, *Org. Lett.* **2017**, *19*, 2770.
- 3 R. Honeker, R. A. Garza-Sanchez, M. N. Hopkinson, F. Glorius, *Chem. Eur. J.* **2016**, *22*, 4395.
- 4 S. Luo, X. Zhang, Y. Zheng, K. Harms, L. Zhang, E. Meggers, *J. Org. Chem.* **2017**, *82*, 8995.
- 5 a) H. Huang, G. Zhang, L. Gong, S. Zhang, Y. Chen, *J. Am. Chem. Soc.* **2014**, *136*, 2280; b) J. Yang, J. Zhang, L. Qi, C. Hu, Y. Chen, *Chem. Commun.* **2015**, *51*, 5275.
- 6 H. Zhang, P. Zhang, M. Jiang, H. Yang, H. Fu, *Org. Lett.* **2017**, *19*, 1016.

Chapter 5: Experimental Part

5.1 Materials and Methods

All reactions were carried out under an atmosphere of nitrogen with magnetic stirring. The catalysis reactions were performed using standard Schlenk glassware techniques.

Solvents and Reagents

Solvents were distilled under nitrogen from calcium hydride (CHCl_3 , CH_2Cl_2 , CH_3CN and DMF), magnesium turnings/iodine (MeOH) or sodium/benzophenone (Et_2O , THF and toluene). HPLC grade solvents, such as 2-methoxyethanol, ethanol and 1,4-dioxane used directly without further drying. All reagents were purchased from Acros, Alfa Aesar, Sigma Aldrich, TCI, ChemPur and Fluorochem and used without further purification.

Chromatographic Methods

The course of the reactions and the column chromatographic elution were monitored by thin layer chromatography (TLC) [Macherey-Nagel (ALUGRAM®Xtra Sil G/UV254)]. Flash column chromatography was performed with silica gel from Merck (particle size 0.040-0.063 mm).

Nuclear Magnetic Resonance Spectroscopy (NMR)

^1H NMR, proton decoupled ^{13}C NMR, and proton coupled ^{19}F NMR spectra were recorded on Bruker Avance 300 system (^1H NMR: 300 MHz, ^{13}C NMR: 75 MHz, ^{19}F NMR: 282 MHz) spectrometers at ambient temperature. Chemical shifts are given in ppm on the δ scale, and were determined after calibration to the residual signals of the solvents, which were used as an internal standard. NMR standards were used are as follows: ^1H NMR spectroscopy: $\delta = 7.26$ ppm (CDCl_3), $\delta = 5.32$ ppm (CD_2Cl_2), $\delta = 2.50$ ppm (DMSO-*d*6), $\delta = 3.31$ ppm (CD_3OD); ^{13}C -NMR spectroscopy: $\delta = 77.0$ ppm (CDCl_3), $\delta = 53.8$ ppm (CD_2Cl_2), $\delta = 118.26$, 1.32 ppm (CD_3CN), $\delta = 206.26$, $\delta = 39.52$ ppm (DMSO-*d*6), $\delta = 49.0$ ppm (CD_3OD). ^{19}F NMR spectroscopy: $\delta = 0$ ppm (CFCl_3). The characteristic signals were specified from the low field to high field with the chemical shifts (δ in ppm). ^1H NMR spectra peak multiplicities indicated as singlet (s), doublet (d), doublet of doublet (dd), doublet of doublet of doublet (ddd), triplet (t), doublet of triplet (dt), quartet (q), multiplet (m). The coupling

constant J indicated in hertz (Hz).

High-Performance Liquid Chromatography (HPLC)

Chiral HPLC was performed with an Agilent 1200 Series, Agilent 1260 Series HPLC System or Shimadzu Lc-2030c. All the HPLC conditions were detailed in the individual procedures. The type of the columns, mobile phase and the flow rate were specified in the individual procedures.

Infrared Spectroscopy (IR)

IR measurements were recorded on a Bruker Alpha-P FT-IR spectrometer. The absorption bands were indicated a wave numbers ν (cm^{-1}). All substances were measured as films or solids.

Mass Spectrometry (MS)

High-resolution mass spectra were recorded on a Bruker En Apex Ultra 7.0 TFT-MS instrument using ESI or APCI or FD technique. Ionic masses are given in units of m/z for the isotopes with the highest natural abundance.

Circular Dichroism Spectroscopy (CD)

CD spectra were recorded on a JASCO J-810 CD spectropolarimeter. The parameters we used as follows: from 600 nm to 200 nm; data pitch (0.5 nm); band with (1 nm); response (1 second); sensitivity (standard); scanning speed (50 nm/min); accumulation (5 times). The concentration of the compounds for the measurements was 0.2 mM. The formula for converting θ to ϵ is shown as below.

$$\Delta\epsilon = \frac{\theta[m \text{ deg}]}{32980 \times c(\text{mol} / L) \times L(\text{cm})}$$

C = concentration of the sample; L = thickness of the measurement vessel

Crystal Structure Analysis

Crystal X-ray measurements and the crystal structure analysis were carried out by Dr. Klaus Harms (Chemistry Department, Philipps University of Marburg). X-ray data were collected with a Bruker 3 circuit D8 Quest diffractometer with MoK α radiation (microfocus tube with multilayer optics) and Photon 100 CMOS detector. Scaling and absorption correction was performed by using the SADABS

software package of Bruker. Structures were solved using direct methods in SHELXS and refined using the full matrix least squares procedure in SHELXL-2013 or SHELXL-2014. The Flack parameter is a factor used to estimate the absolute configuration of the compounds. The hydrogen atoms were placed in calculated positions and refined as riding on their respective C atom, and Uiso(H) was set at 1.2 Ueq(Csp²) and 1.5 Ueq(Csp³). Disorder of PF₆ ions, solvent molecules or methylene groups was refined using restraints for both the geometry and the anisotropic displacement factors.

UV/Vis Analysis Spectroscopy

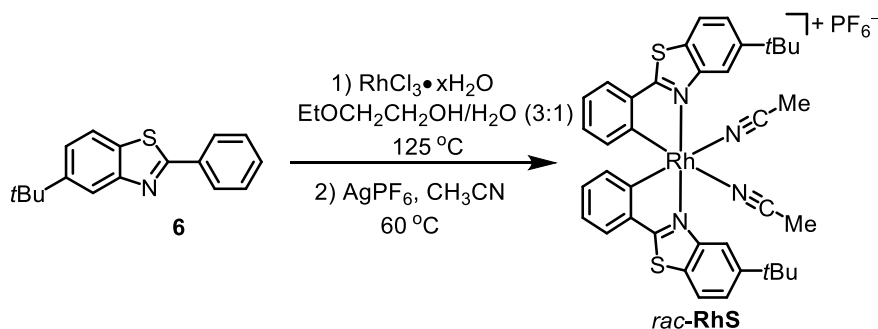
UV/Vis measurements were taken on a Spectra Max M5 microplate reader in a 10.0 mm quartz cuvette.

Optical Rotation Polarimeter

Optical rotations were measured on a Krüss P8000-T or Perkin-Elmer 241 polarimeter with $[\alpha]_D^{20}$ or $[\alpha]_D^{25}$ values reported in degrees with concentrations reported in g/100 mL.

5.2 Synthesis of the New Chiral-at-Rh Lewis Acid Catalyst Λ/Δ -RhS5.2.1 Synthesis of Rhodium-Based Catalysts Λ -RhS and Δ -RhS

1) Racemic Rhodium Catalyst:



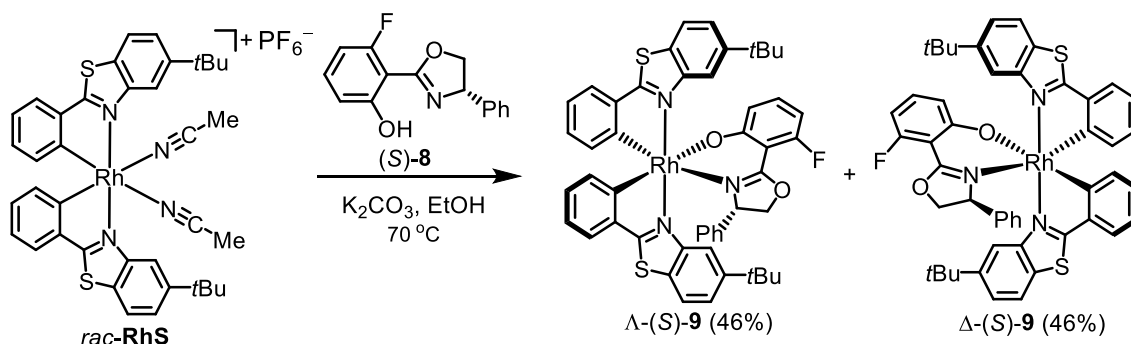
The racemic rhodium catalyst *rac*-**RhS** was synthesized according to a route reported by the Meggers group with some modifications.¹ Accordingly, 5-(*tert*-butyl)-2-phenylbenzo[*d*]thiazole **6** (2000 mg, 7.48 mmol) was added to RhCl₃·*x*H₂O (962 mg, 3.74 mmol) in a mixture of 2-ethoxyethanol and water (v/v = 3:1, 75 mL). The reaction mixture was heated at 125 °C for 4 h under an atmosphere of nitrogen, then concentrated to obtain a brown solid. To the brown solid in CH₃CN (10 mL) was added AgPF₆ (1890 mg, 7.48 mmol) in one portion, then stirred at 60 °C overnight. After cooled to room temperature, the mixture was filtered. The filtrate was collected, evaporated to dryness and purified by column chromatograph on silica gel (100% CH₂Cl₂ to CH₂Cl₂/CH₃CN = 20:1) to give *rac*-**RhS** (1.70 g, 53% yield for two steps) as a pale yellow solid.

¹H NMR (300 MHz, CD₂Cl₂) δ 8.50 (d, *J* = 1.6 Hz, 2H), 8.05 (d, *J* = 8.6 Hz, 2H), 7.73 (dd, *J* = 8.6, 1.8 Hz, 2H), 7.67 (dd, *J* = 7.6, 1.2 Hz, 2H), 7.03 (td, *J* = 7.4, 1.1 Hz, 2H), 6.83 (td, *J* = 7.7, 1.4 Hz, 2H), 6.22 (d, *J* = 7.8 Hz, 2H), 2.18 (s, 6H), 1.47 (s, 18H).

¹³C NMR (75 MHz, CD₂Cl₂) δ 176.9, 176.8, 160.9, 160.5, 152.8 (2C), 150.0 (2C), 140.3 (2C), 133.3 (2C), 131.2 (2C), 129.1 (2C), 126.2 (2C), 125.5 (2C), 124.5 (2C), 123.0 (2C), 122.1 (2C), 116.7 (2C), 35.6 (2C), 31.6 (2C), 3.5 (2C).

HRMS (ESI, *m/z*) calcd for C₃₈H₃₈N₄Rh S₂⁺ [M-PF₆]⁺: 717.1587, found: 717.1596.

IR (film): ν (cm⁻¹) 3118, 2961, 2868, 2282, 1579, 1556, 1477, 1441, 1416, 1364, 1318, 1296, 1281, 1266, 1254, 994, 836, 784, 757, 730, 700, 668, 556, 460.

2) Intermediate Rhodium Auxiliary Complexes Λ -(S)-**9** and Δ -(S)-**9**:

To the racemic rhodium catalyst *rac*-**RhS** (863 mg, 1.0 mmol) and K_2CO_3 (414 mg, 3.0 mmol) in absolute ethanol (40.0 mL) was added (*S*)-3-fluoro-2-(4-phenyl-4,5-dihydrooxazol-2-yl)phenol {(*S*)-**8**} (283 mg, 1.1 mmol) in one portion, and then heated at 60 °C for 6 h. Afterwards, the reaction mixture was cooled to room temperature. The diastereomer Λ -(*S*)-**9** has a lower solubility in ethanol than Δ -(*S*)-**9** and was precipitated selectively. The yellow solid was separated from the solution by centrifugation, and washed for another three times with EtOH (3 \times 10 mL). The combined clear yellow solution was collected and concentrated, and then subjected to a flash chromatography on silica gel (*n*-hexane/EtOAc = 10:1 to 3:1) to give Δ -(*S*)-**9** (410 mg, 46% yield) as a yellow solid. On the other hand, the yellow solid obtained after centrifugation was subjected to a flash chromatography on silica gel (*n*-hexane/ CH_2Cl_2 = 1:10 to 1:1) to provide Λ -(*S*)-**9** with >95% purity as judged by ^1H NMR. The crude complex was recrystallized in *n*-hexane/ CH_2Cl_2 = 10:1 to provide pure Λ -(*S*)-**9** (390 mg, 44% yield) as a yellow solid. The assigned configurations were confirmed by the crystal structure of Δ -(*S*)-**9** (see below).

 Λ -(*S*)-**9**:

^1H NMR (500 MHz, CD_2Cl_2) δ 8.90 (d, J = 1.6 Hz, 1H), 7.98 (d, J = 1.5 Hz, 1H), 7.80 (d, J = 5.1 Hz, 1H), 7.62-7.59 (m, 2H), 7.53 (dd, J = 8.6, 1.8 Hz, 1H), 7.46 (dd, J = 8.6, 1.8 Hz, 1H), 7.40 (dd, J = 7.6, 1.2 Hz, 1H), 6.98 (td, J = 7.3, 1.0 Hz, 1H), 6.92 (td, J = 7.4, 1.0 Hz, 1H), 6.86-6.70 (m, 6H), 6.36-6.15 (m, 4H), 5.88 (d, J = 7.9 Hz, 1H), 5.81 (qd, J = 7.8, 1.1 Hz, 1H), 4.89-4.84 (m, 2H), 4.02-3.97 (m, 1H), 1.45 (s, 9H), 1.28 (s, 9H).

^{13}C NMR (125 MHz, CD_2Cl_2) δ 177.3 (2C), 175.7 (2C), 175.1 (2C), 170.4, 170.1, 168.2, 168.0, 165.9 (2C), 163.6 (d, J = 257.2 Hz), 151.5, 151.4, 151.3, 141.7, 141.4, 141.2, 135.3, 133.2, 132.9, 132.8,

129.9, 129.6, 129.4 (2C), 128.8 (2C), 127.9, 127.6, 125.9 (2C), 123.9, 123.0, 122.4, 122.3, 121.3, 120.4 (2C), 119.6, 116.5, 101.2 (d, $J = 6.3$ Hz), 98.5 (d, $J = 24.0$ Hz), 75.7, 69.4, 35.3, 35.2, 31.7, 31.6.

HRMS (ESI, m/z) calcd for $C_{49}H_{43}FN_3O_2RhS_2Na^+ [M+Na]^+$: 914.1728, found: 914.1731.

IR (film): ν (cm^{-1}) 2956, 2927, 1617, 1591, 1578, 1526, 1474, 1458, 1438, 1414, 1391, 1376, 1292, 1245, 1156, 1092, 1015, 988, 924, 814, 791, 752, 719, 689, 668, 462.

CD {CH₃OH/DCM (4:1)} for Δ -(*S*)-**9**: λ , nm ($\Delta\epsilon$, $M^{-1}cm^{-1}$) 425 (+25), 380 (-10), 362 (-6), 339 (-21), 318 (-2), 299 (+41), 278 (-21), 266 (-15), 254 (-29), 234 (+18), 221 (-30).

Δ -(*S*)-**9**:

¹H NMR (500 MHz, CD₂Cl₂) δ 9.06 (d, $J = 1.8$ Hz, 1H), 8.37 (d, $J = 1.6$ Hz, 1H), 7.93 (d, $J = 8.6$ Hz, 1H), 7.78 (d, $J = 8.6$ Hz, 1H), 7.61 (dd, $J = 7.6, 1.1$ Hz, 1H), 7.58 (dd, $J = 8.6, 1.9$ Hz, 1H), 7.51 (dd, $J = 8.7, 1.9$ Hz, 1H), 7.18 (dd, $J = 7.6, 1.0$ Hz, 1H), 6.95 (td, $J = 7.4, 1.1$ Hz, 1H), 6.92-6.80 (m, 5H), 6.80-6.73 (m, 2H), 6.57 (td, $J = 7.4, 1.0$ Hz, 1H), 6.40 (td, $J = 7.8, 1.4$ Hz, 1H), 6.28 (d, $J = 7.8$ Hz, 1H), 6.24 (d, $J = 8.6$ Hz, 1H), 6.14 (d, $J = 7.8$ Hz, 1H), 5.81 (dd, $J = 11.5, 7.9$ Hz, 1H), 4.30 (t, $J = 9.3$ Hz, 1H), 4.03 (dd, $J = 12.0, 9.4$ Hz, 1H), 3.92 (dd, $J = 12.0, 8.5$ Hz, 1H), 1.37 (s, 9H), 1.23 (s, 9H).

¹³C NMR (125 MHz, CD₂Cl₂) δ 176.5, 176.4 (2C), 174.9 (2C), 169.3, 169.1, 168.7, 168.5, 167.0, 163.0 (d, $J = 254.6$ Hz), 152.5, 151.2, 151.0, 141.0, 140.5, 138.7, 135.2, 133.4, 132.8, 132.7, 130.1, 129.5, 128.7, 128.5, 128.2, 127.6, 127.3, 125.9, 125.6, 124.5, 124.4, 123.0, 122.2, 122.0, 121.9, 119.3 (2C), 118.8, 117.3, 103.7 (d, $J = 8.1$ Hz), 98.4 (d, $J = 22.2$ Hz), 74.9, 70.2, 35.5, 35.4, 31.5, 31.4.

IR (film): ν (cm^{-1}) 2959, 2900, 1618, 1577, 1553, 1530, 1473, 1458, 1436, 1415, 1374, 1292, 1246, 1156, 1092, 1028, 988, 930, 814, 788, 752, 719, 695, 668, 460.

HRMS (ESI, m/z) calcd for $C_{49}H_{44}FN_3O_2RhS_2^+ [M+H]^+$: 892.1909, found: 892.1910.

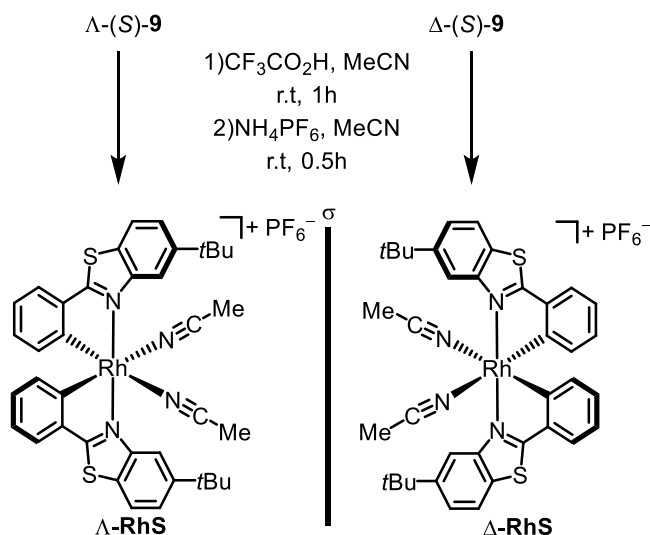
CD {CH₃OH/DCM (4:1)} for Δ -(*S*)-**9**: λ , nm ($\Delta\epsilon$, $M^{-1}cm^{-1}$) 417 (-35), 379 (+33), 362 (+31), 344 (+54), 299 (-58), 274 (+21), 263 (+6), 244 (+36), 233 (-5), 220 (+65).

3) Enantiopure Rhodium Catalysts:

To a suspension of Δ -(*S*)-**9** (178 mg, 0.12 mmol) or Δ -(*S*)-**9** (178 mg, 0.2 mmol) in CH₃CN (5 mL) was added TFA (89 μ L, 1.2 mmol) in one portion, then stirred at room temperature for 0.5 h. The reaction mixture was evaporated to dryness, redissolved in CH₃CN, followed by the addition of excess NH₄PF₆, then stirred at room temperature for another 0.5 h. Afterwards, the reaction mixture was

evaporated to dryness and subjected to a flash chromatography on silica gel. The product was purified as shown below:

- Silica gel flash column chromatography using 200 mL of $\text{CH}_2\text{Cl}_2/\text{CH}_3\text{CN}$ (99/1, vol/vol) with 0.1% of TFA (0.2 mL); then switched to 200 mL $\text{CH}_2\text{Cl}_2/\text{CH}_3\text{CN}$ (95/5, vol/vol) to wash out the residual TFA.
- After the solvent was almost completely used, changed the eluent to first 100 mL of $\text{CH}_2\text{Cl}_2/\text{CH}_3\text{CN}$ (95/5, vol/vol), and then 300 mL of $\text{CH}_2\text{Cl}_2/\text{CH}_3\text{CN}$ (90/10, vol/vol) to elute a purple band which has been characterized as the chiral auxiliary together with some coloured impurities.
- Afterwards, added 326 mg of NH_4PF_6 (2.0 mmol, 10 equiv.) atop the seasand.
- Used 200 mL $\text{CH}_2\text{Cl}_2/\text{CH}_3\text{CN}$ (50/50, vol/vol) to elute residual pale yellow band on the column.
- Collected the pale yellow band, then removed the solvent *in vacuo* to give a pale yellow solid containing desired Δ -**RhS** with a hexafluorophosphate counterion and additional salts.
- Subjected the obtained yellow solid to a thin pad (~1 cm) of silica gel to remove excess salts using 50 mL of $\text{CH}_2\text{Cl}_2/\text{CH}_3\text{CN}$ (99/1, vol/vol) as eluent.
- Collected the filtrate, then removed the solvent *in vacuo* to obtain Δ -**RhS** in 90% yield (155 mg) as a pale yellow solid. Λ -**RhS** can also be obtained using the identical procedure in a 90% yield.



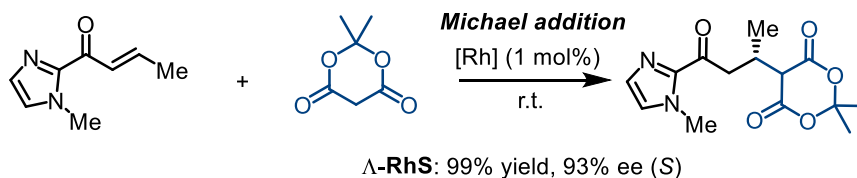
CD (CH_3OH) for Λ -**RhS**: λ , nm ($\Delta\epsilon$, $\text{M}^{-1}\text{cm}^{-1}$) 408 (−45), 368 (+77), 357 (+66), 347 (+65), 300 (−99), 265 (+36), 253 (+36), 240 (+60), 229 (−24), 217 (+83).

CD (CH_3OH) for Δ -**RhS**: λ , nm ($\Delta\epsilon$, $\text{M}^{-1}\text{cm}^{-1}$) 407 (+51), 367 (−79), 360 (−71), 348 (−67), 301 (−107), 262 (−32), 253 (−35), 242 (−68), 231 (+22), 216 (−93).

All other spectroscopic data of Λ -**RhS** and Δ -**RhS** were in agreement with the *rac*-**RhS**.

5.2.2 Rhodium-Catalyzed Asymmetric Reactions

Michael addition reaction:

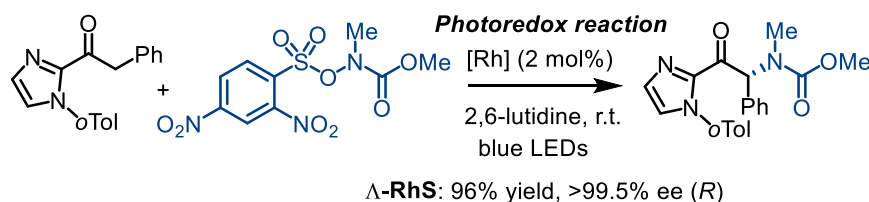


To a solution of catalyst Λ -**RhS** (1.7 mg, 0.002 mmol, 1 mol%) in distilled, anhydrous THF (0.20 mL, 1.0 M) was added the acylimidazole (30.2 mg, 0.20 mmol) in a Schlenk tube. After being stirred at room temperature for 20 min, the nucleophile (86.5 mg, 0.60 mmol) was added at room temperature. The reaction was stirred at room temperature for 16 h under nitrogen atmosphere. Afterwards, the mixture was concentrated under reduced pressure. The residue was purified by flash chromatography on silica gel (EtOAc/*n*-hexane = 1:2 to 2:1) to afford the product (58.0 mg, 99% yield, 93% e.e.). Enantiomeric excess established by HPLC analysis by using a Chiralpak AD-H column, e.e. = 93% (HPLC: AD-H, 254 nm, *n*-hexane/isopropanol = 90:10, flow rate = 0.8 mL/min, 40 °C, t_r (minor) = 24.3 min, t_r (major) = 26.1 min), $[\alpha]_D^{20} = +4.1^\circ$ (c 1.0, CH₂Cl₂).

¹H NMR (300 MHz, CDCl₃) δ 7.13 (d, J = 0.9 Hz, 1H), 7.03 (s, 1H), 4.22-4.16 (m, 1H), 3.98 (s, 3H), 3.56 (dd, J = 7.2, 5.0 Hz, 2H), 3.24-3.10 (m, 1H), 1.77 (d, J = 5.8 Hz, 6H), 1.21 (d, J = 7.0 Hz, 3H).

All other spectroscopic data were in agreement with the literature.^{1b}

Photoredox reaction:



To an oven-dried 10 mL Schlenk tube equipped with a magnetic stir bar was added Λ -**RhS** (3.5 mg, 0.004 mmol, 2 mol%), 2-acyl imidazole (104.8 mg, 0.4 mmol, 2.0 equiv), and the nitrogen reagent (67.0 mg, 0.20 mmol, 1.0 equiv). The Schlenk tube was then degassed by alternative evacuation and back filling with nitrogen. DMSO (0.25 mL), CH₃CN (0.75 mL), and 2,6-lutidine (36.4 mg, 40 μ L, 0.34 mmol, 1.7 equiv) were then added to the Schlenk tube via syringe addition. The resulting clear solution was degassed for 5 min by bubbling nitrogen through the reaction medium. The reaction

mixture was stirred at room temperature and positioned approximately 10 cm from 24 W blue LEDs. 2 hours later, the reaction mixture was concentrated in *vacuo*. The resulting crude oil was purified by flash chromatography on silica gel (EtOAc/ n-hexane = 1:4 to 1:2) to provide the target product (2 hours, 69.7 mg, 0.192 mmol, 96% yield). Enantiomeric excess established by HPLC analysis using a Chiralpak OD-H column, e.e. = 97% (HPLC: OD-H, 254 nm, n-hexane /isopropanol = 85:15, flow rate 1.0 mL/min, 25 °C), t_r (major) = 7.9 min, t_r (minor) = 13.0 min).

^1H NMR (300 MHz, CDCl_3) δ 7.46 -7.17 (m, 10H), 7.17-6.97 (m, 2H), 3.70 (s, 3H), 2.73 and 2.69 (s and s, 3H, contained the rotamer), 2.04 and 1.97 (s and s, 3H, contained the rotamer).

All other spectroscopic data were in agreement with the literature.²

5.2.3 Determination of Enantiomeric Purities of the Rhodium Catalysts

The analysis was performed with a Daicel Chiralpak IB (250 × 4.6 mm) HPLC column on a Shimadzu Lc-2030c HPLC system. The column temperature was 25 °C and UV-absorption was measured at 254 nm. Solvent A = 0.1% TFA in H_2O , solvent B = MeCN.

<Chromatogram>

mV

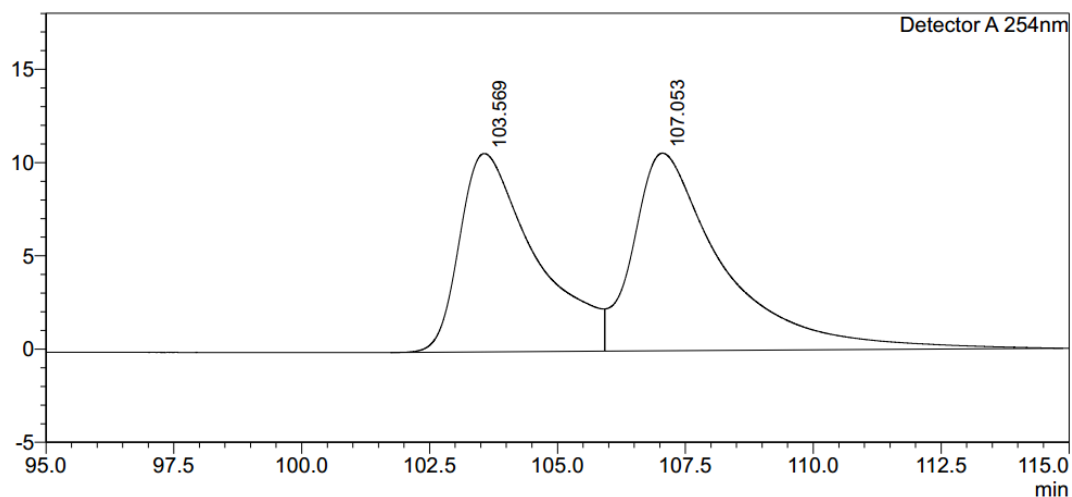


Figure 82. HPLC trace for the racemic reference complexes Δ/Λ -RhS. (Daicel Chiralpak IB, with a linear gradient of 40% to 50% B in 180 min, flow rate = 0.6 mL/min).

<Chromatogram>

mV

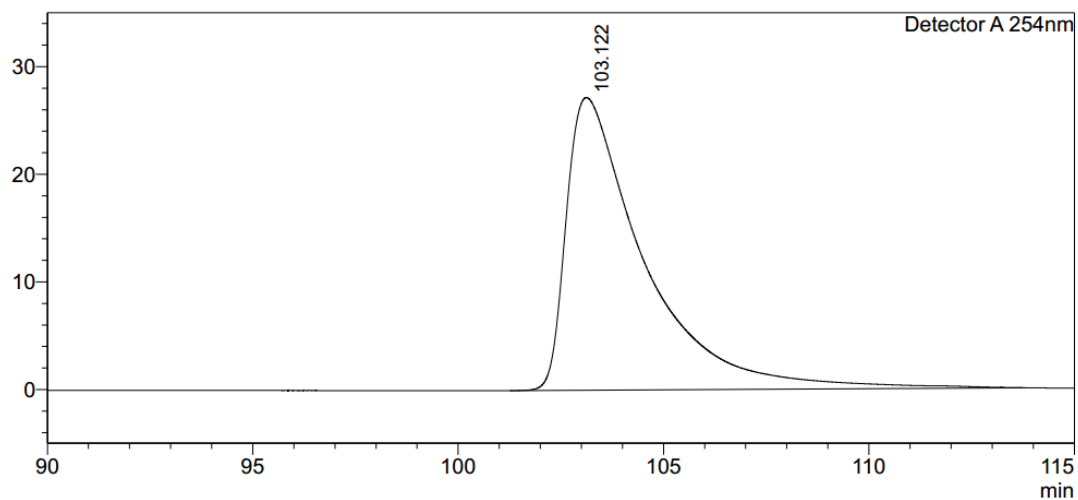
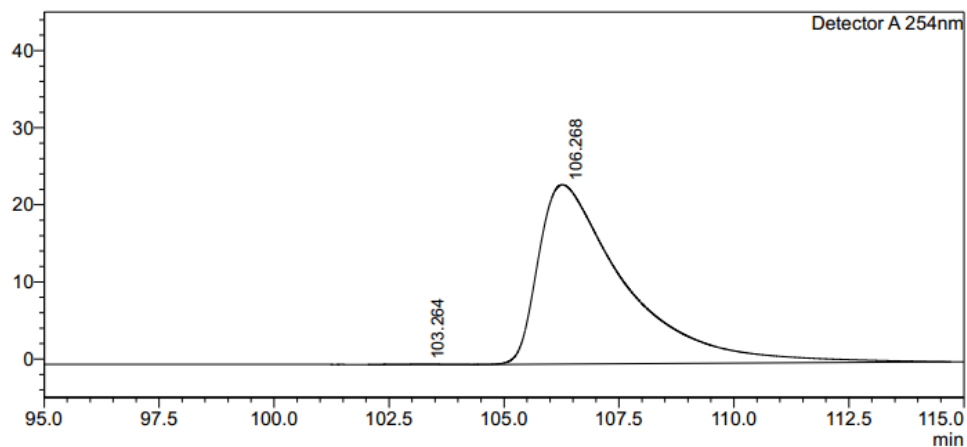


Figure 83. HPLC trace for the complex Δ -RhS. Integration of peak areas > 99% ee.

<Chromatogram>

mV



<Peak Table>

Detector A 254nm

Peak#	Ret. Time	Area	Height	Area%
1	103.264	2809	47	0.092
2	106.268	3037937	23259	99.908
Total		3040746	23306	100.000

Figure 84. HPLC trace for the complex Δ -RhS. Integration of peak areas = 99.8% ee.

5.2.4 Investigation of the Configurational Stability of the Rhodium Catalyst

1) Catalyst Stability Investigated by ^1H NMR

The rhodium complex Λ -**RhS** (20.0 mg) was stored in a brown glass vial and kept on the bench at room temperature. ^1H NMR spectra were recorded after 2, 4, 6, and 8 days.

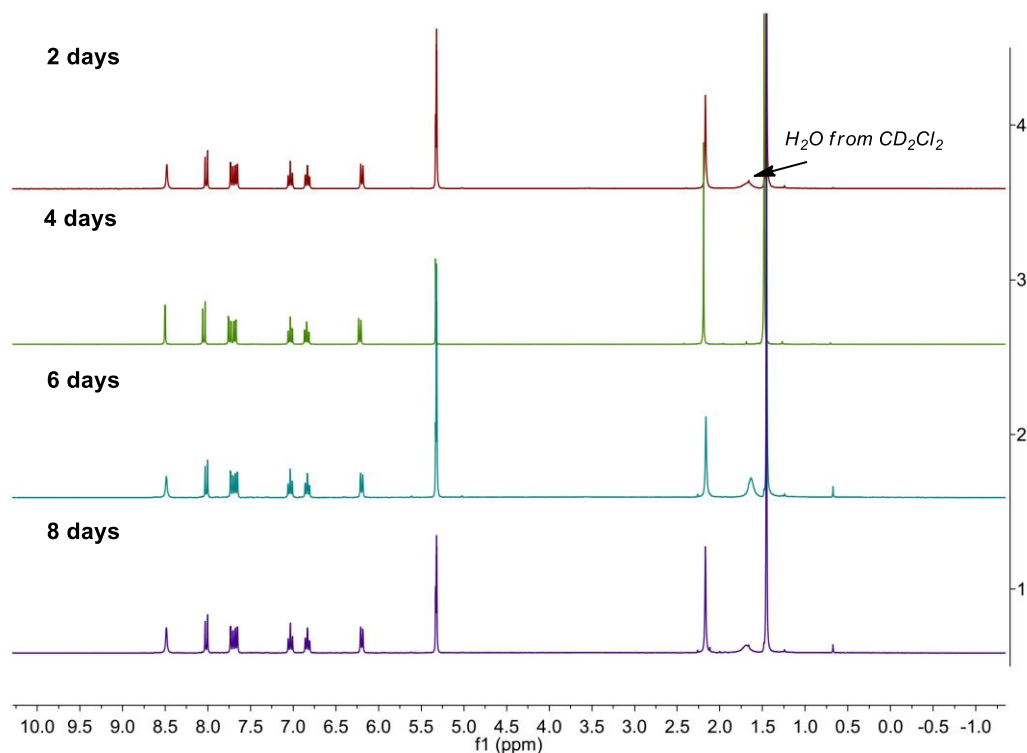


Figure 85. ^1H NMR of Λ -**RhS** recorded in CD_2Cl_2 over 8 days.

2) Catalyst Stability Investigated by HPLC on Chiral Stationary Phase

Enantiopure rhodium complex Λ -**RhS** (20.0 mg) was stored in a brown vial and kept on the bench at room temperature. The HPLC traces were collected after 2, 4, 6 and 8 days. HPLC conditions: Daicel Chiralpak IB (250 \times 4.6 mm) column, the column temperature was 25 $^\circ\text{C}$ and UV-absorption was measured at 254 nm. Solvent A = 0.1% TFA, solvent B = MeCN with a linear gradient of 40% to 50% B in 180 min with a flow rate = 0.6 mL/min.

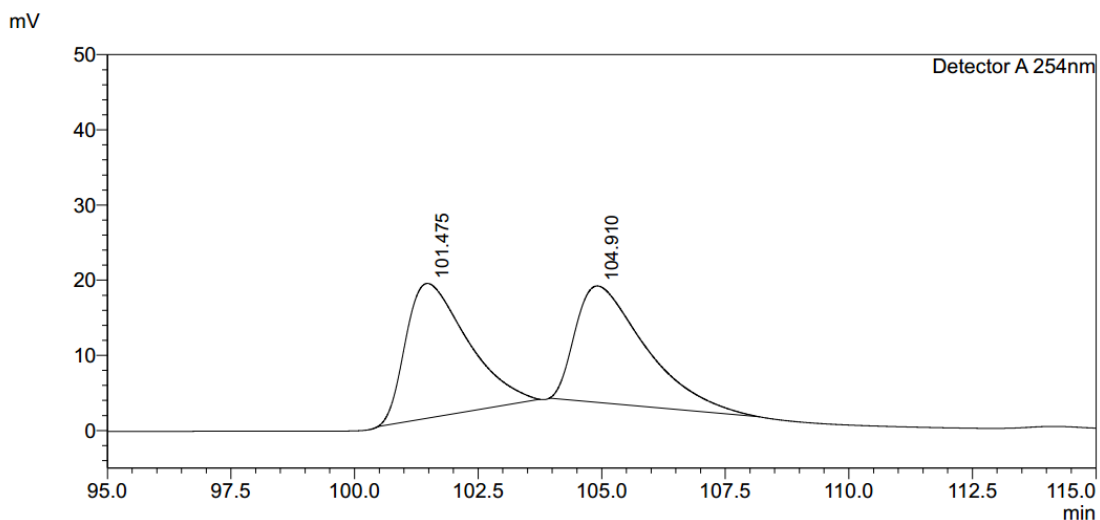
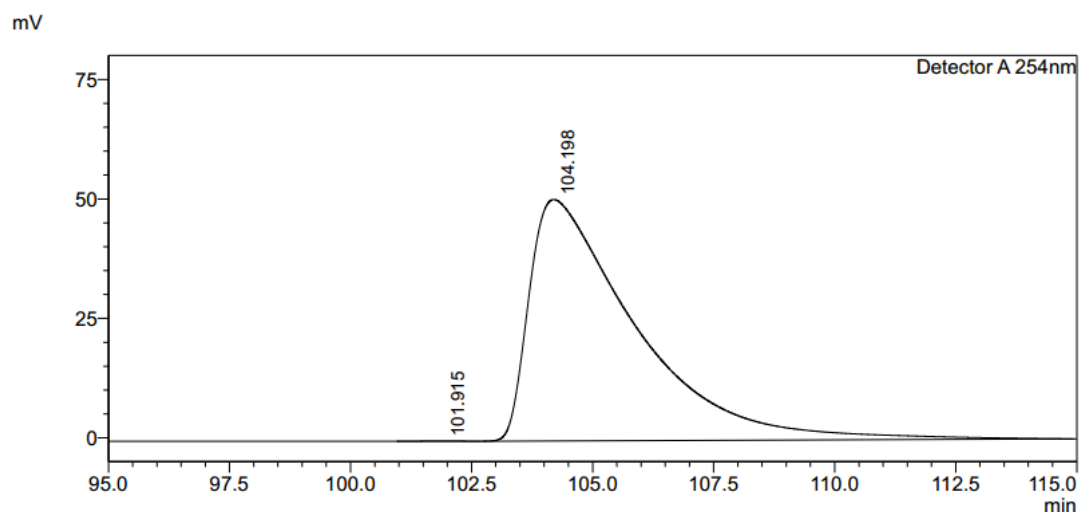


Figure 86. HPLC trace for the racemic reference complexes Δ/Λ -RhS. (Daicel Chiralpak IB, with a linear gradient of 40% to 50% B in 180 min, flow rate = 0.6 mL/min), (the retention time changed compared with former when the HPLC conditions were reproduced).

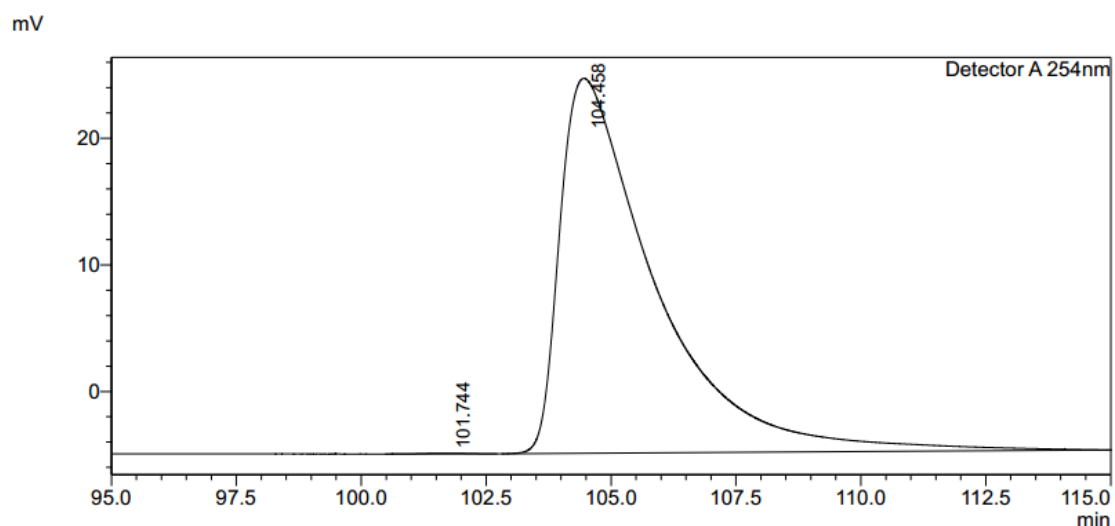


<Peak Table>

Detector A 254nm

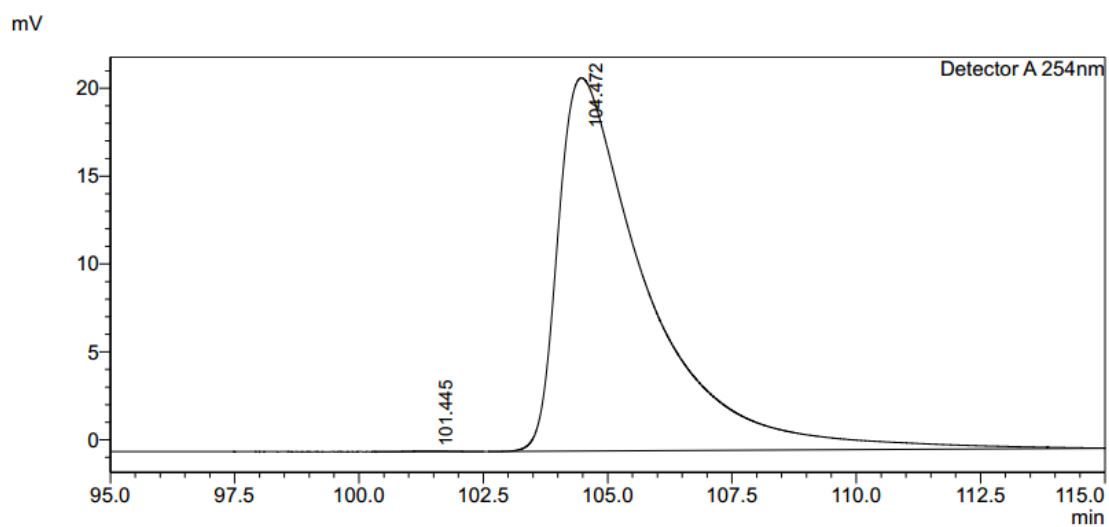
Peak#	Ret. Time	Area	Area%
1	101.915	3119	0.040
2	104.198	7720649	99.960
Total		7723768	100.000

Figure 87. HPLC trace of the freshly prepared Λ -RhS (99.9% ee).

**<Peak Table>**

Detector A 254nm

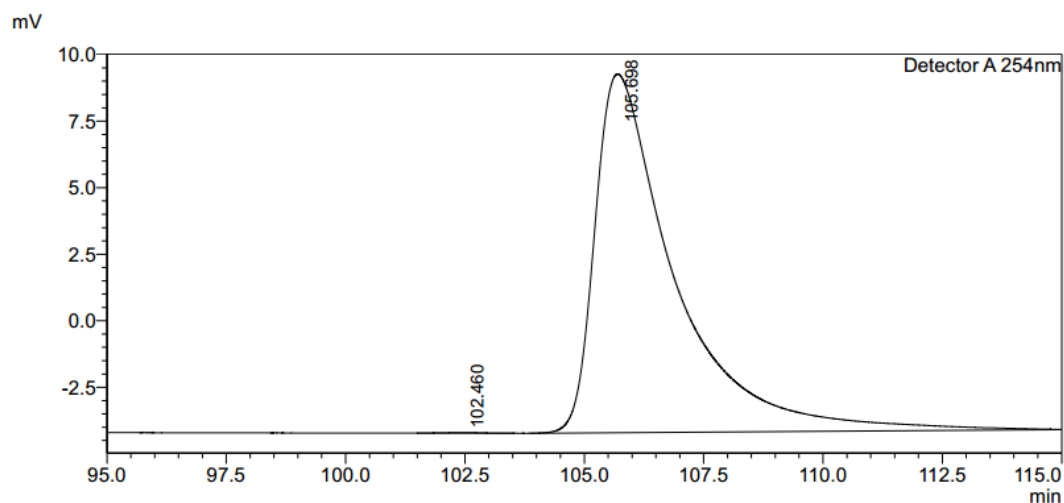
Peak#	Ret. Time	Area	Area%
1	101.744	3485	0.088
2	104.458	3943796	99.912
Total		3947282	100.000

Figure 88. HPLC trace of the Λ -RhS after 2 days (99.8% ee).**<Peak Table>**

Detector A 254nm

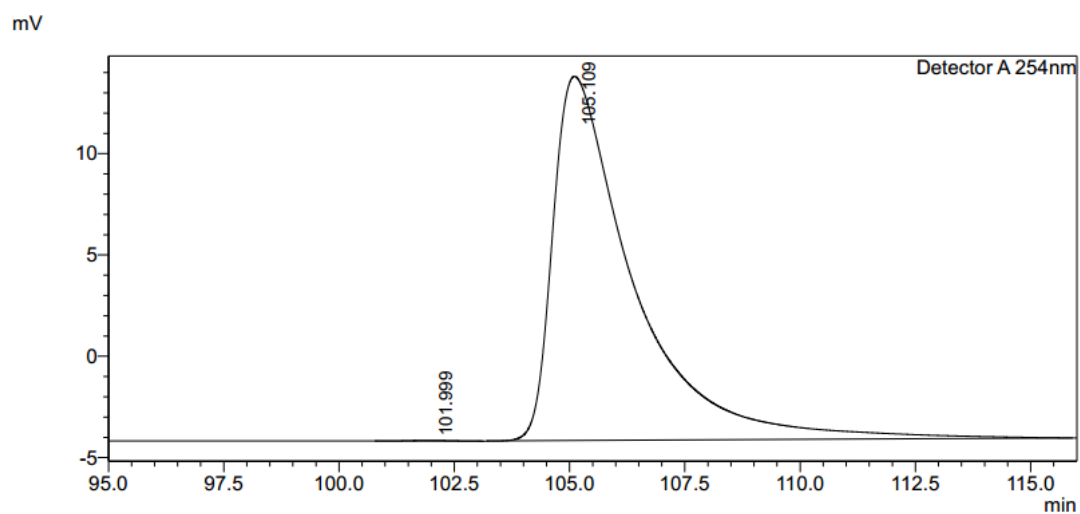
Peak#	Ret. Time	Area	Area%
1	101.445	2766	0.104
2	104.472	2650355	99.896
Total		2653121	100.000

Figure 89. HPLC trace of the Λ -RhS after 4 days (99.8% ee).

**<Peak Table>**

Detector A 254nm			
Peak#	Ret. Time	Area	Area%
1	102.460	1399	0.089
2	105.698	1576676	99.911
Total		1578075	100.000

Figure 90. HPLC trace of the Λ -RhS after 6 days (99.8% ee).

**<Peak Table>**

Detector A 254nm			
Peak#	Ret. Time	Area	Area%
1	101.999	2206	0.101
2	105.109	2191386	99.899
Total		2193592	100.000

Figure 91. HPLC trace of the Λ -RhS after 8 days (99.8% ee).

5.2.5 Single Crystal X-Ray Diffraction Studies

Crystals of Λ -(*S*)-**9** and Λ -**RhS** were obtained by slow diffusion from a solution of the compounds in CH_2Cl_2 layered with *n*-hexane at room temperature for several days.

Crystal data and details of the structure determination are presented in **Table 10**. X-ray data were collected with a Bruker 3 circuit D8 Quest diffractometer with MoKa radiation (microfocus tube with multilayer optics) and Photon 100 CMOS detector at 115 K. Scaling and absorption correction was performed by using the SADABS³ software package of Bruker. Structures were solved using direct methods in SHELXS or SHELXT⁴ and refined using the full matrix least squares procedure in SHELXL-2014⁵. The hydrogen atoms were placed in calculated positions and refined as riding on their respective C atom, and Uiso(H) was set at 1.2 Ueq(Csp²) and 1.5 Ueq(Csp³). Disorder of PF₆ ions, solvent molecules or phenyl and *tert*-butyl groups was refined using restraints for both the geometry and the anisotropic displacement factors.

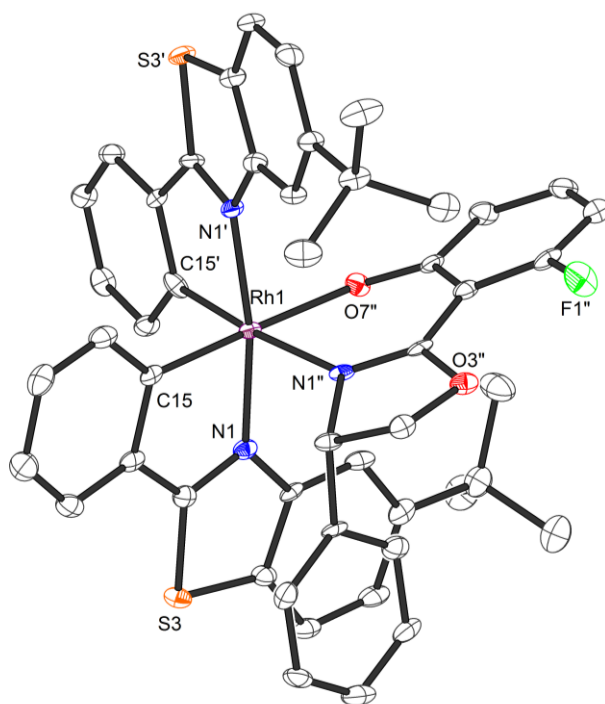


Figure 92. Crystal structure of Λ -(*S*)-**9**. ORTEP drawing with 50 % probability thermal ellipsoids.

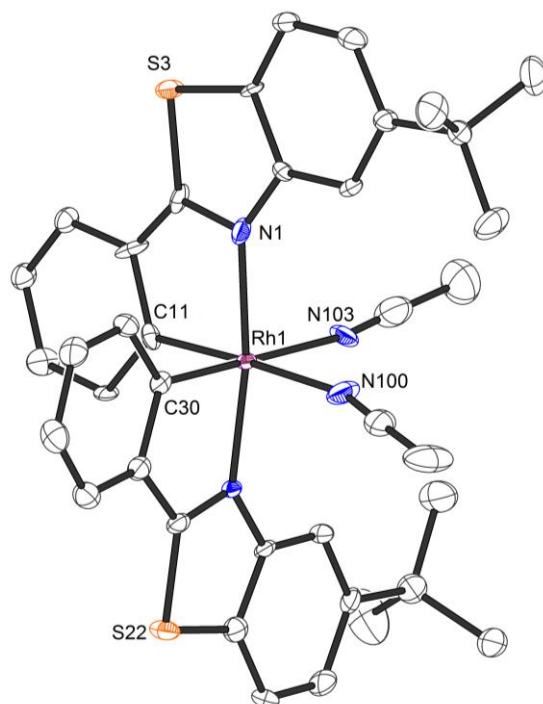


Figure 93. Crystal structure of Λ -RhS. The hexafluorophosphate counteranion and the solvent molecules are omitted for clarity. ORTEP drawing with 50 % probability thermal ellipsoids.

Table 10 Crystal data and details of the structure determination.

	Λ -(S)- 9	Λ - RhS
Empiric formula	C ₄₉ H ₄₃ F N ₃ O ₂ Rh S ₂	C ₄₀ H ₄₂ Cl ₄ F ₆ N ₄ P Rh S ₂
Formula weight	891.89	1032.57
Crystal system, space group	Monoclinic, P2 ₁	Triclinic, P1
<i>a</i> , <i>b</i> , <i>c</i> (Å)	9.9533(7), 13.4582(10), 12.1722(7)	12.3943(5), 13.2600(6), 14.1991(6)
α , β , γ (°)	90, 102.666(2), 90	102.772(2), 104.015(2), 90.825(2)
<i>V</i> (Å ³)	2068.3(3)	2202.41(16)
<i>Z</i>	2	2
μ (mm ⁻¹)	0.563	0.822
Crystal size (mm)	0.15 x 0.13 x 0.06	0.43 x 0.18 x 0.03
<i>T</i> _{min} , <i>T</i> _{max}	0.79, 0.97	0.77, 0.98
No. of measured, independent and observed [<i>I</i> > 2 σ (<i>I</i>)] reflections	11397, 7003, 6335	87967, 15931, 15144
<i>R</i> _{int}	0.0335	0.0483
Goodness-of-fit on <i>F</i> ²	1.035	1.070
R index (all data)	wR2 = 0.0938	wR2 = 0.0915
R index conventional [<i>I</i> > 2 σ (<i>I</i>)]	R1 = 0.0406	R1 = 0.0371
No. of reflections	7003	15931

No. of parameters	529	1133
No. of restraints	1	417
$\Delta\rho_{\max}, \Delta\rho_{\min}$ ($e \text{ \AA}^{-3}$)	1.556, -0.668	2.017, -0.659
Absolute structure parameter	-0.02(2)	0.010(7)
CCDC	1455732	1455731

References

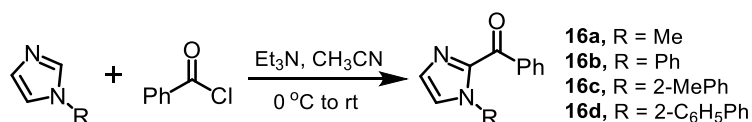
- 1 a) L.-A. Chen, W. Xu, B. Huang, J. Ma, L. Wang, J. Xi, K. Harms, L. Gong, E. Meggers, *J. Am. Chem. Soc.* **2013**, *135*, 10598; b) C. Wang, L.-A. Chen, H. Huo, X. Shen, K. Harms, L. Gong, E. Meggers, *Chem. Sci.* **2015**, *6*, 1094.
- 2 X. Shen, K. Harms, M. Marsch, E. Meggers, *Chem. Eur. J.* **2016**, *22*, 9102.
- 3 *SADABS. Bruker AXS area detector scaling and absorption correction*, Bruker AXS Inc., Madison, Wisconsin, USA, 2014.
- 4 G. M. Sheldrick, *Acta Cryst. A*, **2008**, *64*, 112.
- 5 G. M. Sheldrick, *SHELXT*, Universität Göttingen, Göttingen, Germany, 2014.

5.3 Cooperative Rhodium/Ruthenium Asymmetric Photoredox Catalysis to Access Chiral 1,2-Aminoalcohols

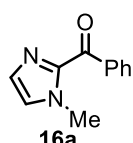
5.3.1 Synthesis of Substrates

1) Synthesis of 2-acyl imidazoles

Method A



General procedure for the preparation of 16a-d with method A. To a mixture of imidazole (2.0 mmol) in CH₃CN (8 mL) was added benzoyl chloride (348 μ L, 3.0 mmol) dropwise at 0 °C, followed by the addition of Et₃N (420 μ L, 3.0 mmol), then stirred at room temperature for 12h. Afterwards, the reaction mixture was poured into H₂O (50 mL), extracted by EtOAc (3 \times 20 mL). The organic layer was collected and dried over anhydrous Na₂SO₄, filtered, then concentrated under reduced pressure. The residue was purified by flash chromatography on silica gel (EtOAc/*n*-hexane = 1:3).



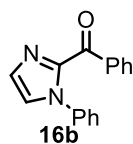
1-Methyl-1*H*-imidazole was converted to 2-acyl imidazole **16a** (316 mg, 1.70 mmol, 85% yield) as a pale yellow oil.

¹H NMR (300 MHz, CDCl₃) δ 8.23-8.21 (m, 2H), 7.50 (tt, J = 7.3, 2.3 Hz, 1H), 7.43-7.39 (m, 2H), 7.15 (d, J = 0.6 Hz, 1H), 7.01 (s, 1H), 3.96 (s, 3H).

¹³C NMR (75 MHz, CDCl₃) δ 183.9, 142.9, 137.1, 132.4, 130.5, 129.0, 127.8, 126.6, 36.1.

IR (film): ν (cm⁻¹) 3107, 3063, 2956, 1706, 1639, 1597, 1507, 1448, 1393, 1292, 1257, 1165, 1077, 999, 935, 897, 770, 735, 681, 651, 618, 554.

HRMS (ESI, m/z) calcd for C₁₁H₁₁N₂O⁺ [M+H]⁺: 187.0866, found: 187.0866.



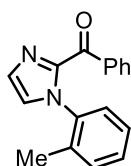
1-Phenyl-1*H*-imidazole was converted to 2-acyl imidazole **16b** (456 mg, 1.84 mmol, 92% yield) as a pale yellow oil.

¹H NMR (300 MHz, CDCl₃) δ 8.28-8.25 (m, 2H), 7.59 (tt, J = 7.3, 2.4 Hz, 1H), 7.51-7.45 (m, 5H), 7.36 (d, J = 0.9 Hz, 1H), 7.35-7.32 (m, 2H), 7.28 (d, J = 0.9 Hz, 1H).

^{13}C NMR (75 MHz, CDCl_3) δ 182.9, 143.2, 138.5, 136.8, 133.0, 130.8, 129.6, 129.1, 128.5, 128.1, 126.3, 125.6.

IR (film): ν (cm^{-1}) 3061, 1647, 1594, 1494, 1445, 1395, 1337, 1302, 1240, 1162, 1100, 1073, 1001, 928, 893, 759, 687, 656, 576, 532.

HRMS (ESI, m/z) calcd for $\text{C}_{16}\text{H}_{13}\text{N}_2\text{O}^+$ $[\text{M}+\text{H}]^+$: 249.1022, found: 249.1023.

**16c**

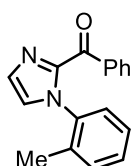
1-(*o*-Tolyl)-1*H*-imidazole was converted to 2-acyl imidazole **16c** (424 mg, 1.62 mmol, 81% yield) as a colorless oil.

^1H NMR (300 MHz, CDCl_3) δ 8.32-8.28 (m, 2H), 7.57 (tt, $J = 7.4, 2.4$ Hz, 1H), 7.50-7.44 (m, 2H), 7.40 (d, $J = 1.0$ Hz, 1H), 7.39-7.27 (m, 3H), 7.22 (dd, $J = 7.6, 1.0$ Hz, 1H), 7.17 (d, $J = 1.0$ Hz, 1H).

^{13}C NMR (75 MHz, CDCl_3) δ 182.6, 143.7, 138.2, 136.7, 134.5, 132.9, 130.9, 130.8, 129.9, 129.0, 128.2, 126.6, 126.4, 126.1, 17.4.

IR (film): ν (cm^{-1}) 3062, 2922, 1646, 1592, 1494, 1447, 1395, 1334, 1300, 1243, 1203, 1161, 1087, 1038, 1002, 930, 894, 762, 688, 658, 551, 458.

HRMS (ESI, m/z) calcd for $\text{C}_{17}\text{H}_{15}\text{N}_2\text{O}^+$ $[\text{M}+\text{H}]^+$: 263.1179, found: 263.1180.

**16d**

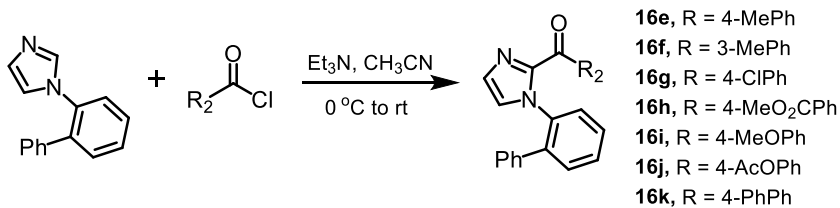
1-([1,1'-Biphenyl]-2-yl)-1*H*-imidazole was converted to 2-acyl imidazole **16d** (640 mg, 1.98 mmol, 99% yield) as a white solid.

^1H NMR (300 MHz, CDCl_3) δ 7.81-7.78 (m, 2H), 7.57-7.47 (m, 5H), 7.34 (t, $J = 7.6$ Hz, 2H), 7.24 (br, 1H), 7.19 (br, 1H), 7.15-7.08 (m, 3H), 7.00-6.96 (m, 2H).

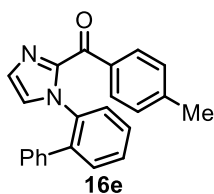
^{13}C NMR (75 MHz, CDCl_3) δ 183.1, 144.1, 138.5, 137.8, 136.4, 136.3, 132.7, 130.9, 130.5, 129.5, 129.0, 128.4, 128.3, 128.2, 127.8, 127.5, 126.4, 126.2.

IR (film): ν (cm^{-1}) 3131, 3061, 1732, 1650, 1590, 1480, 1440, 1402, 1302, 1237, 1159, 1080, 1002, 930, 893, 763, 690, 653, 574, 523, 465.

HRMS (ESI, m/z) calcd for $\text{C}_{22}\text{H}_{16}\text{N}_2\text{NaO}^+$ $[\text{M}+\text{Na}]^+$: 347.1155, found: 347.1156.



General procedure for the preparation of 16e-g with method A. To a mixture of imidazole (220 mg, 1.0 mmol) in CH₃CN (4 mL) was added acyl chloride (1.5 mmol) portionwise at 0 °C, followed by the addition of Et₃N (210 μL, 1.5 mmol), then stirred at room temperature for 12 h. Afterwards, the reaction mixture was poured into H₂O (25 mL), extracted by EtOAc (3 × 20 mL). The organic layer was collected and dried over anhydrous Na₂SO₄, filtered, then concentrated under reduced pressure. The residue was purified by flash chromatography on silica gel (EtOAc/*n*-hexane = 3:1).



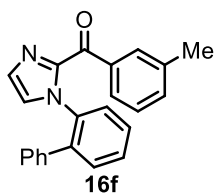
4-Methylbenzoyl chloride was converted to 2-acyl imidazole **16e** (275 mg, 0.82 mmol, 82% yield) as a white solid.

¹H NMR (300 MHz, CDCl₃) δ 7.77-7.73 (m, 2H), 7.56-7.40 (m, 4H), 7.22 (d, *J* = 1.1 Hz, 1H), 7.18-7.08 (m, 6H), 7.02-7.00 (m, 2H), 2.38 (s, 3H).

¹³C NMR (75 MHz, CDCl₃) δ 182.7, 144.2, 143.4, 138.3, 137.8, 136.4, 133.7, 130.7, 130.6, 129.2, 128.9, 128.4, 128.2 (2C), 128.1, 127.4, 126.4, 126.0, 21.6.

IR (film): ν (cm⁻¹) 3131, 3076, 3028, 1650, 1605, 1570, 1503, 1482, 1455, 1434, 1411, 1334, 1304, 1267, 1253, 1182, 1162, 1090, 994, 898, 832, 792, 778, 761, 735, 697, 658, 555, 482, 433.

HRMS (ESI, *m/z*) calcd for C₂₃H₁₈N₂NaO⁺ [M+Na]⁺: 361.1311, found: 361.1311.



3-Methylbenzoyl chloride was converted to 2-acyl imidazole **16f** (326 mg, 0.97 mmol, 97% yield) as a white solid.

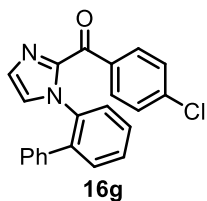
¹H NMR (300 MHz, CDCl₃) δ 7.48 (d, *J* = 7.6 Hz, 1H), 7.43-7.36 (m, 3H), 7.35-7.30 (m, 2H), 7.19 (d, *J* = 8.0 Hz, 1H), 7.14-7.10 (m, 2H), 7.06 (d, *J* = 1.1 Hz, 1H), 7.04-6.96 (m, 3H), 6.89-6.85 (m, 2H), 2.23 (s, 3H).

¹³C NMR (75 MHz, CDCl₃) δ 183.5, 144.3, 138.5, 137.9, 137.4, 136.4 (2C), 133.6, 131.0, 130.9,

129.4, 129.1, 128.4, 128.3 (2C), 127.8, 127.5, 126.5, 126.1, 21.3.

IR (film): ν (cm⁻¹) 3129, 3113, 1646, 1582, 1481, 1456, 1443, 1304, 1271, 1261, 1204, 1151, 1134, 1089, 1010, 942, 833, 778, 766, 736, 706, 698, 674, 584, 560, 536, 430.

HRMS (ESI, m/z) calcd for C₂₃H₁₉N₂O⁺ [M+H]⁺: 339.1492, found: 339.1491.



16g

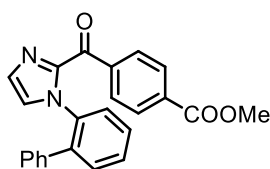
4-Chlorobenzoyl chloride was converted to 2-acyl imidazole **16g** (304 mg, 0.85 mmol, 85% yield) as a pale yellow solid.

¹H NMR (300 MHz, CDCl₃) δ 7.76-7.72 (m, 2H), 7.57-7.50 (m, 2H), 7.48-7.42 (m, 2H), 7.31 (dt, J = 8.8, 2.0 Hz, 2H), 7.24 (d, J = 1.1 Hz, 1H), 7.22 (d, J = 1.1 Hz, 1H), 7.15-7.07 (m, 3H), 7.00-6.93 (m, 2H).

¹³C NMR (75 MHz, CDCl₃) δ 181.6, 143.8, 139.2, 138.4, 137.8, 136.2, 134.6, 131.9, 130.9, 129.6, 129.1, 128.4, 128.3, 128.2, 128.1, 127.5, 126.4, 126.3.

IR (film): ν (cm⁻¹) 3094, 3059, 1656, 1584, 1504, 1482, 1448, 1434, 1409, 1393, 1235, 1168, 1143, 1083, 1007, 926, 899, 870, 827, 795, 734, 697, 683, 655, 592, 538, 499, 477.

HRMS (ESI, m/z) calcd for C₂₂H₁₅ClN₂NaO⁺ [M+Na]⁺: 381.0765, found: 381.0766.



16h

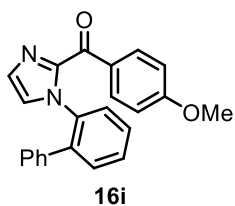
Methyl 4-(chlorocarbonyl)benzoate was converted to 2-acyl imidazole **16h** (305 mg, 0.80 mmol, 80% yield) as a white solid.

¹H NMR (300 MHz, CDCl₃) δ 8.03 (d, J = 8.5 Hz, 2H), 7.83 (d, J = 8.5 Hz, 2H), 7.59-7.53 (m, 2H), 7.51-7.45 (m, 2H), 7.28 (d, J = 2.4 Hz, 2H), 7.19-7.08 (m, 3H), 6.99-6.95 (m, 2H), 3.95 (s, 3H).

¹³C NMR (75 MHz, CDCl₃) δ 182.3, 166.4, 143.7, 139.8, 138.5, 137.8, 136.2, 133.3, 130.9, 130.3, 129.8, 129.2, 128.9, 128.5, 128.4, 128.2, 127.6, 126.6, 126.3, 52.3.

IR (film): ν (cm⁻¹) 3120, 3060, 2948, 1712, 1655, 1569, 1506, 1481, 1436, 1409, 1276, 1231, 1168, 1101, 1007, 924, 895, 865, 820, 776, 743, 700, 647, 613, 534, 495, 462.

HRMS (ESI, m/z) calcd for C₂₄H₁₈N₂NaO₃⁺ [M+Na]⁺: 405.1210, found: 405.1212.



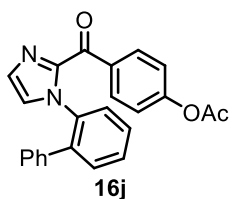
4-Methoxybenzoyl chloride was converted to 2-acyl imidazole **16i** (258 mg, 0.73 mmol, 73% yield) as a pale yellow oil.

^1H NMR (300 MHz, CDCl_3) δ 7.88 (d, $J = 9.0$ Hz, 2H), 7.54-7.40 (m, 4H), 7.20 (d, $J = 0.8$ Hz, 1H), 7.14-7.06 (m, 4H), 7.00-6.97 (m, 2H), 6.84 (d, $J = 8.8$ Hz, 2H), 3.84 (s, 3H).

^{13}C NMR (75 MHz, CDCl_3) δ 181.7, 163.5, 144.4, 138.4, 137.9, 136.5, 133.0, 130.8, 129.2 (2C), 129.0, 128.4, 128.3 (2C), 127.5, 126.5, 125.9, 113.2, 55.4 .

IR (film): ν (cm^{-1}) 3061, 2906, 2935, 1643, 1595, 1507, 1481, 1444, 1399, 1306, 1249, 1154, 1026, 923, 898, 843, 763, 730, 695, 652, 619, 579, 562, 517.

HRMS (ESI, m/z) calcd for $\text{C}_{23}\text{H}_{18}\text{N}_2\text{NaO}_2^+$ $[\text{M}+\text{Na}]^+$: 377.1260, found: 377.1262.



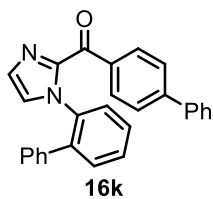
4-(Chlorocarbonyl)phenyl acetate was converted to 2-acyl imidazole **16j** (263 mg, 0.70 mmol, 70% yield) as a pale yellow solid.

^1H NMR (300 MHz, CDCl_3) δ 7.89 (d, $J = 8.7$ Hz, 2H), 7.55-7.40 (m, 4H), 7.20 (d, $J = 10.7$ Hz, 2H), 7.13-7.07 (m, 5H), 6.97-6.94 (m, 2H), 2.29 (s, 3H).

^{13}C NMR (75 MHz, CDCl_3) δ 181.6, 168.6, 154.2, 143.9, 138.4, 137.7, 136.3, 133.7, 132.2, 130.9, 129.4, 129.0, 128.4, 128.3, 128.2, 127.6, 126.4, 126.3, 120.9, 21.1..

IR (film): ν (cm^{-1}) 3120, 3060, 2948, 1712, 1655, 1506, 1481, 1436, 1276, 1231, 1168, 1101, 1007, 924, 896, 866, 821, 777, 744, 700, 647, 613, 534, 495, 462.

HRMS (ESI, m/z) calcd for $\text{C}_{24}\text{H}_{18}\text{N}_2\text{NaO}_3^+$ $[\text{M}+\text{Na}]^+$: 405.1210, found: 405.1212.



[1,1'-Biphenyl]-4-carbonyl chloride was converted to 2-acylimidazole **16k** (293 mg, 0.73 mmol, 73% yield) as a white solid.

^1H NMR (300 MHz, CDCl_3) δ 7.91 (dt, $J = 8.5, 1.8$ Hz, 2H), 7.66-7.58 (m, 4H), 7.56-7.45 (m, 6H),

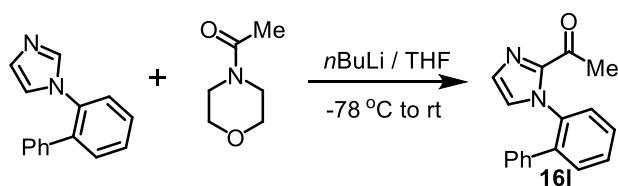
7.41 (dt, $J = 6.1, 1.4$ Hz, 1H), 7.27 (d, $J = 1.1$ Hz, 1H), 7.21 (d, $J = 1.1$ Hz, 1H), 7.18-7.10 (m, 3H), 7.04-7.00 (m, 2H).

^{13}C NMR (75 MHz, CDCl_3) δ 182.6, 145.3, 144.2, 140.2, 138.4, 137.8, 136.4, 135.1, 131.0, 130.8, 129.4, 128.9, 128.8, 128.3 (2C), 128.2, 128.0, 127.5, 127.2, 126.5, 126.4, 126.2.

IR (film): ν (cm^{-1}) 1648, 1598, 1480, 1443, 1402, 1305, 1238, 1166, 1143, 1002, 929, 897, 847, 751, 727, 692, 655, 587, 558, 528, 490.

HRMS (ESI, m/z) calcd for $\text{C}_{28}\text{H}_{21}\text{N}_2\text{O}^+$ $[\text{M}+\text{H}]^+$: 401.1648, found: 401.1651.

Method B



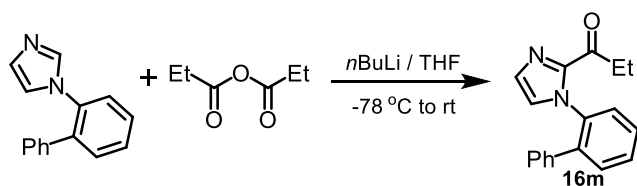
Preparation of 16l with method B. To a solution of imidazole (220 mg, 1.0 mmol) in THF (4 mL) was added $n\text{BuLi}$ (0.48 mL, 2.5 M in n -hexane, 1.2 mmol) at $-78\text{ }^\circ\text{C}$ dropwise. After stirred at this temperature for 1 h, 1-morpholinoethan-1-one (0.13 mL, 1.1 mmol) was added slowly. The reaction mixture was warmed to room temperature gradually, then stirred for another 15 h. Afterwards, the mixture was poured into saturated aqueous solution of NH_4Cl and extracted with EtOAc (3×20 mL). The combined organic layers were dried over anhydrous Na_2SO_4 , filtered, and concentrated under reduced pressure. The residue was purified by flash chromatography on silica gel (EtOAc/ n -hexane = 1:1) to give **16l** (197 mg, 0.75 mmol, 75% yield) as a white solid.

^1H NMR (300 MHz, CDCl_3) δ 7.54-7.32 (m, 3H), 7.32-7.29 (m, 1H), 7.23-7.20 (m, 3H), 7.13 (d, $J = 0.9$ Hz, 1H), 7.05 (d, $J = 0.9$ Hz, 1H), 7.00-6.94 (m, 2H), 2.31 (s, 3H).

^{13}C NMR (75 MHz, CDCl_3) δ 188.8, 143.9, 138.6, 137.8, 136.2, 130.7, 129.3, 129.0, 128.1 (2C), 127.4, 126.8, 126.4, 26.6.

IR (film): ν (cm^{-1}) 3032, 2921, 2851, 1682, 1504, 1483, 1447, 1434, 1403, 1357, 1337, 1304, 1267, 1224, 1158, 1145, 1128, 1101, 1085, 1017, 763, 714, 702, 680, 610, 563, 430.

HRMS (ESI, m/z) calcd for $\text{C}_{17}\text{H}_{15}\text{N}_2\text{O}^+$ $[\text{M}+\text{H}]^+$: 263.1179, found: 263.1180.

Method C

Preparation of 16i with method C. To a solution of imidazole (220 mg, 1.0 mmol) in THF (4 mL) was added *n*BuLi (0.48 mL, 2.5 M in *n*-hexane, 1.2 mmol) at -78 °C dropwise. After stirred at this temperature for 1 h, propionic anhydride (0.16 mL, 1.2 mmol) was added slowly. The reaction mixture was warmed to room temperature gradually, then stirred for another 15 h. Afterwards, the mixture was poured into saturated aqueous solution of Na₂CO₃ and extracted with EtOAc (3 × 20 mL). The combined organic layers were dried over anhydrous Na₂SO₄, filtered, and concentrated under reduced pressure. The residue was purified by flash chromatography on silica gel (EtOAc/*n*-hexane = 1:1) to give **16m** (180 mg, 0.66 mmol, 66% yield) as a colorless oil.

¹H NMR (300 MHz, CDCl₃) δ 7.54-7.42 (m, 3H), 7.34-7.30 (m, 1H), 7.23-7.18 (m, 3H), 7.13 (d, *J* = 1.0 Hz, 1H), 7.07 (d, *J* = 1.1 Hz, 1H), 6.98-6.94 (m, 2H), 2.99-2.85 (m, 1H), 2.63-2.50 (m, 1H), 0.93 (t, *J* = 7.3 Hz, 3H).

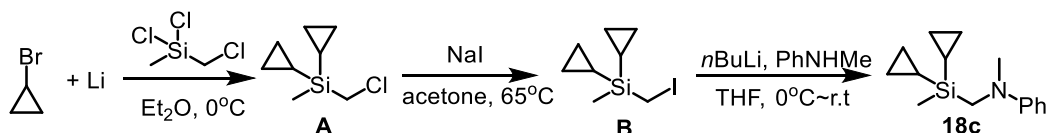
¹³C NMR (75 MHz, CDCl₃) δ 192.1, 143.7, 138.7, 138.0, 136.4, 130.7, 129.2, 129.0, 128.2 (2C), 127.4, 126.5, 126.4, 32.0, 7.7.

IR (film): ν (cm⁻¹) 2975, 2936, 1683, 1505, 1482, 1455, 1446, 1378, 1324, 1303, 1210, 1145, 1075, 1021, 1009, 938, 909, 803, 763, 735, 699, 645, 611, 573, 554, 505.

HRMS (ESI, *m/z*) calcd for C₁₈H₁₇N₂O⁺ [M+H]⁺: 277.1335, found: 277.1335.

2) Synthesis of Aniline Derivatives

The anilines **2a**¹, **2d-g**¹, and **2h-i**² were prepared according to the published procedure.

Preparation of 2b:

Procedure for the preparation of (chloromethyl)dicyclopropyl(methyl)silane (A). To a stirred suspension of granular lithium (278 mg, 40 mmol) in diethyl ether (10 mL) at 0 °C was added a solution of bromocyclopropane (1.60 mL, 20 mmol) in diethyl ether (10 mL) dropwise within 10 min,

and the resulting mixture was stirred at 0 °C for another 60 min. Afterwards, a solution of dichloro(chloromethyl)methylsilane (1.31 mL, 10 mmol) in diethyl ether (5 mL) was added dropwise with 10 min at 0 °C. Subsequently, the reaction mixture was stirred at this temperature for another 45 min, then poured into water (30 mL). The organic phase was separated and the aqueous layer was extracted with diethyl ether (3 × 20 mL). The combined organic extracts were dried over anhydrous Na₂SO₄, filtered, and concentrated under reduced pressure to furnish **A** (1.40 g, 8.0 mmol, 80% yield, > 95% purity judged by ¹H NMR) as a pale yellow oil.

¹H NMR (300 MHz, CDCl₃) δ 2.83 (s, 2H), 0.63-0.57 (m, 4H), 0.35-0.30 (m, 4H), -0.11 (s, 3H), -0.39 (tt, *J* = 9.8, 6.9 Hz, 2H).

All spectroscopic data was in agreement with the literature.³

Procedure for the preparation of dicyclopropyl(iodomethyl)(methyl)silane (B). A suspension of **A** (1.40 g, 8.0 mmol) and NaI (6.01 g, 40 mmol) in acetone (15 mL) was heated at 65 °C for 6h. Afterwards, the reaction mixture was poured into water (100 mL), extracted with diethyl ether (3 × 30 mL). The combined organic extracts were dried over anhydrous Na₂SO₄, filtered, and concentrated under reduced pressure to furnish **B** (1.75 g, 6.56 mmol, 82% yield, >95% purity judged by ¹H-NMR) as a pale yellow oil.

¹H NMR (300 MHz, CDCl₃) δ 2.03 (s, 2H), 0.65-0.58 (m, 4H), 0.34-0.28 (m, 4H), -0.10 (s, 3H), -0.38 (tt, *J* = 9.8, 6.9 Hz, 2H).

¹³C NMR (75 MHz, CDCl₃) δ 1.3, 1.1, -7.3, -7.7, -15.2.

IR (film): ν (cm⁻¹) 3070, 2997, 1287, 1252, 1186, 1099, 1078, 1053, 1032, 896, 822, 790, 773, 784, 722, 690, 661, 516.

Procedure for the preparation of *N*-((dicyclopropyl(methyl)silyl)methyl)-*N*-methylaniline (18c).

To a stirred solution of *N*-methylaniline (0.43 mL, 4.0 mmol) in THF (10 mL) at 0 °C was added *n*BuLi (2.4 mL, 2.5 M in *n*-hexane, 6.0 mmol) dropwise. After stirred at 0 °C for 2 h, **B** (1.28 g, 4.80 mmol) was added to the mixture slowly, and the resulting solution was stirred for another 15 h. The reaction was then quenched by slow addition of a saturated solution of NH₄Cl (15 mL) and extracted with EtOAc (3 × 20 mL). The combined organic extracts were dried over anhydrous Na₂SO₄, filtered, and concentrated under reduced pressure. The residue was subjected to a flash chromatography on

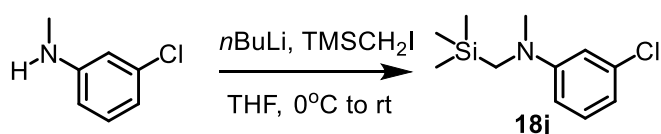
silica gel (EtOAc/*n*-hexane = 1:30) to give **18c** (785 mg, 3.20 mmol, 80% yield) as a pale yellow oil.

^1H NMR (300 MHz, CDCl_3) δ 7.47-7.40 (m, 2H), 6.96-6.93 (m, 2H), 6.85 (tt, $J = 7.3, 0.8$ Hz, 1H), 3.22 (s, 3H), 3.17 (s, 2H), 0.83-0.77 (m, 4H), 0.53-0.50 (m, 4H), 0.00 (s, 3H), -0.23 (tt, $J = 9.8, 6.9$ Hz, 2H).

^{13}C NMR (75 MHz, CDCl_3) δ 150.7, 128.8, 115.0, 111.9, 42.2, 40.2, 1.4, 1.0, -7.1, -8.5.

IR (film): ν (cm^{-1}) 3068, 2996, 2925, 2802, 1597, 1504, 1365, 1286, 1251, 1233, 1192, 1097, 1032, 989, 897, 821, 799, 772, 743, 689, 631, 512, 400.

HRMS (ESI, m/z) calcd for $\text{C}_{15}\text{H}_{24}\text{NSi}^+$ [$\text{M}+\text{H}$] $^+$: 246.1673, found: 246.1673.



Procedure for the preparation of 3-chloro-N-methyl-N-((trimethylsilyl)methyl)aniline (18j**).** To a stirred solution of 3-Chloro-*N*-methylaniline (0.61 mL, 5.0 mmol) in THF (12 mL) at 0°C was added $n\text{BuLi}$ (2.4 mL, 2.5 M in *n*-hexane, 6.0 mmol) dropwise. After stirred at 0°C for 2 h, (Iodomethyl)trimethylsilane (1.11 mL, 7.50 mmol) was added to the mixture slowly, and the resulting solution was stirred for another 15 h. The reaction was then quenched by slow addition of a saturated solution of NH_4Cl (15 mL) and extracted with EtOAc (3×20 mL). The combined organic extracts were dried over anhydrous Na_2SO_4 , filtered, and concentrated under reduced pressure. The residue was subjected to a flash chromatography on silica gel (EtOAc/*n*-hexane = 1:30) to give **18j** (830 mg, 3.64 mmol, 73% yield) as a pale yellow oil.

^1H NMR (300 MHz, CDCl_3) δ 7.10 (t, $J = 8.0$ Hz, 2H), 6.60-6.48 (m, 3H), 2.94 (s, 3H), 2.87 (s, 2H), 0.11 (s, 9H).

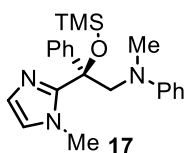
^{13}C NMR (75 MHz, CDCl_3) δ 151.2, 134.9, 129.8, 114.8, 111.4, 109.8, 43.9, 40.1, -1.2.

IR (film): ν (cm^{-1}) 2953, 2894, 2809, 1591, 1557, 1493, 1366, 1247, 1232, 1195, 1099, 986, 837, 753, 680, 661, 443.

HRMS (ESI, m/z) calcd for $\text{C}_{11}\text{H}_{19}\text{ClNSi}^+$ [$\text{M}+\text{H}$] $^+$: 228.0970, found: 228.0970.

5.3.2 Rhodium-Catalyzed Redox Coupling Reactions Activated by Visible Light

General procedure for entries 1-6 of Table 2. A dried 10 mL Schlenk tube was charged with the catalyst Λ -**RhO** (4 mol%) (entries 1-5) or Λ -**IrO** (4 mol%) (entry 6), the photosensitizer [Ru(bpy)₃](PF₆)₂ (0.86 mg, 0.001 mmol, 1 mol%) and the corresponding 2-acyl imidazoles (0.10 mmol, 1.0 eq.). A solution of **2a** (29.0 mg, 0.15 mmol, 1.5 eq.) in MeCN/DMAC (v/v = 4:1, 1 mL) was added in one portion. The reaction mixture was degassed *via* freeze-pump-thaw for three cycles. After the mixture was thoroughly degassed, the vial was sealed and positioned approximately 5 cm from a 23 W compact fluorescent lamp. The reaction was stirred at room temperature for the indicated time (monitored by TLC) under nitrogen atmosphere. Afterwards, the mixture was concentrated under reduced pressure. The residue was redissolved in THF (2 mL), and then TBAF (0.5 mL, 1.0 M in THF, 0.5 mmol) was added (except entry 1). The mixture was stirred at room temperature for another 0.5 h and quenched by the addition of saturated aqueous solution of NH₄Cl, extracted by EtOAc (3 × 10 mL). The combined organic layers were concentrated and subjected to a flash chromatography on silica gel (EtOAc/*n*-hexane = 1:7 to 1:4) to afford the products **17**, **19a-d**. Racemic samples were obtained by carrying out the reactions with *rac*-**RhO**. The enantiomeric excess was determined by chiral HPLC analysis.



As for entry 1, starting from **16a** (18.6 mg, 0.10 mmol) and **18a** (29.0 mg, 0.15 mmol)

according to the general procedure without treating with TBAF to give **17** as a pale yellow oil (27.0 mg, 0.68 mmol, 68% yield). Enantiomeric excess established by HPLC analysis by using a Chiralpak OD-H column, ee = 41% (HPLC: OD-H, 254 nm, *n*-hexane/isopropanol = 95: 5, flow rate 0.5 mL/min, 25 °C, *t_r* (minor) = 9.6 min, *t_r* (major) = 11.2 min); [α]_D²⁰ = +38.0° (*c* 1.0, CH₂Cl₂)

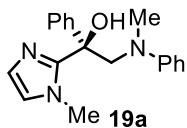
¹H NMR (300 MHz, CD₂Cl₂) δ 7.28-7.23 (m, 2H), 7.19-7.07 (m, 3H), 7.00 (d, *J* = 1.2 Hz, 1H), 6.97-6.90 (m, 2H), 6.82 (d, *J* = 1.1 Hz, 1H), 6.50-6.44 (m, 3H), 4.76 (d, *J* = 15.1 Hz, 1H), 4.02 (d, *J* = 15.1 Hz, 1H), 2.97 (s, 6H), 0.02 (s, 9H).

¹³C NMR (75 MHz, CD₂Cl₂) δ 151.0, 149.5, 144.0, 128.5, 127.9, 127.2, 126.7, 126.4, 123.3, 116.1, 112.8, 79.7, 62.6, 39.4, 34.7.

IR (film): ν (cm⁻¹) 3060, 3025, 2953, 2897, 1598, 1505, 1448, 1403, 1368, 1343, 1279, 1262, 1251,

1195, 1125, 1088, 1064, 1016, 992, 959, 883, 840, 744, 725, 690, 582, 462.

HRMS (ESI, m/z) calcd for $C_{22}H_{30}N_3OSi^+$ $[M+H]^+$: 380.2153, found: 380.2158.



As for entry 2, starting from **16a** (18.6 mg, 0.10 mmol) and **18a** (29.0 mg, 0.15 mmol) according to the general procedure to give **19a** as a pale yellow oil (22.4 mg, 0.729 mmol, 73% yield).

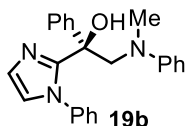
Enantiomeric excess established by HPLC analysis by using a Chiralpak OD-H column, ee = 41% (HPLC: OD-H, 254 nm, *n*-hexane/isopropanol = 95: 5, flow rate 0.5 mL/min, 25 °C, t_r (minor) = 20.4 min, t_r (major) = 15.2 min); $[\alpha]_D^{20} = +50.4^\circ$ (*c* 1.0, CH_2Cl_2)

1H NMR (300 MHz, $CDCl_3$) δ 7.40-7.32 (m, 4H), 7.30-7.19 (m, 3H), 7.01 (d, $J = 1.2$ Hz, 1H), 6.94-6.90 (m, 2H), 6.83-6.78 (m, 2H), 4.82 (d, $J = 14.9$ Hz, 1H), 3.96 (br, 1H), 3.74 (d, $J = 14.9$ Hz, 1H), 3.41 (s, 3H), 2.76 (s, 3H).

^{13}C NMR (75 MHz, $CDCl_3$) δ 152.0, 149.4, 144.3, 129.2, 128.7, 127.5, 126.0, 125.2, 123.1, 118.8, 114.5, 74.7, 65.1, 39.8, 34.4.

IR (film): ν (cm^{-1}) 3059, 2952, 2870, 2758, 1597, 1503, 1448, 1407, 1346, 1279, 1256, 1174, 1145, 1123, 1092, 1064, 1031, 991, 966, 938, 900, 745, 730, 696, 645, 589, 562, 470.

HRMS (ESI, m/z) calcd for $C_{19}H_{22}N_3O^+$ $[M+H]^+$: 308.1757, found: 308.1753.



As for entry 3, starting from **16b** (24.8 mg, 0.10 mmol) and **18a** (29.0 mg, 0.15 mmol) according to the general procedure to give **19b** as a white solid (27.0 mg, 0.740 mmol, 74% yield).

Enantiomeric excess established by HPLC analysis by using a Chiralpak AD-H column, ee = 82% (HPLC: AD-H, 254 nm, *n*-hexane/isopropanol = 90: 10, flow rate 1.0 mL/min, 25 °C, t_r (minor) = 14.0 min, t_r (major) = 9.9 min); $[\alpha]_D^{20} = +56.6^\circ$ (*c* 1.0, CH_2Cl_2)

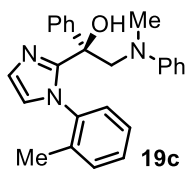
1H NMR (300 MHz, CD_2Cl_2) δ 7.26-7.18 (m, 6H), 7.17-7.12 (m, 4H), 7.11 (d, $J = 1.2$ Hz, 1H), 6.97 (d, $J = 1.3$ Hz, 1H), 6.89-6.83 (m, 4H), 6.73 (tt, $J = 7.3, 0.8$ Hz, 1H) 4.78 (d, $J = 14.9$ Hz, 1H), 3.75 (d, $J = 14.9$ Hz, 1H), 3.54 (br, 1H), 2.70 (s, 3H).

^{13}C NMR (75 MHz, CD_2Cl_2) δ 152.3, 150.4, 145.2, 139.2, 129.2, 128.5, 128.4, 128.2, 127.7, 127.3, 126.7, 125.6, 124.4, 118.4, 114.4, 75.6, 65.5, 39.7.

IR (film): ν (cm^{-1}) 3059, 3025, 2870, 2729, 1597, 1496, 1446, 1352, 1302, 1253, 1175, 1138, 1122,

1096, 1065, 1031, 990, 937, 897, 746, 727, 689, 595, 538, 514.

HRMS (ESI, m/z) calcd for $C_{24}H_{23}N_3NaO^+$ $[M+Na]^+$: 392.1733, found: 392.1732.



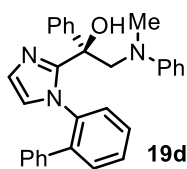
As for entry 4, starting from **16c** (26.2 mg, 0.10 mmol) and **18a** (29.0 mg, 0.15 mmol) according to the general procedure to give **19c** as a white solid (28.0 mg, 0.73 mmol, 73% yield). Enantiomeric excess established by HPLC analysis by using a Chiralpak OD-H column, ee = 88% (HPLC: OD-H, 254 nm, *n*-hexane/isopropanol = 95: 5, flow rate 0.5 mL/min, 25 °C, t_r (minor) = 12.3 min, t_r (major) = 13.7 min); $[\alpha]_D^{20} = +70.2^\circ$ (c 1.0, CH_2Cl_2).

1H NMR (300 MHz, $CDCl_3$, mixture of rotamers) δ 7.32-7.28 (m, 1H), 7.57 (tt, $J = 7.3, 1.3$ Hz, 0.8 H), 7.47 (tt, $J = 7.7, 1.4$ Hz, 0.2 H, other rotamer), 7.42-7.30 (m, 1H), 7.36-7.25 (m, 1H), 7.24-7.21 (m, 2H), 7.20-7.18 (m, 3H), 7.17-7.15 (m, 2H), 7.15-7.12 (m, 1H), 6.92-6.83 (m, 2H), 6.82-6.74 (m, 2H), 6.12 (d, $J = 7.8$ Hz, 0.8 H, other rotamer), 4.92 (d, $J = 14.7$ Hz, 0.8 H), 4.78 (d, $J = 14.7$ Hz, 0.2 H, other rotamer), 3.83 (d, $J = 2.7$ Hz, 0.8 H), 3.78 (d, $J = 2.8$ Hz, 0.2 H, other rotamer), 2.56 (br, 0.8 H), 2.51 (br, 0.2 H, other rotamer), 2.72 (s, 2.4 H), 2.64 (s, 0.6 H, other rotamer), 2.08 (s, 2.4 H), 2.06 (s, 0.6 H, other rotamer).

^{13}C NMR (125 MHz, CD_2Cl_2 , mixture of rotamers) δ 152.4 (2C), 150.3, 150.2, 145.4, 144.3, 138.5, 138.0, 136.5, 135.8, 130.5, 130.3, 129.9, 129.2, 128.8 (2C), 128.5, 128.2, 128.1, 127.5, 127.1, 126.9, 126.7, 125.9, 125.7, 123.8, 123.6, 118.7, 118.5, 114.6, 115.5, 75.5, 75.2, 66.0, 65.4, 39.6, 17.6, 17.0.

IR (film): ν (cm^{-1}) 3058, 3025, 2924, 2855, 1598, 1495, 1446, 1351, 1301, 1253, 1175, 1139, 1120, 1093, 1064, 1032, 991, 938, 848, 747, 721, 693, 674, 645, 602, 547, 516, 456.

HRMS (ESI, m/z) calcd for $C_{25}H_{26}N_3O^+$ $[M+H]^+$: 384.2070, found: 384.2071.



As for entry 5, starting from **16d** (32.4 mg, 0.10 mmol) and **18a** (29.0 mg, 0.15 mmol) according to the general procedure to give **19d** as a white solid (32.0 mg, 0.072 mmol, 72% yield). Enantiomeric excess established by HPLC analysis by using a Chiralpak OD-H column, ee = 93% (HPLC: OD-H, 254 nm, *n*-hexane/isopropanol = 95: 5, flow rate 0.5 mL/min, 25 °C, t_r (minor) = 15.8 min, t_r (major) = 13.3 min).

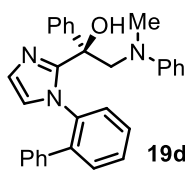
^1H NMR (300 MHz, CDCl_3) δ 7.46-7.26 (m, 9H), 7.24-7.16 (m, 3H), 7.12-6.98 (m, 3H), 6.87-6.74 (m, 4H), 6.67 (d, $J = 1.1$ Hz, 1H), 6.39 (d, $J = 7.8$ Hz, 1H), 4.70 (d, $J = 14.8$ Hz, 1H), 3.72 (d, $J = 14.8$ Hz, 1H), 3.50 (br, 1H), 2.66 (s, 3H).

^{13}C NMR (75 MHz, CDCl_3) δ 151.6, 149.8, 145.0, 138.8, 138.7, 137.1, 130.3, 128.9, 128.6, 128.3 (2C), 128.2, 128.1, 127.3, 127.2, 127.1, 126.3, 125.0, 124.2, 118.4, 114.2, 75.4, 65.2, 39.1.

IR (film): ν (cm^{-1}) 3060, 3020, 1596, 1572, 1502, 1485, 1447, 1436, 1356, 1341, 1327, 1255, 1182, 1097, 1068, 1031, 1008, 992, 958, 940, 909, 767, 751, 732, 699, 672, 547, 463.

HRMS (ESI, m/z) calcd for $\text{C}_{30}\text{H}_{27}\text{N}_3\text{NaO}^+$ $[\text{M}+\text{Na}]^+$: 468.2046, found: 468.2047.

General procedure for entries 7 and 10 of Table 2. A dried 10 mL Schlenk tube was charged with the catalyst Λ -IrO (3.70 mg, 0.004 mmol, 4 mol%) (entry 7) or Λ -RhS (3.50 mg, 0.004 mmol, 4 mol%) (entry 10) and the 2-acyl imidazole **16d** (32.4 mg, 0.10 mmol, 1.0 eq.). A solution of **18a** (29.0 mg, 0.15 mmol, 1.5 eq.) in MeCN/DMAC (v/v = 4:1, 1 mL) was added in one portion. The reaction mixture was degassed *via* freeze-pump-thaw for three cycles. After the mixture was thoroughly degassed, the vial was sealed and positioned approximately 5 cm from a 23 W compact fluorescent lamp. The reaction was stirred at room temperature for 24 h or 20 h under nitrogen atmosphere. Afterwards, the mixture was concentrated under reduced pressure. The residue was redissolved in THF (2 mL), then TBAF (0.5 mL, 1.0 M in THF, 0.5 mmol) was added. The mixture was stirred at room temperature for another 0.5 h and quenched by the addition of saturated aqueous solution of NH_4Cl , extracted by EtOAc (3×10 mL). The combined organic layers were concentrated. The conversion was determined by the crude ^1H NMR analysis.



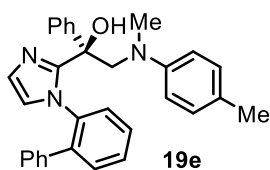
As for entry 7, starting from **16d** (32.4 mg, 0.10 mmol) and **18a** (29.0 mg, 0.15 mmol) according to the general procedure to give **19d** as a white solid (19.0 mg, 0.430 mmol, 43% yield). Enantiomeric excess established by HPLC analysis by using a Chiralpak OD-H column, ee = 3% (HPLC: OD-H, 254 nm, *n*-hexane/isopropanol = 95: 5, flow rate 0.5 mL/min, 25 °C, t_r (minor) = 15.1 min, t_r (major) = 13.3 min).

General procedure for entries 8-9 and 11 of Table 2. A dried 10 mL Schlenk tube was charged with

the catalyst Λ -**RhS** (3.50 mg, 0.004 mmol, 4 mol%), the photosensitizer [Ru(bpy)₃](PF₆)₂ (0.86 mg, 0.001 mmol, 1 mol%) and 2-acyl imidazole **16d** (32.4 mg, 0.10 mmol, 1.0 eq.). A solution of **18a-b** (0.15 mmol, 1.5 eq.) in MeCN/DMAC (v/v = 4:1, 1 mL) was added in one portion. The reaction mixture was degassed *via* freeze-pump-thaw for three cycles. After the mixture was thoroughly degassed, the vial was sealed and positioned approximately 5 cm from a 23 W compact fluorescent lamp (the catalytic reaction of entry 8 was conducted in the dark). The reaction was stirred at room temperature for the indicated time (monitored by TLC) under nitrogen atmosphere. Afterwards, the mixture was concentrated under reduced pressure. The residue was redissolved in THF (2 mL), then TBAF (0.5 mL, 1.0 M in THF, 0.5 mmol) was added. The mixture was stirred at room temperature for another 0.5 h and quenched by the addition of saturated aqueous solution of NH₄Cl, extracted by EtOAc (3 × 10 mL). The combined organic layers were concentrated. The conversion was determined by the crude ¹H NMR analysis. If the product was detected in the crude ¹H NMR, the residue was subjected to a flash chromatography on silica gel (EtOAc/*n*-hexane = 1:7 to 1:4) to afford the products **19d**. The enantiomeric excess was determined by chiral HPLC analysis.

As for entry 8, starting from **1d** (32.4 mg, 0.10 mmol) and **2a** (29.0 mg, 0.15 mmol) according to the general procedure to give **3d** as a white solid (33.8 mg, 0.760 mmol, 76% yield). Enantiomeric excess established by HPLC analysis by using a Chiralpak OD-H column, ee = 95% (HPLC: OD-H, 254 nm, *n*-hexane/isopropanol = 95: 5, flow rate 0.5 mL/min, 25 °C, t_r (minor) = 15.1 min, t_r (major) = 13.3 min); [α]_D²⁰ = -6.6° (*c* 1.0, CH₂Cl₂).

General procedure for Figure 44. A dried 10 mL Schlenk tube was charged with the catalyst Λ -**RhS** (5.2 mg, 0.0060 mmol, 4 mol%), the photosensitizer $[\text{Ru}(\text{bpy})_3](\text{PF}_6)_2$ (1.30 mg, 0.0015 mmol, 1 mol%) and 2-acyl imidazole **16d** (48.6 mg, 0.150 mmol, 1.0 eq.). A solution of **18d** (0.45 mmol, 3.0 eq.) or **18e-i** (0.225 mmol, 1.5 eq.) in MeCN/DMAC (v/v = 4:1, 1.5 mL) was added in one portion. The reaction mixture was degassed *via* freeze-pump-thaw for three cycles. After the mixture was thoroughly degassed, the vial was sealed and positioned approximately 5 cm from a 23 W compact fluorescent lamp. The reaction was stirred at room temperature for the indicated time (monitored by TLC) under nitrogen atmosphere. Afterwards, the mixture was concentrated under reduced pressure. The residue was redissolved in THF (2 mL), then TBAF (1.0 mL, 1.0 M in THF, 1.0 mmol) was added. The mixture was stirred at room temperature for another 0.5 h and quenched by the addition of saturated aqueous solution of NH_4Cl , extracted by EtOAc (3 \times 10 mL). The combined organic layers were concentrated. The residue was subjected to a flash chromatography on silica gel (EtOAc/*n*-hexane = 1:7 to 1:4) to afford the products **19e-j**. The enantiomeric excess was determined by chiral HPLC analysis.



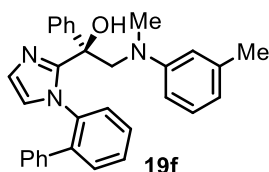
Starting from **16d** (48.9 mg, 0.15 mmol) and **18d** (93.2 mg, 0.45 mmol) with Λ -**RhS** for 5 h according to the general procedure to give **19e** as a pale yellow oil (55.0 mg, 0.120 mmol, 80% yield). Enantiomeric excess established by HPLC analysis by using a Chiralpak AD-H column, ee = 98% (HPLC: AD-H, 254 nm, *n*-hexane/isopropanol = 90: 10, flow rate 1.0 mL/min, 25 °C, t_r (minor) = 9.9 min, t_r (major) = 6.0 min); $[\alpha]_{\text{D}}^{20} = -24.0^\circ$ (c 1.0, CH_2Cl_2).

^1H NMR (500 MHz, CD_2Cl_2) δ 7.42-7.32 (m, 6H), 7.30-7.22 (m, 6H), 7.07 (td, J = 8.3, 2.3 Hz, 1H), 6.98 (d, J = 8.5 Hz, 2H), 6.91 (d, J = 0.8 Hz, 1H), 6.73 (d, J = 8.7 Hz, 2H), 6.63 (d, J = 1.0 Hz, 1H), 6.35 (d, J = 7.9 Hz, 1H), 4.63 (d, J = 14.7 Hz, 1H), 3.73 (br, 1H), 3.58 (d, J = 14.7 Hz, 1H), 2.62 (s, 3H), 2.22 (s, 3H).

^{13}C NMR (125 MHz, CD_2Cl_2) δ 150.2, 145.8, 139.2, 139.0, 137.5, 130.6, 129.7, 128.8, 128.7, 128.6, 128.5 (2C), 128.2, 128.1, 127.6, 127.5, 126.4, 125.8, 125.4, 124.5, 114.9, 75.5, 66.4, 39.4, 20.3.

IR (film): ν (cm^{-1}) 3059, 3028, 2924, 2860, 1615, 1599, 1517, 1483, 1446, 1352, 1303, 1252, 1177, 1139, 1117, 1097, 1068, 806, 765, 739, 699, 526, 514, 450, 410, 391.

HRMS (ESI, m/z) calcd for $C_{31}H_{30}N_3O^+$ $[M+H]^+$: 460.2383, found: 460.2385.



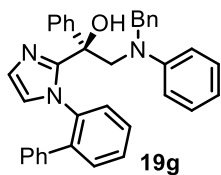
Starting from **16d** (48.9 mg, 0.15 mmol) and **28g** (46.6 mg, 0.225 mmol) with Λ -**RhS** for 10 h according to the general procedure to give **19f** as a pale yellow oil (56.0 mg, 0.122 mmol, 81% yield). Enantiomeric excess established by HPLC analysis by using a Chiralpak AD-H column, ee = 97% (HPLC: AD-H, 254 nm, *n*-hexane/isopropanol = 90: 10, flow rate 1.0 mL/min, 25 °C, t_r (minor) = 6.8 min, t_r (major) = 6.0 min); $[\alpha]_D^{20} = -30.4^\circ$ (*c* 1.0, CH_2Cl_2).

1H NMR (500 MHz, CD_2Cl_2) δ 7.41-7.33 (m, 6H), 7.31-7.23 (m, 6H), 7.08-7.06 (m, 1H), 7.04 (d, $J = 7.8$ Hz, 1H), 6.92 (d, $J = 1.0$ Hz, 1H), 6.64-6.60 (m, 3H), 6.58 (d, $J = 7.4$ Hz, 1H), 6.33 (d, $J = 7.7$ Hz, 1H), 4.65 (d, $J = 14.7$ Hz, 1H), 3.66 (d, $J = 14.7$ Hz, 1H), 3.56 (s, 1H), 2.64 (s, 3H), 2.25 (s, 3H).

^{13}C NMR (125 MHz, CD_2Cl_2) δ 152.2, 150.1, 145.7, 139.1, 139.0, 138.9, 137.5, 130.6, 129.0, 128.8, 128.7, 128.6, 128.5, 127.6, 127.5 (2C), 126.4, 125.4, 124.5, 119.6, 115.3, 111.7, 75.8, 65.8, 39.4, 21.9.

IR (film): ν (cm^{-1}) 3058, 2922, 2859, 2811, 1601, 1581, 1494, 1482, 1352, 1303, 1257, 1172, 1139, 1095, 1067, 1030, 1009, 995, 961, 945, 841, 764, 737, 698, 675, 610, 559, 446.

HRMS (ESI, m/z) calcd for $C_{31}H_{30}N_3O^+$ $[M+H]^+$: 460.2383, found: 460.2386.



Starting from **16d** (48.9 mg, 0.15 mmol) and **18f** (60.6 mg, 0.225 mmol) with Λ -**RhS** for 10 h according to the general procedure to give **19g** as a pale white solid (61.0 mg, 0.117 mmol, 78% yield). Enantiomeric excess established by HPLC analysis by using a Chiralpak OD-H column, ee = 93% (HPLC: OD-H, 254 nm, *n*-hexane/isopropanol = 90: 10, flow rate 0.5 mL/min, 25 °C, t_r (minor) = 11.2 min, t_r (major) = 10.0 min); $[\alpha]_D^{20} = -5.2^\circ$ (*c* 1.0, CH_2Cl_2).

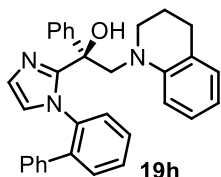
1H NMR (500 MHz, CD_2Cl_2) δ 7.44 (dd, $J = 7.6, 1.6$ Hz, 1H), 7.42 (dd, $J = 7.3, 0.8$ Hz, 1H), 7.38-7.36 (m, 2H), 7.32-7.28 (m, 6H), 7.24-7.21 (m, 5H), 7.19-7.18 (m, 1H), 7.12 (t, $J = 7.3$ Hz, 2H), 7.07 (td, $J = 7.9, 1.7$ Hz, 1H), 7.01 (d, $J = 7.2$ Hz, 2H), 6.97 (s, 1H), 6.79 (d, $J = 8.2$ Hz, 2H), 6.67 (d, $J = 1.0$ Hz, 1H), 6.35 (d, $J = 7.7$ Hz, 1H), 4.89 (d, $J = 15.0$ Hz, 1H), 4.47 (d, $J = 17.3$ Hz, 1H), 4.09 (d, $J = 17.3$ Hz, 1H), 4.04 (d, $J = 15.0$ Hz, 1H), 3.31 (br, 1H).

^{13}C NMR (125 MHz, $CDCl_3$) δ 149.7 (2C), 144.9, 138.9, 138.6, 137.7, 136.8, 130.4, 128.9, 128.7,

128.4, 128.3 (2C), 128.1, 127.4, 127.3, 127.2, 126.7, 126.4, 126.3, 125.3, 125.1, 124.2, 118.1, 114.5, 76.1, 62.3, 53.5.

IR (film): ν (cm⁻¹) 3060, 3027, 2930, 1964, 1598, 1503, 1483, 1450, 1384, 1450, 1384, 1360, 1303, 1265, 1231, 1197, 1138, 1070, 990, 767, 748, 728, 697, 675, 608, 557, 535, 512, 458.

HRMS (ESI, m/z) calcd for C₃₆H₃₂N₃O⁺ [M+H]⁺: 522.2540, found: 522.2545.



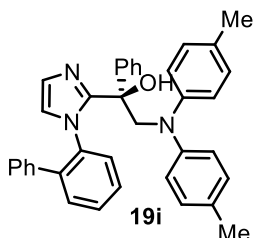
Starting from **16d** (48.9 mg, 0.15 mmol) and **18g** (49.4 mg, 0.225 mmol) with Λ -**RhS** for 15 h according to the general procedure to give **19h** as a pale yellow oil (49.0 mg, 0.105 mmol, 70% yield). Enantiomeric excess established by HPLC analysis by using a Chiralpak OD-H column, ee = 95% (HPLC: OD-H, 254 nm, *n*-hexane/isopropanol = 90: 10, flow rate 0.5 mL/min, 25 °C, t_r (minor) = 12.0 min, t_r (major) = 8.8 min); $[\alpha]_D^{20} = -17.4^\circ$ (c 1.0, CH₂Cl₂).

¹H NMR (500 MHz, CD₂Cl₂) δ 7.43-7.33 (m, 6H), 7.32-7.23 (m, 6H), 7.04 (td, $J = 7.8, 1.7$ Hz, 1H), 6.94-6.90 (m, 3H), 6.70 (d, $J = 8.5$ Hz, 1H), 6.66-6.60 (m, 2H), 6.27 (d, $J = 7.9$ Hz, 1H), 4.69 (d, $J = 14.8$ Hz, 1H), 3.64 (d, $J = 14.8$ Hz, 1H), 3.59 (br, 1H), 3.19-3.14 (m, 1H), 3.00-2.82 (m, 1H), 2.77-2.66 (m, 2H), 1.84-1.77 (m, 1H), 1.75-1.70 (m, 1H).

¹³C NMR (125 MHz, CD₂Cl₂) δ 149.9, 147.5, 145.6, 138.8, 138.5, 137.0, 130.3, 129.3, 128.5, 128.3 (2C), 128.2, 128.1, 127.3, 127.2, 127.1, 126.7, 126.0, 125.0, 124.1 (2C), 117.8, 114.0, 75.2, 64.7, 51.1, 28.0, 22.0.

IR (film): ν (cm⁻¹) 3060, 3023, 2929, 2841, 1671, 1600, 1575, 1493, 1482, 1444, 1343, 1326, 1301, 1191, 1171, 1137, 1097, 1063, 763, 739, 697, 675, 647, 563, 440.

HRMS (ESI, m/z) calcd for C₃₂H₃₀N₃O⁺ [M+H]⁺: 472.2383, found: 472.2386.



Starting from **16d** (48.9 mg, 0.15 mmol) and **18h** (63.9 mg, 0.225 mmol) with

Λ -**RhS** for 5 h according to the general procedure to give **19i** as a pale yellow solid (68.0 mg, 0.128 mmol, 85% yield). Enantiomeric excess established by HPLC analysis by using a Chiralpak OD-H column, ee = 91% (HPLC: OD-H, 254 nm, *n*-hexane/isopropanol = 90: 10, flow rate 0.5 mL/min,

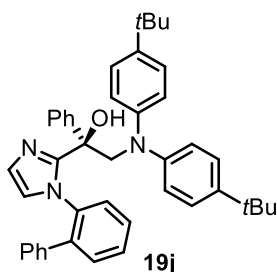
25 °C, t_r (minor) = 8.9 min, t_r (major) = 8.4 min); $[\alpha]_D^{20} = +11.6^\circ$ (c 1.0, CH_2Cl_2).

^1H NMR (500 MHz, CD_2Cl_2) δ 7.40-7.34 (m, 2H), 7.31-7.24 (m, 5H), 7.23-7.19 (m, 5H), 7.00 (td, $J = 8.1, 2.0$ Hz, 1H), 6.91 (d, $J = 8.3$ Hz, 4H), 6.77 (d, $J = 0.9$ Hz, 1H), 6.60 (d, $J = 8.3$ Hz, 4H), 6.57 (d, $J = 0.8$ Hz, 1H), 6.19 (d, $J = 7.8$ Hz, 1H), 4.98 (d, $J = 15.2$ Hz, 1H), 4.40 (d, $J = 15.2$ Hz, 1H), 3.39 (s, 1H), 2.22 (s, 6H).

^{13}C NMR (125 MHz, CD_2Cl_2) δ 149.3, 147.2, 144.6, 138.6, 138.5, 136.5, 131.2, 130.1, 129.3, 129.2, 128.3, 128.1, 127.9, 127.7, 127.1, 126.8, 126.7, 125.7, 125.1, 123.6, 121.7, 76.1, 64.0, 20.0.

IR (film): ν (cm^{-1}) 3057, 3026, 2977, 2858, 1687, 1507, 1482, 1439, 1341, 1302, 1264, 1172, 1137, 1101, 1069, 1010, 880, 811, 764, 736, 697, 676, 581, 565, 530, 444.

HRMS (ESI, m/z) calcd for $\text{C}_{37}\text{H}_{34}\text{N}_3\text{O}^+$ $[\text{M}+\text{H}]^+$: 536.2696, found: 536.2699.



Starting from **16d** (48.9 mg, 0.15 mmol) and **18i** (82.6 mg, 0.225 mmol) with Λ -**RhS** for 30 h according to the general procedure to give **19j** as a white solid (64.0 mg, 0.104 mmol, 69% yield). Enantiomeric excess established by HPLC analysis by using a Chiralpak IA column, ee = 93% (HPLC: IA, 254 nm, *n*-hexane/isopropanol = 95: 5, flow rate 0.3 mL/min, 25 °C, t_r (minor) = 18.3 min, t_r (major) = 20.3 min); $[\alpha]_D^{20} = +24.6^\circ$ (c 1.0, CH_2Cl_2).

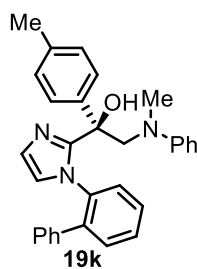
^1H NMR (300 MHz, CDCl_3 , mixture of two rotamers) δ 7.45-7.35 (m, 2H), 7.33-7.24 (m, 4H), 7.23-7.11 (m, 7H), 7.10 (br, 2H), 7.04-6.95 (m, 2H), 6.78 (d, $J = 1.2$ Hz, 1H), 6.75-6.66 (m, 4H), 6.58 (br, 1H), 6.19 (d, $J = 7.6$ Hz, 1H), 5.02 (d, $J = 15.4$ Hz, 0.2 H), 4.92 (d, $J = 15.1$ Hz, 0.8 H, other rotamer), 4.47 (d, $J = 15.1$ Hz, 0.8 H), 4.15 (d, $J = 14.8$ Hz, 0.2 H, other rotamer), 3.44 (br, 0.8 H), 3.27 (br, 0.2 H, other rotamer), 1.17 (s, 18H).

^{13}C NMR (75 MHz, CDCl_3) δ 149.6, 146.9, 144.7, 144.5, 138.9, 138.7, 136.7, 130.3, 128.6, 128.5, 128.4, 128.1, 127.8, 127.7, 127.6, 127.3, 126.9, 126.8, 126.5, 126.1, 126.0, 125.7, 125.4, 123.7, 121.5, 75.9, 64.3, 34.0, 31.4.

IR (film): ν (cm^{-1}) 3058, 2959, 2902, 2865, 1603, 1509, 1483, 1445, 1393, 1363, 1303, 1266, 1201, 1172, 1138, 1100, 1068, 1011, 882, 826, 766, 736, 697, 677, 656, 609, 583, 571, 556.

HRMS (ESI, m/z) calcd for $\text{C}_{43}\text{H}_{46}\text{N}_3\text{O}^+$ $[\text{M}+\text{H}]^+$: 620.3635, found: 620.3643.

General procedure for Figure 45. A dried 10 mL Schlenk tube was charged with the catalyst Λ -**RhS** (5.20 mg, 0.0060 mmol, 4 mol%), the photosensitizer [Ru(bpy)₃](PF₆)₂ (1.30 mg, 0.0015 mmol, 1 mol%) and 2-acyl imidazole **16e-m** (0.150 mmol, 1.0 eq.). A solution of **18a** (87.0 mg, 0.450 mmol, 3.0 eq.) or **18j** (103 mg, 0.450 mmol, 3.0 eq.) in MeCN/DMAC (v/v = 4:1, 1 mL) was added in one portion. The reaction mixture was degassed *via* freeze-pump-thaw for three cycles. After the mixture was thoroughly degassed, the vial was sealed and positioned approximately 5 cm from a 23 W compact fluorescent lamp. The reaction was stirred at room temperature for the indicated time (monitored by TLC) under nitrogen atmosphere. Afterwards, the mixture was concentrated under reduced pressure. The residue was redissolved in THF (2 mL), then TBAF (1.0 mL, 1.0 M in THF, 1.0 mmol) was added. The mixture was stirred at room temperature for another 0.5 h and quenched by the addition of saturated aqueous solution of NH₄Cl, extracted by EtOAc (3 × 10 mL). The combined organic layers were concentrated. The residue was subjected to a flash chromatography on silica gel (EtOAc/*n*-hexane = 1:7 to 1:4) to afford the products **19k-s**. The enantiomeric excess was determined by chiral HPLC analysis.



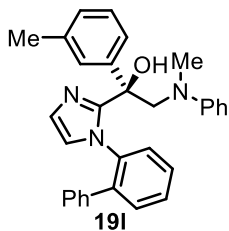
Starting from **16e** (50.7 mg, 0.15 mmol) and **18a** (87.4 mg, 0.45 mmol) with Λ -**RhS** for 5h according to the general procedure to give **19k** as a white solid (51.6 mg, 0.113 mmol, 75% yield). Enantiomeric excess established by HPLC analysis by using a Chiralpak OD-H column, ee = 98% (HPLC: OD-H, 254 nm, *n*-hexane/isopropanol = 95: 5, flow rate 0.5 mL/min, 25 °C, *t_r* (minor) = 14.8 min, *t_r* (major) = 10.6 min); [α]_D²⁰ = -40.0° (*c* 1.0, CH₂Cl₂).

¹H NMR (500 MHz, CD₂Cl₂, mixture of rotamers) δ 7.41-7.37 (m, 2H), 7.30-7.20 (m, 6H), 7.19-7.14 (m, 4H), 7.10-7.07 (m, 1H), 6.92 (d, *J* = 1.0 Hz, 1H), 6.81 (d, *J* = 8.2 Hz, 2H), 6.74 (t, *J* = 7.3 Hz, 1H), 6.64 (d, *J* = 0.9 Hz, 1H), 6.41 (d, *J* = 7.8 Hz, 1H), 4.63 (d, *J* = 14.7 Hz, 0.8 H), 4.46 (d, *J* = 14.7 Hz, 0.2 H, other rotamer), 3.64 (d, *J* = 14.7 Hz, 1H), 3.42 (br, 0.8 H), 3.32 (br, 0.2 H, other rotamer), 2.66 (s, 2.4 H), 2.56 (s, 0.6 H, other rotamer), 2.36 (s, 2.4 H), 2.28 (s, 0.6 H, other rotamer).

¹³C NMR (125 MHz, CD₂Cl₂) δ 152.2, 150.2, 142.6, 139.1, 139.0, 137.6, 137.3, 130.6, 129.3, 129.1, 128.8, 128.7, 128.6, 128.5, 127.6, 127.5, 126.4, 125.3, 124.5, 118.5, 114.4, 75.9, 65.7, 39.2, 21.1.

IR (film): ν (cm⁻¹) 3059, 3026, 2921, 2867, 2813, 1598, 1503, 1482, 1438, 1411, 1351, 1303, 1252, 1172, 1139, 1113, 1088, 1034, 992, 952, 927, 915, 816, 765, 735, 695, 559, 469.

HRMS (ESI, m/z) calcd for C₃₁H₃₀N₃O⁺ [M+H]⁺: 460.2383, found: 460.2387.



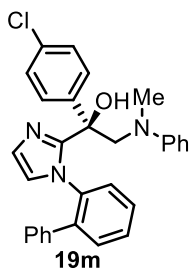
Starting from **16f** (50.7 mg, 0.15 mmol) and **18a** (87.4 mg, 0.45 mmol) with Λ -**RhS** for 5h according to the general procedure to give **19i** as a white solid (55.0 mg, 0.12 mmol, 80% yield). Enantiomeric excess established by HPLC analysis by using a Chiralpak OD-H column, ee = 97% (HPLC: OD-H, 254 nm, *n*-hexane/isopropanol = 90: 10, flow rate 0.5 mL/min, 25 °C, t_r (minor) = 11.7 min, t_r (major) = 10.3 min); $[\alpha]_D^{20} = -18.2^\circ$ (*c* 1.0, CH₂Cl₂).

¹H NMR (500 MHz, CD₂Cl₂, mixture of rotamers) δ 7.40-7.38 (m, 2H), 7.28-7.20 (m, 5H), 7.18-7.04 (m, 6H), 6.92 (d, $J = 0.7$ Hz, 1H), 6.81 (d, $J = 8.1$ Hz, 2H), 6.74 (t, $J = 7.3$ Hz, 1H), 6.64 (d, $J = 0.9$ Hz, 1H), 6.38 (d, $J = 7.9$ Hz, 1H), 4.65 (d, $J = 14.8$ Hz, 0.8 H), 4.52 (d, $J = 14.3$ Hz, 0.2 H, other rotamer), 3.67 (d, $J = 14.7$ Hz, 1H), 3.46 (br, 0.8 H), 3.43 (br, 0.2 H, other rotamer), 2.66 (s, 2.4 H), 2.56 (s, 0.6 H, other rotamer), 2.33 (s, 2.4 H), 2.21 (s, 0.6 H, other rotamer).

¹³C NMR (75 MHz, CD₂Cl₂) δ 152.2, 150.1, 145.5, 139.1, 139.0, 138.4, 137.5, 130.6, 129.1, 128.9, 128.7, 128.6, 128.5 (2C), 128.3, 128.1, 127.6, 127.4, 126.4, 126.0, 124.5, 122.5, 118.5, 114.4, 75.8, 65.7, 39.3, 21.7.

IR (film): ν (cm⁻¹) 3055, 3025, 2920, 2861, 1598, 1503, 1482, 1438, 1350, 1303, 1256, 1180, 1034, 992, 942, 788, 747, 736, 695, 676, 649, 609, 556, 514, 438.

HRMS (ESI, m/z) calcd for C₃₁H₃₀N₃O⁺ [M+H]⁺: 460.2383, found: 460.2386.



Starting from **16g** (53.8 mg, 0.15 mmol) and **18a** (87.4 mg, 0.45 mmol) with Λ -**RhS** for 5h according to the general procedure to give **19m** as a white solid (63.2 mg, 0.13 mmol, 88% yield). Enantiomeric excess established by HPLC analysis by using a Chiralpak OD-H column, ee = 93% (HPLC: OD-H, 254 nm, *n*-hexane/isopropanol = 90: 10, flow rate 1.0 mL/min, 25 °C, t_r (minor)

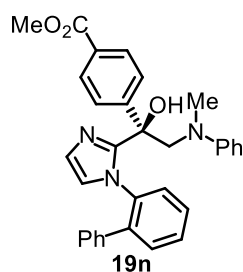
= 6.5 min, t_r (major) = 5.0 min); $[\alpha]_D^{20} = +11.4^\circ$ (c 1.0, CH_2Cl_2).

^1H NMR (500 MHz, CD_2Cl_2) δ 7.44-7.43 (m, 2H), 7.37-7.31 (m, 4H), 7.29-7.23 (m, 5H), 7.22-7.19 (m, 3H), 7.17-7.12 (m, 1H), 7.01 (d, $J = 1.2$ Hz, 1H), 6.82-6.80 (m, 3H), 6.72 (d, $J = 1.2$ Hz, 1H), 6.45 (d, $J = 7.8$ Hz, 1H), 4.67 (d, $J = 14.8$ Hz, 1H), 3.63 (d, $J = 14.8$ Hz, 1H), 3.54 (s, 1H), 2.64 (s, 3H).

^{13}C NMR (125 MHz, CDCl_3) δ 151.5, 149.3, 143.5, 138.8, 138.6, 136.9, 133.1, 130.4, 129.0 (2C), 128.8, 128.4, 128.3, 128.0, 127.4, 127.2, 126.5, 126.4, 124.4, 118.7, 114.3, 75.0, 65.2, 39.0.

IR (film): ν (cm^{-1}) 3137, 2923, 2853, 1652, 1583, 1568, 1504, 1481, 1445, 1434, 1395, 1341, 1305, 1280, 1256, 1233, 1165, 1141, 1084, 1011, 928, 872, 794, 755, 737, 721, 695, 653, 612, 593, 550, 497, 427.

HRMS (ESI, m/z) calcd for $\text{C}_{30}\text{H}_{27}\text{ClN}_3\text{O}^+$ $[\text{M}+\text{H}]^+$: 480.1837, found: 480.1835.



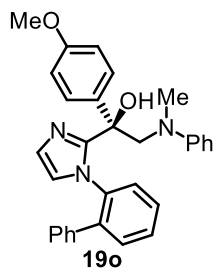
Starting from **16h** (57.3 mg, 0.15 mmol) and **18a** (87.4 mg, 0.45 mmol) with Λ -**RhS** for 5h according to the general procedure to give **19n** as a white solid (59.1 mg, 0.118 mmol, 79% yield). Enantiomeric excess established by HPLC analysis by using a Chiralpak OD-H column, $ee = 54\%$ (HPLC: OD-H, 254 nm, n -hexane/isopropanol = 90: 10, flow rate 1.0 mL/min, 25 °C, t_r (minor) = 6.1 min, t_r (major) = 4.8 min); $[\alpha]_D^{20} = -6^\circ$ (c 1.0, CH_2Cl_2).

^1H NMR (500 MHz, CD_2Cl_2 , mixture of rotamers) δ 8.00 (d, $J = 8.4$ Hz, 2H), 7.76 (d, $J = 8.1$ Hz, 2H, other rotamer), 7.48 (d, $J = 8.4$ Hz, 2H), 7.43-7.38 (m, 2H), 7.37-7.31 (m, 1H), 7.23-7.20 (m, 3H), 7.19-7.16 (m, 2H), 7.09-7.06 (m, 1H), 7.02 (br, 1H), 6.81 (t, $J = 8.2$ Hz, 1H), 6.82-6.76 (m, 3H), 6.70 (br, 1H), 6.34 (d, $J = 7.8$ Hz, 1H), 4.71 (d, $J = 15.0$ Hz, 0.8 H), 4.51 (d, $J = 14.8$ Hz, 0.2 H, other rotamer), 3.93 (s, 3H), 3.65 (d, $J = 14.6$ Hz, 1H), 3.60 (br, 1H), 2.60 (s, 2.4 H), 2.57 (s, 0.6 H, other rotamer).

^{13}C NMR (125 MHz, CDCl_3) δ 167.0, 151.6, 149.2, 139.0, 138.7, 136.9, 130.5, 129.8, 129.3, 129.1, 129.0, 128.4 (2C), 128.0, 127.5, 127.4, 126.5, 125.5, 125.2, 124.6, 118.9, 114.4, 75.3, 65.2, 52.2, 39.2.

IR (film): ν (cm^{-1}) 2953, 2897, 2807, 1722, 1599, 1504, 1441, 1410, 1362, 1275, 1246, 1186, 1106, 846, 743, 693, 516.

HRMS (ESI, m/z) calcd for $\text{C}_{32}\text{H}_{29}\text{N}_3\text{NaO}_3^+$ $[\text{M}+\text{Na}]^+$: 526.2101, found: 526.2101.



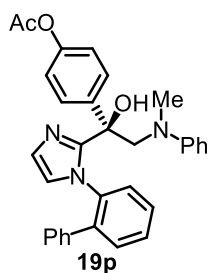
Starting from **16i** (53.1 mg, 0.15 mmol) and **18a** (87.4 mg, 0.45 mmol) with Λ -**RhS** for 15h according to the general procedure to give **19o** as a white solid (50.5 mg, 0.106 mmol, 71% yield). Enantiomeric excess established by HPLC analysis by using a Chiralpak OD-H column, ee = 86% (HPLC: OD-H, 254 nm, *n*-hexane/isopropanol = 90: 10, flow rate 1.0 mL/min, 25 °C, t_r (minor) = 7.5 min, t_r (major) = 5.8 min); $[\alpha]_D^{20} = -33^\circ$ (*c* 1.0, CH₂Cl₂).

¹H NMR (500 MHz, CD₂Cl₂, mixture of rotamers) δ 7.44-7.38 (m, 2H), 7.33-7.22 (m, 6H), 7.17 (dd, *J* = 7.3, 1.3 Hz, 2H), 7.11-7.08 (m, 1H), 7.00-6.90 (m, 3H), 6.83-6.80 (m, 3H), 6.74 (t, *J* = 7.3 Hz, 1H), 6.64 (d, *J* = 0.9 Hz, 1H), 6.41 (d, *J* = 7.9 Hz, 1H), 4.66 (d, *J* = 14.8 Hz, 0.8 H), 4.52 (d, *J* = 14.4 Hz, 0.2 H, other rotamer), 3.76 (s, 2.4 H), 3.67 (d, *J* = 14.8 Hz, 1H), 3.65 (s, 0.6 H, other rotamer), 3.50 (br, 1H), 2.66 (s, 2.4 H), 2.58 (s, 0.6 H, other rotamer).

¹³C NMR (125 MHz, CDCl₃) δ 159.8, 151.8, 149.7, 146.9, 138.8, 137.1, 130.3, 129.3, 128.8, 128.5, 128.3, 128.2, 127.3, 127.1, 126.1, 124.2, 118.3, 117.4, 114.1, 112.7, 110.5, 75.3, 65.3, 55.2, 38.9.

IR (film): ν (cm⁻¹) 3059, 2925, 2862, 1599, 1503, 1445, 1413, 1352, 1301, 1246, 1172, 1085, 1031, 951, 828, 737, 695, 559, 521, 470.

HRMS (ESI, *m/z*) calcd for C₃₁H₂₉N₃NaO₂⁺ [M+Na]⁺: 498.2152, found: 498.2148.



Starting from **16j** (57.3 mg, 0.15 mmol) and **18a** (87.4 mg, 0.45 mmol) with Λ -**RhS** for 15h according to the general procedure to give **19p** as a pale yellow oil (60.4 mg, 0.120 mmol, 80% yield). Enantiomeric excess established by HPLC analysis by using a Chiralpak OD-H column, ee = 96% (HPLC: OD-H, 254 nm, *n*-hexane/isopropanol = 90: 10, flow rate 1.0 mL/min, 25 °C, t_r (minor) = 9.4 min, t_r (major) = 7.2 min); $[\alpha]_D^{20} = -40^\circ$ (*c* 1.0, CH₂Cl₂).

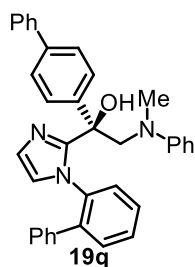
¹H NMR (500 MHz, CDCl₃, mixture of rotamers) 7.44-7.40 (m, 3H), 7.34-7.32 (m, 1H), 7.28-7.19 (m, 6H), 7.16-7.10 (m, 1H), 7.09-7.06 (m, 2H), 7.00 (br, 1H), 6.88-6.74 (m, 4H), 6.70 (d, *J* = 1.1 Hz, 1H),

6.45 (d, $J = 7.9$ Hz, 1H), 4.70 (d, $J = 14.7$ Hz, 0.75 H), 4.45 (d, $J = 14.1$ Hz, 0.25 H, other rotamer), 3.67 (d, $J = 14.8$ Hz, 1H), 3.57 (br, 1H), 2.66 (s, 2.25 H), 2.60 (s, 0.75 H, other rotamer), 2.34 (s, 2.25 H), 2.31 (s, 0.75 H, other rotamer).

^{13}C NMR (125 MHz, CDCl_3) δ 169.4, 151.6, 149.9, 149.6, 138.8, 138.7, 130.3, 129.0 (2C), 128.8, 128.3 (2C), 128.2, 128.0, 127.4, 127.3, 126.5, 126.2, 124.4, 121.4, 118.7, 114.3, 75.1, 65.2, 39.0, 21.2.

IR (film): ν (cm^{-1}) 3059, 2925, 2869, 1757, 1598, 1499, 1443, 1363, 1304, 1256, 1195, 1116, 1084, 1012, 954, 909, 845, 737, 695, 554, 521.

HRMS (ESI, m/z) calcd for $\text{C}_{32}\text{H}_{29}\text{N}_3\text{NaO}_3^+$ $[\text{M}+\text{Na}]^+$: 526.2101, found: 526.2098.



Starting from **16k** (60.0 mg, 0.15 mmol) and **18a** (87.4 mg, 0.45 mmol) with Λ -**RhS**

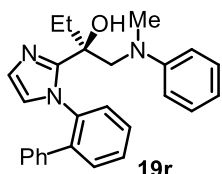
for 15 h according to the general procedure to give **19q** as a white solid (46.4 mg, 0.105 mmol, 70% yield). Enantiomeric excess established by HPLC analysis by using a Chiralpak OD-H column, ee = 96% (HPLC: OD-H, 254 nm, hexane/isopropanol = 90: 10, flow rate 0.5 mL/min, 25 °C, t_r (minor) = 16.5 min, t_r (major) = 11.5 min); $[\alpha]_D^{20} = -26.2^\circ$ (c 1.0, CH_2Cl_2).

^1H NMR (500 MHz, CD_2Cl_2 , mixture of rotamers) δ 7.69 (d, $J = 7.7$ Hz, 2H), 7.64 (d, $J = 8.4$, 2H), 7.51-7.43 (m, 5H), 7.42-7.27 (m, 6H), 7.22 (t, $J = 8.7$ Hz, 2H), 7.16-7.12 (m, 1H), 7.00 (d, $J = 1.1$ Hz, 1H) 6.87 (d, $J = 8.4$ Hz, 2H), 6.79 (t, $J = 7.4$ Hz, 1H), 6.72 (d, $J = 1.0$, 1H), 6.51 (d, $J = 8.0$, 1H), 4.74 (d, $J = 14.8$ Hz, 0.8 H), 4.51 (d, $J = 14.8$ Hz, 0.2 H, other rotamer), 3.74 (d, $J = 14.7$ Hz, 1H), 3.57 (br, 0.8 H), 3.43 (br, 0.2 H, other rotamer), 2.72 (s, 2.4 H), 2.63 (s, 0.6 H, other rotamer).

^{13}C NMR (125 MHz, CD_2Cl_2) δ 152.2, 150.0, 144.6, 140.9, 140.2, 139.1 (2C), 137.5, 130.7, 129.2, 129.1, 128.9, 128.7, 128.6 (2C), 127.7, 127.6, 127.3, 127.2, 126.6, 125.9, 124.6, 118.6, 114.5, 75.8, 65.7, 39.3.

IR (film): ν (cm^{-1}) 3383, 3060, 2967, 2878, 1597, 1494, 1446, 1366, 1303, 1268, 1193, 1161, 1132, 1104, 1070, 951, 740, 696, 608, 533, 457.

HRMS (ESI, m/z) calcd for $\text{C}_{36}\text{H}_{32}\text{N}_3\text{O}^+$ $[\text{M}+\text{H}]^+$: 522.2540, found: 522.2543.



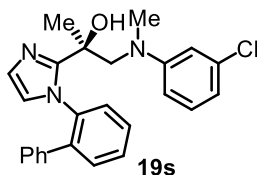
Starting from **16l** (40.8 mg, 0.15 mmol) and **18a** (87.4 mg, 0.45 mmol) with Λ -**RhS** for 5h according to the general procedure to give **19r** as a white solid (52.4 mg, 0.132 mmol, 88% yield). Enantiomeric excess established by HPLC analysis by using a Chiralpak OD-H column, ee = 97% (HPLC: OD-H, 254 nm, *n*-hexane/isopropanol = 95: 5, flow rate 0.5 mL/min, 25 °C, t_r (minor) = 19.2 min, t_r (major) = 15.9 min); $[\alpha]_D^{20} = +19.2^\circ$ (*c* 1.0, CH₂Cl₂).

¹H NMR (300 MHz, CDCl₃, mixture of rotamers) δ 7.52-7.46 (m, 1H), 7.44-7.32 (m, 2H), 7.30-7.24 (m, 2H), 7.23-7.18 (m, 2H), 7.17-7.11 (m, 4H), 7.09 (d, *J* = 1.1 Hz, 1H), 7.03 (d, *J* = 1.1 Hz, 1H, other rotamer), 6.95-6.91 (m, 1H), 6.70 (dd, *J* = 12.5, 6.9 Hz, 1H), 6.62 (d, *J* = 8.3 Hz, 1H), 6.51 (d, *J* = 8.3 Hz, 1H), 3.64 (d, *J* = 14.8 Hz, 0.4 H), 3.55 (d, *J* = 14.9 Hz, 0.6 H, other rotamer), 3.47 (d, *J* = 14.8 Hz, 0.4 H), 3.39 (d, *J* = 14.9 Hz, 0.6 H, other rotamer), 2.70 (br, 0.4 H), 2.62 (s, 1.8 H), 2.42 (s, 1.2 H, other rotamer), 2.26 (br, 0.6 H, other rotamer), 1.86-1.73 (m, 1.2 H), 1.58-1.48 (m, 0.8 H, other rotamer), 0.67 (t, *J* = 7.5 Hz, 1.2 H), 0.40 (t, *J* = 7.4 Hz, 1.8 H, other rotamer).

¹³C NMR (125 MHz, CDCl₃, mixture of rotamers) δ 151.5, 150.8, 150.6, 150.3, 139.7 (2C), 138.6, 138.5, 137.7, 137.4, 130.9, 130.6, 129.1, 129.0 (2C), 128.8, 128.7, 128.6, 128.5, 128.4, 127.9, 127.7, 127.6, 127.5, 127.0, 126.7, 124.9, 124.6, 117.4, 117.2, 113.4, 112.8, 78.2, 64.5, 64.3, 39.8, 39.1, 33.7, 31.3, 8.0, 6.8.

IR (film): ν (cm⁻¹) 3060, 2965, 2932, 2874, 1598, 1504, 1481, 1439, 1371, 1330, 1303, 1277, 1256, 1213, 1191, 1166, 1129, 1118, 1100, 1025, 989, 926, 879, 761, 700, 692, 610, 556, 526, 484.

HRMS (ESI, *m/z*) calcd for C₂₆H₂₈N₃O⁺ [M+H]⁺: 398.2227, found: 398.2226.



Starting from **16m** (39.3 mg, 0.15 mmol) and **18j** (103 mg, 0.45 mmol) with Λ -**RhS** for 15h according to the general procedure to give **19s** as a white solid (54.2 mg, 0.130 mmol, 86% yield). Enantiomeric excess established by HPLC analysis by using a Chiralpak OD-H column, ee = 99% (HPLC: OD-H, 254 nm, *n*-hexane/isopropanol = 90: 10, flow rate 1.0 mL/min, 25 °C, t_r (minor) = 8.3 min, t_r (major) = 7.4 min); $[\alpha]_D^{20} = -8.2^\circ$ (*c* 1.0, CH₂Cl₂).

¹H NMR (300 MHz, CDCl₃, mixture of rotamers) δ 7.58-7.47 (m, 2H), 7.46-7.27 (m, 3H), 7.26-7.09

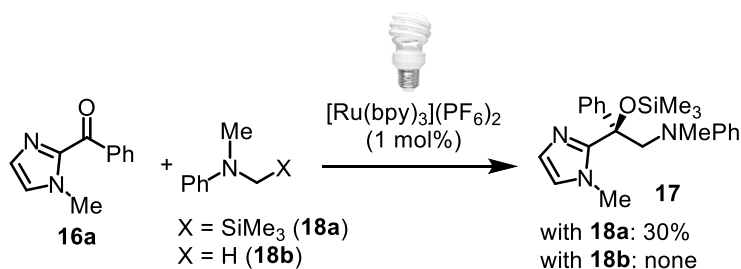
(m, 4H), 7.07-7.01 (m, 1H), 6.99 (dd, $J = 8.0, 1.2$ Hz, 1H), 6.92 (dd, $J = 13.2, 1.2$ Hz, 1H), 6.62 (dt, $J = 7.8, 1.8$ Hz, 1H), 6.56 (dt, $J = 12.2, 2.4$ Hz, 1H), 6.47 (qd, $J = 17.7, 8.5, 2.4$ Hz, 1H), 3.60-3.50 (m, 1H), 3.48-3.28 (m, 1H), 3.00 (br, 0.6 H), 2.65 (s, 1.8 H), 2.60 (s, 1.2 H, other rotamer), 2.30 (br, 0.4 H, other rotamer), 1.23 (s, 1.2 H), 1.13 (s, 1.8 H, other rotamer).

^{13}C NMR (75 MHz, CD_2Cl_2 , mixture of rotamers) δ 152.4, 152.2, 151.7, 151.3, 140.1, 140.0, 138.8, 138.7, 137.8, 137.6, 135.1, 134.9, 131.4, 131.0, 130.2, 130.1, 129.8, 129.6, 129.0, 128.8 (3C), 128.3 (2C), 128.2, 128.1, 127.4, 126.8, 125.3, 124.8, 116.9, 116.7, 112.9, 112.8, 111.4, 111.3, 75.7, 74.8, 64.8, 63.4, 40.0 (2C), 26.5, 26.3.

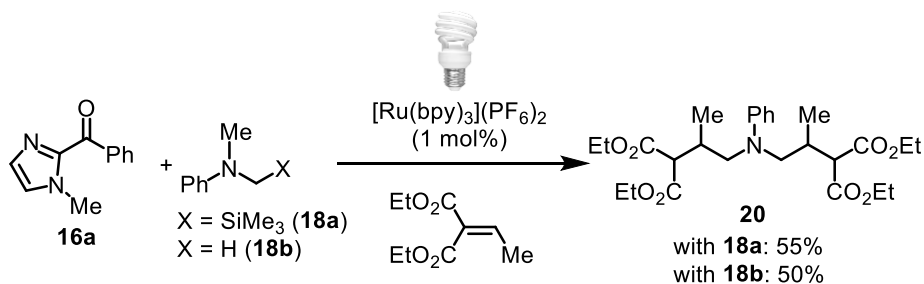
IR (film): ν (cm^{-1}) 2971, 2918, 2849, 1594, 1558, 1497, 1481, 1373, 1339, 1308, 1263, 1195, 1179, 1126, 1098, 1080, 1001, 988, 979, 948, 921, 819, 773, 762, 752, 732, 699, 675, 603, 572, 546, 499, 442.

HRMS (ESI, m/z) calcd for $\text{C}_{25}\text{H}_{25}\text{ClN}_3\text{O}^+$ $[\text{M}+\text{H}]^+$: 418.1681, found: 418.1684.

5.3.3 Mechanistic Studies

1) α -Aminoalkyl radical trapping experiments

A dried 10 mL Schlenk tube was charged with the photosensitizer $[\text{Ru}(\text{bpy})_3](\text{PF}_6)_2$ (0.86 mg, 0.001 mmol, 1 mol%) and the 2-acyl imidazole **16a** (0.10 mmol, 1.0 eq.). A solution of **18a** (58.0 mg, 0.30 mmol, 3.0 eq.) or **18b** (36.4 mg, 0.30 mmol, 3.0 eq.) in MeCN/DMAC (v/v = 4:1, 1 mL) was added in one portion. The reaction mixture was degassed *via* freeze-pump-thaw for three cycles. After the mixture was thoroughly degassed, the vial was sealed and positioned approximately 5 cm from a 23 W compact fluorescent lamp. The reaction was stirred at room temperature for 15h under nitrogen atmosphere. Afterwards, the mixture was concentrated under reduced pressure. With **18a**, the residue was subjected to a flash chromatography on silica gel (EtOAc/*n*-hexane = 1:20 to 1:10) to afford the product **17** (11.3 mg, 0.030 mmol, 30% yield). With **18b**, no product was formed.



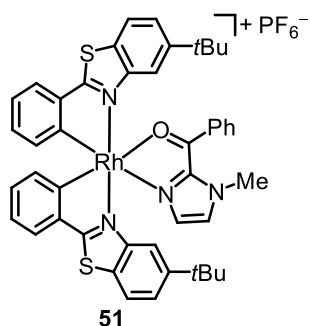
A dried 10 mL Schlenk tube was charged with the photosensitizer $[\text{Ru}(\text{bpy})_3](\text{PF}_6)_2$ (0.86 mg, 0.001 mmol, 1 mol%) and the 2-acyl imidazole **16a** (0.10 mmol, 1.0 eq.). A solution of **18a** (58.0 mg, 0.30 mmol, 3.0 eq.) or **18b** (36.4 mg, 0.30 mmol, 3.0 eq.) in MeCN/DMAC (v/v = 4:1, 1 mL) was added in one portion, followed by the addition of Diethyl 2-ethylidenemalonate (18 μL , 0.1 mmol, 1 eq.). The reaction mixture was degassed *via* freeze-pump-thaw for three cycles. After the mixture was thoroughly degassed, the vial was sealed and positioned approximately 5 cm from a 23 W compact fluorescent lamp. The reaction was stirred at room temperature for 15h under nitrogen atmosphere. Afterwards, the reaction was quenched by the addition of saturated aqueous NH_4Cl solution, then

extracted by EtOAc (3 × 10 mL). The organic layer was collected and concentrated under reduced pressure. The residue was subjected to a flash chromatography on silica gel (EtOAc/*n*-hexane = 1:20 to 1:10) to afford the product **20** (with **18a**: 27.0 mg, 0.055 mmol, 55% yield; with **18b**: 24.6 mg, 0.050 mmol, 50% yield).

¹H NMR (300 MHz, C₆D₆) δ 7.28-7.21 (m, 2H), 7.10-7.00 (m, 2H), 6.76-6.70 (m, 1H), 4.02-3.86 (m, 8H), 3.81 (dd, *J* = 14.3, 5.1 Hz, 1H), 3.68 (dd, *J* = 14.6, 6.9 Hz, 1H), 3.43 (d, *J* = 6.5 Hz, 1H), 3.36 (d, *J* = 6.8 Hz, 1H), 3.32 (dd, *J* = 14.6, 8.1 Hz, 1H), 3.13 (dd, *J* = 14.3, 9.2 Hz, 1H), 3.05-2.93 (m, 2H), 1.021 (d, *J* = 7.0 Hz, 3H), 1.017 (d, *J* = 6.8 Hz, 3H), 0.94-0.87 (m, 12H).

All spectroscopic data were in agreement with the literature.⁴

2) Synthesis of the intermediate complex **51**



The racemic complex **51** was obtained by reacting substrate **16a** (13.0 mg, 0.049 mmol) with *rac*-**RhS** (40.0 mg, 0.043 mmol) at room temperature for 10 min in CH₂Cl₂ (1.0 mL). After the slow addition of *n*-hexane (5.0 mL), crystals were collected after several days (32.2 mg, yield: 68%).

¹H NMR (500 MHz, CD₂Cl₂) δ 7.92 (dd, *J* = 8.5, 0.4 Hz, 1H), 7.86 (d, *J* = 8.7 Hz, 1H), 7.81 (dd, *J* = 7.7, 0.2 Hz, 1H), 7.78 (dd, *J* = 7.7, 0.4 Hz, 1H), 7.72 (tt, *J* = 7.1, 1.5 Hz, 1H), 7.58-7.50 (m, 8H), 7.16 (dd, *J* = 7.5, 1.0 Hz, 1H), 7.12 (dd, *J* = 7.5, 1.0 Hz, 1H), 7.09 (d, *J* = 1.1 Hz, 1H), 6.95-6.90 (m, 3H), 6.47 (dt, *J* = 7.9, 0.9 Hz, 1H), 6.40 (d, *J* = 7.5 Hz, 1H), 3.67 (s, 3H), 1.20 (s, 9H), 1.15 (s, 9H).

¹³C NMR (125 MHz, CD₂Cl₂) 190.0, 178.2 (2C), 174.9, 174.8, 163.3, 163.0, 159.5, 159.2, 152.5, 152.3, 149.4, 149.1, 145.8, 141.2, 139.6, 135.9, 135.1, 134.6, 134.3, 132.5, 131.7, 131.4, 131.3, 130.0, 129.6, 126.8, 126.5, 125.3, 124.8, 124.7, 124.5, 123.2, 123.1, 115.6, 115.4, 38.7, 35.2 (2C), 31.5, 31.4.

5.3.4 Single Crystal X-Ray Diffraction Studies

Crystals of **19s** and complex **51** were obtained by slow diffusion from a solution of the compounds in CH₂Cl₂ layered with *n*-hexane at room temperature for several days.

Crystal data and details of the structure determination are presented in **Table 11**. X-ray data were collected with a Bruker 3 circuit D8 Quest diffractometer with MoK α radiation (microfocus tube with multilayer optics) and Photon 100 CMOS detector at 115 K. Scaling and absorption correction was performed by using the SADABS⁵ software package of Bruker. Structures were solved using direct methods in SHELXT⁶ and refined using the full matrix least squares procedure in SHELXL-2014⁷. The hydrogen atoms were placed in calculated positions and refined as riding on their respective C atom, and Uiso(H) was set at 1.2 Ueq(Csp²) and 1.5 Ueq(Csp³). Disorder of PF₆ ions, solvent molecules or phenyl and *tert*-butyl groups was refined using restraints for both the geometry and the anisotropic displacement factors.

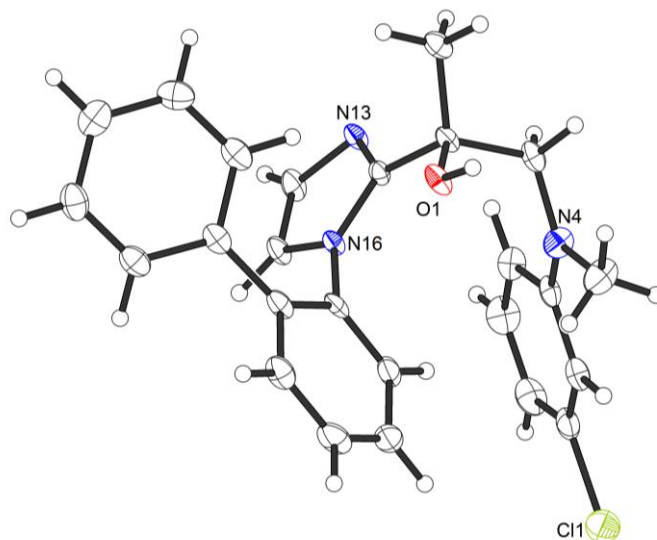


Figure 94. Crystal structure of **16s**. ORTEP drawing with 50 % probability thermal ellipsoids.

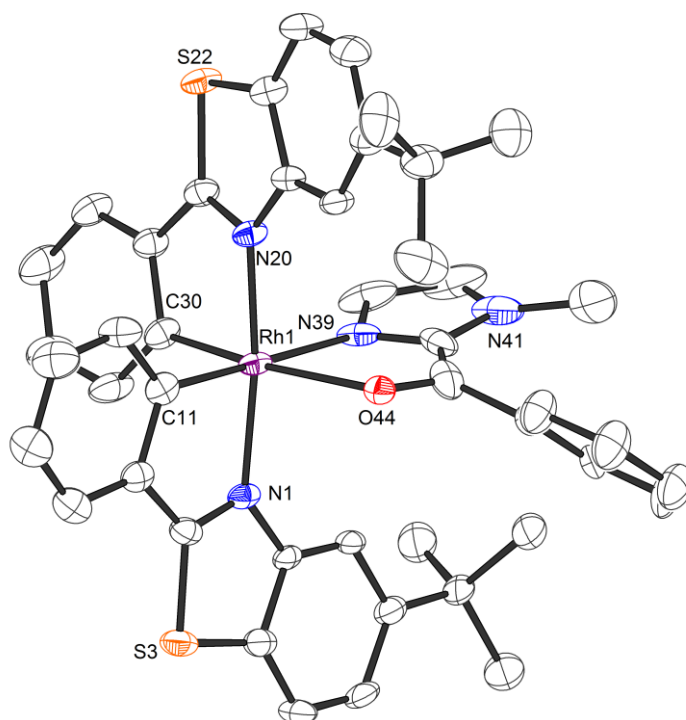


Figure 95. One of the two independent ions of complex **51** in the asymmetric unit. The hexafluorophosphate counteranion and the solvent molecules (*n*-hexane and CH₂Cl₂) are omitted for clarity. No disorder shown. ORTEP drawing with 50 % probability thermal ellipsoids.

Table 11. Crystal data and details of the structure determination.

	16s	complex 51
Empiric formula	C ₂₅ H ₂₄ Cl N ₃ O	C _{48.4} H _{49.6} Cl ₂ F ₆ N ₄ O P Rh S ₂
Formula weight	417.92	1086.22
Crystal system, space group	Orthorhombic, P2 ₁ 2 ₁ 2 ₁	Triclinic, P-1
<i>a</i> , <i>b</i> , <i>c</i> (Å)	10.3206(4), 11.6585(5), 18.3971(8)	17.1583(11), 17.7095(11), 18.8292(12)
α , β , γ (°)	90, 90, 90	66.918(2), 69.054(2), 76.796(2)
<i>V</i> (Å ³)	2213.59(16)	4889.7(5)
<i>Z</i>	4	4
μ (mm ⁻¹)	0.194	0.640
Crystal size (mm)	0.43 x 0.09 x 0.04	0.37 x 0.37 x 0.03
<i>T</i> _{min} , <i>T</i> _{max}	0.92, 0.99	0.98, 0.86
No. of measured, independent and observed [<i>I</i> > 2σ(<i>I</i>)] reflections	12569, 4006, 3552	112817, 17855, 13904
<i>R</i> _{int}	0.0336	0.0533
<i>R</i> [<i>F</i> ² > 2σ(<i>F</i> ²)], <i>wR</i> (<i>F</i> ²), <i>S</i>	0.0352, 0.0736, 1.060	0.0565, 0.1437, 1.039
No. of used reflections	4006	17855
No. of parameters	277	1548
No. of restraints	0	582
$\Delta\rho_{\max}$, $\Delta\rho_{\min}$ (e Å ⁻³)	0.148, -0.212	1.691, -0.833
Absolute structure parameter	0.08(3)	-
CCDC	1480694	1480695

References

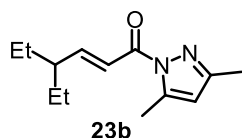
- 1 L. Ruiz Espelt, I. S. McPherson, E. M. Wiensch, T. P. Yoon, *J. Am. Chem. Soc.* **2015**, *137*, 2452.
- 2 C. Wang, Y. Zheng, H. Huo, P. Röse, L. Zhang, K. Harms, G. Hilt, E. Meggers, *Chem. Eur. J.* **2015**, *21*, 7355.
- 3 A. Sunderkötter, S. Lorenzen, R. Tacke, P. Kraft, *Chem. Eur. J.* **2010**, *16*, 7404.
- 4 Y. Miyake, K. Nakajima, Y. Nishibayashi, *J. Am. Chem. Soc.* **2012**, *134*, 3338.
- 5 *SADABS. Bruker AXS area detector scaling and absorption correction*, Bruker AXS Inc., Madison, Wisconsin, USA, 2014.
- 6 G. M. Sheldrick, *Acta Cryst. A*, **2008**, *64*, 112.
- 7 G. M. Sheldrick, *SHELXT*, Universität Göttingen, Göttingen, Germany, 2014.

5.4 Synthesis of Fluoroalkyl-Containing Compounds through Enantioselective Three-Component Photoredox Reaction

5.4.1 Synthesis of Substrates

α,β -Unsaturated 2-acyl pyrazoles **23a-j** were synthesized according to our published procedures¹⁻².

The experimental data of **23b-c**, **23e**, **23g** are shown below.

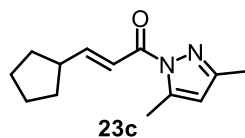


¹H NMR (300 MHz, CDCl₃) δ 7.28 (d, J = 15.6 Hz, 1H), 7.00 (dd, J = 15.6, 9.3 Hz, 1H), 5.97 (s, 1H), 2.57 (s, 3H), 2.25 (s, 3H), 2.22-2.10 (m, 1H), 1.61-1.48 (m, 2H), 1.45-1.33 (m, 2H), 0.88 (t, J = 7.4 Hz, 6H).

¹³C NMR (75 MHz, CDCl₃) δ 165.3, 155.8, 151.8, 144.5, 121.1, 111.3, 46.4, 27.0, 14.7, 13.9, 11.7.

IR (film): ν (cm⁻¹) 2959, 2926, 2869, 1705, 1636, 1580, 1452, 1411, 1370, 1339, 1290, 1257, 1177, 1140, 1011, 987, 963, 858, 801, 770, 743, 707, 625, 585, 474, 403.

HRMS (ESI, m/z) calcd for C₁₃H₂₁N₂O⁺ [M+H]⁺: 221.1648, found: 221.1646.

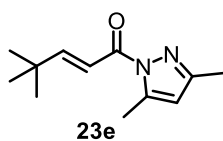


¹H NMR (300 MHz, CDCl₃) δ 7.27 (d, J = 15.6 Hz, 1H), 7.00 (dd, J = 15.5, 7.7 Hz, 1H), 5.95 (s, 1H), 2.81-2.68 (m, 1H), 2.56 (s, 3H), 2.24 (s, 3H), 1.92-1.83 (m, 2H), 1.76-1.55 (m, 4H), 1.51-1.40 (m, 2H).

¹³C NMR (75 MHz, CDCl₃) δ 165.6, 155.9, 151.7, 144.4, 119.3, 111.2, 43.4, 32.7, 25.4, 14.7, 13.9.

IR (film): ν (cm⁻¹) 2952, 2867, 1703, 1634, 1579, 1476, 1445, 1410, 1371, 1341, 1230, 1170, 1137, 987, 961, 856, 801, 752, 707, 623, 588, 462, 413.

HRMS (ESI, m/z) calcd for C₁₃H₁₈N₂ONa⁺ [M+Na]⁺: 241.1311, found: 241.1307.

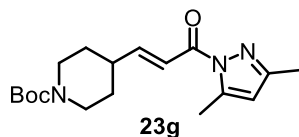


¹H NMR (300 MHz, CDCl₃) δ 7.20 (s, 2H), 5.95 (s, 1H), 2.56 (s, 3H), 2.25 (s, 3H), 1.15 (s, 9H).

¹³C NMR (75 MHz, CDCl₃) δ 165.9, 161.2, 151.8, 144.4, 116.6, 111.3, 34.4, 28.8, 14.7, 13.9.

IR (film): ν (cm^{-1}) 2958, 1706, 1633, 1579, 1474, 1411, 1372, 1341, 1301, 1236, 1176, 1014, 964, 926, 836, 800, 764, 727, 624, 448, 414.

HRMS (ESI, m/z) calcd for $\text{C}_{12}\text{H}_{18}\text{N}_2\text{ONa}^+$ $[\text{M}+\text{Na}]^+$: 229.1311, found: 229.1308.



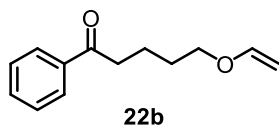
^1H NMR (300 MHz, CDCl_3) δ 7.30 (d, $J = 15.7$ Hz, 1H), 7.00 (dd, $J = 15.8, 6.7$ Hz, 1H), 5.97 (s, 1H), 4.12 (br, 2H), 2.78 (t, $J = 12.2$ Hz, 2H), 2.56 (s, 3H), 2.48-2.34 (m, 1H), 2.24 (s, 3H), 1.80-1.77 (m, 2H), 1.50-1.40 (m, 11H).

^{13}C NMR (75 MHz, CDCl_3) δ 165.3, 154.8, 153.7, 152.0, 144.5, 120.1, 111.5, 79.6, 43.5, 39.3, 30.8, 28.5, 14.7, 13.9.

IR (film): ν (cm^{-1}) 3390, 2965, 2929, 2858, 1679, 1637, 1587, 1428, 1372, 1340, 1278, 1236, 1168, 1112, 1012, 958, 866, 834, 798, 760, 699, 605, 540.

HRMS (ESI, m/z) calcd for $\text{C}_{18}\text{H}_{27}\text{N}_3\text{O}_3\text{Na}^+$ $[\text{M}+\text{Na}]^+$: 356.1945, found: 356.1939.

Vinyl ethers **22a-22q** were synthesized according to the published procedures.³ The experimental data of **22b-c**, **22e-q** are shown below.

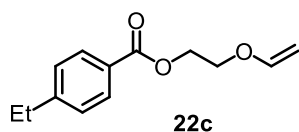


^1H NMR (300 MHz, CDCl_3) δ 7.98-7.14 (m, 2H), 7.61-7.53 (m, 1H), 7.49-7.43 (m, 2H), 6.45 (dd, $J = 14.3, 6.8$ Hz, 1H), 4.17 (dd, $J = 14.4, 1.9$ Hz, 1H), 3.98 (dd, $J = 6.8, 1.9$ Hz, 1H), 3.73 (t, $J = 6.2$ Hz, 2H), 3.02 (t, $J = 6.9$ Hz, 2H), 1.91-1.71 (m, 4H).

^{13}C NMR (75 MHz, CDCl_3) δ 200.0, 151.9, 137.1, 133.0, 128.7, 128.1, 86.5, 67.8, 38.2, 28.7, 21.0.

IR (film): ν (cm^{-1}) 3055, 2995, 2942, 2872, 1682, 1611, 1447, 1409, 1360, 1318, 1234, 1196, 1076, 972, 928, 886, 816, 748, 690, 654, 568.

HRMS (ESI, m/z) calcd for $\text{C}_{13}\text{H}_{16}\text{O}_2\text{Na}^+$ $[\text{M}+\text{Na}]^+$: 227.1043, found: 227.1039.



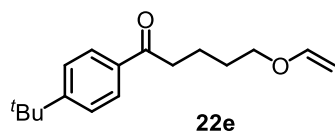
^1H NMR (300 MHz, CD_2Cl_2) δ 7.98 (d, $J = 8.3$ Hz, 2H), 7.32 (d, $J = 8.3$ Hz, 2H), 6.55 (dd, $J = 14.3,$

6.8 Hz, 1H), 4.55-4.53 (m, 2H), 4.28 (dd, $J = 14.3, 2.2$ Hz, 1H), 4.10-4.03 (m, 3H), 2.74 (q, $J = 7.6$ Hz, 2H), 1.28 (t, $J = 7.6$ Hz, 3H).

^{13}C NMR (75 MHz, CDCl_3) δ 166.4, 151.8, 150.2, 129.7, 128.0, 127.6, 86.9, 66.3, 63.1, 29.0, 15.1.

IR (film): ν (cm^{-1}) 3055, 2995, 2942, 2872, 1682, 1611, 1447, 1409, 1360, 1318, 1234, 1196, 1076, 972, 928, 886, 816, 748, 690, 654, 568.

HRMS (ESI, m/z) calcd for $\text{C}_{13}\text{H}_{16}\text{O}_3\text{Na}^+$ $[\text{M}+\text{Na}]^+$: 243.0992, found: 243.0995.

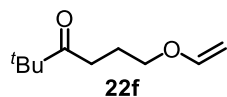


^1H NMR (300 MHz, CDCl_3) δ 7.91-7.88 (m, 2H), 7.49-7.45 (m, 2H), 6.46 (dd, $J = 14.3, 6.8$ Hz, 1H), 4.17 (dd, $J = 14.3, 1.9$ Hz, 1H), 3.98 (dd, $J = 6.8, 2.0$ Hz, 1H), 3.72 (t, $J = 6.2$ Hz, 2H), 3.00 (t, $J = 6.9$ Hz, 2H), 1.91-1.70 (m, 4H), 1.34 (s, 9H).

^{13}C NMR (75 MHz, CDCl_3) δ 199.7, 156.8, 152.0, 134.6, 128.1, 125.6, 86.5, 67.9, 38.1, 35.2, 31.2, 28.8, 21.1.

IR (film): ν (cm^{-1}) 3002, 2947, 2868, 1679, 1606, 1402, 1355, 1321, 1236, 1194, 977, 919, 837, 737, 578, 535, 458.

HRMS (ESI, m/z) calcd for $\text{C}_{17}\text{H}_{24}\text{O}_2\text{Na}^+$ $[\text{M}+\text{Na}]^+$: 283.1669, found: 283.1664.

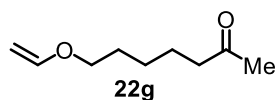


^1H NMR (300 MHz, CDCl_3) δ 6.44 (dd, $J = 14.4, 6.9$ Hz, 1H), 4.16 (dd, $J = 14.4, 2.0$ Hz, 1H), 3.97 (dd, $J = 6.8, 2.0$ Hz, 1H), 3.68 (t, $J = 6.0$ Hz, 2H), 2.61 (t, $J = 7.1$ Hz, 2H), 1.96-1.87 (m, 2H), 1.14 (s, 9H).

^{13}C NMR (75 MHz, CDCl_3) δ 215.4, 151.8, 86.6, 67.2, 44.2, 32.8, 26.5, 23.4.

IR (film): ν (cm^{-1}) 2999, 2946, 1704, 1615, 1476, 1402, 1358, 1321, 1195, 1056, 979, 920, 831, 567, 510, 462.

HRMS (ESI, m/z) calcd for $\text{C}_{10}\text{H}_{18}\text{O}_2\text{Na}^+$ $[\text{M}+\text{Na}]^+$: 193.1199, found: 193.1196.



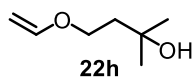
^1H NMR (300 MHz, CDCl_3) δ 6.43 (dd, $J = 14.4, 6.8$ Hz, 1H), 4.15 (dd, $J = 14.3, 1.8$ Hz, 1H), 3.95 (dd, $J = 6.8, 1.9$ Hz, 1H), 3.66 (t, $J = 6.4$ Hz, 2H), 2.43 (t, $J = 7.3$ Hz, 2H), 2.12 (s, 3H), 1.70-1.55 (m,

4H), 1.43-1.32 (m, 2H).

^{13}C NMR (75 MHz, CDCl_3) δ 208.9, 152.0, 86.4, 67.8, 43.6, 29.9, 28.9, 25.7, 23.6.

IR (film): ν (cm^{-1}) 2938, 2868, 1712, 1613, 1463, 1414, 1361, 1318, 1196, 1162, 1074, 964, 814, 718, 594, 526.

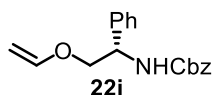
HRMS (ESI, m/z) calcd for $\text{C}_9\text{H}_{16}\text{O}_2\text{Na}$ $[\text{M}+\text{Na}]^+$: 179.1043, found: 179.1040.



^1H NMR (300 MHz, CDCl_3) δ 6.49 (dd, $J = 14.3, 6.8$ Hz, 1H), 4.25 (dd, $J = 14.4, 2.1$ Hz, 1H), 4.06 (dd, $J = 6.8, 2.0$ Hz, 1H), 3.92 (t, $J = 6.3$ Hz, 2H), 2.43 (t, $J = 7.3$ Hz, 2H), 2.15 (br, 1H), 1.30 (s, 6H).

^{13}C NMR (75 MHz, CDCl_3) δ 151.4, 86.9, 63.0, 31.7, 29.4, 21.6 (2C).

IR (film): ν (cm^{-1}) 3363, 2969, 2932, 1727, 1672, 1465, 1371, 1138, 1096, 1066, 1027, 979, 915, 879, 539, 463.

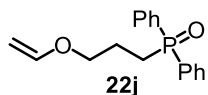


^1H NMR (300 MHz, CDCl_3) δ 7.38-7.27 (m, 10H), 6.44 (dd, $J = 14.3, 6.8$ Hz, 1H), 5.45 (br, 1H), 5.15-4.95 (m, 3H), 4.19 (dd, $J = 14.3, 2.3$ Hz, 1H), 4.04 (dd, $J = 6.8, 2.3$ Hz, 1H), 4.00-3.86 (m, 2H).

^{13}C NMR (75 MHz, CDCl_3) δ 155.9, 151.3, 139.4, 136.4, 128.7, 128.6, 128.2, 127.9, 126.8, 87.4, 70.3, 67.1.

IR (film): ν (cm^{-1}) 3333, 3059, 3035, 2922, 2871, 1679, 1613, 1531, 1458, 1381, 1351, 1322, 1283, 1255, 1195, 1147, 1054, 1001, 961, 913, 813, 755, 727, 694, 636, 609, 596, 526, 486.

HRMS (ESI, m/z) calcd for $\text{C}_{18}\text{H}_{19}\text{NO}_3\text{Na}$ $[\text{M}+\text{Na}]^+$: 320.1257, found: 320.1252.

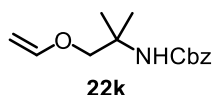


^1H NMR (300 MHz, CDCl_3) δ 7.72-7.66 (m, 4H), 7.46-7.35 (m, 6H), 6.35 (dd, $J = 14.4, 6.8$ Hz, 1H), 4.07 (dd, $J = 14.4, 2.0$ Hz, 1H), 3.89 (dd, $J = 6.8, 2.0$ Hz, 1H), 3.65 (t, $J = 5.9$ Hz, 2H), 2.37-2.28 (m, 2H), 1.98-1.86 (m, 2H).

^{13}C NMR (75 MHz, CDCl_3) δ 151.3, 131.6, 130.6, 130.5, 128.6, 86.7, 67.6, 26.7, 21.4.

IR (film): ν (cm^{-1}) 3453, 3059, 2915, 1619, 1479, 1436, 1400, 1318, 1169, 1115, 1064, 966, 845, 749, 697, 539, 507, 398.

HRMS (ESI, m/z) calcd for $\text{C}_{17}\text{H}_{19}\text{O}_2\text{PNa}$ $[\text{M}+\text{Na}]^+$: 309.1015, found: 309.1011.

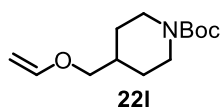


^1H NMR (300 MHz, CDCl_3) δ 7.37-7.29 (m, 5H), 6.45 (dd, $J = 14.3, 6.7$ Hz, 1H), 5.06 (s, 2H), 4.90 (br, 1H), 4.20 (dd, $J = 14.3, 2.1$ Hz, 1H), 3.99 (dd, $J = 6.8, 2.1$ Hz, 1H), 3.68 (s, 2H), 1.36 (s, 6H).

^{13}C NMR (75 MHz, CDCl_3) δ 168.7, 151.8, 136.7, 128.6, 128.1, 87.0, 73.6, 66.3, 52.8, 24.3.

IR (film): ν (cm^{-1}) 2995, 2944, 1710, 1617, 1507, 1454, 1395, 1357, 1323, 1263, 1196, 1075, 1010, 973, 926, 830, 776, 740, 697, 579, 507, 464.

HRMS (ESI, m/z) calcd for $\text{C}_{15}\text{H}_{21}\text{NO}_3\text{Na}$ $[\text{M}+\text{Na}]^+$: 286.1412, found: 286.1412.

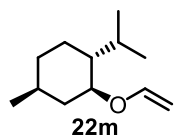


^1H NMR (300 MHz, CDCl_3) δ 6.45 (dd, $J = 14.3, 6.8$ Hz, 1H), 4.18-4.04 (m, 3H), 3.98 (dd, $J = 6.8, 2.0$ Hz, 1H), 3.51 (d, $J = 6.3$ Hz, 2H), 2.70 (t, $J = 12.2$ Hz, 2H), 1.89-1.66 (m, 3H), 1.45 (s, 9H), 1.25-1.11 (m, 2H).

^{13}C NMR (75 MHz, CDCl_3) δ 154.9, 152.0, 86.5, 79.4, 72.5, 43.7, 36.1, 28.9, 28.6.

IR (film): ν (cm^{-1}) 2927, 2856, 1688, 1614, 1415, 1364, 1319, 1242, 1174, 1071, 1003, 916, 863, 815, 766, 527, 460.

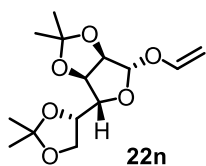
HRMS (ESI, m/z) calcd for $\text{C}_{13}\text{H}_{23}\text{NO}_3\text{Na}$ $[\text{M}+\text{Na}]^+$: 264.1570, found: 264.1566.



^1H NMR (300 MHz, CDCl_3) δ 6.32 (dd, $J = 14.1, 6.5$ Hz, 1H), 4.28 (dd, $J = 14.1, 1.4$ Hz, 1H), 3.94 (dd, $J = 6.5, 1.4$ Hz, 1H), 3.57-3.48 (m, 1H), 2.16-2.02 (m, 2H), 1.70-1.63 (m, 2H), 1.45-1.22 (m, 3H), 1.04-0.98 (m, 1H), 0.94-0.90 (m, 5H), 0.89-0.87 (m, 2H), 0.77 (d, $J = 6.9$ Hz, 3H).

^{13}C NMR (75 MHz, CDCl_3) δ 151.4, 87.6, 79.9, 47.9, 41.0, 34.5, 31.6, 25.9, 23.6, 22.2, 20.8, 16.4.

IR (film): ν (cm^{-1}) 2920, 2864, 1729, 1651, 1453, 1373, 1328, 1239, 1177, 1125, 1082, 1027, 907, 840, 503, 572, 447.



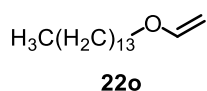
^1H NMR (300 MHz, CDCl_3) δ 6.38 (dd, $J = 14.3, 6.7$ Hz, 1H), 5.88 (d, $J = 6.8$ Hz, 1H), 4.58 (d, $J =$

3.8 Hz, 1H), 4.39 (dd, $J = 14.3, 2.4$ Hz, 1H), 4.35-4.28 (m, 2H), 4.21-4.14 (m, 2H), 4.12-4.00 (m, 2H), 1.51 (s, 3H), 1.43 (s, 3H), 1.34 (s, 3H), 1.31 (s, 3H).

^{13}C NMR (75 MHz, CDCl_3) δ 150.1, 112.1, 109.3, 105.3, 89.6, 82.2, 80.6, 80.5, 72.2, 67.2, 27.0, 26.8, 26.3, 25.4.

IR (film): ν (cm^{-1}) 2986, 2939, 2892, 1623, 1456, 1375, 1326, 1254, 1188, 1163, 1070, 1016, 959, 884, 842, 702, 637, 512, 412.

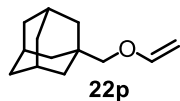
HRMS (ESI, m/z) calcd for $\text{C}_{14}\text{H}_{22}\text{O}_6\text{Na}^+$ $[\text{M}+\text{Na}]^+$: 309.1309, found: 309.1304.



^1H NMR (300 MHz, CDCl_3) δ 6.48 (dd, $J = 14.4, 6.8$ Hz, 1H), 4.19 (dd, $J = 14.3, 1.8$ Hz, 1H), 3.99 (dd, $J = 6.8, 1.8$ Hz, 1H), 3.69 (t, $J = 6.6$ Hz, 2H), 1.72-1.63 (m, 2H), 1.36-1.24 (m, 22H), 0.91 (t, $J = 6.9$ Hz, 3H).

^{13}C NMR (75 MHz, CDCl_3) δ 152.1, 86.3, 68.3, 32.0, 29.8, 29.7 (2C), 29.5, 29.2, 26.1, 22.8, 14.2.

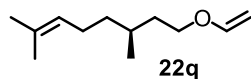
IR (film): ν (cm^{-1}) 2920, 2853, 1641, 1607, 1460, 1374, 1317, 1198, 1074, 968, 810, 721.



^1H NMR (300 MHz, CDCl_3) δ 6.47 (dd, $J = 14.4, 6.9$ Hz, 1H), 4.19 (dd, $J = 14.4, 1.8$ Hz, 1H), 3.99 (dd, $J = 6.8, 1.8$ Hz, 1H), 3.76 (t, $J = 7.3$ Hz, 2H), 1.96 (br, 3H), 1.71-1.67 (m, 4H), 1.55-1.54 (m, 6H), 1.48 (t, $J = 7.4$ Hz, 3H).

^{13}C NMR (75 MHz, CDCl_3) δ 152.1, 86.3, 64.2, 42.9, 42.8, 37.2, 31.9, 28.8.

IR (film): ν (cm^{-1}) 2897, 2845, 1639, 1605, 1447, 1316, 1197, 1101, 1070, 991, 960, 809.

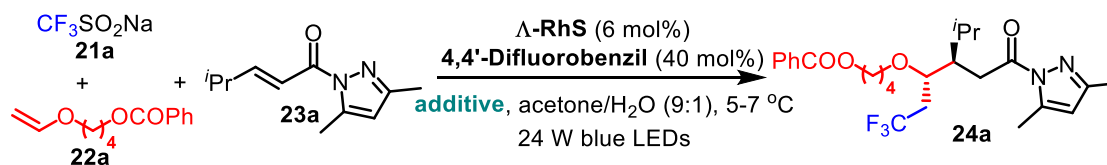


^1H NMR (300 MHz, CDCl_3) δ 6.48 (dd, $J = 14.3, 6.8$ Hz, 1H), 5.15-5.09 (m, 1H), 4.19 (dd, $J = 14.4, 1.8$ Hz, 1H), 3.99 (dd, $J = 6.8, 1.8$ Hz, 1H), 3.76-3.70 (m, 2H), 2.08-1.92 (m, 2H), 1.78-1.68 (m, 4H), 1.66-1.57 (m, 4H), 1.54-1.47 (m, 1H), 1.43-1.32 (m, 1H), 1.27-1.13 (m, 1H), 0.93 (d, $J = 6.5$ Hz, 3H).

^{13}C NMR (75 MHz, CDCl_3) δ 152.1, 131.3, 124.8, 86.3, 66.5, 37.2, 36.1, 29.6, 25.8, 25.5, 19.6, 17.7.

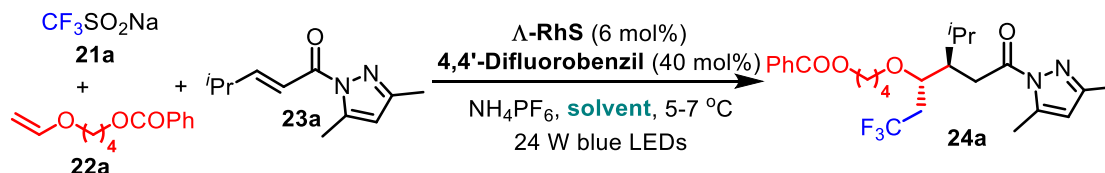
IR (film): ν (cm^{-1}) 2919, 2870, 1609, 1452, 1376, 1317, 1197, 1071, 967, 813.

5.4.2 Optimization of Conditions

Table 12. Effect of NH_4PF_6 .^a

	additive	yield (%) ^b	dr ^c	ee (%) ^d
1	NH_4PF_6 (10 equiv.)	64% (28 h)	2:1	96/96
2	NH_4PF_6 (5 equiv.)	27% (48 h)	2:1	85/85
3	none	21% (48 h)	2:1	70/77

^aReaction conditions: **21a** (0.60 mmol), **22a** (0.30 mmol) and **23a** (0.10 mmol), $\Delta\text{-RhS}$ (5.2 mg, 6 mol%), 4,4'-difluorobenzil (9.8 mg, 0.04 mmol, 40 mol%), and the corresponding amount of NH_4PF_6 in acetone/ H_2O (9:1, 0.1 M) were stirred at 5-7 °C under irradiation with 24 W blue LEDs for the indicated time. ^bIsolated yield. ^cDetermined by ^{19}F NMR analysis of the crude product. ^dDetermined by HPLC on chiral stationary phase. The ee values of both diastereomers are shown.

Table 13. Effect of H_2O .^a

	solvent	yield (%) ^b	dr ^c	ee (%) ^d
1	acetone/ H_2O (0.8 mL: 0.2 mL)	27% (48 h)	2:1	50/50
2	acetone/ H_2O (0.9 mL: 0.1 mL)	64% (28 h)	2:1	96/96
3	acetone/ H_2O (0.95 mL: 0.05 mL)	31% (48 h)	2:1	64/64
4	only acetone (1 mL)	35% (48 h)	2:1	60/60

^aReaction conditions: **21a** (0.60 mmol), **22a** (0.30 mmol) and **23a** (0.10 mmol), $\Delta\text{-RhS}$ (5.2 mg, 6 mol%), 4,4'-difluorobenzil (9.8 mg, 0.04 mmol, 40 mol%), NH_4PF_6 (163 mg, 1.0 mmol) in the indicated solvent mixture acetone/ H_2O (0.1 M) were stirred at 5-7 °C under irradiation with 24 W blue LEDs for the indicated time. ^bIsolated yield. ^cDetermined by ^{19}F NMR analysis of the crude product. ^dDetermined by HPLC on chiral stationary phase. The ee values of both diastereomers are shown.

Table 14. Comparison of different photoredox mediators^a.

	photoredox mediator	yield (%) ^b	dr ^c	ee (%) ^d
1	4,4'-difluorobenzil (40 mol%)	64 (28h)	2:1	96/96
2	none	0 (48h)	n.a.	n.a.
3	benzil (40 mol%)	35 (48h)	2:1	82/82
4	anthraquinone (40 mol%)	0 (48h)	n.a.	n.a.
5	9-fluorenone (40 mol%)	0 (48h)	n.a.	n.a.
6	acetophenone (40 mol%)	0 (48h)	n.a.	n.a.
7	[Acr-Mes]ClO ₄ (2 mol%)	30 (28h)	2:1	91/91
8	[Ru(bpy) ₃](PF ₆) ₂ (2 mol%)	<5% (48h)	n.d.	n.d.
9	Ir[dF(CF ₃)ppy] ₂ (bpy)PF ₆ (2 mol%)	66% (28h)	2:1	81/81

^aReaction conditions: **21a** (0.60 mmol), **22a** (0.30 mmol) and **23a** (0.10 mmol), Δ -**RhS** (5.2 mg, 6 mol%), the corresponding photoredox mediator, NH₄PF₆ (163 mg, 1.0 mmol) in acetone/H₂O (9:1, 0.1 M) were stirred at 5-7 °C under irradiation with 24 W blue LEDs for the indicated time.

^bIsolated yield. ^cDetermined by ¹⁹F NMR analysis of the crude product. ^dDetermined by HPLC on chiral stationary phase. The ee values of both diastereomers are shown. n.a. = not applicable; n.d. = not determined.

Table 15. Comparison of different light sources^a.

	light source	yield (%) ^b	dr ^c	ee (%) ^d
1	24W blue LEDs	64 (28h)	2:1	96/96
2	21W CFL	<5 (48h)	n.d.	n.d.
3	6W blue LEDs	50% (38h)	2:1	95/95
4	12W blue LEDs (reaction temperature 8-11 °C)	64% (28h)	2:1	91/91

^aReaction conditions: **21a** (0.60 mmol), **22a** (0.30 mmol) and **23a** (0.10 mmol), Λ -**RhS** (5.2 mg, 6 mol%), 4,4'-difluorobenzil (9.8 mg, 0.04 mmol, 40 mol%), NH_4PF_6 (163 mg, 1.0 mmol) in acetone/ H_2O (9:1, 0.1 M) were stirred at 5-7 °C under irradiation with the indicated light source for the indicated time. ^bIsolated yield. ^cDetermined by ^{19}F NMR analysis of the crude product. ^dDetermined by HPLC on chiral stationary phase. The ee values of both diastereomers are shown. n.d. = not determined.

Table 16. Control experiments with triplet quencher^a.

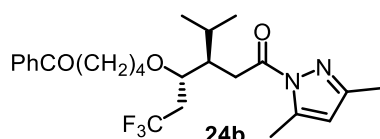
	quencher	yield (%) ^b	dr ^c	ee (%) ^d
1	none	64 (28h)	2:1	96/96
2	2,5-dimethylhexa-2,4-diene (40 mol%)	<5 (48h)	n.d.	n.d.
3	pyridazine (40 mol%)	<5 (48h)	n.d.	n.d.

^aReaction conditions: **21a** (0.60 mmol), **22a** (0.30 mmol) and **23a** (0.10 mmol), Λ -**RhS** (5.2 mg, 6 mol%), 4,4'-difluorobenzil (9.8 mg, 0.04 mmol, 40 mol%), NH_4PF_6 (163 mg, 1.0 mmol) in acetone/ H_2O (9:1, 0.1 M), and in the presence of the indicated quenchers, were stirred at 5-7 °C under irradiation with 24 W blue LEDs for the indicated time. ^bIsolated yield. ^cDetermined by ^{19}F NMR analysis of the crude product. ^dDetermined by HPLC on chiral stationary phase. The ee values of both diastereomers are shown. n.d. = not determined.

5.4.3 Rhodium-Catalyzed Asymmetric Three-Component Photoredox Reactions

1) General Procedure for Table 4:

A dried 10 mL Schlenk tube was charged with the catalyst Λ or Δ -**RhS** (4–8 mol% as indicated), 4,4'-difluorobenzil (9.80 mg, 0.04 mmol, 40 mol%), sodium perfluoroalkyl sulfonates **21a-c** (0.6 mmol), vinyl ethers **22a-c** (0.3 mmol) and *N*-acylpyrazoles **23a-g** (0.1 mmol) in acetone/H₂O (v/v = 9:1, 1.0 mL). The reaction mixture was degassed *via* freeze-pump-thaw for three cycles. After the mixture was thoroughly degassed, the vial was sealed and positioned approximately 10 cm from 24 W blue LEDs. The reaction was stirred at 5–7 °C for the indicated time (14–66 h) (monitored by TLC) under nitrogen atmosphere. Afterwards, the mixture was concentrated under reduced pressure. The residue was subjected to a flash chromatography on silica gel to afford the products **24b-j**. The dr value was determined by ¹⁹F NMR analysis after purification. The enantiomeric excess was determined by chiral HPLC analysis.



Starting from **21a** (94.0 mg, 0.60 mmol), **22b** (61.0 mg, 0.30 mmol)

and **23a** (19.2 mg, 0.10 mmol) with Λ -**RhS** (4 mol%) and 4,4'-difluorobenzil (40 mol%) for 30 h according to the general procedure to give **24b** as a pale yellow oil (32.5 mg, 0.070 mmol, 70% yield, dr = 2.1:1). Enantiomeric excess established by HPLC analysis by using a Chiralpak OD-H column, ee = 92% / 93%. $[\alpha]_D^{20} = -3.0^\circ$ (*c* 1.0, CH₂Cl₂). The dr value was determined by ¹⁹F NMR of **24b** after purified by flash chromatography.

HPLC for major diastereomer: OD-H, 254 nm, *n*-hexane/isopropanol = 98:2, flow rate 0.5 mL/min, 25 °C, *t_r* (minor) = 16.8 min, *t_r* (major) = 20.6 min.

HPLC for minor diastereomer: OD-H, 254 nm, *n*-hexane/isopropanol = 98:2, flow rate 0.5 mL/min, 25 °C, *t_r* (minor) = 15.5 min, *t_r* (major) = 16.3 min.

¹H NMR (500 MHz, CDCl₃, major diastereoisomer) δ 7.95–7.92 (m, 2H), 7.58–7.52 (m, 1H), 7.48–7.43 (m, 2H), 5.91 (s, 1H), 3.62–3.58 (m, 1H), 3.54–3.38 (m, 2H), 3.25 (dd, *J* = 17.2, 7.2 Hz, 1H), 2.94–2.86 (m, 3H), 2.51 (s, 3H), 2.48–2.22 (m, 3H), 2.21 (s, 3H), 1.88–1.78 (m, 1H), 1.72–1.62 (m, 2H), 1.48–1.38 (m, 2H), 1.0 (d, *J* = 6.8 Hz, 3H), 0.92 (d, *J* = 6.8 Hz, 3H).

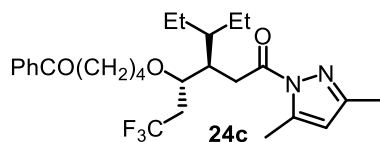
¹³C NMR (125 MHz, CDCl₃, major diastereoisomer) δ 200.2, 174.0, 151.7, 144.1, 137.1, 133.0, 128.7, 128.1, 126.6 (q, *J* = 277.1 Hz), 111.1, 75.2, 70.3, 45.6, 38.3, 37.9 (q, *J* = 26.9 Hz), 32.6, 29.4, 28.8,

21.2, 21.0, 19.3, 14.7, 13.8.

^{19}F NMR (282 MHz, CDCl_3 , major diastereoisomer) δ -63.5 (s, 3F).

IR (film): ν (cm^{-1}) 3001, 2941, 1723, 1683, 1585, 1443, 1381, 1338, 1250, 1138, 1079, 974, 915, 845, 795, 744, 690, 571.

HRMS (ESI, m/z) calcd for $\text{C}_{25}\text{H}_{33}\text{F}_3\text{N}_2\text{O}_3\text{Na}^+$ $[\text{M}+\text{Na}]^+$: 489.2335, found: 489.2334.



Starting from **21a** (94.0 mg, 0.60 mmol), **22b** (61.0 mg, 0.30 mmol)

and **23b** (22.0 mg, 0.10 mmol) with Λ -**RhS** (6 mol%) and 4,4'-difluorobenzil (40 mol%) for 48 h according to the general procedure to give **24c** as a pale yellow oil (28.0 mg, 0.057 mmol, 57% yield, dr = 1.7:1). Enantiomeric excess established by HPLC analysis by using a Chiralpak AD-H column, ee = 95% / 95%. $[\alpha]_{\text{D}}^{20} = -5.2^\circ$ (c 1.0, CH_2Cl_2). The dr value was determined by ^{19}F NMR of **24c** after purified by flash chromatography.

HPLC for major diastereomer: AD-H, 254 nm, n -hexane/isopropanol = 95: 5, flow rate 0.5 mL/min, 25 °C, t_{r} (minor) = 16.5 min, t_{r} (major) = 17.5 min.

HPLC for minor diastereomer: AD-H, 254 nm, n -hexane/isopropanol = 95: 5, flow rate 0.5 mL/min, 25 °C, t_{r} (minor) = 14.1 min, t_{r} (major) = 13.2 min.

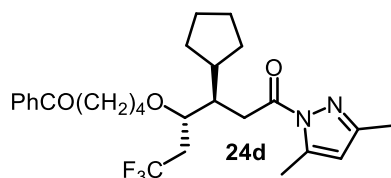
^1H NMR (500 MHz, CDCl_3 , minor diastereoisomer) δ 7.94-7.91 (m, 2H), 7.58-7.50 (m, 1H), 7.47-7.42 (m, 2H), 5.91 (s, 1H), 3.80-3.72 (m, 1H), 3.55-3.48 (m, 1H), 3.37-3.29 (m, 1H), 3.13 (dd, $J = 16.2, 7.5$ Hz, 1H), 2.98 (dd, $J = 16.3, 5.2$ Hz, 1H), 2.91 (t, $J = 7.4$ Hz, 2H), 2.71-2.65 (m, 1H), 2.50 (s, 3H), 2.49-2.35 (m, 1H), 2.30-2.10 (m, 4H), 1.72-1.62 (m, 2H), 1.50-1.32 (m, 5H), 1.28-1.20 (m, 2H), 0.91-0.86 (m, 6H),.

^{13}C NMR (125 MHz, CDCl_3 , major diastereoisomer) δ 200.3, 173.8, 151.8, 144.1, 137.1, 133.0, 128.6, 128.1, 126.7 (q, $J = 275.8$ Hz), 111.2, 76.1, 70.3, 43.8, 42.1, 38.3, 37.7, 37.4 (q, $J = 27.2$ Hz), 34.6, 31.6, 30.8, 29.6, 25.2, 24.7, 21.0, 14.7, 13.8.

^{19}F NMR (282 MHz, CDCl_3) δ -64.3 (s, 3F, minor).

IR (film): ν (cm^{-1}) 3060, 2933, 2874, 1723, 1684, 1585, 1451, 1376, 1333, 1250, 1135, 1095, 1017, 963, 843, 804, 743, 689, 574.

HRMS (ESI, m/z) calcd for $\text{C}_{27}\text{H}_{37}\text{F}_3\text{N}_2\text{O}_3\text{Na}^+$ $[\text{M}+\text{Na}]^+$: 517.2648, found: 517.2661.



Starting from **21a** (94.0 mg, 0.60 mmol), **22b** (61.0 mg, 0.30 mmol)

and **23c** (21.8 mg, 0.10 mmol) with Λ -**RhS** (8 mol%) and 4,4'-difluorobenzil (40 mol%) for 30 h according to the general procedure to give **24d** as a pale yellow oil (26.0 mg, 0.0530 mmol, 53% yield, dr = 1.9:1). Enantiomeric excess established by HPLC analysis by using a Chiralpak OD-H column, ee = 97% / 94%. $[\alpha]_D^{20} = -1.6^\circ$ (*c* 1.0, CH₂Cl₂). The dr value was determined by ¹⁹F NMR of **24d** after purified by flash chromatography.

HPLC for major diastereomer: OD-H, 254 nm, *n*-hexane/isopropanol = 98:2, flow rate 0.2 mL/min, 25 °C, *t_r* (minor) = 41.4 min, *t_r* (major) = 48.5 min.

HPLC for minor diastereomer: OD-H, 254 nm, *n*-hexane/isopropanol = 98:2, flow rate 0.2 mL/min, 25 °C, *t_r* (minor) = 37.2 min, *t_r* (major) = 38.9 min.

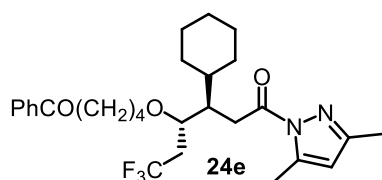
¹H NMR (500 MHz, CDCl₃, mixture of diastereoisomers) δ 8.00-7.92 (m, 2H), 7.58-7.52 (m, 1H), 7.48-7.43 (m, 2H), 5.93 (s, 1H), 3.73-3.65 (m, 1H), 3.56-3.47 (m, 2H), 3.20-3.13 (m, 1H), 3.07 (d, *J* = 17.4, 4.9 Hz, 1H), 2.98-2.93 (m, 2H), 2.52 (s, 3H), 2.47-2.22 (m, 3H), 2.22 (s, 3H), 2.00-1.70 (m, 4H), 1.70-1.57 (m, 4H), 1.55-1.46 (m, 3H), 1.29-1.22 (m, 1H), 1.20-1.10 (m, 1H).

¹³C NMR (125 MHz, CDCl₃, mixture of diastereoisomers) δ 200.3, 173.8, 151.8, 144.1, 137.1, 133.0, 128.6, 128.1, 126.7 (q, *J* = 275.9 Hz), 111.2, 76.1, 70.3, 43.8, 42.1, 38.3, 37.7, 37.5 (q, *J* = 27.2 Hz), 34.6, 31.6, 30.8, 29.6, 25.2, 24.7, 21.0, 14.7, 13.8.

¹⁹F NMR (282 MHz, CDCl₃, major diastereoisomer) δ -63.9 (s, 3F).

IR (film): ν (cm⁻¹) 2947, 2866, 1722, 1684, 1585, 1477, 1444, 1408, 1377, 1331, 1252, 1204, 1141, 1089, 1029, 1004, 961, 842, 804, 749, 689, 568, 414.

HRMS (ESI, *m/z*) calcd for C₂₇H₃₅F₃N₂O₃Na⁺[M+Na]⁺: 515.2492, found: 515.2492.



Starting from **21a** (94.0 mg, 0.60 mmol), **22b** (61.0 mg, 0.30 mmol)

and **23d** (23.2 mg, 0.10 mmol) with Λ -**RhS** (8 mol%) and 4,4'-difluorobenzil (40 mol%) for 30 h according to the general procedure to give **24e** as a pale yellow oil (33.0 mg, 0.0652 mmol, 65% yield, dr = 2:1). Enantiomeric excess established by HPLC analysis by using a Chiralpak OD-H column, ee

= 96% / 90%. $[\alpha]_{\text{D}}^{20} = -13.6^{\circ}$ (c 1.0, CH_2Cl_2). The dr value was determined by ^{19}F NMR of **24e** after purified by flash chromatography.

HPLC for major diastereomer: OD-H, 254 nm, *n*-hexane/isopropanol = 95:5, flow rate 0.5 mL/min, 25 °C, t_{r} (minor) = 10.8 min, t_{r} (major) = 14.1 min.

HPLC for minor diastereomer: OD-H, 254 nm, *n*-hexane/isopropanol = 95:5, flow rate 0.5 mL/min, 25 °C, t_{r} (minor) = 12.8 min, t_{r} (major) = 10.0 min.

^1H NMR (500 MHz, CDCl_3 , major diastereoisomer) δ 7.95-7.93 (m, 2H), 7.57-7.54 (m, 1H), 7.47-7.44 (m, 2H), 5.91 (s, 1H), 3.63-3.61 (m, 1H), 3.51-3.47 (m, 1H), 3.43-3.39 (m, 1H), 3.24 (dd, $J = 17.3, 7.3$ Hz, 1H), 2.95-2.88 (m, 3H), 2.51 (s, 3H), 2.43-2.33 (m, 2H), 2.26-2.22 (m, 1H), 2.21 (s, 3H), 1.78-1.72 (m, 3H), 1.68-1.62 (m, 4H), 1.45-1.40 (m, 2H), 1.28-1.15 (m, 3H), 1.13-1.00 (m, 3H).

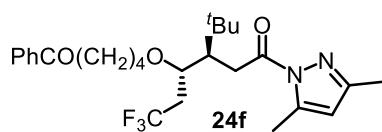
^{13}C NMR (125 MHz, CDCl_3 , major diastereoisomer) δ 200.2, 174.0, 151.7, 144.1, 137.1, 133.0, 128.6, 128.1, 126.6 (q, $J = 276.6$ Hz), 111.1, 74.9, 70.2, 45.0, 39.2, 38.3, 38.2 (q, $J = 27.0$ Hz), 33.0, 31.6, 29.9, 29.4, 26.7 (2C), 26.6, 21.0, 14.7, 13.8.

^1H NMR (500 MHz, CDCl_3 , minor diastereoisomer) δ 7.94-7.91 (m, 2H), 7.56-7.52 (m, 1H), 7.46-7.41 (m, 2H), 5.91 (s, 1H), 3.84-3.80 (m, 1H), 3.56-3.46 (m, 2H), 3.34-3.27 (m, 1H), 3.08 (t, $J = 5.1$ Hz, 2H), 2.91 (t, $J = 7.4$ Hz, 2H), 2.56-2.43 (m, 4H), 2.43-2.33 (m, 1H), 2.26-2.22 (m, 4H), 1.76-1.66 (m, 7H), 1.26-0.95 (m, 7H).

^{19}F NMR (282 MHz, CDCl_3) δ -64.37 (s, 3F, major), -64.41 (s, 3F, minor).

IR (film): ν (cm^{-1}) 2925, 2854, 1723, 1684, 1585, 1445, 1408, 1378, 1332, 1251, 1204, 1138, 1096, 1022, 961, 841, 804, 748, 689, 571, 406.

HRMS (ESI, m/z) calcd for $\text{C}_{28}\text{H}_{37}\text{F}_3\text{N}_2\text{O}_3\text{Na}^+$ $[\text{M}+\text{Na}]^+$: 529.2659, found: 529.2648.



Starting from **21a** (94.0 mg, 0.60 mmol), **22b** (61.0 mg, 0.30 mmol)

and **23e** (20.6 mg, 0.10 mmol) with Λ -**RhS** (6 mol%) and 4,4'-difluorobenzil (40 mol%) for 66 h according to the general procedure to give **24f** as a pale yellow oil (22.7 mg, 0.471 mmol, 47% yield, dr = 6:1). Enantiomeric excess established by HPLC analysis by using a Chiralpak OD-H column, ee = 96%. $[\alpha]_{\text{D}}^{20} = -18.2^{\circ}$ (c 1.0, CH_2Cl_2). The dr value was determined by ^1H NMR of **24f** after purified by flash chromatography.

HPLC for major diastereomer: OD-H, 254 nm, *n*-hexane/isopropanol = 98:2, flow rate 0.5 mL/min,

25 °C, t_r (minor) = 12.7 min, t_r (major) = 16.5 min.

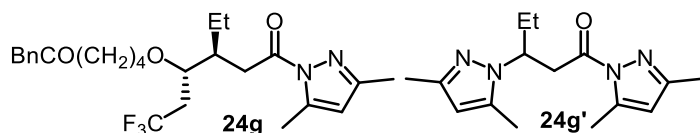
^1H NMR (500 MHz, CDCl_3) δ 7.94-7.93 (m, 2H), 7.57-7.54 (m, 1H), 7.47-7.44 (m, 2H), 5.90 (s, 1H), 3.70-3.68 (m, 1H), 3.50-3.39 (m, 2H), 3.25 (dd, J = 18.0, 7.4 Hz, 1H), 3.05 (dd, J = 18.0, 5.0 Hz, 1H), 2.88 (t, J = 7.3 Hz, 2H), 2.50 (s, 3H), 2.48-2.30 (m, 2H), 2.28-2.15 (m, 4H), 1.72-1.62 (m, 2H), 1.48-1.39 (m, 2H), 0.95 (s, 9H).

^{13}C NMR (125 MHz, CDCl_3) δ 200.2, 174.7, 151.6, 144.1, 137.1, 133.0, 128.6, 128.1, 126.5 (q, J = 277.0 Hz), 111.1, 73.3, 70.2, 49.8, 40.4 (q, J = 26.4 Hz), 38.3, 33.4, 31.4, 29.4, 28.1, 21.0, 14.7, 13.9.

^{19}F NMR (282 MHz, CDCl_3) δ -64.6 (s, 3F).

IR (film): ν (cm^{-1}) 2954, 2873, 1723, 1684, 1586, 1449, 1375, 1323, 1247, 1139, 1090, 963, 840, 804, 737, 690, 572, 479.

HRMS (ESI, m/z) calcd for $\text{C}_{26}\text{H}_{35}\text{F}_3\text{N}_2\text{O}_3\text{Na}^+[\text{M}+\text{Na}]^+$: 503.2492, found: 503.2491.



Starting from **21a** (94.0 mg, 0.60 mmol),

22c (62.0 mg, 0.30 mmol) and **23f** (17.8 mg, 0.10 mmol) with Λ -**RhS** (6 mol%) and 4,4'-difluorobenzil (40 mol%) for 14 h according to the general procedure to give **24g** as a pale yellow oil (11.80 mg, 0.0260 mmol, 26% yield, dr = 1.7:1), and **24g'** as a white solid (6.85 mg, 0.025 mmol, 50% yield). Enantiomeric excess of **24g** was established by HPLC analysis using a Chiralpak OD-H column, ee = 70% / 78%. $[\alpha]_D^{20} = -19.6^\circ$ (c 1.0, CH_2Cl_2). The dr value was determined by ^1H NMR of **24g** after purified by flash chromatography.

24g:

HPLC for major diastereomer: OD-H, 254 nm, *n*-hexane/isopropanol = 99:1, flow rate 1.0 mL/min, 25 °C, t_r (minor) = 10.7 min, t_r (major) = 14.2 min.

HPLC for minor diastereomer: OD-H, 254 nm, *n*-hexane/isopropanol = 99:1, flow rate 1.0 mL/min, 25 °C, t_r (minor) = 12.7 min, t_r (major) = 11.5 min.

^1H NMR (500 MHz, CDCl_3 , major diastereoisomer) δ 7.35-7.32 (m, 5H), 5.95 (s, 1H), 4.49 (s, 2H), 3.63-3.60 (m, 1H), 3.50-3.48 (m, 2H), 3.12 (dd, J = 17.0, 6.7 Hz, 1H), 2.99 (dd, J = 17.0, 6.1 Hz, 1H), 2.53 (s, 3H), 2.40-2.34 (m, 1H), 2.22 (s, 3H), 1.67-1.58 (m, 7H), 1.44-1.37 (m, 1H), 1.35-1.27 (m, 2H), 0.95 (t, J = 7.5 Hz, 3H).

^{13}C NMR (125 MHz, CDCl_3 , major diastereoisomer) δ 173.4, 152.0, 144.1, 138.7, 128.4, 127.7, 127.6,

127.5, 126.8 (q, $J = 276.8$ Hz), 111.2, 75.4, 72.9, 70.2, 40.2, 36.5 (q, $J = 27.2$ Hz), 35.4, 34.9, 26.8, 26.5, 23.1, 14.7, 13.9, 12.0.

^{19}F NMR (282 MHz, CDCl_3) δ -63.6 (s, 3F, major), -63.8 (s, 3F, minor).

IR (film): ν (cm^{-1}) 2930, 2868, 1719, 1584, 1452, 1379, 1341, 1260, 1097, 1023, 960, 842, 801, 709, 600, 470.

HRMS (ESI, m/z) calcd for $\text{C}_{24}\text{H}_{33}\text{F}_3\text{N}_2\text{O}_3\text{Na}^+$ $[\text{M}+\text{H}]^+$: 477.2335, found: 477.2336.

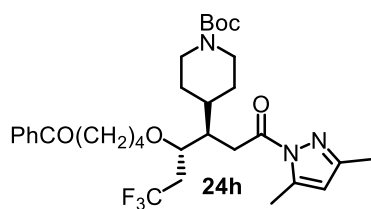
24g':

^1H NMR (500 MHz, CDCl_3) δ 5.95 (s, 1H), 5.76 (s, 1H), 4.62-4.56 (m, 1H), 4.01 (dd, $J = 18.1, 8.5$ Hz, 1H), 3.52 (dd, $J = 17.7, 4.3$ Hz, 1H), 2.48 (s, 3H), 2.33 (s, 3H), 2.25 (s, 3H), 2.24 (s, 3H), 1.92-1.84 (m, 2H), 0.77 (t, $J = 7.3$ Hz, 3H).

^{13}C NMR (125 MHz, CDCl_3) δ 171.5, 152.1, 147.4, 143.8, 111.1, 105.2, 104.3, 55.2, 41.0, 28.6, 14.4, 13.8, 11.2, 10.7.

IR (film): ν (cm^{-1}) 2933, 2877, 1590, 1458, 1341, 1260, 1097, 965, 801, 600, 470.

HRMS (ESI, m/z) calcd for $\text{C}_{15}\text{H}_{23}\text{N}_4\text{O}$ $[\text{M}+\text{H}]^+$: 275.1866, found: 275.1867.



Starting from **21a** (94.0 mg, 0.60 mmol), **22b** (61.0 mg, 0.30 mmol)

and **23g** (33.3 mg, 0.10 mmol) with Λ -**RhS** (6 mol%) and 4,4'-difluorobenzil (40 mol%) for 28 h according to the general procedure to give **24h** as a pale yellow oil (52.0 mg, 0.86 mmol, 86% yield, dr = 2:1). Enantiomeric excess established by HPLC analysis by using a Chiralpak AD-H column, ee = 94% / 92%. $[\alpha]_{\text{D}}^{20} = +15.8^\circ$ (c 1.0, CH_2Cl_2). The dr value was determined by ^{19}F NMR of **24h** after purified by flash chromatography.

HPLC for major diastereomer: AD-H, 254 nm, n -hexane/isopropanol = 90:10, flow rate 1.0 mL/min, 25 °C, t_{r} (minor) = 16.2 min, t_{r} (major) = 6.9 min.

HPLC for minor diastereomer: AD-H, 254 nm, n -hexane/isopropanol = 90:10, flow rate 1.0 mL/min, 25 °C, t_{r} (minor) = 10.1 min, t_{r} (major) = 8.3 min.

^1H NMR (500 MHz, CDCl_3 , major diastereoisomer) δ 7.96-7.92 (m, 2H), 7.57-7.53 (m, 1H), 7.47-7.43 (m, 2H), 5.93 (s, 1H), 4.11 (br, 2H), 3.66 (dd, $J = 5.2, 4.4$ Hz, 1H), 3.53-3.48 (m, 1H), 3.41 (td, $J = 6.2, 3.7, 2.5$ Hz, 1H), 3.18 (dd, $J = 11.3, 6.2$ Hz, 1H), 3.03 (dd, $J = 17.3, 5.9$ Hz, 1H), 2.94-2.91 (m,

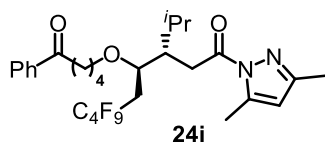
2H), 2.63 (br, 2H), 2.51 (s, 3H), 2.47-2.22 (m, 3H), 2.21 (s, 3H), 1.77-1.62 (m, 4H), 1.57-1.48 (m, 3H), 1.44 (s, 9H), 1.28-1.20 (m, 2H).

^{13}C NMR (125 MHz, CDCl_3 , major diastereoisomer) δ 200.0, 173.5, 154.8, 151.9, 144.2, 137.0, 133.0, 128.7, 128.1, 126.5 (q, $J = 278$ Hz, 1C), 111.3, 79.5, 74.4, 70.0, 44.0, 41.3, 38.3, 37.9, 37.6, 35.4 (q, $J = 28$ Hz), 32.9, 29.5, 28.5, 21.0, 17.4, 13.8.

^{19}F NMR (282 MHz, CDCl_3 , major diastereoisomer) δ -64.6 (s, 3F).

IR (film): ν (cm^{-1}) 2928, 2861, 1723, 1685, 1586, 1417, 1375, 1333, 1249, 1139, 1091, 1023, 964, 860, 804, 752, 690, 570, 534, 471, 412.

HRMS (ESI, m/z) calcd for $\text{C}_{32}\text{H}_{44}\text{F}_3\text{N}_3\text{O}_5\text{Na}^+$ $[\text{M}+\text{Na}]^+$: 630.3125, found: 630.3127.



Starting from **21b** (183.0 mg, 0.60 mmol), **22b** (61.0 mg, 0.30 mmol) and **23a** (19.2 mg, 0.10 mmol) with Δ -**RhS** (4 mol%) and 4,4'-difluorobenzil (25 mol%) for 38 h according to the general procedure to give **24i** as a pale yellow oil (31.4 mg, 0.0510 mmol, 51% yield, dr = 2.7:1).

Enantiomeric excess established by HPLC analysis by using a Chiralpak OD-H column, ee = 91% / 91%. $[\alpha]_{\text{D}}^{20} = -8.2^\circ$ (c 1.0, CH_2Cl_2). The dr value was determined by ^{19}F NMR of **24i** after purified by flash chromatography.

HPLC for major diastereomer: OD-H, 254 nm, n -hexane/isopropanol = 95:5, flow rate 0.5 mL/min, 25 $^\circ\text{C}$, t_{r} (minor) = 9.5 min, t_{r} (major) = 8.9 min.

HPLC for minor diastereomer: OD-H, 254 nm, n -hexane/isopropanol = 98:2, flow rate 0.3 mL/min, 25 $^\circ\text{C}$, t_{r} (minor) = 18.4 min, t_{r} (major) = 17.0 min.

^1H NMR (500 MHz, CD_2Cl_2 , major diastereoisomer) δ 7.93-7.91 (m, 2H), 7.56 (tt, $J = 6.8, 1.3$ Hz, 1H), 7.48-7.45 (m, 2H), 5.91 (s, 1H), 3.77 (q, $J = 4.7$ Hz, 1H), 3.53-3.48 (m, 1H), 3.43-3.38 (m, 1H), 3.26 (dd, $J = 17.0, 6.8$ Hz, 1H), 2.94-2.88 (m, 3H), 2.49 (s, 3H), 2.45-2.31 (m, 2H), 2.26-2.21 (m, 1H), 2.18 (s, 3H), 1.86-1.79 (m, 1H), 1.67-1.61 (m, 2H), 1.48-1.38 (m, 2H), 1.00 (d, $J = 6.8$ Hz, 3H), 0.91 (d, $J = 6.8$ Hz, 3H).

^1H NMR (500 MHz, CDCl_3 , minor diastereoisomer) δ 7.93-7.90 (m, 2H), 7.60-7.51 (m, 1H), 7.46-7.41 (m, 2H), 5.94 (s, 1H), 3.94-3.91 (m, 1H), 3.58-3.50 (m, 2H), 3.36-3.29 (m, 1H), 3.19 (dd, $J = 16.0, 7.0$ Hz, 1H), 2.99 (dd, $J = 16.0, 5.6$ Hz, 1H), 2.90 (t, $J = 7.2$ Hz, 2H), 2.50-2.38 (m, 5H), 2.25-2.13 (m, 4H), 1.73-1.64 (m, 2H), 1.48-1.42 (m, 2H), 0.98 (d, $J = 3.4$ Hz, 3H), 0.96 (d, $J = 3.4$ Hz, 3H).

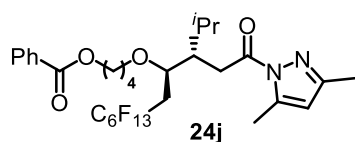
^{13}C NMR (125 MHz, CDCl_3 , major diastereoisomer) δ 200.1, 174.1, 151.8, 144.3, 137.5, 133.1, 128.8, 128.2, 111.2, 74.2, 70.3, 46.5, 38.5, 35.1 (t, $J = 21.0$ Hz), 32.7, 29.7, 29.3, 21.1, 21.0, 19.5, 14.7, 13.8.

^{19}F NMR (282 MHz, CDCl_3 , major diastereoisomer) δ -81.51 to -81.59 (m, 3F), -113.07 to -113.23 (m, 2F), -124.65 to -124.75 (m, 2F), -126.17 to -126.27 (m, 2F).

^{19}F NMR (282 MHz, CDCl_3 , minor diastereoisomer) δ -83.95 to -84.03 (m, 3F), -116.07 to -116.43 (m, 2F), -127.28 to -127.35 (m, 2F), -128.71 to -128.80 (m, 2F).

IR (film): ν (cm^{-1}) 2960, 2931, 2874, 1725, 1686, 1584, 1450, 1412, 1380, 1347, 1224, 1129, 1021, 962, 878, 803, 740, 692, 653, 596, 528.

HRMS (ESI, m/z) calcd for $\text{C}_{28}\text{H}_{33}\text{F}_9\text{N}_2\text{O}_3\text{Na}^+$ $[\text{M}+\text{Na}]^+$: 639.2240, found: 639.2241.



Starting from **21c** (243.0 mg, 0.60 mmol), **22a** (66.0 mg, 0.30 mmol)

and **23a** (19.2 mg, 0.10 mmol) with Δ -**RhS** (4 mol%) and 4,4'-difluorobenzil (25 mol%) for 30 h according to the general procedure to give **24j** as a pale yellow oil (30.6 mg, 0.0418 mmol, 42% yield, dr = 2.6:1). Enantiomeric excess established by HPLC analysis by using a Chiralpak AD-H column, ee = 90% / 87%. $[\alpha]_{\text{D}}^{20} = -9.6^\circ$ (c 1.0, CH_2Cl_2). The dr value was determined by ^{19}F NMR of **24j** after purified by flash chromatography.

HPLC for major diastereomer: AD-H, 254 nm, n -hexane/isopropanol = 99:1, flow rate 0.5 mL/min, 25 $^\circ\text{C}$, t_{r} (minor) = 8.7 min, t_{r} (major) = 9.2 min.

HPLC for minor diastereomer: AD-H, 254 nm, n -hexane/isopropanol = 99:1, flow rate 0.3 mL/min, 25 $^\circ\text{C}$, t_{r} (minor) = 14.5 min, t_{r} (major) = 17.3 min.

^1H NMR (500 MHz, CDCl_3 , major diastereoisomer) δ 8.06-8.03 (m, 2H), 7.56 (tt, $J = 7.4, 1.4$ Hz, 1H), 7.48-7.43 (m, 2H), 5.94 (s, 1H), 4.25 (t, $J = 6.5$ Hz, 2H), 3.79 (q, $J = 5.4$ Hz, 1H), 3.58-3.43 (m, 2H), 3.33 (dd, $J = 17.0, 7.3$ Hz, 1H), 2.93 (dd, $J = 17.0, 5.0$ Hz, 1H), 2.53 (s, 3H), 2.45-2.26 (m, 3H), 2.23 (s, 3H), 1.92-1.79 (m, 1H), 1.75-1.66 (m, 2H), 1.55-1.46 (m, 2H), 1.04 (d, $J = 6.8$ Hz, 3H), 0.96 (d, $J = 6.8$ Hz, 3H).

^1H NMR (500 MHz, CD_2Cl_2 , minor diastereoisomer) δ 8.01-7.98 (m, 2H), 7.59-7.54 (m, 1H), 7.46-7.41 (m, 2H), 5.94 (s, 1H), 4.22 (td, $J = 6.5, 1.5$ Hz, 2H), 3.97-3.93 (m, 1H), 3.58-3.51 (m, 1H), 3.37-3.30 (m, 1H), 3.21 (dd, $J = 16.0, 7.6$ Hz, 1H), 2.98 (dd, $J = 15.9, 5.4$ Hz, 1H), 2.62-2.40 (m, 5H), 2.30-2.11 (m, 4H), 1.75-1.63 (m, 2H), 1.1.62-1.53 (m, 3H), 1.02-0.94 (m, 6H).

^{13}C NMR (125 MHz, CDCl_3 , major diastereoisomer) δ 173.9, 166.6, 151.6, 144.0, 132.8, 130.4, 129.5, 128.3, 111.1, 74.1, 69.8, 64.8, 46.3, 35.2 (t, $J = 21.3$ Hz), 32.4, 28.8, 26.4, 25.4, 21.0, 19.3, 14.6, 13.7.

^{19}F NMR (282 MHz, CDCl_3 , minor diastereoisomer) δ -80.94 to -81.01 (m, 3F), -113.03 to -116.45 (m, 2F), -121.85 to -121.96 (m, 2F), -122.96 to -123.08 (m, 2F), -123.66 to -123.60 (m, 2F), -126.24 to -126.32 (m, 2F).

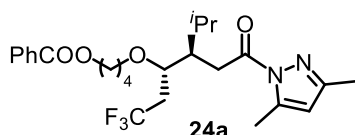
^{19}F NMR (282 MHz, CDCl_3 , major diastereoisomer) δ -80.75 (t, $J = 9.5$ Hz, 3F), -112.50 to -112.69 (m, 2F), -121.62 to -121.74 (m, 2F), -122.74 to -122.84 (m, 2F), -123.28 to -123.38 (m, 2F), -126.00 to -126.10 (m, 2F).

IR (film): ν (cm^{-1}) 2960, 2931, 2874, 1725, 1686, 1584, 1450, 1412, 1380, 1347, 1224, 1129, 1021, 962, 878, 803, 740, 692, 653, 596, 528.

HRMS (ESI, m/z) calcd for $\text{C}_{30}\text{H}_{33}\text{F}_{13}\text{N}_2\text{O}_4\text{Na}^+$ $[\text{M}+\text{Na}]^+$: 755.2125, found: 755.2133.

2) General Procedure for Figure 51:

A dried 10 mL Schlenk tube was charged with the catalyst Λ or Δ -**RhS** (6 mol%) as indicated, 4,4'-difluorobenzil (9.80 mg, 0.04 mmol, 40 mol%), Langlois reagent **21a** (94.0 mg, 0.6 mmol), vinyl ethers **22a**, **22c-q** (0.3 mmol) and *N*-acylpyrazoles **23a**, **23g** (0.1 mmol) in acetone/ H_2O (v/v = 9:1, 1.0 mL). The reaction mixture was degassed *via* freeze-pump-thaw for three cycles. After the mixture was thoroughly degassed, the vial was sealed and positioned approximately 10 cm from 24 W blue LEDs. The reaction was stirred at 5-7 °C for the indicated time (24–48 h) (monitored by TLC) under nitrogen atmosphere. Afterwards, the mixture was concentrated under reduced pressure. The residue was subjected to a flash chromatography on silica gel to afford the products **24a**, **24k-y**. The dr value was determined by ^{19}F NMR analysis after purification, except that **24q**, **24u** and **24v** were determined by the crude ^{19}F NMR. The dr value of **24y** was determined by ^{19}F NMR and chiral HPLC analysis. The enantiomeric excess was determined by chiral HPLC analysis.



Starting from **21a** (94.0 mg, 0.60 mmol), **22a** (66.0 mg, 0.30 mmol) and **23a** (19.2 mg, 0.10 mmol) with Λ -**RhS** (6 mol%) and 4,4'-difluorobenzil (40 mol%) for 32 h according to the general procedure to give **24a** as a pale yellow oil (31.0 mg, 0.0643 mmol, 64% yield, dr = 2:1). Enantiomeric excess established by HPLC analysis by using a Chiralpak OD-H column, ee

= 96% / 96% (major/minor). $[\alpha]_D^{20} = +1.4^\circ$ (c 1.0, CH_2Cl_2). The dr value was determined by crude ^{19}F NMR of **24a**.

HPLC for major diastereomer: OD-H, 254 nm, *n*-hexane/isopropanol = 99: 1, flow rate 0.4 mL/min, 25 °C, t_r (minor) = 19.4 min, t_r (major) = 29.2 min.

HPLC for minor diastereomer: OD-H, 254 nm, *n*-hexane/isopropanol = 99: 1, flow rate 0.4 mL/min, 25 °C, t_r (minor) = 23.2 min, t_r (major) = 21.1 min.

^1H NMR (300 MHz, CDCl_3 , major diastereoisomer) δ 8.06-8.03 (m, 2H), 7.58 (tt, $J = 7.4, 2.1$ Hz, 1H), 7.48-7.43 (m, 2H), 5.93 (s, 1H), 4.25 (t, $J = 6.6$ Hz, 2H), 3.62-3.58 (m, 1H), 3.56-3.46 (m, 2H), 3.31 (dd, $J = 17.1, 7.4$ Hz, 1H), 2.91 (dd, $J = 17.1, 4.7$ Hz, 1H), 2.53 (s, 3H), 2.50-2.35 (m, 2H), 2.34-2.26 (m, 1H), 2.24 (s, 3H), 1.92-1.80 (m, 1H), 1.76-1.65 (m, 2H), 1.54-1.48 (m, 2H), 1.03 (d, $J = 6.8$ Hz, 3H), 0.94 (d, $J = 6.8$ Hz, 3H).

^1H NMR (300 MHz, CDCl_3 , minor diastereoisomer) δ 8.03-8.00 (m, 2H), 7.55 (tt, $J = 7.4, 2.1$ Hz, 1H), 7.45-7.40 (m, 2H), 5.92 (s, 1H), 4.25 (td, $J = 6.5, 1.7$ Hz, 2H), 3.84-3.78 (m, 1H), 3.60-3.53 (m, 1H), 3.38-3.30 (m, 1H), 3.15 (dd, $J = 16.4, 6.8$ Hz, 1H), 3.03 (dd, $J = 16.3, 5.7$ Hz, 1H), 2.50 (s, 3H), 2.48-2.35 (m, 2H), 2.30-2.15 (m, 4H), 1.80-1.66 (m, 2H), 1.64-1.56 (m, 3H), 0.98 (d, $J = 4.6$ Hz, 3H), 0.96 (d, $J = 4.5$ Hz, 3H).

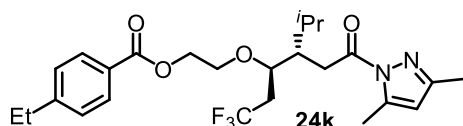
^{13}C NMR (125 MHz, CDCl_3 , major diastereoisomer) δ 174.0, 166.7, 151.7, 144.1, 132.9, 133.5, 129.6, 128.4, 126.6 (q, $J = 278.2$ Hz), 111.1, 75.3, 70.1, 64.9, 45.6, 38.3 (q, $J = 27.2$ Hz), 32.5, 28.7, 26.4, 25.4, 21.2, 19.1, 14.7, 13.9..

^{19}F NMR (282 MHz, CDCl_3 , major diastereoisomer) δ -63.48 (s, 3F).

^{19}F NMR (282 MHz, CDCl_3 , minor diastereoisomer) δ -63.67 (s, 3F).

IR (film): ν (cm^{-1}) 2958, 2875, 1718, 1583, 1453, 1379, 1338, 1265, 1133, 1102, 1028, 961, 842, 804, 746, 711, 675, 587, 474.

HRMS (ESI, m/z) calcd for $\text{C}_{25}\text{H}_{33}\text{F}_3\text{N}_2\text{O}_4\text{Na}^+$ $[\text{M}+\text{Na}]^+$: 505.2285, found: 505.2293.



Starting from **21a** (94.0 mg, 0.60 mmol), **22c** (66.0 mg, 0.30

mmol) and **23a** (19.2 mg, 0.10 mmol) with Δ -**RhS** (6 mol%) and 4,4'-difluorobenzil (40 mol%) for 30 h according to the general procedure to give **24k** as a pale yellow oil (31.8 mg, 0.0660 mmol, 66% yield, dr = 2.1:1). Enantiomeric excess established by HPLC analysis by using a Chiralpak OD-H

column, ee = 98% / 96. $[\alpha]_{\text{D}}^{20} = -13.4^{\circ}$ (*c* 1.0, CH₂Cl₂). The dr value was determined by ¹⁹F NMR of **24k** after purified by flash chromatography.

HPLC for major diastereomer: OD-H, Daicel column (250 x 4.6 mm), 254 nm, *n*-hexane/isopropanol = 99:1, flow rate 0.3 mL/min, 25 °C, *t_r* (minor) = 37.2 min, *t_r* (major) = 33.1 min.

HPLC for minor diastereomer: OD-H, Daicel column (250 x 4.6 mm), 254 nm, *n*-hexane/isopropanol = 99:1, flow rate 0.3 mL/min, 25 °C, *t_r* (minor) = 26.9 min, *t_r* (major) = 35.6 min.

¹H NMR (300 MHz, CD₂Cl₂) δ 7.93 (d, *J* = 8.2 Hz, 2H), 7.28 (d, *J* = 8.2 Hz, 2H), 5.98 (s, 1H), 4.33-4.18 (m, 2H), 3.90-3.75 (m, 3H), 3.26 (dd, *J* = 17.2, 6.6 Hz, 1H), 3.02 (dd, *J* = 17.4, 5.6 Hz, 1H), 2.73 (q, *J* = 7.6 Hz, 2H) 2.58-2.43 (m, 5H), 2.33-2.25 (m, 1H), 2.21 (s, 3H), 1.94-1.80 (m, 1H), 1.28 (t, *J* = 7.5 Hz, 3H), 1.20 (d, *J* = 6.8 Hz, 3H), 0.94 (d, *J* = 6.8 Hz, 3H).

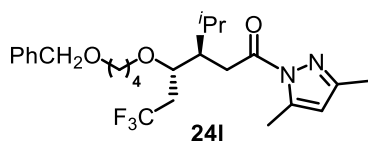
¹³C NMR (75 MHz, CDCl₃) δ 173.6, 166.3, 151.6, 149.8, 143.9, 129.6, 127.8, 127.7, 128.4, 126.6 (q, *J* = 276.9 Hz), 111.9, 75.5 (d, *J* = 2.5 Hz), 68.3, 63.8, 45.1, 37.6 (q, *J* = 26.8 Hz), 32.5, 28.9 (2C), 20.8, 19.2, 14.9, 14.2, 13.4.

¹⁹F NMR (282 MHz, CDCl₃, major diastereoisomer) δ -63.7 (s, 3F).

¹⁹F NMR (282 MHz, CDCl₃, major diastereoisomer, under proton irradiation) δ -63.7 (t, *J* = 11.2 Hz, 3F).

IR (film): ν (cm⁻¹) 2952, 2874, 1718, 1582, 1453, 1379, 1340, 1265, 1133, 1105, 1029, 960, 832, 802, 746, 711, 675, 587, 474.

HRMS (ESI, *m/z*) calcd for C₂₅H₃₃F₃N₂O₄Na⁺ [M+Na]⁺: 505.2285, found: 505.2279.



Starting from **21a** (94.0 mg, 0.60 mmol), **22d** (62.0 mg, 0.30 mmol)

and **23a** (19.2 mg, 0.10 mmol) with Λ -**RhS** (6 mol%) and 4,4'-difluorobenzil (40 mol%) for 32 h according to the general procedure to give **24l** as a pale yellow oil (26.6 mg, 0.0568 mmol, 57% yield, dr = 2:1). Enantiomeric excess established by HPLC analysis by using a Chiralpak OD-H column, ee = 96% / 96%. $[\alpha]_{\text{D}}^{20} = +2.8^{\circ}$ (*c* 1.0, CH₂Cl₂). The dr value was determined by ¹⁹F NMR of **24l** after purified by flash chromatography.

HPLC for major diastereomer: OD-H, 254 nm, *n*-hexane/isopropanol = 99: 1, flow rate 0.5 mL/min, 25 °C, *t_r* (minor) = 16.4 min, *t_r* (major) = 18.3 min.

HPLC for minor diastereomer: OD-H, 254 nm, *n*-hexane/isopropanol = 99: 1, flow rate 0.5 mL/min,

25 °C, t_r (minor) = 13.3min, t_r (major) = 12.5 min.

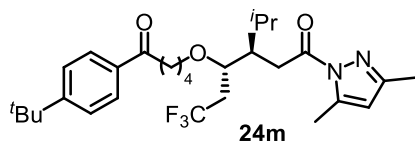
^1H NMR (500 MHz, CDCl_3 , major diastereoisomer) δ 7.35-7.28 (m, 5H), 5.92 (s, 1H), 4.47 (s, 2H), 3.60-3.57 (m, 1H), 3.49-3.43 (m, 1H), 3.40-3.36 (m, 3H), 3.24 (dd, J = 17.2, 7.1 Hz, 1H), 3.24 (dd, J = 17.2, 5.1 Hz, 1H), 2.52 (s, 3H), 2.44-2.31 (m, 2H), 2.22 (s, 3H), 1.85-1.79 (m, 1H), 1.59-1.55 (m, 3H), 1.44-1.38 (m, 2H), 0.99 (d, J = 6.8 Hz, 3H), 0.91 (d, J = 6.8 Hz, 3H).

^{13}C NMR (125 MHz, CDCl_3 , major diastereoisomer) δ 174.0, 151.7, 144.1, 138.7, 128.4, 127.7, 127.6, 111.1, 75.0, 72.9, 70.2 (2C), 45.5, 38.1 (q, J = 26.5 Hz), 32.5, 28.8, 26.6, 26.4, 21.1, 19.3, 14.7, 13.9.

^{19}F NMR (282 MHz, CDCl_3 , major diastereoisomer) δ -63.54 (s, 3F).

IR (film): ν (cm^{-1}) 2999, 2945, 2864, 1722, 1583, 1484, 1444, 1384, 1341, 1259, 1138, 1088, 1027, 971, 899, 844, 798, 740, 707, 594, 463, 407.

HRMS (ESI, m/z) calcd for $\text{C}_{25}\text{H}_{35}\text{F}_3\text{N}_2\text{O}_3\text{Na}^+$ $[\text{M}+\text{Na}]^+$: 491.2492, found: 491.2494.



Starting from **21a** (94.0 mg, 0.60 mmol), **22e** (78.0 mg, 0.30 mmol)

and **23a** (19.2 mg, 0.10 mmol) with Λ -**RhS** (6 mol%) and 4,4'-difluorobenzil (40 mol%) for 30 h according to the general procedure to give **24m** as a pale yellow oil (34.4 mg, 0.0670 mmol, 67% yield, dr = 2.2:1). Enantiomeric excess established by HPLC analysis by using Chiralpak OD-H / AD-H columns, ee = 93% / 93%. $[\alpha]_{\text{D}}^{20} = -2.6^\circ$ (c 1.0, CH_2Cl_2). The dr value was determined by ^{19}F NMR of **24m** after purified by flash chromatography.

HPLC for major diastereomer: OD-H, 254 nm, n -hexane/isopropanol = 98:2, flow rate 0.3 mL/min, 25 °C, t_r (minor) = 19.6 min, t_r (major) = 21.6 min.

HPLC for minor diastereomer: AD-H, 254 nm, n -hexane/isopropanol = 95:5, flow rate 0.5 mL/min, 25 °C, t_r (minor) = 10.4min, t_r (major) = 11.0 min.

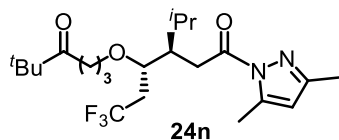
^1H NMR (300 MHz, CDCl_3 , major diastereoisomer) δ 7.91-7.88 (m, 2H), 7.50-7.47 (m, 2H), 5.93 (s, 1H), 3.62 (q, J = 5.0 Hz, 1H), 3.55-3.40 (m, 2H), 3.27 (dd, J = 17.1, 7.1 Hz, 1H), 2.96-2.85 (m, 3H), 2.53 (s, 3H), 2.49-2.32 (m, 2H), 2.30-2.16 (m, 4H), 1.90-1.80 (m, 1H), 1.74-1.64 (m, 2H), 1.50-1.40 (m, 2H), 1.36 (s, 9H), 1.01 (d, J = 6.8 Hz, 3H), 0.93 (d, J = 6.8 Hz, 3H).

^{13}C NMR (125 MHz, CDCl_3 , major diastereoisomer) δ 199.9, 174.0, 156.7, 151.7, 144.1, 134.5, 128.1, 126.6 (q, J = 276.9 Hz), 125.6, 111.1, 75.2, 70.3, 64.9, 45.6, 38.19, 38.16 (q, J = 26.8 Hz), 35.2, 32.5, 31.2, 29.5, 28.8, 21.2, 19.2, 14.7, 13.9.

^{19}F NMR (282 MHz, CDCl_3 , major diastereoisomer) δ -63.54 (s, 3F).

IR (film): ν (cm^{-1}) 2961, 2873, 1725, 1682, 1604, 1468, 1379, 1341, 1255, 1138, 1099, 1026, 962, 842, 809, 740, 669, 580, 543, 488, 409.

HRMS (ESI, m/z) calcd for $\text{C}_{29}\text{H}_{41}\text{F}_3\text{N}_2\text{O}_3\text{Na}^+$ $[\text{M}+\text{Na}]^+$: 545.2961, found: 545.2964.



Starting from **21a** (94.0 mg, 0.60 mmol), **22f** (51.0 mg, 0.30 mmol) and **23a** (19.2 mg, 0.10 mmol) with Λ -**RhS** (6 mol%) and 4,4'-difluorobenzil (40 mol%) for 30 h according to the general procedure to give **24n** as a pale yellow oil (30.2 mg, 0.0699 mmol, 70% yield, dr = 2:1). Enantiomeric excess established by HPLC analysis by using a Chiralpak OJ-H / OD-H column, ee = 98% / 93%. $[\alpha]_{\text{D}}^{20} = -10.0^\circ$ (c 1.0, CH_2Cl_2). The dr value was determined by ^{19}F NMR of **24n** after purified by flash chromatography.

HPLC for major diastereomer: OJ-H, 254 nm, n -hexane/isopropanol = 99:1, flow rate 0.1 mL/min, 15 $^\circ\text{C}$, t_{r} (minor) = 47.7 min, t_{r} (major) = 51.0 min.

HPLC for minor diastereomer: OD-H, 254 nm, n -hexane/isopropanol = 95:5, flow rate 0.2 mL/min, 25 $^\circ\text{C}$, t_{r} (minor) = 20.3 min, t_{r} (major) = 21.8 min.

^1H NMR (300 MHz, CDCl_3 , major diastereoisomer) δ 5.96 (s, 1H), 3.63-3.57 (m, 1H), 3.46-3.41 (m, 2H), 3.23 (dd, $J = 17.3, 7.1$ Hz, 1H), 2.94 (dd, $J = 17.3, 5.2$ Hz, 1H), 2.53 (s, 3H), 2.50-2.32 (m, 4H), 2.28-2.16 (m, 4H), 1.88-1.78 (m, 1H), 1.65-1.56 (m, 2H), 1.11 (s, 9H), 1.00 (d, $J = 6.8$ Hz, 3H), 0.92 (d, $J = 6.8$ Hz, 3H).

^1H NMR (300 MHz, CDCl_3 , minor diastereoisomer) δ 5.95 (s, 1H), 3.82-3.75 (m, 1H), 3.56-3.46 (m, 1H), 3.30-3.20 (m, 1H), 3.14 (dd, $J = 16.4, 6.6$ Hz, 1H), 3.02 (dd, $J = 16.5, 5.9$ Hz, 1H), 2.52 (s, 3H), 2.50-2.38 (m, 4H), 2.23 (s, 3H), 2.20-2.10 (m, 1H), 1.76-1.58 (m, 2H), 1.53-1.48 (m, 1H), 1.10 (s, 9H), 0.97 (d, $J = 5.0$ Hz, 3H), 0.95 (d, $J = 4.9$ Hz, 3H).

^{13}C NMR (125 MHz, CDCl_3 , major diastereoisomer) δ 215.7, 173.9, 151.7, 144.0, 126.5 (q, $J = 276.5$ Hz), 111.1, 75.0, 69.5, 45.2, 44.0, 37.9 (q, $J = 26.9$ Hz), 33.0, 32.5, 28.8, 26.5, 24.0, 21.1, 19.4, 14.7, 13.8.

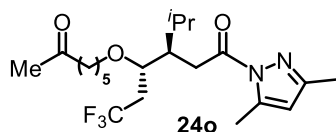
^{19}F NMR (282 MHz, CDCl_3 , major diastereoisomer) δ -63.41 (s, 3F).

^{19}F NMR (282 MHz, CDCl_3 , minor diastereoisomer) δ -63.50 (s, 3F).

IR (film): ν (cm^{-1}) 2963, 2875, 1715, 1586, 1471, 1377, 1339, 1253, 1138, 1093, 1055, 961, 842, 804,

742, 669, 586.

HRMS (ESI, m/z) calcd for $C_{22}H_{35}F_3N_2O_3Na^+$ $[M+Na]^+$: 455.2492, found: 455.2490.



Starting from **21a** (94.0 mg, 0.60 mmol), **22g** (47.0 mg, 0.30 mmol) and

23a (19.2 mg, 0.10 mmol) with Λ -**RhS** (6 mol%) and 4,4'-difluorobenzil (40 mol%) for 40 h according to the general procedure to give **24o** as a pale yellow oil (28.4 mg, 0.0679 mmol, 68% yield, dr = 2.7:1). Enantiomeric excess established by HPLC analysis by using a Chiralpak OD-H column, ee = 95% / 93%. $[\alpha]_D^{20} = +14.4^\circ$ (c 1.0, CH_2Cl_2). The dr value was determined by ^{19}F NMR of **24o** after purified by flash chromatography.

HPLC for major diastereomer: OD-H, 254 nm, n -hexane/isopropanol = 98:2, flow rate 0.5 mL/min, 25 °C, t_r (minor) = 11.4 min, t_r (major) = 12.0 min.

HPLC for minor diastereomer: OD-H, 254 nm, n -hexane/isopropanol = 98:2, flow rate 0.5 mL/min, 25 °C, t_r (minor) = 11.6 min, t_r (major) = 11.1 min.

1H NMR (300 MHz, $CDCl_3$, major diastereoisomer) δ 5.96 (s, 1H), 3.60-3.54 (m, 1H), 3.48-3.32 (m, 2H), 3.25 (dd, $J = 17.1, 7.3$ Hz, 1H), 2.89 (dd, $J = 17.2, 5.0$ Hz, 1H), 2.53 (s, 3H), 2.48-2.32 (m, 4H), 2.23 (s, 3H), 2.12 (s, 3H), 1.90-1.78 (m, 1H), 1.51-1.46 (m, 2H), 1.38-1.18 (m, 5H), 1.00 (d, $J = 6.8$ Hz, 3H), 0.91 (d, $J = 6.8$ Hz, 3H).

1H NMR (300 MHz, $CDCl_3$, minor diastereoisomer) δ 5.95 (s, 1H), 3.81-3.74 (m, 1H), 3.52-3.42 (m, 1H), 3.30-3.22 (m, 1H), 3.13 (dd, $J = 16.6, 6.7$ Hz, 1H), 3.03 (dd, $J = 16.4, 6.0$ Hz, 1H), 2.52 (s, 3H), 2.48-2.32 (m, 4H), 2.23 (s, 3H), 2.20-2.08 (m, 4H), 1.52-1.32 (m, 4H), 1.30-1.20 (m, 3H), 0.98-0.94 (m, 6H).

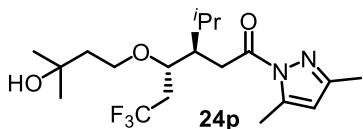
^{13}C NMR (125 MHz, $CDCl_3$, major diastereoisomer) δ 209.2, 174.0, 151.6, 144.1, 126.6 (q, $J = 276.8$ Hz), 111.1, 75.2, 70.4, 45.5, 43.7, 38.2 (q, $J = 26.8$ Hz), 32.5, 30.0, 29.6, 28.7, 25.6, 23.7, 21.2, 19.2, 14.8, 13.9.

^{19}F NMR (282 MHz, $CDCl_3$, major diastereoisomer) δ -63.50 (s, 3F).

^{19}F NMR (282 MHz, $CDCl_3$, minor diastereoisomer) δ -63.65 (s, 3F).

IR (film): ν (cm^{-1}) 2935, 2872, 1719, 1585, 1465, 1377, 1342, 1254, 1138, 1095, 961, 841, 804, 740, 670, 591, 524, 477, 414.

HRMS (ESI, m/z) calcd for $C_{21}H_{33}F_3N_2O_3Na^+$ $[M+Na]^+$: 441.2335, found: 441.2335.



Starting from **21a** (94.0 mg, 0.60 mmol), **22h** (39.0 mg, 0.30 mmol)

and **23a** (19.2 mg, 0.10 mmol) with Λ -**RhS** (6 mol%) and 4,4'-difluorobenzil (40 mol%) for 28 h according to the general procedure to give **24p** as a pale yellow oil (20.2 mg, 0.0515 mmol, 52% yield, dr = 2:1). Enantiomeric excess established by HPLC analysis by using a Chiralpak AD-H column, ee = 94% / 95%. $[\alpha]_D^{20} = +24.4^\circ$ (*c* 1.0, CH₂Cl₂). The dr value was determined by ¹⁹F NMR of **24p** after purified by flash chromatography.

HPLC for major diastereomer: AD-H, 254 nm, *n*-hexane/isopropanol = 90:10, flow rate 0.5 mL/min, 25 °C, *t_r* (minor) = 7.9 min, *t_r* (major) = 8.2 min.

HPLC for minor diastereomer: AD-H, 254 nm, *n*-hexane/isopropanol = 98:2, flow rate 0.5 mL/min, 25 °C, *t_r* (minor) = 19.3 min, *t_r* (major) = 17.3 min.

¹H NMR (300 MHz, CDCl₃, major diastereoisomer) δ 5.96 (s, 1H), 3.79-3.70 (m, 1H), 3.66-3.58 (m, 2H), 3.24 (dd, *J* = 17.3, 7.6 Hz, 1H), 2.91 (dd, *J* = 17.3, 4.8 Hz, 1H), 2.57-2.35 (m, 6H), 2.32-2.26 (m, 1H), 2.23 (s, 3H), 1.90-1.78 (m, 1H), 1.53-1.47 (m, 2H), 1.18 (s, 3H), 1.14 (s, 3H), 1.02 (d, *J* = 6.8 Hz, 3H), 0.92 (d, *J* = 6.8 Hz, 3H).

¹H NMR (300 MHz, CDCl₃, minor diastereoisomer) δ 5.96 (s, 1H), 3.86-3.74 (m, 2H), 3.59-3.50 (m, 1H), 3.09 (dd, *J* = 6.5, 3.5 Hz, 2H), 2.53-2.38 (m, 6H), 2.30-2.16 (m, 5H), 1.67-1.64 (m, 2H), 1.18 (s, 3H), 1.15 (s, 3H), 1.00-0.96 (m, 6H).

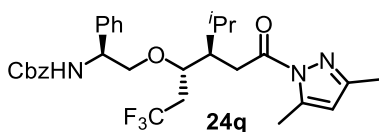
¹³C NMR (125 MHz, CDCl₃, major diastereoisomer) δ 173.7, 151.9, 144.4, 126.5 (q, *J* = 276.6 Hz), 111.2, 76.1, 70.1, 67.9, 45.1, 41.9, 38.1 (q, *J* = 27.1 Hz), 32.5, 29.6, 29.1, 28.7, 21.3, 19.3, 14.7, 13.8.

¹⁹F NMR (282 MHz, CDCl₃, major diastereoisomer) δ -63.53 (s, 3F).

¹⁹F NMR (282 MHz, CDCl₃, minor diastereoisomer) δ -63.64 (s, 3F).

IR (film): ν (cm⁻¹) 2966, 2930, 2879, 1724, 1583, 1469, 1380, 1341, 1254, 1136, 1086, 1031, 989, 961, 888, 841, 804, 741, 669, 587, 463, 415.

HRMS (ESI, *m/z*) calcd for C₁₉H₃₁F₃N₂O₃Na⁺ [M+ Na]⁺: 415.2179, found: 415.2177.



Starting from **21a** (94.0 mg, 0.60 mmol), **22i** (89.0 mg, 0.30 mmol)

and **23a** (19.2 mg, 0.10 mmol) with Λ -**RhS** (6 mol%) and 4,4'-difluorobenzil (40 mol%) for 26 h

according to the general procedure to give **24q** as a pale yellow oil (32.1 mg, 0.0574 mmol, 57% yield, dr > 28:5:1). $[\alpha]_D^{20} = +10.0^\circ$ (*c* 1.0, CH₂Cl₂). The dr value was determined by crude ¹⁹F NMR of **24q**.

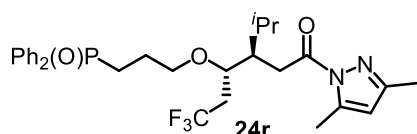
¹H NMR (300 MHz, CDCl₃, major diastereoisomer) δ 7.40-7.28 (m, 5H), 7.25-7.19 (m, 3H), 7.16-7.12 (m, 2H), 5.90 (s, 1H), 5.67 (br, 1H), 5.07 (s, 2H), 4.62 (br, 1H), 3.70-3.58 (m, 3H), 3.33 (dd, *J* = 17.0, 8.1 Hz, 1H), 2.82 (dd, *J* = 17.0, 4.5 Hz, 1H), 2.48 (s, 3H), 2.42-2.22 (m, 3H), 2.20 (s, 3H), 1.84-1.72 (m, 1H), 0.96 (d, *J* = 6.8 Hz, 3H), 0.88 (d, *J* = 6.8 Hz, 3H).

¹³C NMR (125 MHz, CDCl₃, major diastereoisomer) δ 173.7, 155.9, 152.0, 144.3, 128.4, 128.3, 128.1, 128.0, 127.4, 126.6, 111.3, 75.3, 72.7, 66.6, 54.9, 45.5, 38.1 (q, *J* = 27.0 Hz), 32.3, 28.8, 21.0, 18.9, 14.6, 13.8.

¹⁹F NMR (282 MHz, CDCl₃, major diastereoisomer) δ -63.32 (s, 3F).

IR (film): ν (cm⁻¹) 2961, 2930, 2875, 1718, 1585, 1504, 1461, 1381, 1338, 1252, 1138, 1054, 992, 963, 914, 843, 806, 744, 698, 585, 535, 479, 412.

HRMS (ESI, *m/z*) calcd for C₃₀H₃₆F₃N₃O₄Na⁺ [M+H]⁺: 582.2550, found: 582.2556.



Starting from **21a** (94.0 mg, 0.60 mmol), **22j** (87.0 mg, 0.30 mmol)

and **23a** (19.2 mg, 0.10 mmol) with Λ -**RhS** (6 mol%) and 4,4'-difluorobenzil (40 mol%) for 26 h according to the general procedure to give **24r** as a pale yellow oil (45.0 mg, 0.0821 mmol, 82% yield, dr = 1.7:1). Enantiomeric excess established by HPLC analysis by using a Chiralpak OD-H column, ee = 92% / 93%. $[\alpha]_D^{20} = -3.8^\circ$ (*c* 1.0, CH₂Cl₂). The dr value was determined by ¹⁹F NMR of **24r** after purified by flash chromatography.

HPLC for major diastereomer: OD-H, 254 nm, *n*-hexane/isopropanol = 95:5, flow rate 0.5 mL/min, 25 °C, *t_r* (minor) = 45.9 min, *t_r* (major) = 56.7 min.

HPLC for minor diastereomer: OD-H, 254 nm, *n*-hexane/isopropanol = 95:5, flow rate 0.5 mL/min, 25 °C, *t_r* (minor) = 35.6 min, *t_r* (major) = 38.9 min.

¹H NMR (300 MHz, CDCl₃, major diastereoisomer) δ 7.75-7.68 (m, 4H), 7.56-7.40 (m, 6H), 5.89 (s, 1H), 3.65-3.58 (m, 1H), 3.57-3.45 (m, 2H), 3.25 (dd, *J* = 17.3, 6.9 Hz, 1H), 2.96 (dd, *J* = 17.3, 5.3 Hz, 1H), 2.46 (s, 3H), 2.42-2.35 (m, 2H), 2.30-2.24 (m, 2H), 2.20 (s, 3H), 1.86-1.80 (m, 4H), 0.98 (d, *J* = 6.8 Hz, 3H), 0.92 (d, *J* = 6.8 Hz, 3H).

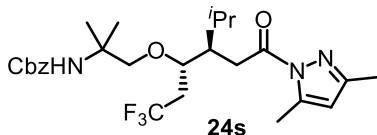
¹³C NMR (125 MHz, CDCl₃, major diastereoisomer) δ 173.8, 151.8, 144.0, 131.9, 130.94, 130.91,

130.87, 130.83, 128.8, 128.7, 126.5 (q, $J = 277.2$ Hz), 111.3, 75.3, 70.3, 45.2, 37.9 (q, $J = 27.1$ Hz), 32.6, 32.5, 29.0, 22.3, 21.1, 19.4, 14.7, 13.8.

^{19}F NMR (282 MHz, CDCl_3) δ -63.35 (s, 3F, major diastereoisomer), -63.42 (s, 3F, minor diastereoisomer).

IR (film): ν (cm^{-1}) 3000, 2942, 1717, 1429, 1343, 1251, 1181, 1137, 984, 915, 843, 713, 545, 476.

HRMS (ESI, m/z) calcd for $\text{C}_{29}\text{H}_{36}\text{F}_3\text{N}_2\text{O}_3\text{PNa}^+ [\text{M}+\text{Na}]^+$: 571.2308, found: 571.2304.



Starting from **21a** (94.0 mg, 0.60 mmol), **22k** (75.0 mg, 0.30 mmol)

and **23a** (19.2 mg, 0.10 mmol) with Λ -**RhS** (6 mol%) and 4,4'-difluorobenzil (40 mol%) for 38 h according to the general procedure to give **24s** as a pale yellow oil (26.0 mg, 0.0508 mmol, 51% yield, dr = 1.8:1). Enantiomeric excess established by HPLC analysis by using a Chiralpak OD-H column, ee = 90% / 90%. $[\alpha]_{\text{D}}^{20} = +3.2^\circ$ (c 1.0, CH_2Cl_2). The dr value was determined by ^{19}F NMR of **24s** after purified by flash chromatography.

HPLC for major diastereomer: OD-H, 254 nm, n -hexane/isopropanol = 95:5, flow rate 0.2 mL/min, 25 °C, t_{r} (minor) = 24.0 min, t_{r} (major) = 24.7 min.

HPLC for minor diastereomer: OD-H, 254 nm, n -hexane/isopropanol = 95:5, flow rate 0.4 mL/min, 25 °C, t_{r} (minor) = 12.7 min, t_{r} (major) = 12.0 min.

^1H NMR (300 MHz, CDCl_3 , major diastereoisomer) δ 7.35-7.30 (m, 5H), 5.93 (s, 1H), 5.00-4.95 (m, 3H), 3.70-3.64 (m, 1H), 3.48-3.40 (m, 2H), 3.21 (dd, $J = 17.3, 6.9$ Hz, 1H), 2.99 (dd, $J = 17.3, 5.4$ Hz, 1H), 2.51 (s, 3H), 2.47-2.36 (m, 2H), 2.30-2.24 (m, 1H), 2.21 (s, 3H), 1.89-1.76 (m, 1H), 1.23 (s, 3H), 1.21 (s, 3H), 0.98 (d, $J = 6.8$ Hz, 3H), 0.91 (d, $J = 6.8$ Hz, 3H).

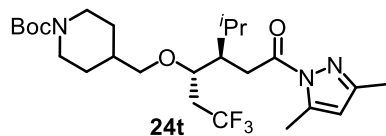
^1H NMR (300 MHz, CDCl_3 , minor diastereoisomer) δ 7.36-7.29 (m, 5H), 5.91 (s, 1H), 5.05-5.00 (m, 3H), 3.90-3.83 (m, 1H), 3.67-3.40 (m, 2H), 3.33 (d, $J = 8.8$ Hz, 1H), 3.17 (dd, $J = 16.7, 5.9$ Hz, 1H), 3.04 (dd, $J = 16.8, 6.2$ Hz, 1H), 2.54-2.32 (m, 5H), 2.30-2.14 (m, 4H), 1.27 (s, 3H), 1.20 (s, 3H), 0.97 (d, $J = 6.6$ Hz, 3H), 0.94 (d, $J = 6.6$ Hz, 3H).

^{13}C NMR (125 MHz, CDCl_3 , major diastereoisomer) δ 173.8, 152.0, 144.2, 136.9, 128.5, 128.1, 128.0, 127.9, 126.5 (q, $J = 277.0$ Hz), 111.3, 75.5, 75.1, 66.1, 53.0, 44.6, 37.4 (q, $J = 27.1$ Hz), 32.9, 29.0, 24.2, 24.1, 21.1, 19.9, 14.7, 13.8.

^{19}F NMR (282 MHz, CDCl_3 , major diastereoisomer) δ -63.29 (s, 3F).

IR (film): ν (cm⁻¹) 2999, 2945, 1721, 1509, 1385, 1342, 1254, 1140, 1074, 973, 918, 848, 739, 580, 529, 456.

HRMS (ESI, m/z) calcd for C₂₆H₃₆F₃N₃O₄Na⁺ [M+ Na]⁺: 534.2556, found: 534.2550.



Starting from **21a** (94.0 mg, 0.60 mmol), **22l** (72.0 mg, 0.30 mmol)

and **23a** (19.2 mg, 0.10 mmol) with Λ -**RhS** (6 mol%) and 4,4'-difluorobenzil (40 mol%) for 38 h according to the general procedure to give **24t** as a pale yellow oil (23.0 mg, 0.0457 mmol, 46% yield, dr = 1.3:1). Enantiomeric excess established by HPLC analysis by using Chiralpak OD-H / OJ-H columns, ee = 91% / 93%. $[\alpha]_D^{20} = +1.4^\circ$ (c 1.0, CH₂Cl₂). The dr value was determined by ¹⁹F NMR of **24t** after purified by flash chromatography.

HPLC for major diastereomer: OJ-H, 254 nm, *n*-hexane/isopropanol = 95:5, flow rate 0.2 mL/min, 25 °C, t_r (minor) = 19.8 min, t_r (major) = 21.9 min.

HPLC for minor diastereomer: OD-H, 254 nm, *n*-hexane/isopropanol = 99:1, flow rate 0.3 mL/min, 25 °C, t_r (minor) = 21.9 min, t_r (major) = 19.9 min.

¹H NMR (500 MHz, CDCl₃, major diastereoisomer) δ 5.96 (s, 1H), 4.03 (br, 2H), 3.78-3.75 (m, 1H), 3.36 (dd, $J = 8.4, 5.7$ Hz, 1H), 3.15-3.08 (m, 2H), 3.02 (dd, $J = 16.4, 5.9$ Hz, 1H), 2.65-2.55 (m, 2H), 2.52 (s, 3H), 2.46-2.37 (m, 2H), 2.23 (s, 3H), 2.22-2.16 (m, 1H), 1.62-1.60 (m, 1H), 1.56-1.48 (m, 3H), 1.44 (s, 9H), 1.09-1.01 (m, 2H), 0.97 (d, $J = 6.7$ Hz, 3H), 0.94 (d, $J = 6.8$ Hz, 3H).

¹H NMR (300 MHz, CDCl₃, minor diastereoisomer) δ 5.98 (s, 1H), 4.05 (br, m, 2H), 3.82-3.75 (m, 1H), 3.39 (dd, $J = 8.5, 5.7$ Hz, 1H), 3.20-3.00 (m, 3H), 2.70-2.54 (m, 2H), 2.54 (s, 3H), 2.50-2.34 (m, 2H), 2.30-2.12 (m, 4H), 1.68-1.60 (m, 1H), 1.55-21.50 (m, 4H), 1.46 (s, 9H), 1.12-1.05 (m, 1H), 1.00-0.96 (m, 6H).

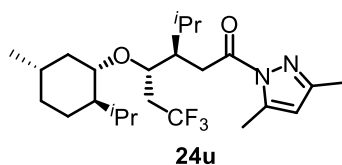
¹³C NMR (125 MHz, CDCl₃, major diastereoisomer) δ 173.8, 154.9, 151.8, 144.0, 127.0 (q, $J = 277.0$ Hz), 111.2, 79.3, 74.9, 74.2, 43.1, 36.7, 35.1 (q, $J = 27.5$ Hz), 33.0, 29.4, 28.9, 28.8, 28.5, 21.2, 20.9, 14.7, 13.9.

¹⁹F NMR (282 MHz, CDCl₃, major diastereoisomer) δ -63.40 (s, 3F).

¹⁹F NMR (282 MHz, CDCl₃, minor diastereoisomer) δ -63.58 (s, 3F).

IR (film): ν (cm⁻¹) 2966, 2926, 2863, 1725, 1690, 1584, 1471, 1417, 1375, 1342, 1316, 1250, 1138, 1095, 962, 922, 861, 803, 765, 743, 670, 589, 539.

HRMS (ESI, m/z) calcd for $C_{25}H_{40}F_3N_3O_4Na^+$ $[M+Na]^+$: 526.2863, found: 526.2862.



Starting from **21a** (94.0 mg, 0.60 mmol), **22m** (54.6 mg, 0.30 mmol) and **23a** (19.2 mg, 0.10 mmol) with Λ -**RhS** (6 mol%) and 4,4'-difluorobenzil (40 mol%) for 24 h according to the general procedure to give **24u** as a pale yellow oil (33.3 mg, 0.0748 mmol, 75% yield, dr > 38:1:1). $[\alpha]_D^{20} = -54.2^\circ$ (c 1.0, CH_2Cl_2). The dr value was determined by crude ^{19}F NMR of **24u**.

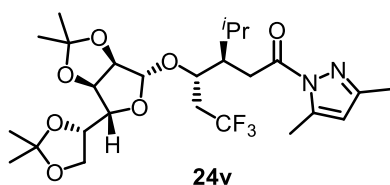
1H NMR (300 MHz, $CDCl_3$, major diastereoisomer) δ 5.97 (s, 1H), 3.88-3.81 (m, 1H), 3.35 (dd, $J = 16.5, 7.6$ Hz, 1H), 3.14-3.11 (m, 1H), 2.74 (dd, $J = 16.3, 4.3$ Hz, 1H), 2.60-2.50 (m, 4H), 2.35-2.21 (m, 5H), 2.10-1.95 (m, 2H), 1.92-1.82 (m, 1H), 1.54-1.48 (m, 1H), 1.04 (d, $J = 6.7$ Hz, 3H), 0.95-0.92 (m, 7H), 0.81-0.76 (m, 4H), 0.75-0.60 (m, 7H).

^{13}C NMR (75 MHz, $CDCl_3$, major diastereoisomer) δ 174.5, 151.2, 144.1, 111.0, 74.7, 68.9, 48.2, 47.1, 39.0, 38.7 (q, $J = 26.5$ Hz), 34.6, 32.3, 31.4, 28.3, 24.6, 22.9, 22.6, 21.6, 21.3, 18.6, 15.8, 14.8, 13.8.

^{19}F NMR (282 MHz, $CDCl_3$, major diastereoisomer) δ -63.6 (s, 3F).

IR (film): ν (cm^{-1}) 2999, 2944, 1726, 1589, 1447, 1385, 1333, 1249, 1183, 1139, 1043, 973, 920, 843, 795, 745, 510, 461.

HRMS (ESI, m/z) calcd for $C_{24}H_{39}F_3N_2O_2Na^+$ $[M+Na]^+$: 467.2856, found: 467.2854.



Starting from **21a** (94.0 mg, 0.60 mmol), **22n** (86.0 mg, 0.30 mmol) and **23a** (19.2 mg, 0.10 mmol) with Λ -**RhS** (6 mol%) and 4,4'-difluorobenzil (40 mol%) for 36 h according to the general procedure to give **24v** as a pale yellow oil (20.0 mg, 0.0365 mmol, 36% yield, dr > 19:1). $[\alpha]_D^{20} = -7.8^\circ$ (c 1.0, CH_2Cl_2). The dr value was determined by crude 1H NMR of **24v**.

1H NMR (500 MHz, $CDCl_3$, major diastereoisomer) δ 5.96 (s, 1H), 5.78 (d, $J = 3.7$ Hz, 1H), 4.50 (d, $J = 3.7$ Hz, 1H), 4.23-4.19 (m, 1H), 4.14 (d, $J = 3.3$ Hz, 1H), 4.11-4.08 (m, 2H), 3.94 (d, $J = 5.6$ Hz, 2H), 3.20-3.11 (m, 2H), 2.61-2.56 (m, 1H), 2.53 (s, 3H), 2.35-2.29 (m, 2H), 2.23 (s, 3H), 1.52-1.47 (m, 4H), 1.33 (s, 3H), 1.30 (s, 3H), 1.01 (d, $J = 6.7$ Hz, 3H), 0.97 (s, 3H), 0.92 (d, $J = 6.7$ Hz, 3H).

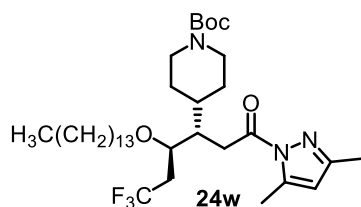
^{13}C NMR (125 MHz, $CDCl_3$, major diastereoisomer) δ 173.2, 151.8, 144.0, 126.9 (q, $J = 277.9$ Hz), 120.0, 111.2, 108.9, 105.4, 81.9, 81.2, 78.9, 72.5, 71.8, 67.2, 40.5, 35.1 (q, $J = 27.3$ Hz), 32.8, 30.2,

27.0, 26.7, 26.4, 24.4, 21.5, 20.6, 14.8, 13.9.

^{19}F NMR (282 MHz, CDCl_3 , major diastereoisomer) δ -63.37 (s, 3F).

IR (film): ν (cm^{-1}) 2979, 2935, 2885, 1728, 1585, 1465, 1378, 1337, 1252, 1216, 1139, 1071, 1018, 960, 846, 802, 750, 636, 512, 416.

HRMS (ESI, m/z) calcd for $\text{C}_{26}\text{H}_{39}\text{F}_3\text{N}_2\text{O}_7\text{Na}^+$ $[\text{M}+\text{Na}]^+$: 571.2602, found: 571.2603.



Starting from **21a** (94.0 mg, 0.60 mmol), **22o** (72.0 mg, 0.30 mmol) and

23g (33.3 mg, 0.10 mmol) with Δ -**RhS** (6 mol%) and 4,4'-difluorobenzil (40 mol%) for 48 h according to the general procedure to give **24w** as a pale yellow oil (45.0 mg, 0.070 mmol, 70% yield, dr = 2:1). Enantiomeric excess established by HPLC analysis by using Chiralpak AD-H / IC columns, ee = 97% / 95%. $[\alpha]_{\text{D}}^{20} = -10.0^\circ$ (c 1.0, CH_2Cl_2). The dr value was determined by ^1H NMR of **24w** after purified by flash chromatography.

HPLC for major diastereomer: AD-H, 254 nm, n -hexane/isopropanol = 95:5, flow rate 0.5 mL/min, 25 °C, t_{r} (minor) = 6.7 min, t_{r} (major) = 9.9 min.

HPLC for minor diastereomer: IC, 254 nm, n -hexane/isopropanol = 95:5, flow rate 0.5 mL/min, 25 °C, t_{r} (minor) = 11.9 min, t_{r} (major) = 17.5 min.

^1H NMR (500 MHz, CDCl_3 , major diastereoisomer) δ 5.96 (s, 1H), 4.14 (br, 2H), 3.65-3.62 (m, 4H), 3.46-3.42 (m, 1H), 3.35-3.31 (m, 1H), 3.19 (dd, $J = 17.3, 6.2$ Hz, 1H), 3.01 (dd, $J = 17.4, 5.9$ Hz, 1H), 2.68-2.60 (m, 2H), 2.53 (s, 3H), 2.50-2.32 (m, 2H), 2.31-2.26 (m, 1H), 2.23 (s, 3H), 1.77-1.74 (m, 1H), 1.59-1.53 (m, 4H), 1.45 (s, 9H), 1.35-1.28 (m, 11H), 1.24-1.18 (m, 6H), 0.89-0.86 (m, 7H).

^1H NMR (300 MHz, CDCl_3 , minor diastereoisomer) δ 5.95 (s, 1H), 4.11 (br, 2H), 3.80-3.77 (m, 1H), 3.64 (t, $J = 6.6$ Hz, 1H), 3.50-3.40 (m, 3H), 3.18-3.03 (m, 2H), 2.67-2.58 (m, 2H), 2.52-2.35 (m, 5H), 2.22-2.12 (m, 4H), 1.68-1.62 (m, 2H), 1.45 (s, 9H), 1.42-1.28 (m, 9H), 1.24-1.16 (m, 14H), 0.90-0.86 (m, 5H).

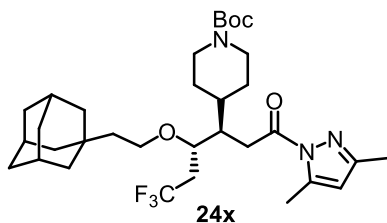
^{13}C NMR (125 MHz, CDCl_3 , major diastereoisomer) δ 173.6, 154.8, 151.9, 144.2, 126.5 (q, $J = 277.1$ Hz), 111.3, 79.5, 74.3, 70.4, 63.2, 44.0, 37.9, 37.7 (q, $J = 26.2$ Hz), 32.9, 32.0, 29.86, 29.79, 29.77, 29.76, 29.75, 29.72, 29.71, 29.69, 29.67, 29.56, 29.52, 29.45, 28.5, 26.1, 25.8, 22.8, 14.7, 14.2, 13.9.

^{19}F NMR (282 MHz, CDCl_3 , major diastereoisomer) δ -64.48 (s, 3F).

^{19}F NMR (282 MHz, CDCl_3 , minor diastereoisomer) δ -63.68 (s, 3F).

IR (film): ν (cm^{-1}) 3000, 2923, 2853, 1692, 1582, 1422, 1336, 1247, 1173, 1145, 976, 919, 866, 793, 523, 458.

HRMS (ESI, m/z) calcd for $\text{C}_{35}\text{H}_{60}\text{F}_3\text{N}_3\text{O}_4\text{Na}^+$ [$\text{M} + \text{Na}$] $^+$: 666.4428, found: 666.4431.



Starting from **21a** (94.0 mg, 0.60 mmol), **22p** (57.6 mg, 0.30 mmol)

and **23g** (33.3 mg, 0.10 mmol) with Λ -**RhS** (6 mol%) and 4,4'-difluorobenzil (40 mol%) for 48 h according to the general procedure to give **24x** as a pale yellow oil (42.2 mg, 0.0696 mmol, 70% yield, dr = 1.9:1). Enantiomeric excess was established by HPLC analysis using a Chiralpak OD-H column, ee = 91%. $[\alpha]_{\text{D}}^{20} = -5.2^\circ$ (c 1.0, CH_2Cl_2). The dr value was determined by ^1H NMR of **24x** after purified by flash chromatography.

HPLC for major diastereomer: IC, 254 nm, n -hexane/isopropanol = 97:3, flow rate 0.5 mL/min, 25 $^\circ\text{C}$, t_{r} (minor) = 18.3 min, t_{r} (major) = 19.9 min.

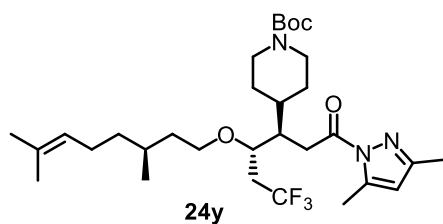
^1H NMR (500 MHz, CD_2Cl_2 , major diastereoisomer) δ 6.02 (s, 1H), 4.15 (br, 2H), 3.71-3.65 (m, 2H), 3.59-3.54 (m, 1H), 3.43-3.38 (m, 1H), 3.22 (dd, $J = 17.4, 6.2$ Hz, 1H), 3.01 (dd, $J = 17.4, 5.9$ Hz, 1H), 2.67 (br, 2H), 2.55 (s, 3H), 2.52-2.37 (m, 2H), 2.31-2.27 (m, 1H), 2.24 (s, 3H), 1.96-1.92 (m, 2H), 1.76-1.74 (m, 2H), 1.56 (d, $J = 2.3$ Hz, 2H), 1.48 (d, $J = 2.1$ Hz, 6H), 1.46 (s, 9H), 1.38 (t, $J = 7.6$ Hz, 6H), 1.30-1.22 (m, 2H), 1.17-1.11 (m, 1H).

^{13}C NMR (125 MHz, CD_2Cl_2 , major diastereoisomer) δ 173.4, 154.5, 151.6, 144.0, 127.7 (q, $J = 277.6$ Hz), 111.0, 79.0, 74.4, 66.2, 58.5, 47.4, 44.0, 43.7, 42.7, 42.6, 38.0, 37.5 (q, $J = 27.0$ Hz), 37.1, 32.8, 31.5, 28.9, 28.2, 14.4, 13.6.

^{19}F NMR (282 MHz, CDCl_3 , major diastereoisomer) δ -63.86 (s, 3F).

IR (film): ν (cm^{-1}) 2901, 2848, 1725, 1690, 1584, 1419, 1378, 1330, 1250, 1143, 1091, 1024, 965, 860, 803, 757, 674, 531.

HRMS (ESI, m/z) calcd for $\text{C}_{33}\text{H}_{50}\text{F}_3\text{N}_3\text{O}_4\text{Na}^+$ [$\text{M} + \text{Na}$] $^+$: 632.3646, found: 632.3643.



Starting from **21a** (94.0 mg, 0.60 mmol), **22q** (54.6 mg, 0.30

mmol) and **23a** (33.3 mg, 0.10 mmol) with Λ -**RhS** (6 mol%) and 4,4'-difluorobenzil (40 mol%) for 48 h according to the general procedure to give **24y** as a pale yellow oil (38.1 mg, 0.0650 mmol, 65% yield, dr > 43:21:1). The dr value was determined by ^{19}F NMR and HPLC analysis of **24y** after purified by flash chromatography.

HPLC for major spot: IC, 254 nm, *n*-hexane/isopropanol = 95:5, flow rate 0.5 mL/min, 25 °C, t_r (minor) = 12.7 min, t_r (major) = 11.4 min. Dr > 99:1.

HPLC for minor spot: IC, 254 nm, *n*-hexane/isopropanol = 95:5, flow rate 0.5 mL/min, 25 °C, t_r (minor) = 13.2 min, t_r (major) = 14.0 min. Dr = 40:1.

^1H NMR (500 MHz, CDCl_3 , major diastereoisomer) δ 5.96 (s, 1H), 5.07 (t, J = 6.1 Hz, 1H) 4.13 (br, 2H), 3.65-3.62 (m, 1H), 3.52-3.44 (m, 1H), 3.39-3.34 (m, 1H), 3.22-3.17 (m, 1H), 3.01 (dt, J = 17.4, 5.7 Hz, 1H), 2.63 (br, 2H), 2.53 (s, 3H), 2.49-2.32 (m, 2H), 2.29-2.27 (m, 1H), 2.22 (s, 3H), 1.99-1.85 (m, 2H), 1.79-1.71 (m, 1H), 1.67 (s, 3H), 1.65-1.58 (m, 5H), 1.45 (s, 9H), 1.40-1.36 (m, 1H), 1.34-1.04 (m, 6H), 0.81(d, J = 6.6 Hz, 3H) .

^{13}C NMR (125 MHz, CDCl_3 , major diastereoisomer) δ 173.6, 154.8, 151.9, 144.2, 131.3, 126.5 (q, J = 273.8 Hz), 124.8, 111.3, 79.5, 74.4, 68.6, 44.0, 37.9, 37.3, 37.2, 36.8, 36.7, 32.9, 29.4, 28.5, 25.8, 25.5 (2C), 19.6, 19.5, 17.7, 14.7, 13.9, .

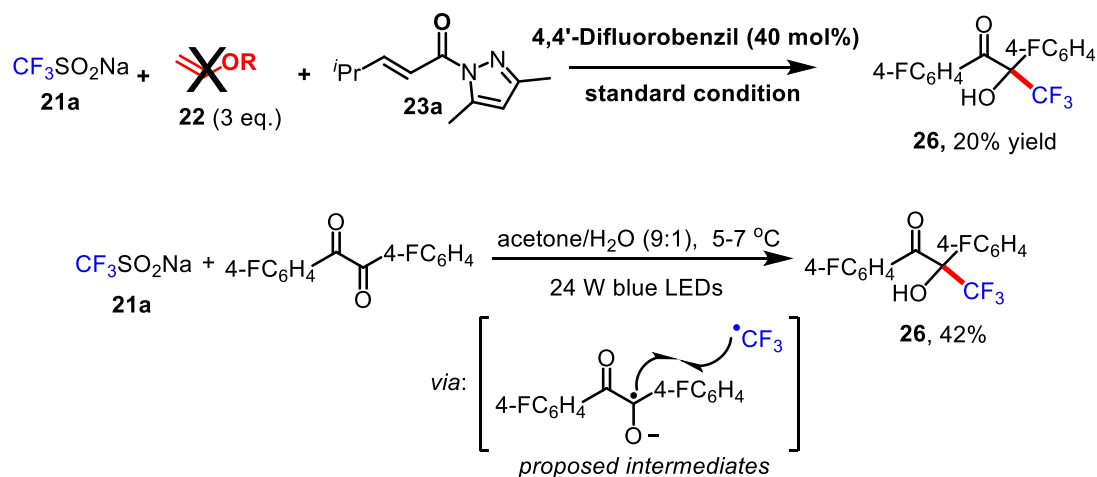
^{19}F NMR (282 MHz, CDCl_3 , major diastereoisomer) δ -63.57 (s, 3F).

IR (film): ν (cm^{-1}) 3274, 3226, 3109, 2992, 2927, 2862, 2771, 2729, 2680, 2637, 2617, 2555, 2513, 2480, 2446, 2360, 2267, 2198.

HRMS (ESI, m/z) calcd for $\text{C}_{31}\text{H}_{50}\text{F}_3\text{N}_3\text{O}_4\text{Na}^+$ $[\text{M}+\text{Na}]^+$: 608.3646, found: 608.3643.

5.4.4 Mechanistic Experiments

1) Side Products Isolation and Key Intermediates Trapping



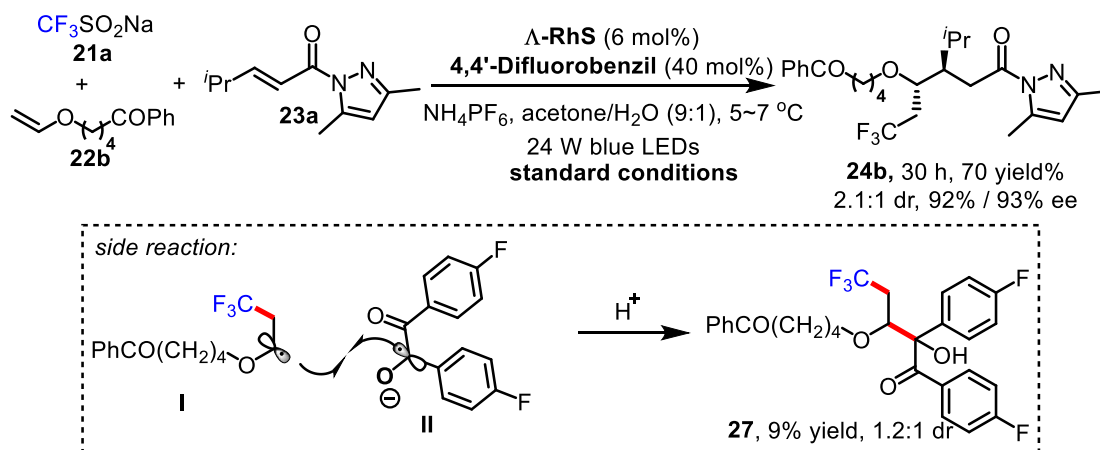
As shown herein, without the addition of substrate **22**, a side product **26** was isolated with 20% yield {2.5 mg, refer to 4,4'-difluorobenzil (0.04 mmol)} under the standard conditions, or a higher yield of 42% {13.2 mg refer to 4,4'-difluorobenzil (0.1 mmol)} obtained by combining **21a** and 4,4'-difluorobenzil under visible light irradiation.

Analytic data of **26** is shown below:

¹H NMR (500 MHz, CDCl₃) δ 7.81-7.78 (m, 2H), 7.55-7.52 (m, 2H), 7.16-7.11 (m, 2H), 7.03-6.99 (m, 2H), 4.65 (br, 1H).

¹³C NMR (125 MHz, CDCl₃) δ 191.8, 167.0, 165.0, 164.3, 162.3, 133.9, 133.8, 128.8, 128.7, 116.4, 116.2, 115.8, 115.6.

¹⁹F NMR (282 MHz, CDCl₃) δ -73.76 (s, 3F), -102.26 (s, F), -110.87 (s, F).



A side product **27** was isolated with 9% yield {1.9 mg, refer to 4,4'-difluorobenzil (0.4 mmol)} and 1.2:1 dr under the standard conditions. Compound **27** was proposed to be formed by the radical-radical recombination between two key intermediates **I** and **II**.

Analytic data of **27** is shown below:

^1H NMR (500 MHz, CDCl_3 , major diastereoisomer) δ 8.07-8.03 (m, 2H), 7.98-7.94 (m, 2H), 7.59 (tt, $J = 6.8, 1.3$ Hz, 1H), 7.51-7.42 (m, 4H), 7.10-7.05 (m, 4H), 5.81 (br, 1H), 4.94 (t, $J = 5.3$ Hz, 1H), 3.58-3.40 (m, 2H), 2.98 (t, $J = 7.2$ Hz, 2H), 2.63-2.46 (m, 3H), 2.32-2.22 (m, 1H), 1.83-1.75 (m, 2H).

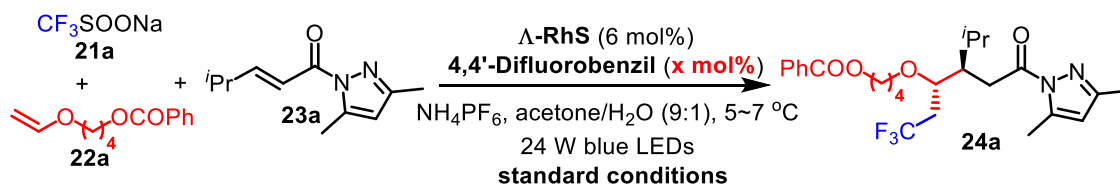
^{13}C NMR (125 MHz, CDCl_3 , major diastereoisomer) δ 199.8, 194.4, 166.7, 164.7, 163.8, 161.9, 136.9, 133.1, 132.2, 132.1, 131.93, 131.85, 131.06, 131.04, 130.9, 129.0, 128.9, 128.6, 128.0, 116.1, 116.0, 115.8, 115.6, 80.5, 66.7, 38.8 (q, $J = 27.9$ Hz), 37.9, 29.0, 20.7.

^{19}F NMR (282 MHz, CDCl_3 , mixture of diastereoisomers) δ -63.05 (s, 3F), -63.27 (s, F), -111.08 (s, F), -111.19 (s, F), -111.31 (s, F), -111.42 (s, F).

2) Stern-Volmer Quenching Experiments

The solution of 4,4'-difluorobenzil in acetone/ H_2O (9:1, 4 mM) was excited at $\lambda = 400$ nm and the emission was measured at 500 nm (emission maximum). For each quenching experiment, after degassing with a nitrogen stream for 5 minutes, the emission intensity of the solution (1 mL) of 4,4'-difluorobenzil with different concentrations of quencher (0, 0.1, 0.2, 0.3, 0.4, 0.5 mM) in a screw-top 10.0 mm quartz cuvette was collected.

3) Kinetic Profile for 4,4'-Difluorobenzil



The catalytical reactions were conducted under the standard conditions except that with different loading of 4,4'-difluorobenzil (0, 20 mol%, 40 mol%, 60 mol%, 80 mol%, 100 mol%), respectively. All of the reactions were quenched after 6 h, and yields were determined by the crude ^{19}F NMR analysis with PhCF_3 as internal standard. See **Figure 96** for the results.

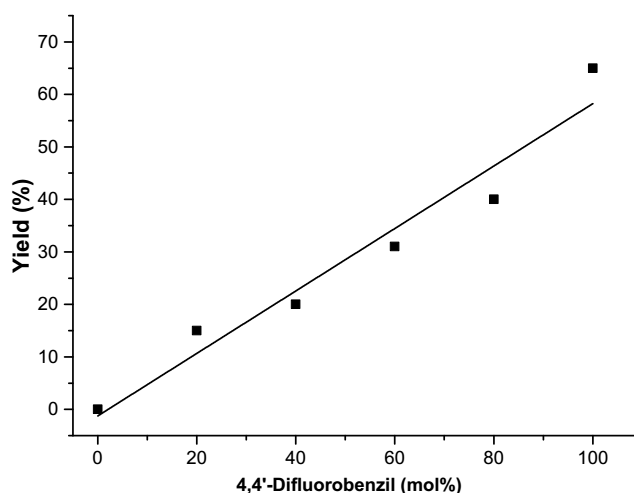
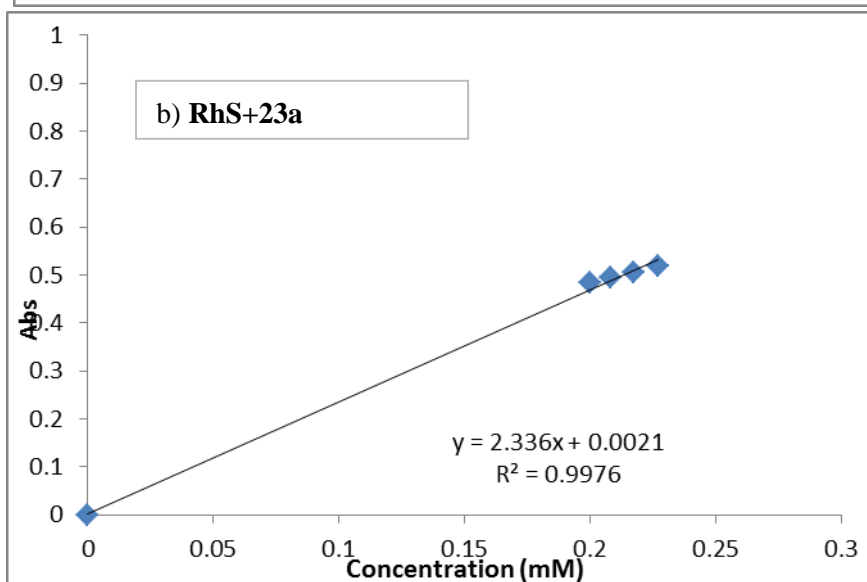
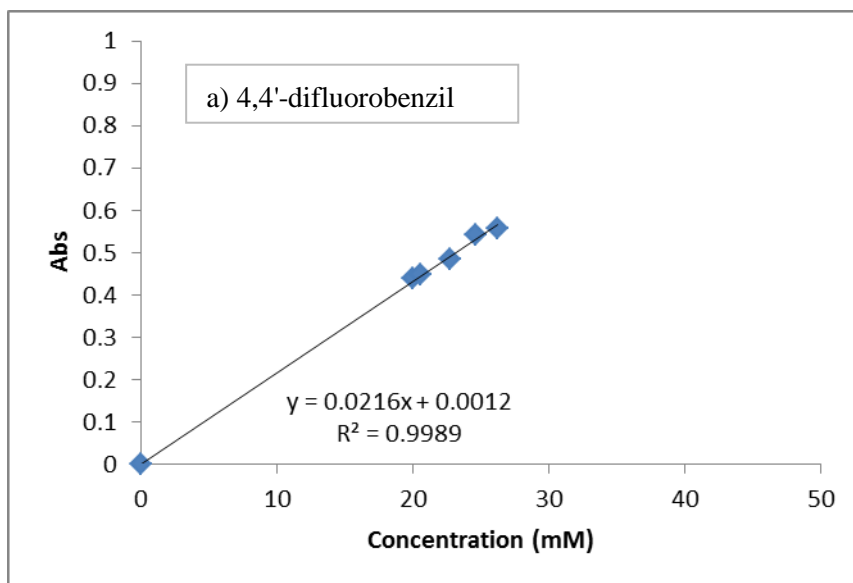


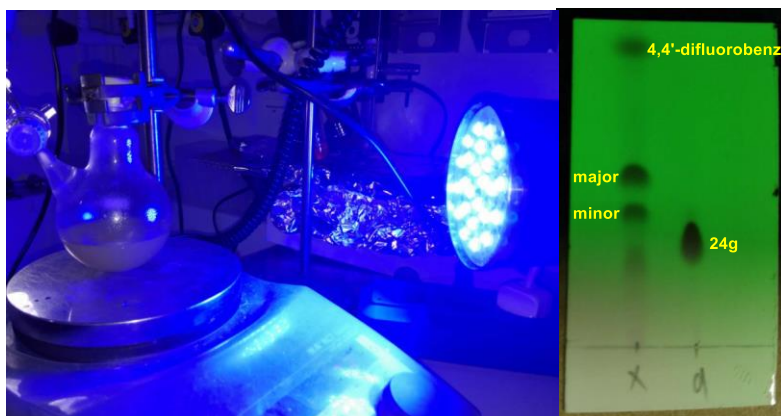
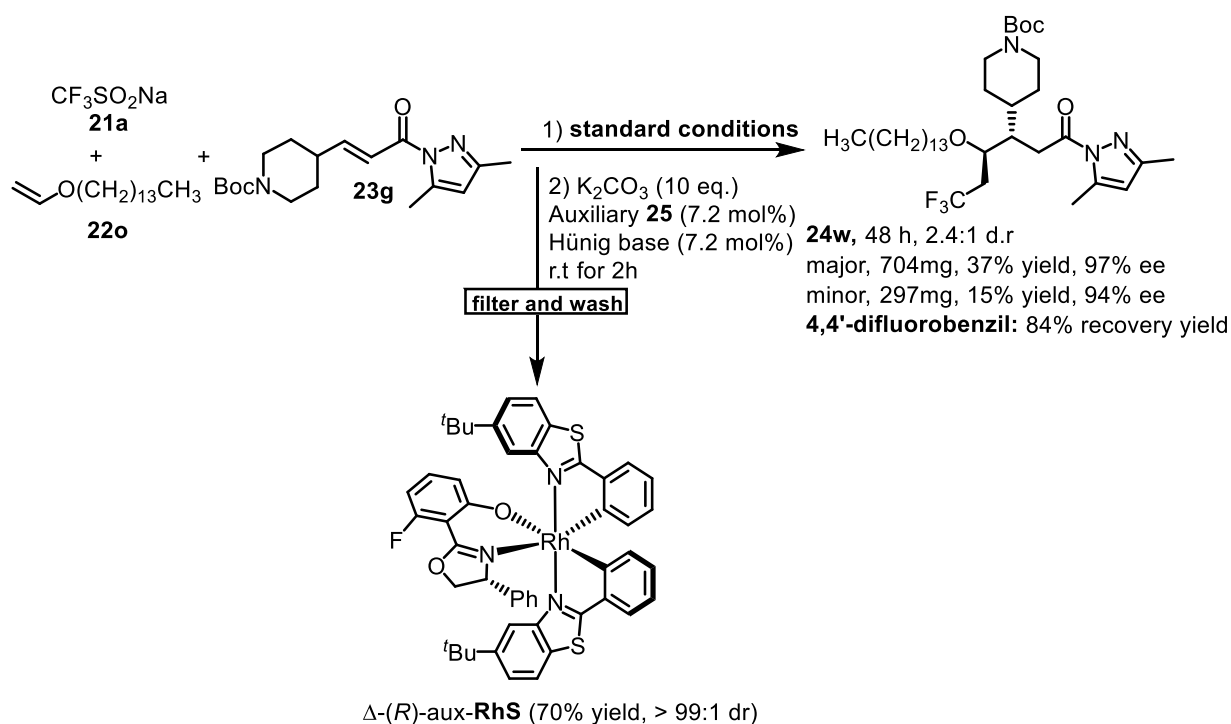
Figure 96. Kinetic profile of the visible-light-induced three-component reaction catalyzed by individual amounts of 4,4'-difluorobenzil.

4) Determination of Extinction Coefficient of 4,4'-Difluorobenzil and RhS-3a

The absorbance values of 4,4'-difluorobenzil and **RhS-23a** complex were collected at different concentrations at 420 nm in acetone using 1.0 cm quartz cuvette and the extinction coefficients determined according to the Lambert-Beer law. As a result, the extinction coefficient of 4,4'-difluorobenzil was calculated as: $\epsilon_{420} = 22.8 \text{ M}^{-1}\text{cm}^{-1}$ and the extinction coefficient of **RhS-23a** as: $\epsilon_{420} = 2338 \text{ M}^{-1}\text{cm}^{-1}$.



5.4.5 Gram Scale Reaction and Catalyst Recovery



A solution of **21a** (2.80 g, 18.0 mmol), **22o** (2.16 g, 9.0 mmol) and **23g** (1.0 g, 3.0 mmol), Δ -RhS (156.0 mg, 0.18 mmol, 6 mol%), 4,4'-difluorobenzil (295.0 mg, 1.20 mmol, 40 mol%), NH_4PF_6 (4.89 g, 30.0 mmol) in acetone/ H_2O (9:1, v/v, 30 mL, 0.1 M) were stirred at 5-7 °C under an atmosphere of nitrogen and an irradiation with 24 W blue LEDs for 48 h. Upon completion, K_2CO_3 (4.14 g, 30.0 mmol), Hünig base (36 μL , 0.216 mmol, 7.2 mol%), and the chiral auxiliary **25** (55.5 mg, 0.216 mmol, 7.2 mol%) were added stepwise, then stirred for another 2 h at r.t. Afterwards, the solvent was concentrated to dryness, and the residue was filtered by a thin pad of silica gel to remove the inorganic salts. The organic filtrate was concentrated to around 3 mL. After the addition of *n*-hexane/ Et_2O (1:1, 10 mL), yellow solid was precipitated immediately. The precipitation was washed by *n*-hexane/ Et_2O

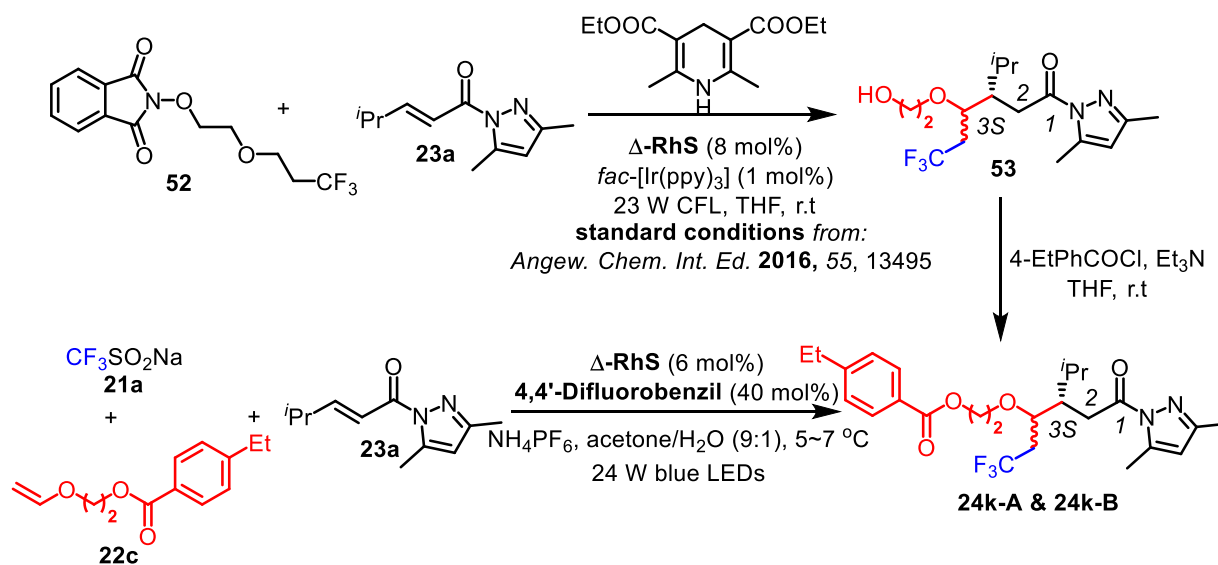
(1:1, v/v, 3 × 10 mL) to give Δ -(*R*)-aux-**RhS** (111 mg, 70%, > 99:1 dr from the ^{19}F NMR analysis) as a yellow solid⁶. Additionally, all the organic phase was concentrated and purified by flash column chromatography to give 4,4'-difluorobenzil as a pale yellow solid (249 mg, 84% recovery yield), the minor diastereomer of **24w** as a pale oil (297 mg, 15% yield, 94% ee), and the major diastereomer of **24w** as a pale oil (704 mg, 37% yield, 97% ee).

HPLC for minor diastereomer: IG Daicel column (250 x 4.6 mm), 254 nm, *n*-hexane/isopropanol = 98:2, flow rate 1 mL/min, 25 °C, t_r (minor) = 5.9 min, t_r (major) = 6.4 min. Area integration = 96.9:3.1 (93.8% ee).

HPLC for major diastereomer: IC Daicel column (250 x 4.6 mm), 254 nm, *n*-hexane/isopropanol = 95:5, flow rate 0.3 mL/min, 25 °C, t_r (minor) = 21.5 min, t_r (major) = 20.4 min. Area integration = 98.7:1.3 (97.4% ee).

5.4.6 Assignment of Absolute and Relative Configurations

1) Assignment of the Absolute Configuration



As shown herein, compound **52** was synthesized according to a recently published method.² The product **53** (mixture of two diastereomers) was isolated with 56% yield, 94% / 92% ee for two isomers and 2.8:1 dr by column chromatography. The absolute configuration was assigned as 3S in following previous report.²

Starting from **53**, compound **24k-A** was obtained by one-step transformation with an unchanged enantiomeric excess (94% / 92% ee for two isomers) in which the absolute configuration was assigned

to be 3*S* consistent with the starting material. $[\alpha]_D^{20} = -12.0^\circ$ (*c* 1.0, CH₂Cl₂). Enantiomeric excess was established by HPLC analysis by using a Daicel Chiralpak OD-H column, ee = 94% / 92%.

HPLC for diastereomer 1: OD-H, Daicel column (250 x 4.6 mm), 254 nm, *n*-hexane/isopropanol = 99:1, flow rate 0.3 mL/min, 25 °C, *t_r* (minor) = 26.2 min, *t_r* (major) = 35.2 min.

HPLC for diastereomer 2: OD-H, Daicel column (250 x 4.6 mm), 254 nm, *n*-hexane/isopropanol = 99:1, flow rate 0.3 mL/min, 25 °C, *t_r* (minor) = 36.4 min, *t_r* (major) = 33.0 min.

As for the hereby described asymmetric three-component fluoroalkylation reaction, **24k-B** was synthesized under the developed standard conditions with Δ -**RhS**. The two diastereomers were isolated. $[\alpha]_D^{20} = -13.4^\circ$ (*c* 1.0, CH₂Cl₂). Enantiomeric excess was established by HPLC analysis by using a Chiralpak OD-H column, ee = 98% / 96% {OD-H, 254 nm, *n*-hexane/isopropanol = 99:1, flow rate 0.3 mL/min, 25 °C}.

After comparing the HPLC traces and optical rotation of **24k-A** and **24k-B** synthesized by individual methods, the absolute configuration of **24k-B** obtained from asymmetric three-component fluoroalkylation reaction was assigned as 3*S*. See the HPLC traces of **24k-A** and **24k-B** below:

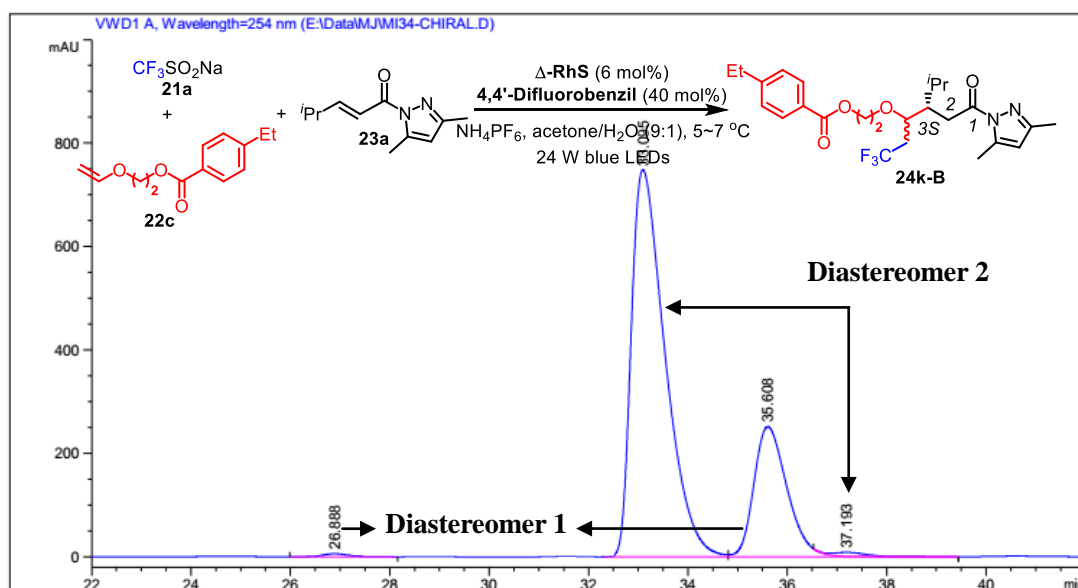
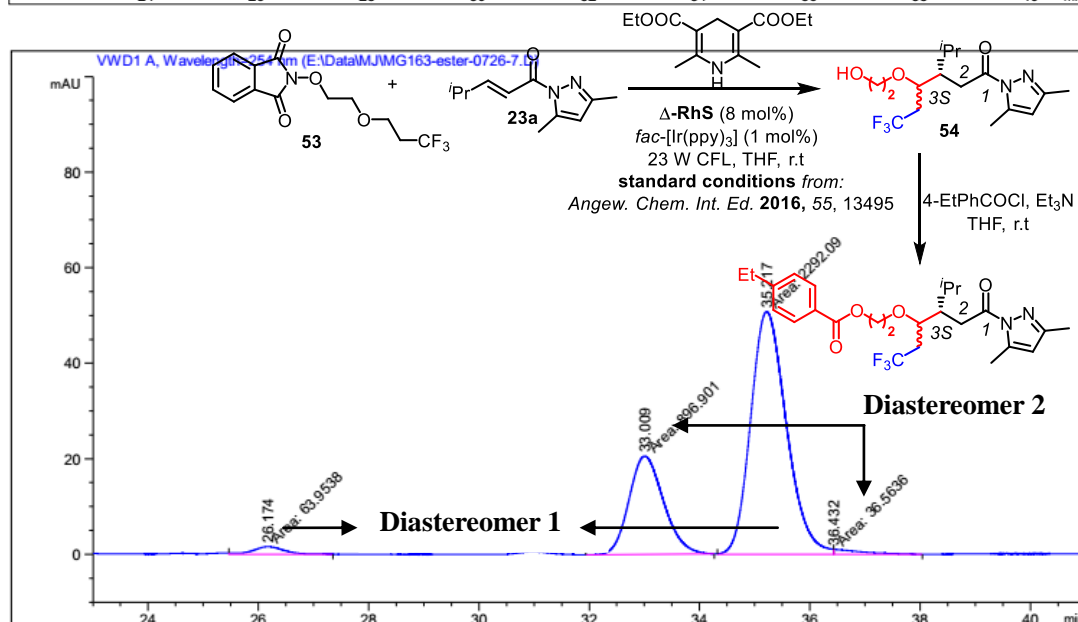
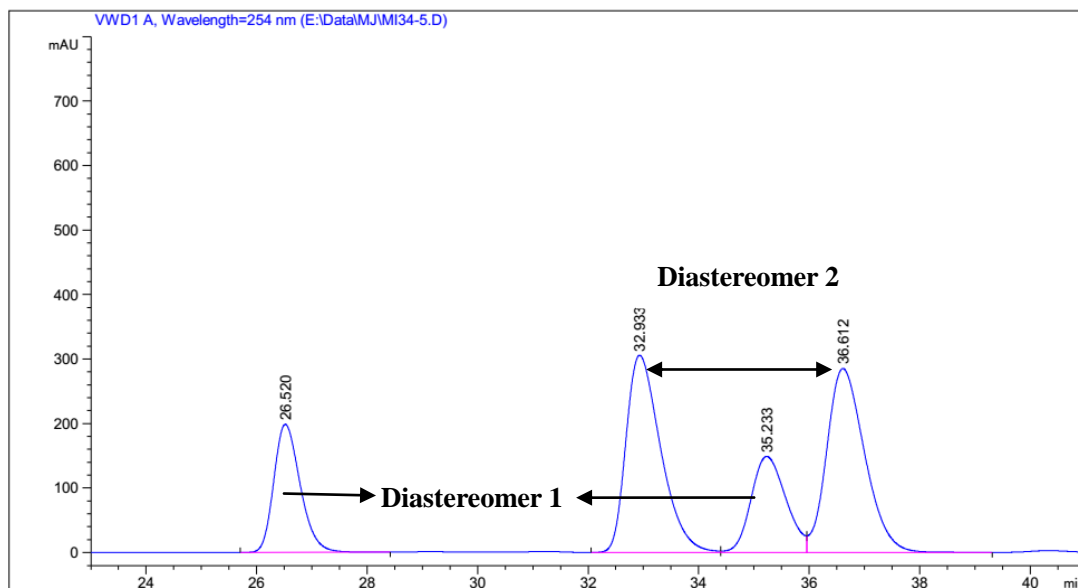
Compound **52**:

¹H NMR (500 MHz, CDCl₃) δ 5.97 (s, 1H), 3.89-3.86 (m, 1H), 3.61-3.46 (m, 4H), 3.25 (dd, , *J* = 16.1, 7.5 Hz, 1H), 2.97 (dd, , *J* = 16.1, 5.3 Hz, 1H), 2.52 (s, 3H), 2.50-2.41 (m, 2H), 2.33 (br, 1H), 2.29-2.16 (m, 4H), 1.55-1.48 (m, 1H), 0.99 (d, *J* = 6.6 Hz, 6H).

¹³C NMR (125 MHz, CDCl₃) δ 174.3, 152.1, 144.2, 127.0 (q, *J* = 277 Hz), 111.5, 75.5, 71.6, 61.9, 44.0, 34.8 (q, *J* = 27.3 Hz), 32.9, 29.5, 21.4, 20.8, 14.8, 13.9.

¹⁹F NMR (282 MHz, CDCl₃, major diastereoisomer) δ -64.5 (s, 3F).

HRMS (ESI, *m/z*) calcd for C₁₆H₂₅F₃N₂O₃Na⁺ [M+Na]⁺: 373.1709, found: 373.1709.



2) Assignment of the Relative Configuration by NOE Analysis

This part of work was conducted by Dr. Xiulan Xie in the NMR-Abteilung.

Product **24k-B** was obtained under asymmetric three-component fluoroalkylation conditions catalyzed by Δ -**RhS** to provide absolute configuration as *3S*. Whereas, **24s** was obtained under the identical conditions except employing Λ -**RhS**, thus, with the absolute configuration of *3R*.

Configuration and conformation of the two neighboring chiral centers of **24s** was determined by NMR spectroscopy.

Experimental:

Sample for NMR measurements was about 16 mg of substance dissolved in 0.6 mL of CDCl₃. Experiments were performed on a Bruker AVHD 500 MHz spectrometer equipped with a 5 mm TXI probe with z-gradient. NOESY experiments were performed with mixing times of 0.5, 0.8, and 1.5 s, while ROESY spectrum with mixing time 0.2 and 0.3 s was recorded in order to confirm the NOESY results.

Results and Discussion:

The ¹H signals of hydrogen atoms attached to positions 2 – 15 appear in chemical shift region 0.5 – 4.0 ppm, well resolved with coupling patterns from doublet to multiplet. Signal assignment was fulfilled by using 1D experiments ¹H and ¹³C, as well as the 2D experiments ¹H, ¹H DQF-COSY and ¹H, ¹³C HSQC experiments. Signals for the two diastereotopic hydrogen atoms on C-2 are separated for more than 0.2 ppm, which allowed us for an unambiguous stereospecific assignment of them.

Figure 97 shows section of the NOESY spectrum in the range of 0.5 – 4.0 ppm. Numerous cross peaks were observed. These were correlations (in the order of chemical shift from low to high field) H-4/H13, H-4/H13', H-4/H-12, H-4/H-3, H-4/H-6; H-6/H-15, H-6/H-15', H-6/H-3; H-2^{proS}/H-14, H-2^{proS}/H-2^{proR}, H-2^{proS}/H-6, H-2^{proR}/H-13, H-2^{proR}/H-13', H-2^{proR}/H-12, H-2^{proR}/H-3; H-14/H-12; H-3/H-13, H-3/H-13', H-3/H-12; H-12/H-13, H-12/H-13'.

Given the known absolute configuration of C-3 (*3R*), observation of NOE contact between H-3 and H-4 is expected to reveal a *cis*- (with NOE contact) or a *trans*- (without NOE contact) configuration of them. Nevertheless, a closer consideration of the observed NOE contacts among the neighboring groups revealed that neither a *cis*- nor a *trans*-configuration between H-3 and H-4 could fulfill those NOE contacts. Since the backbone of this molecule consists of 12 chemical bonds, and the two chiral

centers are built in the middle of the molecule, no free rotation along the bond between C-3 and C-4 is possible and this restriction in conformation came into play for the structural property of the molecule and resulted in the observed NOE contacts.

The possible conformation between H-3 and H-4 are *trans*, *gauche* (+), and *gauche* (-). The characteristic NOE contacts H-4/H-3, H-4/H-12; H-6/H-3, H-6/H-2^{proS}, H-2^{proS}/H-14; and H-14/H-12 provided us a unique *gauche* (+) conformation, as shown in Figure 97, which led further to an absolute configuration of (3*R*, 4*S*) of this molecule (24s).

The only unequivocally determined vicinal coupling constants were those between H-2 and H-3. Thus 6.8 Hz and 5.5 Hz were measured for ${}^3J_{\text{H2proSH3}}$ and ${}^3J_{\text{H2proRH3}}$, respectively. These measured vicinal coupling constants were apparent averaged values, which confirmed that restrict rotations still exist within the preferred conformation. See Figures 97 and 98.

Taken together, the absolute and relative configuration of compound 24k-B was determined as (3*S*, 4*R*), and all other compounds were assigned accordingly based on the employed Λ -RhS or Δ -RhS.

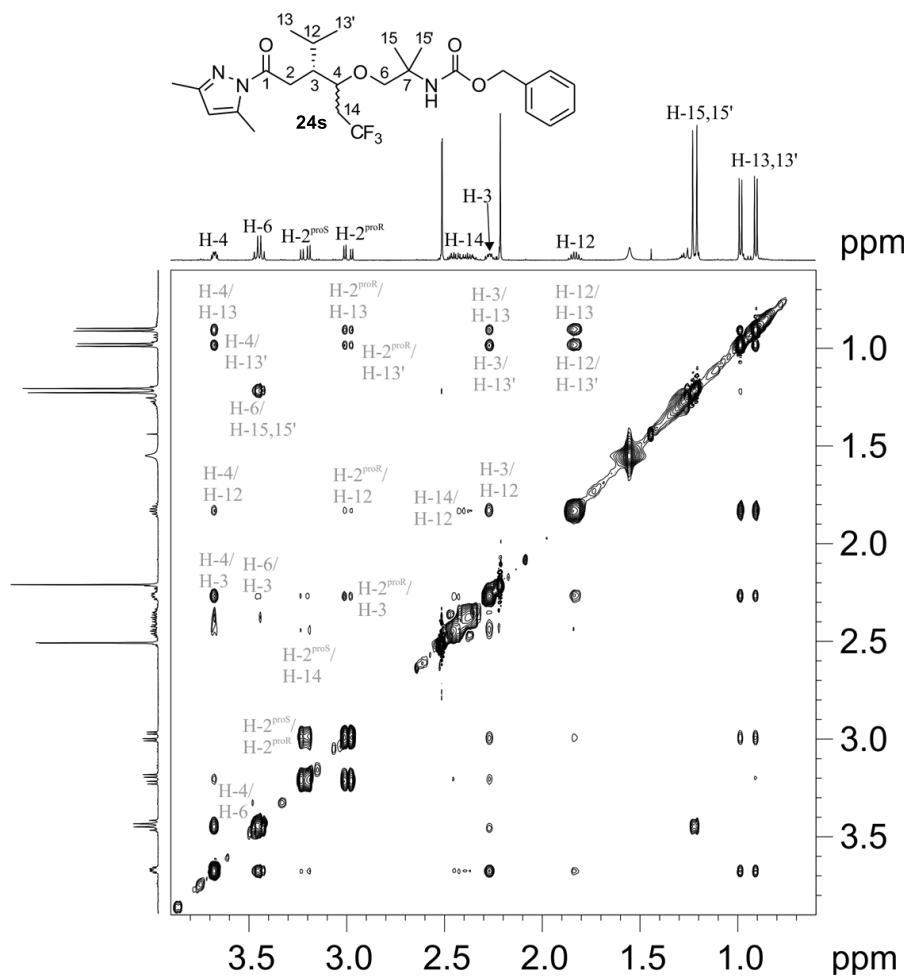


Figure 97. Section of NOESY spectrum of **24s** in CDCl_3 at 300 K, mixing time 1.5 s.

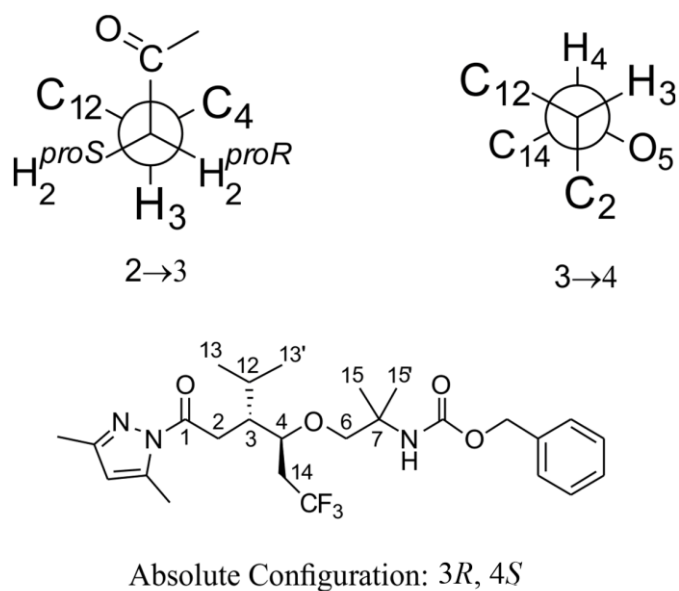


Figure 98. Structural scheme of **24s**, with partial conformation sketch.

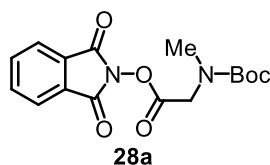
References

- 1 H. Huo, K. Harms, E. Meggers, *J. Am. Chem. Soc.* **2016**, *138*, 6936.
- 2 C. Wang, K. Harms, E. Meggers, *Angew. Chem. Int. Ed.* **2016**, *55*, 13495.
- 3 P. M. Weintraub, C.-H. R. King, *J. Org. Chem.* **1997**, *62*, 1560.
- 4 L. Q. Hu, D. D. DesMarteau, *Inorg. Chem.* **1993**, *32*, 5007.
- 5 L. Cui, Y. Matusaki, N. Tada, T. Miura, B. Uno, A. Itoh, *Adv. Synth. Catal.* **2013**, *355*, 2203.
- 6 a) J. Ma, X. Shen, K. Harms, E. Meggers, *Dalton Trans.* **2016**, *45*, 8320; b) J. Ma, X. Zhang, X. Huang, S. Luo, E. Meggers, *Nat. Protoc.* **2018**, *13*, 605.

5.5 Synthesis of β -Substituted γ -Aminobutyric Acid Derivatives via Enantioselective Photoredox Catalysis

5.5.1 Synthesis of Substrates

N-(Acyloxy)phthalimides **28a-g** were synthesized according to a published procedure with some modifications.³ Analytical data of **28b** and **28g** were consistent with the report.³ The experimental data of **1a**, **1c-f** are shown below.

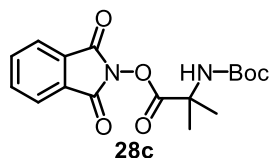


¹H NMR (300 MHz, CDCl₃, two rotamers) δ 8.00–7.87 (m, 2H), 7.80–7.70 (m, 2H), 4.44 (s, 2H), 4.29 (s, 2H, other rotamer), 3.02 (s, 3H), 2.98 (s, 3H, other rotamer), 1.49 (s, 9H).

¹³C NMR (75 MHz, CDCl₃, two rotamers) δ 166.6, 161.6, 155.1, 134.9, 128.9, 124.1, 81.3, 80.8 (other rotamer), 49.0, 48.1 (other rotamer), 35.7, 35.3 (other rotamer), 28.3, 28.1 (other rotamer).

IR (film): ν (cm⁻¹)_{2978, 2934, 1831, 1789, 1736, 1712, 1475, 1367, 1294, 1241, 1155, 1053, 966, 874, 781, 696, 597, 556, 513.}

HRMS (ESI, *m/z*) calcd for C₂₇H₂₅N₂O₄ [M+H]⁺: 357.1057, found: 357.1074.

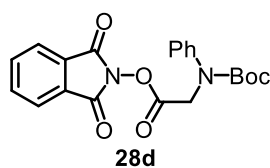


¹H NMR (300 MHz, CDCl₃) δ 7.91–7.88 (m, 2H), 7.81–7.78 (m, 2H), 5.06 (br, 1H), 1.73 (s, 6H), 1.53 (s, 9H).

¹³C NMR (75 MHz, CDCl₃) δ 171.2, 161.7, 154.3, 134.7, 129.1, 123.9, 81.0, 55.9, 34.0, 28.2.

IR (film): ν (cm⁻¹)_{3265, 2977, 1815, 1786, 1733, 1709, 1618, 1468, 1364, 1259, 1169, 1133, 1082, 1048, 968, 872, 824, 781, 694, 639, 590, 515, 459.}

HRMS (ESI, *m/z*) calcd for C₁₇H₂₀N₂O₆Na [M+ Na]⁺: 371.1214, found: 371.1225.

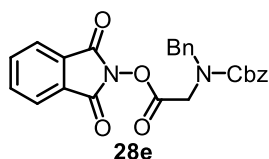


^1H NMR (300 MHz, CDCl_3 , two rotamers) δ 7.91–7.87 (m, 2H), 7.81–7.78 (m, 2H), 7.40–7.20 (m, 5H), 4.69 (s, 2H), 1.52 (s, 9H).

^{13}C NMR (75 MHz, CDCl_3) δ 166.8, 161.6, 153.9, 142.2, 134.9, 129.1, 129.0, 126.8, 126.4, 124.1, 82.3, 50.2, 28.1.

IR (film): ν (cm^{-1}) 2978, 1828, 1789, 1739, 1710, 1600, 1467, 1365, 1283, 1238, 1151, 1078, 1050, 965, 872, 776, 693, 590, 556, 513, 411.

HRMS (ESI, m/z) calcd for $\text{C}_{21}\text{H}_{20}\text{N}_2\text{O}_6\text{Na}$ $[\text{M}+\text{Na}]^+$: 419.1214, found: 419.1226.

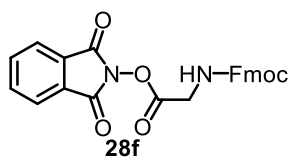


^1H NMR (300 MHz, CDCl_3 , two rotamers) δ 7.91–7.89 (m, 2H), 7.82–7.79 (m, 2H), 7.50–7.25 (m, 10H), 5.31 (s, 2H), 5.30 (s, 2H, other rotamer), 4.72 (s, 2H), 4.70 (s, 2H, other rotamer), 4.44 (s, 2H), 4.32 (s, 2H, other rotamer).

^{13}C NMR (75 MHz, CDCl_3 , two rotamers) δ 166.2, 161.4, 156.2, 155.9, 136.1, 136.0, 134.8, 128.8, 128.7, 128.5, 128.3, 128.1, 128.0, 127.9, 123.9, 68.1, 51.4, 50.9 (other rotamer), 45.5, 45.3 (other rotamer).

IR (film): ν (cm^{-1}) 3064, 3031, 2945, 1827, 1790, 1741, 1706, 1607, 1586, 1496, 1466, 1453, 1425, 1402, 1365, 1314, 1233, 1186, 1124, 1079, 1029, 1014, 971, 911, 875, 821, 770, 734, 694, 634, 597, 567, 542, 517, 471, 403.

HRMS (ESI, m/z) calcd for $\text{C}_{25}\text{H}_{20}\text{N}_2\text{O}_6\text{Na}$ $[\text{M}+\text{Na}]^+$: 467.1214, found: 467.1228.



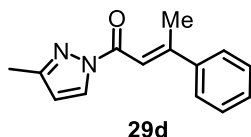
^1H NMR (300 MHz, CDCl_3 , two rotamers) δ 7.93–7.90 (m, 2H), 7.83–7.75 (m, 4H), 7.61 (d, $J = 7.4$ Hz, 2H), 7.41 (t, $J = 7.4$ Hz, 2H), 7.33 (t, $J = 7.4$ Hz, 2H), 5.41 (m, 1H), 4.60–4.20 (m, 5H).

^{13}C NMR (75 MHz, CDCl_3) δ 167.0, 161.5, 156.1, 143.7, 141.3, 135.0, 128.8, 127.8, 127.2, 125.1, 124.2, 120.0, 67.6, 47.1, 40.7.

IR (film): ν (cm^{-1}) 3369, 1827, 1789, 1736, 1520, 1451, 1363, 1247, 1176, 1131, 1078, 1001, 965, 876, 732, 694, 517, 418.

HRMS (ESI, m/z) calcd for $\text{C}_{25}\text{H}_{18}\text{N}_2\text{O}_6\text{Na}$ $[\text{M}+\text{Na}]^+$: 465.1057, found: 465.1069.

α,β -Unsaturated *N*-acylpyrazoles **29a-y** were synthesized according to our recent published procedure. Analytical data of **29a**⁴, **29b-c**⁵, **29f-g**⁴ were consistent with the report. The experimental data of **29d-f**, **2i-y** are shown below.

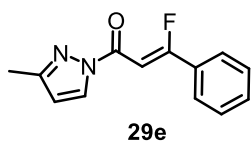


¹H NMR (300 MHz, CDCl₃) δ 8.27 (d, *J* = 2.7 Hz, 1H), 7.61–7.59 (m, 2H), 7.54–7.52 (m, 1H), 7.45–7.38 (m, 3H), 6.26 (d, *J* = 2.7 Hz, 1H), 2.71 (d, *J* = 1.2 Hz, 3H), 2.34 (s, 3H).

¹³C NMR (75 MHz, CDCl₃) δ 163.2, 159.7, 153.3, 142.5, 129.6, 129.2, 128.6, 126.8, 115.3, 110.2, 19.0, 14.0.

IR (film): ν (cm⁻¹) 2924, 1687, 1605, 1545, 1438, 1395, 1352, 1318, 1267, 1197, 1073, 1036, 967, 918, 873, 830, 753, 684, 566, 516, 475, 404.

HRMS (ESI, *m/z*) calcd for C₁₄H₁₄N₂ONa [M+Na]⁺: 249.0998, found: 249.1004.



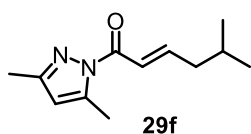
¹H NMR (300 MHz, CDCl₃) δ 8.29 (d, *J* = 2.7 Hz, 1H), 7.87–7.83 (m, 2H), 7.60–7.48 (m, 3H), 7.34 (d, *J* = 29.3 Hz, 1H), 6.31 (d, *J* = 2.8 Hz, 1H), 2.38 (s, 3H).

¹³C NMR (75 MHz, CDCl₃) δ 168.9 (d, *J* = 284.1 Hz, 1C), 160.2, 153.6, 132.2, 130.8 (d, *J* = 25.5 Hz, 1C), 129.1, 128.8 (d, *J* = 2.0 Hz, 1C), 126.3 (d, *J* = 8.4 Hz, 1C), 110.7, 95.1 (d, *J* = 1.8 Hz, 1C), 14.0.

¹⁹F NMR (282 MHz, CDCl₃) δ -92.5.

IR (film): ν (cm⁻¹) 2924, 2856, 1701, 1631, 1547, 1493, 1403, 1351, 1321, 1287, 1196, 1051, 936, 883, 832, 762, 676, 607, 515, 440.

HRMS (ESI, *m/z*) calcd for C₁₃H₁₁FN₂ONa [M+Na]⁺: 253.0748, found: 253.0758.



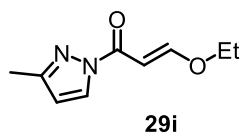
¹H NMR (300 MHz, CDCl₃) δ 7.35–7.18 (m, 2H), 6.00 (s, 1H), 2.61 (s, 3H), 2.29–2.24 (m, 5H), 1.86 (m, 1H), 0.99 (d, *J* = 6.7 Hz, 6H).

¹³C NMR (75 MHz, CDCl₃) δ 165.3, 151.8, 150.7, 144.5, 122.2, 111.3, 42.0, 28.1, 22.5, 14.7, 13.9.

IR (film): ν (cm⁻¹) 2958, 2927, 2873, 1706, 1638, 1580, 1467, 1439, 1410, 1376, 1343, 1296, 1267,

1243, 1170, 1138, 989, 961, 892, 850, 803, 752, 695, 623, 483.

HRMS (ESI, m/z) calcd for $C_{12}H_{18}N_2ONa$ $[M+Na]^+$: 229.1318, found: 229.1318.

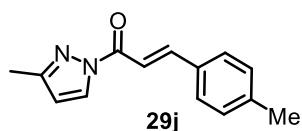


1H NMR (300 MHz, $CDCl_3$) δ 8.20 (d, $J = 2.6$ Hz, 1H), 7.88 (d, $J = 12.6$ Hz, 1H), 6.59 (d, $J = 12.6$ Hz, 1H), 6.23 (d, $J = 2.7$ Hz, 1H), 4.08 (q, $J = 7.0$ Hz, 2H), 2.32 (s, 3H), 1.39 (t, $J = 7.1$ Hz, 3H).

^{13}C NMR (75 MHz, $CDCl_3$) δ 165.2, 164.6, 153.2, 129.0, 109.9, 95.2, 67.5, 14.4, 14.0.

IR (film): ν (cm^{-1}) 2984, 1697, 1602, 1547, 1447, 1350, 1299, 1233, 1187, 1044, 959, 894, 831, 773, 727, 685, 518, 410.

HRMS (ESI, m/z) calcd for $C_9H_{12}N_2O_2Na$ $[M+Na]^+$: 203.0796, found: 203.0796.

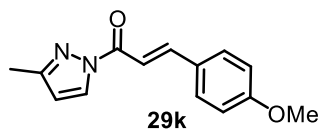


1H NMR (300 MHz, $CDCl_3$) δ 8.28 (d, $J = 2.6$ Hz, 1H), 7.98 (d, $J = 16.0$ Hz, 1H), 7.82 (d, $J = 16.0$ Hz, 1H), 7.59 (d, $J = 8.1$ Hz, 2H), 7.22 (d, $J = 8.0$ Hz, 2H), 6.29 (d, $J = 2.8$ Hz, 1H), 2.39 (s, 3H), 2.38 (s, 3H).

^{13}C NMR (75 MHz, $CDCl_3$) δ 163.6, 153.7, 147.5, 141.5, 132.0, 129.7, 129.5, 128.9, 115.0, 110.6, 21.6, 14.1.

IR (film): ν (cm^{-1}) 2858, 1694, 1612, 1546, 1407, 1377, 1343, 1202, 1054, 946, 884, 803, 769, 728, 680, 543, 516, 487, 446, 402.

HRMS (ESI, m/z) calcd for $C_{14}H_{14}N_2ONa$ $[M+Na]^+$: 249.0998, found: 249.1005.

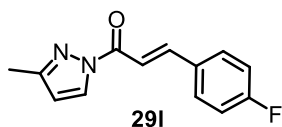


1H NMR (300 MHz, $CDCl_3$) δ 7.91 (d, $J = 15.9$ Hz, 1H), 7.83 (d, $J = 15.9$ Hz, 1H), 7.65–7.60 (m, 3H), 6.92 (d, $J = 8.8$ Hz, 2H), 6.19 (m, 1H), 3.85 (s, 3H), 2.67 (s, 3H).

^{13}C NMR (75 MHz, $CDCl_3$) δ 166.1, 161.9, 146.6, 143.7, 142.1, 130.6, 127.6, 115.1, 114.5, 110.4, 55.5, 14.8.

IR (film): ν (cm^{-1}) 2860, 1697, 1614, 1571, 1509, 1422, 1351, 1307, 1290, 1249, 1227, 1204, 1187, 1152, 1116, 1010, 983, 950, 904, 888, 808, 776, 731, 674, 636, 556, 518, 450, 394.

HRMS (ESI, m/z) calcd for $C_{14}H_{14}N_2O_2Na$ $[M+Na]^+$: 265.0947, found: 265.0953.

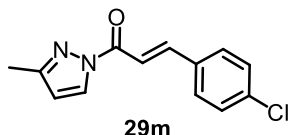


1H NMR (300 MHz, $CDCl_3$) δ 8.29 (d, $J = 2.7$ Hz, 1H), 7.97 (d, $J = 16.0$ Hz, 1H), 7.80 (d, $J = 16.1$ Hz, 1H), 7.73–7.68 (m, 2H), 7.16–7.10 (m, 2H), 6.32 (d, $J = 2.8$ Hz, 1H), 2.39 (s, 3H).

^{13}C NMR (75 MHz, $CDCl_3$) δ 164.4 (d, $J = 253.1$ Hz, 1C), 163.3, 153.9, 145.9, 131.0, 130.9, 130.7, 129.5, 116.2 (d, $J = 22.2$ Hz, 1C), 110.7, 14.0.

IR (film): ν (cm^{-1}) 3156, 1695, 1624, 1593, 1550, 1503, 1412, 1349, 1287, 1202, 1154, 1096, 1055, 978, 944, 887, 821, 772, 734, 680, 600, 545, 505, 451, 404.

HRMS (ESI, m/z) calcd for $C_{13}H_{11}FN_2ONa$ $[M+Na]^+$: 253.0748, found: 253.0754.

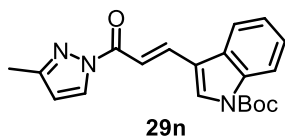


1H NMR (300 MHz, $CDCl_3$) δ 8.27 (d, $J = 2.8$ Hz, 1H), 7.93 (d, $J = 16.0$ Hz, 1H), 7.83 (d, $J = 16.0$ Hz, 1H), 7.62 (d, $J = 8.5$ Hz, 2H), 7.39 (d, $J = 8.5$ Hz, 2H), 6.30 (d, $J = 2.8$ Hz, 1H), 2.37 (s, 3H).

^{13}C NMR (75 MHz, $CDCl_3$) δ 163.2, 154.0, 145.7, 136.9, 133.2, 130.0, 129.5, 129.3, 116.8, 110.8, 14.0.

IR (film): ν (cm^{-1}) 3074, 1684, 1599, 1548, 1508, 1403, 1376, 1338, 1275, 1205, 1063, 1039, 971, 939, 856, 827, 772, 742, 708, 588, 530, 480, 437.

HRMS (ESI, m/z) calcd for $C_{13}H_{11}ClN_2ONa$ $[M+Na]^+$: 269.0452, found: 269.0461.

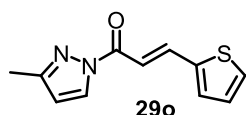


1H NMR (300 MHz, $CDCl_3$) δ 8.30 (d, $J = 2.7$ Hz, 1H), 8.23–8.20 (m, 1H), 8.16 (d, $J = 16.1$ Hz, 1H), 8.03 (s, 1H), 8.01–7.98 (m, 1H), 7.93 (d, $J = 16.1$ Hz, 1H), 7.45–7.36 (m, 2H), 6.31 (d, $J = 2.8$ Hz, 1H), 2.40 (s, 3H), 1.70 (s, 9H).

^{13}C NMR (75 MHz, $CDCl_3$) δ 163.8, 153.8, 149.2, 138.9, 136.4, 129.8, 129.5, 128.0, 125.5, 123.9, 120.6, 117.4, 115.7, 115.1, 110.5, 84.9, 28.3, 14.1.

IR (film): ν (cm^{-1}) 2978, 2930, 1733, 1697, 1615, 1548, 1451, 1411, 1351, 1303, 1243, 1200, 1150, 1093, 1065, 1043, 978, 947, 846, 811, 759, 736, 634, 552, 509, 451, 416.

HRMS (ESI, m/z) calcd for $C_{20}H_{22}N_3O_3$ $[M+H]^+$: 352.1656, found: 352.1667.

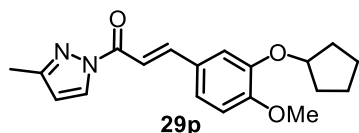


1H NMR (300 MHz, $CDCl_3$) δ 8.26 (d, $J = 2.8$ Hz, 1H), 8.09 (d, $J = 15.6$ Hz, 1H), 7.63 (d, $J = 15.6$ Hz, 1H), 7.46 (d, $J = 5.1$ Hz, 1H), 7.41 (d, $J = 3.6$ Hz, 1H), 7.10 (dd, $J = 5.0, 3.7$ Hz, 1H), 6.29 (d, $J = 2.8$ Hz, 1H), 2.38 (s, 3H).

^{13}C NMR (75 MHz, $CDCl_3$) δ 163.4, 153.9, 140.2, 139.5, 132.2, 129.7, 129.4, 128.3, 114.9, 110.7, 14.1.

IR (film): ν (cm^{-1}) 2921, 1693, 1612, 1545, 1508, 1407, 1378, 1342, 1201, 1112, 1052, 945, 883, 803, 768, 727, 679, 599, 542, 515, 486, 444.

HRMS (ESI, m/z) calcd for $C_{11}H_{10}N_2OSNa$ $[M+Na]^+$: 241.0406, found: 241.0412.

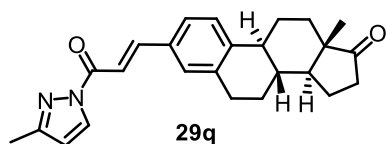


1H NMR (300 MHz, $CDCl_3$) δ 8.28 (d, $J = 2.7$ Hz, 1H), 7.94 (d, $J = 15.9$ Hz, 1H), 7.80 (d, $J = 15.9$ Hz, 1H), 7.29–7.26 (m, 1H), 7.20 (d, $J = 2.0$ Hz, 1H), 6.88 (d, $J = 8.4$ Hz, 1H), 6.29 (d, $J = 2.7$ Hz, 1H), 4.86 (m, 1H), 3.89 (s, 3H), 2.38 (s, 3H), 2.22–1.80 (m, 6H), 1.70–1.58 (m, 2H).

^{13}C NMR (75 MHz, $CDCl_3$) δ 163.7, 153.7, 153.0, 148.0, 147.8, 129.5, 127.7, 123.3, 114.7, 113.4, 111.7, 110.4, 80.8, 56.1, 32.9, 24.2, 14.0.

IR (film): ν (cm^{-1}) 2950, 2950, 1697, 1597, 1504, 1433, 1408, 1348, 1265, 1195, 1162, 1134, 1066, 1041, 990, 952, 848, 804, 764, 509, 450, 417.

HRMS (ESI, m/z) calcd for $C_{19}H_{22}N_2O_3Na$ $[M+Na]^+$: 349.1523, found: 349.1533.

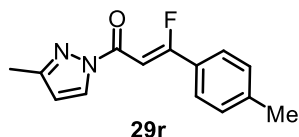


1H NMR (300 MHz, $CDCl_3$) δ 8.28 (d, $J = 2.7$ Hz, 1H), 7.96 (d, $J = 15.9$ Hz, 1H), 7.80 (d, $J = 15.9$ Hz, 1H), 7.48 (d, $J = 8.1$ Hz, 1H), 7.44 (s, 1H), 7.35 (d, $J = 8.0$ Hz, 1H), 6.30 (d, $J = 2.7$ Hz, 1H), 2.99–2.96 (m, 2H), 2.56–2.30 (m, 6H), 2.19–1.97 (m, 4H), 1.70–1.40 (m, 6H), 0.92 (s, 3H).

^{13}C NMR (75 MHz, $CDCl_3$) δ 220.7, 163.6, 153.8, 147.4, 143.4, 137.3, 132.3, 129.5, 126.5, 126.0, 115.2, 110.6, 50.7, 48.0, 44.8, 38.1, 35.9, 31.7, 29.3, 26.4, 25.7, 21.7, 14.1, 13.9.

IR (film): ν (cm⁻¹) 2923, 2863, 1732, 1693, 1618, 1550, 1409, 1345, 1209, 1062, 1002, 949, 821, 781, 730, 587, 563, 440.

HRMS (ESI, m/z) calcd for C₂₅H₂₉N₂O₂ [M+H]⁺: 389.2224, found: 389.2232.



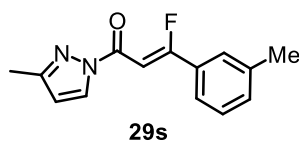
¹H NMR (300 MHz, CDCl₃) δ 8.28 (d, J = 2.7 Hz, 1H), 7.73 (d, J = 8.3 Hz, 2H), 7.37 (d, J = 33.7 Hz, 1H), 7.29 (d, J = 7.2 Hz, 2H), 6.29 (d, J = 2.7 Hz, 1H), 2.44 (s, 3H), 2.37 (s, 3H).

¹³C NMR (75 MHz, CDCl₃) δ 169.3 (d, J = 284.1 Hz, 1C), 160.3 (d, J = 2.2 Hz, 1C), 153.5, 143.0, 129.7 (d, J = 2.0 Hz, 1C), 129.1, 128.0 (d, J = 25.0 Hz, 1C), 126.3 (d, J = 8.4 Hz, 1C), 110.6, 94.1 (d, J = 1.8 Hz, 1C), 21.7, 14.0.

¹⁹F NMR (282 MHz, CDCl₃) δ -92.5.

IR (film): ν (cm⁻¹) 3114, 2924, 1700, 1633, 1545, 1511, 1443, 1404, 1347, 1319, 1286, 1191, 1128, 1075, 1041, 940, 886, 815, 779, 717, 680, 635, 597, 561, 511, 464.

HRMS (ESI, m/z) calcd for C₁₄H₁₃FN₂ONa [M+Na]⁺: 267.0904, found: 267.0911.

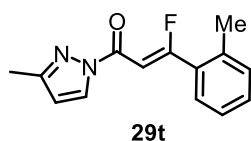


¹H NMR (300 MHz, CDCl₃) δ 8.30 (d, J = 2.7 Hz, 1H), 7.69–7.64 (m, 2H), 7.47–7.30 (m, 3H), 6.32 (d, J = 2.7 Hz, 1H), 2.46 (s, 3H), 2.39 (s, 3H).

¹³C NMR (75 MHz, CDCl₃) δ 169.2 (d, J = 284.8 Hz, 1C), 160.2 (d, J = 2.2 Hz, 1C), 153.5, 138.7 (d, J = 2.0 Hz, 1C), 133.0, 130.6 (d, J = 25.2 Hz, 1C), 129.0, 128.8 (d, J = 1.9 Hz, 1C), 126.6 (d, J = 8.3 Hz, 1C), 123.5 (d, J = 8.4 Hz, 1C), 110.6, 94.7 (d, J = 1.8 Hz, 1C), 21.4, 13.9.

IR (film): ν (cm⁻¹) 2956, 1709, 1632, 1545, 1445, 1405, 1347, 1317, 1202, 1049, 947, 893, 856, 830, 775, 719, 683, 648, 538, 511, 467, 424.

HRMS (ESI, m/z) calcd for C₁₄H₁₃FN₂ONa [M+Na]⁺: 267.0904, found: 267.0914.



¹H NMR (300 MHz, CDCl₃) δ 8.28 (d, J = 2.7 Hz, 1H), 7.58 (d, J = 8.1 Hz, 1H), 7.40 (m, 1H), 7.30–7.22 (m, 2H), 7.11 (d, J = 32.3 Hz, 1H), 6.29 (d, J = 2.8 Hz, 1H), 2.53 (d, J = 3.8 Hz, 3H), 2.33

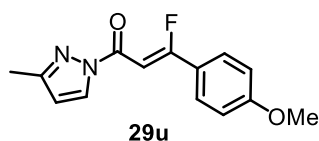
(s, 3H).

^{13}C NMR (75 MHz, CDCl_3) δ 171.2 (d, $J = 290.0$ Hz, 1C), 160.0 (d, $J = 2.6$ Hz, 1C), 153.6, 137.6, 131.4, 131.1 (d, $J = 22.5$ Hz, 1C), 129.3 (d, $J = 6.2$ Hz, 1C), 129.0, 126.1, 110.7, 99.4 (d, $J = 2.8$ Hz, 1C), 20.8 (d, $J = 4.4$ Hz, 1C), 13.9.

^{19}F NMR (282 MHz, CDCl_3) δ -75.3.

IR (film): ν (cm^{-1}) 3108, 2927, 1733, 1696, 1632, 1547, 1484, 1447, 1407, 1386, 1345, 1306, 1263, 1202, 1119, 1058, 1020, 938, 883, 845, 811, 765, 720, 655, 617, 512, 453, 406.

HRMS (ESI, m/z) calcd for $\text{C}_{14}\text{H}_{13}\text{FN}_2\text{ONa}$ $[\text{M}+\text{Na}]^+$: 267.0904, found: 267.0910.



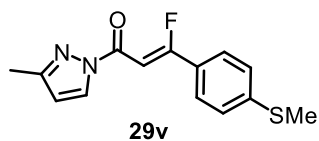
^1H NMR (300 MHz, CDCl_3) δ 8.17 (d, $J = 2.7$ Hz, 1H), 7.68 (d, $J = 9.0$ Hz, 2H), 7.16 (d, $J = 8.0$ Hz, 1H), 6.88 (d, $J = 8.7$ Hz, 2H), 6.18 (d, $J = 2.7$ Hz, 1H), 3.79 (s, 3H), 2.26 (s, 3H).

^{13}C NMR (75 MHz, CDCl_3) δ 169.3 (d, $J = 282.8$ Hz, 1C), 160.4 (d, $J = 2.3$ Hz, 1C), 162.9, 153.4, 129.1, 128.2 (d, $J = 8.9$ Hz, 1C), 123.1 (d, $J = 25.3$ Hz, 1C), 114.4 (d, $J = 2.0$ Hz, 1C), 110.5, 92.5 (d, $J = 1.9$ Hz, 1C), 55.6, 14.0.

^{19}F NMR (282 MHz, CDCl_3) δ -92.3.

IR (film): ν (cm^{-1}) 3153, 3005, 2932, 2845, 1705, 1637, 1602, 1549, 1510, 1461, 1409, 1349, 1263, 1194, 1045, 1014, 943, 883, 825, 769, 719, 685, 633, 579, 508, 446.

HRMS (ESI, m/z) calcd for $\text{C}_{14}\text{H}_{13}\text{FN}_2\text{O}_2\text{Na}$ $[\text{M}+\text{Na}]^+$: 283.0853, found: 283.0863.



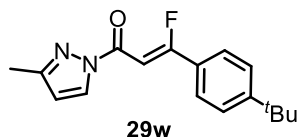
^1H NMR (300 MHz, CDCl_3) δ 8.28 (d, $J = 2.7$ Hz, 1H), 7.58 (d, $J = 8.1$ Hz, 1H), 7.40 (m, 1H), 7.30–7.22 (m, 2H), 7.11 (d, $J = 32.3$ Hz, 1H), 6.29 (d, $J = 2.8$ Hz, 1H), 2.53 (d, $J = 3.8$ Hz, 3H), 2.33 (s, 3H).

^{13}C NMR (75 MHz, CDCl_3) δ 168.7 (d, $J = 283.0$ Hz, 1C), 160.1 (d, $J = 2.1$ Hz, 1C), 153.4, 144.9, 128.9, 126.7 (d, $J = 25.8$ Hz, 1C), 126.4 (d, $J = 8.5$ Hz, 1C), 125.5 (d, $J = 2.0$ Hz, 1C), 110.5, 93.8 (d, $J = 1.8$ Hz, 1C), 14.8, 13.9.

^{19}F NMR (282 MHz, CDCl_3) δ -93.7 (t, $J = 15.9$ Hz).

IR (film): ν (cm⁻¹) 3122, 2923, 1702, 1628, 1591, 1544, 1487, 1441, 1402, 1341, 1196, 1096, 1051, 939, 885, 849, 818, 767, 721, 658, 590, 471, 416.

HRMS (ESI, m/z) calcd for C₁₄H₁₃FN₂OSNa [M+ Na]⁺: 299.0625, found: 299.0632.



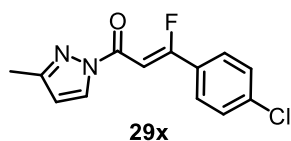
¹H NMR (300 MHz, CDCl₃) δ 8.27 (d, J = 2.7 Hz, 1H), 7.76 (d, J = 8.6 Hz, 2H), 7.48 (d, J = 8.4 Hz, 2H), 7.37 (d, J = 33.8 Hz, 1H), 6.28 (d, J = 2.7 Hz, 1H), 2.35 (s, 3H), 1.35 (s, 9H).

¹³C NMR (75 MHz, CDCl₃) δ 169.3 (d, J = 282.9 Hz, 1C), 160.4 (d, J = 2.2 Hz, 1C), 156.1, 153.5, 129.1, 128.0 (d, J = 25.4 Hz, 1C), 126.2 (d, J = 8.4 Hz, 1C), 126.0 (d, J = 2.0 Hz, 1C), 110.6, 94.2 (d, J = 1.7 Hz, 1C), 35.2, 31.2, 14.0.

¹⁹F NMR (282 MHz, CDCl₃) δ -92.5.

IR (film): ν (cm⁻¹) 2952, 2903, 2866, 1702, 1628, 1551, 1513, 1451, 1403, 1343, 1267, 1193, 1115, 1045, 939, 884, 830, 763, 725, 671, 643, 596, 513.

HRMS (ESI, m/z) calcd for C₁₇H₂₀FN₂O [M+H]⁺: 287.1554, found: 287.1562.



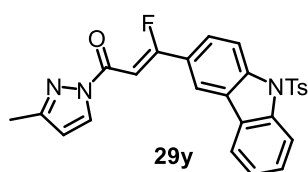
¹H NMR (300 MHz, CDCl₃) δ 8.25 (d, J = 2.7 Hz, 1H), 7.76–7.73 (m, 2H), 7.46–7.32 (m, 3H), 6.28 (d, J = 2.7 Hz, 1H), 2.35 (s, 3H).

¹³C NMR (75 MHz, CDCl₃) δ 167.7 (d, J = 283.6 Hz, 1C), 160.0 (d, J = 2.4 Hz, 1C), 153.7, 138.5, 129.4, 129.3 (d, J = 2.0 Hz, 1C), 129.1, 127.5 (d, J = 8.3 Hz, 1C), 110.9, 95.5 (d, J = 1.9 Hz, 1C), 14.0.

¹⁹F NMR (282 MHz, CDCl₃) δ -94.7.

IR (film): ν (cm⁻¹) 3108, 2922, 2856, 1699, 1634, 1550, 1485, 1408, 1350, 1319, 1275, 1197, 936, 880, 821, 769, 720, 664, 635, 594, 503, 467, 419.

HRMS (ESI, m/z) calcd for C₁₃H₁₀ClFN₂ONa [M+Na]⁺: 287.0358, found: 287.0365.



^1H NMR (300 MHz, CDCl_3) δ 8.43–8.34 (m, 3H), 8.29 (d, $J = 2.7$ Hz, 1H), 7.99 (d, $J = 7.5$ Hz, 1H), 7.94 (dd, $J = 8.9, 1.8$ Hz, 1H), 7.73 (d, $J = 8.5$ Hz, 2H), 7.60–7.40 (m, 3H), 7.15 (d, $J = 8.1$ Hz, 2H), 6.31 (d, $J = 2.7$ Hz, 1H), 2.39 (s, 3H), 2.29 (s, 3H).

^{13}C NMR (75 MHz, CDCl_3) δ 168.9 (d, $J = 282.7$ Hz, 1C), 160.1 (d, $J = 2.0$ Hz, 1C), 153.6, 145.5, 140.5, 139.0, 134.8, 129.9, 129.1, 128.4, 126.8 (d, $J = 1.6$ Hz, 1C), 126.6, 126.3 (d, $J = 25.5$ Hz, 1C), 125.5, 125.4 (d, $J = 8.4$ Hz, 1C), 124.4, 120.5, 118.3 (d, $J = 8.8$ Hz, 1C), 115.4 (d, $J = 1.8$ Hz, 1C), 115.2, 110.7, 94.6 (d, $J = 1.6$ Hz, 1C), 21.6, 14.0.

^{19}F NMR (282 MHz, CDCl_3) δ -91.9.

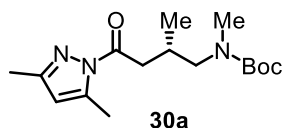
IR (film): ν (cm^{-1}) 1699, 1621, 1546, 1483, 1441, 1406, 1363, 1335, 1299, 1264, 1234, 1191, 1175, 1146, 1081, 1047, 976, 945, 885, 809, 770, 741, 684, 660, 634, 586, 563, 536, 514, 465, 416.

HRMS (ESI, m/z) calcd for $\text{C}_{26}\text{H}_{20}\text{FN}_3\text{O}_3\text{SNa}$ [$\text{M}+\text{Na}$] $^+$: 496.1102, found: 496.1115.

5.5.2 Rhodium-Catalyzed Giese-Type Reaction Activated by Visible Light

A dried 10 mL Schlenk tube was charged with *N*-hydroxyphthalimide esters **28a-f** (1.5 equiv.), *N*-acyl pyrazoles **29a-y** (1.0 equiv.), Δ -**RhS** (8 mol%) or Δ -**RhS** (8 mol%), and Hantzsch ester (2.0 equiv.) in acetone (0.1 M or 0.2 M). The reaction mixture was degassed via freeze-pump-thaw for two cycles. After the mixture was thoroughly degassed, the Schlenk tube was sealed tightly with a Teflon septum and positioned close to 23 W CFL. The reaction was stirred at room temperature for the indicated time (monitored by TLC) under an atmosphere of nitrogen. Afterwards, the mixture was diluted with CH_2Cl_2 . The organic solutions were concentrated under reduced pressure. The crude material was purified by flash chromatography on silica gel (*n*-hexane/EtOAc or *n*-hexane/ Et_2O) to afford the C–C formation products **30a-c**, **30e-30ad**. Racemic samples were obtained by carrying out the reactions with *rac*-**RhS**. The enantiomeric excess was determined by chiral HPLC analysis.

Remark: In case of the synthesis of **30l**, **30u** and **30z**, the C–C formation products showed the similar R_f values with the unconsumed Hantzsch ester (HE), thus couldn't be separated completely from HE on silica gel chromatography column. Therefore, the Hantzsch ester could be consumed through *in situ* oxidation to the corresponding pyridine derivative by opening the Schlenk tube to the air and stirring for another 2–3 hours under the irradiation of 23 W CFL.



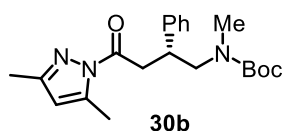
According to the general procedure, a mixture of **28a** (100.2 mg, 0.30 mmol, 1.5 equiv.), **29a** (32.8 mg, 0.20 mmol), Λ -**RhS** (13.8 mg, 0.016 mmol, 8 mol%), and HE (101.0 mg, 0.40 mmol, 2.0 equiv.) in acetone (1.0 mL, 0.2 M) was stirred under nitrogen atmosphere for 16 hours under irradiation with 23 W CFL at room temperature to afford **30a** as a colorless oil (53.0 mg, 86% yield, 94% ee). Purification conditions: *n*-hexane/EtOAc = 20:1 to 10:1, R_f = 0.7 in *n*-hexane/EtOAc (5:1). Enantiomeric excess was established by HPLC analysis using a Chiralpak AD-H column, ee = 94% (HPLC: 254 nm, *n*-hexane/isopropanol = 99:1, flow rate 0.3 mL/min, 25 °C, t_r (major) = 32.8 min, t_r (minor) = 37.4 min). $[\alpha]_D^{22} = -6.2^\circ$ (*c* 1.0, CH₂Cl₂).

¹H NMR (300 MHz, CD₂Cl₂) δ 5.96 (s, 1H), 3.24 (dd, *J* = 13.9, 7.7 Hz, 1H), 3.14–3.05 (m, 2H), 2.90–2.80 (m, 4H), 2.51 (s, 3H), 2.48–2.38 (m, 1H), 2.19 (s, 3H), 1.42 (s, 9H), 0.96 (d, *J* = 6.7 Hz, 3H).

¹³C NMR (125 MHz, CD₂Cl₂) δ 173.3, 156.0, 151.9, 144.1, 111.1, 79.4, 54.9, 40.2, 34.7, 29.2, 28.4, 17.8, 14.6, 13.8.

IR (film): ν (cm⁻¹) 2968, 2927, 1726, 1693, 1583, 1456, 1384, 1335, 1247, 1216, 1086, 1044, 995, 962, 877, 801, 770, 745, 713, 641, 527.

HRMS (ESI, *m/z*) calcd for C₁₆H₂₇N₃O₃Na [M+Na]⁺: 332.1945, found: 332.1952.



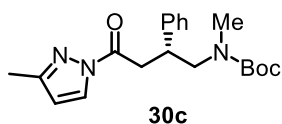
According to the general procedure, a mixture of **28a** (100.2 mg, 0.30 mmol, 1.5 equiv.), **29b** (45.2 mg, 0.20 mmol), Λ -**RhS** (13.8 mg, 0.016 mmol, 8 mol%), and HE (101.0 mg, 0.40 mmol, 2.0 equiv.) was stirred under nitrogen atmosphere for 16 hours under irradiation with 23 W CFL at room temperature to afford **30b** as a colorless oil (40.3 mg, 54% yield, 90% ee). Purification conditions: *n*-hexane/Et₂O = 20:1 to 10:1, R_f = 0.4 in *n*-hexane/EtOAc (5:1). Enantiomeric excess was established by HPLC analysis using a Chiralpak IG column, ee = 90% (HPLC: 254 nm, *n*-hexane/isopropanol = 95:5, flow rate 1.0 mL/min, 25 °C, t_r (major) = 11.0 min, t_r (minor) = 11.8 min). $[\alpha]_D^{22} = +70.0^\circ$ (*c* 1.0, CH₂Cl₂).

¹H NMR (300 MHz, CD₂Cl₂) δ 7.38–7.20 (m, 5H), 5.97 (s, 1H), 3.70–3.25 (m, 5H), 2.75 (s, 3H), 2.45 (s, 3H), 2.24 (s, 3H), 1.40 (s, 9H).

^{13}C NMR (125 MHz, CD_2Cl_2) δ 172.4, 155.6, 152.1, 144.2, 142.5, 128.7, 128.3, 127.1, 111.2, 79.5, 55.1, 40.5, 38.9, 34.7, 28.3, 14.5, 13.8.

IR (film): ν (cm^{-1}) 2971, 2926, 1694, 1457, 1384, 1340, 1229, 1165, 963, 880, 762, 700, 654, 520, 422.

HRMS (ESI, m/z) calcd for $\text{C}_{21}\text{H}_{29}\text{N}_3\text{O}_3\text{Na}$ $[\text{M}+\text{Na}]^+$: 394.2101, found: 394.2106.



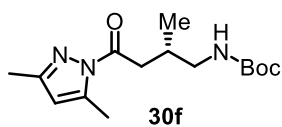
According to the general procedure, a mixture of **28a** (100.2 mg, 0.30 mmol, 1.5 equiv.) and **29c** (42.4 mg, 0.20 mmol), Λ -**RhS** (13.8 mg, 0.016 mmol, 8 mol%), and HE (101.0 mg, 0.40 mmol, 2.0 equiv.) was stirred under nitrogen atmosphere for 16 hours under irradiation with 23 W CFL at room temperature to afford **30c** as a colorless oil (59.9 mg, 84% yield, 95% ee). Purification conditions: *n*-hexane/ Et_2O = 20:1 to 10:1, R_f = 0.4 in *n*-hexane/ EtOAc (5:1). Enantiomeric excess was established by HPLC analysis using a Chiralpak IG column, ee = 95% (HPLC: IG, 254 nm, *n*-hexane/isopropanol = 95:5, flow rate 1.0 mL/min, 25 °C, t_r (major) = 15.4 min, t_r (minor) = 23.6 min). $[\alpha]_D^{22} = +89.8^\circ$ (*c* 1.0, CH_2Cl_2).

^1H NMR (300 MHz, CD_2Cl_2) δ 8.06 (d, J = 2.7 Hz, 1H), 7.40–7.20 (m, 5H), 6.25 (d, J = 2.8 Hz, 1H), 3.80–3.25 (m, 5H), 2.75 (s, 3H), 2.32 (s, 3H), 1.40 (s, 9H).

^{13}C NMR (125 MHz, CD_2Cl_2) δ 170.1, 153.8, 141.9, 128.7, 128.6, 128.5, 127.9, 126.9, 110.2, 79.3, 54.8, 40.3, 37.3, 34.4, 28.0, 13.7.

IR (film): ν (cm^{-1}) 2960, 2925, 1708, 1552, 1481, 1454, 1414, 1372, 1268, 1212, 1142, 1060, 875, 775, 699, 525.

HRMS (ESI, m/z) calcd for $\text{C}_{20}\text{H}_{27}\text{N}_3\text{O}_3\text{Na}$ $[\text{M}+\text{Na}]^+$: 380.1945, found: 380.1954.



According to the general procedure, a mixture of **28b** (96.0 mg, 0.30 mmol, 1.5 equiv.), **29a** (32.8 mg, 0.20 mmol), Λ -**RhS** (13.8 mg, 0.016 mmol, 8 mol%), and HE (101.0 mg, 0.40 mmol, 2.0 equiv.) in acetone (1.0 mL, 0.2 M) was stirred under nitrogen atmosphere for 16 hours under irradiation with 23 W CFL at room temperature to afford **30f** as a colorless oil (52.0 mg, 88% yield, 94% ee). Purification conditions: *n*-hexane/ EtOAc = 20:1 to 10:1, R_f = 0.6 in *n*-hexane/ EtOAc (5:1). Enantiomeric excess was established by HPLC analysis using a Chiralpak AD-H column, ee =

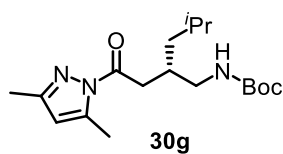
94% (HPLC: 254 nm, *n*-hexane/isopropanol = 97:3, flow rate 0.5 mL/min, 25 °C, t_r (major) = 25.2 min, t_r (minor) = 28.0 min). $[\alpha]_D^{22} = -11.8^\circ$ (c 1.0, CH_2Cl_2).

^1H NMR (300 MHz, CD_2Cl_2) δ 5.98 (s, 1H), 5.02 (br, 1H), 3.13 (dd, $J = 15.7, 6.5$ Hz, 1H), 3.06 (t, $J = 6.3$ Hz, 2H), 2.86 (d, $J = 15.7, 7.1$ Hz, 1H), 2.51 (s, 3H), 2.28–2.16 (m, 4H), 1.40 (s, 9H), 1.00 (d, $J = 6.8$ Hz, 3H).

^{13}C NMR (75 MHz, CD_2Cl_2) δ 173.4, 156.3, 152.1, 144.3, 111.2, 78.9, 46.2, 40.0, 31.4, 28.4, 18.1, 14.7, 13.8.

IR (film): ν (cm^{-1}) 3341, 2977, 2928, 1723, 1684, 1535, 1476, 1453, 1438, 1412, 1382, 1372, 1364, 1338, 1309, 1278, 1252, 1169, 1123, 1036, 982, 932, 886, 841, 766, 749, 657, 550, 461, 390.

HRMS (ESI, m/z) calcd for $\text{C}_{15}\text{H}_{25}\text{N}_3\text{O}_3\text{Na}$ $[\text{M}+\text{Na}]^+$: 318.1788, found: 318.1798.



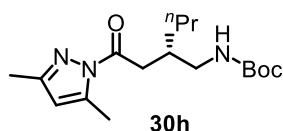
According to the general procedure, a mixture of **28b** (96.0 mg, 0.30 mmol, 1.5 equiv.), **29f** (41.2 mg, 0.20 mmol), Λ -**RhS** (13.8 mg, 0.016 mmol, 8 mol%), and HE (101.0 mg, 0.40 mmol, 2.0 equiv.) in acetone (1.0 mL, 0.2 M) was stirred under nitrogen atmosphere for 16 hours under irradiation with 23 W CFL at room temperature to afford **30g** as a colorless oil (58.6 mg, 87% yield, 92% ee). Purification conditions: *n*-hexane/EtOAc = 20:1 to 10:1, $R_f = 0.6$ in *n*-hexane/EtOAc (5:1). Enantiomeric excess was established by HPLC analysis using a Chiralpak AD-H column, ee = 92% (HPLC: 254 nm, *n*-hexane/isopropanol = 95:5, flow rate 0.4 mL/min, 25 °C, t_r (major) = 17.6 min, t_r (minor) = 14.6 min). $[\alpha]_D^{22} = -24.0^\circ$ (c 1.0, CH_2Cl_2).

^1H NMR (300 MHz, CD_2Cl_2) δ 5.89 (s, 1H), 5.16 (br, 1H), 3.13–2.90 (m, 3H), 2.85 (dd, $J = 15.4, 5.2$ Hz, 1H), 2.47 (s, 3H), 2.28–2.12 (m, 4H), 1.66 (s, 1H), 1.34 (s, 9H), 1.17 (t, $J = 6.9$ Hz, 2H), 0.85 (d, $J = 3.7$ Hz, 3H), 0.82 (d, $J = 3.7$ Hz, 3H).

^{13}C NMR (125 MHz, CD_2Cl_2) δ 173.6, 156.2, 152.1, 144.2, 111.2, 78.9, 44.0, 41.9, 38.2, 33.9, 28.5, 25.2, 22.8, 22.7, 14.7, 13.8.

IR (film): ν (cm^{-1}) 3368, 2959, 2928, 2872, 1714, 1584, 1513, 1448, 1375, 1336, 1245, 1168, 1105, 1038, 962, 861, 804, 775, 747, 649, 586.

HRMS (ESI, m/z) calcd for $\text{C}_{18}\text{H}_{31}\text{N}_3\text{O}_3\text{Na}$ $[\text{M}+\text{Na}]^+$: 360.2258, found: 360.2267.



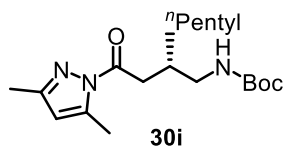
According to the general procedure, a mixture of **28b** (72.0 mg, 0.225 mmol, 1.5 equiv.), **29g** (28.8 mg, 0.15 mmol), Λ -**RhS** (10.3 mg, 0.012 mmol, 8 mol%), and HE (76.0 mg, 0.30 mmol, 2.0 equiv.) in acetone (0.75 mL, 0.2 M) was stirred under nitrogen atmosphere for 16 hours under irradiation with 23 W CFL at room temperature to afford **30h** as a colorless oil (41.3 mg, 85% yield, 92% ee). Purification conditions: *n*-hexane/EtOAc = 20:1 to 10:1, $R_f = 0.7$ in *n*-hexane/EtOAc (5:1). Enantiomeric excess was established by HPLC analysis using a Chiralpak IG column, ee = 92% (HPLC: 254 nm, *n*-hexane/isopropanol = 97:3, flow rate 1.0 mL/min, 25 °C, t_r (major) = 16.0 min, t_r (minor) = 17.3 min). $[\alpha]_D^{22} = -18.6^\circ$ (*c* 1.0, CH₂Cl₂).

¹H NMR (300 MHz, CD₂Cl₂) δ 6.00 (s, 1H), 5.20 (br, 1H), 3.20–3.02 (m, 3H), 2.94 (dd, $J = 15.6, 5.7$ Hz, 1H), 2.54 (d, $J = 0.8$ Hz, 3H), 2.30–2.15 (m, 4H), 1.48–1.34 (m, 13H), 0.94 (t, $J = 6.8$ Hz, 3H).

¹³C NMR (125 MHz, CD₂Cl₂) δ 173.4, 156.0, 151.9, 144.1, 111.0, 78.5, 43.8, 37.9, 35.8, 34.7, 28.1, 20.0, 14.4, 14.0, 13.5.

IR (film): ν (cm⁻¹) 3366, 2962, 2927, 2868, 1712, 1582, 1513, 1454, 1376, 1336, 1245, 1168, 1035, 962, 859, 800, 743, 643, 588, 525.

HRMS (ESI, *m/z*) calcd for C₁₇H₂₉N₃O₃Na [M+ Na]⁺: 346.2101, found: 346.2115.



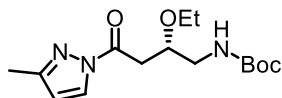
According to the general procedure, a mixture of **28b** (72.0 mg, 0.225 mmol, 1.5 equiv.), **29h** (33.0 mg, 0.15 mmol), Λ -**RhS** (10.3 mg, 0.012 mmol, 8 mol%), and HE (76.0 mg, 0.30 mmol, 2.0 equiv.) in acetone (0.75 mL, 0.2 M) was stirred under nitrogen atmosphere for 16 hours under irradiation with 23 W CFL at room temperature to afford **30i** as a colorless oil (42.7 mg, 81% yield, 94% ee). Purification conditions: *n*-hexane/EtOAc = 20:1 to 10:1, $R_f = 0.7$ in *n*-hexane/EtOAc (5:1). Enantiomeric excess was established by HPLC analysis using a Chiralpak AD-H column, ee = 94% (HPLC: 254 nm, *n*-hexane/isopropanol = 98:2, flow rate 0.5 mL/min, 25 °C, t_r (major) = 20.5 min, t_r (minor) = 18.3 min). $[\alpha]_D^{22} = -31.4^\circ$ (*c* 1.0, CH₂Cl₂).

¹H NMR (300 MHz, CD₂Cl₂) δ 6.00 (s, 1H), 5.20 (br, 1H), 3.21–3.02 (m, 3H), 2.94 (dd, $J = 15.6, 5.6$ Hz, 1H), 2.54 (d, $J = 0.8$ Hz, 3H), 2.30–2.10 (m, 4H), 1.45–1.36 (m, 13H), 1.35–1.25 (m, 4H), 0.91 (t, $J = 6.6$ Hz, 3H).

^{13}C NMR (125 MHz, CD_2Cl_2) δ 173.5, 156.0, 151.8, 144.1, 111.0, 78.5, 43.8, 37.9, 36.0, 32.4, 32.0, 28.1, 26.5, 22.6, 14.4, 13.9, 13.5.

IR (film): ν (cm^{-1}) 3363, 2957, 2927, 2858, 1716, 1583, 1511, 1455, 1411, 1378, 1364, 1340, 1245, 1168, 983, 962, 801, 746.

HRMS (ESI, m/z) calcd for $\text{C}_{19}\text{H}_{33}\text{N}_3\text{O}_3\text{Na}$ $[\text{M}+\text{Na}]^+$: 374.2414, found: 374.2423.



30j

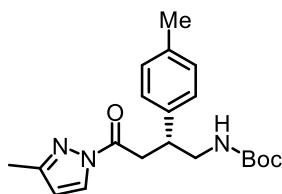
According to the general procedure, a mixture of **28b** (72.0 mg, 0.225 mmol, 1.5 equiv.), **29i** (27.0 mg, 0.15 mmol), Λ -**RhS** (10.3 mg, 0.012 mmol, 8 mol%), and HE (76.0 mg, 0.30 mmol, 2.0 equiv.) in acetone (0.75 mL, 0.2 M) was stirred under nitrogen atmosphere for 20 hours under irradiation with 23 W CFL at room temperature to afford **30j** as a colorless oil (41.6 mg, 89% yield, 97% ee). Purification conditions: *n*-hexane/EtOAc = 20:1 to 10:1, R_f = 0.6 in *n*-hexane/EtOAc (10:1). Enantiomeric excess was established by HPLC analysis using a Chiralpak AD-H column, ee = 97% (HPLC: 254 nm, *n*-hexane/isopropanol = 90:10, flow rate 1.0 mL/min, 25 °C, t_r (major) = 7.0 min, t_r (minor) = 8.6 min). $[\alpha]_D^{22}$ = +11.0° (*c* 1.0, CH_2Cl_2).

^1H NMR (300 MHz, CDCl_3) δ 8.07 (d, J = 2.8 Hz, 1H), 6.17 (d, J = 2.7 Hz, 1H), 4.87 (br, 1H), 3.98 (m, 1H), 3.59–3.44 (m, 2H), 3.35–3.20 (m, 3H), 3.13 (dd, J = 16.2, 5.7 Hz, 1H), 2.24 (s, 3H), 1.37 (s, 9H), 1.08 (t, J = 6.9 Hz, 3H).

^{13}C NMR (125 MHz, CDCl_3) δ 169.5, 156.1, 154.0, 129.0, 110.7, 79.4, 74.4, 65.3, 43.4, 37.1, 28.5, 15.5, 14.0.

IR (film): ν (cm^{-1}) 3359, 2975, 2930, 1717, 1548, 1513, 1413, 1388, 1342, 1249, 1169, 1101, 1048, 937, 774.

HRMS (ESI, m/z) calcd for $\text{C}_{15}\text{H}_{25}\text{N}_3\text{O}_4\text{Na}$ $[\text{M}+\text{Na}]^+$: 334.1737, found: 334.1752.



30k

According to the general procedure, a mixture of **28b** (72.0 mg, 0.225 mmol, 1.5 equiv.), **29j** (33.9 mg, 0.15 mmol), Λ -**RhS** (10.3 mg, 0.012 mmol, 8 mol%), and HE (76.0 mg, 0.30 mmol, 2.0 equiv.) in acetone (0.75 mL, 0.2 M) was stirred under nitrogen atmosphere for 16 hours under irradiation with 23 W CFL at room temperature to afford **30k** as a colorless oil (45.5 mg,

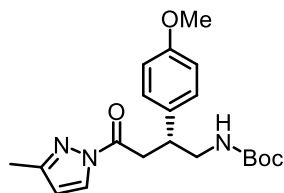
85% yield, 95% ee). Purification conditions: *n*-hexane/EtOAc = 20:1 to 10:1, $R_f = 0.5$ in *n*-hexane/EtOAc (10:1). Enantiomeric excess was established by HPLC analysis using a Chiralpak OD-H column, ee = 95% (HPLC: 254 nm, *n*-hexane/isopropanol = 95:5, flow rate 1.0 mL/min, 25 °C, t_r (major) = 11.4 min, t_r (minor) = 15.8 min). $[\alpha]_D^{22} = +54.4^\circ$ (c 1.0, CH_2Cl_2).

^1H NMR (300 MHz, CD_2Cl_2) δ 8.07 (d, $J = 2.7$ Hz, 1H), 7.14 (dd, $J = 15.0, 8.1$ Hz, 4H), 6.20 (d, $J = 2.7$ Hz, 1H), 4.57 (br, 1H), 3.56–3.40 (m, 4H), 3.33 (m, 1H), 2.31 (m, 6H), 1.39 (s, 9H).

^{13}C NMR (125 MHz, CD_2Cl_2) δ 170.2, 155.9, 153.9, 138.4, 136.7, 129.5, 129.1, 127.7, 110.4, 79.3, 45.9, 41.3, 37.8, 28.4, 21.1, 14.0.

IR (film): ν (cm^{-1}) 3391, 3192, 2974, 2925, 1720, 1689, 1599, 1551, 1509, 1459, 1412, 1364, 1339, 1303, 1243, 1164, 1085, 1046, 938, 862, 814, 778, 742, 712, 642, 605, 526, 470, 428.

HRMS (ESI, m/z) calcd for $\text{C}_{20}\text{H}_{27}\text{N}_3\text{O}_3\text{Na}$ $[\text{M}+\text{Na}]^+$: 380.1954, found: 380.1954.



301

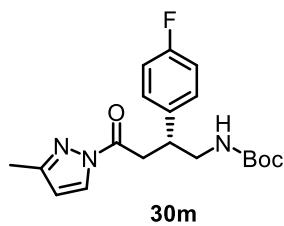
According to the general procedure, a mixture of **28b** (48.0 mg, 0.15 mmol, 1.5 equiv.), **29k** (24.2 mg, 0.10 mmol), Λ -**RhS** (7.0 mg, 0.008 mmol, 8 mol%), and HE (50.4 mg, 0.2 mmol, 2.0 equiv.) in acetone (0.5 mL, 0.2 M) was stirred under nitrogen atmosphere for 16 hours under irradiation with 23 W CFL at room temperature to afford **301** as a colorless oil (30.0 mg, 80% yield, 97% ee). Purification conditions: *n*-hexane/EtOAc = 20:1 to 6:1, $R_f = 0.4$ in *n*-hexane/EtOAc (4:1). Enantiomeric excess was established by HPLC analysis using a Chiralpak AD-H column, ee = 97% (HPLC: 254 nm, *n*-hexane/isopropanol = 90:10, flow rate 1.0 mL/min, 25 °C, t_r (major) = 23.8 min, t_r (minor) = 14.0 min). $[\alpha]_D^{22} = +32.0^\circ$ (c 1.0, CH_2Cl_2).

^1H NMR (300 MHz, CD_2Cl_2) δ 7.54 (d, $J = 0.9$ Hz, 1H), 7.21 (d, $J = 8.7$ Hz, 2H), 6.88 (d, $J = 8.7$ Hz, 2H), 6.16 (m, 1H), 4.61 (br, 1H), 3.80 (s, 3H), 3.49 (m, 4H), 3.34–3.22 (m, 1H), 2.53 (s, 3H), 1.40 (s, 9H).

^{13}C NMR (125 MHz, CD_2Cl_2) δ 172.7, 158.8, 155.7, 143.4, 142.3, 133.8, 128.8, 114.1, 110.2, 79.0, 55.3, 46.1, 41.0, 39.3, 28.1, 14.2.

IR (film): ν (cm^{-1}) 3381, 2930, 1730, 1689, 1611, 1509, 1462, 1376, 1337, 1303, 1239, 1208, 1157, 1083, 1036, 981, 944, 903, 864, 819, 787, 747, 640, 595, 563, 523, 455.

HRMS (ESI, m/z) calcd for $\text{C}_{20}\text{H}_{27}\text{N}_3\text{O}_4\text{Na}$ $[\text{M}+\text{Na}]^+$: 396.1894, found: 396.1903.



According to the general procedure, a mixture of **28b** (72.0 mg, 0.225 mmol, 1.5 equiv.), **29i** (34.5 mg, 0.15 mmol), Λ -**RhS** (10.3 mg, 0.012 mmol, 8 mol%), and HE (76.0 mg, 0.3 mmol, 2.0 equiv.) in acetone (0.75 mL, 0.2 M) was stirred under nitrogen atmosphere for 16 hours under irradiation with 23 W CFL at room temperature to afford **30m** as a pale yellow oil (31.3 mg, 58% yield, 94% ee). Purification conditions: *n*-hexane/EtOAc = 20:1 to 6:1, R_f = 0.4 in *n*-hexane/EtOAc (4:1). Enantiomeric excess was established by HPLC analysis using a Chiralpak OD-H column, ee = 94% (HPLC: 254 nm, *n*-hexane/isopropanol = 90:10, flow rate 1.0 mL/min, 25 °C, t_r (major) = 6.9 min, t_r (minor) = 7.9 min). $[\alpha]_D^{22} = +33.4^\circ$ (*c* 1.0, CH₂Cl₂).

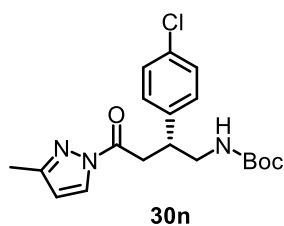
¹H NMR (300 MHz, CD₂Cl₂) δ 8.06 (d, *J* = 2.8 Hz, 1H), 7.28–7.22 (m, 2H), 7.03–6.97 (m, 2H), 6.24 (d, *J* = 2.8 Hz, 1H), 4.67 (br, 1H), 3.54–3.40 (m, 4H), 3.33–3.24 (m, 1H), 2.29 (s, 3H), 1.37 (s, 9H).

¹³C NMR (125 MHz, CD₂Cl₂) δ 170.3, 162.2 (d, *J* = 244.6 Hz, 1C), 154.3, 137.8, 129.8, 129.7, 129.1, 115.6 (d, *J* = 21.4 Hz, 1C), 110.7, 79.3, 46.0, 41.4, 37.9, 28.4, 14.0.

¹⁹F NMR (282 MHz) δ -116.8.

IR (film): ν (cm⁻¹) 3397, 2924, 2857, 1721, 1689, 1604, 1553, 1514, 1453, 1416, 1389, 1334, 1290, 1221, 1164, 1056, 933, 829, 781, 741, 692, 584, 545, 478, 435.

HRMS (ESI, *m/z*) calcd for C₁₉H₂₄FN₃O₃Na [M+Na]⁺: 384.1694, found: 384.1704.



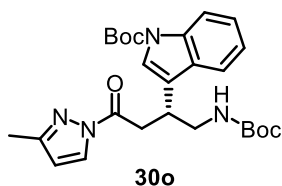
According to the general procedure, a mixture of **28b** (96.0 mg, 0.3 mmol, 1.5 equiv.), **29m** (49.3 mg, 0.20 mmol), Λ -**RhS** (13.8 mg, 0.016 mmol, 8 mol%), and HE (101 mg, 0.2 mmol, 2.0 equiv.) in acetone (1.0 mL, 0.2 M) was stirred under nitrogen atmosphere for 16 hours under irradiation with 23 W CFL at room temperature to afford **30n** as a pale yellow solid (61.8 mg, 82% yield, 90% ee). Purification conditions: *n*-hexane/EtOAc = 20:1 to 6:1, R_f = 0.4 in *n*-hexane/EtOAc (4:1). Enantiomeric excess was established by HPLC analysis using a Chiralpak AS-H column, ee = 90% (HPLC: 254 nm, *n*-hexane/isopropanol = 90:10, flow rate 1.0 mL/min, 25 °C, t_r (major) = 10.3 min, t_r (minor) = 8.9 min). $[\alpha]_D^{22} = +16.8^\circ$ (*c* 1.0, CH₂Cl₂).

^1H NMR (300 MHz, CD_2Cl_2) δ 8.07 (d, $J = 2.8$ Hz, 1H), 7.32 (d, $J = 8.5$ Hz, 2H), 7.25 (d, $J = 8.6$ Hz, 2H), 6.27 (d, $J = 2.8$ Hz, 1H), 4.68 (br, 1H), 3.60–2.26 (m, 5H), 2.32 (s, 3H), 1.40 (s, 9H).

^{13}C NMR (125 MHz, CD_2Cl_2) δ 170.2, 156.0, 154.3, 140.6, 132.9, 129.6, 129.1, 129.0, 110.7, 79.4, 45.9, 41.6, 37.7, 28.3, 14.0.

IR (film): ν (cm^{-1}) 3398, 2974, 2927, 1719, 1688, 1517, 1414, 1391, 1332, 1245, 1219, 1163, 931, 826, 775, 581, 535, 494, 462, 401.

HRMS (ESI, m/z) calcd for $\text{C}_{19}\text{H}_{24}\text{ClN}_3\text{O}_3\text{Na}$ $[\text{M}+\text{Na}]^+$: 400.1398, found: 400.1410.



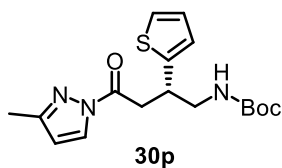
According to the general procedure, a mixture of **28b** (32.2 mg, 0.1 mmol, 1.0 equiv.), **29n** (42.2 mg, 0.12 mmol, 1.2 equiv.), Λ -**RhS** (6.5 mg, 0.008 mmol, 8 mol%), and HE (37.8 mg, 0.15 mmol, 1.5 equiv.) in acetone (0.5 mL, 0.2 M) was stirred under nitrogen atmosphere for 16 hours under irradiation with 23 W CFL at room temperature to afford **30o** as a pale yellow solid (33.8 mg, 70% yield, 90% ee). Purification conditions: *n*-hexane/EtOAc = 20:1 to 5:1, $R_f = 0.3$ in *n*-hexane/EtOAc (4:1). Enantiomeric excess was established by HPLC analysis using a Chiralpak AD-H column, ee = 90% (HPLC: 254 nm, *n*-hexane/isopropanol = 95:5, flow rate 1.0 mL/min, 25 °C, t_r (major) = 17.1 min, t_r (minor) = 19.3 min). $[\alpha]_D^{22} = +17.8^\circ$ (c 1.0, CH_2Cl_2).

^1H NMR (300 MHz, CD_2Cl_2) δ 8.13–8.10 (m, 2H), 7.67 (d, $J = 7.6$ Hz, 1H), 7.49 (s, 1H), 7.35–7.28 (m, 1H), 7.25–7.21 (m, 1H), 6.23 (d, $J = 2.7$ Hz, 1H), 4.71 (br, 1H), 3.88 (m, 1H), 3.60–3.50 (m, 4H), 2.32 (s, 3H), 1.66 (s, 9H), 1.38 (s, 9H).

^{13}C NMR (125 MHz, CD_2Cl_2) δ 170.5, 156.1, 154.3, 149.9, 136.0, 130.0, 129.2, 124.8, 123.2, 122.7, 121.2, 119.6, 115.6, 110.8, 84.0, 79.3, 44.7, 37.0, 33.4, 28.4, 28.3, 14.0.

IR (film): ν (cm^{-1}) 2922, 2853, 1722, 1512, 1453, 1411, 1366, 1308, 1250, 1218, 1153, 1101, 1068, 1048, 1018, 934, 855, 764, 745, 465, 446, 418, 383.

HRMS (ESI, m/z) calcd for $\text{C}_{26}\text{H}_{34}\text{N}_4\text{O}_5\text{Na}$ $[\text{M}+\text{Na}]^+$: 505.2421, found: 505.2434.



According to the general procedure, a mixture of **28b** (32.2 mg, 0.1 mmol, 1.0 equiv.), **29o** (32.7 mg, 0.15 mmol, 1.5 equiv.), Λ -**RhS** (6.5 mg, 0.008 mmol, 8 mol%), and HE (50.4

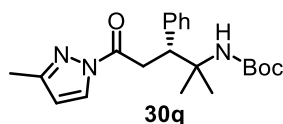
mg, 0.2 mmol, 2.0 equiv.) in acetone (0.5 mL, 0.2 M) was stirred under nitrogen atmosphere for 16 hours under irradiation with 23 W CFL at room temperature to afford **30p** as a pale yellow solid (15.0 mg, 42% yield, 91% ee). Purification conditions: *n*-hexane/EtOAc = 20:1 to 5:1, $R_f = 0.3$ in *n*-hexane/EtOAc (4:1). Enantiomeric excess was established by HPLC analysis using a Chiralpak AD-H column, ee = 91% (HPLC: 254 nm, *n*-hexane/isopropanol = 90:10, flow rate 1.0 mL/min, 25 °C, t_r (major) = 12.1 min, t_r (minor) = 14.5 min). $[\alpha]_D^{22} = +11.2^\circ$ (*c* 1.0, CH₂Cl₂).

¹H NMR (300 MHz, CD₂Cl₂) δ 8.10 (d, $J = 2.8$ Hz, 1H), 7.18–7.16 (m, 1H), 6.95–6.91 (m, 2H), 6.23 (d, $J = 2.8$ Hz, 1H), 4.73 (br, 1H), 3.89 (m, 1H), 3.56–3.36 (m, 4H), 2.31 (s, 3H), 1.40 (s, 9H).

¹³C NMR (125 MHz, CD₂Cl₂) δ 169.6, 155.8, 154.0, 144.8, 129.1, 126.9, 124.8, 124.0, 110.6, 79.5, 46.2, 38.5, 37.2, 28.3, 14.0.

IR (film): ν (cm⁻¹) 2921, 2854, 1719, 1550, 1510, 1458, 1412, 1364, 1249, 1167, 1045, 936, 773, 697.

HRMS (ESI, *m/z*) calcd for C₁₇H₂₃N₃O₃SNa [M+Na]⁺: 372.1352, found: 372.1361.



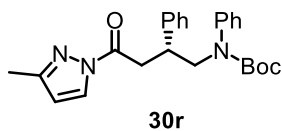
According to the general procedure, a mixture of **28c** (78.3 mg, 0.225 mmol, 1.5 equiv.), **29c** (31.8 mg, 0.15 mmol), Λ -**RhS** (10.3 mg, 0.012 mmol, 8 mol%), and HE (76.0 mg, 0.3 mmol, 2.0 equiv.) in acetone (0.75 mL, 0.2 M) was stirred under nitrogen atmosphere for 16 hours under irradiation with 23 W CFL at room temperature to afford **30q** as a pale yellow oil (30.6 mg, 55% yield, 93% ee). Purification conditions: *n*-hexane/EtOAc = 20:1 to 10:1, $R_f = 0.5$ in *n*-hexane/EtOAc (6:1). Enantiomeric excess was established by HPLC analysis using a Chiralpak IG column, ee = 93% (HPLC: 254 nm, *n*-hexane/isopropanol = 90:10, flow rate 1.0 mL/min, 40 °C, t_r (major) = 12.6 min, t_r (minor) = 8.9 min). $[\alpha]_D^{22} = +75.0^\circ$ (*c* 1.0, CH₂Cl₂).

¹H NMR (300 MHz, CD₂Cl₂) δ 8.03 (d, $J = 2.8$ Hz, 1H), 7.34–7.24 (m, 5H), 6.26 (d, $J = 2.7$ Hz, 1H), 4.80 (br, 1H), 4.01 (dd, $J = 10.6, 4.0$ Hz, 1H), 3.72 (dd, $J = 10.6, 16.3$ Hz, 1H), 3.56 (dd, $J = 16.4, 4.1$ Hz, 1H), 2.37 (s, 3H), 1.48 (s, 9H), 1.40 (s, 3H), 1.25 (s, 3H).

¹³C NMR (75 MHz, CD₂Cl₂) δ 170.6, 153.8, 140.5, 129.7, 128.9, 127.9, 126.9, 110.2, 55.4, 48.8, 35.0, 28.3, 13.8.

IR (film): ν (cm⁻¹) 2972, 2928, 1719, 1550, 1499, 1453, 1408, 1386, 1354, 1245, 1164, 1068, 935, 772, 707, 566, 511, 460.

HRMS (ESI, *m/z*) calcd for C₂₁H₃₀N₃O₃ [M+H]⁺: 372.2282, found: 372.2293.



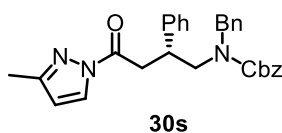
According to the general procedure, a mixture of **28d** (90.0 mg, 0.225 mmol, 1.5 equiv.), **29c** (31.8 mg, 0.15 mmol), Λ -**RhS** (10.3 mg, 0.012 mmol, 8 mol%), and HE (76.0 mg, 0.3 mmol, 2.0 equiv.) in acetone (0.75 mL, 0.2 M) was stirred under nitrogen atmosphere for 16 hours under irradiation with 23 W CFL at room temperature to afford **30r** as a pale yellow solid (45.4 mg, 72% yield, 95% ee). Purification conditions: *n*-hexane/EtOAc = 20:1 to 10:1, R_f = 0.6 in *n*-hexane/EtOAc (5:1). Enantiomeric excess was established by HPLC analysis using a Chiralpak IG column, ee = 95% (HPLC: 254 nm, *n*-hexane/isopropanol = 90:10, flow rate 1.0 mL/min, 25 °C, t_r (major) = 8.9 min, t_r (minor) = 10.7 min). $[\alpha]_D^{22} = +29.2^\circ$ (*c* 1.0, CH₂Cl₂).

¹H NMR (300 MHz, CD₂Cl₂) δ 8.00 (d, *J* = 2.8 Hz, 1H), 7.32–7.15 (m, 8H), 7.07–7.04 (m, 2H), 6.20 (d, *J* = 2.8 Hz, 1H), 4.07 (dd, *J* = 14.0, 7.6 Hz, 1H), 3.85 (dd, *J* = 13.9, 7.3 Hz, 1H), 3.64–3.52 (m, 1H), 3.46 (dd, *J* = 7.9, 6.7 Hz, 2H), 2.28 (s, 3H), 1.37 (s, 9H).

¹³C NMR (125 MHz, CD₂Cl₂) δ 170.0, 154.5, 153.8, 142.4, 141.5, 128.7, 128.6, 128.4, 128.2, 127.4, 126.9, 126.0, 110.2, 80.2, 54.8, 40.5, 37.7, 27.9, 13.7.

IR (film): ν (cm⁻¹) 2975, 2928, 1724, 1694, 1596, 1552, 1495, 1454, 1386, 1365, 1345, 1328, 1298, 1281, 1251, 1226, 1207, 1163, 1103, 1070, 1047, 1008, 935, 860, 758, 697, 646, 561, 549, 533.

HRMS (ESI, *m/z*) calcd for C₂₅H₂₉N₃O₃Na [M+Na]⁺: 442.2109, found: 442.2109.



According to the general procedure, a mixture of **28e** (66.7 mg, 0.15 mmol, 1.5 equiv.), **29c** (21.2 mg, 0.10 mmol), Λ -**RhS** (7.0 mg, 0.008 mmol, 8 mol%), and HE (50.4 mg, 0.2 mmol, 2.0 equiv.) in acetone (0.5 mL, 0.2 M) was stirred under nitrogen atmosphere for 16 hours under irradiation with 23 W CFL at room temperature to afford **30s** as a colorless oil (37.6 mg, 80% yield, 96% ee). Purification conditions: *n*-hexane/EtOAc = 20:1 to 6:1, R_f = 0.5 in *n*-hexane/EtOAc (5:1). Enantiomeric excess was established by HPLC analysis using a Chiralpak AS-H column, ee = 96% (HPLC: 254 nm, *n*-hexane/isopropanol = 90:10, flow rate 1.0 mL/min, 25 °C, t_r (major) = 9.5 min, t_r (minor) = 12.2 min). $[\alpha]_D^{22} = +51.4^\circ$ (*c* 1.0, CH₂Cl₂).

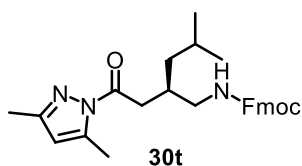
¹H NMR (300 MHz, CDCl₃) δ 8.06 (d, *J* = 2.8 Hz, 1H), 7.45–7.30 (m, 6H), 7.29–7.06 (m, 9H), 6.22 (d, *J* = 2.4 Hz, 1H), 5.26–5.00 (m, 2H), 4.57 (d, *J* = 15.6 Hz, 1H), 4.14–4.06 (m, 1H), 3.90–3.34 (m,

5H), 2.33 (s, 3H).

^{13}C NMR (125 MHz, CDCl_3 , two rotamers) δ 170.1, 169.9, 156.7, 156.5, 153.9, 153.8, 141.5, 141.4, 137.5, 136.7, 134.4, 129.0, 128.7, 128.6 (2C), 128.5, 128.2, 128.1, 128.0, 127.9, 127.8, 127.5, 127.4, 127.1, 110.5, 110.4, 67.5, 67.3, 52.1, 51.4, 50.4, 50.3, 40.2, 39.8, 37.5, 37.4, 14.1.

IR (film): ν (cm^{-1}) 2923, 1693, 1487, 1443, 1366, 1207, 1169, 1087, 974, 811, 742, 708, 661, 632, 575, 537, 492, 407.

HRMS (ESI, m/z) calcd for $\text{C}_{29}\text{H}_{29}\text{N}_3\text{O}_3\text{Na}$ [$\text{M} + \text{Na}$] $^+$: 490.2101, found: 490.2116.



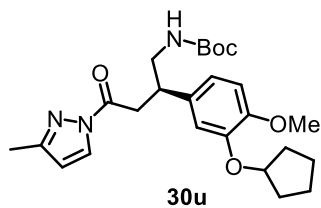
According to the general procedure, a mixture of **28f** (66.3 mg, 0.15 mmol, 1.5 equiv.), **29f** (20.6 mg, 0.10 mmol), Δ -**RhS** (7.0 mg, 0.008 mmol, 8 mol%), and HE (50.4 mg, 0.2 mmol, 2.0 equiv.) in acetone (0.5 mL, 0.2 M) was stirred under nitrogen atmosphere for 24 hours under irradiation with 23 W CFL at room temperature to afford **30t** as a colorless oil (40.0 mg, 87% yield, 91% ee). Purification conditions: *n*-hexane/ Et_2O = 10:1 to 3:1, R_f = 0.6 in *n*-hexane/ Et_2O (30:1). Enantiomeric excess was established by HPLC analysis using a Chiralpak IA column, ee = 91% (HPLC: 254 nm, *n*-hexane/isopropanol = 90:10, flow rate 1.0 mL/min, 25 °C, t_r (major) = 21.8 min, t_r (minor) = 23.5 min). $[\alpha]_D^{22} = -14.0^\circ$ (c 1.0, CH_2Cl_2).

^1H NMR (300 MHz, CDCl_3) δ 7.80 (d, J = 7.4 Hz, 2H), 7.80 (d, J = 7.5 Hz, 2H), 7.43 (t, J = 7.4 Hz, 2H), 7.43 (td, J = 7.4, 1.1 Hz, 2H), 6.00 (s, 1H), 5.60 (br, 1H), 4.38 (m, 2H), 4.23 (t, J = 6.8 Hz, 1H), 3.30–3.10 (m, 3H), 2.97 (dd, J = 15.4, 5.3 Hz, 1H), 2.54 (s, 3H), 2.38–2.16 (m, 4H), 1.77 (m, 1H), 1.28 (t, J = 7.2 Hz, 2H), 0.95 (d, J = 4.3 Hz, 3H), 0.93 (d, J = 4.3 Hz, 3H).

^{13}C NMR (125 MHz, CDCl_3) δ 173.4, 156.5, 152.1, 144.3, 144.2, 141.4, 127.7, 127.1, 125.1, 120.0, 111.1, 66.4, 47.5, 44.5, 41.8, 38.1, 34.1, 25.3, 22.6, 22.5, 14.4, 13.6.

IR (film): ν (cm^{-1}) 3343, 2953, 2924, 1716, 1582, 1524, 1448, 1378, 1330, 1239, 1137, 996, 961, 806, 738, 646, 585, 539, 421.

HRMS (ESI, m/z) calcd for $\text{C}_{28}\text{H}_{33}\text{N}_3\text{O}_3\text{Na}$ [$\text{M} + \text{Na}$] $^+$: 482.2414, found: 482.2426.



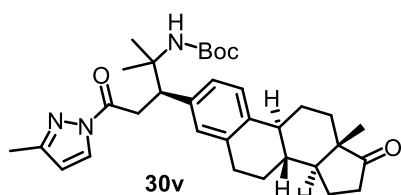
According to the general procedure, a mixture of **28b** (48.0 mg, 0.15 mmol, 1.5 equiv.), **29p** (32.6 mg, 0.10 mmol), Λ -**RhS** (7.0 mg, 0.008 mmol, 8 mol%), and HE (50.4 mg, 0.2 mmol, 2.0 equiv.) in acetone (1.0 mL, 0.1 M) was stirred under nitrogen atmosphere for 16 hours under irradiation with 23 W CFL at room temperature to afford **30u** as a colorless solid (38.9 mg, 85% yield, 95% ee). Purification conditions: *n*-hexane/EtOAc = 20:1 to 6:1, R_f = 0.3 in *n*-hexane/EtOAc (5:1). Enantiomeric excess was established by HPLC analysis using a Chiralpak IG column, ee = 95% (HPLC: 254 nm, *n*-hexane/isopropanol = 90:10, flow rate 1.0 mL/min, 25 °C, t_r (major) = 27.0 min, t_r (minor) = 25.5 min). $[\alpha]_D^{22} = +32.0^\circ$ (*c* 1.0, CH₂Cl₂).

¹H NMR (300 MHz, CDCl₃) δ 8.09 (d, *J* = 2.7 Hz, 1H), 6.85–6.75 (m, 3H), 6.26 (d, *J* = 2.8 Hz, 1H), 4.80–4.60 (m, 2H), 3.81 (s, 3H), 3.56–3.30 (m, 5H), 2.32 (s, 3H), 1.95–1.72 (m, 6H), 1.68–1.60 (m, 2H), 1.41 (s, 9H).

¹³C NMR (125 MHz, CDCl₃) δ 170.2, 155.6, 153.8, 149.0, 147.6, 133.8, 128.7, 119.6, 114.5, 112.1, 110.3, 80.1, 78.9, 55.9, 45.8, 41.4, 37.5, 32.72, 32.69, 28.04, 24.0, 13.6.

IR (film): ν (cm⁻¹) 3385, 2955, 2927, 2867, 1722, 1688, 1553, 1511, 1413, 1362, 1334, 1253, 1215, 1164, 1138, 1049, 1021, 992, 936, 902, 863, 804, 771, 735, 638, 604, 535, 443.

HRMS (ESI, *m/z*) calcd for C₂₅H₃₅N₃O₅Na [M+Na]⁺: 480.2469, found: 480.2481.



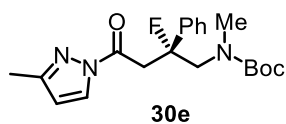
According to the general procedure, a mixture of **28c** (52.0 mg, 0.15 mmol, 1.5 equiv.), **29q** (38.8 mg, 0.10 mmol), Λ -**RhS** (7.0 mg, 0.008 mmol, 8 mol%), and HE (50.4 mg, 0.2 mmol, 2.0 equiv.) in acetone (1.0 mL, 0.1 M) was stirred under nitrogen atmosphere for 16 hours under irradiation with 23 W CFL at room temperature to afford **30v** as a colorless oil (46.4 mg, 85% yield, 92% de). Purification conditions: *n*-hexane/EtOAc = 10:1 to 2:1, R_f = 0.3 in *n*-hexane/EtOAc (3:1). Enantiomeric excess was established by HPLC analysis using a Chiralpak AD-H column, de = 92% (HPLC: 254 nm, *n*-hexane/isopropanol = 80:20, flow rate 1.0 mL/min, 40 °C, t_r (major) = 6.5 min, t_r (minor) = 9.8 min). $[\alpha]_D^{22} = +94.2^\circ$ (*c* 1.0, CH₂Cl₂).

^1H NMR (300 MHz, CD_2Cl_2) δ 7.92 (d, $J = 2.7$ Hz, 1H), 7.19–7.08 (m, 2H), 6.94–6.87 (m, 2H), 6.13 (d, $J = 2.7$ Hz, 1H), 4.73 (br, 1H), 3.76 (dd, $J = 10.6, 3.8$ Hz, 1H), 3.55 (dd, $J = 10.6, 16.3$ Hz, 1H), 3.39 (dd, $J = 16.3, 3.7$ Hz, 1H), 2.86–2.74 (m, 2H), 2.40–2.14 (m, 6H), 2.08–1.78 (m, 5H), 1.58–1.46 (m, 3H), 1.40–1.30 (m, 11H), 1.27 (s, 3H), 1.11 (s, 3H), 0.88 (s, 3H).

^{13}C NMR (125 MHz, CD_2Cl_2) δ 220.4, 170.3, 155.3, 153.7, 139.1, 138.6, 136.7, 128.7, 128.4, 125.4, 125.1, 110.2, 79.2, 54.8, 50.5, 47.9, 44.4, 39.6, 38.2, 37.2, 35.8, 34.4, 31.7, 29.5, 28.0, 26.5, 25.8, 21.5, 13.7.

IR (film): ν (cm^{-1}) 2926, 2864, 1727, 1501, 1457, 1407, 1361, 1340, 1290, 1250, 1212, 1162, 1072, 1008, 934, 775, 730, 585, 455.

HRMS (ESI, m/z) calcd for $\text{C}_{33}\text{H}_{45}\text{N}_3\text{O}_4\text{Na}$ $[\text{M}+\text{Na}]^+$: 570.3302, found: 570.3320.



According to the general procedure, a mixture of **28a** (50.1 mg, 0.30 mmol, 1.5 equiv.), **29e** (23.0 mg, 0.20 mmol), Δ -**RhS** (13.8 mg, 0.016 mmol, 8 mol%), and HE (101.0 mg, 0.4 mmol, 2.0 equiv.) in acetone (2.0 mL, 0.2 M) was stirred under nitrogen atmosphere for 16 hours under irradiation with 23 W CFL at room temperature to afford **30e** as a pale yellow oil (52.0 mg, 70% yield, 93% ee). Purification conditions: *n*-hexane/EtOAc = 20:1 to 10:1, $R_f = 0.6$ in *n*-hexane/EtOAc (5:1). Enantiomeric excess was established by HPLC analysis using a Chiralpak IC column, ee = 93% (HPLC: 254 nm, *n*-hexane/isopropanol = 97:3, flow rate 1.0 mL/min, 25 °C, t_r (major) = 20.6 min, t_r (minor) = 17.7 min). $[\alpha]_D^{22} = -10.6^\circ$ (c 1.0, CH_2Cl_2).

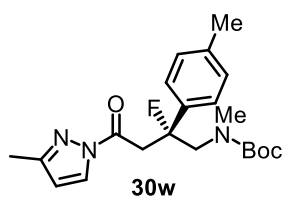
^1H NMR (300 MHz, CD_2Cl_2) δ 8.02 (d, $J = 2.7$ Hz, 1H), 7.49–7.29 (m, 5H), 6.24 (m, 1H), 4.30–3.50 (m, 4H), 2.93 (d, $J = 1.5$ Hz, 3H), 2.31 (s, 3H), 1.49 (s, 9H), 1.44 (s, 9H, other rotamer).

^{13}C NMR (125 MHz, CD_2Cl_2 , two rotamers) δ 166.8, 155.2, 153.8 (d, $J = 15.3$ Hz, 1C), 140.2 (d, $J = 20.8$ Hz, 1C), 128.5, 128.3, 128.1, 127.8 (2C), 124.6 (d, $J = 9.4$ Hz, 1C), 110.5, 99.5 (d, $J = 184.1$ Hz, 1C), 80.1, 58.4 (d, $J = 22.6$ Hz, 1C), 40.0 (d, $J = 21.6$ Hz, 1C), 36.0, 27.9, 13.6.

IR (film): ν (cm^{-1}) 2972, 2927, 1735, 1694, 1552, 1450, 1396, 1362, 1325, 1213, 1152, 1104, 1045, 939, 879, 769, 699, 609, 568.

^{19}F NMR (282 MHz) δ -157.1, -158.2 (other rotamer).

HRMS (ESI, m/z) calcd for $\text{C}_{20}\text{H}_{26}\text{FN}_3\text{O}_3\text{Na}$ $[\text{M}+\text{Na}]^+$: 398.1858, found: 398.1858.



According to the general procedure, a mixture of **28a** (78.3 mg, 0.225 mmol, 1.5 equiv.), **29r** (36.6 mg, 0.15 mmol), Δ -**RhS** (10.3 mg, 0.012 mmol, 8 mol%), and HE (76.0 mg, 0.3 mmol, 2.0 equiv.) in acetone (1.5 mL, 0.1 M) was stirred under nitrogen atmosphere for 16 hours under irradiation with 23 W CFL at room temperature to afford **30w** as a pale yellow solid (41.5 mg, 74% yield, 94% ee). Purification conditions: *n*-hexane/EtOAc = 20:1 to 10:1, R_f = 0.6 in *n*-hexane/EtOAc (5:1). Enantiomeric excess was established by HPLC analysis using a Chiralpak IG column, ee = 94% (HPLC: 254 nm, *n*-hexane/isopropanol = 90:10, flow rate 1.0 mL/min, 25 °C, t_r (major) = 14.3 min, t_r (minor) = 10.5 min). $[\alpha]_D^{22} = -21.8^\circ$ (c 1.0, CH_2Cl_2).

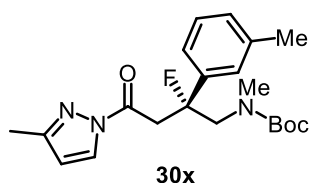
^1H NMR (300 MHz, CD_2Cl_2) δ 8.02 (d, J = 2.7 Hz, 1H), 7.40–7.26 (m, 2H), 7.20–7.17 (m, 2H), 6.25 (m, 1H), 4.30–3.70 (m, 3H), 3.53 (dd, J = 18.4, 15.8 Hz, 1H), 2.93 (s, 3H), 2.35 (s, 3H), 2.31 (s, 3H), 1.49 (s, 9H), 1.44 (s, 9H, other rotamer).

^{13}C NMR (125 MHz, CD_2Cl_2 , two rotamers) δ 166.9, 156.2, 155.2 (other rotamer), 153.7 (d, J = 16.4 Hz, 1C), 137.7, 137.2 (d, J = 21.4 Hz, 1C), 128.9, 128.7, 128.5, 124.6 (d, J = 9.6 Hz, 1C), 124.4 (other rotamer, d, J = 9.3 Hz, 1C), 110.5, 110.4 (other rotamer), 99.1 (d, J = 181.6 Hz, 1C), 98.5 (other rotamer, d, J = 183.2 Hz, 1C), 80.0, 79.6 (other rotamer), 58.4 (d, J = 22.4 Hz, 1C), 57.1 (other rotamer, d, J = 22.4 Hz, 1C), 39.9 (d, J = 22.3 Hz, 1C), 36.2, 36.0 (other rotamer), 28.0, 27.9 (other rotamer), 20.8, 13.6.

^{19}F NMR (282 MHz) δ -156.7, -157.8 (other rotamer).

IR (film): ν (cm^{-1}) 2973, 2927, 1740, 1693, 1553, 1480, 1452, 1409, 1388, 1364, 1327, 1311, 1247, 1212, 1150, 1084, 1043, 1001, 939, 903, 881, 814, 769, 725, 682, 669, 612, 569.

HRMS (ESI, m/z) calcd for $\text{C}_{21}\text{H}_{28}\text{FN}_3\text{O}_3\text{Na}$ $[\text{M} + \text{Na}]^+$: 412.2017, found: 412.2017.



According to the general procedure, a mixture of **28a** (78.3 mg, 0.225 mmol, 1.5 equiv.), **29s** (36.6 mg, 0.15 mmol), Δ -**RhS** (10.3 mg, 0.012 mmol, 8 mol%), and HE (76.0 mg, 0.3 mmol, 2.0 equiv.) in acetone (1.5 mL, 0.1 M) was stirred under nitrogen atmosphere for 16 hours under irradiation with 23 W CFL at room temperature to afford **30x** as a pale yellow solid (43.4 mg, 74%

yield, 94% ee). Purification conditions: *n*-hexane/EtOAc = 20:1 to 10:1, R_f = 0.6 in *n*-hexane/EtOAc (5:1). Enantiomeric excess was established by HPLC analysis using a Chiralpak IA column, ee = 94% (HPLC: 254 nm, *n*-hexane/isopropanol = 98:2, flow rate 1.0 mL/min, 25 °C, t_r (major) = 17.6 min, t_r (minor) = 13.0 min). $[\alpha]_D^{22} = -16.6^\circ$ (*c* 1.0, CH₂Cl₂).

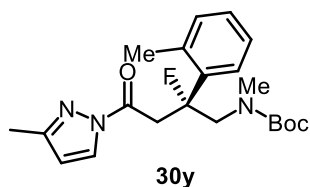
¹H NMR (300 MHz, CD₂Cl₂) δ 7.91 (d, J = 2.7 Hz, 1H), 7.20–7.00 (m, 4H), 6.13 (m, 1H), 4.20–3.59 (m, 3H), 3.41 (dd, J = 19.1, 15.3 Hz, 1H), 2.82 (d, J = 1.5 Hz, 3H), 2.25 (s, 3H), 2.20 (s, 3H), 1.38 (s, 9H), 1.36 (s, 9H, other rotamer).

¹³C NMR (125 MHz, CD₂Cl₂) δ 166.9, 156.3, 155.2 (other rotamer), 153.7 (d, J = 16.4 Hz, 1C), 140.2 (d, J = 20.8 Hz, 1C), 138.1, 137.9 (other rotamer), 128.5, 128.2, 128.0, 125.4 (d, J = 9.3 Hz, 1C), 125.2 (other rotamer, d, J = 9.1 Hz, 1C), 121.7 (d, J = 9.8 Hz, 1C), 121.5 (other rotamer, d, J = 9.5 Hz, 1C), 110.5, 110.4 (other rotamer), 99.1 (d, J = 181.6 Hz, 1C), 98.5 (other rotamer, d, J = 183.3 Hz, 1C), 80.0, 79.7 (other rotamer), 58.4 (d, J = 22.2 Hz, 1C), 57.2 (other rotamer, d, J = 22.4 Hz, 1C), 39.9 (d, J = 22.1 Hz, 1C), 36.1, 36.0 (other rotamer), 29.7, 28.1, 27.9 (other rotamer), 13.6.

¹⁹F NMR (282 MHz) δ -157.1, -158.0 (other rotamer).

IR (film): ν (cm⁻¹) 2965, 2926, 2855, 1738, 1694, 1553, 1481, 1452, 1409, 1389, 1364, 1328, 1310, 1247, 1212, 1150, 1076, 1043, 940, 907, 876, 829, 770, 704, 684.

HRMS (ESI, *m/z*) calcd for C₂₁H₂₈FN₃O₃Na [M+Na]⁺: 412.2016, found: 412.2016.



According to the general procedure, a mixture of **28a** (78.3 mg, 0.225 mmol, 1.5 equiv.), **29t** (36.6 mg, 0.15 mmol), Δ -**RhS** (10.3 mg, 0.012 mmol, 8 mol%), and HE (76.0 mg, 0.3 mmol, 2.0 equiv.) in acetone (1.5 mL, 0.1 M) was stirred under nitrogen atmosphere for 16 hours under irradiation with 23 W CFL at room temperature to afford **30y** as a pale yellow solid (39.6 mg, 68% yield, 96% ee). Purification conditions: *n*-hexane/EtOAc = 20:1 to 10:1, R_f = 0.7 in *n*-hexane/EtOAc (5:1). Enantiomeric excess was established by HPLC analysis using a Chiralpak IA column, ee = 96% (HPLC: 254 nm, *n*-hexane/isopropanol = 98:2, flow rate 0.7 mL/min, 25 °C, t_r (major) = 21.4 min, t_r (minor) = 14.9 min). $[\alpha]_D^{22} = -71.4^\circ$ (*c* 1.0, CH₂Cl₂).

¹H NMR (500 MHz, CD₂Cl₂) δ 8.02 (d, J = 2.7 Hz, 1H), 7.39 (dd, J = 16.3, 6.5 Hz, 1H), 7.25–7.15 (m, 3H), 6.25 (m, 1H), 4.52–4.09 (m, 2H), 3.39 (dt, J = 53.9, 16.7 Hz, 1H), 3.50–3.38 (m, 1H), 2.98 (d, J

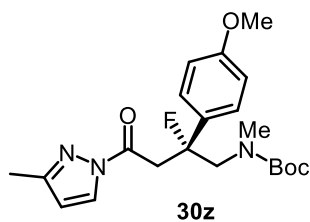
= 1.4 Hz, 3H), 2.54 (s, 3H), 2.50 (s, 3H, other rotamer), 2.31 (s, 3H), 2.30 (s, 3H, other rotamer), 1.55 (s, 9H), 1.48 (s, 9H, other rotamer).

^{13}C NMR (125 MHz, CD_2Cl_2) δ 167.0, 156.5, 155.4 (other rotamer), 153.7 (d, $J = 15.6$ Hz, 1C), 138.0 (d, $J = 18.8$ Hz, 1C), 134.6, 134.2 (other rotamer), 132.4, 132.3 (other rotamer), 128.5, 127.9, 127.8, 125.9, 125.8, 125.6, 110.4, 100.4 (d, $J = 181.6$ Hz, 1C), 99.9 (other rotamer, d, $J = 182.5$ Hz, 1C), 80.4, 79.8 (other rotamer), 56.9 (d, $J = 21.7$ Hz, 1C), 56.2 (other rotamer, d, $J = 21.3$ Hz, 1C), 39.6 (d, $J = 22.9$ Hz, 1C), 39.6 (other rotamer, d, $J = 23.1$ Hz, 1C), 36.43, 36.41 (other rotamer), 28.1, 21.8 (d, $J = 6.0$ Hz, 1C), 13.6.

^{19}F NMR (282 MHz) δ -149.9, -151.2 (other rotamer).

IR (film): ν (cm^{-1}) 2966, 2928, 2856, 1738, 1694, 1481, 1452, 1409, 1389, 1364, 1328, 1310, 1247, 1212, 1150, 1077, 1043, 940, 906, 876, 829, 771, 704, 684.

HRMS (ESI, m/z) calcd for $\text{C}_{21}\text{H}_{28}\text{FN}_3\text{O}_3\text{Na}$ $[\text{M}+\text{Na}]^+$: 412.2007, found: 412.2017.



According to the general procedure, a mixture of **28a** (78.3 mg, 0.225 mmol, 1.5 equiv.), **29u** (39.0 mg, 0.15 mmol), Δ -**RhS** (10.3 mg, 0.012 mmol, 8 mol%), and HE (76.0 mg, 0.3 mmol, 2.0 equiv.) in acetone (1.5 mL, 0.1 M) was stirred under nitrogen atmosphere for 16 hours under irradiation with 23 W CFL at room temperature to afford **30z** as a pale yellow solid (48.5 mg, 80% yield, 94% ee). Enantiomeric excess was established by HPLC analysis using a Chiralpak IB column, ee = 94% (HPLC: 254 nm, *n*-hexane/isopropanol = 90:10, flow rate 0.7 mL/min, 25 °C, t_r (major) = 8.1 min, t_r (minor) = 7.5 min). $[\alpha]_D^{22} = -20.4^\circ$ (c 1.0, CH_2Cl_2).

^1H NMR (300 MHz, CD_2Cl_2) δ 8.03 (d, $J = 2.7$ Hz, 1H), 7.33 (m, 2H), 6.90 (d, $J = 8.5$ Hz, 2H), 6.25 (d, $J = 1.8$ Hz, 1H), 4.25–3.86 (m, 2H), 3.80–3.50 (m, 5H), 2.93 (d, $J = 1.5$ Hz, 3H), 2.31 (s, 3H), 1.49 (s, 9H), 1.44 (s, 9H, other rotamer).

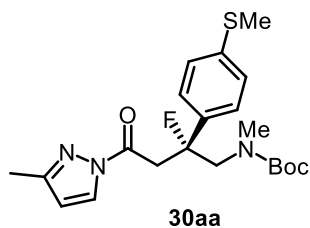
^{19}F NMR (282 MHz) δ -155.1, -156.4 (other rotamer).

^{13}C NMR (125 MHz, CD_2Cl_2 , two rotamers) δ 166.9, 159.3, 156.2, 155.2 (other rotamer), 153.7 (d, $J = 16.4$ Hz, 1C), 132.1 (d, $J = 22.2$ Hz, 1C), 128.5, 126.1 (d, $J = 9.3$ Hz, 1C), 125.8 (other rotamer, d, $J = 9.2$ Hz, 1C), 113.6, 113.4 (other rotamer), 110.5, 110.4 (other rotamer), 99.0 (d, $J = 180.1$ Hz, 1C), 98.4 (other rotamer, d, $J = 182.8$ Hz, 1C), 80.0, 79.6 (other rotamer), 58.3 (d, $J = 22.4$ Hz, 1C), 56.9

(other rotamer, d, $J = 21.6$ Hz, 1C), 55.2, 40.0 (d, $J = 21.7$ Hz, 1C), 36.1, 36.0 (other rotamer), 28.0, 27.9 (other rotamer), 20.8, 13.6.

IR (film): ν (cm^{-1}) 2968, 2928, 1736, 1693, 1613, 1553, 1514, 1453, 1392, 1360, 1323, 1248, 1213, 1151, 1080, 1038, 938, 879, 830, 773, 735, 569.

HRMS (ESI, m/z) calcd for $\text{C}_{21}\text{H}_{28}\text{FN}_3\text{O}_4\text{Na}$ $[\text{M}+\text{Na}]^+$: 428.1956, found: 428.1761.



According to the general procedure, a mixture of **28a** (78.3 mg, 0.225 mmol, 1.5 equiv.), **29v** (41.4 mg, 0.15 mmol), Δ -**RhS** (10.3 mg, 0.012 mmol, 8 mol%), and HE (76.0 mg, 0.3 mmol, 2.0 equiv.) in acetone (1.5 mL, 0.1 M) was stirred under nitrogen atmosphere for 16 hours under irradiation with 23 W CFL at room temperature to afford **30aa** as a pale yellow oil (36.1 mg, 57% yield, 95% ee). Enantiomeric excess was established by HPLC analysis using a Chiralpak IA column, ee = 95% (HPLC: 254 nm, *n*-hexane/isopropanol = 90:10, flow rate 0.5 mL/min, 25 °C, t_r (major) = 21.6 min, t_r (minor) = 16.8 min). $[\alpha]_D^{22} = -20.2^\circ$ (c 1.0, CH_2Cl_2).

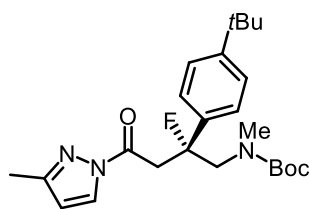
^1H NMR (300 MHz, CD_2Cl_2) δ 8.02 (d, $J = 2.8$ Hz, 1H), 7.40–7.20 (m, 4H), 6.25 (m, 1H), 4.35–3.50 (m, 4H), 2.93 (d, $J = 1.5$ Hz, 3H), 2.49 (s, 3H), 2.31 (s, 3H), 1.48 (s, 9H), 1.44 (s, 9H, other rotamer).

^{19}F NMR (282 MHz) δ -156.5, -157.6 (other rotamer).

^{13}C NMR (125 MHz, CD_2Cl_2 , two rotamers) δ 166.8, 156.2, 155.2 (other rotamer), 153.7 (d, $J = 16.0$ Hz, 1C), 138.5, 138.4 (other rotamer), 136.8 (d, $J = 22.1$ Hz, 1C), 125.9, 125.8 (other rotamer), 125.3 (d, $J = 9.5$ Hz, 1C), 125.1 (other rotamer, d, $J = 9.2$ Hz, 1C), 110.6, 110.5 (other rotamer), 99.0 (d, $J = 183.6$ Hz, 1C), 98.3 (other rotamer, d, $J = 182.7$ Hz, 1C), 80.1, 79.7 (other rotamer), 58.2 (d, $J = 22.5$ Hz, 1C), 56.9 (other rotamer, d, $J = 21.3$ Hz, 1C), 40.0 (d, $J = 22.5$ Hz, 1C), 39.9 (other rotamer, d, $J = 21.8$ Hz, 1C), 36.13, 36.07 (other rotamer), 29.7, 28.02, 27.95 (other rotamer), 15.3, 13.6.

IR (film): ν (cm^{-1}) 2962, 2924, 2857, 1730, 1692, 1553, 1483, 1449, 1390, 1363, 1326, 1211, 1149, 1088, 1044, 973, 937, 878, 816, 770, 736, 668, 634, 574, 539.

HRMS (ESI, m/z) calcd for $\text{C}_{21}\text{H}_{28}\text{FN}_3\text{O}_3\text{SNa}$ $[\text{M}+\text{Na}]^+$: 444.1728, found: 444.1737.

**30ab**

According to the general procedure, a mixture of **28a** (78.3 mg, 0.225 mmol, 1.5 equiv.), **29w** (42.9 mg, 0.15 mmol), Δ -**RhS** (10.3 mg, 0.012 mmol, 8 mol%), and HE (76.0 mg, 0.3 mmol, 2.0 equiv.) in acetone (1.5 mL, 0.1 M) was stirred under nitrogen atmosphere for 16 hours under irradiation with 23 W CFL at room temperature to afford **30ab** as a pale yellow oil (51.7 mg, 80% yield, 92% ee). Enantiomeric excess was established by HPLC analysis using a Chiralpak IG column, ee = 92% (HPLC: 254 nm, *n*-hexane/isopropanol = 90:10, flow rate 1.0 mL/min, 25 °C, t_r (major) = 10.5 min, t_r (minor) = 8.8 min). $[\alpha]_D^{22} = -18.0^\circ$ (*c* 1.0, CH₂Cl₂).

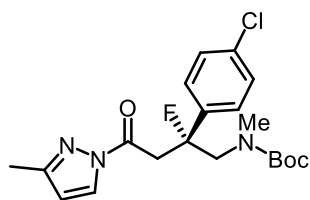
¹H NMR (300 MHz, CD₂Cl₂) δ 8.04 (d, *J* = 2.8 Hz, 1H), 7.42–7.30 (m, 4H), 6.25 (m, 1H), 4.30–3.50 (m, 4H), 2.94 (d, *J* = 1.6 Hz, 3H), 2.31 (s, 3H), 1.46 (m, 9H), 1.33 (s, 9H).

¹³C NMR (125 MHz, CD₂Cl₂, two rotamers) δ 166.9, 156.2, 155.2 (other rotamer), 153.7 (d, *J* = 19.0 Hz, 1C), 150.8, 137.2 (d, *J* = 22.1 Hz, 1C), 128.5, 125.2, 125.0 (other rotamer), 124.4 (d, *J* = 9.2 Hz, 1C), 124.3 (other rotamer, d, *J* = 9.0 Hz, 1C), 110.5, 110.4 (other rotamer), 99.1 (d, *J* = 182.3 Hz, 1C), 98.5 (other rotamer, d, *J* = 182.3 Hz, 1C), 80.0, 79.6 (other rotamer), 58.2 (d, *J* = 22.4 Hz, 1C), 56.9 (other rotamer, d, *J* = 21.0 Hz, 1C), 40.1 (d, *J* = 23.5 Hz, 1C), 40.0 (other rotamer, d, *J* = 21.3 Hz, 1C), 36.15, 36.05 (other rotamer), 34.4, 31.1, 28.0, 27.9 (other rotamer), 13.6.

¹⁹F NMR (282 MHz) δ -156.6, -157.7 (other rotamer).

IR (film): ν (cm⁻¹) 2961, 2927, 2864, 1736, 1696, 1553, 1454, 1393, 1360, 1325, 1267, 1153, 1080, 1045, 938, 880, 832, 770, 612, 582.

HRMS (ESI, *m/z*) calcd for C₂₄H₃₄FN₃O₃Na [M+ Na]⁺: 454.2476, found: 454.2487.

**30ac**

According to the general procedure, a mixture of **28a** (78.3 mg, 0.225 mmol, 1.5 equiv.), **29x** (39.6mg, 0.15 mmol), Δ -**RhS** (10.3 mg, 0.012 mmol, 8 mol%), and HE (76.0 mg, 0.3 mmol, 2.0 equiv.) in acetone (1.5 mL, 0.1 M) was stirred under nitrogen atmosphere for 16 hours under irradiation with 23 W CFL at room temperature to afford **30ac** as a pale yellow oil (32.6 mg, 53% yield, 93% ee). Enantiomeric excess was established by HPLC analysis using a Chiralpak OD-H

column, ee = 93% (HPLC: 254 nm, *n*-hexane/isopropanol = 95:5, flow rate 1.0 mL/min, 25 °C, t_r (major) = 10.3 min, t_r (minor) = 8.8 min). $[\alpha]_D^{22} = -25.4^\circ$ (c 1.0, CH_2Cl_2).

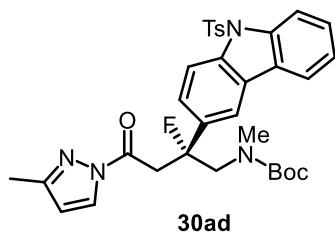
^1H NMR (300 MHz, CD_2Cl_2) δ 8.02 (d, $J = 2.6$ Hz, 1H), 7.36 (m, 4H), 6.26 (d, $J = 1.5$ Hz, 1H), 4.23–3.52 (m, 4H), 2.93 (d, $J = 1.2$ Hz, 3H), 2.31 (s, 3H), 1.49 (s, 9H), 1.43 (s, 9H, other rotamer).

^{19}F NMR (282 MHz) δ -155.8, -156.9 (other rotamer).

^{13}C NMR (125 MHz, CD_2Cl_2 , two rotamers) δ 166.6, 156.2, 155.1 (other rotamer), 153.9 (d, $J = 14.7$ Hz, 1C), 138.9 (d, $J = 24.0$ Hz, 1C), 133.7 (d, $J = 13.2$ Hz, 1C), 128.6, 128.4, 128.2 (other rotamer), 126.5 (d, $J = 9.5$ Hz, 1C), 126.2 (other rotamer, d, $J = 9.0$ Hz, 1C), 110.5, 98.9 (d, $J = 185.5$ Hz, 1C), 98.2 (other rotamer, d, $J = 185.0$ Hz, 1C), 80.2, 79.8 (other rotamer), 58.1 (d, $J = 21.7$ Hz, 1C), 56.7 (other rotamer, d, $J = 21.4$ Hz, 1C), 40.2 (d, $J = 21.8$ Hz, 1C), 40.0 (other rotamer, d, $J = 21.4$ Hz, 1C), 36.1, 28.0, 13.6.

IR (film): ν (cm^{-1}) 2974, 2929, 1733, 1693, 1554, 1491, 1453, 1410, 1388, 1365, 1327, 1310, 1246, 1214, 1151, 1091, 1045, 1013, 1000, 938, 904, 882, 826, 770, 723, 608, 565, 548.

HRMS (ESI, m/z) calcd for $\text{C}_{20}\text{H}_{25}\text{ClFN}_3\text{O}_3\text{Na}$ $[\text{M}+\text{Na}]^+$: 432.1461, found: 432.1469.



According to the general procedure, a mixture of **28a** (96.0 mg, 0.30 mmol, 1.5 equiv.), **29y** (94.6 mg, 0.20 mmol), Δ -**RhS** (13.8 mg, 0.016 mmol, 8 mol%), and HE (101.0 mg, 0.40 mmol, 2.0 equiv.) in acetone (2.0 mL, 0.1 M) was stirred under nitrogen atmosphere for 16 hours under irradiation with 23 W CFL at room temperature to afford **30ad** as pale yellow solid (76.0 mg, 62% yield, 93% ee). Enantiomeric excess was established by HPLC analysis using a Chiralpak IG column, ee = 93% (HPLC: 254 nm, *n*-hexane/isopropanol = 70:30, flow rate 1 mL/min, 25 °C, t_r (major) = 23.2 min, t_r (minor) = 29.1 min). $[\alpha]_D^{22} = -22.0^\circ$ (c 1.0, CH_2Cl_2).

^1H NMR (300 MHz, CD_2Cl_2) δ 8.18 (dd, $J = 11.5, 8.4$ Hz, 2H), 8.00–7.80 (m, 3H), 7.62 (d, $J = 8.2$ Hz, 2H), 7.50–7.35 (m, 2H), 7.29 (t, $J = 7.4$ Hz, 1H), 7.06 (d, $J = 8.2$ Hz, 2H), 6.08 (m, 1H), 4.30–3.90 (m, 2H), 3.78–3.40 (m, 2H), 2.83 (d, $J = 1.3$ Hz, 3H), 2.20 (m, 6H), 1.34 (s, 9H), 1.26 (s, 9H, other rotamer).

^{19}F NMR (282 MHz) δ -154.5, -155.4 (other rotamer).

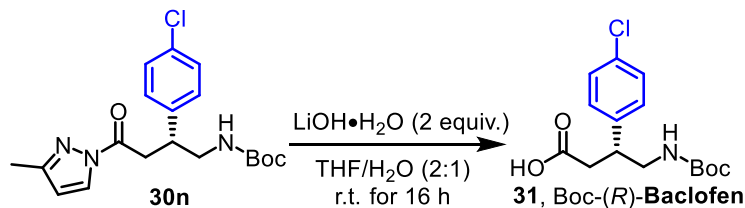
^{13}C NMR (125 MHz, two rotamers) δ 166.8, 156.2, 155.2 (other rotamer), 153.8 (d, $J = 16.0$ Hz, 1C),

145.5, 138.6, 137.7, 136.0 (d, $J = 22.3$ Hz, 1C), 134.8, 129.8, 128.5, 127.7, 127.6 (other rotamer), 126.5, 126.1, 126.0 (other rotamer), 124.0 (2C), 120.2, 116.8 (d, $J = 24.4$ Hz, 1C), 116.7 (other rotamer, d, $J = 25.3$ Hz, 1C), 114.9, 114.6, 114.4 (other rotamer), 110.6, 110.5 (other rotamer), 99.3 (d, $J = 182.1$ Hz, 1C), 98.7 (other rotamer, d, $J = 183.3$ Hz, 1C), 80.1, 79.7 (other rotamer), 58.5 (d, $J = 21.3$ Hz, 1C), 57.2 (other rotamer, d, $J = 20.5$ Hz, 1C), 40.4 (d, $J = 19.1$ Hz, 1C), 40.2 (other rotamer, d, $J = 20.9$ Hz, 1C), 36.2, 36.1 (other rotamer), 27.9, 21.3, 13.6.

IR (film): ν (cm^{-1}) 2923, 2169, 2054, 1691, 1597, 1553, 1481, 1444, 1414, 1367, 1208, 1170, 1143, 1089, 1036, 974, 905, 876, 814, 747, 702, 665, 576, 539, 463, 421.

HRMS (ESI, m/z) calcd for $\text{C}_{33}\text{H}_{35}\text{FN}_4\text{O}_5\text{SNa}$ $[\text{M}+\text{Na}]^+$: 641.2222, found: 641.2222.

5.5.3 Synthetic Applications

1) Synthesis of Boc-(*R*)-Baclofen (**4**) and Boc-(*S*)-Pregabalin (**5**)

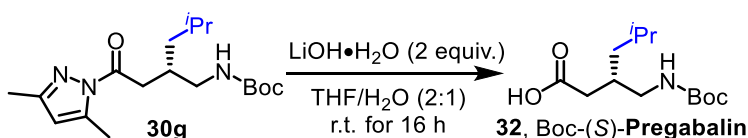
To **30n** (50.0 mg, 0.132 mmol, 1.0 equiv.) in THF/H₂O (2:1, 1 mL) was added LiOH·H₂O (11.1 mg, 2 equiv.) in one portion. The reaction mixture was stirred for 16 h at room temperature. Afterwards, the reaction was quenched by the addition of two drops of acetic acid. The volatiles were removed by evaporation and the resulted material was purified by flash chromatography column. Purification conditions: *n*-hexane/EtOAc = 10:1 to 3:1 containing 1% acetic acid, *R_f* = 0.3 in EtOAc. Boc-(*R*)-baclofen (**31**) was obtained as a white solid (37.5 mg, 0.120 mmol, 90% yield, 90% ee). Enantiomeric excess was established by HPLC analysis using a Chiralpak AD-H column, ee = 90% (HPLC: 254 nm, *n*-hexane/isopropanol = 80:20, flow rate 1 mL/min, 40 °C, *t_r* (major) = 6.8 min, *t_r* (minor) = 5.6 min). $[\alpha]_{\text{D}}^{22} = -14.0^\circ$ (*c* 0.1, CH₂Cl₂).

¹H NMR (300 MHz, CDCl₃) δ 7.22 (d, *J* = 8.4 Hz, 2H), 7.06 (d, *J* = 7.9 Hz, 2H), 5.95 (br, 1H), 4.45 (br, 1H, other rotamer), 3.38–3.21 (m, 3H), 2.64 (dd, *J* = 16.3, 5.7 Hz, 1H), 2.53 (dd, *J* = 15.9, 7.1 Hz, 1H), 1.33 (s, 9H).

¹³C NMR (125 MHz, CDCl₃, two rotamers) δ 176.5, 157.3, 156.1, 140.1, 139.6, 132.9, 129.0, 128.9, 128.8, 81.1, 79.8, 47.5, 45.4, 41.5, 38.1, 37.9, 29.7, 28.3.

IR (film): ν (cm⁻¹) 3372, 2976, 2926, 2610, 1684, 1523, 1406, 1358, 1325, 1275, 1246, 1216, 1164, 1089, 1061, 1008, 928, 879, 822, 780, 737, 690, 635, 585, 457.

HRMS (ESI, *m/z*) calcd for C₁₅H₂₀ClNO₄Na [M+ Na]⁺: 336.0982, found: 336.0982.



To **30g** (58.6 mg, 0.174 mmol, 1.0 equiv.) in THF/H₂O (2:1, 1 mL) was added LiOH·H₂O (15.0 mg, 2 equiv.) in one portion. The reaction mixture was stirred for 16 h at room temperature. Afterwards, the reaction was quenched by the addition of two drops of acetic acid. The volatiles were removed by evaporation and the resulted material was purified by flash chromatography column. Purification

conditions: *n*-hexane/EtOAc = 10:1 to 3:1 containing 1% acetic acid, $R_f = 0.3$ in EtOAc. Boc-(*S*)-pregabalin (**32**) was obtained as a white solid (41.9 mg, 0.161 mmol, 93% yield). $[\alpha]_D^{22} = -23.0^\circ$ (*c* 1.0, CH_2Cl_2).

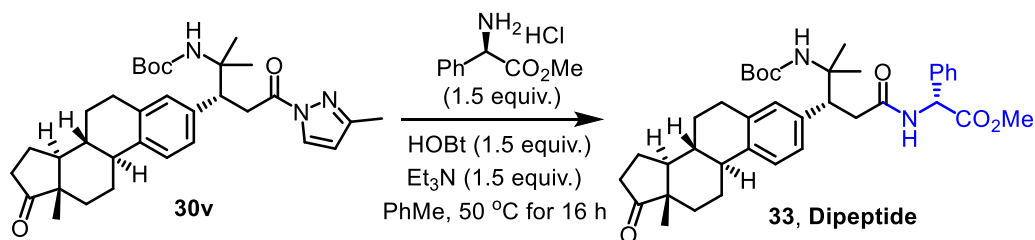
^1H NMR (300 MHz, CDCl_3) δ 10.13 (br, 1H), 6.13 (br, 1H), 4.80 (br, 1H, other rotamer), 3.28–3.18 (m, 1H), 3.11–2.80 (m, 1H), 2.36–2.02 (m, 3H), 1.65 (m, 1H), 1.44 (s, 9H), 1.17 (m, 2H), 0.90 (m, 6H).

^{13}C NMR (125 MHz, CDCl_3 , two rotamers) δ 177.9, 157.8, 156.6, 80.7, 79.6, 46.0, 43.8, 41.8, 41.3, 38.0, 37.1, 33.7, 33.6, 28.4, 25.1, 22.7, 22.6.

IR (film): ν (cm^{-1}) 3309, 3247, 3094, 2986, 2958, 2929, 2868, 2207, 2185, 1650, 1469, 1416, 1366, 1321, 1309, 1278, 1263, 1228, 1113, 1081, 1063, 1007, 965, 728, 664, 576, 442, 411, 396, 379.

HRMS (ESI, m/z) calcd for $\text{C}_{13}\text{H}_{25}\text{NO}_4\text{Na}$ $[\text{M} + \text{Na}]^+$: 282.1683, found: 282.1683.

2) Synthesis of a Dipeptide (**33**)



To a mixture of **30v** (45 mg, 0.0823 mmol, 1.0 equiv.), D-phenylglycine methyl ester hydrochloride (27.0 mg, 1.5 equiv.), 1-hydroxybenzotriazole (17.1 mg, 1.5 equiv.) in PhMe (1 mL) was added Et_3N (18 μL , 1.5 equiv.). The reaction mixture was stirred for 16 h at 50 °C. Afterwards, the volatiles were removed by evaporation and the resulted material was purified by flash chromatography column. Purification conditions: *n*-hexane/EtOAc = 8:1 to 1:1, $R_f = 0.2$ in *n*-hexane/EtOAc (1:1). Compound **33** was obtained as a white solid (42.7 mg, 0.0677 mmol, 83% yield, > 20:1 dr). $[\alpha]_D^{22} = +185.8^\circ$ (*c* 0.1, CH_2Cl_2).

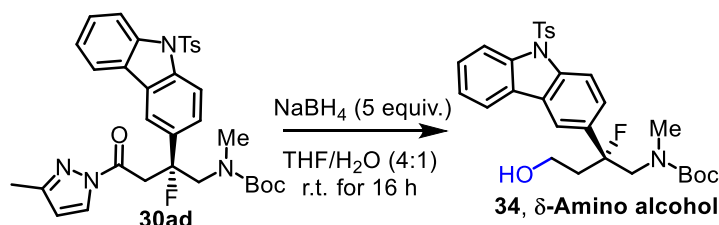
^1H NMR (300 MHz, CD_2Cl_2) δ 7.32–7.20 (m, 4H), 7.15–6.90 (m, 4H), 6.38 (br, 1H), 5.83 (br, 1H, other rotamer), 4.78 (br, 1H), 3.68 (s, 3H), 3.63–3.20 (m, 3H), 3.10–2.82 (m, 4H), 2.74 (m, 3H), 2.58–2.24 (m, 5H), 2.18–2.00 (m, 3H), 1.95–1.88 (m, 1H), 1.66–1.30 (m, 17H), 0.87 (s, 3H).

^{13}C NMR (125 MHz, CD_2Cl_2 , two rotamers) δ 220.4, 171.8, 170.8, 170.3, 156.2, 155.2, 139.1, 138.7, 138.5, 136.7, 136.3, 136.0, 129.3, 128.5, 128.4, 126.9, 125.4, 125.2, 79.2, 79.0, 52.1, 50.5, 47.8, 44.3, 40.7, 40.6, 40.4, 40.2, 38.2, 37.8, 35.8, 34.6, 31.6, 29.4, 28.1, 26.6, 25.7, 21.5, 13.6.

IR (film): ν (cm⁻¹) 3309, 2923, 2855, 1737, 1687, 1662, 1532, 1497, 1453, 1392, 1364, 1257, 1214, 1165, 1139, 1082, 1051, 1030, 1007, 876, 821, 765, 733, 700, 580, 491, 446.

HRMS (ESI, m/z) calcd for C₃₈H₅₀N₂O₆Na [M+ Na]⁺: 653.3561, found: 653.3571.

3) Synthesis of a δ -Amino Alcohol (**34**)



To **30ad** (45 mg, 0.0727 mmol, 1.0 equiv.) in THF/H₂O (4:1, 1 mL) was added NaBH₄ (14.0 mg, 5 equiv.) in one portion. The reaction mixture was stirred for 16 h at room temperature. Afterwards, the volatiles were removed by evaporation and the resulted material was purified by flash chromatography column. Purification conditions: *n*-hexane/EtOAc = 5:1 to 1:1, R_f = 0.3 in *n*-hexane/EtOAc (1:1). Compound **34** was obtained as a white solid (36.1 mg, 0.0669 mmol, 92% yield, 93 % ee). Enantiomeric excess was established by HPLC analysis using a Chiralpak IA column, ee = 93% (HPLC: 254 nm, *n*-hexane/isopropanol = 80:20, flow rate 1 mL/min, 25 °C, t_r (major) = 10.5 min, t_r (minor) = 9.1 min). $[\alpha]_D^{22} = +9.6^\circ$ (c 1.0, CH₂Cl₂).

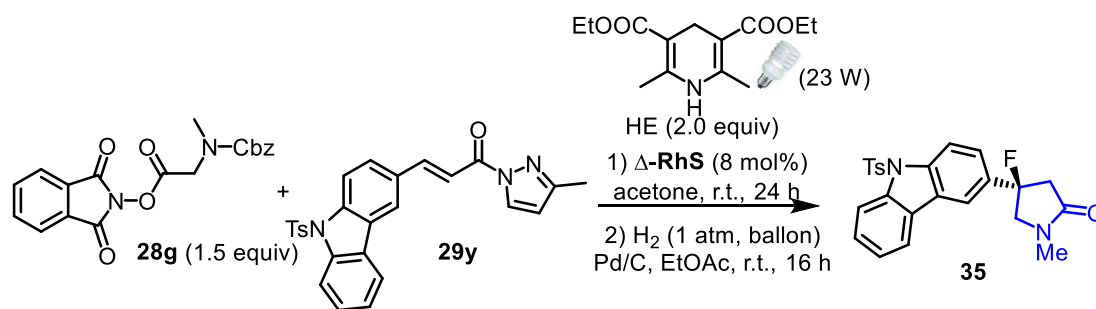
¹H NMR (500 MHz, CD₂Cl₂) δ 8.35 (d, J = 8.4 Hz, 2H), 8.02–7.95 (m, 2H), 7.76 (d, J = 8.2 Hz, 2H), 7.58–7.41 (m, 3H), 7.19 (d, J = 8.2 Hz, 2H), 4.14–3.86 (m, 1H), 3.75–3.42 (m, 3H), 2.91 (s, 3H), 2.48–2.30 (m, 5H), 2.16 (s, 1H), 1.37 (s, 9H), 1.34 (s, 9H, other rotamer).

¹⁹F NMR (282 MHz) δ -154.8, -159.2 (other rotamer).

¹³C NMR (125 MHz, two rotamers) δ 156.5, 155.2 (other rotamer), 153.8 (d, J = 16.0 Hz, 1C), 145.5, 138.6, 137.7, 136.3 (d, J = 21.9 Hz, 1C), 134.8, 129.8, 127.8, 127.7 (other rotamer), 126.5, 126.3, 126.2 (other rotamer), 124.2, 124.0, 120.2, 116.6 (m, 1C), 115.0, 114.9, 114.7 (other rotamer), 101.6 (d, J = 176.6 Hz, 1C), 101.2 (other rotamer, d, J = 178.8 Hz, 1C), 79.7, 79.6 (other rotamer), 58.0 (m, 2C, containing one rotamer), 57.0 (d, J = 21.2 Hz, 1C), 39.8 (d, J = 21.2 Hz, 1C), 39.5 (other rotamer, d, J = 22.2 Hz, 1C), 36.3, 35.9 (other rotamer), 27.9, 21.3.

IR (film): ν (cm⁻¹) 2923, 2169, 2054, 1691, 1597, 1553, 1481, 1444, 1414, 1367, 1208, 1170, 1143, 1089, 1036, 974, 905, 876, 814, 747, 702, 665, 576, 539, 463, 421.

HRMS (ESI, m/z) calcd for C₂₉H₃₃FN₂O₅SNa [M+Na]⁺: 563.1986, found: 563.1997.

4) Synthesis of a γ -Lactam (**35**)

According to the general procedure, a mixture of **28g** (110.5 mg, 0.30 mmol, 1.5 equiv.), **29y** (94.6 mg, 0.20 mmol), Δ -**RhS** (13.8 mg, 0.016 mmol, 8 mol%), and HE (101.0 mg, 0.40 mmol, 2.0 equiv.) in acetone (2.0 mL, 0.1 M) was stirred under nitrogen atmosphere for 24 hours under irradiation with 23 W CFL at room temperature. The C–C formation product was obtained by flash chromatography on silica gel. The obtained compound was dissolved in EtOAc (2 mL) and treated with Pd/C (10% Pd, 50 mg), then stirred under an atmosphere of H₂ (1 atm, with a balloon) at room temperature for 14 h. Afterwards, the insoluble solid was filtered off and washed by DCM (10 mL). The combined organic solution was concentrated in vacuo. The resulting residue was purified by column chromatography to afford **35** as a white solid (52.0 mg, 0.119 mmol, 60% yield for two steps). Purification conditions: *n*-hexane/EtOAc = 3:1 to 1:2, R_f = 0.2 in *n*-hexane/EtOAc (1:3). Enantiomeric excess was established by HPLC analysis using a Chiralpak OD-H column, ee = 94% (HPLC: 254 nm, *n*-hexane/isopropanol = 50:50, flow rate 1 mL/min, 40 °C, t_r (major) = 12.8 min, t_r (minor) = 18.1 min). $[\alpha]_D^{22} = +3.8^\circ$ (*c* 1.0, CH₂Cl₂).

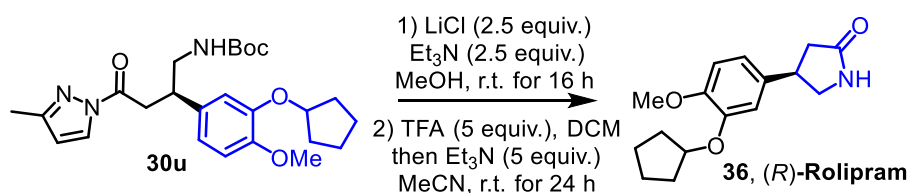
¹H NMR (500 MHz, CD₂Cl₂) δ 8.39 (d, *J* = 8.7 Hz, 1H), 8.35 (d, *J* = 8.4 Hz, 1H), 8.04 (m, 1H), 8.01–7.99 (m, 1H), 7.75–7.74 (m, 2H), 7.60–7.55 (m, 2H), 7.45–7.42 (m, 1H), 7.18 (d, *J* = 8.0 Hz, 2H), 3.95–3.90 (m, 2H), 3.15–2.96 (m, 5H), 2.3 (s, 3H).

¹³C NMR (125 MHz) δ 170.5, 145.6, 138.9, 138.3, 135.0 (d, *J* = 23.1 Hz, 1C), 134.8, 129.9, 128.1, 126.6, 126.5, 125.9, 124.2, 123.9 (d, *J* = 7.3 Hz, 1C), 120.3, 116.5 (d, *J* = 8.9 Hz, 1C), 115.2 (d, *J* = 19.8 Hz, 1C), 96.9 (d, *J* = 179.4 Hz, 1C), 61.9 (d, *J* = 28.3 Hz, 1C), 45.0 (d, *J* = 27.1 Hz, 1C), 29.2, 21.3.

¹⁹F NMR (282 MHz) δ –138.9.

IR (film): ν (cm⁻¹) 2923, 1693, 1487, 1443, 1366, 1207, 1169, 1087, 974, 811, 742, 708, 661, 632, 575, 537, 492, 407.

HRMS (ESI, *m/z*) calcd for C₂₄H₂₁FN₂O₃SNa [M+ Na]⁺: 459.1149, found: 459.1162.

5) Synthesis of (*R*)-Rolipram (**36**)

To a solution of **30u** (92.0 mg, 0.201 mmol, 1.0 equiv.) in MeOH (3 mL) was added LiCl (21.2 mg, 2.5 equiv.) in one portion, followed by Et₃N (70 μL, 2.5 equiv.). The reaction mixture was stirred for 16 h at room temperature. Afterwards, the volatiles were removed by evaporation and the resulted material was purified by flash chromatography column to afford the corresponding ester. To the ester in CH₂Cl₂ (2 mL) was added TFA (75 μL, 5 equiv.), then stirred at room temperature for 2 h. Upon the starting material consumed, the volatiles were removed by evaporation thoroughly. The mixture was redissolved in MeCN and treated with Et₃N (140 μL, 5 equiv.), then stirred at room temperature for 24 h. After concentration, the resulted material was purified by flash chromatography column to afford **36** as a white solid (51.0 mg, 0.185 mmol, 92% yield, 95 % ee). Enantiomeric excess was established by HPLC analysis using a Chiralpak IG column, ee = 95% (HPLC: 254 nm, *n*-hexane/isopropanol = 90:10, flow rate 1 mL/min, 25 °C, *t_r* (major) = 23.8 min, *t_r* (minor) = 27.6 min). [α]_D²² = -25.2° (*c* 1.0, MeOH). [Compound **9** with >99% ee shown optical rotation as [α]_D²⁵ = -33.9° (*c* 1.09, MeOH) in a previous report, see: *J. Am. Chem. Soc.* **2002**, *124*, 13394–13395].

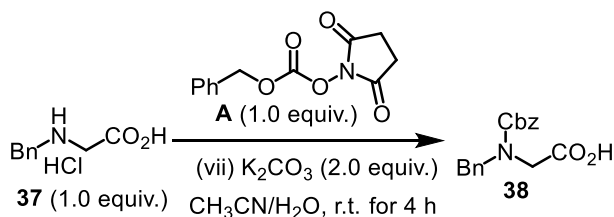
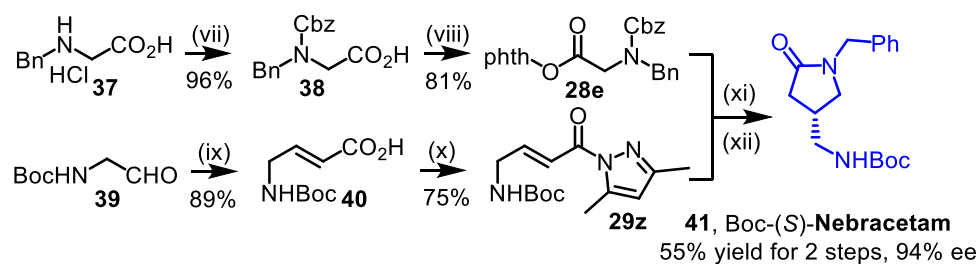
¹H NMR (300 MHz, CDCl₃) δ 6.84–6.76 (m, 3H), 6.05 (br, 1H), 4.76 (m, 1H), 3.79 (s, 3H), 3.75–3.55 (m, 2H), 3.34 (dd, *J* = 8.8, 7.2 Hz, 1H), 2.63 (dd, *J* = 16.9, 8.8 Hz, 1H), 2.40 (dd, *J* = 16.8, 9.0 Hz, 1H), 1.94–1.73 (m, 6H), 1.62 (m, 2H).

¹³C NMR (125 MHz, CDCl₃) δ 177.5, 149.6, 148.3, 135.3, 119.2, 114.3, 112.8, 80.8, 56.4, 49.9, 40.4, 38.3, 33.2, 24.4.

IR (film): *ν* (cm⁻¹) 3191, 3088, 2955, 2868, 1685, 1583, 1510, 1452, 1413, 1348, 1235, 1162, 1136, 1027, 998, 967, 852, 809, 773, 682, 609, 576, 521.

HRMS (ESI, *m/z*) calcd for C₁₆H₂₁NO₃Na [M+Na]⁺: 298.1414, found: 298.1421.

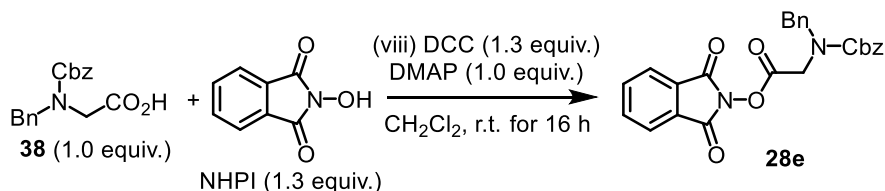
6) Synthesis of Boc-(S)-Nebracetam (14)



Synthesis of compound 38: to a solution of compound A (2.02 g, 10.0 mmol, 1.0 equiv.) in CH_3CN (20 ml) was added *N*-benzylglycine hydrochloride (compound 37, 2.49 g, 10.0 mmol, 1.0 equiv.), followed by K_2CO_3 (2.76 g, 20.0 mmol, 2.0 equiv.) in H_2O (15 ml). The reaction mixture was stirred vigorously for 4 hours. Afterwards, the mixture was poured into H_2O (100 mL) ml and the aqueous layer was washed with Et_2O (2 x 20 ml). Then, the aqueous layer was acidified to about $\text{pH} = 1$ by careful addition of concentrated HCl and the product was extracted with EtOAc (3 x 40 ml). The organic layers were combined and dried over Na_2SO_4 , filtered and concentrated under reduced pressure to afford a colorless oil as compound 38 (2.87 g, 96% yield).

$^1\text{H NMR}$ (300 MHz, CDCl_3) δ 7.35–7.22 (m, 10H), 5.10 (s, 2H), 4.49 (m, 2H), 3.90 (s, 2H).

All other analytical data were consistent with the report.⁶



Synthesis of compound 28e: to a solution of 38 (1.50 g, 5.0 mmol, 1.0 equiv.) and NHPI (1.06 g, 6.5 mmol, 1.3 equiv.) in CH_2Cl_2 (20 mL) was added DCC (1.34 g, 6.5 mmol, 1.3 equiv.), followed by DMAP (0.61 g, 5.0 mmol, 1.0 equiv.). Then the reaction mixture was stirred for 16 h at room temperature. Afterwards, the insoluble solid was filtered off and washed by DCM (20 mL). The

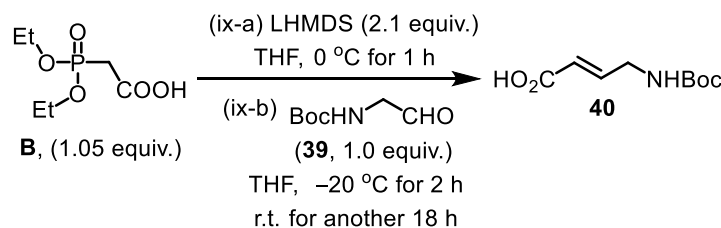
combined organic solution was concentrated in vacuo. The resulting residue was purified by column chromatography to afford **28e** as a colorless oil (1.80 g, 4.06 mmol, 81% yield). Purification conditions: DCM/EtOAc = 50:1 to 20:1, R_f = 0.6 in DCM/EtOAc (20:1).

^1H NMR (300 MHz, CDCl_3 , two rotamers) δ 7.91–7.89 (m, 2H), 7.82–7.79 (m, 2H), 7.50–7.25 (m, 10H), 5.31 (s, 2H), 5.30 (s, 2H, other rotamer), 4.72 (s, 2H), 4.70 (s, 2H, other rotamer), 4.44 (s, 2H), 4.32 (s, 2H, other rotamer).

^{13}C NMR (75 MHz, CDCl_3 , two rotamers) δ 166.2, 161.4, 156.2, 155.9, 136.1, 136.0, 134.8, 128.8, 128.7, 128.5, 128.3, 128.1, 128.0, 127.9, 123.9, 68.1, 51.4, 50.9 (other rotamer), 45.5, 45.3 (other rotamer).

IR (film): ν (cm^{-1}) 3064, 3031, 2945, 1827, 1790, 1741, 1706, 1607, 1586, 1496, 1466, 1453, 1425, 1402, 1365, 1314, 1233, 1186, 1124, 1079, 1029, 1014, 971, 911, 875, 821, 770, 734, 694, 634, 597, 567, 542, 517, 471, 403.

HRMS (ESI, m/z) calcd for $\text{C}_{25}\text{H}_{20}\text{N}_2\text{O}_6\text{Na}$ [$\text{M} + \text{Na}$] $^+$: 467.1214, found: 467.1228.

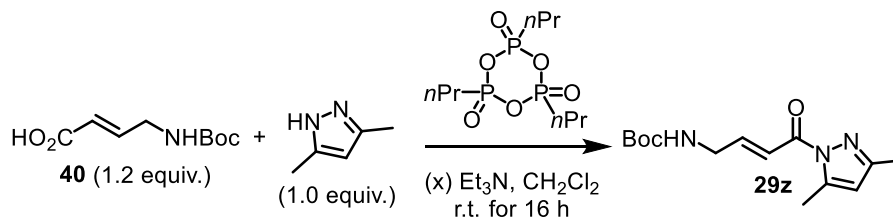


Synthesis of compound 40: to a solution of **B** (1.29 g, 6.59 mmol, 1.05 equiv.) in THF (20 mL) cooled to $0\text{ }^\circ\text{C}$ was added a solution of LHMDS (13.2 mL, 13.2 mmol, 1.0 M in THF, 2.10 equiv.) dropwise and the mixture was stirred for 1 h at this temperature. Compound **39** (1.00 g, 6.28 mmol, 1.0 equiv) in THF (10 mL) was subsequently added at $-20\text{ }^\circ\text{C}$ and the reaction was left to stir for 2 h at $-20\text{ }^\circ\text{C}$, after which time the cooling was removed and the reaction was stirred at room temperature for a further 18 h. The reaction was then quenched by the addition of acetic acid (2 ml), and then poured onto cool water (40 mL). The aqueous layer was extracted with EtOAc (3 x 30 mL). The combined organic extracts were dried (Na_2SO_4) and concentrated in vacuo. The resulting residue was purified by column chromatography to afford **40** as a pale yellow solid (1.13 g, 5.62 mmol, 89% yield, E/Z = >20:1). Purification conditions: *n*-hexane/EtOAc = 5:1 to 1:1 with 0.1% AcOH, R_f = 0.1 in *n*-hexane/EtOAc (1:1).

^1H NMR (300 MHz, CDCl_3) δ 6.93 (dt, J = 15.7, 4.8 Hz, 1H), 6.35 (br, 1H), 5.93 (dt, J = 15.7, 1.7 Hz,

1H), 3.90 (m, 2H), 1.44 (s, 9H).

All other analytical data were consistent with the report.⁷



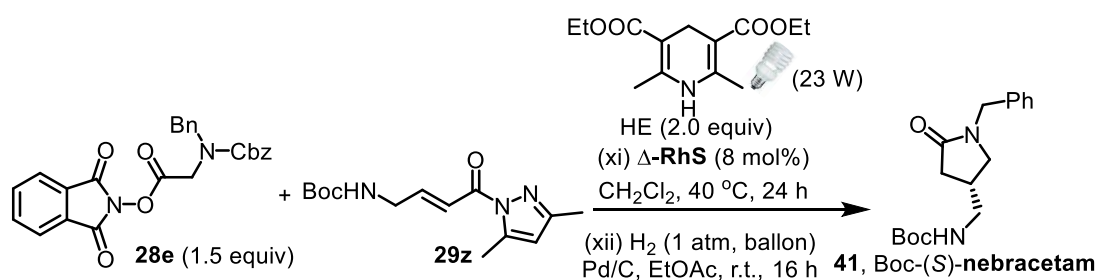
Synthesis of compound 1y: to a solution of 3,5-dimethylpyrazole (150 mg, 1.53 mmol, 1.0 equiv.) and **40** (370 mg, 1.84 mmol, 1.2 equiv.) in CH₂Cl₂ (10 mL) at room temperature was added 1-propanephosphonic acid cyclic anhydride (T₃P, 1.5 g, 1.84 mmol, 50% solution in EtOAc, 1.2 equiv.) dropwise. After stirring for 15 min at room temperature, Et₃N (430 μL, 3.07 mmol, 2.0 equiv) was added dropwise. Then the reaction mixture was stirred for 16 h at room temperature. Afterwards, the mixture was poured into saturated NH₄Cl solution (aqueous, 30 mL) and extracted with EtOAc (3 x 30 mL). The combined organic extracts were dried (Na₂SO₄) and concentrated in vacuo. The resulting residue was purified by column chromatography to afford **29z** as a pale yellow solid (320 mg, 1.15 mmol, 75% yield, single *E* isomer). Purification conditions: *n*-hexane/EtOAc = 10:1 to 4:1, R_f = 0.3 in *n*-hexane/EtOAc (4:1).

¹H NMR (300 MHz, CDCl₃) δ 7.39 (dt, *J* = 15.7, 1.7 Hz, 1H), 7.10 (dt, *J* = 15.7, 4.9 Hz, 1H), 5.96 (s, 1H), 4.81 (br, 1H), 4.02 (m, 2H), 2.55 (m, 3H), 2.23 (s, 3H), 1.46 (s, 9H).

¹³C NMR (75 MHz, CDCl₃) δ 164.7, 155.7, 152.1, 146.4, 144.5, 121.4, 111.5, 79.9, 42.0, 28.4, 14.6, 13.8.

IR (film): ν (cm⁻¹) 3355, 2981, 2922, 1706, 1682, 1648, 1523, 1436, 1407, 1340, 1274, 1243, 1163, 1096, 1039, 1004, 960, 929, 864, 840, 803, 749, 694, 644, 586, 458, 434, 404.

HRMS (ESI, *m/z*) calcd for C₁₄H₂₁N₃O₃Na [M+Na]⁺: 302.1475, found: 302.1484.



Synthesis of Boc-(R)-Nberacetam (41): a dried 50 mL Schlenk tube was charged with *N*-(acyloxy)phthalimide **28e** (200.0 mg, 0.45 mmol, 1.5 equiv.), *N*-acyl pyrazole **29z** (83.8 mg, 0.3 mmol, 1.0 equiv.), Δ -**RhS** (21.0 mg, 0.024 mmol, 8 mol%), and Hantzsch ester (151 mg, 0.6 mmol, 2.0 equiv.) in CH₂Cl₂ (6 mL, 0.1 M). The reaction mixture was degassed via freeze-pump-thaw for two cycles. After the mixture was thoroughly degassed, the Schlenk tube was sealed tightly with a Teflon septum and immersed into a preheated oil bath (40 °C). The reaction was stirred at 40 °C under the irradiation of 23 W CFL for 24 h. Afterwards, the mixture was diluted with CH₂Cl₂. The organic solutions were concentrated under reduced pressure. The crude material was purified by flash chromatography on silica gel to afford the C–C formation product. The obtained compound was dissolved in EtOAc (2 mL) and treated with Pd/C (10% Pd, 50 mg), then stirred under an atmosphere of H₂ (1 atm, with a balloon) at room temperature for 14 h. Afterwards, the insoluble solid was filtered off and washed by DCM (10 mL). The combined organic solution was concentrated in vacuo. The resulting residue was purified by column chromatography to afford **41** as a colorless solid (50.0 mg, 0.165 mmol, 55% yield for two steps). Purification conditions: *n*-hexane/EtOAc = 5:1 to 1:2, *R_f* = 0.2 in *n*-hexane/EtOAc (1:2). Enantiomeric excess was established by HPLC analysis using a Chiralpak AS-H column, ee = 94% (HPLC: 254 nm, *n*-hexane/isopropanol = 50:50, flow rate 1 mL/min, 25 °C, *t_r* (major) = 13.5 min, *t_r* (minor) = 7.8 min). [α]_D²² = -17.6° (*c* 1.0, CH₂Cl₂).

¹H NMR (300 MHz, CDCl₃) δ 7.35–7.31 (m, 2H), 7.30–7.27 (m, 1H), 7.23–7.21 (m, 2H), 4.60 (br, 1H), 4.43 (dd, *J* = 33.0, 14.6 Hz, 2H), 3.34 (dd, *J* = 9.9, 7.9 Hz, 1H), 3.13 (t, *J* = 5.9 Hz, 2H), 2.97 (dd, *J* = 10.1, 5.4 Hz, 1H), 2.60–2.50 (m, 2H), 2.20 (dd, *J* = 16.0, 5.4 Hz, 1H), 1.42 (s, 9H).

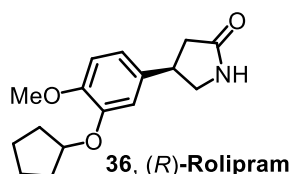
¹³C NMR (125 MHz, CDCl₃) δ 173.6, 156.0, 136.4, 128.8, 128.2, 127.8, 79.8, 50.0, 46.6, 44.0, 35.2, 31.9, 28.4.

IR (film): ν (cm⁻¹) 3372, 2958, 2925, 2862, 1716, 1681, 1519, 1448, 1367, 1255, 1166, 1072, 981, 860, 781, 746, 700, 657, 506.

HRMS (ESI, *m/z*) calcd for C₁₇H₂₄N₂O₃Na [M+Na]⁺: 327.1679, found: 327.1687.

5.5.4 Assignment of Absolute Configuration

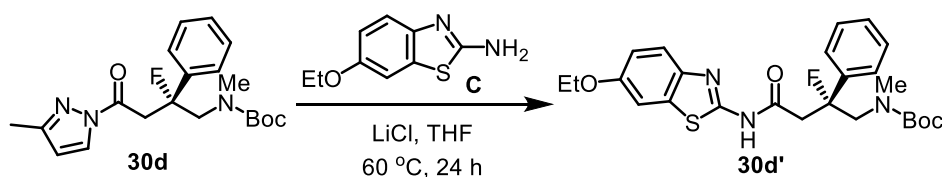
The absolute configuration of (*R*)-rolipram (**36**) was assigned by comparing the optical rotation value with a previous report.⁸ And the absolute configuration of radical conjugate addition products **30a**, **30c**, **30f-v** were assigned accordingly. The optical rotation value of compound **36** was shown as following:



$[\alpha]_{\text{D}}^{22} = -25.2^{\circ}$ (*c* 1.0, MeOH), 95% ee (this study)

$[\alpha]_{\text{D}}^{25} = -33.9^{\circ}$ (*c* 1.09, MeOH), >99% ee (*J. Am. Chem. Soc.* **2002**, *124*, 13394)

The absolute configuration of **30d** was assigned as *R* by the crystal structure of the corresponding derivative **30d'**. And the absolute configuration of radical conjugate addition products **30w-ad** were assigned accordingly. Synthesis and characterization of compound **30d'** was shown as following:



To a solution of **30d** (20 mg, 0.0533 mmol, 1.0 equiv.) and **C** (52.0 mg, 0.267 mmol, 5 equiv) in THF (1 mL) at room temperature was added LiCl (11.5 mg, 0.267 mmol, 5 equiv) in one portion. The reaction mixture was stirred for 24 h at 60 °C. Afterwards, the mixture was concentrated in vacuo. The resulting residue was purified by column chromatography to afford **30d'** as a pale brown solid (12 mg, 0.0245 mmol, 46% yield). Purification conditions: *n*-hexane/EtOAc = 5:1 to 2:1, $R_f = 0.4$ in *n*-hexane/EtOAc (2:1). The product was washed by *n*-hexane to deliver a white solid with 97% ee. Enantiomeric excess was established by HPLC analysis using a Chiralpak IA column, ee = 97% (HPLC: 254 nm, *n*-hexane/isopropanol = 80:20, flow rate 1 mL/min, 40 °C, t_r (major) = 19.2 min, t_r (minor) = 13.2 min). $[\alpha]_{\text{D}}^{22} = +11.2^{\circ}$ (*c* 1.0, CH₂Cl₂).

¹H NMR (300 MHz, CDCl₃) δ 10.5 (br, 1H), 7.55–7.52 (m, 1H), 7.35–7.20 (m, 5H), 7.15 (d, *J* = 2.4 Hz, 1H), 6.90 (dd, *J* = 8.8, 2.54 Hz, 1H), 4.20–3.92 (m, 3H), 3.50–3.42 (m, 1H), 3.24–3.00 (m, 2H), 2.80 (s, 3H), 1.42–1.30 (m, 12H).

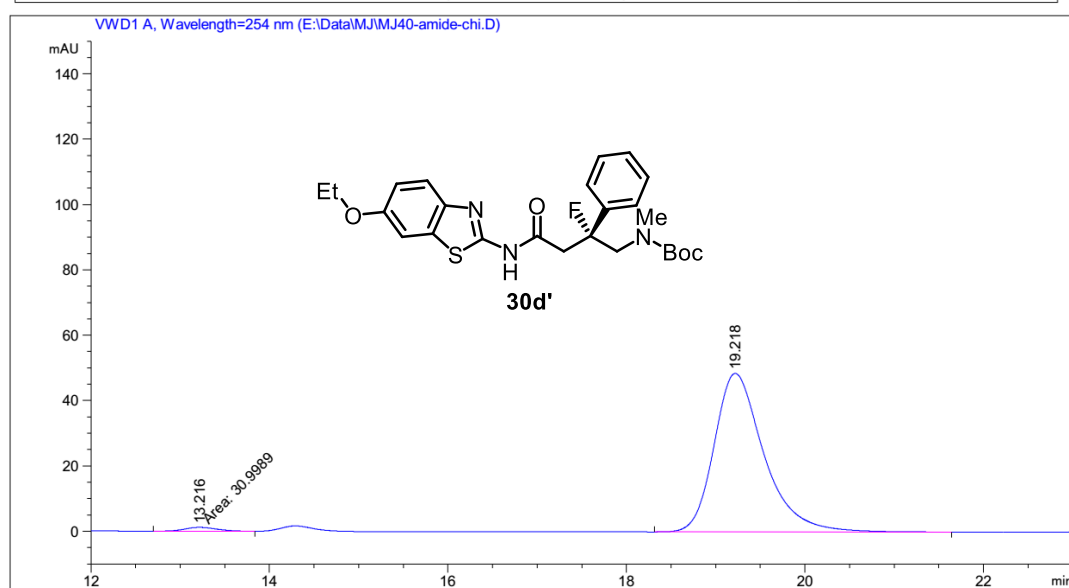
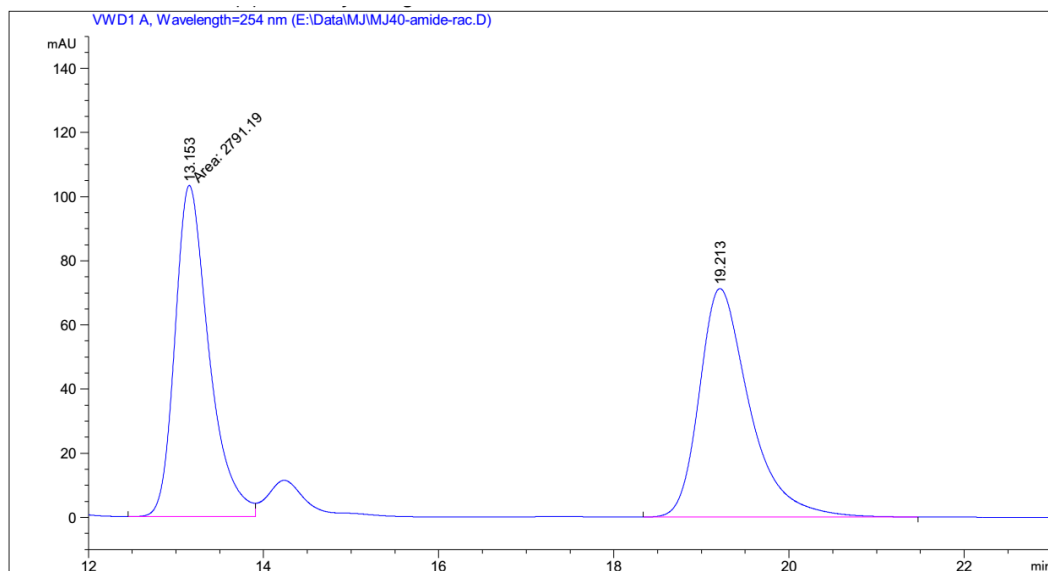
¹³C NMR (125 MHz, CDCl₃) δ 166.6, 157.4, 156.2, 155.4, 142.8, 139.2 (d, *J* = 20.5 Hz, 1C), 133.5, 128.6, 124.4, 124.3, 121.5, 104.8, 98.7 (d, *J* = 181.3 Hz, 1C), 80.9, 64.2, 56.3 (d, *J* = 22.8 Hz, 1C),

44.7 (d, $J = 24.9$ Hz, 1C), 36.9, 28.1, 14.7.

^{19}F NMR (282 MHz) δ -151.5, -155.3 (other rotamer).

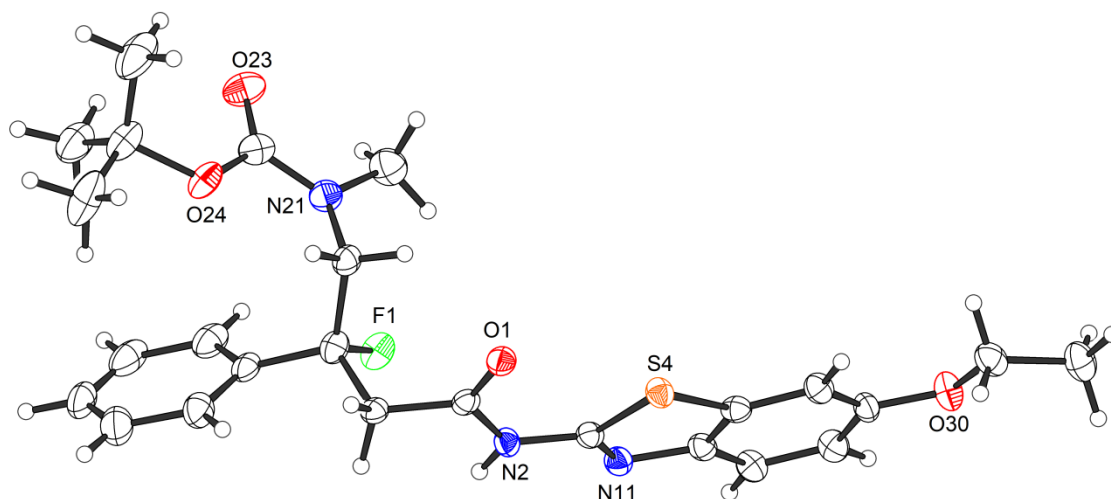
IR (film): ν (cm^{-1}) 3175, 2977, 2926, 1700, 1653, 1604, 1554, 1456, 1396, 1364, 1338, 1310, 1256, 1224, 1152, 1056, 941, 876, 822, 796, 764, 735, 701, 582, 536, 432, 393.

HRMS (ESI, m/z) calcd for $\text{C}_{25}\text{H}_{30}\text{FN}_3\text{O}_4\text{SNa}$ $[\text{M}+\text{Na}]^+$: 510.1833, found: 510.1841.



Peak #	RetTime [min]	Type	Width [min]	Area [mAU*s]	Height [mAU]	Area %
1	13.216	MM	0.4309	30.99891	1.19901	1.6197
2	19.218	BB	0.5867	1882.84448	48.51959	98.3803

HPLC traces of *rac*-**30d'** (reference) and **30d'**. (IA, 254 nm, *n*-hexane/isopropanol = 80:20, flow rate 1.0 mL/min, 40 °C).

**Table 17.** Crystal data and structure refinement for **30d'**.

Crystal data

Identification code	30d'	
Habitus, colour	plate, colourless	
Crystal size	0.230 x 0.080 x 0.030 mm ³	
Crystal system	Orthorhombic	
Space group	P2 ₁ 2 ₁ 2 ₁	Z = 4
Unit cell dimensions	a = 9.4377(2) Å	α = 90°
	b = 9.7762(2) Å	β = 90°
	c = 27.1593(7) Å	γ = 90°
Volume	2505.85(10) Å ³	
Cell determination	17168 peaks with Theta 4.8 to 75.8°	
Empirical formula	C ₂₅ H ₃₀ F N ₃ O ₄ S	
Moiety formula	C ₂₅ H ₃₀ F N ₃ O ₄ S	
Formula weight	487.58	
Density (calculated)	1.292 Mg/m ³	
Absorption coefficient	1.512 mm ⁻¹	
F(000)	1032	
Data collection:		
Diffraction type	STOE STADIVARI	

Chapter 5. Experimental Part

Wavelength	1.54178 Å
Temperature	100(2) K
Theta range for data collection	4.807 to 75.551 °
Index ranges	-11<=h<=11, -5<=k<=11, -33<=l<=34
Data collection software	X-Area Pilatus3_SV 1.31.127.0 (STOE, 2016) ⁹
Cell refinement software	X-Area Recipe 1.33.0.0 (STOE, 2015) ¹⁰
Data reduction software	X-Area Integrate 1.71.0.0 (STOE, 2016) ¹¹ X-Area LANA 1.68.2.0 (STOE, 2016) ¹²
Solution and refinement:	
Reflections collected	21841
Independent reflections	5031 [R(int) = 0.0518]
Completeness to theta = 67.679 °	99.3 %
Observed reflections	3996[I > 2σ(I)]
Reflections used for refinement	5031
Absorption correction	Semi-empirical from equivalents ¹³
Max. and min. transmission	0.8574 and 0.2002
Flack parameter (absolute struct.)	0.010(9) ¹⁴
Largest diff. peak and hole	0.220 and -0.215 e.Å ⁻³
Solution	intrinsic phases ¹⁵
Refinement	Full-matrix least-squares on F ²
Treatment of hydrogen atoms	CH calculated pos., constr., NH located, isotr. ref.
Programs used	XT V2014/1 (Bruker AXS Inc., 2014) ¹⁴ SHELXL-2018/1 (Sheldrick, 2018) ¹⁵ DIAMOND (Crystal Impact) ¹⁶ ShelXle (Hübschle, Sheldrick, Dittrich, 2011) ¹⁷
Data / restraints / parameters	5031 / 0 / 316
Goodness-of-fit on F ²	0.869
R index (all data)	wR2 = 0.0629
R index conventional [I>2sigma(I)] R1 = 0.0330	

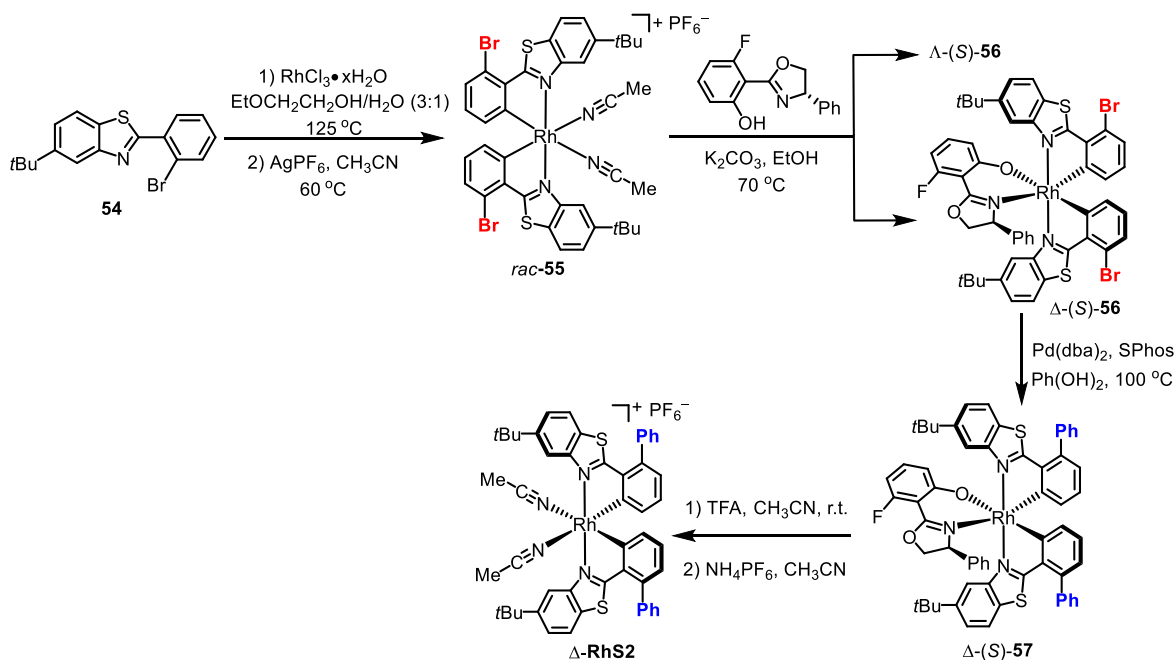
Reference

- 1 J. Ma, X. Zhang, X. Huang, S. Luo, E. Meggers, *Nat. Protoc.* **2018**, *13*, 605-632.
- 2 J. Ma, X. Shen, K. Harms, E. Meggers, *Dalton Trans.* **2016**, *45*, 8320-8323.
- 3 a) J. Schwarz, B. König, *Green Chem.* **2016**, *18*, 4743-4749; b) W. Xue, M. Oestreich, *Angew. Chem. Int. Ed.* **2017**, *56*, 11649.
- 4 H. Huo, K. Harms, E. Meggers, *J. Am. Chem. Soc.* **2016**, *138*, 6936-6939.
- 5 X. Huang, X. Li, X. Xie, K. Harms, R. Riedel, E. Meggers, *Nat. Commun.* **2017**, *8*, 2245.
- 6 C. Fetsch, J. Gaitzsch, L. Messenger, G. Battaglia, R. Luxenhofer, *Sci. Rep.* **2016**, *6*, 33491.
- 7 C. Grison, S. Genève, E. Halbin, P. Coutrot, *Tetrahedron* **2001**, *57*, 4903.
- 8 K. Itoh, S. Kanemasa, *J. Am. Chem. Soc.* **2002**, *124*, 13394.
- 9 *X-Area Pilatus3_SV*, STOE & Cie GmbH, Darmstadt, Germany, **2016**.
- 10 *X-Area Recipe*, STOE & Cie GmbH, Darmstadt, Germany, **2015**.
- 11 *X-Area Integrate*, STOE & Cie GmbH, Darmstadt, Germany, **2016**.
- 12 *X-Area LANA*, STOE & Cie GmbH, Darmstadt, Germany, **2016**.
- 13 S. Parsons, H. D. Flack, T. Wagner, *Acta Cryst. B* **2013**, *69*, 249.
- 14 G. M. Sheldrick, *Acta Cryst. A* **2015**, *71*, 3.
- 15 G. M. Sheldrick, *Acta Cryst. C* **2015**, *71*, 3.
- 16 K. Brandenburg, *Diamond - Crystal and Molecular Structure Visualization*, Crystal Impact - Dr. H. Putz & Dr. K. Brandenburg GbR, Bonn, Germany, **2014**.
- 17 C. B. Hübschle, G. M. Sheldrick, B. Dittrich, *J. Appl. Cryst.* **2011**, *44*, 1281.

5.6 Asymmetric β -C–H Functionalization of Acceptor-Substituted Ketones through Single Rh-based Photoredox Catalysis

5.6.1 Synthesis of a Derived Chiral-at-Rhodium Lewis Acid Catalyst

Chiral-at-rhodium catalyst Δ -**RhS2** was synthesized according to the methodology published recently by our group with some modifications.^{1,3} Accordingly, bromine-substituted racemic rhodium(III) complex *rac*-**55** was first synthesized, and then converted into the corresponding diastereomeric complexes by reacting with a monofluorinated salicyloxazoline as chiral auxiliary. The two diastereomers Λ -(*S*)-**56** and Δ -(*S*)-**56** were resolved relying on their different solubilities in EtOH and by silica gel chromatography. Afterwards, diastereomeric complex Δ -(*S*)-**56** was subjected to Suzuki cross-coupling to provide Δ -(*S*)-**57**. Notably, the post-complexation cross-coupling proceeded smoothly without affecting the optical purity of the rhodium(III) complex. Finally, stereospecific replacement of the auxiliary ligand with acetonitriles induced by trifluoroacetic acid (TFA), followed by anion exchange provided the Δ -**RhS2**.



Synthesis of racemic rhodium complex *rac*-**55**:

The racemic rhodium(III) complex *rac*-**55** was synthesized according to the route reported by Meggers and co-workers recently.¹ Accordingly, **54** (346 mg, 0.90 mmol, 2.0 equiv., prepared according to a previous report^{4a}) was added to $\text{RhCl}_3 \cdot x\text{H}_2\text{O}$ (118 mg, 0.45 mmol, 1.0 equiv.) in a mixture of 2-ethoxyethanol and water (v/v = 3:1, 9.0 mL). The reaction mixture was heated at 125°C for 4 h

under an atmosphere of nitrogen. Then, the solvent was removed *in vacuo* on a rotary evaporator. The flask was kept on the rotary evaporator under vacuum for another 30 min to get rid of the residual water thoroughly to obtain a brown solid. To the brown solid in CH₃CN (5 mL) was added AgPF₆ (230 mg, 0.90 mmol, 2.0 equiv.) in one portion and then stirred at 60 °C. After 15 h, the reaction mixture was allowed to be cooled to room temperature. The solid was filtered off and the filtrate was collected, evaporated to dryness and purified by column chromatograph on silica gel (100% CH₂Cl₂ to CH₂Cl₂/CH₃CN = 20:1) to give *rac*-**55** (312 mg, 0.306 mmol, 68% yield over two steps) as a pale yellow solid.

Remark:

- 1) Weigh out RhCl₃•xH₂O based on the content of metal as 40% which is an average amount calculated from 37–42% (provided by the supplier, Precious Metals Online, website: <http://www.precmet.com.au>).
- 2) The reaction time is critical (4 h).

Synthesis of rhodium(III) complexes Δ -(*S*)-**56** and Λ -(*S*)-**56**:

To the racemic rhodium(III) complex *rac*-**55** (312 mg, 0.306 mmol) and K₂CO₃ (127 mg, 0.919 mmol, 3.0 equiv.) in absolute ethanol (6.0 mL) was added the chiral auxiliary (*S*)-3-fluoro-2-(4-phenyl-4,5-dihydrooxazol-2-yl)phenol (94 mg, 0.367 mmol, 1.2 equiv., prepared according to a previous report^{4b}) in one portion. The mixture was heated at 70 °C for 6 h. Afterwards, the reaction mixture was cooled to room temperature. The diastereomer Λ -(*S*)-**56** has a lower solubility in ethanol than Δ -(*S*)-**56** and was precipitated selectively. The yellow solid was separated from the solution by centrifugation, and washed for another three times with EtOH (3 × 10 mL). The combined clear yellow solution was collected and concentrated, and then subjected to a flash chromatography on silica gel (*n*-hexane/EtOAc = 10:1 to 3:1) to give Δ -(*S*)-**56** (138 mg, 0.131 mmol, 43% yield) as a yellow solid. On the other hand, the yellow solid obtained after centrifugation was subjected to a flash chromatography on silica gel (*n*-hexane/CH₂Cl₂ = 1:10 to 1:1) to provide Λ -(*S*)-**56** with >95% purity as judged by ¹H NMR. The crude complex was recrystallized in *n*-hexane/CH₂Cl₂ = 10:1 to provide pure Λ -(*S*)-**56** (128 mg, 0.122 mmol, 40% yield) as a yellow solid. The assigned configurations were confirmed by the crystal structure of Δ -(*S*)-**56** (see below).

Remark:

- 1) It is recommended to wash the solid until the organic solution becomes colorless after centrifugation to obtain a nearly complete separation of diastereomeric isomers Δ -(*S*)-**56** and Λ -(*S*)-**56**.
- 2) The complexes Δ -(*S*)-**56** and Λ -(*S*)-**56** are acid sensitive. It is therefore recommended to use silica gel of high quality.

Synthesis of rhodium complex Δ -(*S*)-57**:**

To a mixture of rhodium(III) complex Δ -(*S*)-**56** (118.0 mg, 0.1126 mmol), phenylboronic acid (60.0 mg, 0.4903 mmol, 4.0 equiv.), and powdered K_3PO_4 (104.0 mg, 0.4904 mmol, 4.00 equiv.) was added $Pd(dba)_2$ (7.1 mg, 0.01226 mmol, 10 mol%) and SPhos (10.0 mg, 0.02452 mol, 20 mol%). The mixture was evacuated and backfilled with nitrogen for three times. Afterwards, toluene (4.0 mL) was added, and the reaction mixture was heated at 100 °C for 14 h. The reaction was allowed to be cooled to room temperature and the insoluble solid was filtered off. The filtrate was collected and concentrated, and then subjected to a flash chromatography on silica gel (*n*-hexane/EtOAc = 10:1 to 3:1) to give Δ -(*S*)-**57** (96 mg, 0.09233 mmol, 82% yield) as a yellow solid.

Remark:

The complex Δ -(*S*)-**57** is acid sensitive. It is therefore recommend use silica gel of high quality.

Synthesis of chiral-at-rhodium catalyst Δ -RhS2:

To a solution of Δ -(*S*)-**57** (94 mg, 0.09 mmol) in CH_3CN (2 mL) was added TFA (40 μ L, 0.54 mmol, 6 equiv.) in one portion. The clear yellow solution turned to pale yellow within 1 min. The solution was stirred at room temperature for another 30 min. Afterwards, the reaction mixture was evaporated to dryness and subjected to a flash chromatography on silica gel. The product was purified as shown below:

- a) Silica gel flash column chromatography using 200 mL of CH_2Cl_2/CH_3CN (99/1, vol/vol) with 0.1% of TFA (0.2 mL); then switched to 200 mL CH_2Cl_2/CH_3CN (95/5, vol/vol) to wash out the residual TFA.
- b) After the solvent was almost completely used, changed the eluent to first 100 mL of CH_2Cl_2/CH_3CN (95/5, vol/vol), and then 300 mL of CH_2Cl_2/CH_3CN (90/10, vol/vol) to elute a purple band which has

been characterized as the chiral auxiliary together with some coloured impurities.

c) Afterwards, added 150 mg of NH_4PF_6 (0.90 mmol, 10 equiv.) atop the seasand.

d) Used 200 mL $\text{CH}_2\text{Cl}_2/\text{CH}_3\text{CN}$ (50/50, vol/vol) to elute residual pale yellow band on the column.

e) Collected the pale yellow band, then removed the solvent *in vacuo* to give a pale yellow solid containing desired Δ -**RhS2** with a hexafluorophosphate counterion and additional salts.

f) Subjected the obtained yellow solid to a thin pad (~1 cm) of silica gel to remove excess salts using 50 mL of $\text{CH}_2\text{Cl}_2/\text{CH}_3\text{CN}$ (99/1, vol/vol) as eluent.

g). Collected the filtrate, then removed the solvent *in vacuo* to obtain Δ -**RhS2** in 91% yield (83 mg, 0.0819 mmol) as a pale yellow solid.

Remark:

1) Adding TFA (0.1%) in the eluent is crucial to prevent the auxiliary to re-coordinate to the rhodium(III) center, and leads to a separation of the auxiliary and the product band on silica gel chromatography.

2) According to experience of the Meggers lab, the quality of the silica gel is important for obtaining reproducible isolated yields of Δ -**RhS2**.

Analytical data:

54:

^1H NMR (300 MHz, CDCl_3) δ 8.23–8.14 (m, 2H), 7.87 (d, $J = 8.5$ Hz, 1H), 7.56–7.51 (m, 2H), 7.44–7.38 (m, 2H), 1.43 (s, 9H).

^{13}C NMR (75 MHz, CDCl_3) δ 164.3, 152.8, 150.1, 133.1, 132.7, 132.4, 131.7, 131.0, 130.8, 127.1, 123.8, 120.8, 119.8, 35.0, 31.5.

IR (film): ν (cm^{-1}) 3059, 2957, 2865, 1599, 1524, 1431, 1351, 1264, 1063, 1020, 961, 923, 874, 815, 756, 656, 453.

HRMS (ESI, m/z) calcd for $\text{C}_{17}\text{H}_{17}\text{BrNS}$ $[\text{M}+\text{H}]^+$: 348.0240, found: 348.0245.

$R_f = 0.6$ in *n*-hexane/EtOAc = 10:1.

rac-**55:**

^1H NMR (300 MHz, CD_2Cl_2) δ 8.60 (d, $J = 1.5$ Hz, 2H), 8.12 (d, $J = 8.6$ Hz, 2H), 7.81 (dd, $J = 8.6, 1.8$ Hz, 2H), 7.31 (dd, $J = 7.9, 0.7$ Hz, 2H), 6.70 (t, $J = 7.9$ Hz, 2H), 6.12 (d, $J = 7.8$ Hz, 2H), 2.19 (s, 6H), 1.50 (s, 18H).

^{13}C NMR (75 MHz, CD_2Cl_2) δ 174.9, 163.5, 153.1, 148.6, 139.4, 132.3, 131.3, 129.8, 129.2, 125.9, 122.5, 120.4, 116.8, 35.7, 31.6.

IR (film): ν (cm^{-1}) 3060, 2956, 2924, 2861, 2281, 1730, 1600, 1557, 1453, 1403, 1277, 1192, 1132, 1058, 986, 934, 839, 769, 718, 667, 599, 555, 492, 444, 406.

$R_f = 0.4$ in $\text{CH}_2\text{Cl}_2/\text{CH}_3\text{CN}$ (20:1).

Δ -(S)-**56**:

^1H NMR (500 MHz, CD_2Cl_2) δ 9.25 (dd, $J = 1.9, 0.5$ Hz, 1H), 8.55 (dd, $J = 1.8$ Hz, 0.4, 1H), 8.00 (dd, $J = 8.6, 0.4$ Hz, 1H), 7.84 (dd, $J = 8.6, 0.3$ Hz, 1H), 7.64 (dd, $J = 8.5, 1.9$ Hz, 1H), 7.56 (dd, $J = 8.6, 1.8$ Hz, 1H), 7.21 (dd, $J = 7.9, 1.0$ Hz, 1H), 6.94–6.88 (m, 5H), 6.74 (dd, $J = 7.7, 1.1$ Hz, 1H), 6.71–6.67 (m, 1H), 6.60 (t, $J = 7.7$ Hz, 1H), 6.27 (t, $J = 7.6$ Hz, 1H), 6.21 (dt, $J = 7.7, 1.1$ Hz, 1H), 6.15–6.13 (m, 2H), 5.75–5.71 (m, 1H), 4.41–4.34 (m, 1H), 3.90–3.82 (m, 2H), 1.42 (s, 9H), 1.23 (s, 9H).

^{13}C NMR (125 MHz, CD_2Cl_2) δ 175.0, 174.9, 174.9, 174.8, 174.5, 174.4, 172.9, 172.7, 172.6, 172.3, 167.4, 162.8 ($J = 255.1$ Hz), 152.7, 151.4, 149.8, 149.7, 139.8, 139.4, 137.3, 134.0, 133.1, 133.0, 132.1, 130.2, 129.6 (2C), 128.9, 128.7, 128.5, 128.1, 128.0, 127.3, 126.9, 125.0, 124.9, 121.6, 121.5, 120.3, 120.3, 120.0 (2C), 118.9, 118.8, 118.6, 116.9, 104.1 ($J = 8.0$ Hz), 98.7 ($J = 22.2$ Hz), 74.9, 70.7, 35.7, 35.4, 31.6, 32.0.

^{19}F NMR (282 MHz) δ -107.6.

IR (film): ν (cm^{-1}) 3056, 2955, 2900, 1617, 1567, 1530, 1443, 1395, 1270, 1220, 1190, 1151, 1093, 1028, 979, 925, 843, 749, 693, 617, 582, 527, 487, 446, 403.

HRMS (APCI, m/z) calcd for $\text{C}_{49}\text{H}_{42}\text{Br}_2\text{FN}_3\text{O}_2\text{RhS}_2$ [$\text{M}+\text{H}$] $^+$: 1050.0103, found: 1050.0107.

CD { $\text{CH}_3\text{OH}/\text{CH}_2\text{Cl}_2$ (3:2)} for Δ -(S)-**56**: λ , nm ($\Delta\epsilon$, $\text{M}^{-1}\text{cm}^{-1}$) 423 (+58), 368 (+6), 356 (-1), 339 (+9), 290 (+18).

$R_f = 0.4$ in *n*-hexane/EtOAc (1:1).

Λ -(S)-**56**:

^1H NMR (500 MHz, CD_2Cl_2) δ 9.07 (d, $J = 1.6$ Hz, 1H), 8.06 (d, $J = 8.6$ Hz, 1H), 7.87 (d, $J = 8.6$ Hz, 1H), 7.70 (d, $J = 8.5$ Hz, 1H), 7.61 (dd, $J = 8.7, 1.7$ Hz, 1H), 7.55 (dd, $J = 8.6, 1.9$ Hz, 1H), 7.26 (dd, $J = 7.8, 1.0$ Hz, 1H), 7.21 (dd, $J = 7.8, 0.9$ Hz, 1H), 7.03 (br, 1H), 6.87–6.80 (m, 3H), 6.70 (t, $J = 7.8$ Hz, 1H), 6.56 (t, $J = 7.9$ Hz, 1H), 6.34–6.31 (m, 3H), 6.22 (br, 1H), 5.80–5.76 (m, 1H), 5.75 (dt, $J = 7.9, 0.9$ Hz, 1H), 4.95–4.89 (m, 2H), 4.05–4.00 (m, 1H), 1.49 (s, 9H), 1.29 (s, 9H).

^{13}C NMR (125 MHz, CD_2Cl_2) δ 175.0, 174.9, 174.5, 174.4, 174.2, 174.0, 173.7 (2C), 172.0, 171.8, 165.9 (2C), 163.0 ($J = 257.0$ Hz), 151.3, 151.1, 149.9, 149.3, 140.6, 140.2, 139.9, 134.4, 132.7, 132.6, 131.6, 129.5, 129.4 (3C), 129.3 (2C), 128.4 (2C), 128.2, 127.8, 127.5, 127.3, 124.1, 124.0, 121.7, 120.6, 119.9 (2C), 119.8 (2C), 119.4, 115.9, 101.3 ($J = 6.5$ Hz), 98.5 ($J = 23.6$ Hz), 75.7, 69.3, 35.1, 35.0, 31.4, 31.3.

CD { $\text{CH}_3\text{OH}/\text{CH}_2\text{Cl}_2$ (3:2)} for Δ -(*S*)-**56**: λ , nm ($\Delta\epsilon$, $\text{M}^{-1} \text{cm}^{-1}$) 432 (−48), 375 (+20).

$R_f = 0.3$ in *n*-hexane/ CH_2Cl_2 (1:2).

Δ -(*S*)-**57**:

^1H NMR (300 MHz, CD_2Cl_2) δ 9.24 (d, $J = 1.8$ Hz, 1H), 8.54 (d, $J = 1.7$ Hz, 1H), 7.72 (d, $J = 8.6$ Hz, 1H), 7.60–7.50 (m, 8H), 7.49–7.45 (m, 2H), 7.42–7.39 (m, 1H), 7.31 (d, $J = 7.5$ Hz, 1H), 7.19 (dt, $J = 7.4$, 1.3 Hz, 1H), 7.09 (tt, $J = 6.7$, 1.3 Hz, 1H), 6.99–6.96 (m, 2H), 6.94–6.92 (m, 4H), 6.76 (dd, $J = 16.0$, 7.7 Hz, 1H), 6.56–6.53 (m, 2H), 6.46 (dd, $J = 7.3$, 1.1 Hz, 1H), 6.35 (dt, $J = 7.7$, 0.9 Hz, 1H), 6.31 (d, $J = 8.3$ Hz, 1H), 5.78–5.75 (m, 1H), 4.32 (m, 1H), 3.92–3.85 (m, 2H), 1.40 (s, 9H), 1.27 (s, 9H).

^{13}C NMR (75 MHz, CD_2Cl_2) δ 175.2, 175.1, 175.0 (2C), 174.8 (2C), 171.1, 170.9, 170.7, 170.4, 170.0, 162.6 (d, $J = 254.4$ Hz), 161.6, 151.8, 150.6, 149.6, 149.4, 141.7, 141.5, 140.5, 138.9, 138.3, 137.7, 134.2, 132.6, 132.4, 131.9, 130.4, 130.3, 129.4, 129.2 (2C), 129.1 (2C), 129.0, 128.9, 128.8, 128.6, 128.5, 128.3, 128.1, 127.8, 127.3, 126.8, 125.0, 124.0, 123.9, 123.7, 121.0 (2C), 118.6 (2C), 118.1, 116.6, 104.2 (d, $J = 7.9$ Hz), 98.1 (d, $J = 22.3$ Hz), 74.5, 69.8, 35.3, 35.1, 31.3, 31.1.

IR (film): ν (cm^{-1}) 12955, 2143, 1984, 1618, 1544, 1448, 1376, 1269, 1220, 1177, 1097, 1035, 988, 924, 792, 754, 697, 620, 585, 535, 454, 408.

^{19}F NMR (282 MHz) δ −108.8.

HRMS (FD, m/z) calcd for $\text{C}_{61}\text{H}_{51}\text{FN}_3\text{O}_2\text{RhS}_2$ [M]: 1044.2493, found: 1044.2511.

CD { $\text{CH}_3\text{OH}/\text{CH}_2\text{Cl}_2$ (3:2)} for Δ -(*S*)-**57**: λ , nm ($\Delta\epsilon$, $\text{M}^{-1} \text{cm}^{-1}$) 442 (+3), 421 (+2), 375 (+23).

$R_f = 0.4$ in *n*-hexane/EtOAc (1:1).

Δ -**RhS2**:

^1H NMR (500 MHz, CD_2Cl_2) δ 8.58 (br, 2H), 7.79 (d, $J = 8.6$ Hz, 2H), 7.65 (d, $J = 8.7$, 1.8 Hz, 2H), 7.63–7.57 (m, 6H), 7.46–7.43 (m, 2H), 7.45–7.39 (m, 2H), 6.93–6.87 (m, 4H), 6.24 (dt, $J = 7.5$, 1.2 Hz, 2H), 2.20 (s, 6H), 1.46 (s, 18H).

^{13}C NMR (125 MHz, CD_2Cl_2) δ 175.3, 152.1, 148.4, 142.3, 139.6, 138.3, 132.1, 129.7, 129.6 (2C),

129.4, 129.3, 129.2 (2C), 129.1, 126.1, 124.9, 121.8, 116.4, 35.2, 31.3.

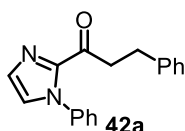
IR (film): ν (cm⁻¹) 2957, 1995, 1550, 1456, 1413, 1318, 1275, 1035, 991, 930, 834, 758, 699, 669, 553, 444, 409.

CD {CH₃OH/CH₂Cl₂ (3:2)} for Δ -**RhS2**: λ , nm ($\Delta\epsilon$, M⁻¹ cm⁻¹) 410 (-97), 369 (+183), 353 (+155), 300 (-281), 247 (+165).

R_f = 0.4 in CH₂Cl₂/CH₃CN (20:1).

5.6.2 Synthesis of Substrates

2-Acyl imidazoles **42a-m** were synthesized according to our recently published procedures.^{5a} Analytical data of **42n** were consistent with the report.^{5a} The experimental data of **42a-m** are shown below.



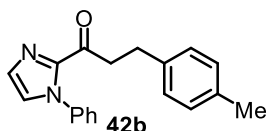
¹H NMR (300 MHz, CDCl₃) δ 7.51–7.47 (m, 3H), 7.31–7.29 (m, 4H), 7.25–7.25 (m, 4H), 7.20 (d, J = 1.0 Hz, 1H), 3.53 (t, J = 7.5 Hz, 2H), 3.02 (t, J = 8.0 Hz, 2H).

¹³C NMR (75 MHz, CDCl₃) δ 190.6, 143.0, 141.1, 138.5, 129.6, 129.0, 128.8, 128.6, 128.5, 127.1, 126.1, 126.0, 40.7, 29.9.

IR (film): ν (cm⁻¹) 3106, 3060, 3028, 3028, 2926, 1682, 1595, 1494, 1445, 1401, 1303, 1146, 1053, 956, 908, 757, 691, 559, 512.

HRMS (ESI, m/z) calcd for C₁₈H₁₇N₂O [M+H]⁺: 277.1335, found: 277.1331.

R_f = 0.5 in *n*-hexane/EtOAc (5:1).



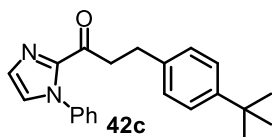
¹H NMR (300 MHz, CDCl₃) δ 7.50–7.47 (m, 3H), 7.31–7.25 (m, 3H), 7.20 (d, J = 0.9 Hz, 1H), 7.17–7.10 (m, 4H), 3.51 (t, J = 7.5 Hz, 2H), 3.00 (t, J = 7.9 Hz, 2H), 1.38 (s, 3H).

¹³C NMR (75 MHz, CDCl₃) δ 190.7, 143.1, 138.5, 138.0, 135.5, 129.6, 129.1, 129.0, 128.8, 128.4, 127.0, 126.0, 40.8, 29.5, 21.0.

IR (film): ν (cm⁻¹) 2932, 1684, 1595, 1492, 1443, 1402, 1340, 1296, 1254, 1207, 1172, 1050, 1008, 955, 909, 868, 805, 763, 690, 540, 497, 434.

HRMS (ESI, m/z) calcd for $C_{19}H_{19}N_2O$ $[M+H]^+$: 291.1492, found: 291.1487.

$R_f = 0.5$ in *n*-hexane/EtOAc (5:1).



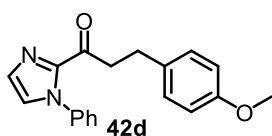
1H NMR (300 MHz, $CDCl_3$) δ 7.52–7.46 (m, 3H), 7.34–7.26 (m, 5H), 7.21–7.19 (m, 3H), 3.53 (t, $J = 7.5$ Hz, 2H), 3.00 (t, $J = 8.0$ Hz, 2H), 1.34 (s, 9H).

^{13}C NMR (75 MHz, $CDCl_3$) δ 190.7, 148.9, 143.1, 138.5, 138.0, 129.6, 129.0, 128.8, 128.2, 127.0, 126.0, 125.3, 40.7, 34.4, 31.5, 29.4.

IR (film): ν (cm^{-1}) 2947, 2863, 1685, 1595, 1493, 1446, 1403, 1337, 1302, 1258, 1207, 1149, 1058, 1011, 959, 909, 819, 763, 690, 642, 557, 508, 433.

HRMS (FD, m/z) calcd for $C_{22}H_{24}N_2O$ $[M]$: 332.1889, found: 332.1883.

$R_f = 0.6$ in *n*-hexane/EtOAc (5:1).

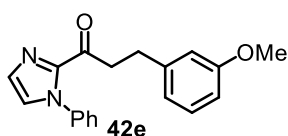


1H NMR (300 MHz, $CDCl_3$) δ 7.50–7.45 (m, 3H), 7.33–7.31 (m, 2H), 7.26 (m, 1H), 7.20 (d, $J = 1.0$ Hz, 1H), 6.88–6.83 (m, 2H), 6.44–6.38 (m, 1H), 6.14 (dt, $J = 15.8, 6.8$ Hz, 1H), 3.83 (s, 3H), 3.36 (t, $J = 7.3$ Hz, 2H), 2.59 (m, 2H).

^{13}C NMR (75 MHz, $CDCl_3$) δ 190.8, 158.9, 143.1, 138.5, 130.6, 129.6, 129.0, 128.8, 127.2, 127.0, 126.0, 114.0, 55.4, 39.0, 27.4.

IR (film): ν (cm^{-1}) 3104, 2972, 2924, 2895, 2837, 1686, 1599, 1499, 1444, 1403, 1299, 1235, 1172, 1101, 1059, 1019, 956, 908, 843, 763, 693, 558, 505, 453, 418.

$R_f = 0.4$ in *n*-hexane/EtOAc (5:1).



1H NMR (300 MHz, $CDCl_3$) δ 7.51–7.46 (m, 3H), 7.31–7.26 (m, 3H), 7.24–7.19 (m, 2H), 6.85 (d, $J = 7.6$ Hz, 1H), 6.81 (m, 1H), 6.76 (dd, $J = 8.1, 2.3$ Hz, 1H), 3.81 (s, 3H), 3.53 (t, $J = 7.5$ Hz, 2H), 2.00 (t, $J = 7.9$ Hz, 2H).

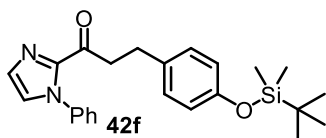
^{13}C NMR (75 MHz, $CDCl_3$) δ 190.5, 159.7, 143.0, 142.7, 138.5, 129.6, 129.4, 129.0, 128.8, 127.1,

125.9, 120.9, 114.1, 111.6, 55.2, 40.6, 30.0.

IR (film): ν (cm⁻¹) 3111, 2938, 2835, 2774, 1683, 1594, 1492, 1445, 1402, 1303, 1255, 1151, 1045, 956, 909, 868, 763, 690, 557, 510, 455.

HRMS (FD, m/z) calcd for C₁₉H₁₈N₂O₂ [M]: 306.1368, found: 306.1374.

R_f = 0.4 in *n*-hexane/EtOAc (5:1).



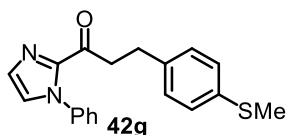
¹H NMR (300 MHz, CDCl₃) δ 7.30–7.26 (m, 3H), 7.10–7.05 (m, 3H), 6.99 (d, J = 1.0 Hz, 1H), 6.91–6.87 (m, 2H), 6.58–6.54 (m, 2H), 3.28 (t, J = 7.5 Hz, 2H), 2.74 (t, J = 8.0 Hz, 2H), 0.80 (s, 9H), 0.00 (s, 6H).

¹³C NMR (75 MHz, CDCl₃) δ 190.7, 153.9, 143.1, 138.5, 133.8, 129.6, 129.4, 129.0, 128.8, 127.0, 126.0, 120.0, 41.0, 29.2, 25.8, 18.3, -4.3.

IR (film): ν (cm⁻¹) 2938, 2858, 1685, 1602, 1503, 1448, 1403, 1251, 1166, 1059, 1013, 956, 910, 833, 765, 689, 638, 524.

HRMS (ESI, m/z) calcd for C₂₄H₃₁N₂O₂Si [M+H]⁺: 407.2149, found: 407.2143.

R_f = 0.5 in *n*-hexane/EtOAc (7:1).



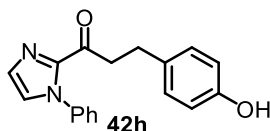
¹H NMR (300 MHz, CDCl₃) δ 7.52–7.47 (m, 3H), 7.29–7.25 (m, 3H), 7.23–7.17 (m, 5H), 3.50 (t, J = 7.4 Hz, 2H), 2.98 (t, J = 7.9 Hz, 2H), 2.49 (s, 3H).

¹³C NMR (75 MHz, CDCl₃) δ 190.4, 143.0, 138.4, 138.3, 135.6, 129.6, 129.1, 129.0, 128.8, 127.3, 127.1, 126.0, 40.6, 29.4, 16.4.

IR (film): ν (cm⁻¹) 2921, 2854, 1731, 1686, 1594, 1491, 1443, 1405, 1336, 1297, 1252, 1206, 1050, 1003, 954, 908, 868, 806, 761, 689, 621, 553, 504, 454.

HRMS (ESI, m/z) calcd for C₁₉H₁₉N₂O₂S [M+H]⁺: 323.1213, found: 323.1205.

R_f = 0.5 in *n*-hexane/EtOAc (4:1).



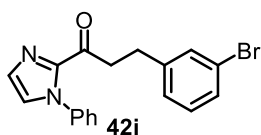
42h was synthesized from **42f** with a TBAF-mediated deprotection of TBS moiety.

^1H NMR (300 MHz, CDCl_3) δ 7.52–7.48 (m, 4H), 7.32 (d, $J = 0.9$ Hz, 1H), 7.31–7.28 (m, 2H), 7.22 (d, $J = 1.0$ Hz, 1H), 7.03–7.00 (m, 2H), 6.76–6.72 (m, 2H), 3.48 (t, $J = 7.4$ Hz, 2H), 2.91 (t, $J = 8.0$ Hz, 2H).

^{13}C NMR (75 MHz, CDCl_3) δ 190.5, 154.5, 142.8, 138.3, 132.5, 129.5, 129.4, 129.1, 129.0, 127.1, 126.0, 115.4, 41.3, 28.9.

IR (film): ν (cm^{-1}) 3005, 2908, 2853, 2162, 1983, 1730, 1676, 1593, 1513, 1449, 1331, 1283, 1203, 1062, 989, 918, 854, 795, 755, 683, 577.

HRMS (ESI, m/z) calcd for $\text{C}_{18}\text{H}_{16}\text{N}_2\text{O}_2$ $[\text{M}+\text{H}]^+$: 293.1285, found: 293.1280.



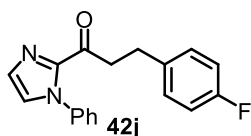
^1H NMR (300 MHz, CDCl_3) δ 7.52–7.48 (m, 3H), 7.41 (m, 1H), 7.43 (dt, $J = 7.0, 2.0$ Hz, 1H), 7.31–7.25 (m, 3H), 7.21 (d, $J = 1.0$ Hz, 1H), 7.18–7.13 (m, 2H), 3.52 (t, $J = 7.4$ Hz, 2H), 3.00 (t, $J = 7.8$ Hz, 2H).

^{13}C NMR (75 MHz, CDCl_3) δ 190.0, 143.5, 142.9, 138.4, 131.6, 130.0, 129.7, 129.2, 129.1, 128.9, 127.2 (2C), 126.0, 122.5, 40.3, 29.5.

IR (film): ν (cm^{-1}) 1685, 1597, 1497, 1442, 1402, 1295, 1237, 1173, 1064, 1022, 954, 909, 845, 763, 691, 561, 511, 435.

HRMS (ESI, m/z) calcd for $\text{C}_{18}\text{H}_{16}\text{BrN}_2\text{O}$ $[\text{M}+\text{H}]^+$: 357.0422, found: 357.0413.

$R_f = 0.5$ in *n*-hexane/EtOAc (5:1).



^1H NMR (300 MHz, CDCl_3) δ 7.50–7.48 (m, 3H), 7.29–7.26 (m, 3H), 7.21–7.19 (m, 3H), 7.00–6.94 (m, 2H), 3.51 (t, $J = 7.5$ Hz, 2H), 2.99 (t, $J = 7.7$ Hz, 2H).

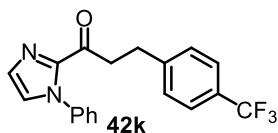
^{13}C NMR (75 MHz, CDCl_3) δ 190.2, 161.4 (d, $J = 243.0$ Hz, 1C), 142.9, 138.4, 136.7 (d, $J = 3.1$ Hz, 1C), 129.9 (d, $J = 7.8$ Hz, 1C), 129.6, 129.0, 128.8, 127.1, 125.9, 115.1 (d, $J = 21.1$ Hz, 1C), 40.7, 29.0.

^{19}F NMR (282 MHz) δ -117.4.

IR (film): ν (cm⁻¹) 3049, 2924, 1682, 1597, 1501, 1444, 1403, 1304, 1219, 1152, 1096, 1058, 1010, 958, 909, 824, 763, 691, 532, 426.

HRMS (ESI, m/z) calcd for C₁₈H₁₆FN₂O [M+H]⁺: 295.1241, found: 295.1242.

R_f = 0.5 in *n*-hexane/EtOAc (5:1).



¹H NMR (300 MHz, CDCl₃) δ 7.51 (dt, J = 8.2 Hz, 2H), 7.48–7.45 (m, 3H), 7.33 (d, J = 8.1 Hz, 2H), 7.27–7.22 (m, 3H), 7.18 (d, J = 0.9 Hz, 1H), 3.52 (t, J = 7.4 Hz, 2H), 3.04 (t, J = 7.6 Hz, 2H).

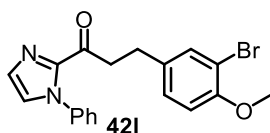
¹³C NMR (75 MHz, CDCl₃) δ 189.9, 145.3, 142.9, 138.4, 129.7, 129.1, 128.9 (2C), 127.3, 126.0, 125.4 (q, J = 3.8 Hz), 124.4 (q, J = 271.7 Hz), 40.2, 29.6.

¹⁹F NMR (282 MHz) δ -62.3.

IR (film): ν (cm⁻¹) 3001, 2943, 2844, 1687, 1493, 1409, 1318, 1213, 1174, 1108, 1057, 1010, 973, 907, 830, 762, 690, 605, 509, 461.

HRMS (ESI, m/z) calcd for C₁₉H₁₆F₃N₂O [M+H]⁺: 345.1209, found: 345.1211.

R_f = 0.6 in *n*-hexane/EtOAc (5:1).



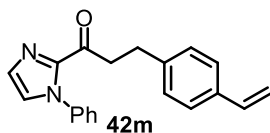
¹H NMR (300 MHz, CDCl₃) δ 7.54–7.48 (m, 3H), 7.43 (d, J = 2.1 Hz, 1H), 7.31–7.25 (m, 3H), 7.20 (d, J = 0.9 Hz, 1H), 7.15 (dd, J = 8.4, 2.2 Hz, 1H), 6.83 (d, J = 8.4 Hz, 1H), 3.89 (s, 3H), 3.48 (t, J = 7.4 Hz, 2H), 2.94 (t, J = 7.7 Hz, 2H).

¹³C NMR (75 MHz, CDCl₃) δ 190.2, 154.3, 142.9, 138.4, 134.8, 133.3, 129.7, 129.1, 128.8, 128.4, 127.2, 125.9, 112.0, 111.5, 56.3, 40.6, 28.7.

IR (film): ν (cm⁻¹) 2908, 2855, 1728, 1681, 1595, 1493, 1447, 1402, 1335, 1296, 1251, 1205, 1172, 1050, 995, 956, 913, 868, 802, 762, 687, 544, 491, 421.

HRMS (ESI, m/z) calcd for C₁₉H₁₈BrN₂O₂ [M+H]⁺: 386.0578, found: 386.0574.

R_f = 0.4 in *n*-hexane/EtOAc (5:1).



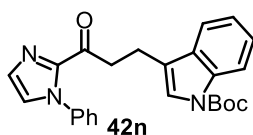
^1H NMR (300 MHz, CDCl_3) δ 7.48–7.41 (m, 3H), 7.33–7.30 (m, 2H), 7.25–7.22 (m, 3H), 7.20–7.16 (m, 3H), 6.68 (dd, $J = 17.6, 11.0$ Hz, 1H), 5.69 (dd, $J = 17.6, 0.9$ Hz, 1H), 5.19 (dd, $J = 10.9, 0.8$ Hz, 1H), 3.49 (t, $J = 7.4$ Hz, 2H), 2.98 (t, $J = 7.9$ Hz, 2H).

^{13}C NMR (75 MHz, CDCl_3) δ 190.5, 143.0, 140.9, 138.5, 136.7, 135.5, 129.6, 129.0, 128.8, 128.7, 127.1, 126.3, 126.0, 113.1, 40.6, 29.6.

IR (film): ν (cm^{-1}) 3113, 3049, 2926, 1688, 1595, 1494, 1407, 1298, 1213, 1055, 1004, 956, 910, 826, 762, 691, 548, 502, 441.

HRMS (ESI, m/z) calcd for $\text{C}_{20}\text{H}_{19}\text{N}_2\text{O}$ $[\text{M}+\text{H}]^+$: 303.1492, found: 303.1486.

$R_f = 0.6$ in *n*-hexane/EtOAc (5:1).



^1H NMR (300 MHz, CDCl_3) δ 8.16 (d, $J = 8.0$ Hz, 1H), 7.59–7.56 (m, 1H), 7.52–7.45 (m, 4H), 7.36–7.22 (m, 5H), 7.22 (d, $J = 1.0$ Hz, 1H), 3.62 (t, $J = 7.4$ Hz, 2H), 3.10 (t, $J = 7.8$ Hz, 2H), 1.70 (s, 9H).

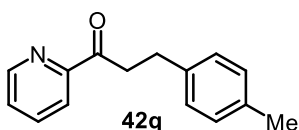
^{13}C NMR (75 MHz, CDCl_3) δ 190.5, 149.8, 143.0, 138.4, 135.6, 130.6, 129.7, 129.2, 128.8, 127.1, 126.0, 124.4, 122.6, 122.4, 119.9, 119.0, 115.2, 83.3, 38.6, 28.3, 19.3.

IR (film): ν (cm^{-1}) 2984, 2924, 1689, 1598, 1495, 1448, 1405, 1374, 1306, 1246, 1210, 1152, 1051, 1020, 959, 909, 843, 760, 691, 554, 508.

HRMS (ESI, m/z) calcd for $\text{C}_{25}\text{H}_{25}\text{N}_3\text{O}_3\text{Na}$ $[\text{M}+\text{Na}]^+$: 438.1788, found: 438.1781.

$R_f = 0.4$ in *n*-hexane/EtOAc (5:1).

2-Acyl pyridines **42p-r** were synthesized according to our recently published procedures.^{5b} Analytical data of **42p**^{5c} and **42r**^{5d} were consistent with the report. The experimental data of **42q** are shown below.



^1H NMR (300 MHz, CDCl_3) δ 8.66 (d, $J = 4.4$ Hz, 1H), 8.04 (d, $J = 7.9$ Hz, 1H), 7.82 (td, $J = 7.7, 1.5$ Hz, 1H), 7.48–7.43 (m, 1H), 7.17 (d, $J = 8.0$ Hz, 2H), 7.09 (d, $J = 7.9$ Hz, 2H), 3.55 (t, $J = 7.5$ Hz, 2H),

3.03 (t, $J = 7.7$ Hz, 2H), 2.3 (s, 3H).

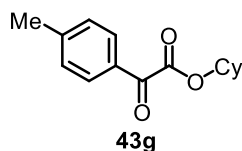
^{13}C NMR (75 MHz, CDCl_3) δ 201.2, 153.5, 149.0, 138.4, 136.9, 135.5, 129.1, 128.4, 127.1, 121.9, 39.6, 29.5, 21.1.

IR (film): ν (cm^{-1}) 3051, 3010, 2923, 1695, 1579, 1514, 1439, 1401, 1360, 1304, 1216, 1096, 1044, 985, 780, 739, 667, 613, 573, 533, 475, 405.

HRMS (ESI, m/z) calcd for $\text{C}_{15}\text{H}_{16}\text{NO}$ $[\text{M}+\text{H}]^+$: 226.1226, found: 226.1230.

$R_f = 0.6$ in *n*-hexane/EtOAc (7:1).

α -Ketoesters **43g-j** were synthesized from acetophenones according to a methodology reported by Jiao.⁶ Analytical data of **43i** were consistent with the report.⁶ The experimental data of **43g**, **43h**, **43j** are shown below.

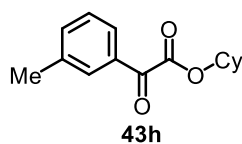


^1H NMR (300 MHz, CDCl_3) δ 7.89 (d, $J = 8.2$ Hz, 2H), 7.30 (d, $J = 8.0$ Hz, 2H), 5.09 (m, 1H), 2.44 (s, 3H), 2.03–1.97 (m, 2H), 1.84–1.75 (m, 2H), 1.66–1.54 (m, 3H), 1.49–1.24 (m, 3H).

^{13}C NMR (75 MHz, CDCl_3) δ 186.6, 164.0, 146.1, 130.3, 130.2, 129.7, 75.4, 31.5, 25.3, 23.7, 22.0.

IR (film): ν (cm^{-1}) 2936, 2859, 1727, 1680, 1603, 1571, 1448, 1296, 1203, 1169, 1117, 989, 900, 834, 794, 732, 619, 478.

$R_f = 0.6$ in *n*-hexane/EtOAc (10:1).



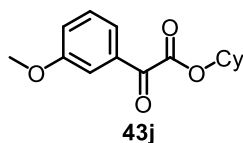
^1H NMR (300 MHz, CDCl_3) δ 7.86–7.76 (m, 2H), 7.49–7.34 (m, 2H), 5.10 (m, 1H), 2.42 (s, 3H), 2.03–1.96 (m, 2H), 1.82–1.76 (m, 2H), 1.64–1.55 (m, 3H), 1.50–1.28 (m, 3H).

^{13}C NMR (75 MHz, CDCl_3) δ 187.1, 163.9, 138.9, 135.7, 132.7, 130.3, 128.8, 127.4, 75.4, 31.5, 25.3, 23.7, 21.4.

IR (film): ν (cm^{-1}) 2961, 1729, 1686, 1407, 1256, 1079, 1013, 866, 792, 687.

HRMS (ESI, m/z) calcd for $\text{C}_{15}\text{H}_{18}\text{O}_3\text{Na}$ $[\text{M}+\text{Na}]^+$: 269.1148, found: 269.1144.

$R_f = 0.6$ in *n*-hexane/EtOAc (10:1).



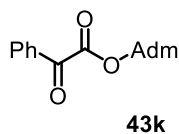
$^1\text{H NMR}$ (300 MHz, CDCl_3) δ 7.56 (dt, $J = 7.7, 1.5$ Hz, 1H), 7.53–7.51 (m, 1H), 7.41 (t, $J = 8.0$ Hz, 1H), 7.22–7.17 (m, 1H), 5.10 (m, 1H), 3.86 (s, 3H), 2.05–1.96 (m, 2H), 1.84–1.74 (m, 2H), 1.67–1.53 (m, 3H), 1.50–1.23 (m, 3H).

$^{13}\text{C NMR}$ (75 MHz, CDCl_3) δ 186.8, 163.8, 160.1, 133.9, 130.0, 123.1, 121.8, 113.3, 75.5, 55.6, 31.5, 25.3, 23.7.

IR (film): ν (cm^{-1}) 2936, 2859, 1728, 1685, 1588, 1483, 1452, 1293, 1245, 1186, 1158, 1119, 1002, 897, 791, 753, 724, 676, 556, 483, 440.

$R_f = 0.6$ in *n*-hexane/EtOAc (10:1).

α -Ketoester **43d** was commercially available, and **43e-f**, **43k-m** were synthesized from glyoxylic acid according to published method.⁷ Analytical data of **43e-f** were consistent with the reported data.^{7,8} The experimental data of **43k-m** are shown below.



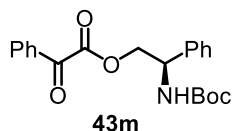
$^1\text{H NMR}$ (300 MHz, CDCl_3) δ 8.00–7.96 (m, 2H), 7.63 (m, 1H), 7.53–7.47 (m, 2H), 2.29 (m, 6H), 2.25 (m, 3H), 1.72 (m, 6H).

$^{13}\text{C NMR}$ (75 MHz, CDCl_3) δ 186.8, 163.5, 134.6, 132.7, 130.0, 128.9, 85.1, 41.5, 36.1, 31.1.

IR (film): ν (cm^{-1}) 2910, 2858, 1718, 1682, 1592, 1450, 1341, 1295, 1201, 1173, 1102, 1040, 988, 934, 873, 838, 758, 725, 688, 541, 441, 397.

HRMS (ESI, m/z) calcd for $\text{C}_{18}\text{H}_{20}\text{O}_3\text{Na}$ $[\text{M}+\text{Na}]^+$: 307.1305, found: 307.1300.

$R_f = 0.5$ in *n*-hexane/EtOAc (15:1).



$^1\text{H NMR}$ (300 MHz, CDCl_3) δ 7.85–7.82 (m, 2H), 7.63 (m, 1H), 7.48–7.42 (m, 2H), 7.38–7.32 (m, 5H), 5.15–4.93 (m, 2H), 4.71–4.58 (m, 2H), 1.41 (s, 9H).

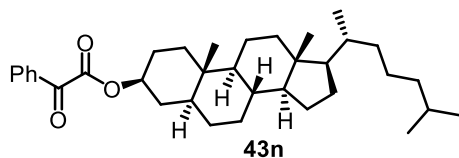
$^{13}\text{C NMR}$ (75 MHz, CDCl_3) δ 185.9, 163.5, 155.1, 135.0, 130.2, 129.0, 129.0, 129.9, 128.2, 126.8,

126.6, 80.3, 67.8, 66.0, 28.4.

IR (film): ν (cm⁻¹) 3377, 2909, 2975, 2859, 1724, 1680, 1516, 1452, 1365, 1289, 1246, 1198, 1165, 1052, 991, 857, 753, 692, 551, 438.

HRMS (ESI, m/z) calcd for C₂₁H₂₃NO₅Na [M+Na]⁺: 392.1468, found: 392.1463.

R_f = 0.4 in *n*-hexane/EtOAc (10:1).



¹H NMR (300 MHz, CDCl₃) δ 8.02–7.97 (m, 2H), 7.64 (m, 1H), 7.53–7.48 (m, 2H), 5.02 (m, 1H), 2.00–1.95 (m, 2H), 2.00–1.95 (m, 2H), 1.83–1.50 (m, 11H), 1.39–1.22 (m, 9H), 1.16–1.07 (m, 5H), 1.00–0.97 (m, 2H), 0.90 (d, J = 6.5 Hz, 3H), 0.87 (d, J = 1.1 Hz, 3H), 0.86 (d, J = 1.0 Hz, 3H), 0.84 (s, 3H), 0.65 (s, 3H).

¹³C NMR (75 MHz, CDCl₃) δ 186.8, 163.8, 134.8, 132.7, 130.0, 128.9, 73.8, 56.5, 56.4, 54.3, 44.9, 42.7, 40.0, 39.6, 36.8, 36.3, 35.9, 35.6, 35.5, 33.9, 32.1, 28.7, 28.3, 28.1, 27.5, 24.3, 23.9, 22.9, 22.6, 21.3, 18.8, 12.3, 12.2.

IR (film): ν (cm⁻¹) 2910, 2856, 1728, 1680, 1516, 1452, 1331, 1291, 1203, 1171, 1040, 991, 922, 855, 754, 686.

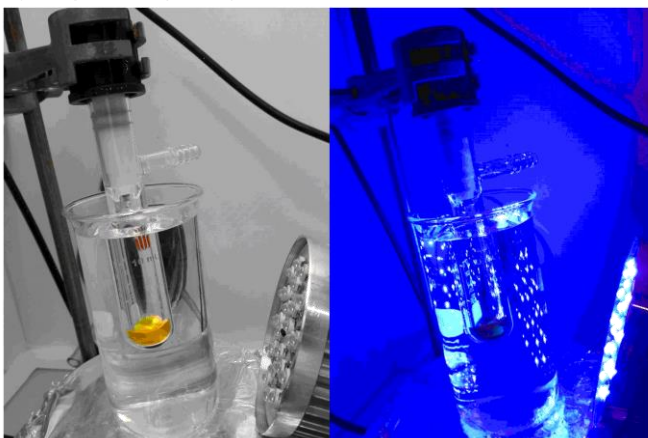
HRMS (ESI, m/z) calcd for C₃₅H₅₂O₃Na [M+Na]⁺: 543.3809, found: 543.3800.

R_f = 0.5 in *n*-hexane/EtOAc (10:1).

5.6.3 Rhodium-Catalyzed β -(sp^3)-C–H Functionalization Activated by Visible Light

A dried 10 mL Schlenk tube was charged with 2-acyl imidazoles **42a-o** (0.10 mmol), Δ -**RhS1** (3.4 mg, 4 mol%) or Δ -**RhS2** (4.0 mg, 4 mol%), and DABCO (2.2 mg, 20 mol%). Acetone (1.0 mL, 0.1 M) was added via syringe, followed by 1,2-dicarbonyl compounds **43d-n** (0.3 mmol, 3 equiv.). While turning to the scope with 2-acyl pyridines, **42p-r** (0.3 mmol, 3 equiv.) and **43d** (0.1 mmol) were employed. The reaction mixture was degassed via freeze-pump-thaw for three cycles. After the mixture was thoroughly degassed, the Schlenk tube was sealed tightly with a Teflon septum and immersed into a water bath which was positioned close to 24 W blue LEDs. The reaction was stirred at room temperature for the indicated time (monitored by TLC) under an atmosphere of nitrogen. Afterwards, the mixture was diluted with CH_2Cl_2 . The combined organic solutions were concentrated under reduced pressure and then subjected to 1H NMR analysis to determine the dr value of the crude products except otherwise noted. Afterwards, the crude material was purified by flash chromatography on silica gel (*n*-hexane/EtOAc) to afford the hetero-coupling products **45a-z**. Racemic samples were obtained by carrying out the reactions with *rac*-**RhS1**. The enantiomeric excess was determined by chiral HPLC analysis.

a) Setup of the reported photoreaction



b) Emission spectrum of the employed 24 W blue LEDs

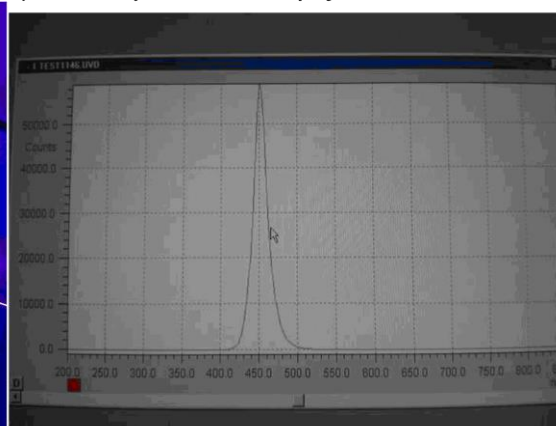
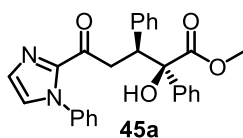
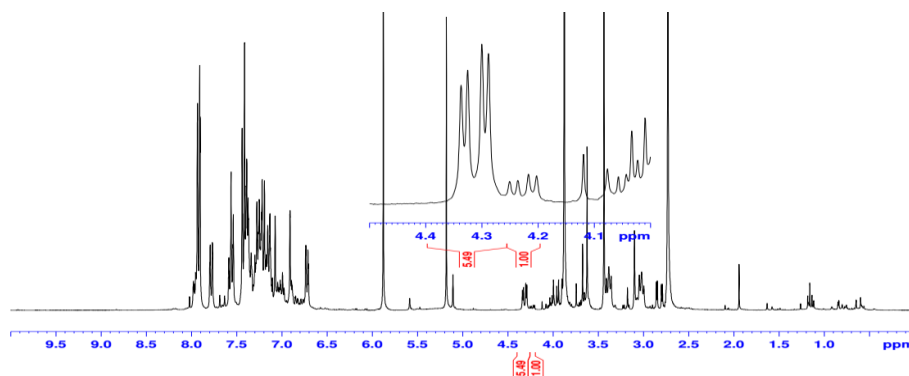


Figure 99 a) Setup of the reported photoreactions; b) emission spectrum of the employed 24 W blue LEDs.



According to the general procedure, a mixture of **42a** (27.6 mg, 0.10 mmol), **43d** (49.0 mg, 3.0 equiv.), Δ -**RhS1** (3.4 mg, 4 mol%), and DABCO (2.2 mg, 20 mol%) in acetone (1.0 mL, 0.1 M) was stirred under nitrogen atmosphere for 16 hours under irradiation with 24 W blue LEDs at room temperature (in a water bath) to afford **45a** as a pale yellow solid (39.1 mg, 89% yield, 5.5:1 dr, 98% ee). Purification conditions: *n*-hexane/EtOAc = 10:1 to 4:1, $R_f = 0.4$ in *n*-hexane/EtOAc (4:1). The NMR yield of 95% was observed before purification. Enantiomeric excess was established by HPLC analysis using a Chiralpak IG column, ee = 98% (HPLC: 254 nm, *n*-hexane/isopropanol = 70:30, flow rate 1 mL/min, 40 °C, t_r (major) = 12.1 min, t_r (minor) = 16.1 min). $[\alpha]_D^{22} = -47.6^\circ$ (*c* 1.0, CH₂Cl₂). The dr value was determined by ¹H NMR analysis of the crude product as shown below:

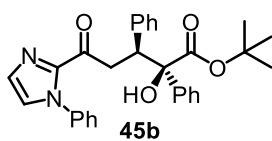


¹H NMR (300 MHz, CD₂Cl₂) δ 7.80–7.77 (m, 2H), 7.41–7.38 (m, 2H), 7.32–7.20 (m, 6H), 7.18–7.12 (m, 3H), 7.10 (d, $J = 0.9$ Hz, 1H), 6.93 (d, $J = 0.9$ Hz, 1H), 6.77–6.74 (m, 2H), 4.34 (dd, $J = 11.1, 3.6$ Hz, 1H), 3.95 (dd, $J = 17.2, 11.1$ Hz, 1H), 3.80 (br, 1H), 3.47 (s, 3H), 2.83 (dd, $J = 17.2, 3.6$ Hz, 1H).

¹³C NMR (75 MHz, CD₂Cl₂) δ 189.9, 174.9, 143.5, 140.3, 139.5, 138.7, 130.2, 129.7, 129.0, 128.7 (2C), 128.3 (2C), 127.6, 127.1, 127.0, 126.0, 81.4, 49.1, 41.5, 39.6.

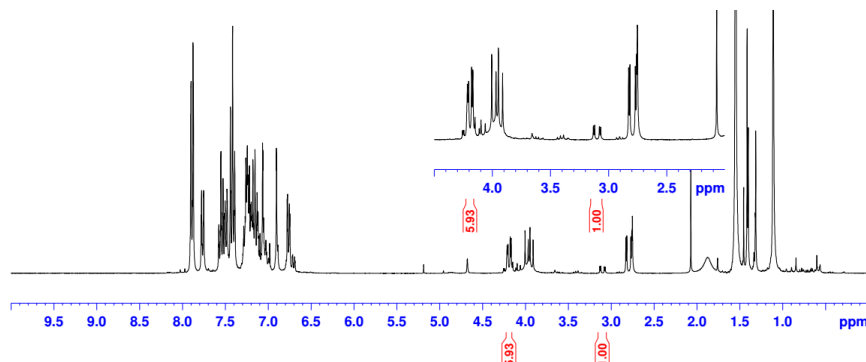
IR (film): ν (cm⁻¹) 3501, 3062, 3030, 2953, 2919, 1731, 1686, 1597, 1494, 1447, 1406, 1303, 1241, 1177, 1121, 1072, 1033, 967, 917, 859, 759, 698, 653, 597, 523.

HRMS (EI, m/z) calcd for C₂₇H₂₅N₂O₄ [M+H]⁺: 441.1809, found: 441.1802.



According to the general procedure, a mixture of **42a** (27.6 mg, 0.10 mmol), **43e** (61.8 mg, 3.0 equiv.), Δ -**RhS1** (3.4 mg, 4 mol%), and DABCO (2.2 mg, 20 mol%) in acetone (1.0 mL, 0.1 M) was stirred under nitrogen atmosphere for 16 hours under irradiation with 24 W blue

LEDs at room temperature (in a water bath) to afford **45b** as a pale yellow solid (43.9 mg, 91% yield, 5.9:1 dr, 98% ee). Purification conditions: *n*-hexane/EtOAc = 10:1 to 5:1, $R_f = 0.5$ in *n*-hexane/EtOAc (4:1). The NMR yield of 95% was observed before purification. Enantiomeric excess was established by HPLC analysis using a Chiralpak AD-H column, ee = 98% (HPLC: 254 nm, *n*-hexane/isopropanol = 80:20, flow rate 1 mL/min, 25 °C, t_r (major) = 13.9 min, t_r (minor) = 18.3 min). $[\alpha]_D^{22} = -32.2^\circ$ (c 1.0, CH_2Cl_2). The dr value was determined by ^1H NMR analysis of the crude product as shown below:

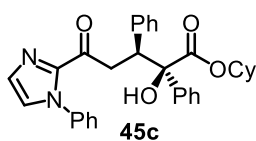


^1H NMR (300 MHz, CD_2Cl_2) δ 7.96–7.86 (m, 2H), 7.58–7.55 (m, 2H), 7.43–7.30 (m, 6H), 7.27–7.22 (m, 3H), 7.14 (d, $J = 0.8$ Hz, 1H), 7.04 (d, $J = 0.9$ Hz, 1H), 6.93–6.89 (m, 2H), 4.25 (dd, $J = 13.4, 3.1$ Hz, 1H), 4.12 (br, 1H), 3.95 (dd, $J = 17.3, 11.3$ Hz, 1H), 2.84 (dd, $J = 17.4, 3.2$ Hz, 1H), 1.23 (s, 9H).

^{13}C NMR (75 MHz, CD_2Cl_2) δ 190.1, 173.5, 143.5, 141.4, 140.2, 138.8, 130.8, 129.7, 129.1, 128.7, 128.5, 128.1, 127.4, 127.1, 126.8, 126.1, 84.0, 81.1, 48.7, 40.4, 27.7.

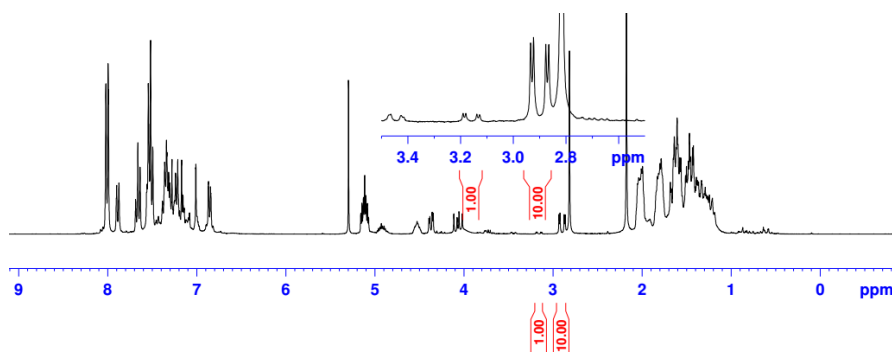
IR (film): ν (cm^{-1}) 3244, 2979, 2929, 1723, 1686, 1595, 1492, 1451, 1406, 1364, 1252, 1160, 1120, 1074, 1032, 960, 918, 843, 755, 695, 635, 594, 536, 425.

HRMS (EI, m/z) calcd for $\text{C}_{30}\text{H}_{31}\text{N}_2\text{O}_4$ $[\text{M}+\text{H}]^+$: 483.2278, found: 483.2271.



According to the general procedure, a mixture of **42a** (27.6 mg, 0.10 mmol), **43f** (69.6 mg, 3.0 equiv.), Δ -**Rhs2** (4.0 mg, 4 mol%), and DABCO (2.2 mg, 20 mol%) in acetone (1.0 mL, 0.1 M) was stirred under nitrogen atmosphere for 16 hours under irradiation with 24 W blue LEDs at room temperature (in a water bath) to afford **45c** as a pale yellow solid (46.2 mg, 91% yield, 10.0:1 dr, >99% ee). Purification conditions: *n*-hexane/EtOAc = 10:1 to 5:1, $R_f = 0.5$ in *n*-hexane/EtOAc (5:1). The NMR yield of 98% was observed before purification. Enantiomeric excess was established by HPLC analysis using a Chiralpak AD-H column, ee = >99% (HPLC: 254 nm, *n*-hexane/isopropanol = 80:20, flow rate 1 mL/min, 25 °C, t_r (major) = 10.6 min, t_r (minor) = 14.1 min). $[\alpha]_D^{22} = -38.4^\circ$ (c 1.0,

CH₂Cl₂). The dr value was determined by ¹H NMR analysis of the crude product as shown below:

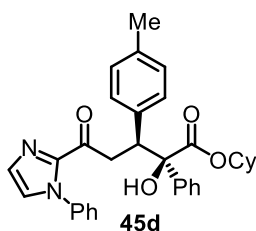


¹H NMR (300 MHz, CDCl₃) δ 7.88–7.85 (m, 2H), 7.55–7.51 (m, 2H), 7.37–7.27 (m, 6H), 7.25–7.18 (m, 3H), 7.16 (d, $J = 0.9$ Hz, 1H), 7.00 (d, $J = 0.9$ Hz, 1H), 6.87–6.83 (m, 2H), 4.51 (m, 1H), 4.35 (dd, $J = 11.0, 3.4$ Hz, 1H), 4.04 (dd, $J = 17.2, 11.0$ Hz, 1H), 3.95 (s, 1H), 2.88 (dd, $J = 17.3, 3.4$ Hz, 1H), 1.70–1.60 (m, 2H), 1.55–1.42 (m, 3H), 1.40–1.28 (m, 2H), 1.24–1.12 (m, 3H).

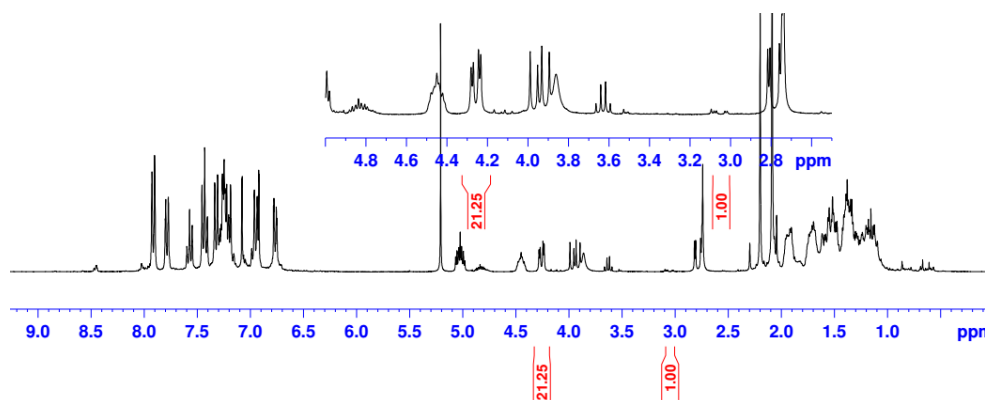
¹³C NMR (75 MHz, CDCl₃) δ 189.7, 173.6, 143.2, 140.7, 139.4, 138.5, 130.3, 129.4, 128.7, 128.4, 128.2, 127.9, 127.8, 127.2, 126.8, 126.6, 125.8, 80.8, 75.7, 48.4, 39.8, 31.3, 31.0, 25.3, 23.6, 23.4.

IR (film): ν (cm⁻¹) 2932, 2857, 1729, 1683, 1492, 1448, 1408, 1333, 1301, 1227, 1162, 1120, 1071, 1032, 1007, 965, 917, 758, 725, 692, 603, 533, 412.

HRMS (EI, m/z) calcd for C₃₂H₃₃N₂O₄ [M+H]⁺: 509.2435, found: 509.2484.



According to the general procedure, a mixture of **42b** (29.0 mg, 0.10 mmol), **43f** (69.6 mg, 3.0 equiv.), Δ -**Rhs2** (4.0 mg, 4 mol%), and DABCO (2.2 mg, 20 mol%) in acetone (1.0 mL, 0.1 M) was stirred under nitrogen atmosphere for 18 hours under irradiation with 24 W blue LEDs at room temperature (in a water bath) to afford **45d** as a pale yellow solid (49.9 mg, 89% yield, >20:1 dr, 98% ee). Purification conditions: *n*-hexane/EtOAc = 10:1 to 4:1, $R_f = 0.5$ in *n*-hexane/EtOAc (5:1). Enantiomeric excess was established by HPLC analysis using a Chiralpak AD-H column, ee = 98% (HPLC: 254 nm, *n*-hexane/isopropanol = 80:20, flow rate 1 mL/min, 40 °C, t_r (major) = 11.9 min, t_r (minor) = 9.3 min). $[\alpha]_D^{22} = +30.2^\circ$ (c 1.0, CH₂Cl₂). The dr value was determined by ¹H NMR analysis of the crude product as shown below:

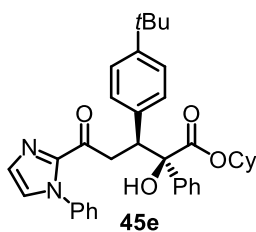


^1H NMR (300 MHz, CD_2Cl_2) δ 7.90–7.86 (m, 2H), 7.42–7.28 (m, 8H), 7.14 (d, $J = 1.0$ Hz, 1H), 7.09–7.04 (m, 3H), 6.90–6.86 (m, 2H), 4.53 (m, 1H), 4.27 (dd, $J = 11.4, 3.3$ Hz, 1H), 4.04 (dd, $J = 11.0, 17.2$ Hz, 1H), 3.97 (s, 1H), 3.91 (dd, $J = 17.3, 11.5$ Hz, 1H), 2.82 (dd, $J = 17.2, 3.3$ Hz, 1H), 2.30 (s, 3H), 1.80–1.66 (m, 2H), 1.55–1.42 (m, 4H), 1.41–1.10 (m, 4H).

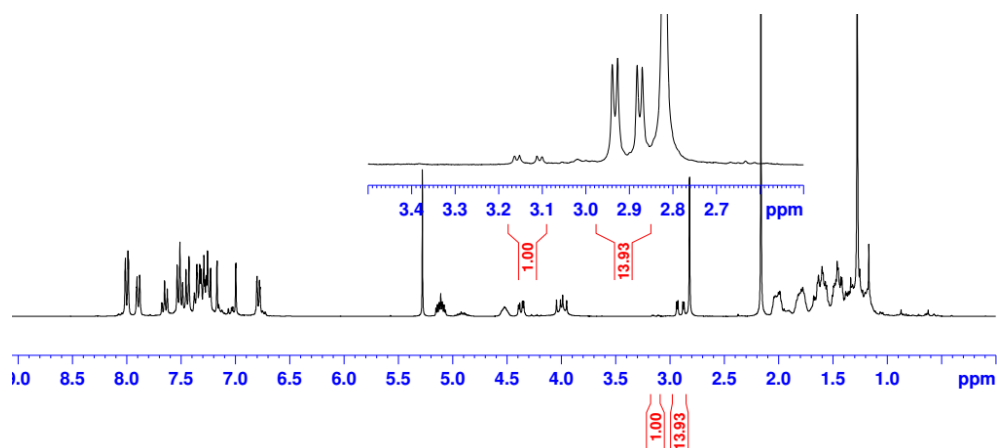
^{13}C NMR (75 MHz, CD_2Cl_2) δ 191.9, 175.7, 145.3, 142.7, 140.5, 138.9, 138.2, 132.1, 131.4, 130.7, 130.5, 130.4, 130.2, 129.8, 128.8, 128.7, 127.8, 82.9, 77.6, 50.0, 41.8, 33.3, 33.0, 27.3, 25.6, 25.4, 22.8.

IR (film): ν (cm^{-1}) 2933, 2857, 1728, 1680, 1594, 1494, 1446, 1406, 1334, 1305, 1229, 1161, 1121, 1070, 1031, 967, 915, 810, 762, 729, 691, 600, 536, 459.

HRMS (ESI, m/z) calcd for $\text{C}_{33}\text{H}_{35}\text{N}_2\text{O}_4$ $[\text{M}+\text{H}]^+$: 523.2591, found: 523.2584.



According to the general procedure, a mixture of **42c** (33.2 mg, 0.10 mmol), **43f** (69.6 mg, 3.0 equiv.), Δ -**RhS2** (4.0 mg, 4 mol%), and DABCO (2.2 mg, 20 mol%) in acetone (1.0 mL, 0.1 M) was stirred under nitrogen atmosphere for 18 hours under irradiation with 24 W blue LEDs at room temperature (in a water bath) to afford **45e** as a pale yellow oil (49.7 mg, 88% yield, 14:1 dr, 99% ee). Purification conditions: *n*-hexane/EtOAc = 10:1 to 5:1, $R_f = 0.5$ in *n*-hexane/EtOAc (6:1). Enantiomeric excess was established by HPLC analysis using a Chiralpak AD-H column, ee = 99% (HPLC: 254 nm, *n*-hexane/isopropanol = 80:20, flow rate 1 mL/min, 40 °C, t_r (major) = 8.3 min, t_r (minor) = 6.7 min). $[\alpha]_D^{22} = +30.2^\circ$ (c 1.0, CH_2Cl_2). The dr value was determined by ^1H NMR analysis of the crude product as shown below:

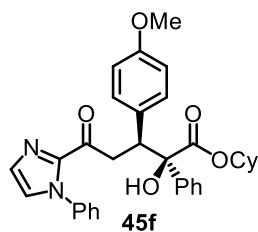


^1H NMR (300 MHz, CD_2Cl_2) δ 7.90–7.87 (m, 2H), 7.42–7.25 (m, 10H), 7.15 (d, $J = 0.9$ Hz, 1H), 7.04 (d, $J = 0.9$ Hz, 1H), 6.87–6.83 (m, 2H), 4.50 (m, 1H), 4.28 (dd, $J = 11.3, 3.2$ Hz, 1H), 3.95–3.85 (m, 2H), 2.82 (dd, $J = 17.2, 3.4$ Hz, 1H), 1.76–1.40 (m, 6H), 1.39–1.50 (m, 13H).

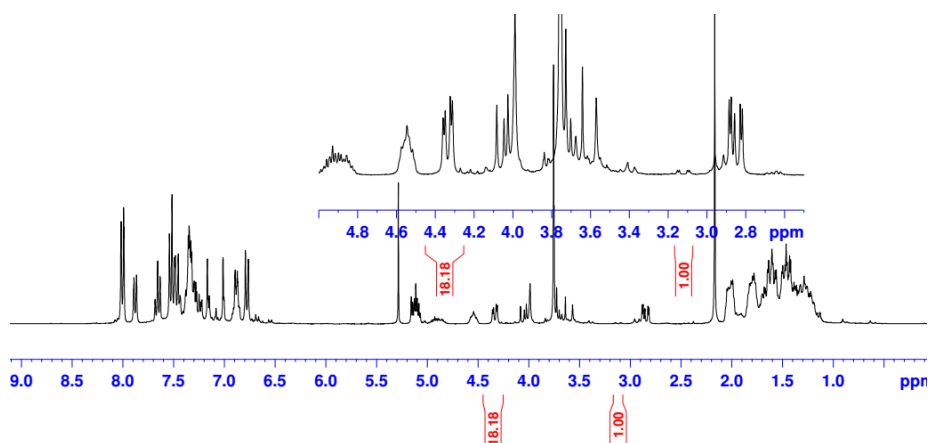
^{13}C NMR (75 MHz, CD_2Cl_2) δ 189.9, 173.5, 150.1, 143.3, 140.8, 138.5, 136.3, 129.9, 129.4, 128.7, 128.4, 128.2, 127.8, 126.7, 126.6, 125.7, 124.7.

IR (film): ν (cm^{-1}) 3348, 2937, 2859, 2178, 2142, 2079, 2031, 1973, 1922, 1730, 1682, 1494, 1446, 1406, 1328, 1230, 1165, 1121, 1073, 1027, 960, 919, 875, 764, 694, 561, 520, 470, 424.

HRMS (EI, m/z) calcd for $\text{C}_{36}\text{H}_{41}\text{N}_2\text{O}_4$ $[\text{M}+\text{H}]^+$: 565.3061, found: 565.3117.



According to the general procedure, a mixture of **42d** (30.6 mg, 0.10 mmol), **43f** (69.6 mg, 3.0 equiv.), Δ -**Rhs2** (4.0 mg, 4 mol%), and DABCO (2.2 mg, 20 mol%) in acetone (1.0 mL, 0.1 M) was stirred under nitrogen atmosphere for 16 hours under irradiation with 24 W blue LEDs at room temperature (in a water bath) to afford **45f** as a pale yellow solid (53.0 mg, 99% yield, 18:1 dr, 97% ee). Purification conditions: *n*-hexane/EtOAc = 10:1 to 5:1, $R_f = 0.5$ in *n*-hexane/EtOAc (4:1). Enantiomeric excess was established by HPLC analysis using a Chiralpak AD-H column, ee = 97% (HPLC: 254 nm, *n*-hexane/isopropanol = 80:20, flow rate 1 mL/min, 25 °C, t_r (major) = 23.7 min, t_r (minor) = 16.9 min). $[\alpha]_D^{22} = +22.6^\circ$ (c 1.0, CH_2Cl_2). The dr value was determined by ^1H NMR analysis of the crude product as shown below:

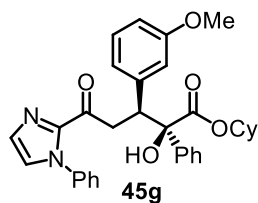


^1H NMR (300 MHz, CD_2Cl_2) δ 7.89–7.86 (m, 2H), 7.48–7.27 (m, 8H), 7.14 (d, $J = 1.0$ Hz, 1H), 7.00 (d, $J = 1.0$ Hz, 1H), 6.92–6.88 (m, 2H), 6.80–6.75 (m, 2H), 4.53 (m, 1H), 4.25 (dd, $J = 11.4, 3.1$ Hz, 1H), 3.97 (s, 1H), 3.89 (dd, $J = 17.2, 11.4$ Hz, 1H), 3.75 (s, 3H), 2.79 (dd, $J = 17.2, 3.3$ Hz, 1H), 1.80–1.62 (m, 2H), 1.54–1.39 (m, 4H), 1.38–1.10 (m, 4H).

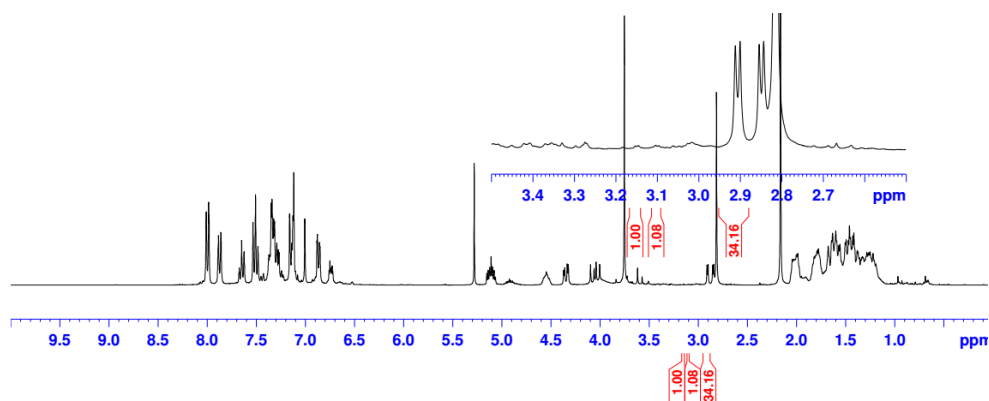
^{13}C NMR (75 MHz, CD_2Cl_2) δ 189.9, 173.7, 158.9, 143.3, 140.7, 138.5, 131.3, 129.4, 128.7, 128.4, 128.2, 127.8, 126.8, 126.6, 125.8, 113.1, 81.0, 75.6, 55.2, 47.6, 39.9, 31.4, 31.0, 25.3, 23.6, 23.4.

IR (film): ν (cm^{-1}) 3121, 3004, 2936, 2855, 1729, 1681, 1602, 1503, 1446, 1406, 1334, 1299, 1233, 1176, 1119, 1073, 1029, 971, 917, 829, 764, 732, 692, 601, 537.

HRMS (EI, m/z) calcd for $\text{C}_{33}\text{H}_{35}\text{N}_2\text{O}_5$ $[\text{M}+\text{H}]^+$: 539.2540, found: 539.2622.



According to the general procedure, a mixture of **42e** (30.6 mg, 0.10 mmol), **43f** (69.6 mg, 3.0 equiv.), Δ -**RhS2** (4.0 mg, 4 mol%), and DABCO (2.2 mg, 20 mol%) in acetone (1.0 mL, 0.1 M) was stirred under nitrogen atmosphere for 16 hours under irradiation with 24 W blue LEDs at room temperature (in a water bath) to afford **45g** as a pale yellow solid (45.2 mg, 84% yield, >20:1 dr, >99% ee). Purification conditions: *n*-hexane/EtOAc = 10:1 to 5:1, $R_f = 0.5$ in *n*-hexane/EtOAc (4:1). Enantiomeric excess was established by HPLC analysis using a Chiralpak AD-H column, ee = >99% (HPLC: 254 nm, *n*-hexane/isopropanol = 80:20, flow rate 1 mL/min, 40 °C, t_r (major) = 9.1 min, t_r (minor) = 11.2 min). $[\alpha]_D^{22} = -35.8^\circ$ (c 1.0, CH_2Cl_2). The dr value was determined by ^1H NMR analysis of the crude product as shown below:

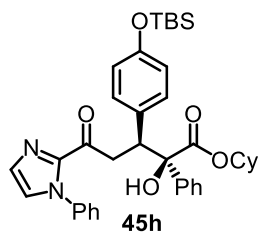


^1H NMR (300 MHz, CD_2Cl_2) δ 7.80–7.77 (m, 2H), 7.30–7.17 (m, 6H), 7.09 (d, $J = 0.7$ Hz, 1H), 7.06–7.00 (m, 3H), 6.93 (d, $J = 0.7$ Hz, 1H), 6.81–6.78 (m, 2H), 6.93 (dt, $J = 7.0, 2.2$ Hz, 1H), 4.46 (m, 1H), 4.26 (dd, $J = 10.9, 3.4$ Hz, 1H), 3.95 (dd, $J = 17.2, 10.9$ Hz, 1H), 3.88 (br, 1H), 3.68 (s, 3H), 2.78 (dd, $J = 17.2, 3.4$ Hz, 1H), 1.66–1.32 (m, 5H), 1.25–1.02 (m, 5H).

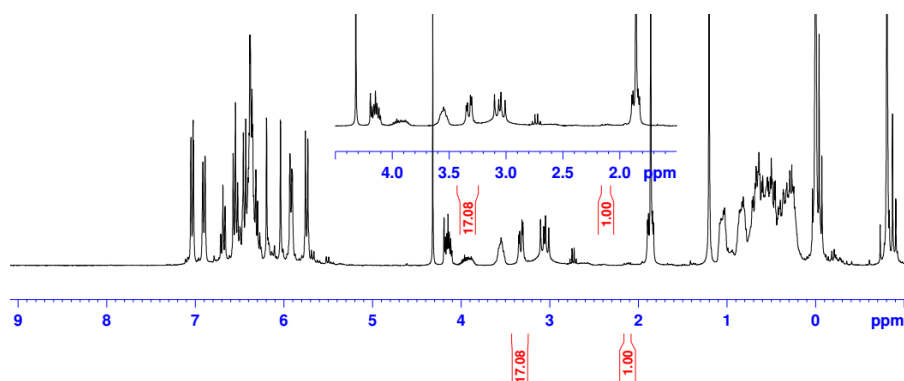
^{13}C NMR (75 MHz, CDCl_3) δ 189.9, 173.6, 159.2, 143.3, 140.9, 140.5, 138.3, 129.5, 128.8, 128.7, 128.5, 128.2, 127.8, 126.7 (2C), 125.7, 122.8, 115.6, 113.0, 80.7, 75.5, 55.3, 48.4, 39.8, 31.3, 31.0, 25.3, 23.6, 23.4.

IR (film): ν (cm^{-1}) 3384, 3284, 2933, 2852, 1724, 1682, 1593, 1489, 1445, 1402, 1327, 1228, 1160, 1114, 1033, 959, 908, 829, 761, 692, 641, 518, 477, 409.

HRMS (ESI, m/z) calcd for $\text{C}_{33}\text{H}_{35}\text{N}_2\text{O}_5$ $[\text{M}+\text{H}]^+$: 539.2540, found: 539.2534.



According to the general procedure, a mixture of **42f** (40.6 mg, 0.10 mmol), **43f** (69.6 mg, 3.0 equiv.), Δ -**RhS2** (4.0 mg, 4 mol%), and DABCO (2.2 mg, 20 mol%) in acetone (1.0 mL, 0.1 M) was stirred under nitrogen atmosphere for 16 hours under irradiation with 24 W blue LEDs at room temperature (in a water bath) to afford **45h** as a pale yellow solid (50.8 mg, 79% yield, 17:1 dr, 98% ee). Purification conditions: *n*-hexane/EtOAc = 10:1 to 5:1, $R_f = 0.5$ in *n*-hexane/EtOAc (6:1). Enantiomeric excess was established by HPLC analysis using a Chiralpak AD-H column, ee = 98% (HPLC: 254 nm, *n*-hexane/isopropanol = 95:5, flow rate 1 mL/min, 40 °C, t_r (major) = 14.1 min, t_r (minor) = 17.5 min). $[\alpha]_D^{22} = -30.0^\circ$ (c 1.0, CH_2Cl_2). The dr value was determined by ^1H NMR analysis of the crude product as shown below:

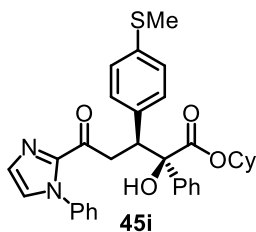


^1H NMR (300 MHz, CD_2Cl_2) δ 7.90–7.82 (m, 2H), 7.42–7.22 (m, 8H), 7.13 (d, $J = 0.9$ Hz, 1H), 7.04 (d, $J = 0.9$ Hz, 1H), 6.93–6.88 (m, 2H), 6.74–6.68 (m, 2H), 4.50 (m, 1H), 4.21 (dd, $J = 11.3, 3.2$ Hz, 1H), 3.99 (s, 1H), 3.90 (dd, $J = 17.1, 11.3$ Hz, 1H), 2.75 (dd, $J = 17.0, 3.2$ Hz, 1H), 1.78–1.60 (m, 2H), 1.58–1.40 (m, 4H), 1.34–1.11 (m, 4H), 0.96 (s, 9H), 0.16 (s, 6H).

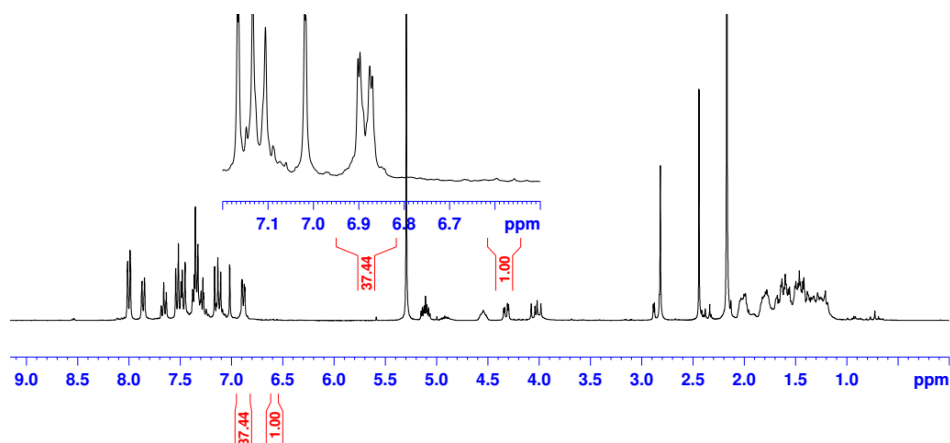
^{13}C NMR (75 MHz, CD_2Cl_2) δ 189.9, 173.6, 154.9, 143.3, 140.8, 138.5, 132.1, 131.3, 129.4, 128.7, 128.4, 128.2, 127.8, 126.8, 126.6, 125.8, 119.3, 81.0, 75.6, 47.9, 39.9, 31.4, 31.1, 25.5, 25.3, 23.3, 18.2, –4.62, –4.66.

IR (film): ν (cm^{-1}) 2930, 2856, 1728, 1683, 1602, 1504, 1449, 1403, 1256, 1233, 1173, 1120, 1021, 915, 812, 765, 724, 690, 600, 541, 516, 473.

HRMS (ESI, m/z) calcd for $\text{C}_{38}\text{H}_{47}\text{N}_2\text{O}_5\text{Si}$ $[\text{M}+\text{H}]^+$: 639.3249, found: 639.3248.



According to the general procedure, a mixture of **42g** (32.2 mg, 0.10 mmol), **43f** (69.6 mg, 3.0 equiv.), Δ -**RhS2** (4.0 mg, 4 mol%), and DABCO (2.2 mg, 20 mol%) in acetone (1.0 mL, 0.1 M) was stirred under nitrogen atmosphere for 16 hours under irradiation with 24 W blue LEDs at room temperature (in a water bath) to afford **45i** as a pale yellow solid (53.5 mg, 97% yield, >20:1 dr, 98% ee). Purification conditions: *n*-hexane/EtOAc = 10:1 to 5:1, $R_f = 0.4$ in *n*-hexane/EtOAc (4:1). Enantiomeric excess was established by HPLC analysis using a Chiralpak AD-H column, ee = 98% (HPLC: 254 nm, *n*-hexane/isopropanol = 80:20, flow rate 1 mL/min, 40 °C, t_r (major) = 11.8 min, t_r (minor) = 16.6 min). $[\alpha]_D^{22} = +35.0^\circ$ (c 1.0, CH_2Cl_2). The dr value²² was determined by ^1H NMR analysis of the crude product as shown below:

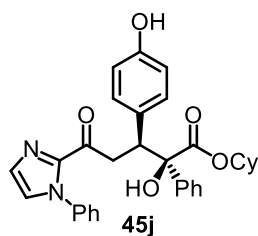


^1H NMR (300 MHz, CD_2Cl_2) δ 7.88–7.85 (m, 2H), 7.45–7.29 (m, 8H), 7.16–7.10 (m, 3H), 7.05 (d, J = 1.0 Hz, 1H), 6.94–6.86 (m, 2H), 4.55 (m, 1H), 4.35 (dd, J = 11.4, 3.3 Hz, 1H), 4.04 (s, 1H), 3.93 (dd, J = 11.4, 17.3 Hz, 1H), 2.82 (dd, J = 17.4, 3.3 Hz, 1H), 2.45 (s, 3H), 1.80–1.64 (m, 2H), 1.58–1.42 (m, 4H), 1.39–1.11 (m, 4H).

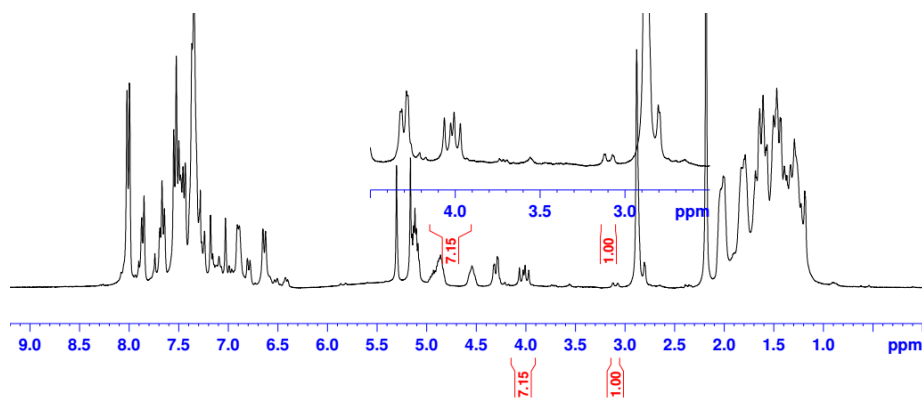
^{13}C NMR (75 MHz, CDCl_3) δ 189.7, 173.6, 143.2, 140.6, 138.4, 137.4, 136.2, 130.8, 129.4, 128.8, 128.4, 128.3, 127.9, 126.9, 126.6, 125.8 (2C), 80.8, 75.7, 47.9, 39.8, 31.4, 31.0, 25.3, 23.6, 23.3, 15.5.

IR (film): ν (cm^{-1}) 2930, 2857, 1729, 1681, 1595, 1491, 1445, 1407, 1333, 1295, 1229, 1162, 1121, 1071, 1031, 964, 917, 838, 761, 729, 692, 591, 540, 424, 3340.

HRMS (ESI, m/z) calcd for $\text{C}_{33}\text{H}_{35}\text{N}_2\text{O}_4\text{S}$ $[\text{M}+\text{H}]^+$: 555.2312, found: 555.2311.



According to the general procedure, a mixture of **42h** (29.2 mg, 0.10 mmol), **43f** (69.6 mg, 3.0 equiv.), Δ -**RhS2** (4.0 mg, 4 mol%), and DABCO (2.2 mg, 20 mol%) in acetone (1.0 mL, 0.1 M) was stirred under nitrogen atmosphere for 16 hours under irradiation with 24 W blue LEDs at room temperature (in a water bath) to afford **45j** as a pale yellow oil (27.2 mg, 52% yield, 7.1:1 dr, 97% ee). Enantiomeric excess was established by HPLC analysis using a Chiralpak AD-H column, ee = 97% (HPLC: AD-H, 254 nm, *n*-hexane/isopropanol = 60:40, flow rate 0.5 mL/min, 40 °C, t_r (major) = 10.5 min, t_r (minor) = 12.0 min). $[\alpha]_{\text{D}}^{22} = -27.2^\circ$ (c 1.0, CH_2Cl_2). The dr value was determined by ^1H NMR analysis of the crude product as shown below:

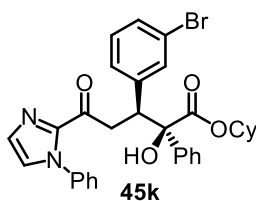


^1H NMR (300 MHz, CD_2Cl_2) δ 7.88–7.84 (m, 2H), 7.41–7.30 (m, 8H), 7.15 (d, $J = 1.0$ Hz, 1H), 7.06 (d, $J = 1.0$ Hz, 1H), 6.98–6.90 (m, 3H), 6.63 (dt, $J = 9.6, 2.3$ Hz, 1H), 5.70 (br, 1H), 4.53 (m, 1H), 4.24 (dd, $J = 11.4, 3.1$ Hz, 1H), 3.97–3.87 (m, 2H), 2.76 (dd, $J = 17.2, 3.2$ Hz, 1H), 1.75–1.60 (m, 2H), 1.55–1.45 (m, 4H), 1.30–1.21 (m, 4H).

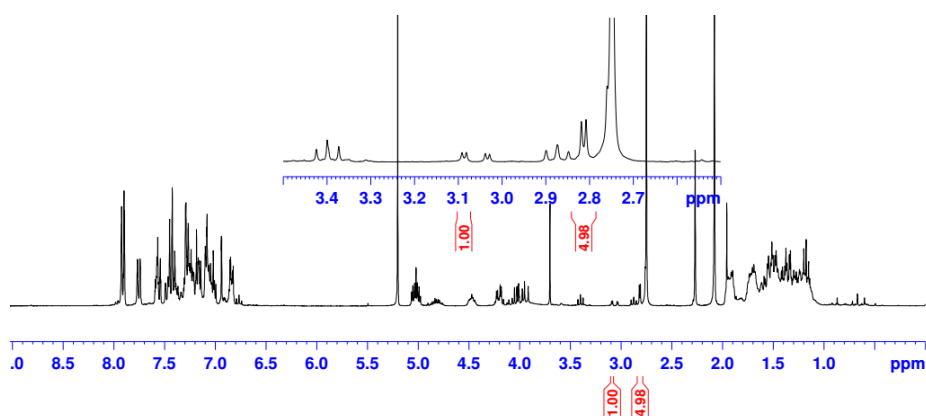
^{13}C NMR (75 MHz, CD_2Cl_2) δ 189.8, 173.7, 155.2, 143.1, 140.6, 138.3, 131.3, 130.9, 129.2, 128.7, 128.4, 128.1, 127.7, 126.8, 126.5, 125.7, 114.6, 80.9, 75.6, 47.5, 39.8, 31.3, 30.9, 25.2, 23.5, 23.3.

IR (film): ν (cm^{-1}) 2927, 2857, 1719, 1684, 1593, 1505, 1446, 1404, 1233, 1172, 1119, 1068, 1034, 966, 914, 824, 761, 731, 692, 608, 516, 464.

HRMS (ESI, m/z) calcd for $\text{C}_{32}\text{H}_{33}\text{N}_2\text{O}_5$ $[\text{M}+\text{H}]^+$: 525.2384, found: 525.2384.



According to the general procedure, a mixture of **42i** (35.6 mg, 0.10 mmol), **43f** (69.6 mg, 3.0 equiv.), Δ -**RhS2** (4.0 mg, 4 mol%), and DABCO (2.2 mg, 20 mol%) in acetone (1.0 mL, 0.1 M) was stirred under nitrogen atmosphere for 24 hours under irradiation with 24 W blue LEDs at room temperature (in a water bath) to afford **45k** as a pale yellow solid (42.8 mg, 73% yield, 5.0:1 dr, 98% ee). Purification conditions: *n*-hexane/EtOAc = 10:1 to 5:1, $R_f = 0.5$ in *n*-hexane/EtOAc (5:1). Enantiomeric excess was established by HPLC analysis using a Chiralpak AD-H column, ee = 98% (HPLC: 254 nm, *n*-hexane/isopropanol = 80:20, flow rate 0.5 mL/min, 25 °C, t_r (major) = 21.4 min, t_r (minor) = 14.9 min). $[\alpha]_D^{22} = +38.2^\circ$ (c 1.0, CH_2Cl_2). The dr value was determined by ^1H NMR analysis of the crude product as shown below:

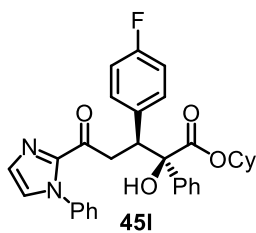


^1H NMR (300 MHz, CD_2Cl_2) δ 7.87–7.82 (m, 2H), 7.64 (t, $J = 1.7$ Hz, 1H), 7.50 (dt, $J = 1.3, 7.8$ Hz, 1H), 7.43–7.28 (m, 6H), 7.16–7.11 (m, 2H), 7.06 (d, $J = 1.0$ Hz, 1H), 7.00 (d, $J = 0.9$ Hz, 1H), 6.97–6.92 (m, 2H), 4.54 (m, 1H), 4.35 (dd, $J = 11.3, 3.1$ Hz, 1H), 4.03 (s, 1H), 3.92 (dd, $J = 11.2, 17.4$ Hz, 1H), 2.83 (dd, $J = 17.5, 3.2$ Hz, 1H), 1.74–1.65 (m, 2H), 1.60–1.54 (m, 1H), 1.52–1.36 (m, 3H), 1.35–1.16 (m, 4H).

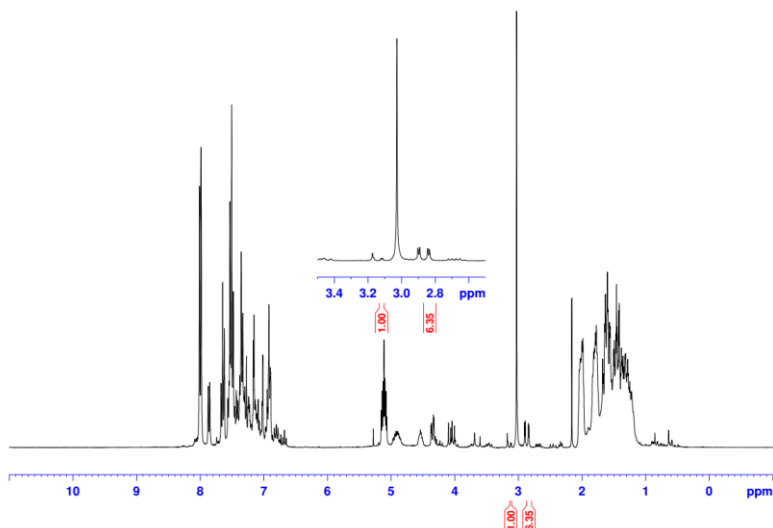
^{13}C NMR (75 MHz, CD_2Cl_2) δ 189.3, 173.4, 143.1, 142.1, 140.4, 138.4, 133.5, 130.2, 129.5, 128.8, 128.5, 128.3, 128.0, 127.0, 126.5, 125.8, 121.7, 125.8, 80.6, 76.0, 48.0, 39.7, 31.4, 31.1, 25.3, 23.7, 23.5.

IR (film): ν (cm^{-1}) 3020, 2937, 2856, 1723, 1683, 1594, 1566, 1491, 1445, 1404, 1335, 1302, 1233, 1172, 1121, 1071, 1035, 1005, 967, 919, 818, 761, 693, 609, 541, 514, 452.

HRMS (ESI, m/z) calcd for $\text{C}_{32}\text{H}_{32}\text{BrN}_2\text{O}_4$ $[\text{M}+\text{H}]^+$: 587.1540, found: 587.1539.



According to the general procedure, a mixture of **42j** (29.4 mg, 0.10 mmol), **43f** (69.6 mg, 3.0 equiv.), Δ -**RhS2** (4.0 mg, 4 mol%), and DABCO (2.2 mg, 20 mol%) in acetone (1.0 mL, 0.1 M) was stirred under nitrogen atmosphere for 24 hours under irradiation with 24 W blue LEDs at room temperature (in a water bath) to afford **45I** as a pale yellow solid (29.8 mg, 57% yield, 6.3:1 dr, 97% ee). Purification conditions: *n*-hexane/EtOAc = 10:1 to 5:1, $R_f = 0.5$ in *n*-hexane/EtOAc (5:1). Enantiomeric excess was established by HPLC analysis using a Chiralpak OD-H column, ee = 97% (HPLC: 254 nm, *n*-hexane/isopropanol = 90:10, flow rate 1 mL/min, 25 °C, t_r (major) = 6.8 min, t_r (minor) = 8.0 min). $[\alpha]_D^{22} = -40.8^\circ$ (c 1.0, CH_2Cl_2). The dr value was determined by ^1H NMR analysis of the crude product as shown below:



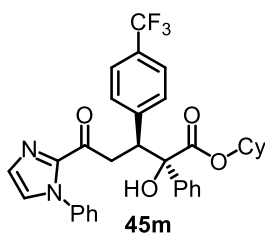
^1H NMR (300 MHz, CD_2Cl_2) δ 7.87–7.85 (m, 2H), 7.52–7.49 (m, 2H), 7.41–7.30 (m, 6H), 7.14 (d, J = 0.9 Hz, 1H), 7.06 (d, J = 0.8 Hz, 1H), 6.96–6.93 (m, 4H), 4.52 (m, 1H), 4.35 (dd, J = 11.4, 3.1 Hz, 1H), 4.04 (s, 1H), 3.93 (dd, J = 17.5, 11.4 Hz, 1H), 2.81 (dd, J = 17.6, 3.2 Hz, 1H), 1.72–1.63 (m, 2H), 1.52–1.38 (m, 4H), 1.31–1.21 (m, 4H).

^{13}C NMR (75 MHz, CD_2Cl_2) δ 189.7, 173.8, 162.3 (J = 245.1 Hz, 1C), 143.3, 140.8, 138.7, 135.6 (J = 3.4 Hz, 1C), 132.2 (J = 7.6 Hz, 1C), 129.7, 129.0, 128.7, 128.5, 128.2, 127.3, 126.8, 126.0, 114.7 (J = 21.0 Hz, 1C), 81.0, 76.1, 47.8, 40.1, 31.6, 31.3, 25.5, 23.9, 23.7.

^{19}F NMR (282 MHz) δ -117.1.

IR (film): ν (cm^{-1}) 2932, 2858, 1724, 1685, 1598, 1503, 1447, 1406, 1304, 1232, 1161, 1121, 1071, 1034, 963, 915, 826, 764, 731, 694, 536.

HRMS (ESI, m/z) calcd for $\text{C}_{32}\text{H}_{32}\text{FN}_2\text{O}_4$ $[\text{M}+\text{H}]^+$: 527.2341, found: 527.2342.



According to the general procedure, a mixture of **42k** (34.4 mg, 0.10 mmol), **43f** (69.6 mg, 3.0 equiv.), Δ -**RhS2** (4.0 mg, 4 mol%), and DABCO (2.2 mg, 20 mol%) in acetone (1.0 mL, 0.1 M) was stirred under nitrogen atmosphere for 26 hours under irradiation with 24 W blue LEDs at 50 °C to afford **45m** as a pale yellow solid (24.6 mg, 43% yield, >20:1 dr, 98% ee). Purification conditions: *n*-hexane/EtOAc = 10:1 to 5:1, R_f = 0.5 in *n*-hexane/EtOAc (5:1). Enantiomeric excess was established by HPLC analysis using a Chiralpak AD-H column, ee = 98% (HPLC: AD-H, 254 nm, *n*-hexane/isopropanol = 80:20, flow rate 1.0 mL/min, 25 °C, t_r (major) = 7.7

min, t_r (minor) = 9.3 min). $[\alpha]_D^{22} = -55.6^\circ$ (c 1.0, CH_2Cl_2). The dr value was determined by ^1H NMR analysis of the pure product.

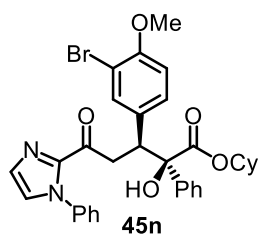
^1H NMR (300 MHz, CDCl_3) δ 7.86–7.83 (m, 2H), 7.67 (d, $J = 8.2$ Hz, 2H), 7.48 (d, $J = 8.2$ Hz, 2H), 7.38–7.28 (m, 6H), 7.17 (d, $J = 0.9$ Hz, 1H), 7.02 (d, $J = 0.9$ Hz, 1H), 6.92–6.87 (m, 2H), 4.53 (m, 1H), 4.39 (dd, $J = 11.1, 3.2$ Hz, 1H), 4.10–3.89 (m, 2H), 2.90 (dd, $J = 17.7, 3.3$ Hz, 1H), 1.70–1.48 (m, 4H), 1.39–1.12 (m, 6H).

^{13}C NMR (75 MHz, CD_2Cl_2) δ 189.3, 173.3, 143.8, 143.0, 140.2, 138.2, 130.7, 129.6 (2C), 128.9, 128.7, 128.4, 128.1, 127.0, 126.5, 125.7, 124.7 (q, $J = 3.7$ Hz), 80.6, 75.8, 47.9, 39.9, 31.3, 31.0, 25.2, 23.6, 23.4.

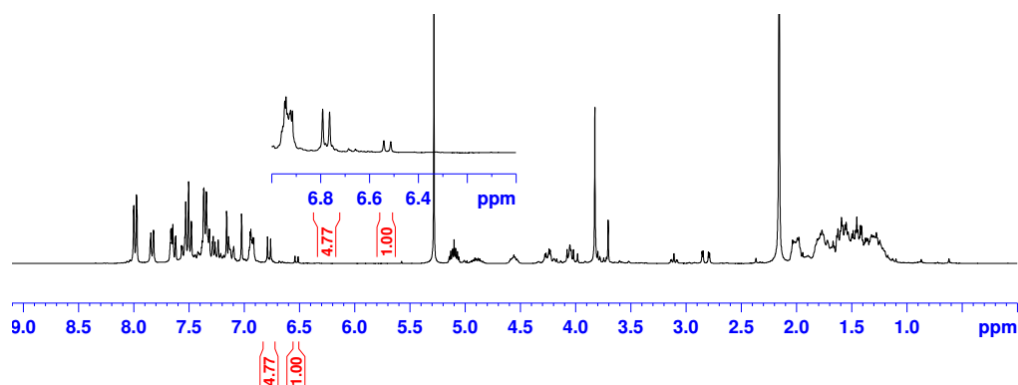
^{19}F NMR (282 MHz) δ -62.4.

IR (film): ν (cm^{-1}) 3106, 3031, 2945, 2847, 1665, 1492, 1445, 1402, 1343, 1254, 1202, 1145, 1051, 974, 919, 737, 693, 613, 522.

HRMS (ESI, m/z) calcd for $\text{C}_{33}\text{H}_{31}\text{F}_3\text{N}_2\text{O}_4\text{Na}$ [$\text{M} + \text{Na}$] $^+$: 599.2128, found: 599.2130.



According to the general procedure, a mixture of **42l** (38.4 mg, 0.10 mmol), **43f** (69.6 mg, 3.0 equiv.), Δ -**RhS2** (4.0 mg, 4 mol%), and DABCO (2.2 mg, 20 mol%) in acetone (1.0 mL, 0.1 M) was stirred under nitrogen atmosphere for 16 hours under irradiation with 24 W blue LEDs at room temperature (in a water bath) to afford **45n** as a pale yellow oil (55.3 mg, 90% yield, 4.8:1 dr, 96% ee). Purification conditions: n -hexane/EtOAc = 10:1 to 5:1, $R_f = 0.4$ in n -hexane/EtOAc (4:1). Enantiomeric excess was established by HPLC analysis using a Chiralpak AD-H column, ee = 96% (HPLC: 254 nm, n -hexane/isopropanol = 80:20, flow rate 1 mL/min, 40 $^\circ\text{C}$, t_r (major) = 18.5 min, t_r (minor) = 13.5 min). $[\alpha]_D^{22} = +27.0^\circ$ (c 1.0, CH_2Cl_2). The dr value was determined by ^1H NMR analysis of the crude product as shown below:

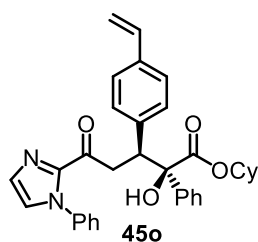


^1H NMR (300 MHz, CD_2Cl_2) δ 7.91–7.87 (m, 2H), 7.69 (d, $J = 2.1$ Hz, 1H), 7.53 (dd, $J = 8.6, 2.2$ Hz, 1H), 7.46–7.33 (m, 7H), 7.19 (d, $J = 1.0$ Hz, 1H), 7.11 (d, $J = 1.0$ Hz, 1H), 7.03–6.97 (m, 2H), 6.86 (d, $J = 8.6$ Hz, 1H), 4.60 (m, 1H), 4.25 (dd, $J = 11.5, 3.2$ Hz, 1H), 4.08 (s, 1H), 3.95 (dd, $J = 17.4, 11.4$ Hz, 1H), 3.88 (s, 3H), 2.83 (dd, $J = 17.4, 3.1$ Hz, 1H), 1.80–1.73 (m, 2H), 1.57–1.46 (m, 4H), 1.43–1.20 (m, 4H).

^{13}C NMR (75 MHz, CD_2Cl_2) δ 189.5, 173.5, 155.1, 143.2, 140.5, 138.4, 135.2, 133.1, 130.1, 129.5, 128.8, 128.5, 128.3, 127.9, 127.0, 126.5, 125.8, 111.3, 110.6, 80.1, 75.9, 56.2, 47.3, 39.7, 31.5, 31.1, 25.3, 23.7, 23.5.

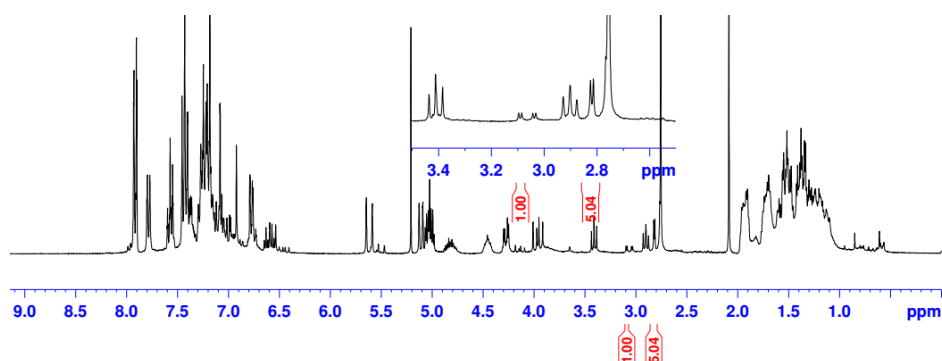
IR (film): ν (cm^{-1}) 3055, 2935, 2854, 1726, 1679, 1597, 1493, 1447, 1402, 1341, 1234, 1179, 1119, 1024, 971, 916, 762, 728, 691, 606, 518, 446.

HRMS (ESI, m/z) calcd for $\text{C}_{33}\text{H}_{34}\text{BrN}_2\text{O}_5$ $[\text{M}+\text{H}]^+$: 618.1678, found: 618.1673.



According to the general procedure, a mixture of **42m** (30.2 mg, 0.10 mmol), **43f** (69.6 mg, 3.0 equiv.), Δ -**RhS2** (4.0 mg, 4 mol%), and DABCO (2.2 mg, 20 mol%) in acetone (1.0 mL, 0.1 M) was stirred under nitrogen atmosphere for 16 hours under irradiation with 24 W blue LEDs at room temperature (in a water bath) to afford **45o** as a pale yellow oil (36.2 mg, 68% yield, 5.0:1 dr, 98% ee). Purification conditions: *n*-hexane/EtOAc = 10:1 to 5:1, $R_f = 0.5$ in *n*-hexane/EtOAc (5:1). Enantiomeric excess was established by HPLC analysis using a Chiralpak AD-H column, ee = 98% (HPLC: 254 nm, *n*-hexane/isopropanol = 85:15, flow rate 1 mL/min, 40 °C, t_r (major) = 12.1 min, t_r (minor) = 18.2 min). $[\alpha]_D^{22} = -31.8^\circ$ (c 1.0, CH_2Cl_2). The dr value was determined by ^1H NMR

analysis of the crude product as shown below:

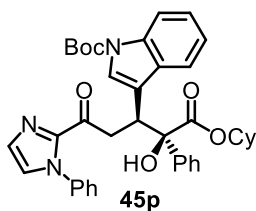


^1H NMR (300 MHz, CD_2Cl_2) δ 7.90–7.86 (m, 2H), 7.47–7.45 (m, 2H), 7.42–7.29 (m, 8H), 7.14 (d, $J = 1.0$ Hz, 1H), 7.05 (d, $J = 1.0$ Hz, 1H), 6.91–6.87 (m, 2H), 6.69 (dd, $J = 17.6, 10.9$ Hz, 1H), 5.73 (dd, $J = 17.6, 0.9$ Hz, 1H), 5.21 (dd, $J = 10.9, 0.9$ Hz, 1H), 4.54 (m, 1H), 4.30 (dd, $J = 11.4, 3.2$ Hz, 1H), 4.02 (br, 1H), 3.94 (dd, $J = 17.3, 11.4$ Hz, 1H), 2.82 (dd, $J = 17.3, 3.3$ Hz, 1H), 1.80–1.62 (m, 2H), 1.55–1.41 (m, 4H), 1.36–1.15 (m, 4H).

^{13}C NMR (75 MHz, CD_2Cl_2) δ 189.7, 173.6, 143.2, 140.6, 139.1, 138.4, 136.7, 136.6, 130.5, 129.4, 128.7, 128.4, 128.3, 127.9, 126.9, 126.6, 125.8, 125.6, 113.4, 80.8, 75.7, 48.2, 39.8, 31.4, 31.0, 25.3, 23.6, 23.4.

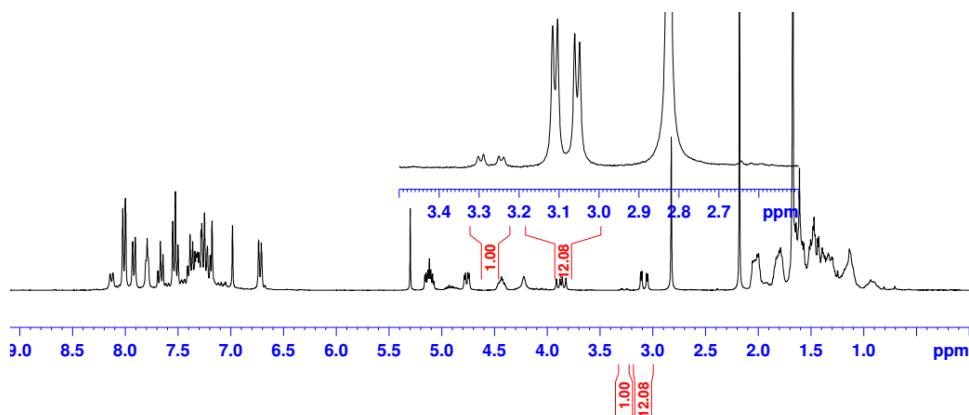
IR (film): ν (cm^{-1}) 3374, 2932, 2857, 1729, 1679, 1632, 1595, 1496, 1448, 1405, 1301, 1230, 1162, 1121, 1071, 1027, 968, 910, 834, 762, 731, 691, 645, 597, 527, 420.

HRMS (ESI, m/z) calcd for $\text{C}_{34}\text{H}_{35}\text{N}_2\text{O}_4$ $[\text{M}+\text{H}]^+$: 535.2591, found: 535.2590.



According to the general procedure, a mixture of **42n** (41.0 mg, 0.10 mmol), **43f** (69.6 mg, 3.0 equiv.), Δ -**RhS2** (4.0 mg, 4 mol%), and DABCO (2.2 mg, 20 mol%) in acetone (1.0 mL, 0.1 M) was stirred under nitrogen atmosphere for 18 hours under irradiation with 24 W blue LEDs at room temperature (in a water bath) to afford **45p** as a pale yellow oil (51.0 mg, 78% yield, 12:1 dr, >99% ee). Purification conditions: *n*-hexane/EtOAc = 10:1 to 5:1, $R_f = 0.4$ in *n*-hexane/EtOAc (5:1). Enantiomeric excess was established by HPLC analysis using a Chiralpak AD-H column, ee = >99% (HPLC: 254 nm, *n*-hexane/isopropanol = 95:5, flow rate 1 mL/min, 40 °C, t_r (major) = 15.6 min, t_r (minor) = 14.4 min). $[\alpha]_D^{22} = +18.4^\circ$ (c 1.0, CH_2Cl_2). The dr value was determined by ^1H NMR

analysis of the crude product as shown below:

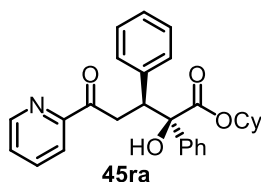


^1H NMR (300 MHz, CD_2Cl_2) δ 8.14 (d, $J = 7.9$ Hz, 1H), 7.95–7.92 (m, 2H), 7.82–7.80 (m, 2H), 7.42–7.27 (m, 7H), 7.24–7.19 (m, 2H), 7.00 (m, 1H), 6.76–6.72 (m, 2H), 4.78 (dd, $J = 10.2, 3.7$ Hz, 1H), 4.45 (m, 1H), 4.21 (s, 1H), 3.88 (dd, $J = 16.6, 10.4$ Hz, 1H), 3.09 (dd, $J = 16.6, 3.7$ Hz, 1H), 1.69 (s, 9H), 1.60–1.30 (m, 6H), 1.28–1.08 (m, 3H), 1.00–0.90 (m, 1H).

^{13}C NMR (75 MHz, CD_2Cl_2) δ 189.7, 173.9, 149.7, 143.1, 140.3, 138.2, 135.1, 130.6, 129.5, 128.7, 128.5, 128.3, 127.9, 126.7 (2C), 125.6, 125.5, 124.1, 122.2, 120.9, 119.3, 114.8, 83.5, 81.0, 75.6, 40.7, 39.4, 30.9, 30.8, 28.3, 25.2, 23.5, 23.4.

IR (film): ν (cm^{-1}) 2936, 2856, 2189, 2072, 2026, 1945, 1725, 1684, 1596, 1492, 1448, 1404, 1366, 1306, 1236, 1154, 1123, 1073, 1026, 962, 916, 850, 758, 693, 580, 519, 468, 412.

HRMS (ESI, m/z) calcd for $\text{C}_{39}\text{H}_{42}\text{N}_3\text{O}_6$ $[\text{M}+\text{H}]^+$: 648.3068, found: 648.3070.



According to the general procedure, a mixture of **42p** (63.3 mg, 0.30 mmol, 3.0 equiv.), **43f** (23.2 mg, 0.30 mmol), Δ -**RhS2** (4.0 mg, 4 mol%), and DABCO (2.2 mg, 20 mol%) in acetone (1.0 mL, 0.1 M) was stirred under nitrogen atmosphere for 24 hours under irradiation with 24 W blue LEDs at room temperature (in a water bath) to afford **45ra** as a pale yellow oil (32.8 mg, 75% yield, >20:1 dr, 97% ee). Purification conditions: *n*-hexane/EtOAc = 10:1 to 6:1, $R_f = 0.5$ in *n*-hexane/EtOAc (6:1). Enantiomeric excess was established by HPLC analysis using a Chiralpak IC column, ee = 97% (HPLC: 254 nm, *n*-hexane/isopropanol = 90:10, flow rate 1 mL/min, 40 °C, t_r (major) = 8.4 min, t_r (minor) = 16.5 min). $[\alpha]_D^{22} = -117.4^\circ$ (c 1.0, CH_2Cl_2). The dr value was determined by ^1H NMR analysis of the product after purification.

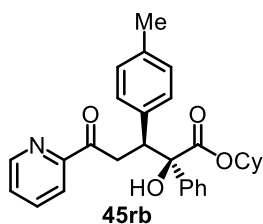
^1H NMR (300 MHz, CD_2Cl_2) δ 8.58 (dt, $J = 4.8, 1.2$ Hz, 1H), 7.91–7.88 (m, 2H), 7.75–7.66 (m, 2H),

7.57–7.53 (m, 2H), 7.41–7.35 (m, 3H), 7.32–7.16 (m, 4H), 4.53 (m, 1H), 4.40 (dd, $J = 11.3, 2.8$ Hz, 1H), 4.10 (dd, $J = 18.4, 11.2$ Hz, 1H), 4.02 (s, 1H), 2.93 (dd, $J = 18.4, 2.8$ Hz, 1H), 1.80–1.64(m, 2H), 1.53–1.41(m, 4H), 1.34–1.20 (m, 4H).

^{13}C NMR (75 MHz, CD_2Cl_2) δ 200.0, 173.7, 153.4, 148.9, 140.8, 139.9, 136.7, 130.2, 128.2, 127.9, 127.8, 127.1, 127.0, 126.6, 121.3, 81.0, 75.7, 48.2, 38.5, 31.3, 31.0, 25.3, 23.7, 23.4.

IR (film): ν (cm^{-1}) 2929, 2857, 1699, 1449, 1355, 1306, 1237, 1119, 1073, 1005, 924, 771, 727, 696, 664, 598, 541.

HRMS (ESI, m/z) calcd for $\text{C}_{28}\text{H}_{29}\text{NO}_4\text{Na}$ $[\text{M}+\text{Na}]^+$: 466.1989, found: 466.1994.



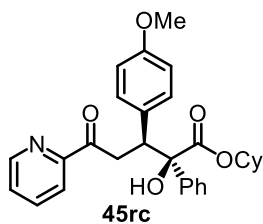
According to the general procedure, a mixture of **42q** (67.6mg, 0.30 mmol, 3.0 equiv.), **43f** (23.2 mg, 0.30 mmol), Δ -**RhS2** (4.0 mg, 4 mol%), and DABCO (2.2 mg, 20 mol%) in acetone (1.0 mL, 0.1 M) was stirred under nitrogen atmosphere for 20 hours under irradiation with 24 W blue LEDs at room temperature (in a water bath) to afford **45rb** as a pale yellow oil (33.2 mg, 73% yield, >20:1 dr, 99% ee). Purification conditions: *n*-hexane/EtOAc = 10:1 to 6:1, $R_f = 0.5$ in *n*-hexane/EtOAc (6:1). Enantiomeric excess was established by HPLC analysis using a Chiralpak IA column, ee = 99% (HPLC: 254 nm, *n*-hexane/isopropanol = 98:2, flow rate 1 mL/min, 25 °C, t_r (major) = 21.2 min, t_r (minor) = 24.9 min). $[\alpha]_D^{22} = -102.2^\circ$ (c 1.0, CH_2Cl_2). The dr value was determined by ^1H NMR analysis of the product after purification.

^1H NMR (300 MHz, CD_2Cl_2) δ 8.58 (dt, $J = 4.7, 1.4$ Hz, 1H), 7.91–7.87 (m, 2H), 7.75–7.66 (m, 2H), 7.43–7.36 (m, 5H), 7.31–7.26 (m, 1H), 7.06 (d, $J = 7.9$ Hz, 2H), 4.55 (m, 1H), 4.37 (dd, $J = 11.3, 2.7$ Hz, 1H), 4.08 (dd, $J = 18.2, 11.4$ Hz, 1H), 3.98 (s, 1H), 2.90 (dd, $J = 18.3, 2.8$ Hz, 1H), 2.28 (s, 3H), 1.85–1.67 (m, 2H), 1.55–1.45 (m, 4H), 1.35–1.12 (m, 4H).

^{13}C NMR (75 MHz, CD_2Cl_2) δ 200.0, 173.8, 153.4, 148.9, 140.8, 136.8, 136.7, 136.6, 129.9, 128.5, 128.2, 127.8, 127.0, 126.7, 121.3, 81.0, 75.6, 47.8, 38.5, 31.4, 31.0, 25.3, 23.7, 23.4, 20.8.

IR (film): ν (cm^{-1}) 2934, 2859, 1700, 1581, 1511, 1446, 1355, 1239, 1176, 1119.7058, 1010, 911, 813, 774, 732, 698, 668, 617, 556, 519.

HRMS (ESI, m/z) calcd for $\text{C}_{29}\text{H}_{31}\text{NO}_4\text{Na}$ $[\text{M}+\text{Na}]^+$: 480.2145, found: 480.2151.



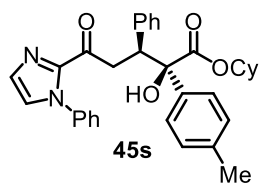
According to the general procedure, a mixture of **42r** (72.3 mg, 0.30 mmol, 3.0 equiv.), **43f** (23.2 mg, 0.30 mmol), Δ -**RhS2** (4.0 mg, 4 mol%), and DABCO (2.2 mg, 20 mol%) in acetone (1.0 mL, 0.1 M) was stirred under nitrogen atmosphere for 20 hours under irradiation with 24 W blue LEDs at room temperature (in a water bath) to afford **45rc** as a pale yellow oil (39.0 mg, 82% yield, >20:1 dr, 99% ee). Purification conditions: *n*-hexane/EtOAc = 10:1 to 6:1, R_f = 0.5 in *n*-hexane/EtOAc (6:1). Enantiomeric excess was established by HPLC analysis using a Chiralpak IA column, ee = 99% (HPLC: 254 nm, *n*-hexane/isopropanol = 90:10, flow rate 1 mL/min, 35 °C, t_r (major) = 11.7 min, t_r (minor) = 15.2 min). $[\alpha]_D^{22} = -86.6^\circ$ (c 1.0, CH_2Cl_2). The dr value was determined by ^1H NMR analysis of the product after purification.

^1H NMR (300 MHz, CD_2Cl_2) δ 8.58 (d, J = 4.1 Hz, 1H), 7.90–7.87 (m, 2H), 7.76 (d, J = 7.8 Hz, 1H), 7.66 (td, J = 7.6, 1.7 Hz, 1H), 7.49 (dt, J = 8.7, 1.9 Hz, 2H), 7.37–7.32 (m, 3H), 7.27–7.22 (m, 1H), 6.76 (dt, J = 8.8, 2.0 Hz, 2H), 4.56 (m, 1H), 4.41 (dd, J = 11.1, 2.7 Hz, 1H), 4.13 (dd, J = 18.3, 11.1 Hz, 1H), 3.99 (s, 1H), 3.74 (s, 3H), 2.94 (dd, J = 18.3, 2.8 Hz, 1H), 1.80–1.65 (m, 2H), 1.55–1.40 (m, 4H), 1.34–1.15 (m, 4H).

^{13}C NMR (75 MHz, CD_2Cl_2) δ 200.1, 173.8, 158.8, 153.4, 148.9, 140.8, 136.7, 131.7, 131.1, 128.2, 127.8, 127.0, 126.6, 121.3, 113.1, 81.1, 75.7, 55.1, 47.4, 38.6, 31.4, 31.1, 25.3, 23.7, 23.4.

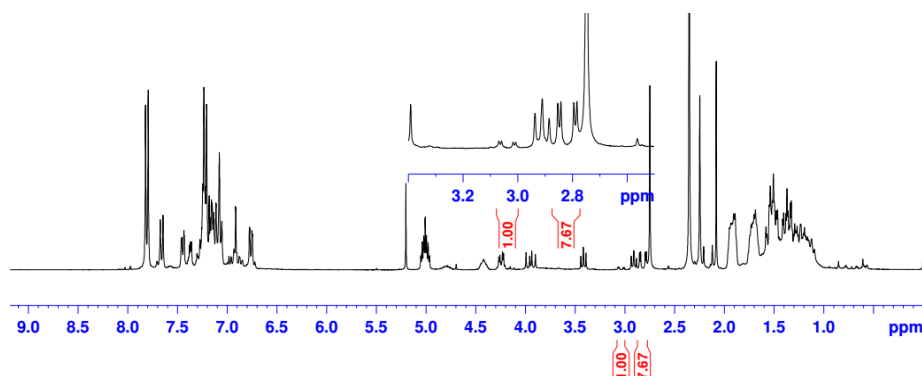
IR (film): ν (cm^{-1}) 2934, 2857, 1699, 1609, 1581, 1510, 1447, 1354, 1241, 1176, 1119, 1070, 1029, 910, 824, 773, 732, 699, 668, 593, 556.

HRMS (ESI, m/z) calcd for $\text{C}_{29}\text{H}_{31}\text{NO}_5\text{Na}$ $[\text{M}+\text{Na}]^+$: 496.2094, found: 496.2100.



According to the general procedure, a mixture of **42a** (27.6 mg, 0.10 mmol), **43g** (74.0 mg, 3.0 equiv.), Δ -**RhS2** (4.0 mg, 4 mol%), and DABCO (2.2 mg, 20 mol%) in acetone (1.0 mL, 0.1 M) was stirred under nitrogen atmosphere for 16 hours under irradiation with 24 W blue LEDs at room temperature (in a water bath) to afford **45s** as a pale yellow solid (48.8 mg, 87% yield, 7.7:1 dr, 99% ee). Purification conditions: *n*-hexane/EtOAc = 10:1 to 5:1, R_f = 0.5 in *n*-hexane/EtOAc (5:1).

Enantiomeric excess was established by HPLC analysis using a Chiralpak AD-H column, ee = 99% (HPLC: 254 nm, *n*-hexane/isopropanol = 80:20, flow rate 1 mL/min, 40 °C, t_r (major) = 8.5 min, t_r (minor) = 14.6 min). $[\alpha]_D^{22} = -54.8^\circ$ (c 1.0, CH_2Cl_2). The dr value was determined by ^1H NMR analysis of the crude product as shown below:

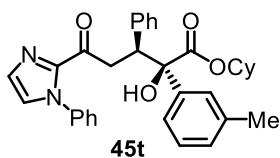


^1H NMR (300 MHz, CD_2Cl_2) δ 7.74 (dt, $J = 8.3, 1.7$ Hz, 2H), 7.50–7.46 (m, 2H), 7.41–7.28 (m, 3H), 7.27–7.17 (m, 5H), 7.14 (d, $J = 1.0$ Hz, 1H), 7.04 (d, $J = 1.0$ Hz, 1H), 6.91–6.86 (m, 2H), 4.49 (m, 1H), 4.26 (dd, $J = 11.3, 3.3$ Hz, 1H), 3.96–3.90 (m, 2H), 2.84 (dd, $J = 17.3, 3.3$ Hz, 1H), 2.35 (s, 3H), 1.80–1.59 (m, 2H), 1.53–1.31 (m, 4H), 1.30–1.10 (m, 4H).

^{13}C NMR (75 MHz, CD_2Cl_2) δ 189.8, 173.7, 143.2, 139.5, 138.5, 137.7, 130.3, 129.3, 128.9, 128.7, 128.4, 127.8, 127.1, 126.8, 126.5, 125.8, 80.7, 75.6, 48.4, 39.8, 31.3, 31.0, 25.3, 23.6, 23.4, 20.8.

IR (film): ν (cm^{-1}) 3030, 2934, 2858, 1724, 1686, 1598, 1498, 1448, 1406, 1335, 1307, 1238, 1170, 1108, 1033, 962, 915, 818, 761, 732, 699, 608, 523.

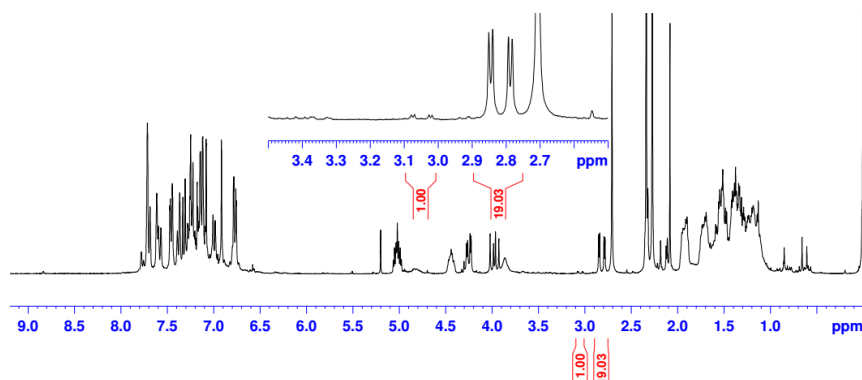
HRMS (ESI, m/z) calcd for $\text{C}_{33}\text{H}_{35}\text{N}_2\text{O}_4$ $[\text{M}+\text{H}]^+$: 523.2591, found: 523.2584.



According to the general procedure, a mixture of **42a** (27.6 mg, 0.10 mmol),

43h (74.0 mg, 3.0 equiv.), Δ -**RhS2** (4.0 mg, 4 mol%), and DABCO (2.2 mg, 20 mol%) in acetone (1.0 mL, 0.1 M) was stirred under nitrogen atmosphere for 16 hours under irradiation with 24 W blue LEDs at room temperature (in a water bath) to afford **45t** as a pale yellow solid (50.5 mg, 97% yield, 19:1 dr, 98% ee). Purification conditions: *n*-hexane/EtOAc = 10:1 to 5:1, $R_f = 0.5$ in *n*-hexane/EtOAc (5:1). Enantiomeric excess was established by HPLC analysis using a Chiralpak AD-H column, ee = 98% (HPLC: 254 nm, *n*-hexane/isopropanol = 85:15, flow rate 1 mL/min, 40 °C, t_r (major) = 12.1 min, t_r (minor) = 18.2 min). $[\alpha]_D^{22} = -44.0^\circ$ (c 1.0, CH_2Cl_2). The dr value was determined by ^1H NMR

analysis of the crude product as shown below:

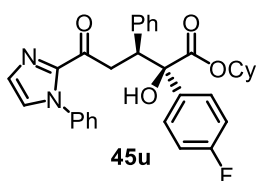


^1H NMR (300 MHz, CD_2Cl_2) δ 7.70–7.65 (m, 2H), 7.51–7.47 (m, 2H), 7.38–7.30 (m, 3H), 7.28–7.18 (m, 4H), 7.14–7.10 (m, 2H), 7.05 (d, $J = 1.0$ Hz, 1H), 6.92–6.86 (m, 2H), 4.51 (m, 1H), 4.27 (dd, $J = 11.3, 3.3$ Hz, 1H), 3.98–3.89 (m, 2H), 2.85 (dd, $J = 17.3, 3.3$ Hz, 1H), 2.38 (s, 3H), 1.80–1.59 (m, 2H), 1.54–1.40 (m, 4H), 1.39–1.12 (m, 4H).

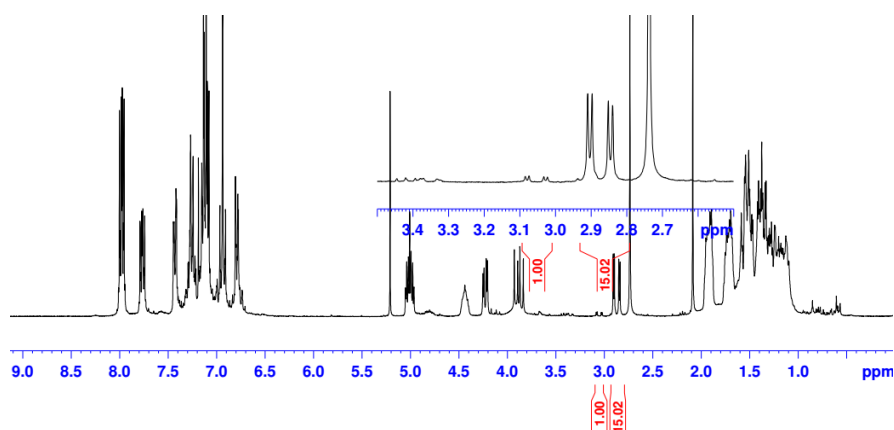
^{13}C NMR (75 MHz, CD_2Cl_2) δ 189.8, 173.7, 143.2, 140.6, 139.6, 138.5, 137.9, 130.3, 129.4, 128.7, 128.6, 128.4, 128.1, 127.8, 127.3, 127.1, 126.8, 125.8, 123.7, 80.8, 75.5, 48.4, 39.8, 31.3, 31.0, 25.3, 23.5, 23.3, 21.4.

IR (film): ν (cm^{-1}) 2856, 1731, 1679, 1596, 1492, 1448, 1405, 1333, 1299, 1226, 1123, 1030, 961, 917, 762, 693, 648, 586, 535, 440.

HRMS (ESI, m/z) calcd for $\text{C}_{33}\text{H}_{35}\text{N}_2\text{O}_4$ + $[\text{M}+\text{H}]^+$: 523.2591, found: 523.2640.



According to the general procedure, a mixture of **42a** (27.6 mg, 0.10 mmol), **43i** (74.4 mg, 3.0 equiv.), Δ -**RhS2** (4.0 mg, 4 mol%), and DABCO (2.2 mg, 20 mol%) in acetone (1.0 mL, 0.1 M) was stirred under nitrogen atmosphere for 14 hours under irradiation with 24 W blue LEDs at room temperature (in a water bath) to afford **45u** as a pale yellow solid (46.2 mg, 88% yield, 15:1 dr, 98% ee). Purification conditions: *n*-hexane/EtOAc = 10:1 to 5:1, $R_f = 0.5$ in *n*-hexane/EtOAc (5:1). Enantiomeric excess was established by HPLC analysis using a Chiralpak AD-H column, ee = 98% (HPLC: 254 nm, *n*-hexane/isopropanol = 90:10, flow rate 1 mL/min, 40 °C, t_r (major) = 12.1 min, t_r (minor) = 16.4 min). $[\alpha]_D^{22} = -51.6^\circ$ (c 1.0, CH_2Cl_2). The dr value was determined by ^1H NMR analysis of the crude product as shown below:



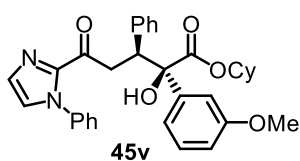
^1H NMR (300 MHz, CD_2Cl_2) δ 7.88–7.84 (m, 2H), 7.49–7.45 (m, 2H), 7.42–7.30 (m, 3H), 7.28–7.20 (m, 3H), 7.15 (d, $J = 1.0$ Hz, 1H), 7.10–7.03 (m, 3H), 6.92–6.86 (m, 2H), 4.51 (m, 1H), 4.03 (br, 1H), 4.26 (dd, $J = 11.0, 3.4$ Hz, 1H), 3.90 (dd, $J = 11.1, 17.3$ Hz, 1H), 2.88 (dd, $J = 17.3, 3.5$ Hz, 1H), 1.76–1.61 (m, 2H), 1.54–1.41 (m, 4H), 1.40–1.10 (m, 4H).

^{13}C NMR (75 MHz, CD_2Cl_2) δ 189.6, 173.4, 162.6 (d, $J = 245.3$ Hz, 1C), 143.2, 139.3, 138.4, 136.4 (d, $J = 3.0$ Hz, 1C), 130.2, 129.4, 128.7 (2C), 128.5 (d, $J = 14.3$ Hz, 1C), 127.9, 127.3, 126.9, 125.8, 114.9 (d, $J = 21.3$ Hz, 1C), 80.5, 75.8, 48.5, 39.7, 31.3, 31.0, 25.2, 23.6, 23.4.

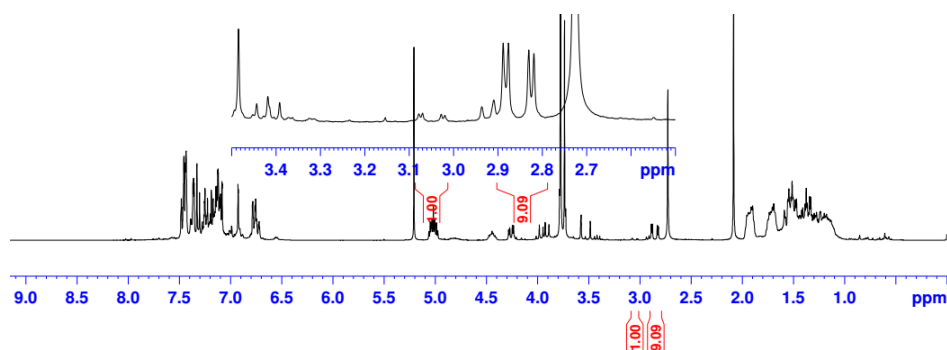
^{19}F NMR (282 MHz) δ -115.2.

IR (film): ν (cm^{-1}) 3336, 2934, 2858, 1730, 1683, 1598, 1499, 1449, 1408, 1335, 1302, 1226, 1159, 1121, 1092, 1033, 1010, 964, 918, 839, 761, 695, 603, 525, 434.

HRMS (EI, m/z) calcd for $\text{C}_{32}\text{H}_{32}\text{FN}_2\text{O}_4$ $[\text{M}+\text{H}]^+$: 527.2341, found: 527.2374.



According to the general procedure, a mixture of **42a** (27.6 mg, 0.10 mmol), **43j** (78.6 mg, 3.0 equiv.), Δ -**RhS2** (4.0 mg, 4 mol%), and DABCO (2.2 mg, 20 mol%) in acetone (1.0 mL, 0.1 M) was stirred under nitrogen atmosphere for 16 hours under irradiation with 24 W blue LEDs at room temperature (in a water bath) to afford **45v** as a pale yellow solid (49.5 mg, 92% yield, 9.1:1 dr, 98% ee). Purification conditions: *n*-hexane/EtOAc = 10:1 to 5:1, $R_f = 0.4$ in *n*-hexane/EtOAc (5:1). Enantiomeric excess was established by HPLC analysis using a Chiralpak AD-H column, ee = 98% (HPLC: 254 nm, *n*-hexane/isopropanol = 90:10, flow rate 1 mL/min, 40 °C, t_r (major) = 17.9 min, t_r (minor) = 23.9 min). $[\alpha]_D^{22} = -36.6^\circ$ (c 1.0, CH_2Cl_2). The dr value was determined by ^1H NMR analysis of the crude product as shown below:

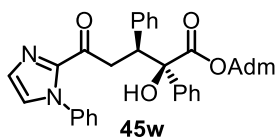


^1H NMR (300 MHz, CD_2Cl_2) δ 7.70–7.44 (m, 4H), 7.38–7.30 (m, 4H), 7.27–7.20 (m, 3H), 7.14 (d, $J = 0.9$ Hz, 1H), 7.05 (d, $J = 0.9$ Hz, 1H), 6.94–6.82 (m, 3H), 4.52 (m, 1H), 4.28 (dd, $J = 11.3, 3.3$ Hz, 1H), 4.00 (s, 1H), 3.91 (dd, $J = 17.3, 11.3$ Hz, 1H), 3.83 (s, 3H), 2.88 (dd, $J = 17.2, 3.3$ Hz, 1H), 1.76–1.61 (m, 2H), 1.55–1.40 (m, 4H), 1.39–1.10 (m, 4H).

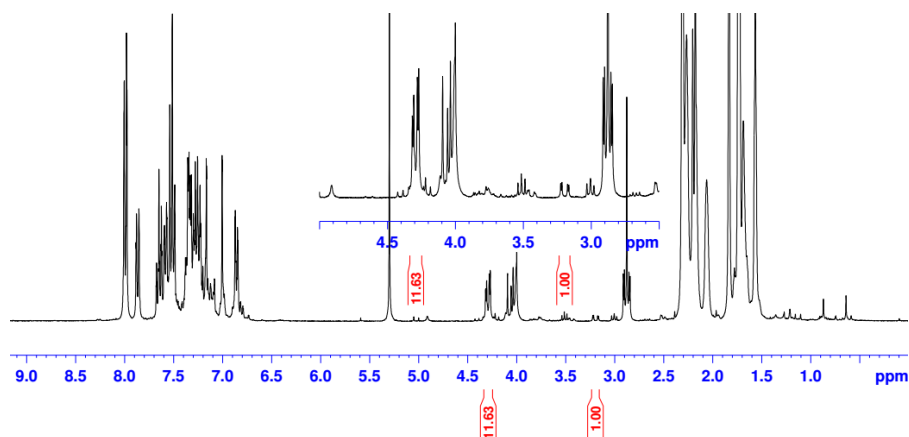
^{13}C NMR (75 MHz, CD_2Cl_2) δ 189.7, 173.5, 159.8, 143.2, 142.4, 139.4, 138.5, 130.3, 129.4, 129.2, 128.7, 128.4, 127.8, 127.2, 126.8, 125.8, 119.0, 113.6, 112.2, 75.7, 55.3, 48.5, 39.9, 31.3, 31.1, 25.3, 23.6, 23.4.

IR (film): ν (cm^{-1}) 2934, 2855, 1729, 1681, 1592, 1490, 1448, 1406, 1333, 1299, 1235, 1122, 1038, 960, 916, 878, 761, 726, 693, 587, 534.

HRMS (ESI, m/z) calcd for $\text{C}_{33}\text{H}_{35}\text{N}_2\text{O}_5$ $[\text{M}+\text{H}]^+$: 539.2540, found: 539.2534.



According to the general procedure, a mixture of **42a** (27.6 mg, 0.10 mmol), **43k** (83.2 mg, 3.0 equiv.), Δ -**Rhs2** (4.0 mg, 4 mol%), and DABCO (2.2 mg, 20 mol%) in acetone (1.0 mL, 0.1 M) was stirred under nitrogen atmosphere for 16 hours under irradiation with 24 W blue LEDs at room temperature (in a water bath) to afford **45w** as a pale yellow solid (49.1 mg, 88% yield, 11:1 dr, 98% ee). Purification conditions: *n*-hexane/EtOAc = 10:1 to 5:1, $R_f = 0.5$ in *n*-hexane/EtOAc (5:1). Enantiomeric excess was established by HPLC analysis using a Chiralpak AD-H column, ee = 98% (HPLC: 254 nm, *n*-hexane/isopropanol = 80:20, flow rate 1 mL/min, 40 °C, t_r (major) = 9.1 min, t_r (minor) = 11.1 min). $[\alpha]_D^{22} = -32.2^\circ$ (c 1.0, CH_2Cl_2). The dr value was determined by ^1H NMR analysis of the crude product as shown below:

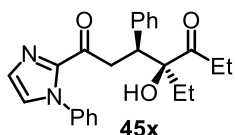


^1H NMR (300 MHz, CD_2Cl_2) δ 7.88–7.84 (m, 2H), 7.55–7.51 (m, 2H), 7.42–7.29 (m, 6H), 7.28–7.20 (m, 3H), 7.13 (d, $J = 0.9$ Hz, 1H), 7.04 (d, $J = 0.9$ Hz, 1H), 6.91–6.87 (m, 2H), 4.21 (dd, $J = 11.4, 3.2$ Hz, 1H), 4.00 (s, 1H), 3.93 (dd, $J = 17.3, 13.4$ Hz, 1H), 2.80 (dd, $J = 17.3, 3.2$ Hz, 1H), 2.05 (m, 3H), 1.84 (d, $J = 2.9$ Hz, 6H), 1.57 (m, 6H).

^{13}C NMR (75 MHz, CD_2Cl_2) δ 189.8, 172.9, 143.2, 141.2, 139.8, 138.5, 130.5, 129.4, 128.7, 128.4, 128.2, 127.7, 127.1, 126.8, 126.5, 125.8, 83.8, 80.8, 48.4, 40.8, 39.9, 36.0, 31.0.

IR (film): ν (cm^{-1}) 2913, 2855, 1728, 1681, 1593, 1491, 1447, 1406, 1333, 1300, 1231, 1163, 1122, 1038, 961, 918, 885, 791, 758, 725, 692, 644, 609, 579, 531, 422.

HRMS (ESI, m/z) calcd for $\text{C}_{36}\text{H}_{37}\text{N}_2\text{O}_4$ $[\text{M}+\text{Na}]^+$: 561.2748, found: 561.2748.



According to the general procedure, a mixture of **42a** (27.6 mg, 0.10 mmol), **43I** (36 μL , 3.0 equiv.), Δ -**RhS2** (4.0 mg, 4 mol%), and DABCO (2.2 mg, 20 mol%) in acetone (1.0 mL, 0.1 M) was stirred under nitrogen atmosphere for 24 hours under irradiation with 24 W blue LEDs at room temperature (in a water bath) to afford **45x** as a pale yellow oil (33.2 mg, 85% yield, 1.8:1 dr, 95%/95% ee). Purification conditions: *n*-hexane/EtOAc = 10:1 to 3:1, $R_f = 0.4$ in *n*-hexane/EtOAc (3:1) for the major diastereomer, $R_f = 0.3$ in *n*-hexane/EtOAc (3:1) for the minor diastereomer. Enantiomeric excess was established by HPLC analysis using a Chiralpak AS-H/IG column, ee = 95%/95% $[\alpha]_D^{22} = +42.2^\circ$ (c 1.0, CH_2Cl_2). The dr value was determined by ^1H NMR analysis of the crude product.

HPLC conditions for major diastereomer: IG, 254 nm, *n*-hexane/isopropanol = 80:20, flow rate 1.0 mL/min, 40 $^\circ\text{C}$, t_r (major) = 16.6 min, t_r (minor) = 24.1 min).

HPLC conditions for minor diastereomer: AS-H, 254 nm, *n*-hexane/isopropanol = 90:10, flow rate 1.0

mL/min, 40 °C, t_r (major) = 7.5 min, t_r (minor) = 11.4 min).

^1H NMR (300 MHz, CD_2Cl_2 , major diastereomer) δ 7.35–7.12 (m, 8H), 7.11 (d, J = 0.9 Hz, 1H), 7.02 (d, J = 0.9 Hz, 1H), 6.82–6.78 (m, 2H), 4.05 (s, 1H), 3.67–3.52 (m, 2H), 2.85–2.71 (m, 2H), 2.60–2.47 (m, 1H), 1.61–1.50 (m, 1H), 1.18–1.10 (m, 1H), 1.04 (t, J = 7.1 Hz, 3H), 0.49 (t, J = 7.3 Hz, 3H).

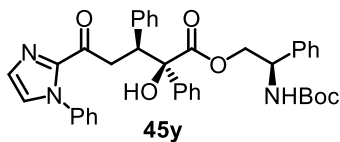
^{13}C NMR (75 MHz, CD_2Cl_2 , major diastereomer) δ 215.1, 189.3, 143.1, 139.6, 138.4, 130.2, 129.5, 128.8, 128.4, 128.0, 127.0, 126.9, 125.7, 84.0, 48.1, 41.0, 30.5, 29.7, 7.5, 7.3.

^1H NMR (300 MHz, CD_2Cl_2 , minor diastereomer) δ 7.43–7.32 (m, 3H), 7.24–7.15 (m, 6H), 7.12 (d, J = 0.9 Hz, 1H), 6.97–6.93 (m, 2H), 4.00 (s, 1H), 3.78–3.60 (m, 3H), 2.60–2.47 (m, 1H), 2.40–2.22 (m, 1H), 2.05–1.80 (m, 2H), 0.79–0.80 (m, 6H).

^{13}C NMR (75 MHz, CD_2Cl_2 , minor diastereomer) δ 213.4, 190.0, 143.3, 140.3, 138.5, 129.5, 129.2, 128.8, 128.5, 128.1, 127.1, 127.0, 125.7, 84.4, 47.7, 40.9, 30.3, 29.7, 7.6, 7.1.

IR (film): ν (cm^{-1}) 3460, 2970, 2933, 1688, 1597, 1495, 1449, 1403, 1338, 1306, 1179, 1125, 1055, 963, 912, 760, 695, 592, 525, 444.

HRMS (ESI, m/z) calcd for $\text{C}_{24}\text{H}_{27}\text{N}_2\text{O}_3$ $[\text{M}+\text{H}]^+$: 391.2016, found: 391.2008.



According to the general procedure, a mixture of **42a** (27.6 mg, 0.10 mmol), **43m** (110.7 mg, 3.0 equiv.), Δ -**RhS2** (4.0 mg, 4 mol%), and DABCO (2.2 mg, 20 mol%) in acetone (1.0 mL, 0.1 M) was stirred under nitrogen atmosphere for 16 hours under irradiation with 24 W blue LEDs at room temperature (in a water bath) to afford **45y** as a pale yellow solid (57.0 mg, 88% yield, 99:1:1:1 dr). Purification conditions: *n*-hexane/EtOAc = 10:1 to 3:1, R_f = 0.5 in *n*-hexane/EtOAc (3:1). The dr value of pure product was established by HPLC analysis using a Chiralpak OD-H column, dr = 99:1:1:1 (HPLC: 254 nm, *n*-hexane/isopropanol = 95:5, flow rate 1 mL/min, 40 °C, t_r (major) = 20.1 min, t_r (minor) = 34.5 min). $[\alpha]_D^{22} = +69.0^\circ$ (c 1.0, CH_2Cl_2).

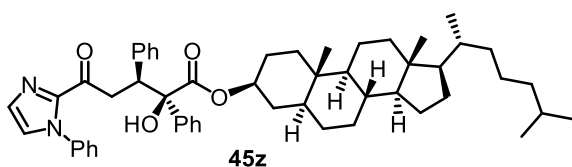
^1H NMR (300 MHz, CD_2Cl_2) δ 7.74–7.70 (m, 2H), 7.42–7.28 (m, 11H), 7.26–7.15 (m, 6H), 7.05 (d, J = 1.0 Hz, 1H), 6.91–6.85 (m, 2H), 5.04–4.80 (m, 2H), 4.22 (dd, J = 11.3, 3.3 Hz, 1H), 4.14 (dd, J = 11.2, 6.1 Hz, 1H), 4.00–3.95 (m, 2H), 3.89 (dd, J = 17.1, 11.4 Hz, 1H), 2.86 (dd, J = 17.1, 3.4 Hz, 1H), 1.43 (s, 9H).

^{13}C NMR (75 MHz, CD_2Cl_2) δ 189.5, 174.0, 154.9, 154.7, 144.5, 143.1, 139.9, 139.4, 138.9, 138.4,

129.8, 129.4, 128.8, 128.8, 128.4 (2C), 128.2, 128.1, 127.9, 127.4, 126.9, 126.7, 126.5, 125.7, 81.2, 79.9, 68.7, 48.7, 39.6, 28.6, 28.2.

IR (film): ν (cm⁻¹) 2931, 2857, 1717, 1686, 1596, 1494, 1448, 1403, 1364, 1302, 1228, 1162, 1115, 1030, 962, 914, 862, 758, 694, 584, 524, 431.

HRMS (ESI, m/z) calcd for C₃₉H₄₀N₃O₆ [M+H]⁺: 647.2944, found: 647.2938.



According to the general procedure, a mixture of **42a**

(27.6 mg, 0.10 mmol), **43n** (156.0 mg, 3.0 equiv.), Δ -**RhS2** (4.0 mg, 4 mol%), and DABCO (2.2 mg, 20 mol%) in acetone/CH₂Cl₂ (1:1, vol/vol, 1.0 mL, 0.1 M) was stirred under nitrogen atmosphere for 40 hours under irradiation with 24 W blue LEDs at room temperature (in a water bath) to afford **45z** as a pale yellow solid (65.2 mg, 82% yield, 99:30:1:1 dr). Purification conditions: *n*-hexane/EtOAc = 10:1 to 3:1, R_f = 0.5 in *n*-hexane/EtOAc (3:1) for the major spot, R_f = 0.6 in *n*-hexane/EtOAc (3:1) for the minor spot. The dr value was established by HPLC analysis using a Chiralpak OD-H/AS-H column in combination with ¹H NMR analysis of the product, dr = 99:30:1:1. $[\alpha]_D^{22} = -67.8^\circ$ (*c* 1.0, CH₂Cl₂).

It's choosed to use chiral HPLC (higher detect limitation) as well as the ¹H NMR to determine the dr value. Theoretically, four diastereomers can be generated in this reaction. As we can't get complete separation of the four diastereomers (A & B and C & D) on a single HPLC trace, diastereomers A & B (identical R_f value) and C & D (identical R_f value) were isolated and separated on individual chiral HPLC conditions, respectively, as shown below:

Two diastereomers (A and B) with identically low R_f value, R_f = 0.5 in *n*-hexane/EtOAc (3:1), were isolated, and the dr value determined by HPLC analysis as 99:1. HPLC conditions: OD-H, 254 nm, *n*-hexane/isopropanol = 95:5, flow rate 1.0 mL/min, 40 °C, t_r (major) = 9.3 min, t_r (minor) = 11.6 min);

Other two diastereomers (C and D) with identically high R_f value, R_f = 0.6 in *n*-hexane/EtOAc (3:1), were isolated, dr value determined by HPLC analysis as 97:3. HPLC conditions: AS-H, 254 nm, *n*-hexane/isopropanol = 95:5, flow rate 1.0 mL/min, 40 °C, t_r (major) = 8.5 min, t_r (minor) = 15.0 min.

Diastereomers A and B (identical ¹H NMR and R_f value), C and D (identical ¹H NMR and R_f value)

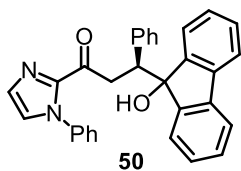
shown a ratio of 3.2:1 as judged by ^1H NMR of the crude material before purification. Combined with the results from chiral HPLC analysis, the exact dr value of the four diastereomers is 99:1: (97/3.2): (3/3.2) = 99:1:30:1.

^1H NMR (300 MHz, CD_2Cl_2) δ 7.80–7.76 (m, 2H), 7.42–7.38 (m, 2H), 7.33–7.20 (m, 6H), 7.18–7.11 (m, 3H), 7.05 (d, $J = 1.0$ Hz, 1H), 6.95 (d, $J = 1.0$ Hz, 1H), 6.81–6.76 (m, 2H), 4.36 (m, 1H), 4.18 (dd, $J = 11.3, 3.3$ Hz, 1H), 3.88–3.78 (m, 2H), 2.73 (dd, $J = 17.3, 3.4$ Hz, 1H), 1.85 (dt, $J = 12.3, 3.0$ Hz, 1H), 1.77–1.50 (m, 4H), 1.45–1.34 (m, 4H), 1.33–1.18 (m, 9H), 1.17–1.09 (m, 4H), 1.08–0.88 (m, 9H), 0.80 (d, $J = 6.6$ Hz, 3H), 0.78 (d, $J = 1.1$ Hz, 3H), 0.76 (d, $J = 1.1$ Hz, 3H), 0.73 (s, 3H), 0.56 (s, 3H).

^{13}C NMR (75 MHz, CD_2Cl_2) δ 189.7, 173.6, 143.2, 140.7, 139.5, 138.5, 130.4, 129.4, 128.7, 128.4, 128.2, 127.9, 127.8, 127.2, 126.8, 126.6, 125.8, 80.8, 76.8, 56.5, 56.4, 48.5, 44.6, 42.7, 40.1, 39.8, 39.6, 36.9, 36.3, 35.9, 35.6, 35.4, 33.7, 32.1, 28.7, 28.3, 28.1, 27.1, 24.3, 23.9, 22.6, 22.3, 21.3, 18.5, 12.0, 11.9.

IR (film): ν (cm^{-1}) 2927, 2855, 1718, 1688, 1493, 1451, 1413, 1243, 1172, 1119, 1068, 1030, 956, 916, 753, 697, 586, 528.

HRMS (ESI, m/z) calcd for $\text{C}_{53}\text{H}_{69}\text{N}_2\text{O}_4$ $[\text{M}+\text{H}]^+$: 798.5285, found: 798.5277.



According to the general procedure, a mixture of **42a** (27.6 mg, 0.10 mmol), **43b** (54.0 mg, 3.0 equiv.), Δ -**RhS1** (3.5 mg, 4 mol%), and DABCO (2.2 mg, 20 mol%) in DMF (1.0 mL, 0.1 M) was stirred under nitrogen atmosphere for 24 hours under irradiation with 24 W blue LEDs at room temperature (in a water bath) to afford **50** as a pale yellow solid (21.6 mg, 55% yield, 94% ee). Purification conditions: *n*-hexane/EtOAc = 8:1 to 2:1, $R_f = 0.3$ in *n*-hexane/EtOAc (2:1) for the major diastereomer. The ee value of pure product was established by HPLC analysis using a Chiralpak AD-H column, ee = 94% (HPLC: 254 nm, *n*-hexane/isopropanol = 80:20, flow rate 1 mL/min, 40 °C, t_r (major) = 12.7 min, t_r (minor) = 21.2 min). $[\alpha]_D^{22} = -14.6^\circ$ (c 1.0, CH_2Cl_2).

^1H NMR (300 MHz, CD_2Cl_2) δ 7.82–7.78 (m, 1H), 7.52–7.31 (m, 8H), 7.30–7.21 (m, 2H), 7.17 (d, $J = 0.9$ Hz, 1H), 7.10 (d, $J = 0.9$ Hz, 1H), 7.04–6.92 (m, 5H), 6.81–6.77 (m, 2H), 4.19 (dd, $J = 8.9, 5.6$ Hz, 1H), 3.74–3.70 (m, 2H), 2.93 (br, 1H).

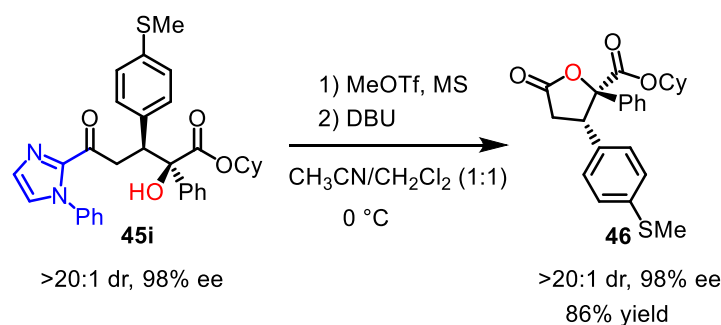
^{13}C NMR (75 MHz, CD_2Cl_2) δ 190.3, 148.4, 147.7, 143.6, 140.8, 140.1, 139.1, 138.8, 130.0, 129.6,

129.5, 129.1 (2C), 128.8, 128.0, 127.8, 127.5, 127.2, 126.8, 126.1, 125.1, 124.7, 120.2, 120.0, 84.6, 50.5, 40.3..

IR (film): ν (cm^{-1}) 2935, 2859, 1732, 1681, 1609, 1494, 1407, 1320, 1230, 1163, 1117, 1067, 1021, 968, 919, 832, 760, 692, 652, 612, 525.

HRMS (ESI, m/z) calcd for $\text{C}_{31}\text{H}_{24}\text{N}_2\text{O}_2\text{Na}$ $[\text{M}+\text{H}]^+$: 479.1730, found: 479.1730.

5.6.4 Removal of Directing Group



The directing group imidazole moiety was cleaved according to our previous report with slight modification.⁹ To a mixture of 4 Å MS (90 mg, 100 mg/0.1 mmol of **45i**) and **45i** (50.0 mg, 0.090 mmol) was added $\text{CH}_3\text{CN}/\text{CH}_2\text{Cl}_2$ (0.09 M, 1 mL) under nitrogen atmosphere. The suspension was stirred vigorously under a positive pressure of nitrogen for 1 hour at room temperature. Then methyl triflate (6.0 μL , 0.054 mmol, 0.6 equiv) was added in one portion at 0 °C. After being stirred at 0 °C for 3 h, another 0.6 equiv of methyl trifluoromethanesulfonate was added, and kept at 0 °C for another 3 h. Afterwards, DBU (23 μL , 0.135 mmol, 1.5 equiv) was added and the mixture was stirred at 0 °C for furthermore 1 h. The reaction was quenched by the addition of water (0.1 mL). Then the mixture was concentrated under vacuum and the residue was purified by flash chromatography on silica gel (EtOAc/*n*-hexane = 1:20) to give **46** (32.0 mg, 86%) as a white solid. $R_f = 0.5$ in *n*-hexane/EtOAc (10:1).

Dr of **46** was determined by the ^1H NMR analysis of pure compound.

Ee of **46** was established by HPLC analysis using a Chiralpak AS-H column to obtain 98% ee (HPLC: AS-H, *n*-hexane/isopropanol = 80:20, flow rate 1 mL/min, 25 °C, t_r (major) = 19.4 min, t_r (minor) = 22.1 min). $[\alpha]_{22}^D = -33.4^\circ$ (c 1.0, CH_2Cl_2).

^1H NMR (300 MHz, CD_2Cl_2) δ 7.23–7.69 (m, 2H), 7.50–7.43 (m, 3H), 7.32–7.22 (m, 4H), 4.55 (m, 1H), 4.11 (dd, $J = 8.3, 4.5$ Hz, 1H), 2.90 (dd, $J = 17.6, 8.4$ Hz, 1H), 2.77 (dd, $J = 17.6, 4.5$ Hz, 1H), 2.53 (s, 3H), 1.52–1.40 (m, 5H) 1.30–1.06 (m, 5H).

^{13}C NMR (75 MHz, CD_2Cl_2) δ 174.9, 167.7, 139.3, 138.6, 135.4, 129.2, 128.8, 127.1, 126.2, 90.8, 75.1, 51.6, 36.6, 31.2, 31.1, 25.5, 23.6, 16.0.

IR (film): ν (cm^{-1}) 2922, 2859, 1795, 1733, 1496, 1468, 1446, 1432, 1417, 1397, 1314, 1276, 1262, 1236, 1170, 1132, 1086, 1056, 1035, 1016, 1005, 977, 937, 899, 885, 844, 801, 790.

HRMS (ESI, m/z) calcd for $\text{C}_{24}\text{H}_{26}\text{O}_4\text{SNa}$ $[\text{M}+\text{Na}]^+$: 433.1444, found: 433.1445.

5.6.5 Mechanistic Experiments

1) UV-Vis Absorption Spectra

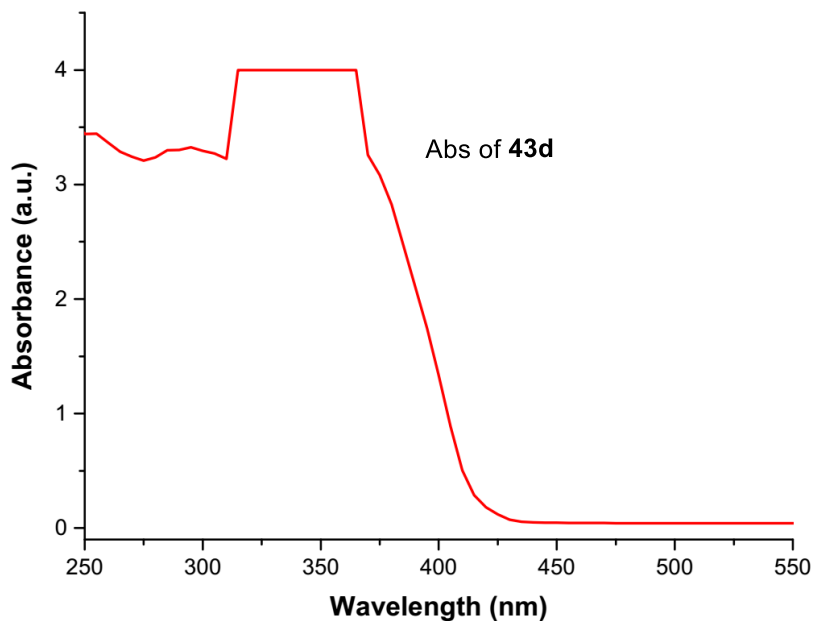


Figure 100. UV-Vis absorption spectrum of α -ketoester **43d** (0.3 M in acetone).

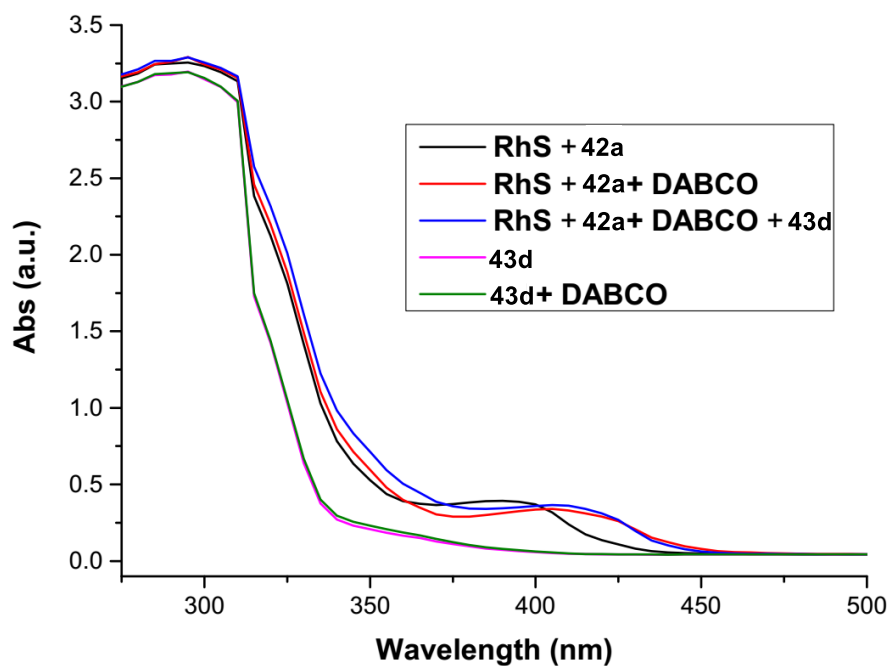


Figure 101. UV-Vis absorption of different compound combinations. Each component was mixed in a ratio that reflects the actual reaction setup. The concentrations are 100-fold lower compared to the actual reaction setup.

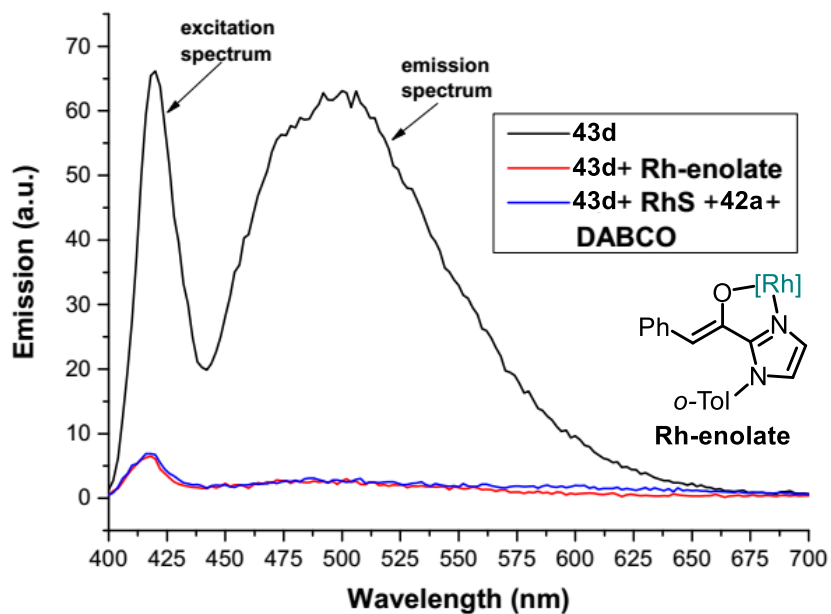


Figure 102. UV-Vis emission (black) spectra of α -ketoester **43d** (0.3 M in acetone) and different combinations. Each component was used in a ratio and concentration that reflects the actual reaction setup. $\lambda_{\text{ex}} = 420$ nm. A **Rh-enolate**⁹ devoid of a β -methylene was employed to rule out a β -H abstraction pathway.

2) Determination of Extinction Coefficient of **43d** and **Rh-enolate**

The absorbance values of **43d** and **Rh-enolate** were collected at different concentrations at 420 nm in acetone and the extinction coefficients determined according to the Lambert-Berr law. As a result, the extinction coefficient of **43d** was calculated as: $\epsilon_{420} = 0.46 \text{ M}^{-1}\text{cm}^{-1}$ and the extinction coefficient of **Rh-enolate**⁹ as: $\epsilon_{420} = 3235 \text{ M}^{-1}\text{cm}^{-1}$.

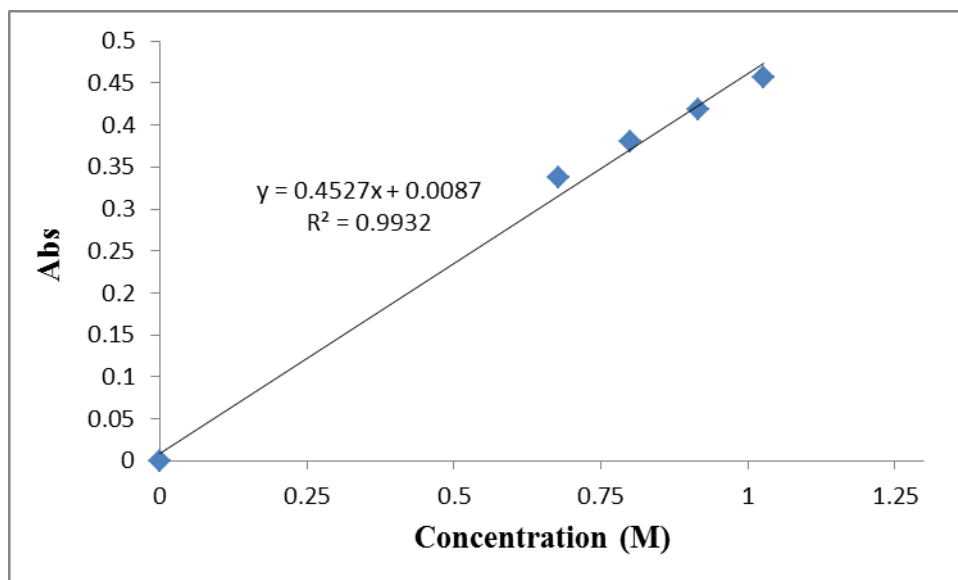


Figure 103. The relation between absorbance at 420 nm and concentrations of **43d** in acetone.

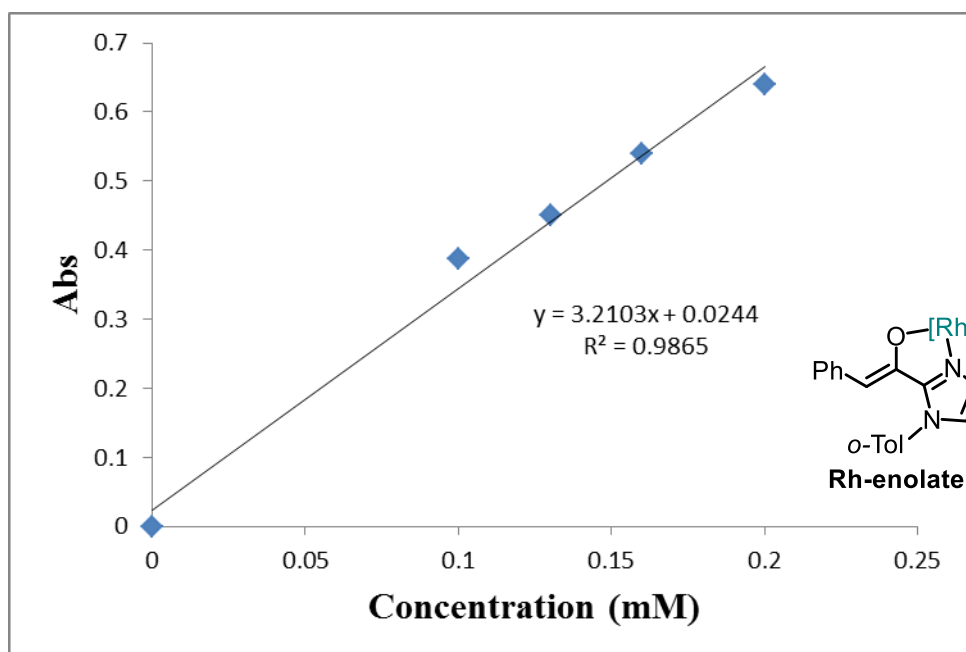


Figure 104. The relation between absorbance at 420 nm and concentrations of **Rh-enolate** in acetone. A **Rh-enolate** devoid of a β -methylene was employed as a model **Rh-enolate** intermediate because of higher chemical stability.

5.6.6 Single Crystal X-Ray Diffraction Studies

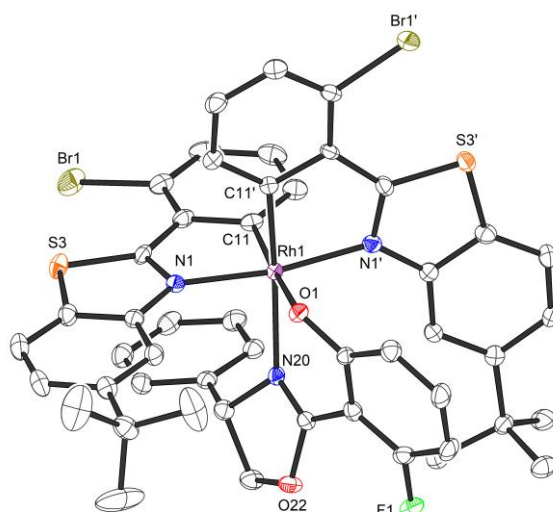


Figure 105. Crystal structure of Δ -(*S*)-**56**. ORTEP drawing with 50 % probability thermal ellipsoids.

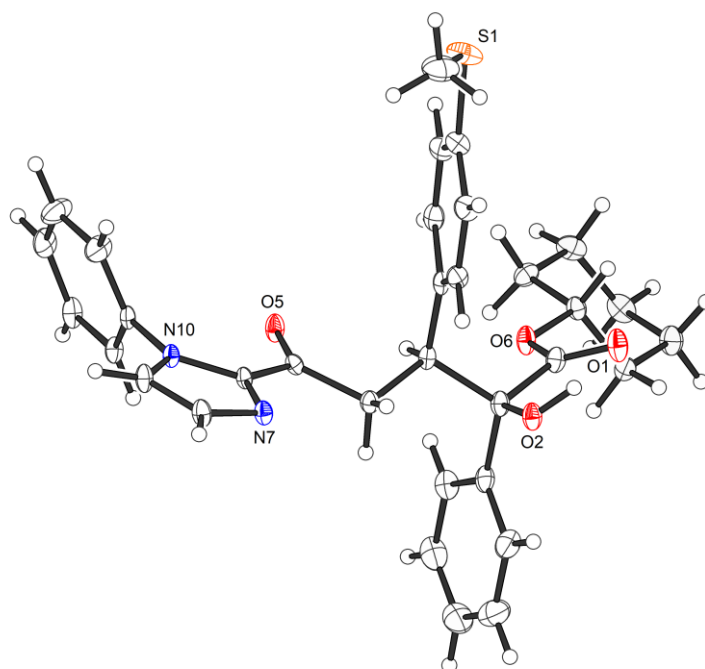


Figure 106. Crystal structure of **45i**. ORTEP drawing with 50 % probability thermal ellipsoids.

Table 18. Crystal data and structure refinement for Δ -(S)-56.

Identification code	Δ -(S)-56	
Habitus, colour	prism, yellow	
Crystal size	0.37 x 0.11 x 0.10 mm ³	
Crystal system	Orthorhombic	
Space group	P2 ₁ 2 ₁ 2 ₁	Z = 4
Unit cell dimensions	a = 12.86140(10) Å	= 90°.
	b = 17.9146(2) Å	= 90°.
	c = 18.8871(2) Å	= 90°.
Volume	4351.72(8) Å ³	
Cell determination	79289 peaks with Theta 2.3 to 75.9 °	
Empirical formula	C ₄₉ H ₄₁ Br ₂ F N ₃ O ₂ Rh S ₂	
Moiety formula	C ₄₉ H ₄₁ Br ₂ F N ₃ O ₂ Rh S ₂	
Formula weight	1049.70	
Density (calculated)	1.602 Mg/m ³	
Absorption coefficient	6.609 mm ⁻¹	
F(000)	2112	
Data collection:		
Diffractometer type	STOE STADIVARI	
Wavelength	1.54178 Å	
Temperature	100(2) K	
Theta range for data collection	3.400 to 76.137 °	
Index ranges	-16<=h<=15, -22<=k<=18, -15<=l<=23	
Data collection software	X-Area Pilatus3_SV 1.31.127.0 (STOE, 2016) ¹⁷	
Cell refinement software	X-Area Recipe 1.33.0.0 (STOE, 2015) ¹⁸	
Data reduction software	X-Area Integrate 1.71.0.0 (STOE, 2016) ¹⁹ X-Area LANA 1.68.2.0 (STOE, 2016) ²⁰	
Solution and refinement:		
Reflections collected	77982	
Independent reflections	8981 [R(int) = 0.0427]	
Completeness to theta = 67.679 °	100.0 %	
Observed reflections	8638[I > 2σ(I)]	
Reflections used for refinement	8981	
Absorption correction	Semi-empirical from equivalents ²⁰	
Max. and min. transmission	1.0000 and 0.2381	

Flack parameter (absolute struct.)	-0.006(4) ²¹
Largest diff. peak and hole	0.538 and -0.573 e.Å ⁻³
Solution	dual space algorithm
Refinement	Full-matrix least-squares on F ²
Treatment of hydrogen atoms	Calculated positions, constr. ref.
Programs used	XT V2014/1 (Bruker AXS Inc., 2014) ²² SHELXL-2016/6 (Sheldrick, 2016) ²³ DIAMOND (Crystal Impact) ²⁴ ShelXle (Hübschle, Sheldrick, Dittrich, 2011) ²⁵
Data / restraints / parameters	8981 / 42 / 578
Goodness-of-fit on F ²	1.063
R index (all data)	wR2 = 0.0687
R index conventional [I>2sigma(I)]	R1 = 0.0265

Table 19. Crystal data and structure refinement for **45i**.

Identification code	45i	
Habitus, colour	nugget, pale yellow	
Crystal size	0.36 x 0.13 x 0.12 mm ³	
Crystal system	Triclinic	
Space group	P1	Z = 4
Unit cell dimensions	a = 10.3202(5) Å	α = 78.028(1) °
	b = 15.5911(6) Å	β = 74.768(2) °
	c = 19.1946(8) Å	γ = 83.519(2) °
Volume	2909.6(2) Å ³	
Cell determination	9758 peaks with Theta 2.4 to 27.5 °	
Empirical formula	C ₃₃ H ₃₄ N ₂ O ₄ S	
Moiety formula	C ₃₃ H ₃₄ N ₂ O ₄ S	
Formula weight	554.68	
Density (calculated)	1.266 Mg/m ³	
Absorption coefficient	0.151 mm ⁻¹	
F(000)	1176	
Data collection:		
Diffraction type	Bruker D8 QUEST area detector	
Wavelength	0.71073 Å	

Temperature	100(2) K
Theta range for data collection	2.238 to 27.588 °
Index ranges	-13<=h<=13, -20<=k<=20, -24<=l<=24
Data collection software	APEX3 (Bruker AXS Inc., 2015) ¹⁷
Cell refinement software	SAINT V8.37A (Bruker AXS Inc., 2015) ¹⁸
Data reduction software	SAINT V8.37A (Bruker AXS Inc., 2015)

Solution and refinement:

Reflections collected	176522
Independent reflections	25501 [R(int) = 0.0409]
Completeness to theta = 25.242 °	99.9 %
Observed reflections	23537[I > 2σ(I)]
Reflections used for refinement	25501
Absorption correction	Semi-empirical from equivalents ¹⁹
Max. and min. transmission	0.7456 and 0.7256
Flack parameter (absolute struct.)	0.002(9) ²⁰
Largest diff. peak and hole	0.525 and -0.416 e.Å ⁻³
Solution	dual space method
Refinement	Full-matrix least-squares on F ²
Treatment of hydrogen atoms	CH calculated, constr., OH located, isotr. ref.
Programs used	XT V2014/1 (Bruker AXS Inc., 2014) ²¹ SHELXL-2016/6 (Sheldrick, 2016) ²² DIAMOND (Crystal Impact) ²³ ShelXle (Hübschle, Sheldrick, Dittrich, 2011) ²⁴
Data / restraints / parameters	25501 / 3 / 1461
Goodness-of-fit on F ²	1.038
R index (all data)	wR2 = 0.0918
R index conventional [I>2σ(I)]	R1 = 0.0377

References

- 1 a) J. Ma, X. Shen, K. Harms, E. Meggers, *Dalton Trans.* **2016**, 45, 8320; b) J. Ma, X. Zhang, X. Huang, S. Luo, E. Meggers, *Nat. Protoc.* **2018**, 13, 605.
- 2 H. Huo, X. Shen, C. Wang, L. Zhang, P. Röse, L.-A. Chen, K. Harms, M. Marsch, G. Hilt, E. Meggers, *Nature* **2014**, 515, 100.
- 3 T. Mietke, T. Cruchter, E. Winterling, M. Tripp, K. Harms, E. Meggers, *Chem. Eur. J.* **2017**, 23, 12363.
- 4 a) X. Shen, H. Huo, C. Wang, B. Zhang, K. Harms, E. Meggers, *Chem. Eur. J.* **2015**, 21, 9720; b) E. Marchi, R. Sinisi, G. Bergamini, M. Tragni, M. Monari, M. Bandini, P. Ceroni, *Chem. Eur. J.* **2012**,

18, 8765.

5 a) C. Wang, Y. Zheng, H. Huo, P. Röse, L. Zhang, K. Harms, G. Hilt, E. Meggers, *Chem. Eur. J.* **2015**, *21*, 7355; b) H. Huo, C. Wang, K. Harms, E. Meggers, *J. Am. Chem. Soc.* **2015**, *137*, 9551; c) K. N. Boblak, D. A. Klumpp, *J. Org. Chem.* **2014**, *79*, 5852; d) N. Deibl, R. Kempe, *J. Am. Chem. Soc.* **2016**, *138*, 10786.

6 X. Huang, X. Li, M. Zou, J. Pan, N. Jiao, *Org. Chem. Front.* **2015**, *2*, 354.

7 K. Szöri, K. Balázsik, K. Felföldi, M. Bartók, *J. Catal.* **2006**, *241*, 149.

8 T. Igarashi, E. Tayama, H. Iwamoto, E. Hasegawa, *Tetrahedron Lett.* **2013**, *54*, 6874.

9 X. Huang, R. D. Webster, K. Harms, E. Meggers, *J. Am. Chem. Soc.* **2016**, *138*, 12636.

10 L. Lu, B. Xiangbin, Y. Xinyi, Z. Xiaowei, T. Choon-Hong, J. Zhiyong, *Angew. Chem. Int. Ed.* **2017**, *56*, 13842.

11 B. D. Mahoney, N. A. Piro, P. J. Carroll, E. J. Schelter, *Inorg. Chem.* **2013**, *52*, 5970

12 S. Li, M. Aljhdli, H. Thakellapalli, B. Farajidizaji, Y. Zhang, N. G. Akhmedov, C. Milsman, B. V. Popp, K. K. Wang, *Org. Lett.* **2017**, *19*, 4078.

13 G. A. Russell, S. A. Weiner, *J. Am. Chem. Soc.* **1967**, *89*, 6623.

14 M. H. Shaw, V. W. Shurtleff, J. A. Terrett, J. D. Cuthbertson, D. W. C. MacMillan, *Science* **2016**, *352*, 1304.

15 a) R. Braslau, N. Naik, H. Zipse, *J. Am. Chem. Soc.* **2000**, *122*, 8421; b) H. Fischer, H. Paul, *Acc. Chem. Res.* **1987**, *20*, 200.

16 a) U. Megerle, R. Lechner, B. König and E. Riedle, *Photochem. Photobiol. Sci.* **2010**, *9*, 1400; b) X. Huang, S. Luo, O. Burghaus, R. D. Webster, K. Harms, E. Meggers, *Chem. Sci.* **2017**, *8*, 7126.

17 APEX3, Bruker AXS Inc., Madison, Wisconsin, USA, **2016**.

18 SAINT, Bruker AXS Inc., Madison, Wisconsin, USA, **2015**.

19 SADABS. Bruker AXS area detector scaling and absorption correction, Bruker AXS Inc., Madison, Wisconsin, USA, **2016**.

20 S. Parsons, H. D. Flack, T. Wagner, *Acta Cryst. B* **2013**, *69*, 249.

21 G. M. Sheldrick, *Acta Cryst. A* **2015**, *71*, 3.

22 G. Sheldrick, *Acta Cryst. C* **2015**, *71*, 3.

23 K. Brandenburg, *Diamond - Crystal and Molecular Structure Visualization*, Crystal Impact - Dr. H. Putz & Dr. K. Brandenburg GbR, Bonn, Germany, **2014**.

24 C. B. Hübschle, G. M. Sheldrick, B. Dittrich, *J. Appl. Cryst.* **2011**, *44*, 1281.

Chapter 6: Appendices

6.1 List of Abbreviations

^1H NMR	proton nuclear magnetic resonance spectroscopy
^{13}C NMR	carbon nuclear magnetic resonance spectroscopy
^9F NMR	fluorine nuclear magnetic resonance spectroscopy
δ	chemical shift
J	coupling constant
br	broad
s	singlet
d	doublet
t	triplet
q	quartet
m	multiplet
ppm	parts per million
AcOH	acetic acid
aq	aqueous
Ar	argon
bpy	2,2'-bipyridine
CD	circular dichroism
CH_2Cl_2 / DCM	dichloromethane
CD_2Cl_2	dideuteromethylenechloride
CHCl_3	chloroform
CDCl_3	deuteriochloroform
CH_3CN / MeCN	acetonitrile
conc	concentrated
DMAP	4-dimethylaminopyridine
DMF	dimethylformamide
DMSO	dimethyl sulfoxide

Appendices

dr	diastereomeric ratio
EDA	electron donor-acceptor
EDC	1-ethyl-3-(3-dimethylaminopropyl)carbodiimide hydrochloride
ee	enantiomeric excesses
e.g.	exempli gratia (lat.: for example)
et al.	et alii (lat.: and others)
ESI	electrospray ionization
EtOH	ethanol
Et ₂ O	diethyl ether
Et ₃ N	triethyl amine
EtOAc	ethyl acetate
EWG	electron withdrawing group
HAT	hydrogen atom transfer
h	hour(s)
HPLC	high performance liquid chromatography
HRMS	high resolution mass spectrometry
Hz	Hertz
IR spectra	infrared spectra
Ir	iridium
L	liter(s)
M	mol/liter
<i>m</i>	meta-
min	minute(s)
mL	milliliter(s)
mmol	millimole
MS	mass spectroscopy
N ₂	nitrogen
Nu	nucleophile
PCET	proton-coupled electron transfer

Appendices

Ph	phenyl
PPh ₃	triphenylphosphine
ppm	parts per million
ppy	2-phenylpyridine
PC	photoredox catalyst
<i>rac</i>	racemate
Rh	rhodium
rt	room temperature
SET	single-electron transfer
TEMPO	2,2,6,6-tetramethyl-1-piperidinyloxy
TFA	trifluoroacetic acid
THF	tetrahydrofuran
TLC	thin layer chromatography
UV	ultraviolet

6.2 List of Figures

Figure 1. Visible-light-induced photoredox catalytic processes as exemplified by $[\text{Ru}(\text{bpy})_3]^{2+}$. MLCT = metal to ligand charge transfer. ISC = intersystem crossing. SET = single electron transfer	1
Figure 2. Representative photoredox and asymmetric catalysts. The chiral-at-iridium Lewis acid and the chiral amine (only in special cases) constitute dual functions of photoredox/asymmetric catalyst. .	3
Figure 3. α -Alkylation of aldehydes enabled by dual photoredox/enamine catalysis.....	5
Figure 4. Enantioselective α -alkylation of aldehydes through photoexcited EDA and radical chain mechanism. EDA = electron donor acceptor. PET = photoinduced electron transfer	6
Figure 5. Single chiral amine catalyzed enantioselective photoredox chemistry through the direct photoexcitation of enamine. CFL = compact fluorescent lamp.....	7
Figure 6. β -Alkylation of aldehydes through photoexcited iminium ion intermediate enabled by single chiral amine catalyst. TMS = trimethylsilyl. TDS = thexyl-dimethylsilyl.	8
Figure 7. Enantioselective radical conjugate addition reaction enabled by dual photoredox/enamine catalysis. $[\text{Ir}] = \text{Ir}[\text{dF}(\text{CF}_3)\text{ppy}]_2(\text{dtbbpy})\text{PF}_6$	9
Figure 8. β -Arylation of the aldehydes and ketones enabled by dual photoredox/enamine catalysis. $[\text{Ir}] = \text{fac-Ir}(\text{ppy})_3$	10
Figure 9. α -Alkylation of aldehydes enabled by triple photoredox/enamine/HAT catalysis.	11
Figure 10. Proposed mechanism for triple photoredox/enamine/HAT catalysis.	11
Figure 11. Asymmetric α -acylation of tertiary amines enabled by dual photoredox/NHC catalysis. $[\text{Ru}] = \text{Ru}(\text{bpy})_3\text{Cl}_2$. NHC = <i>N</i> -heterocyclic carbene.	12
Figure 12. Enantioselective synthesis of <i>syn</i> 1,2-amino alcohols through dual photoredox/Brønsted acid catalysis. CPA = chiral phosphoric acid. PCET = proton-coupled electron transfer. $[\text{Ir}] = [\text{Ir}(\text{ppy})_2(\text{dtbbpy})]\text{PF}_6$. HE = Hantzsch ester.	13
Figure 13. Radical conjugate addition-enantioselective protonation by dual photoredox/Brønsted acid catalysis.	14
Figure 14. Enantioselective Minisci-type reaction through dual photoredox/Brønsted acid catalysis.	15
Figure 15. Proposed mechanism for dual photoredox/Brønsted acid catalysis promoted Minisci-type reaction.	16

Figure 16. Dual photoredox/Brønsted acid catalysis promoted enantioselective redox coupling of <i>N</i> -arylaminoethanes with <i>N</i> -sulfonyl imines.	17
Figure 17. Enantioselective Mukaiyama Mannich reaction through by sequential photoredox and chiral anion-bonding catalysis.	18
Figure 18. Single chiral phase transfer catalyst (PTC) enabled enantioselective perfluoroalkylation of cyclic β -ketoesters.	19
Figure 19. Enantioselective anti-Markovnikov hydroetherification of alkenols through single chiral ion pair catalyst.	20
Figure 20. Enantioselective decarboxylative Csp^3-Csp^2 cross-coupling reaction enabled by dual photoredox/nickel catalysis.	20
Figure 21. Enantioselective desymmetrization of cyclic <i>meso</i> -anhydrides enabled by dual photoredox/nickel catalysis.	21
Figure 22. Enantioselective cross-coupling of racemic tertiary alkyl chlorides with amines enabled by visible-light-activated single copper catalysis.	22
Figure 23. Enantioselective [2+2] cycloaddition enabled by dual photoredox/Lewis acid catalysis. ..	23
Figure 24. Enantioselective radical conjugate addition reaction eabled by dual photoredox/Lewis acid catalysis.	24
Figure 25. Enantioselective radical conjugate addition reaction enabled by single Ni-based Lewis acid catalyst under visible-light-activated photoredox conditions.	25
Figure 26. Structure of chiral-at-Ir(III) Lewis acid catalyst.	26
Figure 27. Enantioselective photoredox reactions enabled by single chiral-at-Ir Lewis acid catalyst.	27
Figure 28. Single chiral-at-Ir Lewis acid catalyst Λ - IrS mediated asymmetric radical-radical cross-coupling reactions under photoredox conditions.	28
Figure 29. a) Enantioselective cross-dehydrogenative-coupling (CDC) reaction mediated by single chiral-at-rhodium complex Λ - RhO ; b) Enantioselective radical conjugate addition reaction mediated by single Λ - RhO derivative.	29
Figure 30. Single chiral-at-Rh Lewis acid catalyst mediated enantioselective photoredox reaction. ODN = 2,4-dinitrophenylsulfonyloxy.	30
Figure 31. Synthetic strategies for chiral-at-metal iridium and rhodium catalysts.	37
Figure 32. Attempts on resolution of <i>rac</i> - RhS using enantiopure amino acids.	39

Figure 33. Chiral-auxiliary-mediated synthesis of enantiomerically pure Λ - and Δ - RhS	40
Figure 34. Reaction system after first time centrifugation (left) and after washing by EtOH for another three more times (right).....	40
Figure 35. Crystal structure of the auxiliary complex Λ -(<i>S</i>)- 9 . ORTEP drawing with 50% thermal ellipsoids.....	41
Figure 36. CD spectra of Λ - and Δ - RhS recorded in CH ₃ OH:CH ₂ Cl ₂ (4:1).	41
Figure 37. HPLC traces of racemic, Λ - and Δ - RhS . HPLC conditions: Daicel Chiralpak IB, 250 x 4.6 mm, column temp. = 25 °C, abs = 254 nm, flow rate = 0.6 mL/min, solvent A = 0.1% aqueous TFA, solvent B = MeCN, gradient = 40% to 50% B in 180 min.....	42
Figure 38. Comparison of catalytic activity of Λ - RhS and Δ - RhO	42
Figure 39. Superimposed crystal structure of Λ - RhS (grey) with inverted Δ - RhO (green). Fitted are the central metal together with the metal-bound atoms. Atoms are displayed as 50% thermal ellipsoids.	43
Figure 40. Photoinduced catalytic enantioselective radical conjugate addition by Yoon and the former group member H. Huo.....	45
Figure 41. a) Substrate redesign; b) attempt to enantioselective radical conjugate addition. n.d. = not detected. PC = photocatalyst	46
Figure 42. Catalytic enantioselective synthesis of 1,2-aminoalcohol under photoredox conditions. PC = photoredox catalyst.	47
Figure 43. Photoinduced enantioselective redox coupling reaction using the general ketone 16a	48
Figure 44. Substrate scope with respect to α -silylamines.....	50
Figure 45. Substrate scope with respect to 2-acyl imidazoles.	51
Figure 46. Proposed mechanism for the observed silyl effect in the visible-light activated Rh/Ru dual catalysis. SET = single electron transfer.....	52
Figure 47. Crystal structure of a derivative intermediate I and the proposed structure of intermediate III with the indicated stereocontrolled radical-radical recombination.....	53
Figure 48. Mechanistic experiments.....	54
Figure 49. a) H. Huo and C. Wang's work on photoinduced radical conjugate addition reaction; b) proposal for this study. PC = photoredox catalyst. [Ir1] = Ir(dF(CF ₃)ppy) ₂ (bpy)PF ₆ . [Ir2] = <i>fac</i> -Ir(ppy) ₃ . PET = photoinduced electron transfer. EWG = electron withdrawing group. EDG = electron donating	

group.....	56
Figure 50. a) Previous work and this study on visible-light-induced three-component fluoroalkylation reactions; b) Reaction design based on asymmetric Lewis acid catalysis in combination with α -diketone organophotoredox chemistry. PET = photoinduced electron transfer. SET = single electron transfer. .	58
Figure 51. Substrate scope with respect to vinyl ethers. ^a Δ - RhS (6 mol%) was employed. ^b Ee of major diastereomer was available. dmp= 3,5-dimethylpyrazole. The absolute and relative configuration of compound 24k was determined as described in the Experimental Part and all other compounds were assigned accordingly.....	63
Figure 52. Gram-scale reaction and catalysts recovery.	64
Figure 53. UV-Vis absorption (black) and luminescence emission (blue) spectra of 4,4'-difluorobenzil were collected in acetone/H ₂ O (9:1, v/v, 4 mM), $\lambda_{\text{ex}} = 400$ nm.	65
Figure 54. Probing radical pathway.....	65
Figure 55. I_0 and I are respective luminescence intensities in the absence and presence of the indicated concentrations of the corresponding quenchers, 4,4'-difluorobenzil was dissolved in acetone/H ₂ O (9:1, v/v, 4 mM), $\lambda_{\text{ex}} = 375$ nm.	66
Figure 56. Radical trapping experiment.	67
Figure 57. a) Proposal for photoredox-catalyst-free asymmetric radical conjugate addition; b) reports on using Hantzsch ester (HE) as visible-light-activated photoreductant. PC = photoredox catalyst. LG = leaving group. [Rh] = chiral-at-rhodium Lewis acids Λ/Δ - RhS	70
Figure 58. a) Representative β -substituted GABA-based drugs; b) approaches to non-racemic γ -amino carbonyl derivatives through photoinduced radical conjugate addition reaction.	71
Figure 59. Reaction design for the synthesis of β -substituted γ -aminobutyric acid analogs. HE = Hantzsch ester. PG = protecting group. NHPI = <i>N</i> -hydroxyphthalimide.	72
Figure 60. Limitations of the developed methodology.....	74
Figure 61. Scope with respect to synthesis of β -alkyl and β -aryl substituted γ -aminobutyric acid analogs. * Δ - RhS was employed.....	75
Figure 62. Substrate scope with respect to synthesis of β -fluorine- β -aryl substituted γ -aminobutyric acid analogs.....	76
Figure 63. Synthetic applications. Reaction conditions: (i) LiOH, THF/H ₂ O; (ii) LiOH, THF/H ₂ O; (iii) <i>D</i> -Phenylglycine methyl ester hydrochloride, Et ₃ N, HOBT; (iv) NaBH ₄ ; (v) Pd/C, H ₂ (1 atm); (vi) LiCl,	

MeOH then TFA followed by Et ₃ N; (vii) Diethylphosphonoacetic acid, LHMDs; (viii) 3,5-Dimethylpyrazole, T ₃ P, Et ₃ N; (ix) <i>N</i> -Benzyloxycarbonyloxy succinimide; K ₂ CO ₃ ; (x) NHPI, DCC, DMAP; (xi) Δ - RhS , HE, 23 W CFL; (xii) Pd/C, H ₂ (1 atm). More details are available in Experimental Part.	77
Figure 64. a) Production of rhodium stabilized allylic radical intermediate under photoredox conditions as accomplished by the group members Huang, Luo and Zhou; b) MacMillan's report on the β -C(sp ³)-H functionalization through a photogenerated 5 π e ⁻ intermediate.....	80
Figure 65. Proposal for chiral-at-rhodium Lewis acid catalyzed enantioselective β -C(sp ³)-H functionalization under photoredox conditions.	81
Figure 66. Substrate scope with respect to 2-acyl imidazoles and 2-acyl pyridines. Structure of 45i was determined by X-ray crystallography and all other compounds were assigned accordingly. *Reaction was performed at 50 °C.	84
Figure 67. Substrate scope with respect to 1,2-dicarbonyl compounds. *Acetone/CH ₂ Cl ₂ (1:1, vol/vol) was used as solvent. Z = 2-(<i>N</i> -phenyl imidazole).	85
Figure 68. Limitations of the substrate scope.	86
Figure 69. Removal of directing group.	86
Figure 70. Proposed mechanism.	87
Figure 71. An overview of mechanistic studies.	88
Figure 72. Trapping experiments under the conditions with benzil (44c) and α -ketoester (44f).	89
Figure 73. Formation route of cyclobutane product 49	90
Figure 74. Redox potentials vs Normal Hydrogen Electrode (NHE).	94
Figure 75. An overview for this thesis. Only the Δ -configuration is shown. MCR = multicomponent reaction. GABAs = γ -aminobutyric acids	96
Figure 76. Chiral Lewis acid catalysts Λ/Δ - RhS	97
Figure 77. Synthetic route to chiral Lewis acid catalysts Λ/Δ - RhS	97
Figure 78. Cooperative rhodium/ruthenium photoredox catalysis to access chiral 1,2-aminoalcohols.	98
Figure 79. Synthesis of fluoroalkyl-containing compounds through enantioselective three-component photoredox chemistry.	99
Figure 80. Synthesis of β -substituted GABA derivatives through enantioselective photoredox catalysis.	

Appendices

Aux = 3-methyl pyrazole.....	100
Figure 81. Single chiral-at-Rh Lewis acid catalyzed β -C(sp ³)-H functionalization under photoredox conditions.	101
Figure 82. HPLC trace for the racemic reference complexes Δ/Λ - RhS . (Daicel Chiralpak IB, with a linear gradient of 40% to 50% B in 180 min, flow rate = 0.6 mL/min).	112
Figure 83. HPLC trace for the complex Λ - RhS . Integration of peak areas > 99% ee.....	113
Figure 84. HPLC trace for the complex Λ - RhS . Integration of peak areas = 99.8% ee.....	113
Figure 85. ¹ H NMR of Λ - RhS recorded in CD ₂ Cl ₂ over 8 days.....	114
Figure 86. HPLC trace for the racemic reference complexes Δ/Λ - RhS . (Daicel Chiralpak IB, with a linear gradient of 40% to 50% B in 180 min, flow rate = 0.6 mL/min), (the retention time changed compared with former when the HPLC conditions were reproduced).	115
Figure 87. HPLC trace of the freshly prepared Λ - RhS (99.9% ee).	115
Figure 88. HPLC trace of the Λ - RhS after 2 days (99.8% ee).	116
Figure 89. HPLC trace of the Λ - RhS after 4 days (99.8% ee).	116
Figure 90. HPLC trace of the Λ - RhS after 6 days (99.8% ee).	117
Figure 91. HPLC trace of the Λ - RhS after 8 days (99.8% ee).	117
Figure 92. Crystal structure of Λ -(<i>S</i>)- 9 . ORTEP drawing with 50 % probability thermal ellipsoids. .	118
Figure 93. Crystal structure of Λ - RhS . The hexafluorophosphate counteranion and the solvent molecules are omitted for clarity. ORTEP drawing with 50 % probability thermal ellipsoids.	119
Figure 94. Crystal structure of 16s . ORTEP drawing with 50 % probability thermal ellipsoids.....	150
Figure 95. One of the two independent ions of complex 51 in the asymmetric unit. The hexafluorophosphate counteranion and the solvent molecules (<i>n</i> -hexane and CH ₂ Cl ₂) are omitted for clarity. No disorder shown. ORTEP drawing with 50 % probability thermal ellipsoids.	150
Figure 96. Kinetic profile of the visible-light-induced three-component reaction catalyzed by individual amounts of 4,4'-difluorobenzil.	186
Figure 97. Section of NOESY spectrum of 24s in CDCl ₃ at 300 K, mixing time 1.5 s.	194
Figure 98. Structural scheme of 24s , with partial conformation sketch.	194
Figure 99. a) Setup of the reported photoreactions; b) emission spectrum of the employed 24 W blue LEDs.....	255
Figure 100. UV-Vis absorption spectra of α -ketoester 43d (0.3 M in acetone).	284

Figure 101. UV-Vis absorption of different compound combinations. Each component was mixed in a ratio that reflects the actual reaction setup. The concentrations are 100-fold lower compared to the actual reaction setup..... 284

Figure 102. UV-Vis emission (black) spectra of α -ketoester **43d** (0.3 M in acetone) and different combinations. Each component was used in a ratio and concentration that reflects the actual reaction setup. $\lambda_{\text{ex}} = 420$ nm. A **Rh-enolate**⁹ devoid of a β -methylene was employed to rule out a β -H abstraction pathway..... 285

Figure 103. The relation between absorbance at 420 nm and concentrations of **43d** in acetone. 286

Figure 104. The relation between absorbance at 420 nm and concentrations of **Rh-enolate** in acetone. A **Rh-enolate** devoid of a β -methylene was employed as a model Rh-enolate intermediate because of higher chemical stability..... 286

Figure 105. Crystal structure of Δ -(*S*)-**56**. ORTEP drawing with 50 % probability thermal ellipsoids. 287

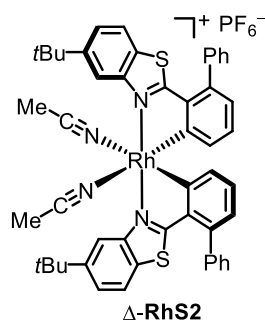
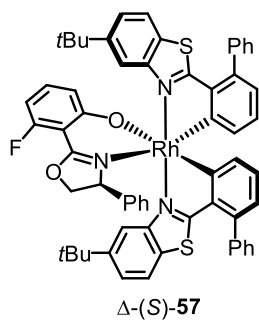
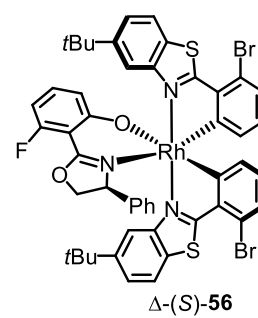
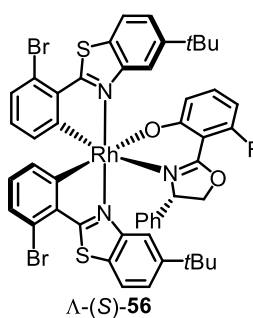
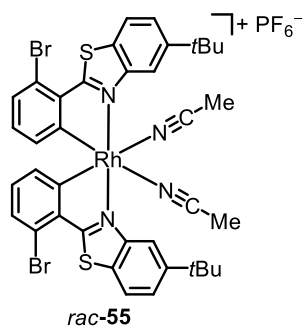
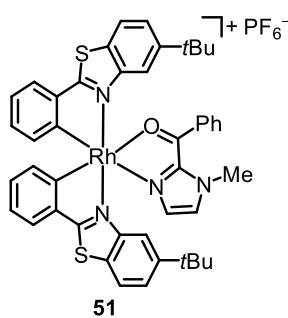
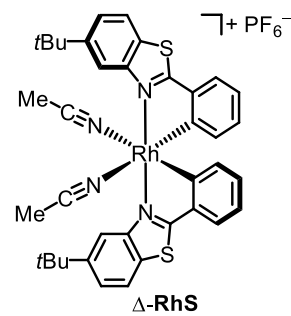
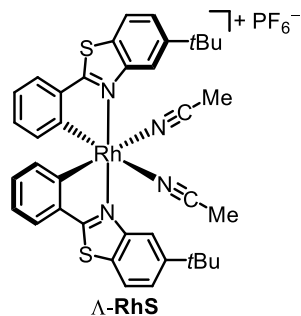
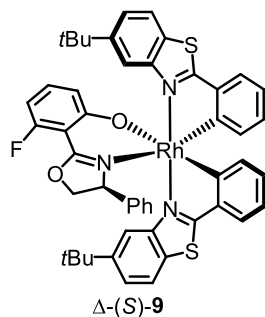
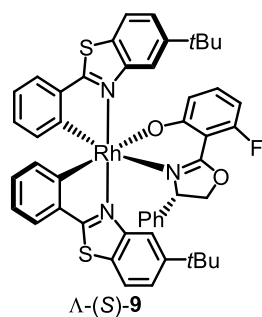
Figure 106. Crystal structure of **45i**. ORTEP drawing with 50 % probability thermal ellipsoids. 287

6.3 List of Tables

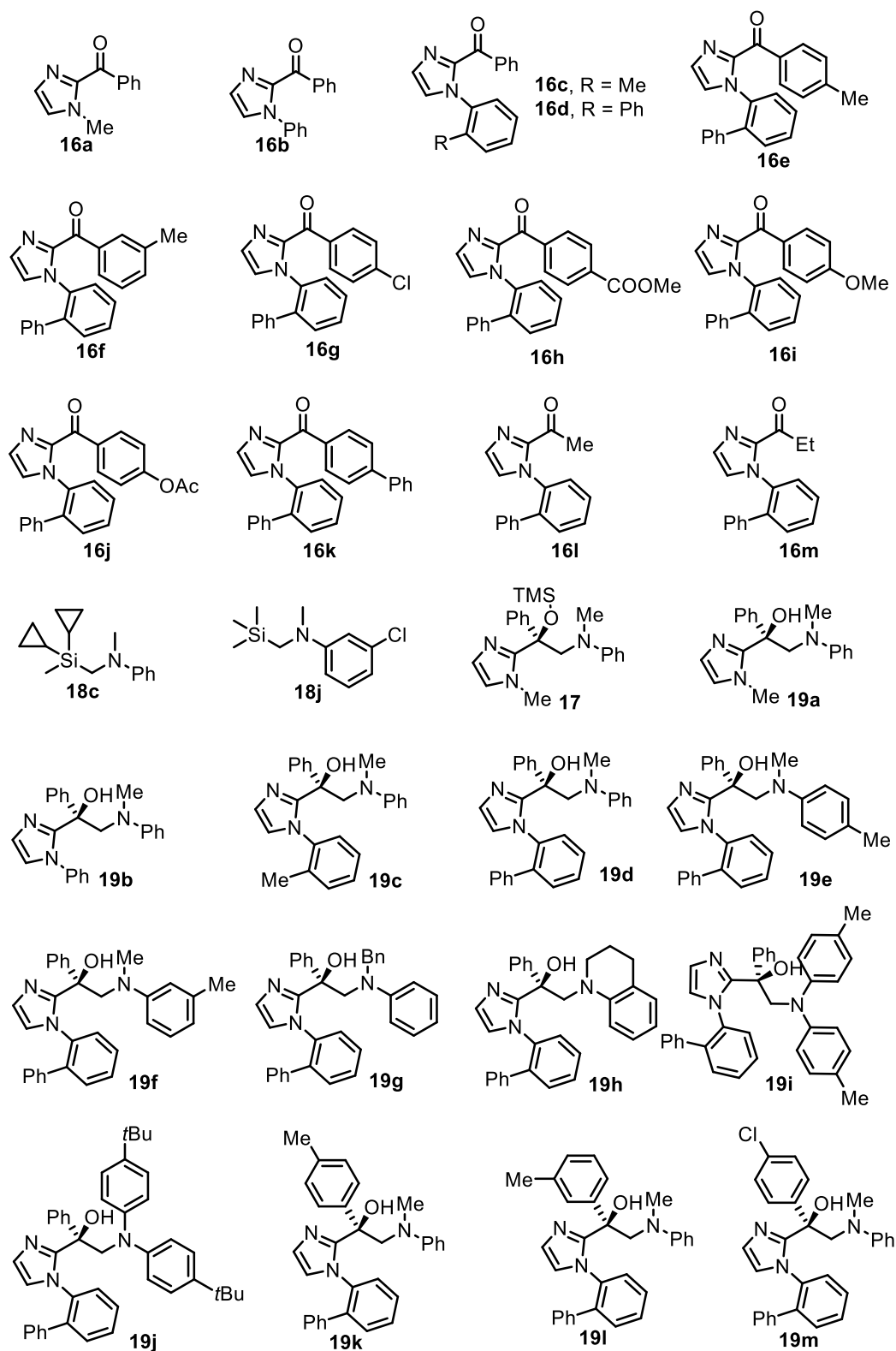
Table 1. Structures of chiral-at-metal Lewis acids.....	34
Table 2. Reaction development and control experiments.	49
Table 3. Reaction development and control experiments ^a	61
Table 4. Substrate scope with respect to <i>N</i> -acylpyrazoles and sodium perfluoroalkyl sulfinates ^a	62
Table 5. Reaction development and control experiments ^a	73
Table 6. Reaction development and control experiments ^a	83
Table 7. Comparison of different light source ^a	90
Table 8. Comparison of different base ^a	91
Table 9. Comparison of different viscous solvents ^a	92
Table 10 Crystal data and details of the structure determination.....	120
Table 11. Crystal data and details of the structure determination.	151
Table 12. Effect of NH ₄ PF ₆ ^a	159
Table 13. Effect of H ₂ O ^a	159
Table 14. Comparison of different photoredox mediators ^a	160
Table 15. Comparison of different light sources ^a	161
Table 16. Control experiments with triplet quencher and TEMPO ^a	161
Table 17. Crystal data and structure refinement for 30d'	237
Table 18. Crystal data and structure refinement for Δ-(<i>S</i>)- 56	288
Table 19. Crystal data and structure refinement for 45i	289

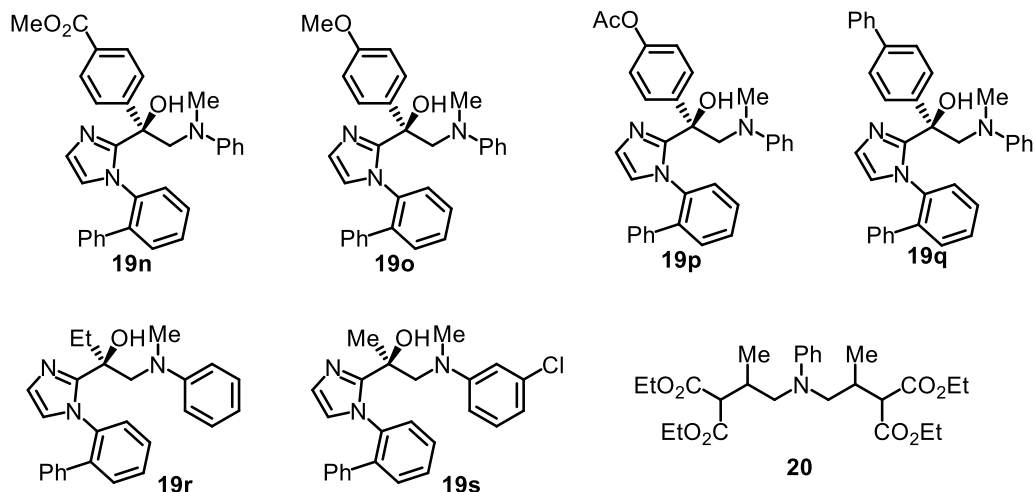
6.4 List of New Compounds

1) Rhodium complexes:

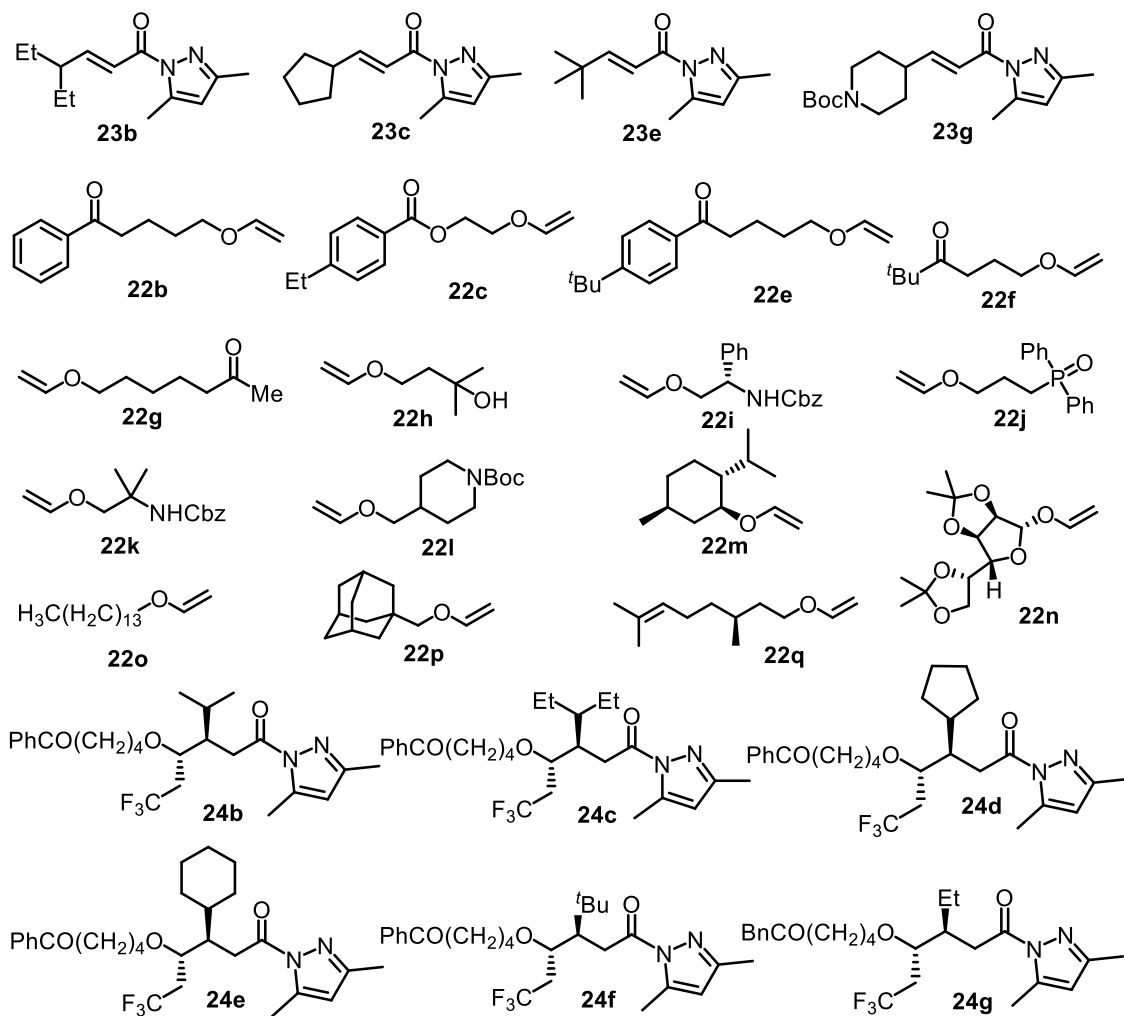


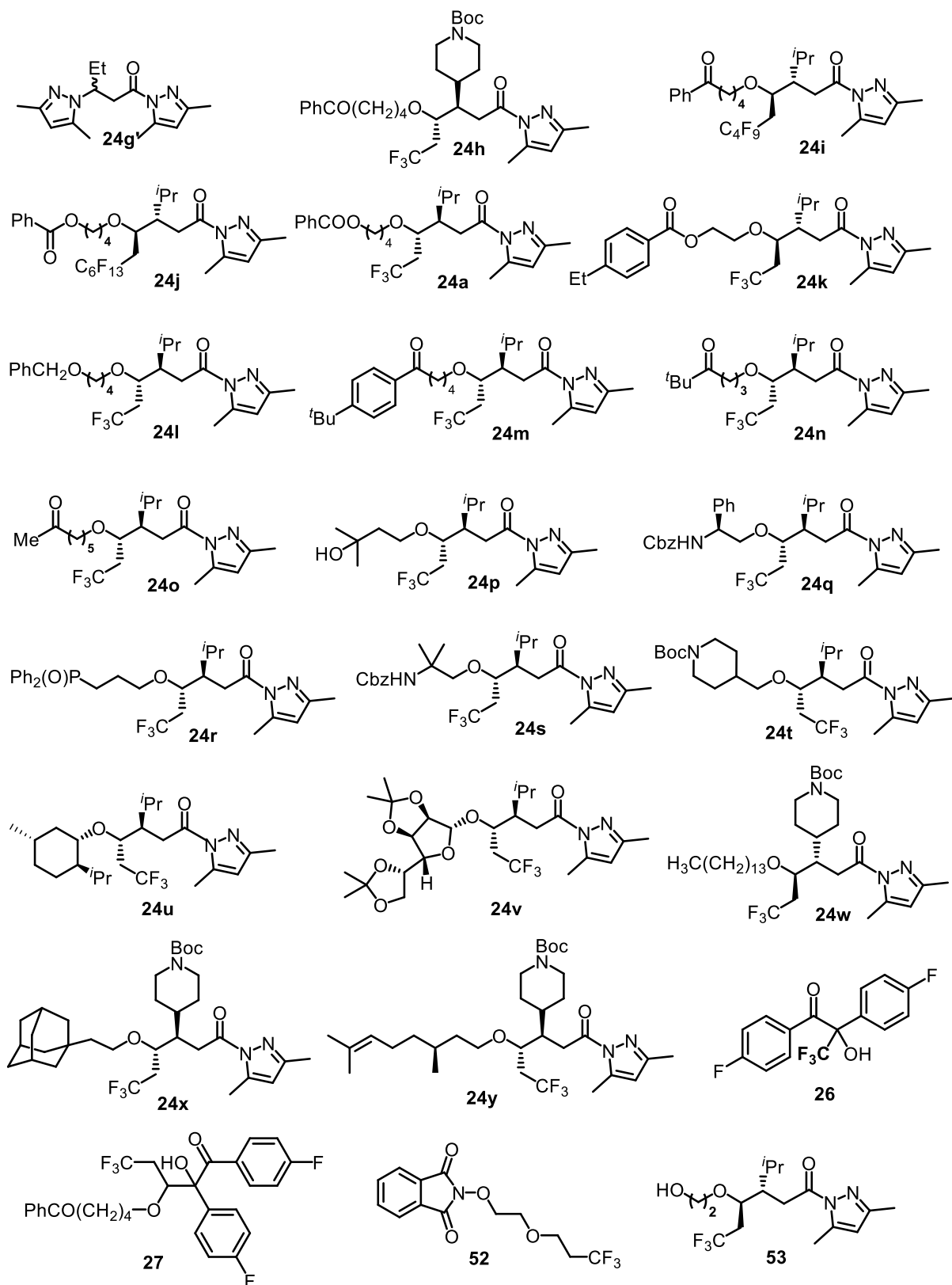
2) Chapter 3.2 and its Experimental Part



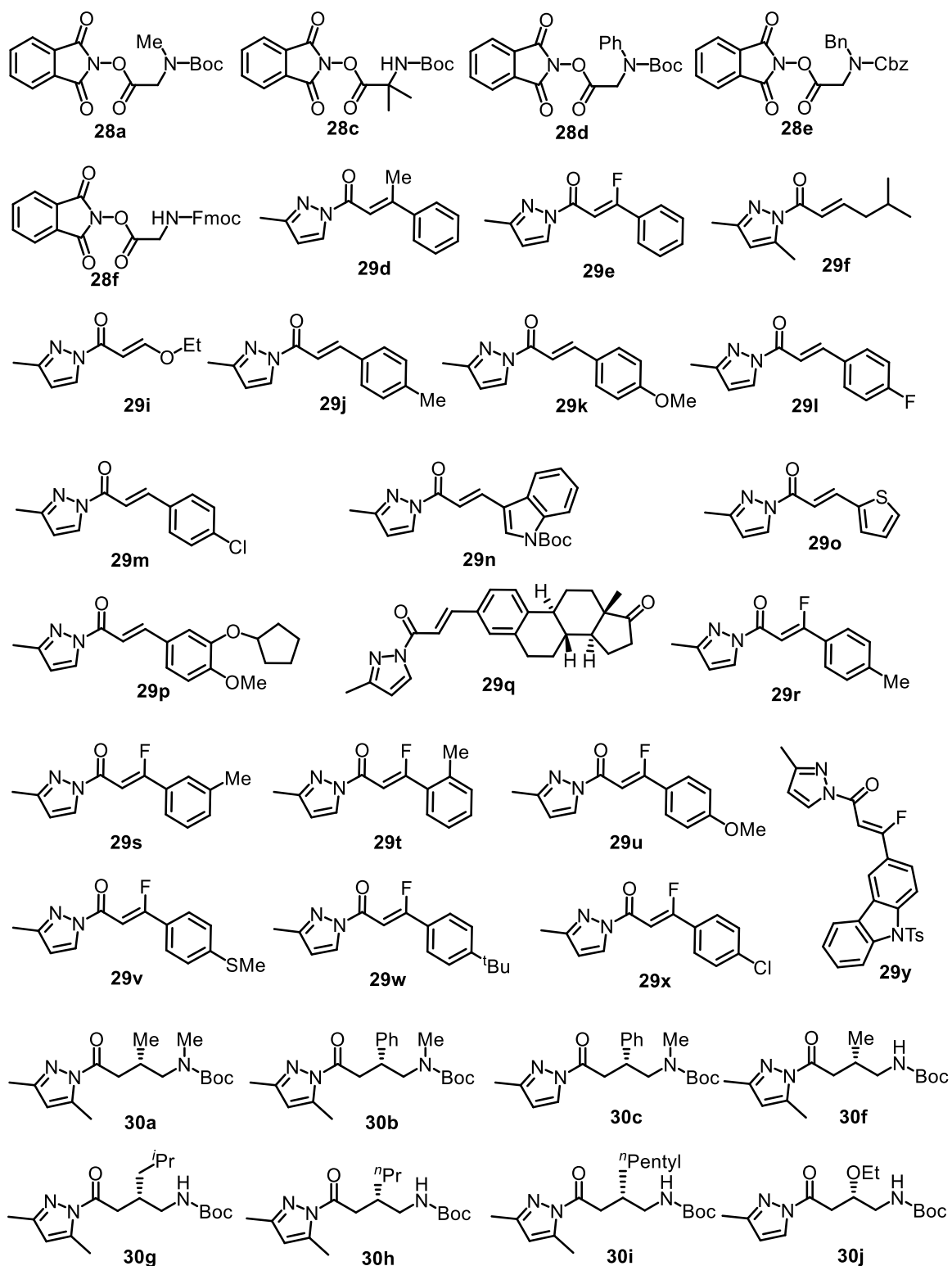


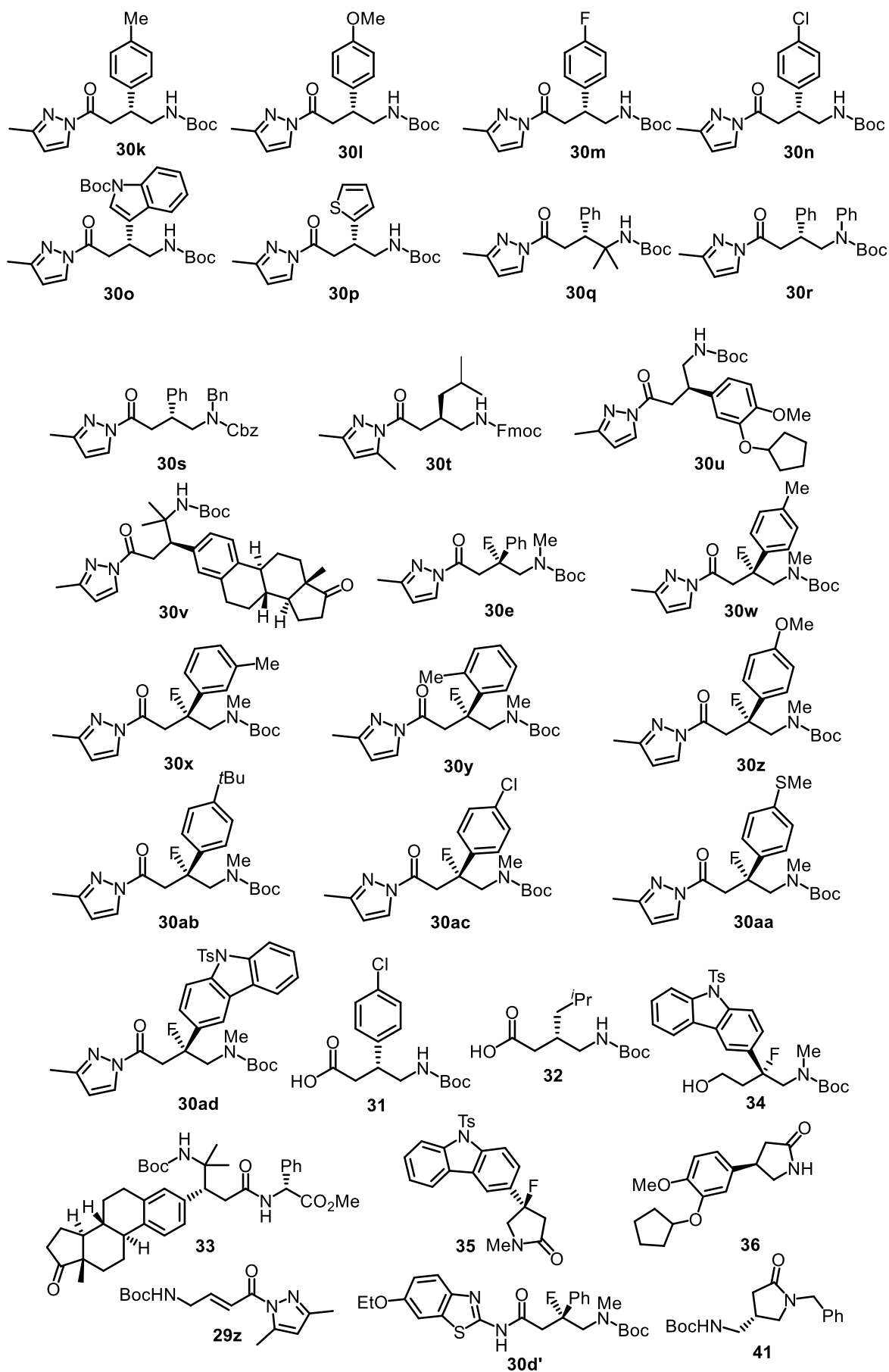
3) Chapter 3.3 and its Experimental Part



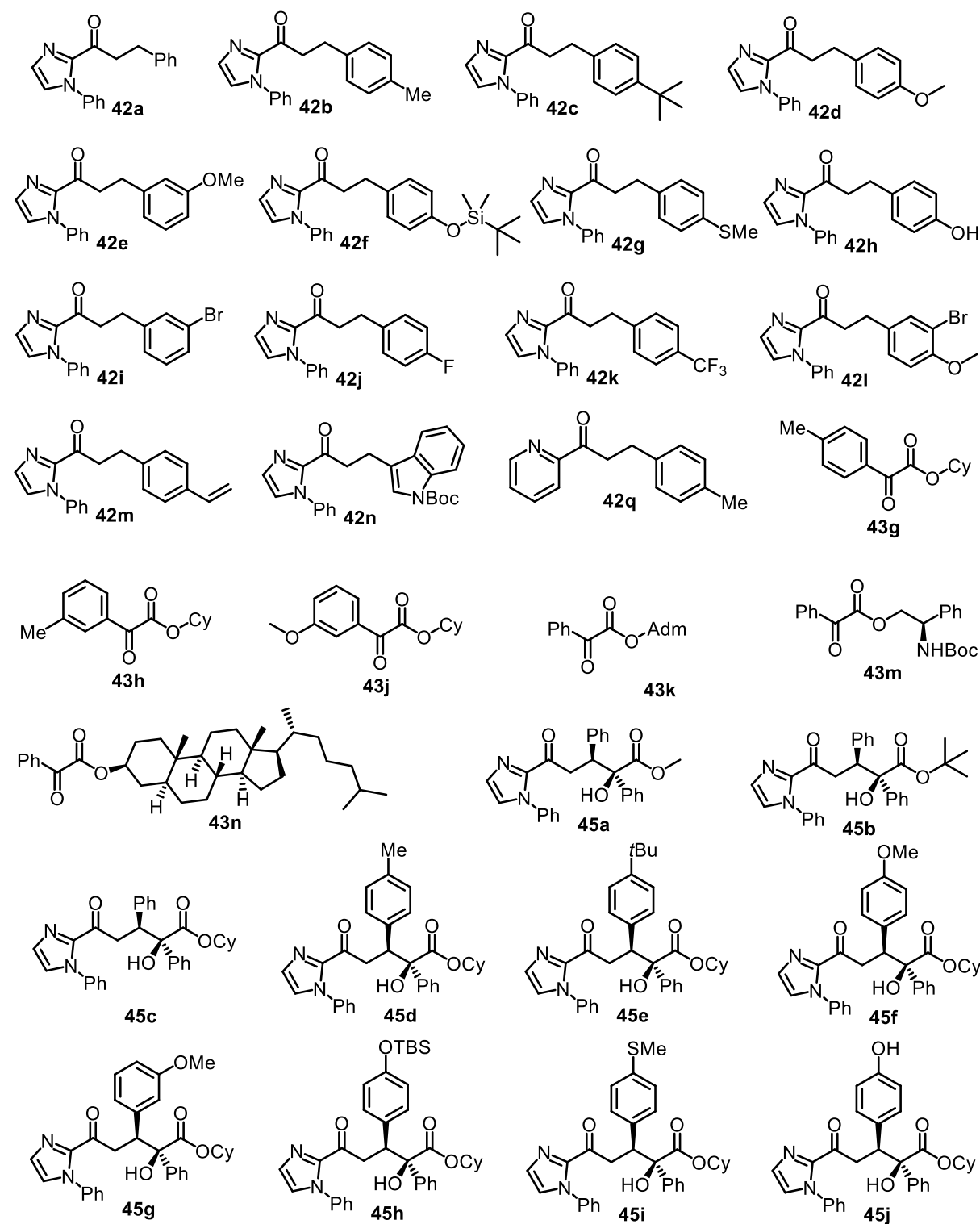


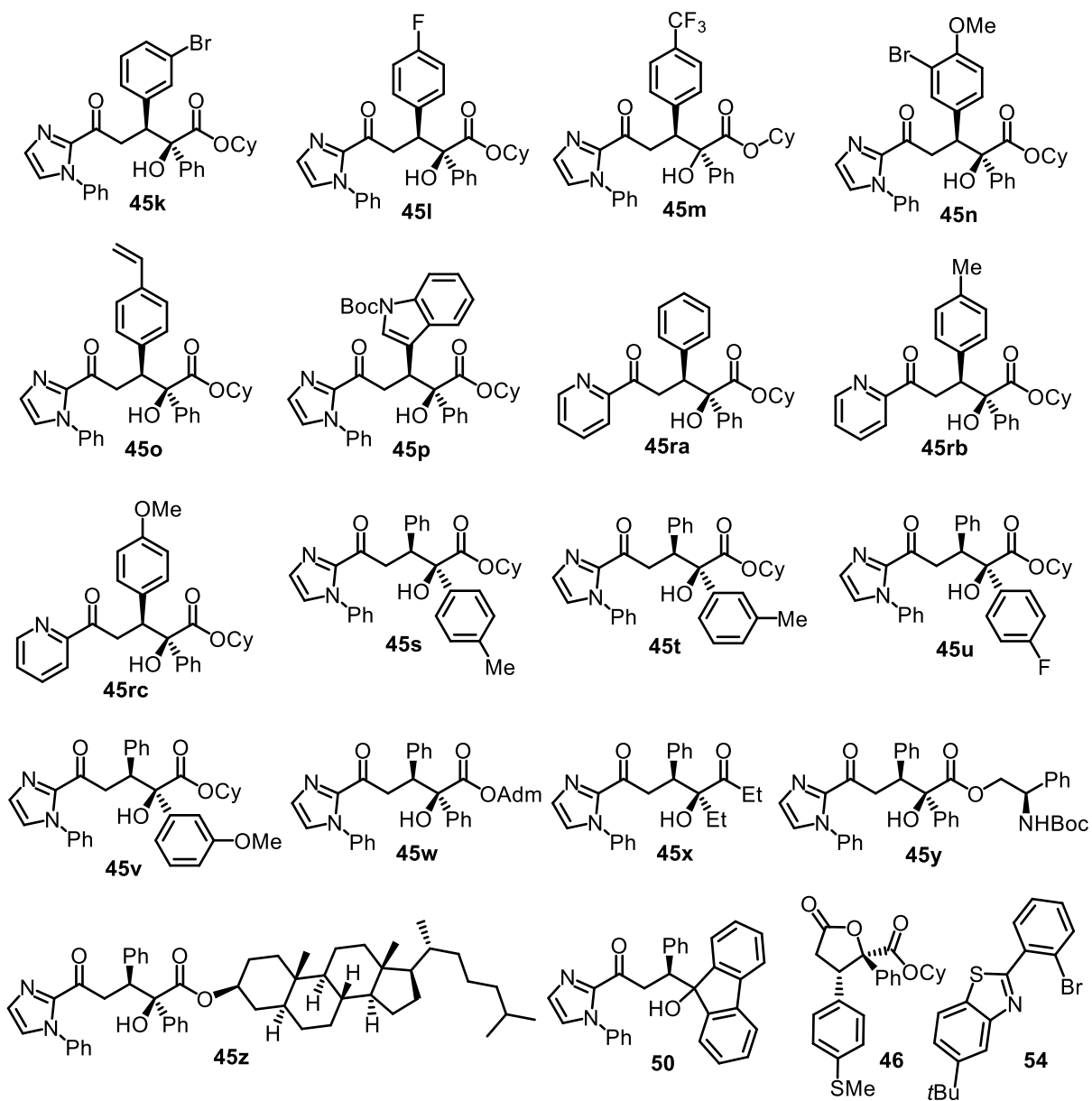
4) Chapter 3.4 and its Experimental Part





5) Chapter 3.5 and its Experimental Part





Statement

gemäß § 10, Abs. 1 der Promotionsordnung der mathematisch-naturwissenschaftlichen Fachbereiche und des Medizinischen Fachbereichs für seine mathematisch-naturwissenschaftlichen Fächer der Philipps-Universität Marburg vom 15.07.2009

Ich erkläre, dass eine Promotion noch an keiner anderen Hochschule als der Philipps-Universität Marburg, Fachbereich Chemie, versucht wurde und versichere, dass ich meine vorgelegte Dissertation

Asymmetric Photoredox Catalysis with Chiral-at-Rhodium Complexes

selbst und ohne fremde Hilfe verfasst, nicht andere als die in ihr angegebenen Quellen oder Hilfsmittel benutz, alle vollständig oder sinngemäß übernommenen Zitate als solche gekennzeichnet sowie die Dissertation in der vorliegenden oder ähnlichen Form noch bei keiner anderen in- oder ausländischen Hochschule anlässlich eines Promotionsgesuchs oder zu anderen Prüfungszwecken eingereicht habe.

Jiajia Ma

Marburg, den 10.07.2018

Curriculum Vitae

Jiajia Ma

Male, born July 19, 1989 in Anhui, P. R. China

Email: majia198908@gmail.com

Education

- 09/2014–present** *Ph.D.* Organic Chemistry, University of Marburg, Germany
Advisor: Prof. Eric Meggers
- 2011/09–2014/07** *M.Sc.* Organic Chemistry, Xiamen University, China
Advisor: Prof. Eric Meggers and Dr. Lei Gong
- 2007/09–2011/07** *B.S.* Bioscience, Northwest A&F University, China

Research Experiences

Ph.D. study: Asymmetric Photoredox Catalysis with Chiral-at-Rhodium Complexes

Publications:

1. J. Ma, J. Lin, L. Zhao, K. Harms, M. Marsch, X. Xie, E. Meggers, *Angew. Chem. Int. Ed.* **2018**, DOI: 10.1002/anie.201804040.
2. J. Ma[‡], X. Zhang[‡], X. Huang, S. Luo, E. Meggers, *Nat. Protoc.* **2018**, *13*, 605. (‡ Equal contribution)
3. J. Ma, X. Xie, E. Meggers, *Chem. Eur. J.* **2018**, *24*, 259.
4. J. Ma, A. R. Rosales, X. Huang, K. Harms, R. Riedel, O. Wiest, E. Meggers, *J. Am. Chem. Soc.* **2017**, *139*, 17245. (featured in *Synfacts* **2018**, 0157)
5. J. Ma, K. Harms, E. Meggers, *Chem. Commun.* **2016**, *52*, 10183.
6. J. Ma, X. Shen, K. Harms, E. Meggers, *Dalton Trans.* **2016**, *45*, 8320.

M.Sc. study: Synthesis of Chiral-at-Metal Brønsted Base Complexes and their Application in Asymmetric aza-Henry Reaction

Publications:

1. J. Ma, X. Ding, Y. Hu, Y. Huang, L. Gong, E. Meggers, *Nat. Commun.* **2014**, *5*, 4531.
2. L.-A. Chen, W. Xu, B. Huang, J. Ma, L. Wang, J. Xi, K. Harms, L. Gong, E. Meggers, *J. Am. Chem. Soc.* **2013**, *135*, 10598.
3. L.-A. Chen, J. Ma, M. A. Celik, H.-L. Yu, Z. Cao, G. Frenking, L. Gong, E. Meggers, *Chem. Asian J.* **2012**, *7*, 2523.